PHOTONITRATION OF AROMATIC COMPOUNDS BY TETRANITROMETHANE

A thesis

presented for the Degree

of

Doctor of Philosophy in Chemistry

in the

University of Canterbury

by

David J. Timmerman-Vaughan

University of Canterbury

Christchurch

New Zealand

1996

PHYSICAL
SCIENCES
LIBRARY
THESIS
copy 2

TABLE OF CONTENTS

Abstract *i*

CHAPTER ONE Introduction

1.1	Aromatic Nitration *via* the Nitronium Ion	1
1.2	Electron Transfer in Aromatic Nitration	2
1.3	Charge-Transfer Complexes	7
1.4	Tetracyanoethylene Charge-Transfer Complexes	8
1.5	Electron Donor-Acceptor Complexes with Tetranitromethane	11
1.6	Photoproducts Formed in the Photolysis of Anthracene Derivatives with Tetranitromethane	17
1.7	Mechanism for the Formation of Photoproducts (4) and (5)	17
1.8	Competitive Reactions of Trinitromethanide Ion and Nitrogen Dioxide with Aromatic Radical Cations	20
1.9	Photochemical Nitration of Naphthalene by Tetranitromethane	23
1.10	Mechanistic Description of the Formation of the Principal Adducts (7)-(10) from the Photolysis of Naphthalene with Tetranitromethane	26
1.11	Photochemical Nitration of 1,4-Dimethylnaphthalene by Tetranitromethane	28
1.12	Solvent and Salt Effects on the Photochemical Nitration of Aromatic Compounds by Tetranitromethane	33
1.13	References for Chapter One	43

CHAPTER TWO Photonitration of 1,4,6,7-Tetramethylnaphthalene (56), 2,6-Dimethylnaphthalene (57) and 1,3-Dimethylnaphthalene (58).

2.1	Introduction	46
2.2	The Photolysis of 1,4,6,7-Tetramethylnaphthalene (56)	56
2.3	The Photochemistry of 1,4,6,7-Tetramethylnaphthalene (56) in Dichloromethane	56
2.4	Rearrangement of 1,4,6,7-Tetramethyl-*r*-1-nitro-*t*-4-trinitromethyl-1,4-dihydronaphthalene (75) on Silica Gel	66
2.5	The Photochemistry of 1,4,6,7-Tetramethylnaphthalene (56) in Acetonitrile	72
2.6	The Photochemistry of 1,4,6,7-Tetramethylnaphthalene (56) in Dichloromethane Containing Trifluoroacetic Acid	75
2.7	Rearrangement of 1,4,6,7-Tetramethyl-*r*-1-nitro-*t*-4-trinitromethyl-1,4-dihydronaphthalene (75) in (D)Chloroform	76
2.8	Rearrangement of 1,4,6,7-Tetramethyl-*r*-1-nitro-*t*-4-trinitromethyl-1,4-dihydronaphthalene (75) in Acetonitrile	79
2.9	Overview of the Photonitration of 1,4,6,7-Tetramethylnaphthalene (56)	80
2.10	The Photolysis of 2,6-Dimethylnaphthalene (57)	86
2.11	The Photochemistry of 2,6-Dimethylnaphthalene (57) in Dichloromethane	87
2.12	The Photochemistry of 2,6-Dimethylnaphthalene (57) in Acetonitrile	108
2.13	Thermal Cycloaddition of *trans*-3,7-Dimethyl-2-nitro-1-trinitromethyl-1,2-dihydronaphthalene (94) to give the Nitrocycloadduct (101)	112

2.14 Thermal Cycloaddition of *trans*-3,7-Dimethyl-1-trinitro-methyl-1,2-dihydronaphthalen-2-ol (102) to give the Hydroxycycloadduct (104) 113

2.15 Overview of the Photonitration of 2,6-Dimethyl-naphthalene (57) 115

2.16 The Photolysis of 1,3-Dimethylnaphthalene (58) 120

2.17 The Photochemistry of 1,3-Dimethylnaphthalene (58) in Dichloromethane 121

2.18 Thermal Cycloaddition of *trans*-5,7-Dimethyl-2-nitro-1-trinitromethyl-1,2-dihydronaphthalene (110) to give the Nitrocycloadduct (122) 137

2.19 The Photochemistry of 1,3-Dimethylnaphthalene (58) in Acetonitrile 140

2.20 The Photochemistry of 1,3-Dimethylnaphthalene (58) in Dichloromethane Containing Trifluoroacetic Acid 143

2.21 Overview of the Photonitration of 1,3-Dimethyl-naphthalene (58) 144

2.22 References for Chapter Two 151

CHAPTER THREE Photonitration of 1,2,3-Trimethylbenzene (137), 1,2,4,5-Tetramethylbenzene (134), Pentamethylbenzene (135) and Hexamethylbenzene (136)

3.1 Introduction 153

3.2 The Photolysis of 1,2,3-Trimethylbenzene (137) 160

3.3 The Photochemistry of 1,2,3-Trimethylbenzene (137) in Dichloromethane 161

3.4 The Photochemistry of 1,2,3-Trimethylbenzene (137) in Dichloromethane Containing Trifluoroacetic Acid 194
3.5 The Photochemistry of 1,2,3-Trimethylbenzene (137) in Acetonitrile 195
3.6 Base Catalysed Decomposition of Nitro/Trinitromethyl Adducts (151), (154)-(156) with 2,6-Di-*tert*-butyl-4-methyl-pyridine in Dichloromethane 200
3.7 Thermal Cycloaddition of 1,2,3-Trimethyl-*r*-5-nitro-*t*-6-tri-nitromethylcyclohexa-1,3-diene (152) to give the Nitro Cycloadduct (153) 201
3.8 Rearrangement of 2,3,4-Trimethyl-4-nitrocyclohexa-2,5-diene-1-one (163) in (D)Chloroform 202
3.9 Overview of the Photonitration of 1,2,3-Trimethylbenzene (137) 203
3.10 The Photolysis of 1,2,4,5-Tetramethylbenzene (134) 225
3.11 The Photochemistry of 1,2,4,5-Tetramethylbenzene (134) in Dichloromethane 225
3.12 The Photochemistry of 1,2,4,5-Tetramethylbenzene (134) in 1,1,1,3,3,3-Hexafluoropropan-2-ol 233
3.13 The Photochemistry of 1,2,4,5-Tetramethylbenzene (134) in Acetonitrile 238
3.14 The Photochemistry of 1,2,4,5-Tetramethylbenzene (134) in Dichloromethane Containing Trifluoroacetic Acid 244
3.15 Rearrangement of 1,3,4,6-Tetramethyl-*r*-3-nitro-*t*-6-trinitro-methylcyclohexa-1,4-diene (216) in Acetonitrile 245
3.16 Rearrangement of 1,3,4,6-Tetramethyl-*r*-3-nitro-*t*-6-trinitro-methylcyclohexa-1,4-diene (216) in (D)Chloroform 248
3.17 Reactions of 1,2,4,5-Tetramethylbenzene (134) with Nitrogen Dioxide in Dichloromethane 250

3.18 Reactions of 1,2,4,5-Tetramethylbenzene (134) with Nitrogen Dioxide in 1,1,1,3,3,3-Hexafluoropropan-2-ol 251
3.19 Overview of the Photonitration of 1,2,4,5-Tetramethylbenzene (134) 253
3.20 The Photolysis of Pentamethylbenzene (135) 265
3.21 The Photochemistry of Pentamethylbenzene (135) in Dichloromethane 265
3.22 The Photochemistry of Pentamethylbenzene (135) in Acetonitrile 279
3.23 The Photochemistry of Pentamethylbenzene (135) in 1,1,1,3,3,3-Hexafluoropropan-2-ol 281
3.24 The Photochemistry of Pentamethylbenzene (135) in Dichloromethane Containing Trifluoroacetic Acid 282
3.25 Reactions of Pentamethylbenzene (135) with Nitrogen Dioxide in Dichloromethane 285
3.26 Rearrangement of 1,2,3,4,6-Pentamethyl-*r*-3-nitro-*t*-6-trinitromethylcyclohexa-1,4-diene (244) in (D_2)Dichloromethane 287
3.27 Overview of the Photonitration of Pentamethylbenzene (135) 288
3.28 The Photolysis of Hexamethylbenzene (136) 300
3.29 The Photochemistry of Hexamethylbenzene (136) in Dichloromethane 300
3.30 The Photochemistry of Hexamethylbenzene (136) in Acetonitrile 308
3.31 The Photochemistry of Hexamethylbenzene (136) in 1,1,1,3,3,3-Hexafluoropropan-2-ol 314
3.32 Reactions of Hexamethylbenzene (136) with Nitrogen Dioxide in Dichloromethane 315

3.33 Reactions of Hexamethylbenzene (136) with Nitrogen Dioxide in Acetonitrile 317
3.34 Overview of the Photonitration of Hexamethylbenzene (136) 318
3.35 References for Chapter Three 325

CHAPTER FOUR Photonitration of 2,3-Dimethylanisole (307)

4.1 Introduction 328
4.2 The Photolysis of 2,3-Dimethylanisole (307) 336
4.3 The Photochemistry of 2,3-Dimethylanisole (307) in Dichloromethane 337
4.4 The Photochemistry of 2,3-Dimethylanisole (307) in Acetonitrile 353
4.5 The Photochemistry of 2,3-Dimethylanisole (307) in 1,1,1,3,3,3-Hexafluoropropan-2-ol 353
4.6 The Photochemistry of 2,3-Dimethylanisole (307) in Dichloromethane Containing Trifluoroacetic Acid 357
4.7 Overview of the Photonitration of 2,3-Dimethylanisole (307) 359
4.8 References for Chapter Four 365

CHAPTER FIVE Experimental and Appendix

5.1 Apparatus, Materials and Instrumentation 367
5.2 Experimental Relating to Chapter Two 370
5.3 Experimental Relating to Chapter Three 393

5.4 Experimental Relating to Chapter Four 434

5.5 Appendix : Crystallography 441

5.6 References for Chapter Five 465

Acknowledgements 467

Abstract

This thesis describes the photochemical reactions of tetranitromethane with aromatic compounds. These reactions are known to occur by initial formation of a triad consisting of an aromatic radical cation, trinitromethanide ion and nitrogen dioxide and the subsequent reactions which occur involve the recombination of these species of the triad.

This thesis is in three major parts. In the first (Chapter 2) the photochemical reactions of tetranitromethane with 1,4,6,7-tetramethylnaphthalene (56), 2,6-dimethylnaphthalene (57) and 1,3-dimethylnaphthalene (58) are described. In all cases the initial recombination step involves the aromatic radical cation and trinitromethanide ion and the reactions of these three naphthalene derivatives further documents the importance of the energy of the delocalized carbon radical formed in the first recombination step. A number of hydroxy/trinitromethyl adducts (84), (98), (102)-(104), (114), (115) and nitro/trinitromethyl adducts (75), (94)-(97), (99)-(101), (110)-(113), (122) were isolated as part of this study.

In the second part of this thesis (Chapter 3) the analogous reactions of 1,2,3-trimethylbenzene (137), 1,2,4,5-tetramethylbenzene (134), pentamethylbenzene (135) and hexamethylbenzene (136) are described. In the photolysis of 1,2,3-trimethylbenzene (137) with tetranitromethane a variety of nitronic esters (159)-(162) are formed in addition to "double" adducts (139), (157), (158) which arise by subsequent addition of nitrogen dioxide to initially formed hydroxy/trinitromethyl adducts (176), (177) and nitro/trinitromethyl adducts (152), (175), and the more usual "single" nitro/trinitromethyl adducts (151)-(156). In the reactions of 1,2,4,5-tetramethylbenzene (134), pentamethylbenzene (135) and hexamethylbenzene (136) evidence was obtained which pointed to increasing instability of initially formed adducts. In particular for pentamethylbenzene (135), nitro/trinitromethyl adducts (244), (245) were

formed at -20, -50 and -78° in dichloromethane but rearranged rapidly in solution. For hexamethylbenzene (136) direct evidence of the formation of nitro/trinitromethyl adducts could not be obtained because of the insolubility of the substrate, hexamethylbenzene (136), in the photolysis solvents. However rearrangement products (279)-(282), (287), (288), analogous to those from pentamethylbenzene (135), were obtained from the photolysis of hexamethylbenzene (136) with tetranitromethane.

The final part of this thesis (Chapter 4) describes the photolysis of 2,3-dimethylanisole (307) with tetranitromethane. The purpose of this section of the work was to explore the effect of replacing one of the flanking methyl groups in 1,2,3-trimethylbenzene (137) with a methoxy group. In the event "single" hydroxy/trinitromethyl adducts (316), (317) and nitro/trinitromethyl adducts (314), (315) were formed but nitronic esters and "double" adducts, characteristic of the reactions of 1,2,3-trimethylbenzene (137), were notably absent from among the products.

CHAPTER ONE

INTRODUCTION

1.1 Aromatic Nitration *via* the Nitronium Ion

In 1903 Euler[1] first proposed that the nitronium ion, NO_2^+, might be the actual nitrating agent under certain conditions of nitration. Substantial work by Ingold and co-workers[2-7] over a considerable number of years confirmed that "The active product for nitration is the nitronium ion, NO_2^+".[5] They studied the kinetics of nitration reactions involving various aromatics with nitric acid using solvents such as sulphuric acid, nitric acid, nitromethane, acetic acid and water.

The mechanism that Hughes *et al.*[5] proposed is illustrated in Scheme 1.1. It involved acid catalysed conversion of nitric acid into the nitric acidium ion, $H_2NO_3^+$ (1), followed by dissociation to form the nitronium ion, NO_2^+ (2). The nitronium ion then underwent direct electrophilic attack by the aromatic substrate (3), followed by the loss of a proton into the solvent (4).

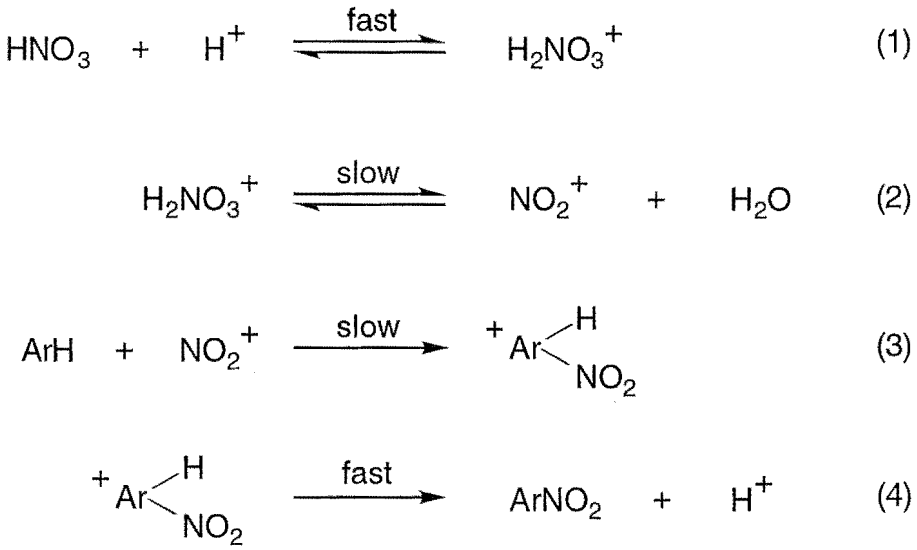

Scheme 1.1

The rate determining step in Scheme 1.1 can be either reaction (2) or reaction (3), depending on the concentration and reactivity of the aromatic substrate. Evidence for reaction *via* the nitronium ion came partly from a zeroth-order kinetic form for nitration in organic solvents[5] and partly from cryoscopic[6] and spectroscopic[7] studies on equilibria involving the nitronium ion in strongly acidic media.

1.2 Electron Transfer in Aromatic Nitration

In 1945 Kenner[8] proposed an electron transfer mechanism for the nitration of benzene. He suggested that the initial interaction of the nitronium ion with benzene could lead to electron transfer resulting in the formation of a benzene radical cation and nitrogen dioxide ($^{\bullet}NO_2$) (1), as seen in Scheme 1.2. Subsequently, loss of a proton from the intermediate benzene radical cation would help "restore the aromatic condition" (2). In the mechanism shown in Scheme 1.2, Kenner used brackets to indicate that the reactants remained "within the sphere of each other's action".

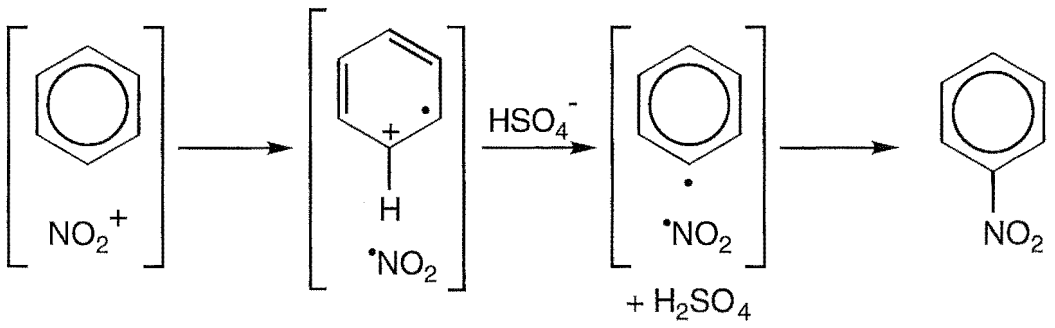

Scheme 1.2

Ingold and co-workers[9] commented on Kenner's proposal stating that although dimerization products due to radical-radical coupling were not seen, this did not automatically imply that the reactants had to be held "within a sphere of each other's action". They also commented that the $^{\bullet}NO_2$ should be within the "sphere of action" of the bisulphate ion and hence react with it as was the case with introduced $^{\bullet}NO_2$.

In a series of electrophilic aromatic nitration reactions involving stable nitronium salts, Olah[10] observed a low substrate (intermolecular) selectivity, but at the same time high positional (intramolecular) selectivity. He suggested that the highest energy transition state was a π-complex (1), formed by overlap of the highest lying occupied aromatic π orbital containing an electron pair with the empty orbital of the electrophile. It was this π-complex which determined the observed intermolecular selectivity. The intramolecular selectivity was due to subsequent formation of the Wheland intermediate (2), as the two-electron, three-centre bond of the π-complex was opened (See Scheme 1.3).

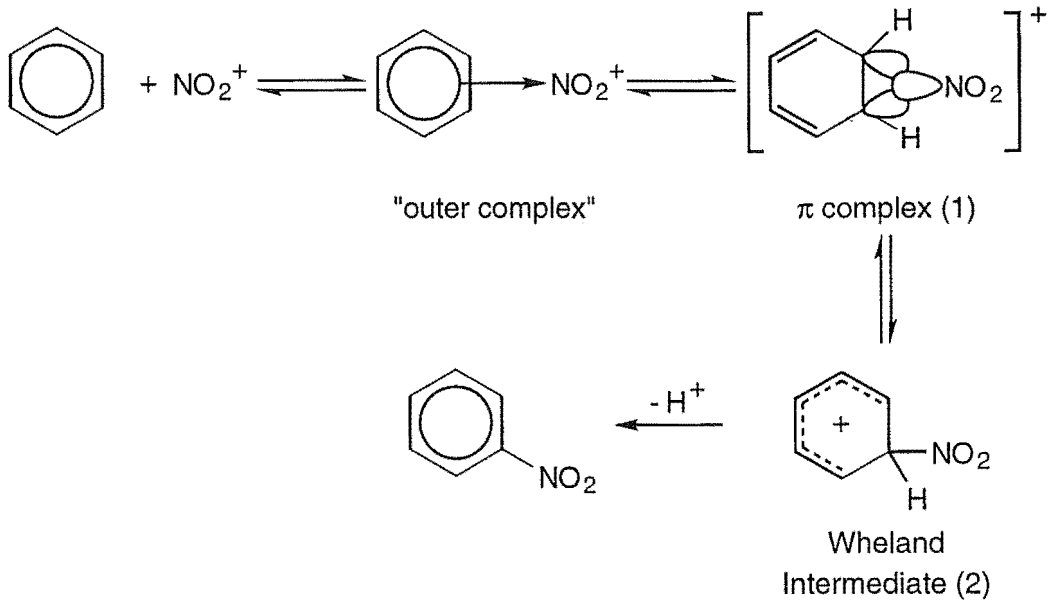

Scheme 1.3

In 1977 Perrin[11] proposed an alternative mechanism to Olah, suggesting that encounter-limited electron transfer from the aromatic compound to the nitronium ion occurred to form a radical cation and $^{\bullet}NO_2$ (1). This was followed by radical-pair collapse to the Wheland intermediate (2), as represented in Scheme 1.4.

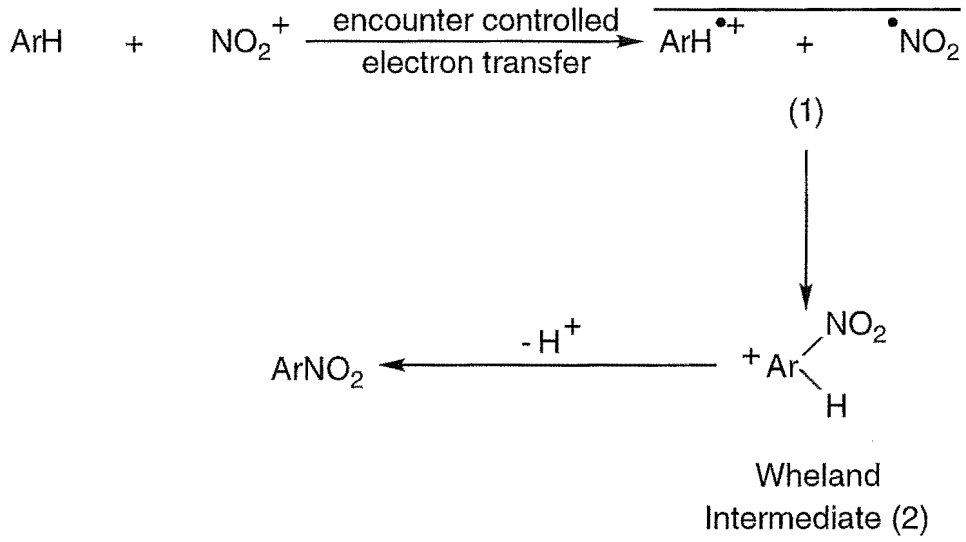

Scheme 1.4

Perrin provided evidence for his mechanism with an electrochemical experiment using a controlled anode potential to oxidise a mixture of naphthalene (1) and $^{\bullet}NO_2$. He assumed that only the naphthalene would react to form the naphthalene radical cation (naph$^{\bullet+}$), since the applied potential was incapable of oxidising $^{\bullet}NO_2$. The radicals would then react to form the Wheland intermediate and products. He obtained a product mixture containing 1-nitronaphthalene (2) and 2-nitronaphthalene (3) in a ratio of 9.2±1, which was within experimental error of the ratio of 10.9±1 that he had observed in the nitration of naphthalene with HNO_3/H_2SO_4, in CH_3CN with urea added (See summary in Scheme 1.5).

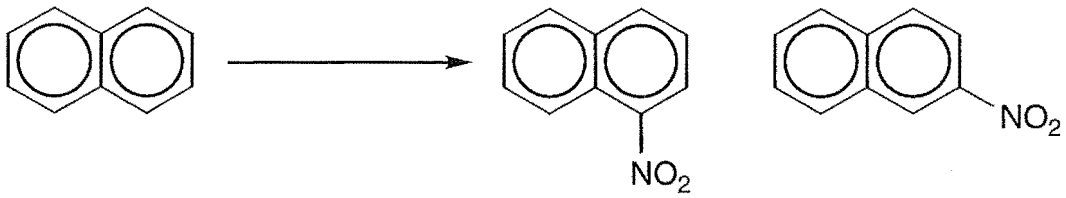

(1) (2) (3)

(a) naph$^{\bullet+}$/ $^{\bullet}NO_2$ generated electrochemically	9.2	:	1
(b) NO_2^+ *via* HNO_3/H_2SO_4 in CH_3CN/urea	10.9	:	1

Scheme 1.5

Perrin interpreted the intramolecular selectivity and positional reactivity in terms of the spin density of the radical cation and Wheland intermediate stability because the attacking species was $^{\bullet}NO_2$ and not NO_2^+.

Eberson *et al.*[12] found major problems with the design and interpretation of Perrin's[11] electrochemical experiment. Repeating Perrin's[11] experiment Eberson *et al.*[12] found that direct nitration of naphthalene by $^{\bullet}NO_2$ accounted for 50-60% of the nitronaphthalenes formed. They also found that the reaction was acid catalysed and that acid was formed at the anode during the reaction, either from trace amounts of water, or due to the formation of dimers and higher oligomers, or *via* proton loss from the Wheland intermediate upon product formation. The nitronium ion may also have formed from $^{\bullet}NO_2$ at the high potentials used in the experiment.

Consequently, Eberson and Radner[13] generated the naphthalene radical cation as its hexafluorophosphate salt and reacted this with $^{\bullet}NO_2$. They obtained a ratio of 1-nitronaphthalene (2) to 2-nitronaphthalene (3) of

≈ 40, clearly different from the ratio of 9.2 which Perrin obtained. Therefore, Eberson and Radner[14] concluded that the naph$^{\bullet+}$/$^{\bullet}NO_2$ reaction could not be the elementary step in the sequence of reactions shown in Scheme 1.4.

Eberson and Radner[14] compared the isomer distribution from their electrochemical experiment with two other nitration procedures - nitration of naphthalene by $^{\bullet}NO_2$ in dichloromethane and nitration of naphthalene by NO_2^+, using HNO_3/acetic anhydride, as seen in Table 1.1.

Table 1.1 Ratio of 1-nitronaphthalene (2) to 2-nitronaphthalene (3) formed *via* various nitration mechanisms.

Reaction	Ratio (1-NO_2 naph : 2-NO_2 naph)
Naph$^{\bullet+}$ + $^{\bullet}NO_2$	40
Naph + $^{\bullet}NO_2$	25
Naph + NO_2^+	11

Later, Johnston *et al.*[15] studied the nitration reaction of naphthalene using ^{15}N CIDNP (Chemically Induced Dynamic Nuclear Polarisation) techniques. For reactions involving electron transfer this technique gives enhanced absorption of the normal n.m.r. signal.[16] Johnston *et al.*[15] found only a slight enhancement in the nitration of naphthalene and hence suggested that only a small percentage of the naphthalene reacts *via* the electron transfer pathway described by Perrin[11] (Scheme 1.4).

1.3 Charge-Transfer Complexes

In 1949 Benesi and Hildebrand[17] discovered that iodine dissolved in various aromatic hydrocarbons absorbed intensely in the region 280-400 nm, as seen in Fig. 1.1. They assumed that the intense absorption peaks were

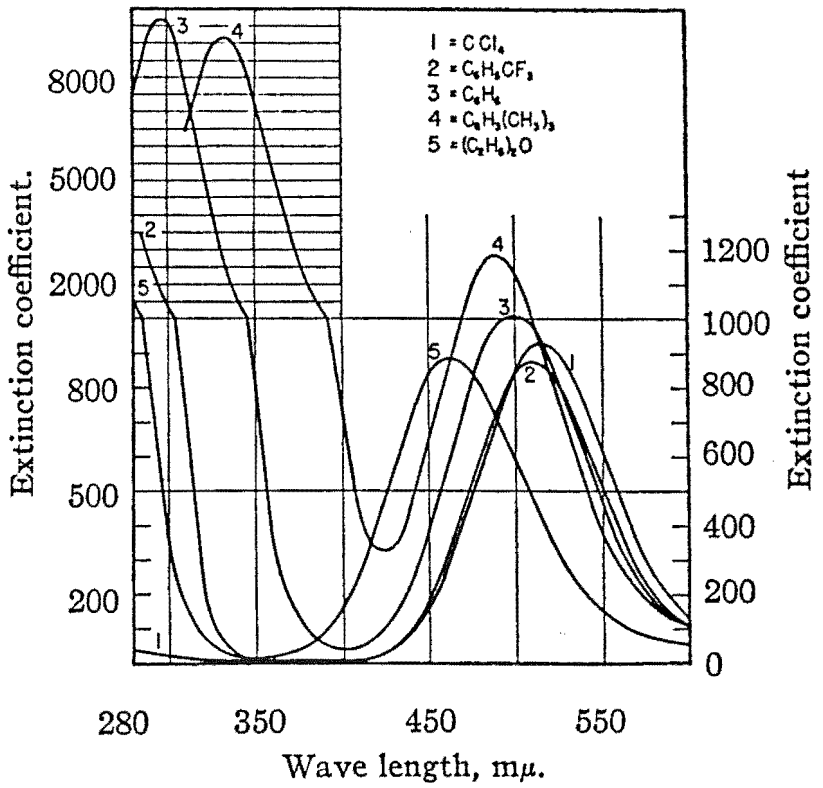

Fig. 1.1 Absorption of iodine in various solvents.

characteristic of an iodine-aromatic hydrocarbon complex, as neither the iodine nor the aromatic hydrocarbon absorbed in this region. Mulliken[18] suggested that "this absorption ... may be due to an intermolecular charge-transfer process during light absorption".

Molecules capable of giving up an electron are electron rich and are called electron donors (D). Molecules which can accept an electron are electrophilic and are called electron acceptors (A). Electron donor ability is

related to ionisation potentials, whereas electron acceptor ability is related to electron affinity and reduction potentials.[19] Mulliken[20] called the electron donor-electron acceptor interactions "donor-acceptor complexes". The donor and acceptor exist together as a weakly bound complex, as illustrated in Scheme 1.6.[19]

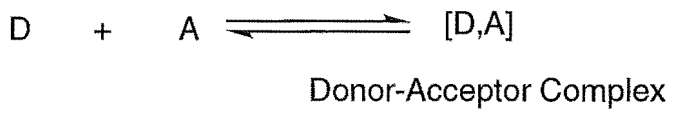

Scheme 1.6

The donor-acceptor complex absorbs light energy corresponding to the absorption band, which causes the transfer of an electron from the donor to the acceptor, to form a radical ion pair called a charge-transfer (CT) complex (See Scheme 1.7).

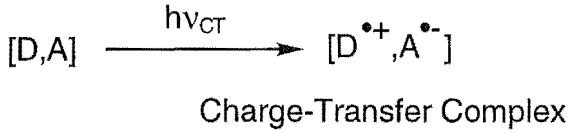

Scheme 1.7

1.4 Tetracyanoethylene Charge-Transfer Complexes

Masnovi *et al.*[21,22] studied a series of anthracene (An) donors with tetracyanoethylene (TCNE) as the acceptor. They found that the charge-transfer absorption bands were exceptionally well resolved from those of the components, as seen in Fig. 1.2. Note that TCNE only absorbs at wavelengths ≤375 nm.

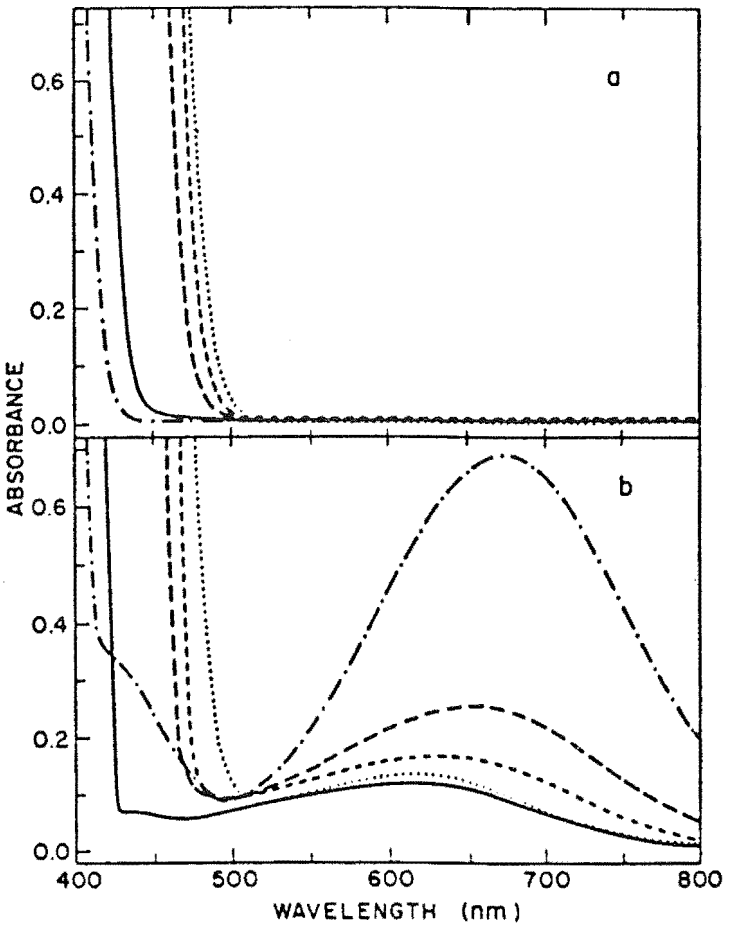

Fig. 1.2 Electronic absorption spectra of (a) various substituted anthracenes and (b) substituted anthracenes with TCNE in dichloromethane.

Transient picosecond absorption techniques[23] were used to study the electron donor-acceptor (EDA) complex of the anthracene with TCNE. Irradiating the EDA complex at a wavelength >500 nm effectively ensured that neither the uncomplexed donor nor the uncomplexed acceptor was excited.[21,22] Fig. 1.3(a) shows the difference absorption spectra after excitation of a solution of 9-cyanoanthracene (CNA) / TCNE EDA complex. Spectra from the electrochemical oxidation of CNA and the electrochemical reduction of TCNE are shown in Fig. 1.3(b) and (c) respectively. It was concluded[22] that Fig. 1.3(a) was a combination of Fig. 1.3(b) and (c), hence the EDA complex consisted of CNA radical cations and TCNE radical anions.

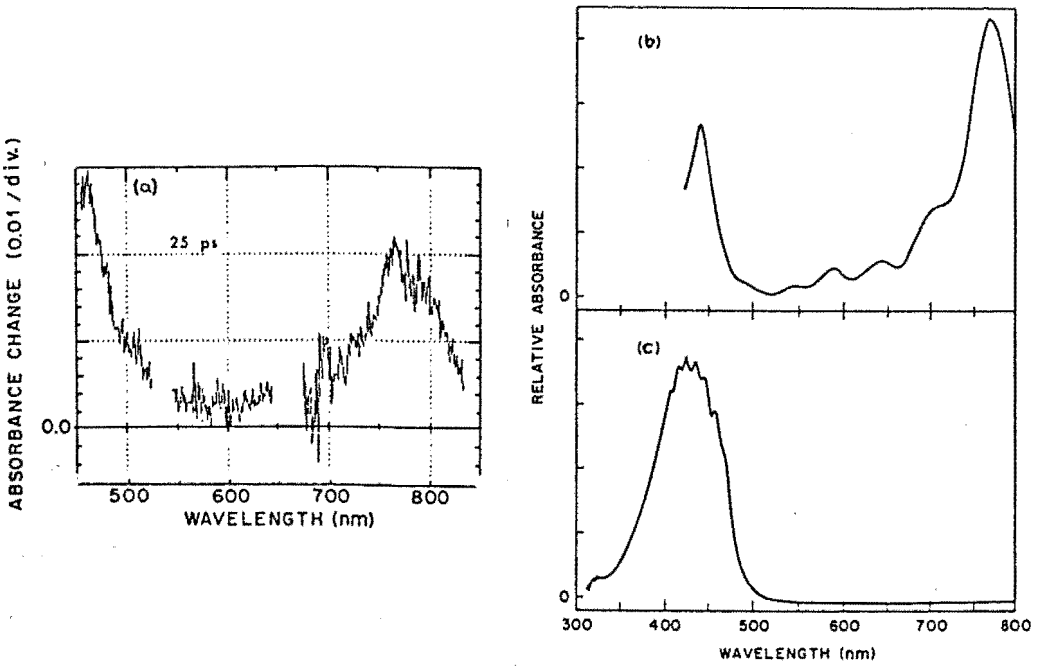

Fig. 1.3 (a) Picosecond absorption spectrum for the CNA/TCNE EDA complex after excitation, (b) and (c) Electronic absorption spectra of the CNA radical cation and the TCNE radical anion, respectively, generated electrochemically.

Similar results were observed for other anthracene donors thus verifying the formation of a charge-transfer complex consisting of a radical ion pair as summarised in Scheme 1.8.

$$An + TCNE \rightleftharpoons [An,TCNE]$$

Donor- Acceptor Complex

$$[An,TCNE] \xrightarrow{h\nu_{CT}} [An^{\bullet+},TCNE^{\bullet-}]$$

Charge-Transfer Complex

Scheme 1.8

The charge-transfer complex was found[22] to undergo rapid back electron transfer to regenerate the original EDA complex without the formation of stable photoproducts, as illustrated in Scheme 1.9.

$$[An^{\bullet+},TCNE^{\bullet-}] \xrightarrow{\sim 60\ ps} [An,TCNE]$$

Scheme 1.9

Tetranitromethane (TNM) was therefore chosen by Masnovi *et al.*[24] as a different acceptor because it was known[25] to be chemically photoactive and form EDA complexes.

1.5 Electron Donor-Acceptor Complexes with TNM

Masnovi *et al.*[24] studied a series of 9-substituted anthracenes with TNM in the presence of dichloromethane. Immediately upon mixing a colourless solution of TNM with the substituted anthracene in dichloro-methane, a brown colour resulted due to the EDA complex, as represented in Scheme 1.10. The charge-transfer absorption spectra were

$$An + C(NO_2)_4 \rightleftharpoons [An,C(NO_2)_4]$$

EDA Complex

Scheme 1.10

characteristically featureless, with a broad tail extending to ≈ 700 nm, as shown in Fig. 1.4.

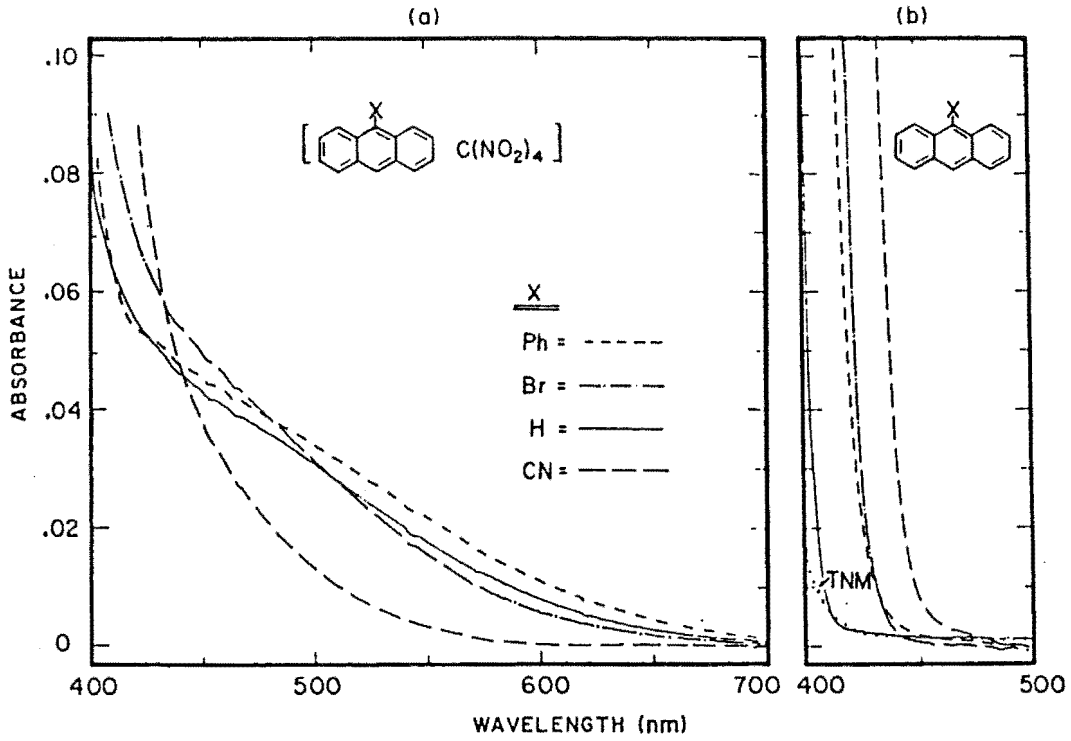

Fig. 1.4 (a) Charge-transfer absorption spectra of the EDA complexes of various 9-substituted anthracenes with TNM in dichloromethane, (b) The absorption spectra of the pure anthracene derivative and pure TNM alone in dichloromethane.

Irradiation at wavelengths >500 nm would selectively excite only the EDA complex and neither the uncomplexed anthracene donor nor the TNM acceptor. Masnovi *et al.*[24] irradiated the EDA complex at 532 nm and using transient picosecond absorption techniques obtained various difference absorption spectra, as observed in Fig. 1.5(a). The absorption bands in Fig. 1.5(a) were assigned to the anthracene radical cations, after comparison with spectra of the radical cations independently generated using electrochemical anodic oxidation [See Fig. 1.5(b)].

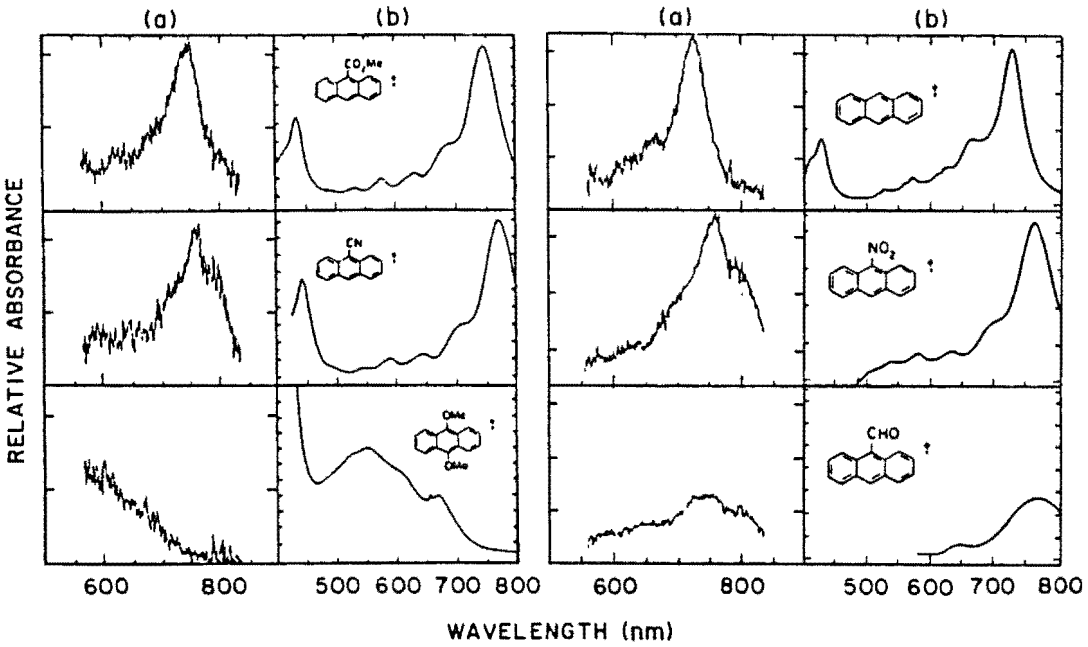

Fig. 1.5 Picosecond absorption spectra of various anthracene/TNM EDA complexes (a) after excitation, compared with (b) the absorption spectra of the corresponding radical cation generated by anodic oxidation.

Masnovi *et al.*[24] found that the radical cations of the anthracene derivatives had substantially longer lifetimes when generated from TNM complexes compared with those generated from TCNE complexes. They also found high yields of photoproducts. This indicated to them that the TNM acceptor radical anion is short lived.

Using pulse radiolysis, Rabani *et al.*[26] showed that electron capture by TNM leads to the formation of the trinitromethanide anion, $(O_2N)_3C^-$, and nitrogen dioxide radical, $^{\bullet}NO_2$, as outlined in Scheme 1.11. In order to

$$C(NO_2)_4 + e^- \longrightarrow (O_2N)_3C^- + {}^{\bullet}NO_2$$

Scheme 1.11

observe the $(O_2N)_3C^-$ absorption, λ_{max} 350 nm,[27] a donor was needed which did not obscure the spectral region below 450 nm, as was the case with the anthracene donors. Hence hexamethylbenzene and hexaethylbenzene, which absorb at wavelengths lower than 300 nm, were chosen as donors.[28]

Absorption spectra produced by time resolved picosecond spectroscopy were characterized by two absorption bands [Fig. 1.6(a)]. When compared with the absorption spectra generated by electrochemical oxidation of hexamethylbenzene, the absorption band centred near 500 nm was assigned to the hexamethylbenzene radical cation [Fig.1.6(b)]. The second absorption band at ~ 350 nm was assigned to $(O_2N)_3C^-$, after comparison with the absorption spectra generated by electrochemical reduction of TNM, also seen in Fig. 1.6(b).

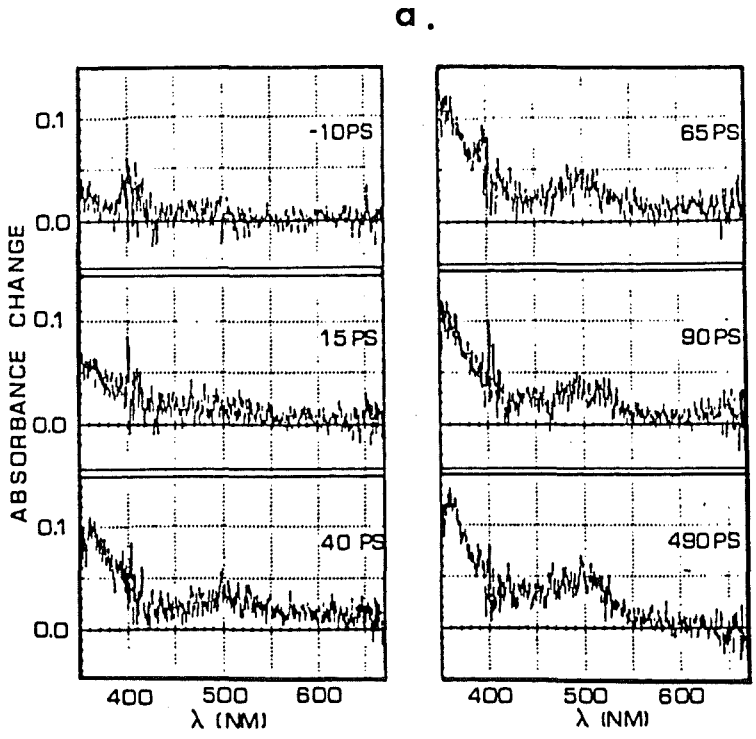

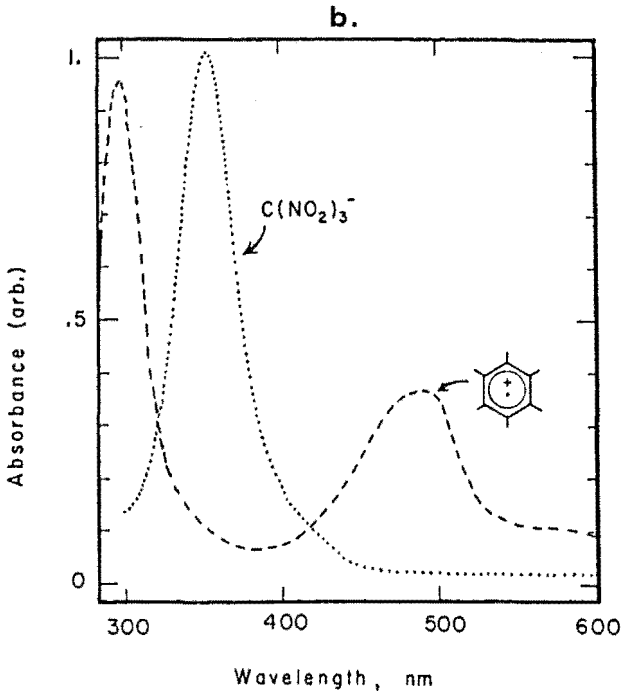

Fig. 1.6 (a) Difference absorption spectra obtained after irradiation of hexamethylbenzene and TNM in dichloromethane,
(b) Absorption spectra of hexamethylbenzene radical cation and trinitromethanide anion generated electrochemically.

Masnovi *et al.*[28] concluded that the tetranitromethane radical anion, formed by irradiation of the EDA complex, is short lived and rapidly dissociates upon electron capture to $(O_2N)_3C^-$ and $^{\bullet}NO_2$, as depicted in Scheme 1.12.

$$C(NO_2)_4 + e^- \longrightarrow (O_2N)_4C^{\bullet-} \xrightarrow{<10\ ps} (O_2N)_3C^- + {}^{\bullet}NO_2$$

Scheme 1.12

The presence of $^{\bullet}NO_2$ could not be confirmed directly in any of the transient absorption spectra due to its weak, broad absorption (250 nm to

greater than 800 nm[29]) being obscured by the more intense absorptions of the radical cation donor and $(O_2N)_3C^-$. The presence of $^{\bullet}NO_2$ was assumed, however, since stable photoadducts were isolated and identified (See Section 1.6).

Using the rates of back-electron transfer and chemical evolution of $(O_2N)_3C^-$, Masnovi *et al.*[28] reasoned an upper limit of ≈ 3 ps for the half-life of the tetranitromethane radical anion in the charge-transfer complex, assuming that the fragmentation, depicted in Scheme 1.12, was responsible for the general photoreactivity of the EDA complexes of TNM (See summary in Scheme 1.13).

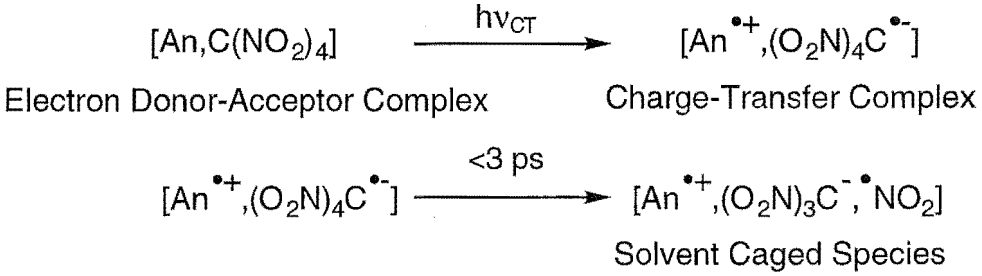

Scheme 1.13

The solvent caged species was consequently termed a triad.[30] Triad formation irreversibly destroys the charge-transfer complex and hence prevents any back electron transfer to reform the EDA complex, as was seen with TCNE. Furthermore, the species in the triad combine to produce photoproducts.

1.6 Photoproducts Formed in the Photolysis of Anthracene Derivatives with TNM

In sharp contrast to the photolysis of TCNE with various anthracene derivatives, where no products were formed, Masnovi *et al.*[24] found that products formed in the photolysis of various anthracene derivatives with TNM. They isolated two major products (4) and (5) and characterised them using X-ray crystallography. The products were derived by addition of $(O_2N)_3C^-$ and $^{\bullet}NO_2$ to the 9,10-positions of the 9-substituted anthracene radical cation.

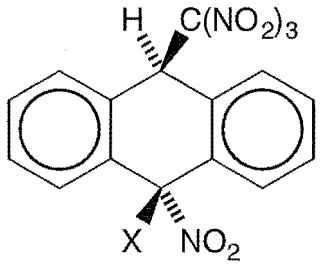

(4) X=Ph
(5) X=Br

The two structures indicated that the attachment of $(O_2N)_3C^-$ was regiospecific with the $(O_2N)_3C^-$ group adding at the unsubstituted 10-position of the 9-substituted anthracene. Also of interest was the overall *anti*-addition of the $(O_2N)_3C^-$ and $^{\bullet}NO_2$ fragments of the triad.

1.7 Mechanism for the Formation of Photoproducts (4) and (5)

In the picosecond absorption spectra of the EDA complex of various 9-substituted anthracenes with TNM, Masnovi *et al.*[24] observed that an

absorption band formed near 550 nm as the radical cations decayed. This was particularly clear for 9-nitroanthracene, as observed in Fig. 1.7.

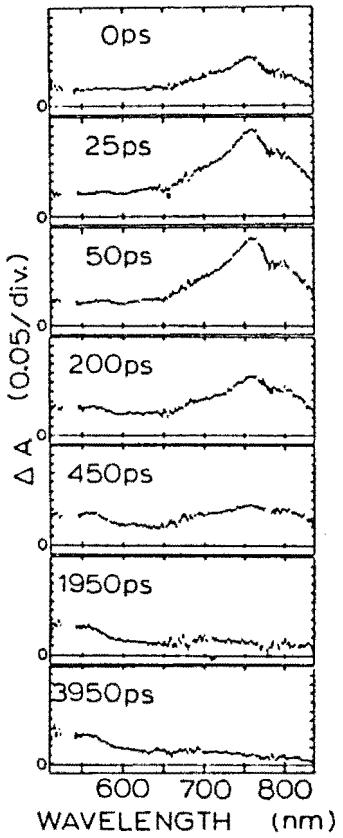

Fig. 1.7 Time resolved picosecond absorption spectra following excitation of the EDA complex of 9-nitroanthracene with TNM.

Masnovi *et al.*[24] proposed that the absorption band was due to the 9-substituted-10-trinitromethyl-10-hydranthryl radical (6), after comparison with the previously reported[31] 9-cyano-10-hydranthryl radical, generated by pulse radiolysis of 9-cyanoanthracene in ethanol. Masnovi *et al.*[24] proposed that the 9-substituted-10-trinitromethyl-10-hydranthryl radical (6) arose by attack of $(O_2N)_3C^-$ on the 9-substituted anthracene derivatives radical cation, as seen in Scheme 1.14.

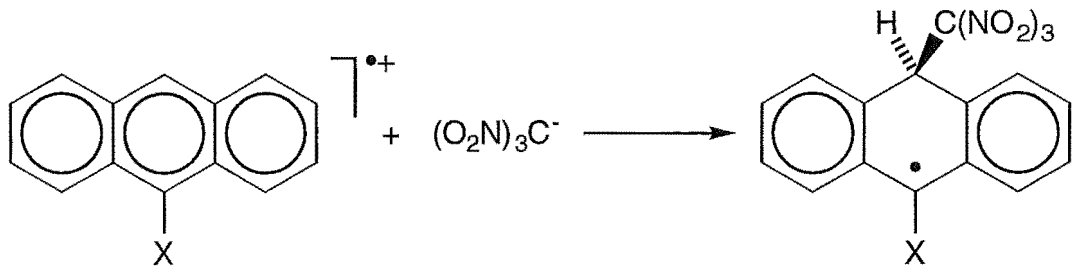

(6)

Scheme 1.14

Addition of $(O_2N)_3C^-$ at the 10-position to produce (6), irrespective of the electron donating/withdrawing group, was consistent with formation of the most stable radical (6).[32]

The final step to form photoproducts (4) and (5) was the coupling of the radical (6) with $^{\bullet}NO_2$, as outlined in Scheme 1.15.

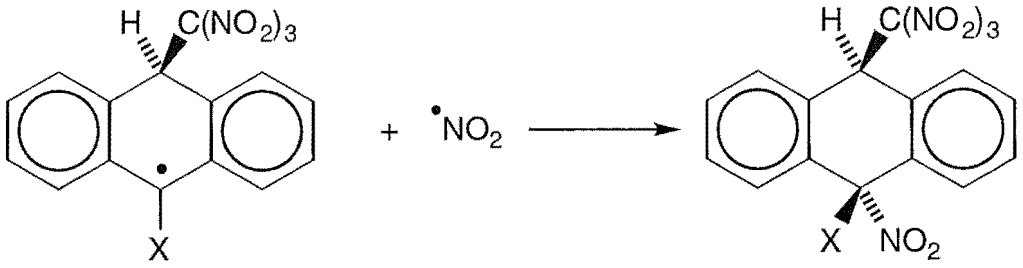

(6)

(4) X=Ph
(5) X=Br

Scheme 1.15

Single crystal X-ray studies[24] showed that the trinitromethyl group occupied a *pseudo*-axial position and that the $^{\bullet}NO_2$ was added stereoselectively, from the sterically less hindered face opposite the bulky

trinitromethyl group, resulting in an overall *anti*-addition of the TNM fragments.

1.8 Competitive Reactions of Trinitromethanide Ion and Nitrogen Dioxide with Aromatic Radical Cations

As discussed previously in Section 1.5, Masnovi *et al.*[28] showed that a charge-transfer (CT) complex was formed upon irradiation of the EDA complex between an aromatic compound (ArH) and TNM. Within 3 ps this led to a triad consisting of $ArH^{\bullet+}$, $(O_2N)_3C^-$ and $^{\bullet}NO_2$, as summarised in Scheme 1.16.

$$\underset{\text{EDA Complex}}{[An,C(NO_2)_4]} \xrightarrow{h\nu_{CT}} \underset{\text{CT Complex}}{[An^{\bullet+},(O_2N)_4C^{\bullet-}]} \xrightarrow{<3\ ps} \underset{\text{Triad}}{[An^{\bullet+},(O_2N)_3C^-,{}^{\bullet}NO_2]}$$

Scheme 1.16

The formation of adducts raised the question as to which of the components in the triad would react with $ArH^{\bullet+}$ in the first chemical step of the reaction. Would the reaction occur (a) with $(O_2N)_3C^-$ attack on $ArH^{\bullet+}$ or (b) with $^{\bullet}NO_2$ attack on $ArH^{\bullet+}$, as depicted in Scheme 1.17?

$$ArH^{\bullet+} + (O_2N)_3C^- \longrightarrow {}^{\bullet}Ar(H)C(NO_2)_3 \qquad (a)$$

$$ArH^{\bullet+} + {}^{\bullet}NO_2 \longrightarrow {}^{+}Ar(H)NO_2 \qquad (b)$$

Scheme 1.17

Eberson *et al.*[33] attempted to solve this problem by removing one reactant of the triad as soon as it formed and observing the chemical changes. By adding trifluoroacetic acid (TFA), it would be possible to protonate $(O_2N)_3C^-$ forming the less nucleophilic nitroform, as illustrated in Scheme 1.18.

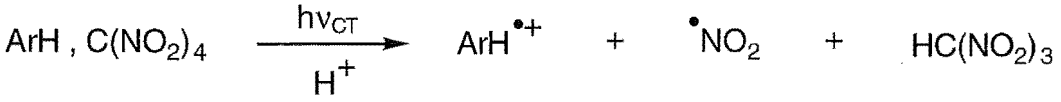

Scheme 1.18

By monitoring the reaction using EPR spectroscopy they found that without TFA present it was not possible to detect the $ArH^{\bullet+}$. However, with TFA present a rapid build up of the $ArH^{\bullet+}$ signal usually occurred.

The results of the study are shown in Table 1.2, which contains the aromatic substrates listed approximately in order of decreasing $E^{\circ}(ArH^{\bullet+}/ArH)$. The substrates range from very reactive radical cations, like naphthalene and 1-methylnaphthalene, to radical cations which have high stability like tris(4-bromophenyl)amine.

Without TFA present, only the least reactive radical cations [9,10-diphenylanthracene, perylene and tris(4-bromophenyl)amine] gave a radical cation EPR signal visible above the noise level. However with TFA present, radical cation EPR signals were observed for all but the most reactive substrates (naphthalene and 1-methylnaphthalene). Similar results were obtained in acetonitrile using methanesulphonic acid, but only for the less reactive radical cations.

Eberson *et al.*[33] suggested that when TFA is present $(O_2N)_3C^-$ is protonated rapidly and the radical cation is observed because it is much less reactive toward $^{\bullet}NO_2$. They therefore interpreted the results as showing that the radical cation $(ArH^{\bullet+})$ is much more reactive towards $(O_2N)_3C^-$ than

Table 1.2 EPR spectral intensities after irradiation of ArH/TNM solutions in dichloromethane with and without TFA present.[a]

ArH	EPR spectral intensity[b]		
	With $C(NO_2)_4$	With $C(NO_2)_4$ and TFA[c]	Ratio
Naphthalene	<2	<2[d] (<2)	1
1-Methylnaphthalene	<2	<2 (<2)	1
1,4-Dimethylnaphthalene	<2	10 (<1.5)	>5
1,2-Dimethylnaphthalene	<2.5	54 (<2)	>22
1,8-Dimethylnaphthalene	<2	16 (4)	>8
1,4,6,7-Tetramethylnaphthalene	<0.7	52 (4)	>74
1,4,5,8-Tetramethylnaphthalene	<1.8	100 (5)	>55
1,3,5,8-Tetramethylnaphthalene	<2	44 (2.6)	>22
1,4-Dimethoxybenzene	<2	540 (<2)	>270
9-Phenylanthracene	<1.8	100 (8)	>56
9,10-Diphenylanthracene	2.6	300 (6.5)	115
Perylene	8	230 (25)	106
Tris(4-bromophenyl)amine	19	181 (3.2)	9.5
9,10-Dimethylanthracene	<1	600 (4.6)	>600

[a] Irradiation time 6 min (during which100 spectra were accumulated), λ>435 nm, [ArH] = 20-40 mmol L^{-1}, $[C(NO_2)_4]$ = 0.8 mol L^{-1}, [TFA] = 0.4 mol L^{-1}, T = -60°. [b] < indicates intensity corresponding to noise level. [c] The number within the parentheses refers to a identical check experiment with only TFA (0.4 mol L^{-1}) added. [d] At [TFA] = 1 mol L^{-1}, the naphthalene radical cation concentration was above noise level (intensity ≈ 3.5).

$^{\bullet}NO_2$. This indicated that the first chemical step which occurs, leading to the formation of adducts, is the reaction between $ArH^{\bullet+}$ and $(O_2N)_3C^-$ to give a carbon radical, which then reacts with $^{\bullet}NO_2$ to give adducts, as summarized in Scheme 1.19.

$$ArH^{\bullet+} + (O_2N)_3C^- \longrightarrow {}^{\bullet}Ar(H)C(NO_2)_3$$

$$^{\bullet}Ar(H)C(NO_2)_3 + {}^{\bullet}NO_2 \longrightarrow \text{adducts}$$

Scheme 1.19

1.9 Photochemical Nitration of Naphthalene by TNM

Sankararaman and Kochi[34] studied the photochemical reaction between naphthalene and TNM in acetonitrile. Using g.l.c. detection, they found that only two products were formed, 1-nitronaphthalene (2) and 2-nitronaphthalene (3), in a ratio of 1-/2-nitronaphthalene of 7.4. The thermal

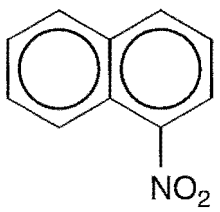

(2)

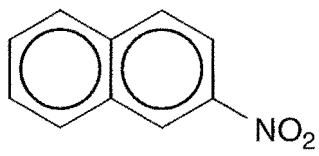

(3)

reaction between naphthalene and *N*-nitropyridinium tetrafluoroborate, i.e. NO_2^+, in acetonitrile gave a ratio of 1-/2-nitronaphthalene of 9.8 and hence they concluded that both the electrophilic (thermal) reaction with NO_2^+ and the charge-transfer (photochemical) reaction between $ArH^{\bullet+}$ and $^{\bullet}NO_2$ were indistinguishable.

Earlier work by Eberson and Radner,[13] however, showed that reaction between $ArH^{\bullet+}$ and $^{\bullet}NO_2$ gave an isomer ratio of ≈ 40 and hence this led Eberson and Radner[35] to study further the reaction between naphthalene and TNM in order to try and identify any possible discrepancies. They detected adducts in the photochemical reaction between naphthalene and TNM, using dichloromethane as solvent, and later[36] one adduct was isolated and a single crystal X-ray analysis revealed the structure of one of the major adducts as cis-1-nitro-4-trinitromethyl-1,4-dihydronaphthalene (7).

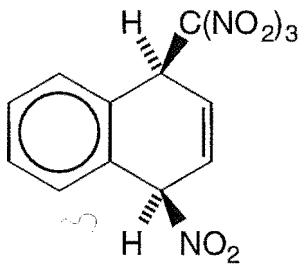

(7)

Eberson *et al.*[37] then undertook an intensive product study using both dichloromethane and acetonitrile as solvents to assess if the solvent had any effect on the products formed in the reaction, which Sankararaman *et al.*[30] previously postulated during photochemical reactions between various substituted anisoles and TNM. Masnovi and Kochi[32] earlier found that the products formed in the photochemical reactions between anthracene derivatives and TNM were thermally unstable and so Eberson *et al.*[37] performed the reactions between naphthalene and TNM at both +20 and -20°.

In the event, adduct formation was found to be predominant in the photolysis of the naphthalene/TNM charge-transfer complex. Adducts (8), (9) and (10) were identified by their n.m.r. spectral properties. A number of other adducts were detected in the n.m.r. spectra of the crude reaction mixture but not isolated or identified. An overview of the product yields from

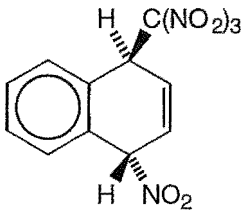

(8)

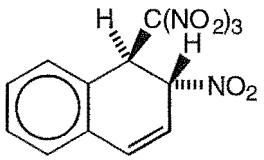

(9)

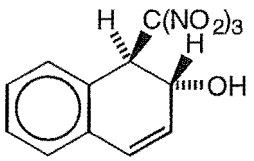

(10)

the photochemical reactions between naphthalene and TNM for both solvents and at different temperatures are given in Table 1.3.

Table 1.3 Overview of product yields from the photolysis of naphthalene (1.0 mol L^{-1}) and TNM (2.0 mol L^{-1}).

				Yield (%)						
Solvent	Temp (°)	t (h)	Conversion (%)	(7)	(8)	(9)	(10)	Total Adducts	Nitronaphthalene (2)	(3)
CH_2Cl_2	-20	24	≈ 90	26.8	16.8	17.7	12.7	86.5	13.5	≤0.5[a]
	20	24	100	24.0	20.4	17.1	≤2[a]	95.6	4.4	≤0.5[a]
CH_3CN	-20	28.5	82	27.3	16.7	16.7	11.5	88.8	10.3	0.9
	20	28.2	100	21.1	22.7	19.8	≤2[a]	87.4	10.6	2.0

[a] Limit of detection

The results showed that there was no significant difference in the observed adduct yields at either temperature or between the two different solvents. The dichloromethane results at -20° gave a ratio of 1-/2-nitronaphthalene of at least ≥27. This was consistent with the formation of nitronaphthalene substantially by coupling of the naphthalene radical cation and $^{\bullet}NO_2$ as previously determined by Eberson and Radner.[13]

Eberson *et al.*[37] found that pure adduct (7) placed in acetonitrile underwent a spontaneous decomposition into 1-nitronaphthalene (2), with a half-life of ≈ 43 h. They also found that by injecting pure adduct (7) into a

g.l.c. at 100° they obtained 1-nitronaphthalene (2), as represented in Scheme 1.20.

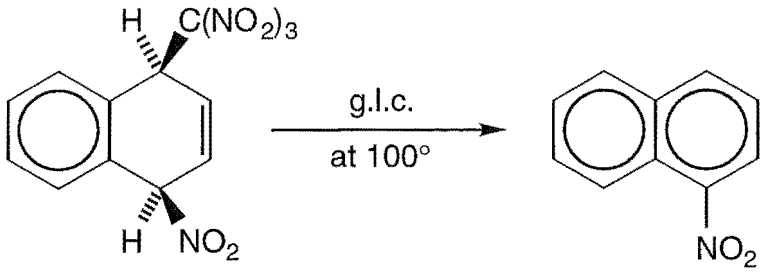

(7) (2) - 100%

Scheme 1.20

It was therefore clear that the conclusions Sankararaman and Kochi[34] made with respect to the photochemical reaction between naphthalene and TNM were invalid, since their analysis of the thermally unstable products was based upon inappropriate g.l.c. detection.

1.10 Mechanistic Description of the Formation of the Principal Adducts (7)-(10) from Photolysis of Naphthalene with TNM.

Adducts (7)-(9) were envisaged as being formed by attack of $(O_2N)_3C^-$ at C1 of the naphthalene radical cation to give the delocalized carbon radical (11), as outlined in Scheme 1.21. Attack of $^{\bullet}NO_2$ at C4 could occur *cis* or *trans* to the trinitromethyl group to give adducts (7) and (8) respectively, while attack of $^{\bullet}NO_2$ at C2 gives the 1-trinitromethyl-2-nitro adduct (9). The *trans*-stereochemistry of adduct (9) was assumed to be due to the presence of the bulky trinitromethyl group shielding the *syn*-face of the delocalized carbon radical (11) from attack by the incoming $^{\bullet}NO_2$.

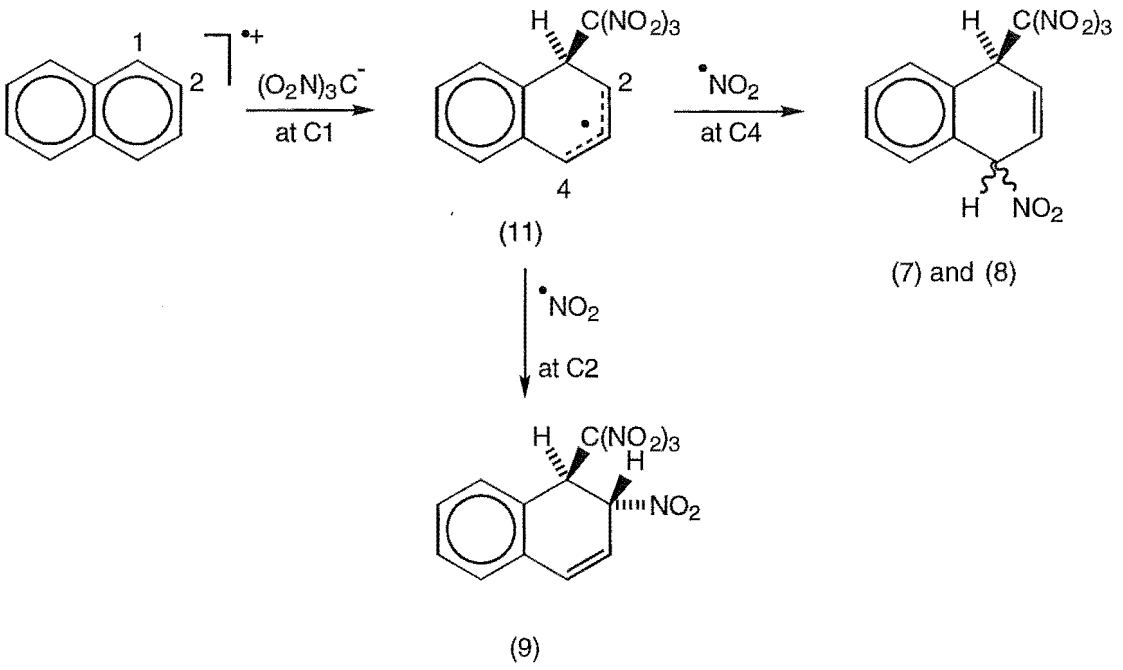

Scheme 1.21

Adduct (10) also arises *via* initial attack of $(O_2N)_3C^-$ at C1 of the naphthalene radical cation, to give the delocalized radical (11). However,

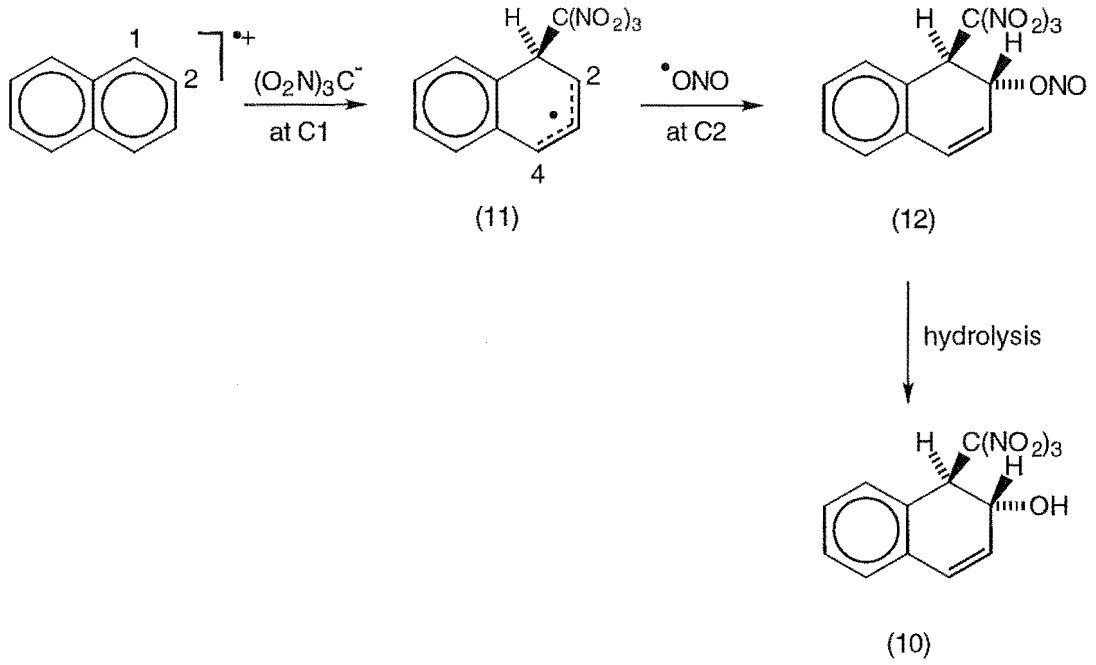

Scheme 1.22

subsequent $^{\bullet}NO_2$ attack at C2 with C-O bond formation would give the trinitromethyl/nitrite adduct (12). Hydrolysis of the nitrite adduct (12), either in the acidic reaction conditions or during workup, would yield the hydroxy/trinitromethyl adduct (10) (See Scheme 1.22).

1.11 Photochemical Nitration of 1,4-Dimethylnaphthalene by TNM

Sankararaman *et al*[34] studied the photochemical reaction of 1,4-dimethylnaphthalene with TNM in both dichloromethane and acetonitrile. They characterised two epimeric 1,4-adducts, (13) and (14), and were able to confirm the absolute stereochemistry of the major adduct (13) as *anti* by X-ray crystallography.

Two further products were identified as the side-chain nitro derivative (15) and 1,4-dimethyl-2-nitronaphthalene (16), with the latter being a minor product.

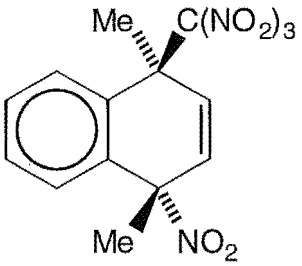

(13)

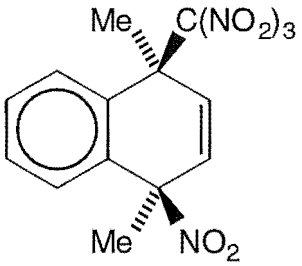

(14)

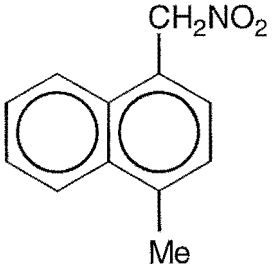

(15)

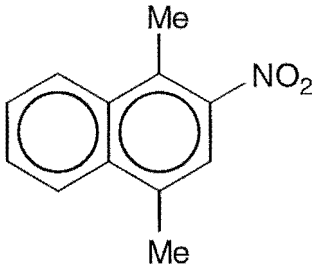

(16)

The product composition was found to be temperature dependent, with adduct formation dominant at lower temperatures and the side-chain nitro compound (15) dominating at higher temperatures. When a mixture of the *syn-* and *anti-* adducts were placed into acetonitrile at room temperature, they converted slowly into the side-chain nitro derivative (15). The various products in the photonitration between 1,4-dimethylnaphthalene and TNM were proposed to arise *via* a competitive process between (a) adduct formation and (b) ring nitration, as illustrated in Scheme 1.23.

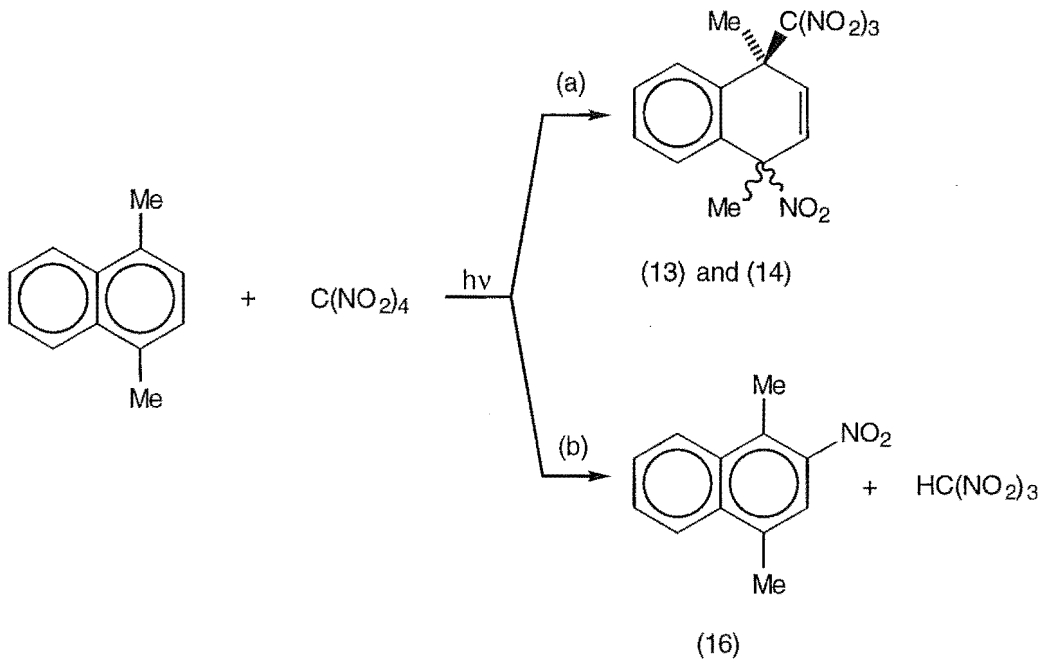

Scheme 1.23

A more detailed study of the 1,4-dimethylnaphthalene/TNM/*hν* reaction was carried out by Eberson *et al.*[38] They also found that adduct formation dominated at lower temperatures, reaching 90% in dichloro-methane at -50°. However, in acetonitrile a new epimeric pair of adducts was observed and identified as 1,4-hydroxy/trinitromethyl adducts (17) and (18).

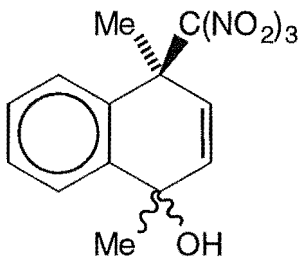

(17) and (18)

The product yields from the photonitration of 1,4-dimethylnaphthalene and TNM, in both dichloromethane and acetonitrile and at different temperatures are shown in Table 1.4.

Table 1.4 Overview of product yields from the photolysis of 1,4-dimethyl-naphthalene (1.0 mol L^{-1}) and TNM (2.0 mol L^{-1}).

				Yield (%)					
Solvent	Temp (°)	t (h)	Conversion (%)	(13)	(14)	(15)	(16)	(17)	(18)
CH_2Cl_2	-50	5.25	74	81	9	7	-	-	-
	-20	5.25	81	73.3	7.7	15.4	-	-	-
	20	5.25	100	29.5	3.8	64.9	-	-	-
CH_3CN	-20	6.25	60.8	71.5	17.0	6.8	-	3.3	1.4
	20	6.25	97.7	33.7	9.1	43.0	14.1	trace	-

To understand more fully the observed results, Eberson *et al.*[38] studied the thermal rearrangement of adduct (13) in both acetonitrile and dichloromethane. In acetonitrile, adduct (13) epimerized to give adduct (14), which then underwent further rearrangement to give adducts (17) and (18). Also during the course of the rearrangements the side-chain nitro compound (15) steadily increased. Using dichloromethane, they found that adduct (13)

rearranged to form both adduct (14) and the side-chain nitro compound (15). The rearrangement of adduct (13) to adduct (14) in dichloromethane was ~ $1.4x10^2$ times slower compared with using acetonitrile.

Eberson *et al.*[38] therefore proposed that the rearrangement of adduct (13) to adduct (14) was polar, with the trinitromethyl group as the leaving group and leading to the intermediate nitrocyclohexadienyl cation/trinitro-methanide ion pair (19), as outlined in Scheme 1.24.

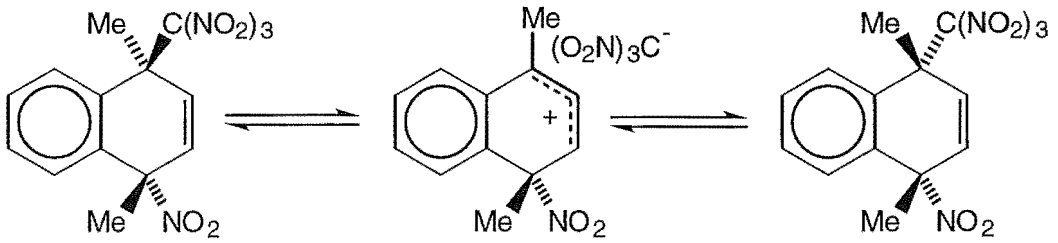

(13) (19) (14)

Scheme 1.24

Loss of nitroform from the intermediate nitrocyclohexadienyl cation/ trinitromethanide ion pair (19), by abstraction of an acidic proton from the methyl group by $(O_2N)_3C^-$, would lead to the formation of the side-chain nitro compound (15), as illustrated in Scheme 1.25.

The formation of adducts (17) and (18) was proposed to proceed *via* a trinitromethylcyclohexadienyl radical (20), formed by loss of $^{\bullet}NO_2$ from adduct (14) (See Scheme 1.26). Subsequently, addition of $^{\bullet}NO_2$ to the trinitromethylcyclohexadienyl radical (20) with C-O bond formation, followed by hydrolysis of the resulting nitrites (17a) and (18a), would yield adducts (17) and (18).

The observation that the 2-nitro compound (16) only appeared in the later stages of the acetonitrile reaction, at which time photolysis mixtures were always acidic, led Eberson *et al.*[38] to perform an acid catalysed

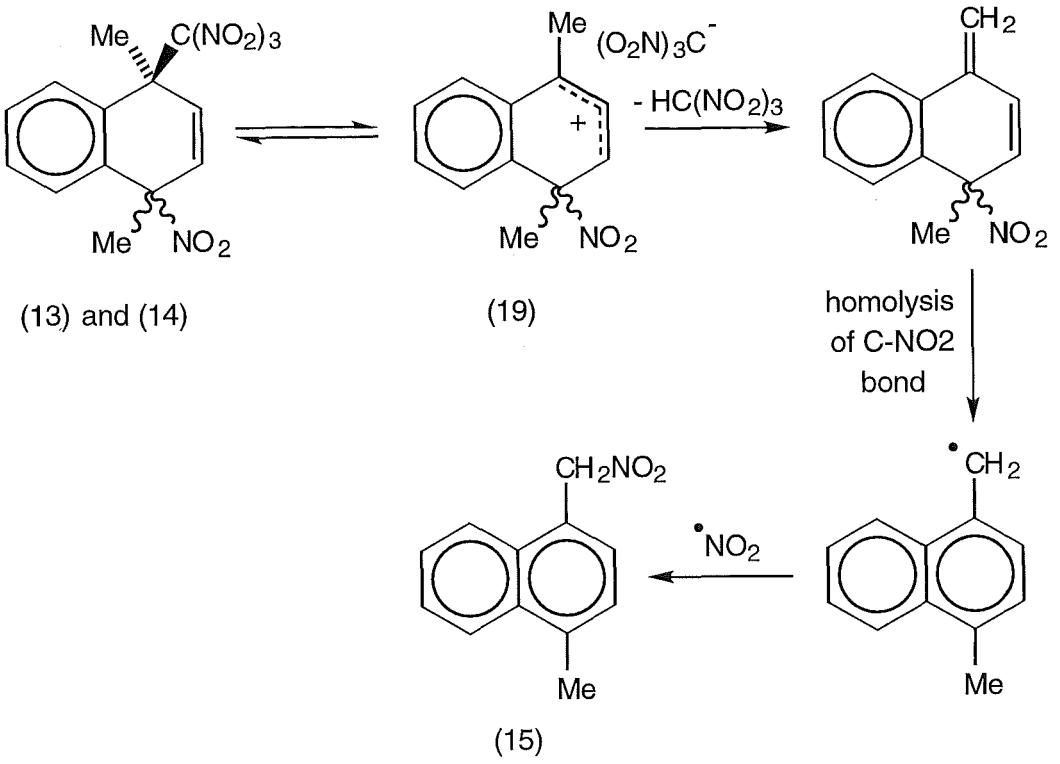

Scheme 1.25

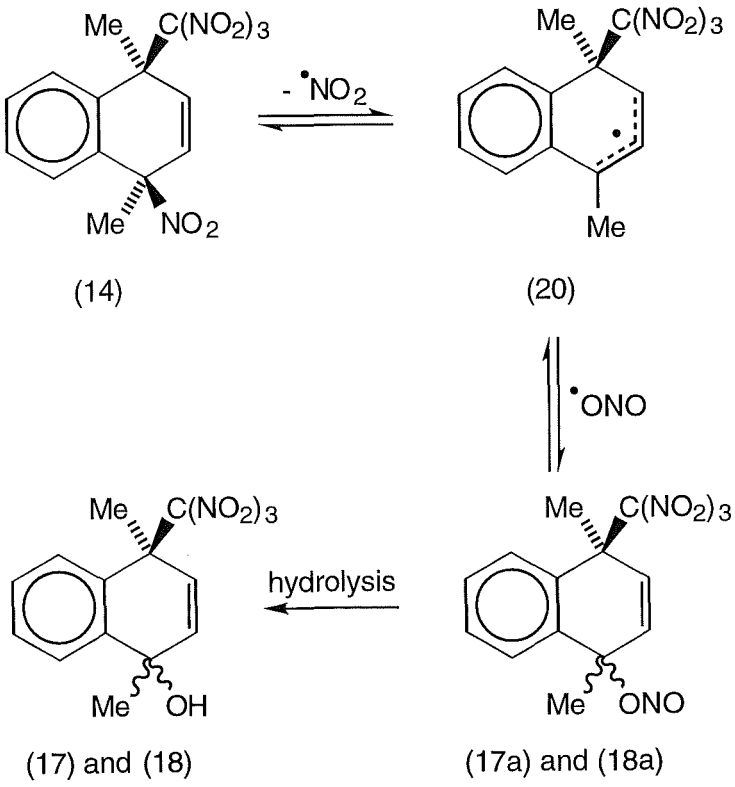

Scheme 1.26

rearrangement of adduct (13) using methanesulfonic acid in acetonitrile. Adduct (13) was found to rearrange to give the side-chain nitro compound (15), 1,4-dimethylnaphthalene and the 2-nitro compound (16). This led them to propose that the 2-nitro compound (16) was formed *via* the trinitromethyl-cyclohexadienyl radical (20) in an acid-promoted process involving $^{\bullet}NO_2$ coupling at C2, followed by loss of nitroform, as shown in Scheme 1.27.

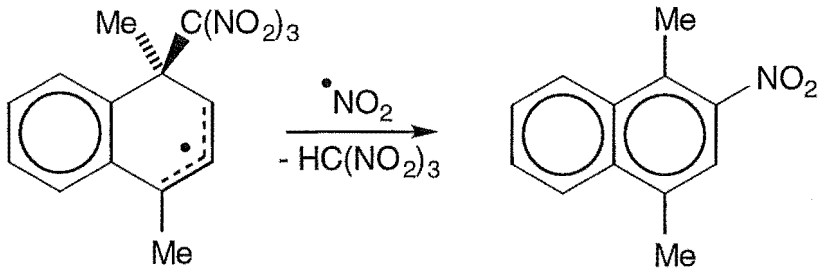

(20) (16)

Scheme 1.27

1.12 Solvent and Salt Effects on the Photochemical Nitration of Aromatic Compounds by TNM

1.12.1 Solvent Effects in the Reactions of the Trinitromethanide Ion.

Masnovi *et al.*[39,40] observed that solvent polarity played an important but selective role during the photochemical nitration of various aromatic donors with TNM. While studying a series of time resolved absorption spectra involving substituted anthracene donors and TNM, formed *via* laser-flash photolytic techniques, they found that different results were obtained when using dichloromethane and acetonitrile. In the non-polar dichloro-methane, the radical cation lifetime was too short to be observed on the microsecond time scale, whereas in the polar acetonitrile the radical cation was readily observed.

Rate measurements indicated that the decay of the substituted anthracene radical cation in acetonitrile was consistently slower than in dichloromethane by at least two orders of magnitude.[39] Similar results were obtained by Sankararaman *et al.*[30] while studying various substituted anisoles, except differences up to three orders of magnitude were observed. This "solvent effect" was causing $(O_2N)_3C^-$ to react with the radical cation 10^2-10^3 times faster in dichloromethane than in acetonitrile.

More recent work by Wang *et al.*,[41] with 9-substituted anthracene radical cations, found inconsistencies in some of the results obtained by Masnovi *et al.*[40] They found that the reaction of $(O_2N)_3C^-$ with the radical cation was less than 10 times faster in dichloromethane than in acetonitrile,[41] the expected difference due to the change in solvent polarity.

1.12.2 Solvent Effects on Product Formation.

While studying the reactions of various monosubstituted anisoles with TNM, Sankararaman *et al.*[30] found that the products formed were highly dependent on the solvent polarity. In dichloromethane the principal product was derived by addition of a single trinitromethyl group onto the aromatic ring, with minor amounts of aromatic nitro compounds formed. In acetonitrile however, nitration was predominant, with only minor amounts of trinitromethyl aromatics sometimes formed.

It was therefore concluded that a change in solvent polarity, from non-polar dichloromethane to polar acetonitrile, caused a change in the mechanism of reactions within the triad from (a) ion-pair collapse to (b) radical-pair collapse respectively, as depicted in Scheme 1.28.

In the reactions of 1,4-dimethylnaphthalene, Eberson *et al.*[38] found that adducts which had arisen by addition of $(O_2N)_3C^-$ and $^{\bullet}NO_2$ to the radical cation had a greater tendency to decompose in acetonitrile at +20° to give nitro compounds than in dichloromethane. The rate of rearrangement

(a) Ion-Pair Collapse :

(non polar solvent, CH_2Cl_2)

$$ArH^{\bullet+} + (O_2N)_3C^- \longrightarrow {}^{\bullet}Ar(H)C(NO_2)_3 \xrightarrow{{}^{\bullet}NO_2} ArC(NO_2)_3 + HNO_2$$

(b) Radical-Pair Collapse :

(polar solvent, CH_3CN)

$$ArH^{\bullet+} + {}^{\bullet}NO_2 \longrightarrow {}^{+}Ar(H)NO_2 \xrightarrow{(O_2N)_3C^-} ArNO_2 + HC(NO_2)_3$$

Scheme 1.28

of adduct (13) into the side-chain nitro compound (15) was at least 100 times faster in acetonitrile than in dichloromethane (See Scheme 1.29).

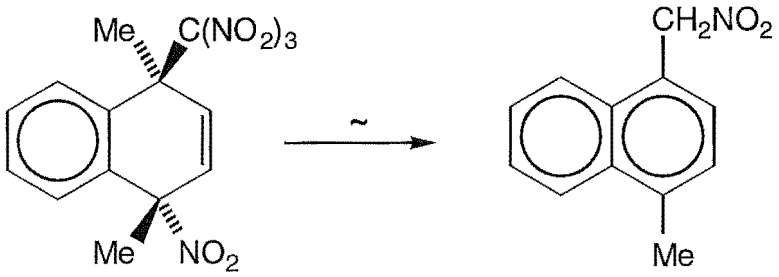

(13) (15)

Scheme 1.29

Butts *et al.*[42] re-examined the photochemical reactions of 4-methyl-anisole with TNM, initially studied by Sankararaman *et al.*[30] and discussed earlier in Part 1.12.2 of this Section. They too found[42] that at +20° in dichloromethane the major product of the reaction was the 4-methyl-2-trinitromethylanisole (21), whereas in acetonitrile the major product was 4-methyl-2-nitroanisole (22).

However in dichloromethane Butts *et al.*[42] also observed the

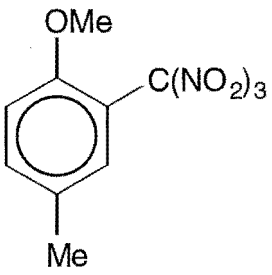

(21)

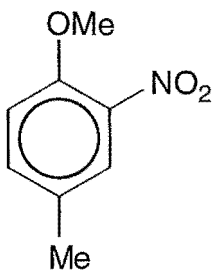

(22)

formation of four unstable isomeric adducts (23)-(26), which decomposed as the reaction proceeded. In acetonitrile only the epimeric adducts (25) and (26) were seen at low temperatures (-20 and -50°).

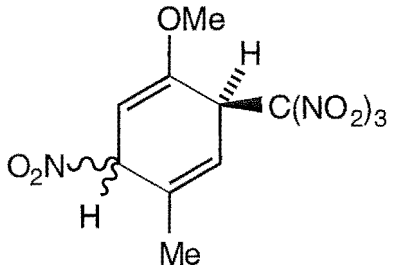

(23) and (24)

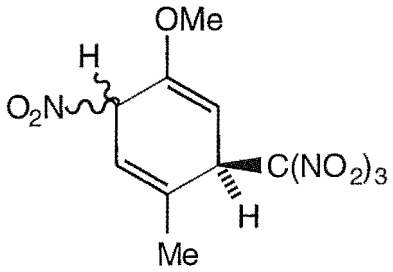

(25) and (26)

It was proposed that the products were formed by two competing mechanisms. In Scheme 1.30, attack of $(O_2N)_3C^-$ at the 2-position of the 4-methylanisole radical cation would give the delocalized radical (27). Attack of $^{\bullet}NO_2$ at C5 would yield adducts (23) and (24). Alternatively, $^{\bullet}NO_2$ could attack *ipso* to the methoxy group at C1, to give the diene (28). Loss of nitrous acid from either the sterically compressed diene (28) or adducts (23) and (24) would give rise to the 4-methyl-2-trinitromethylanisole (21).

Alternatively, attack of $(O_2N)_3C^-$ *ipso* to the methoxy group would give the delocalised carbon radical (29) (See Scheme 1.31). Attack of $^{\bullet}NO_2$ at C2 in the carbon radical (29) would give the diene (30). Loss of nitroform from diene (30) would yield 4-methyl-2-nitroanisole (22). A possible allylic rearrangement of diene (30), with migration of the trinitromethyl group to C5,

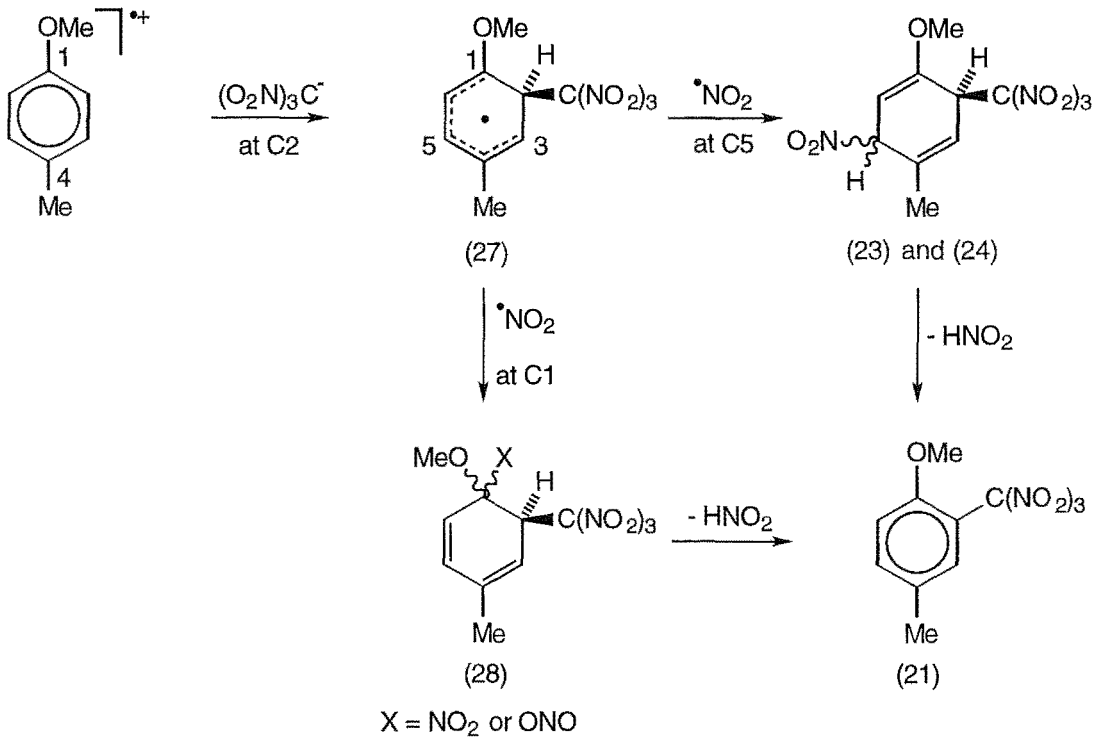

Scheme 1.30

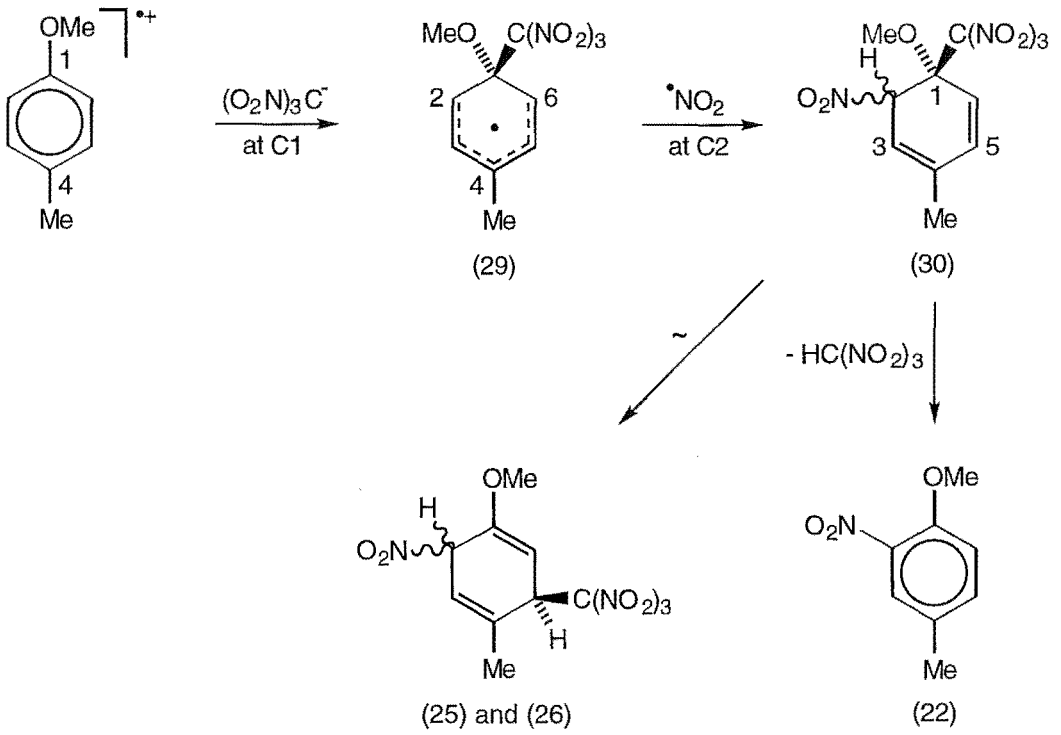

Scheme 1.31

would form adducts (25) and (26).

This type of allylic migration of $(O_2N)_3C^-$ has been observed in the rearrangement of 4,8-dimethyl-*r*-1-nitro-*t*-4-trinitromethyl-1,4-dihydro-naphthalene (31) into 4,8-dimethyl-*r*-1-nitro-*t*-2-trinitromethyl-1,4-dihydro-naphthalene (32),[43] as represented in Scheme 1.32.

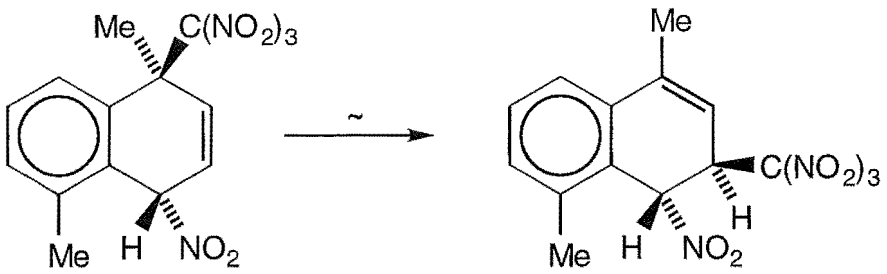

(31) (32)

Scheme 1.32

Butts *et al.*[42] suggested that the "solvent effect" is simply the consequence of the lower reactivity of $(O_2N)_3C^-$ towards the radical cation, due to solvation in the more polar acetonitrile. This would lead to a change in the regiochemistry of attack of $(O_2N)_3C^-$, with attack *ipso* to the methoxy group being favoured due to the high positive charge at that position in the ring.[42] This leads to the reaction pathways, represented in Scheme 1.31, dominating and hence a change in the reaction products observed.

1.12.3 Salt Effects on Product Formation.

During the course of studying the photochemical reactions of 4-methylanisole with TNM, Sankararaman *et al.*[30] examined the effect of added salts on the products formed. They added a non-common ion salt, $Bu_4N^+ClO_4^-$ (0.2 mol L^{-1}), and a common ion salt, $Bu_4N^+C(NO_2)_3^-$ (0.01 mol L^{-1}), to reactions in both dichloromethane and acetonitrile. Their results are summarised in Table 1.5.

Table 1.5 Overview of product yields from the photolysis of 4-methylanisole (0.06-0.6 mol L^{-1}) and TNM (0.66-2.2 mol L^{-1}) with and without added salts.

		Products (%)	
Solvent	Added Salt	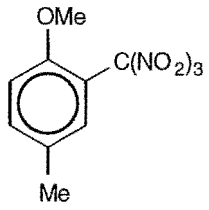 (21)	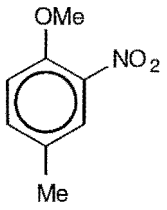 (22)
CH_2Cl_2	-	95	5
	$Bu_4N^+ClO_4^-$	-	100[a]
	$Bu_4N^+C(NO_2)_3^-$	76	24
CH_3CN	-	5	95[a]
	$Bu_4N^+ClO_4^-$	-	100[a]
	$Bu_4N^+C(NO_2)_3^-$	10	90[a]

[a] Including minor amounts of 4-methyl-2-nitrophenol, the rearrangement product of 4-methyl-4-nitroanisole (24), and 2,6-dinitro-4-methylphenol.

In dichloromethane the results showed that addition of the non-common ion salt, $Bu_4N^+ClO_4^-$, at the concentration employed, efficiently diverted the course of the reaction from predominant trinitromethylation to predominant nitration. Adding the common ion salt, $Bu_4N^+C(NO_2)_3^-$, at low concentrations (0.01 mol L^{-1}), had less effect on the products formed. In acetonitrile the added salts had only a minor effect on the products formed. Sankararaman *et al.*[30] proposed that the "salt effects" were due to the competition between ion-pair and radical-pair collapse as previously discussed earlier in Part 1.12.2 of this Section and outlined in Scheme 1.28.

During a later study of the 4-methylanisole system, Butts *et al.*[42] noted that there was a large difference between the concentrations of the two salts [0.2 mol L^{-1} for $Bu_4N^+ClO_4^-$ compared with 0.01 mol L^{-1} for $Bu_4N^+C(NO_2)_3^-$]. They re-interpreted the observed "salt effects" as being due to the consequence of the increased polarity of the solvent system due to the added salt and not the type of salt used. Butts *et al.*[42] suggested that the increase in solvent polarity with added salt would lead to an "acetonitrile-like" solvent environment for the attack of $(O_2N)_3C^-$ on the radical cation of 4-methylanisole. With an "acetonitrile-like" solvent the reaction pathways represented in Scheme 1.31 (Part 1.12.2 of this Section) would now be favoured and hence nitration products would dominate. However with low concentrations of added salt, as in the case of $Bu_4N^+C(NO_2)_3^-$ (0.01 mol L^{-1}), the polarity of the solvent would only be marginally affected. This would lead to a less marked effect on the products formed, as was observed (See Table 1.5).

1.12.4 The Use of 1,1,1,3,3,3-Hexafluoro-2-propanol (HFP) as the Solvent.

Eberson *et al.*[44] studied a wide range of aromatic radical cations ($ArH^{\bullet+}$) generated in HFP. They found that the aromatic radical cations were extremely persistent, even at room temperature, with half-lives often exceeding those found in trifluoroacetic acid (TFA) by greater than 100 times. Subsequently Eberson *et al.*[45] studied the photochemical behaviour of various aromatic compounds with TNM using HFP as solvent. They demonstrated that readily reacting radical cations can persist at room temperature in HFP in the presence of $(O_2N)_3C^-$.

Photolysis of 1,4-dimethylnaphthalene with TNM in HFP was observed to give a broad unresolved EPR signal at +5°, whereas in dichloromethane at -60°, there was no observable signal. A preparative photolysis experiment between 1,4-dimethylnaphthalene and TNM in HFP at +20° resulted in the

quantitative formation of 1,4-dimethyl-2-nitronaphthalene (16), whereas previous studies[38] in dichloromethane at +20° had given rise to the epimeric adducts (13) and (14) and the side chain nitro product (15) (See summary in Scheme 1.33).

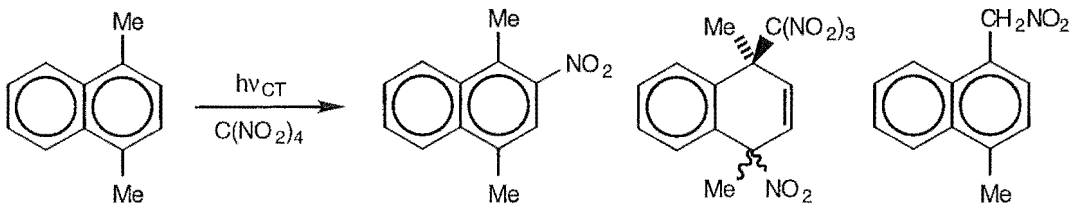

	(16)	(13) and (14)	(15)
CH_2Cl_2	<0.5%	47%	47%
HFP	100%	-	-

Scheme 1.33

It was evident that, in HFP, the usual first chemical reaction step involving attack of $(O_2N)_3C^-$ on the 1,4-dimethylnaphthalene radical cation was eliminated, leaving only the slower radical coupling between $ArH^{\bullet+}$ and $^{\bullet}NO_2$ to occur.

The photochemical reaction of 1-methoxynaphthalene with TNM in HFP at +22° gave an EPR spectrum belonging to the radical cation of the 4,4'-connected dehydrodimer (33). A preparative photolysis experiment in HFP at +20°, between 1-methoxynaphthalene and TNM, gave the dehydrodimer (33) and 1-methoxy-4-nitronaphthalene (34) as products, as summarized in Scheme 1.34.

Once again it was clear that all the products derived from an initial reaction between $(O_2N)_3C^-$ and the 1-methoxynaphthalene radical cation were eliminated in HFP, since neither adducts (35) and (36) nor 1-methoxy-

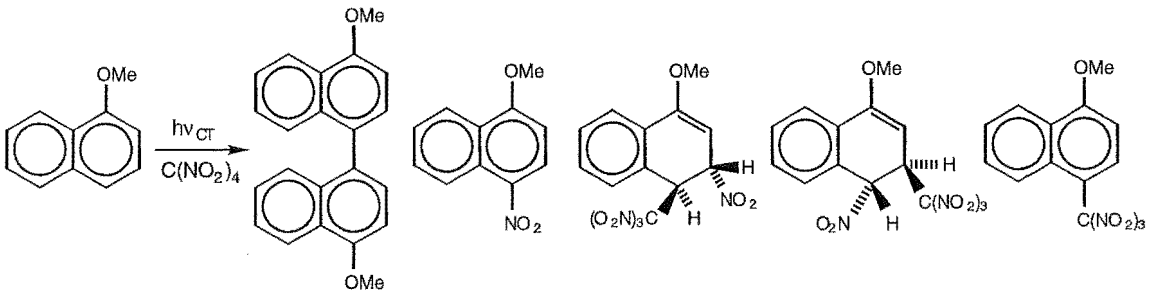

	(33)	(34)	(35)	(36)	(37)
CH_2Cl_2	-	38%	7%	11%	41%
HFP	72%	28%	-	-	-

Scheme 1.34

4-trinitromethylnaphthalene (37), observed in an earlier study,[46] were seen.

Eberson *et al.*[45] found that the reactivity of $(O_2N)_3C^-$ is strongly suppressed in HFP. The radical cation therefore undergoes dehydrodimer formation and/or radical coupling with $^{\bullet}NO_2$ to give the normal product(s) of the $ArH^{\bullet+}/^{\bullet}NO_2$ reaction.

1.13 References for Chapter One

1 Euler, H., *Annalen*, 1903, **330**, 280.

2 Benford, G. A., and Ingold, C. K., *J. Chem. Soc.*, 1938, 929.

3 Hughes, E. D., Ingold, C. K., and Reed, R. I., *Nature*, 1946, **158**, 448.

4 Goddard, D. R., Hughes, E. D., and Ingold, C. K., *Nature*, 1946, **158**, 480.

5 Hughes, E. D., Ingold, C. K., and Reed, R. I., *J. Chem. Soc.*, 1950, 2400.

6 Gillespie, R. J., Graham, J., Hughes, E. D., Ingold, C. K., and Peeling, E. R. A., *J. Chem. Soc.*, 1950, 2504.

7 Ingold, C. K., Millen, D. J., and Poole, H. G., *J. Chem. Soc.*, 1950, 2576.

8 Kenner, J., *Nature*, 1945, **156**, 369.

9 Benford, G. A., Bunton, C. A., Halberstadt, E. S., Hughes, E. D., Ingold, C. K., Minkoff, G.J., and Reid, R. I., *Nature*, 1945, **156**, 688.

10 Olah, G. A., *Acc. Chem. Res.*, 1971, **4**, 240.

11 Perrin, C. L., *J. Am. Chem. Soc.*, 1977, **99**, 5516.

12 Eberson, L., Jonsson, L., and Radner, F., *Acta Chem. Scand. B*, 1978, **32**, 749.

13 Eberson, L., and Radner, F., *Acta Chem. Scand. B*, 1980, **34**, 739.

14 Eberson, L., and Radner, F., *Acta Chem. Scand. B*, 1986, **40**, 71.

15 Johnston, J. F., Ridd, J. H., and Sandall, J. P. B., *J. Chem. Soc., Chem. Commun.*, 1989, 244.

16 Ridd, J. H., *Chem. Soc. Rev.*, 1991, **20**, 149.

17 Benesi, H. A., and Hildebrand, J. H., *J. Am. Chem. Soc.*, 1949, **71**, 2703.

18 Mulliken, R. S., *J. Am. Chem. Soc.*, 1950, **72**, 600.

19 Kosower, E. M., *Prog. Phys. Org. Chem.*, 1965, **3**, 81.

20 Mulliken, R. S., *J. Phys. Chem.*, 1952, **56**, 801.

21 Hilinski, E. F., Masnovi, J. M., Amatore, C., Kochi, J. K., and Rentzepis, P. M., *J. Am. Chem. Soc.*, 1983, **105**, 6167.

22 Hilinski, E. F., Masnovi, J. M., Kochi, J. K., and Rentzepis, P. M., *J. Am. Chem. Soc.*, 1984, **106**, 8071.

23 Hilinski, E. F., and Rentzepis, P. M., *Anal. Chem.*, 1983, **55**, 1121a.

24 Masnovi, J. M., Huffman, J. C., Kochi, J. K., Hilinski, E. F., and Rentzepis, P. M., *Chem. Phys. Lett.*, 1984, **106**, 20.

25 Chaudhuri, J. N., and Basu, S., *J. Chem. Soc.*, 1959, 3085.

26 Rabani, J., Mulac, W. A., and Matheson, M. S., *J. Phys. Chem.*, 1965, **69**, 53.

27 Kamlet, M. J., and Glover, D. J., *J. Org. Chem.*, 1962, **27**, 537.

28 Masnovi, J. M., Kochi, J. K., Hilinski, E. F., and Rentzepis, P. M., *J. Am. Chem. Soc.*, 1986, **108**, 1126.

29 Hall, T. C., and Blacet, F. E., *J. Chem. Phys.*, 1952, **20**, 1745.

30 Sankararaman, S., Haney, W. A., and Kochi, J. K., *J. Am. Chem. Soc.*, 1987, **109**, 7824.

31 Okada, T., Kida, K., and Mataga, N., *Chem. Phys. Lett.*, 1982, **88**, 157.

32 Masnovi, J. M., and Kochi, J. K., *J. Org. Chem.*, 1985, **50**, 5245.

33 Eberson, L., Hartshorn, M. P., and Svensson, J. O., *J. Chem. Soc., Chem. Commun.*, 1993, 1614.

34 Sankararaman, S., and Kochi, J. K., *J. Chem. Soc., Perkin Trans. 2*, 1991, 1.

35 Eberson, L., and Radner, F., *J. Am. Chem. Soc.*, 1991, **113**, 5825.

36 Eberson, L., Hartshorn, M. P., Radner, F., and Robinson, W. T., *J. Chem. Soc., Chem. Commun.*, 1992, 566.

37 Eberson, L., Hartshorn, M. P., and Radner, F., *J. Chem. Soc., Perkin Trans. 2*, 1992, 1793.

38 Eberson, L., Hartshorn, M. P., and Radner, F., *J. Chem.* Soc., Perkin *Trans. 2*, 1992, 1799.

39 Masnovi, J. M., Levine, A., and Kochi, J. K., *J. Am. Chem. Soc.*, 1985, **107**, 4356.

40 Masnovi, J. M., and Kochi, J. K., *J. Am. Chem. Soc.*, 1985, **107**, 7880.

41 Wang, H., Zheng, G., and Parker, V. D., *Acta Chem. Scand.*, 1995, **49**, 311.

42 Butts, C. P., Eberson, L., Hartshorn, M. P., and Robinson, W. T., *Acta Chem. Scand.*, 1996, **50**, 122.

43 Butts, C. P., Eberson, L., Hartshorn, M. P., and Robinson, W. T., *Aust. J. Chem.*, 1995, **48**, 1989.

44 Eberson, L., Hartshorn, M. P., and Persson, O., *J. Chem. Soc., Perkin Trans. 2*, 1995, 1735.

45 Eberson, L., Persson, O., Radner, F., and Hartshorn, M. P., *Res. Chem. Intermediat., in press.*

46 Butts, C. P., Eberson, L., Hartshorn, M. P., Persson, O., and Robinson, W. T., *Acta Chem. Scand.*, 1995, **49**, 253.

CHAPTER TWO

PHOTONITRATION OF 1,4,6,7-TETRAMETHYLNAPHTHALENE, 2,6-DIMETHYLNAPHTHALENE AND 1,3-DIMETHYLNAPHTHALENE

2.1 Introduction

As described in Chapter 1, the photochemical addition of TNM to aromatic compounds (ArH) has been shown[1] to occur by recombination of a triad consisting of $ArH^{\bullet+}$, $(O_2N)_3C^-$ and $^{\bullet}NO_2$. The first chemical step leading to adduct formation is the reaction between $ArH^{\bullet+}$ and $(O_2N)_3C^-$ to give a carbon-centred radical. The carbon radical subsequently reacts with $^{\bullet}NO_2$ to give adducts, as illustrated in Scheme 2.1. The first bond formation,

$$ArH^{\bullet+} + (O_2N)_3C^- \longrightarrow {}^{\bullet}Ar(H)C(NO_2)_3$$

$$^{\bullet}Ar(H)C(NO_2)_3 + {}^{\bullet}NO_2 \longrightarrow \text{adducts}$$

Scheme 2.1

involving reaction of $(O_2N)_3C^-$ with $ArH^{\bullet+}$ is crucial in determining the structures of the adducts formed.[2]

In the photochemical reaction between naphthalene and TNM,[3] it was found that the initial bond formation between the naphthalene radical cation and $(O_2N)_3C^-$ occurred exclusively at C1 on the naphthalene radical cation to give the 1-phenylallylic radical (38), as seen in Scheme 2.2. No adducts were observed arising from initial bond formation at the alternative 2-position of the naphthalene radical cation, which would involve formation of the less stable benzylic radical (39), also seen in Scheme 2.2. Subsequent coupling

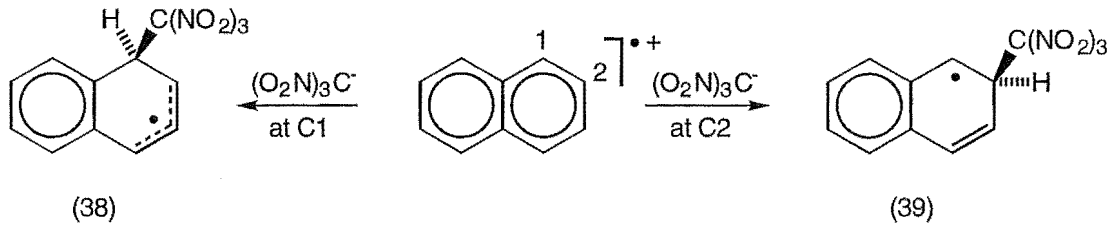

(38) (39)

Scheme 2.2

of $^{\bullet}NO_2$ with the 1-phenylallylic radical (38) gave either nitro/trinitromethyl adducts or hydroxy/trinitromethyl adducts, the latter being formed on hydrolysis of the labile nitrito/trinitromethyl adducts (See Chapter 1, Section 1.10 for mechanistic descriptions).

Photolysis studies on the 1,4-dimethylnaphthalene/TNM system[4] found that adduct formation resulted from addition of $(O_2N)_3C^-$ only at C1 on the 1,4-dimethylnaphthalene radical cation (See Chapter 1, Section 1.11 for further details). The possible initial modes of attack of $(O_2N)_3C^-$ on the 1,4-dimethylnaphthalene radical cation are depicted in Scheme 2.3. Clearly,

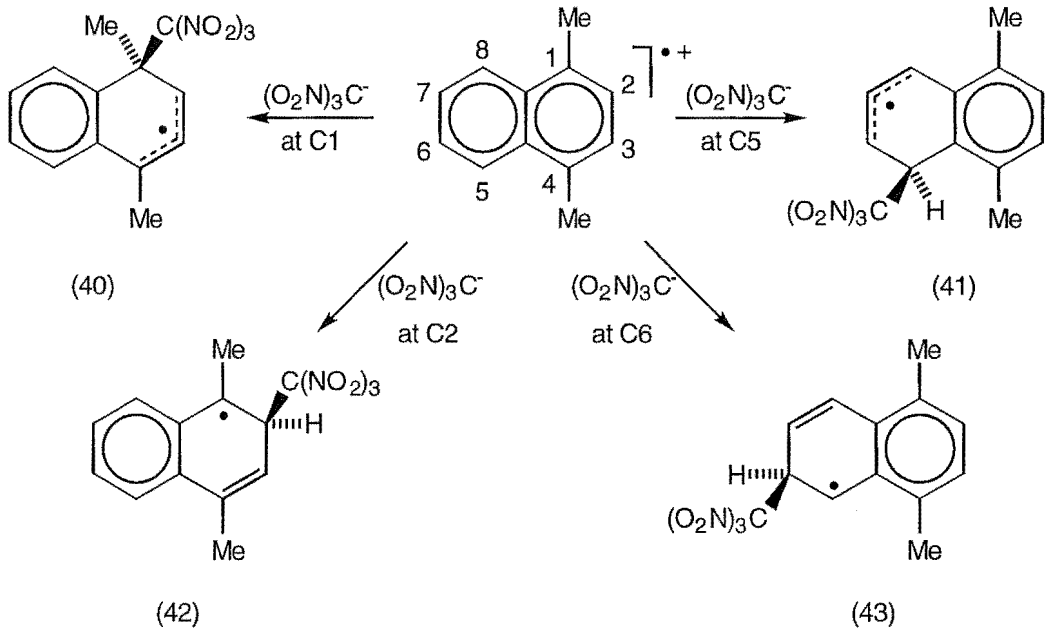

Scheme 2.3

attack of $(O_2N)_3C^-$ at C1 on the 1,4-dimethylnaphthalene radical cation, to give the phenylallylic radical (40), is the energetically favoured pathway, this being stabilized by the 4-methyl group. Formation of the phenylallylic radical (41), arising *via* attack of $(O_2N)_3C^-$ at C5 on the 1,4-dimethylnaphthalene radical cation, would be less favoured due to the steric interaction between the *peri*-methyl and trinitromethyl groups. Similarly the tertiary benzylic radical (42), arising *via* attack of $(O_2N)_3C^-$ at C2 on the 1,4-dimethyl-naphthalene radical cation, would be destabilized by steric interactions between the bulky trinitromethyl group and a β-methyl group. Alternatively, attack of $(O_2N)_3C^-$ at C6 on the 1,4-dimethylnaphthalene radical cation would give the less stable secondary benzylic radical (43).

In the photolysis of the charge-transfer complex of TNM with 2,3-dimethylnaphthalene,[5] in both dichloromethane and acetonitrile at +20°, adducts were found to arise *via* initial attack of $(O_2N)_3C^-$ at both C1 and C5 on the 2,3-dimethylnaphthalene radical cation, in a ratio of *c.* 1:4 for C1:C5. Clearly, attack of $(O_2N)_3C^-$ at C1 and C5 on the 2,3-dimethylnaphthalene radical cation, forming the phenylallylic radicals (44) and (45), respectively, is favoured over attack at C2 and C6 forming the secondary benzylic radicals

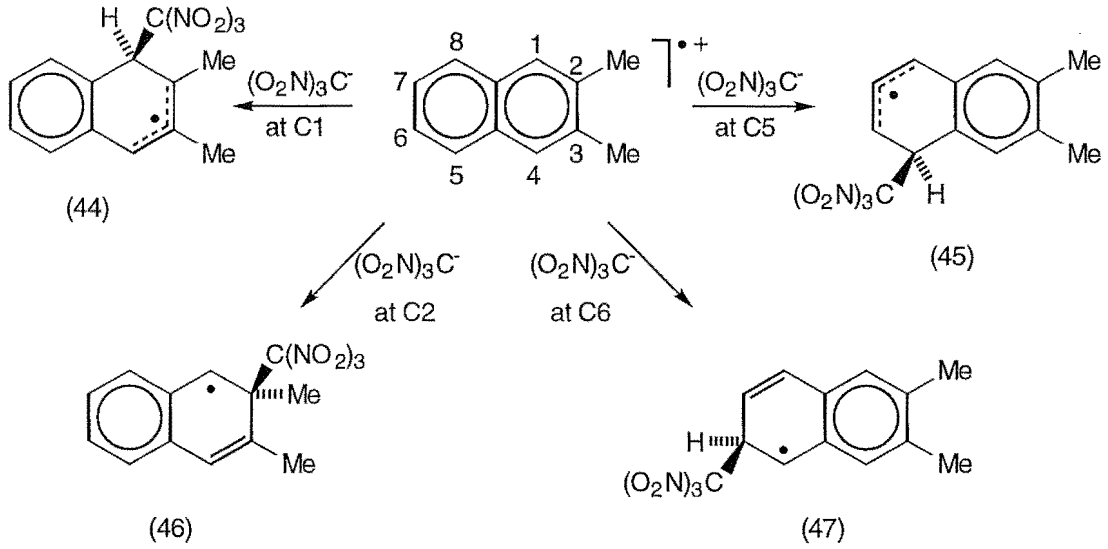

Scheme 2.4

(46) and (47), respectively (See summary in Scheme 2.4). The secondary benzylic radical (46), formed by attack of $(O_2N)_3C^-$ at C2 on the 2,3-dimethylnaphthalene radical cation, would be further destabilized due to steric interactions arising between the bulky trinitromethanide group and both the *ipso* and β-methyl groups. For the phenylallylic radical (44), arising *via* attack of $(O_2N)_3C^-$ at C1 on the 2,3-dimethylnaphthalene radical cation, the enhanced stability due to the 2-methyl group is overshadowed by the steric interaction between the bulky trinitromethyl group and the β-methyl group. It therefore appears that the phenylallylic radical (45), arising from attack of $(O_2N)_3C^-$ at C5 on the 2,3-dimethylnaphthalene radical cation, is the most stable delocalized carbon radical.

In the photochemical reaction between 1-methylnaphthalene and TNM,[6] adduct formation was found to occur predominantly by attack of $(O_2N)_3C^-$ at C4 of the 1-methylnaphthalene radical cation (65% from a total of 69% in dichloromethane at +20°). The remainder of adducts arose *via* attack of $(O_2N)_3C^-$ at C5 on the 1-methylnaphthalene radical cation. The possible phenylallylic radicals are outlined in Scheme 2.5. It appears that

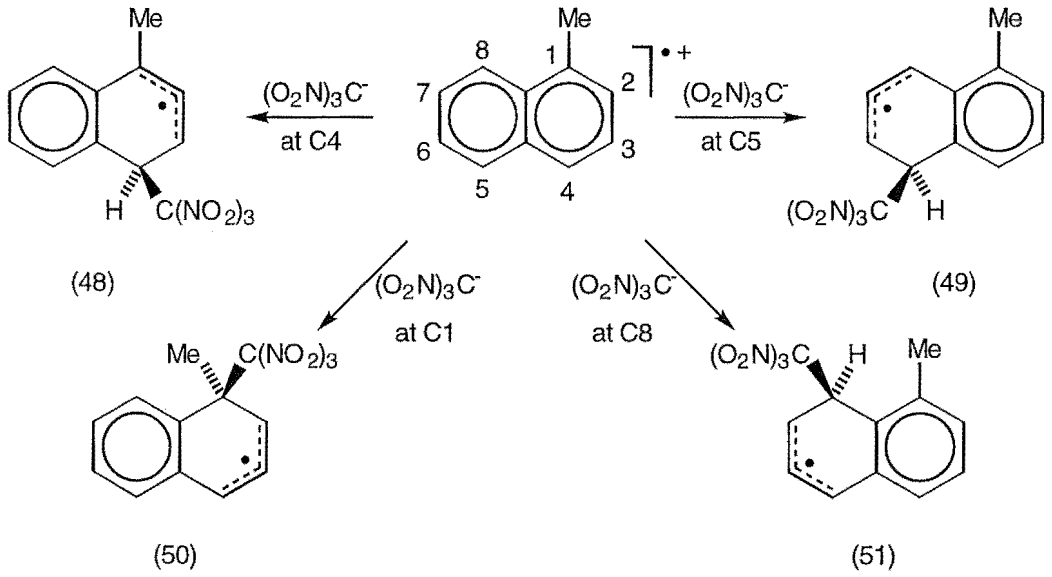

Scheme 2.5

attack of $(O_2N)_3C^-$ at C4 on the 1-methylnaphthalene radical cation leads to the most stable phenylallylic radical (48). This radical (48) has enhanced stability due to the 1-methyl group compared with phenylallylic radical (49), formed *via* attack of $(O_2N)_3C^-$ at C5 on the 1-methylnaphthalene radical cation. Attack on the 1-methylnaphthalene radical cation by $(O_2N)_3C^-$ either *ipso* to the methyl group at C1 or *peri* to the methyl group at C8, yielding phenylallylic radicals (50) and (51), appears to be disfavoured due to the resulting steric interactions between the bulky trinitromethyl and methyl groups. Of the possible benzylic radicals shown in Scheme 2.6, only attack at C2 of the 1-methylnaphthalene radical cation by $(O_2N)_3C^-$ would yield a

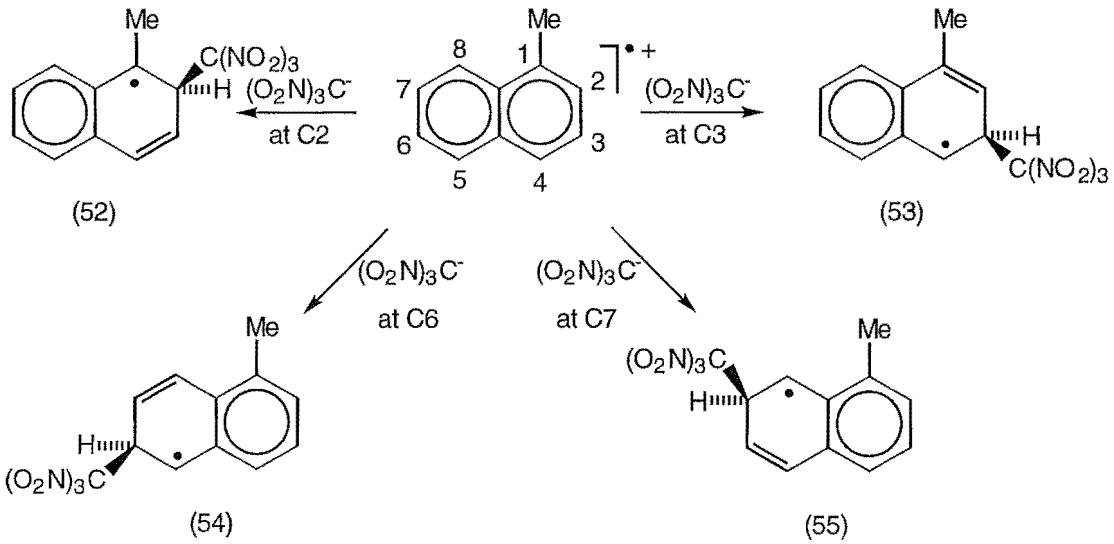

Scheme 2.6

tertiary benzylic radical (52). This would however be destabilized due to the presence of the β-methyl interaction with the trinitromethyl group. Attack of $(O_2N)_3C^-$ on the 1-methylnaphthalene radical cation at C3, C6 and C7 would lead to the less stable secondary benzylic radicals (53), (54) and (55), respectively.

The studies discussed in this Chapter aimed to gain further understanding into the regiochemistry of the photochemical reactions

between aromatic compounds and TNM. In light of the studies discussed above, it appears probable that the relative energies of the various delocalized carbon radicals determine the reaction pathways followed. The energy of the delocalized carbon radical, formed by initial attack of $(O_2N)_3C^-$ on the aromatic radical cation, will be affected in two ways. Firstly, due to steric interactions between the bulky trinitromethyl group and the remainder of the molecule and secondly, by the extent of delocalization of (and stabilization by substitutents on) the discrete carbon-centred radical. To gain further insight into this mechanistic problem, the photolysis reactions of 1,4,6,7-tetramethylnaphthalene (56), 2,6-dimethylnaphthalene (57) and 1,3-dimethylnaphthalene (58) were studied in detail.

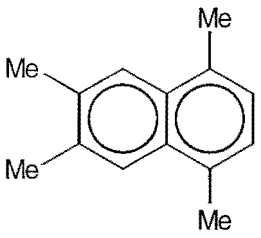

(56)

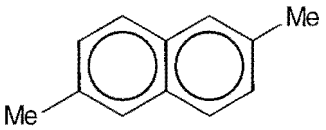

(57)

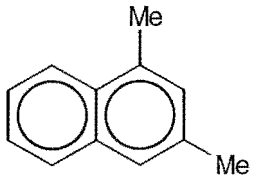

(58)

Attack of $(O_2N)_3C^-$ in the photolysis of 1,4,6,7-tetramethylnaphthalene with TNM was expected to occur predominantly at C1 on the 1,4,6,7-tetramethylnaphthalene radical cation. The potential radicals, represented in Scheme 2.7, fall into two distinct types, those of the phenylallylic type (59) and (60), and those of the benzylic type (61) and (62). While the phenylallylic radical (59), arising *via* attack of $(O_2N)_3C^-$ at C1 on the 1,4,6,7-tetramethylnaphthalene radical cation, may be subject to steric compression arising from the *ipso* attachment of the trinitromethyl group it would have enhanced stability due to the presence of the 4-methyl group. The phenylallylic radical (60), arising from $(O_2N)_3C^-$ attack at C5 on the 1,4,6,7-tetramethylnaphthalene radical cation, would also be stabilised by the methyl group at C6 but steric interactions between the bulky trinitromethyl group and

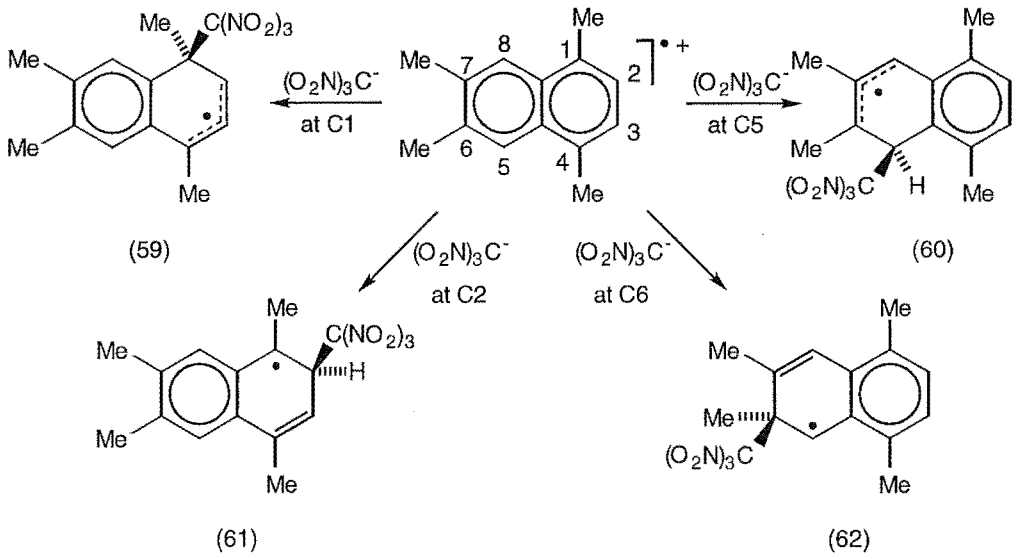

Scheme 2.7

both the β and *peri*-methyl groups would destabilize it. The tertiary benzylic radical (61), formed after C2 attack on the 1,4,6,7-tetramethylnaphthalene radical cation by $(O_2N)_3C^-$, would be destabilized due to the presence of the β-methyl interaction with the trinitromethyl group. Attack of $(O_2N)_3C^-$ at C6 of the 1,4,6,7-tetramethylnaphthalene radical cation not only produces the secondary benzylic radical (62) but also contains an unfavourable β-methyl interaction with the trinitromethyl group and steric compression arising from the *ipso*-methyl attachment. Clearly, the favourable reaction pathway is *via* initial attack of $(O_2N)_3C^-$ at C1, similar to 1,4-dimethylnaphthalene.[4] It was therefore expected that unstable adducts similar to those formed from 1,4-dimethylnaphthalene, would arise and that rearrangement studies of these 1,4,6,7-tetramethylnaphthalene (56) derived adducts might shed further light on the mechanism of product formation.

In the photolysis of 2,6-dimethylnaphthalene (57) with TNM it was expected that the phenylallylic radicals (63) and (64) would be favoured over the less stable secondary benzylic radicals (65) and (66), formed *via* initial attack of $(O_2N)_3C^-$ on the 2,6-dimethylnaphthalene radical cation, at C2 and

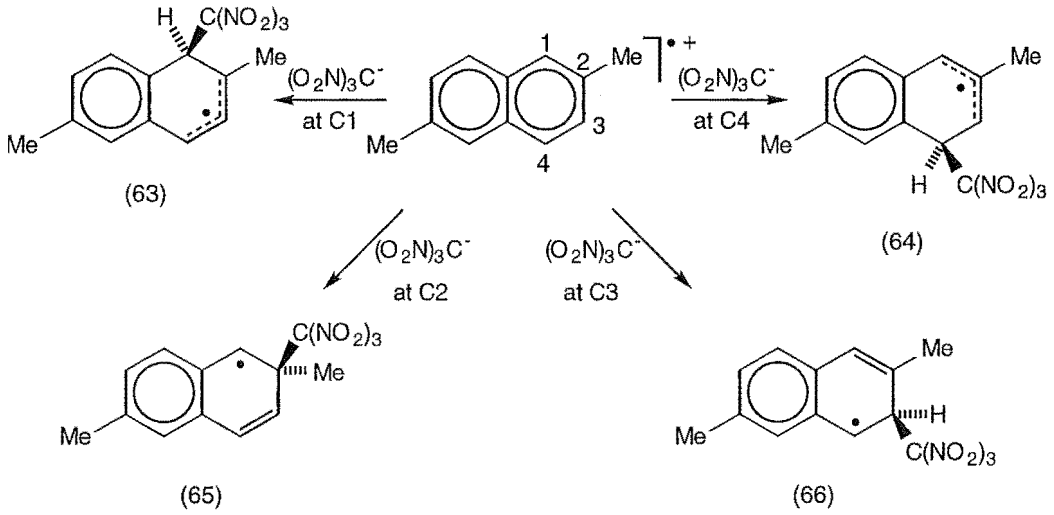

Scheme 2.8

C3, respectively (See Scheme 2.8). The benzylic radicals would be destabilized due to the steric effects between the trinitromethyl group and the presence of an *ipso*-methyl group in the benzylic radical (65) and a β-methyl group in the benzylic radical (66). While attack of $(O_2N)_3C^-$ at C1 on the 2,6-dimethylnaphthalene radical cation would lead to enhanced stability due to the methyl group at C2, the β-methyl interaction with the trinitromethyl group would be expected to destabilize the phenylallylic radical (63). Phenylallylic radical (64), formed after C4 attack on the 2,6-dimethyl-naphthalene radical cation by $(O_2N)_3C^-$, has neither added stability due to suitably positioned methyl groups nor has it any unfavourable steric interactions with the bulky trinitromethyl group. Hence it appears that attack of $(O_2N)_3C^-$ on the 2,6-dimethylnaphthalene radical cation would probably occur predominantly at C4, but that some attack might also occur at C1.

Photolysis of the 1,3-dimethylnaphthalene/TNM system could generate many possible reaction pathways, resulting in either phenylallylic or benzylic radicals. The possible benzylic radicals (67)-(70) are summarized in Scheme 2.9. Attack of $(O_2N)_3C^-$ at C2 on the 1,3-dimethylnaphthalene

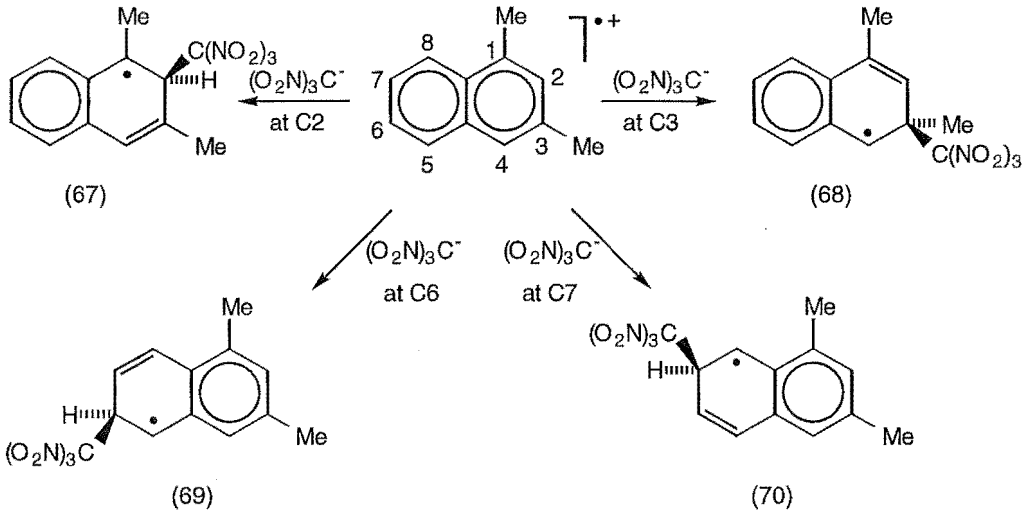

Scheme 2.9

radical cation would give rise to a tertiary benzylic radical (67), however this would be destabilized due to the presence of two β-methyl interactions with the bulky trinitromethyl group. Reaction at C3, C6 or C7 on the 1,3-dimethylnaphthalene radical cation by $(O_2N)_3C^-$ would produce secondary benzylic radicals, (68), (69) and (70), respectively. Benzylic radical (68) would be destabilized by the presence of the *ipso*-attachment of the trinitromethyl group. However, the benzylic radicals (69) and (70), formed *via* attack of $(O_2N)_3C^-$ in the non-methylated ring of the 1,3-dimethylnaphthalene radical cation, have no unfavourable steric interactions.

Scheme 2.10 depicts the possible phenylallylic radicals (71)-(74). The *ipso* attack of $(O_2N)_3C^-$ on the 1,3-dimethylnaphthalene radical cation at C1 produces the phenylallylic radical (71), which has no added stability from the methyl groups. However the stability of the phenylallylic radical (72), formed *via* C4 attack of $(O_2N)_3C^-$ on the 1,3-dimethylnaphthalene radical cation, is enhanced by the presence of the two methyl groups. Radical (72) does, however, contain an unfavourable β-methyl interaction with the trinitromethyl group. Attack of $(O_2N)_3C^-$ at C5 on the 1,3-dimethyl-

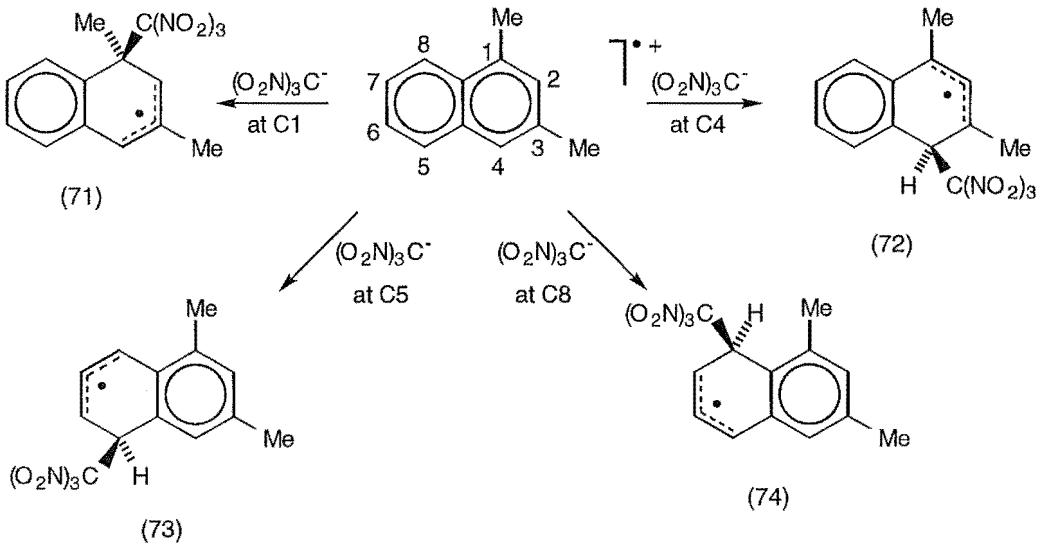

Scheme 2.10

naphthalene radical cation leads to the phenylallylic radical (73), which is neither stabilized by the methyl groups nor destabilized by steric effects due to the bulky trinitromethyl group. Attack at C8 on the 1,3-dimethyl-naphthalene radical cation by $(O_2N)_3C^-$, however, leads to an unfavourable *peri*-methyl interaction with the trinitromethyl group in the resulting phenylallylic radical (74). It therefore appears that many possible options would be open for $(O_2N)_3C^-$ attack on the 1,3-dimethylnaphthalene radical cation, but that attack at C5 might be favoured.

2.2 The Photolysis of 1,4,6,7-Tetramethylnaphthalene (56)

General procedure for the photonitration of 1,4,6,7-tetramethylnaphthalene (56) *with TNM.*

A solution of 1,4,6,7-tetramethylnaphthalene (56) (500 mg, 0.34 mol L^{-1}) and TNM (0.68 mol L^{-1}) in dichloromethane (at +20 or -20°) or acetonitrile (at +20°) was irradiated with filtered light ($\lambda_{cut\text{-}off}$<435 nm) and small samples were withdrawn for analysis at suitable intervals. The work-up procedure, involving evaporation of solvent, TNM and trifluoroacetic acid (if present), was conducted at ≤0°. The crude product mixtures were stored at -20° and were analysed by ^1H n.m.r. spectroscopy as soon as possible (For complete experimental details see Chapter 5, Section 5.2.1).

2.3 The Photochemistry of 1,4,6,7-Tetramethylnaphthalene (56) in Dichloromethane

2.3.1 Photochemistry in dichloromethane at -20° and identification of adducts.

A solution of 1,4,6,7-tetramethylnaphthalene (56) (0.34 mol L^{-1}) and TNM (0.68 mol L^{-1}) in dichloromethane was irradiated at -20° until the strongly red colour of the charge-transfer band was bleached. The composition of the reaction mixture was monitored by withdrawing samples for ^1H n.m.r. spectral analysis. After work-up, the final solution (after 2 h, conversion ≈ 100%) was shown to contain a mixture of adducts (75)-(77) (total 63%), aromatic compounds (78)-(81) (total 36%), and other unidentified aromatic compounds (total 1%).

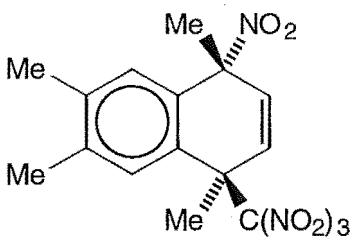

(75)

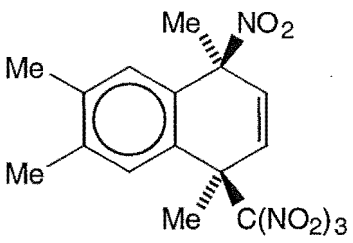

(76)

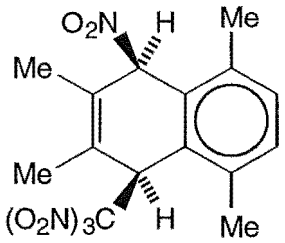

(77)

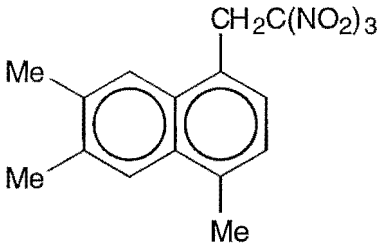

(78)

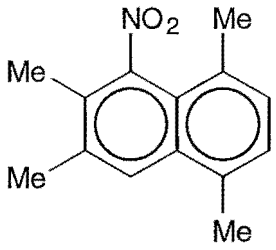

(79)

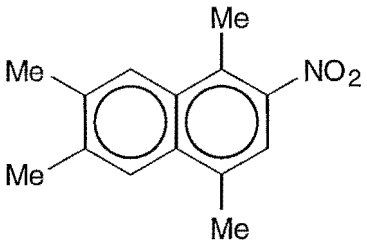

(80)

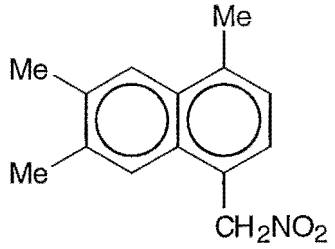

(81)

The major adduct (75) was isolated by crystallization from dichloromethane/pentane and its structure determined by single crystal X-ray analysis. A perspective drawing of 1,4,6,7-tetramethyl-*r*-1-nitro-*t*-4-trinitromethyl-1,4-dihydronaphthalene (75), $C_{15}H_{16}N_4O_8$, m.p. 89° (dec.) is presented in Fig. 2.1, and corresponding atomic coordinates are given in Table 5.1 (See Chapter 5, Section 5.5). In the solid state, the alicyclic ring of adduct (75) is close to planar [torsional angles: C(2)-C(3)-C(4)-C(4a) 1.7(7)°; C(3)-C(2)-C(1)-C(8a) -6.3(7)°]. The orientations of the methyl and trinitromethyl substituents at C(4) relative to the plane of the aromatic ring reflect the difference in the size of the two substituents [torsional angles: C(5)-C(4a)-C(4)-C(10) 52.8(6)°; C(5)-C(4a)-C(4)-C(13) -70.7(6)°], the more

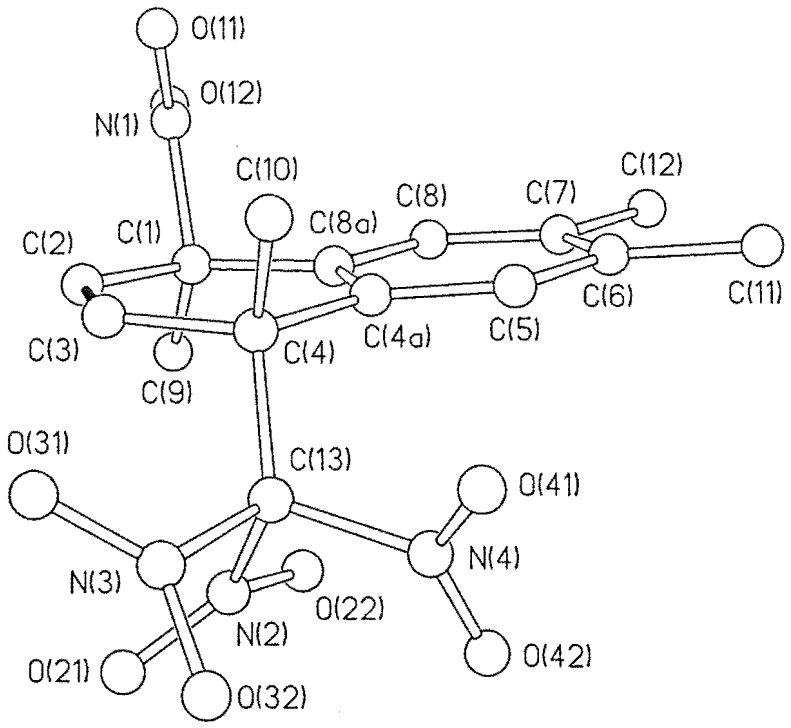

Fig. 2.1 Perspective drawing of adduct (75). Double bond shown in black.

similarly sized substituents at C(1) being more evenly displaced from that plane [torsional angles: C(8)-C(8a)-C(1)-C(9) 56.0(6)°; C(8)-C(8a)-C(1)-N(1) -62.7(6)°]. The plane of the nitro group at C(1) is nearly eclipsed with the C(1)-C(9) bond [torsional angle: C(9)-C(1)-N(1)-O(12) -13.8(6)°]. The spectroscopic data for adduct (75) were in accord with the established structure. In particular the Me-**C**(4)-$C(NO_2)_3$ resonance appeared at δ 48.9, while the Me-**C**(1)-NO_2 resonance appeared at δ 86.7. These assignments were confirmed by long range reverse detected heteronuclear correlation spectra (HMBC). The coupling constant $J_{H2,H3}$ 10.5 Hz indicated the 1,4-substitution and was consistent with the molecule having the same conformation in the solid state and in solution.

The structure of the epimeric 1-nitro-4-trinitromethyl adduct (76), which could not be isolated, was assigned on the basis of its ^1H n.m.r. spectra on comparison with the spectral features of adduct (75), the

structure of which has been determined by single crystal X-ray analysis. In particular, the coupling constant $J_{H2,H3}$ 10.4 Hz indicated the 1,4-substitution, as illustrated in Fig. 2.2. The two sets of spectroscopic data are

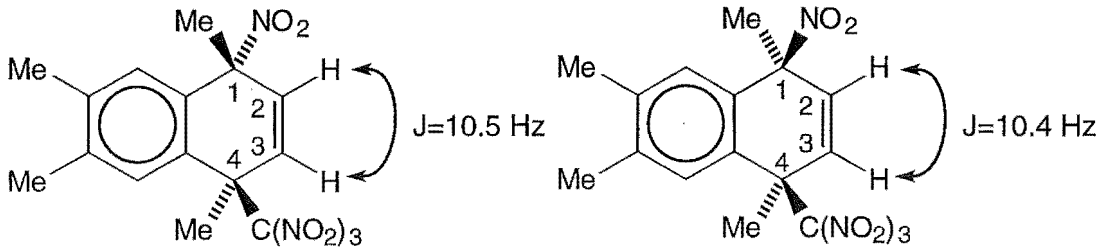

(75) (76)

1-Me	2.07	1-Me	1.99
H2	6.22	H2	6.45
H3	6.64	H3	6.62
4-Me	2.19	4-Me	2.08

Fig. 2.2 Comparison of the characteristic ^{1}H n.m.r. resonances (in ppm) and coupling constants for adducts (75) and (76).

closely similar and consistent with their assignments as epimers.

The structure of the remaining nitro/trinitromethyl adduct (77), which also could not be isolated, was assigned from a comparison of its ^{1}H n.m.r. spectrum with that for *cis*-2,3-dimethyl-1-nitro-4-trinitromethyl-1,4-dihydro-naphthalene (82),[5] as summarized in Fig. 2.3. In particular, the ^{1}H n.m.r. signals due to the C**H**NO_2 (δ 5.91) and C**H**$C(NO_2)_3$ (δ 5.89) appeared as broad singlets, consistent with their location flanking the 2,3-dimethyl structural feature.

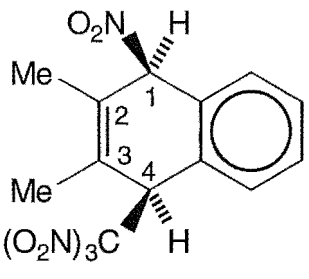

(82)

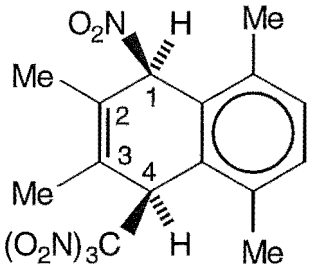

(77)

H1	5.80	H1	5.91
2-Me, 3-Me	2.00, 2.07	2-Me, 3-Me	1.97, 2.15
H4	5.60	H4	5.89

Fig. 2.3 Comparison of the characteristic ^1H n.m.r. resonances (in ppm) for adducts (82) and (77).

2.3.2 Reaction in dichloromethane at +20° and the identification of some of the nitro aromatic compounds.

Reaction of 1,4,6,7-tetramethylnaphthalene (56) / TNM in dichloromethane at +20°, as above, for 2 h gave a product which was shown by ^1H n.m.r. spectra to be a mixture of adducts (75)-(77) (total 17%), aromatic compounds (78)-(81) (total 83%), and a trace of other unidentified aromatic compounds. Chromatography of this mixture on a silica gel Chromatotron plate gave the following in elution order.

The first compound eluted, 4,6,7-trimethyl-1-(2',2',2'-trinitroethyl)-naphthalene (78), was obtained only in low yield but gave a satisfactory parent molecular ion in the mass spectrum, indicating the molecular formula $C_{15}H_{15}N_3O_6$. Nuclear Overhauser enhancement (N.O.e.) experiments confirmed the assignments of the chemical shifts for the protons. In

particular, the site of substitution of the trinitromethyl group was indicated by irradiation at δ 4.84 (CH_2) which gave enhancements at δ 7.16 (H2) and δ 7.44 (H8), as shown in Fig. 2.4. An HMBC experiment confirmed the

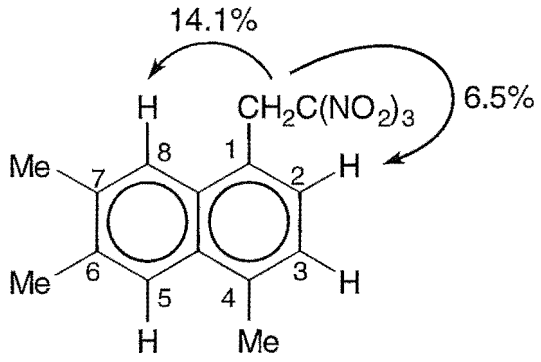

Fig. 2.4 Enhancements (%) from a selected n.O.e. experiment for the side-chain trinitromethyl aromatic compound (78).

assignment of the ^{13}C n.m.r. spectra, except for the methyl groups at C6 and at C7, which had closely similar ^{13}C n.m.r. resonances. Furthermore, the presence of very strong infrared absorptions at 1605 and 1590 cm^{-1} provided evidence for the $-C(NO_2)_3$ substituent.

The second compound eluted, 2,3,5,8-tetramethyl-1-nitro-naphthalene (79), was again isolated only in low yield but gave a satisfactory parent molecular ion in the mass spectrum, indicating the molecular formula $C_{14}H_{15}NO_2$. Again, the connectivity in the structure was established by the complete assignment of the ^1H and ^{13}C NMR spectra *via* a combination of n.O.e. and HMBC experiments. In particular, the site of substitution of the nitro group was indicated by irradiation at δ 2.31 (2-Me) which led to enhancement at δ 2.50 (3-Me), irradiation at δ 7.88 (H4) led to enhancements at δ 2.50 (3-Me) and at δ 2.64 (5-Me), and irradiation at δ 7.20 (H6 and H7) led to enhancements at δ 2.64 (5-Me) and at δ 2.53 (8-Me), as represented in Fig. 2.5. The characteristic infrared absorption at 1531 cm^{-1} for a $-NO_2$ substituent provided further evidence for product (79).

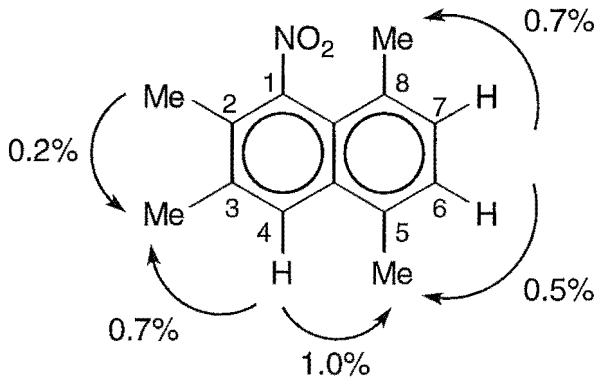

Fig. 2.5 Enhancements (%) from selected n.O.e. experiments for the 1-nitro aromatic compound (79).

The third compound eluted, 1,4,6,7-tetramethyl-2-nitronaphthalene (80), was identified from its ^{1}H and ^{13}C n.m.r. spectra which again allowed the complete connectivity in the structure to be determined. N.O.e. experiments confirmed the assignments of the chemical shifts for the protons. In particular, the position of the NO_2 group was indicated by irradiation at δ 2.77 (1-Me) which led to enhancement at δ 7.93 (H8), and irradiation at δ 7.57 (H3) which led to enhancement at δ 2.66 (4-Me), as seen in Fig. 2.6. The mass spectrum gave a satisfactory parent molecular ion

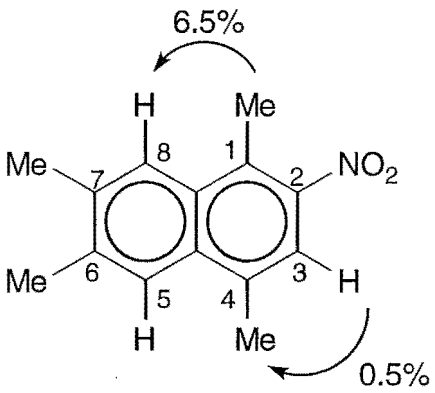

Fig. 2.6 Enhancements (%) from selected n.O.e. experiments for the 2-nitro aromatic compound (80).

indicating the molecular formula $C_{14}H_{15}NO_2$ and further evidence for the $-NO_2$ substituent was seen with the characteristic infrared absorption at 1586 cm^{-1}.

The final compound eluted, 4,6,7-trimethyl-1-nitromethylnaphthalene (81), appeared to be unstable on a silica gel Chromatotron plate and could be isolated only in admixture with other materials. The structure of compound (81) was assigned from a comparison of its ^1H n.m.r. spectrum with that for 4-methyl-1-nitromethyl-naphthalene (83),[4] as outlined in Fig. 2.7.

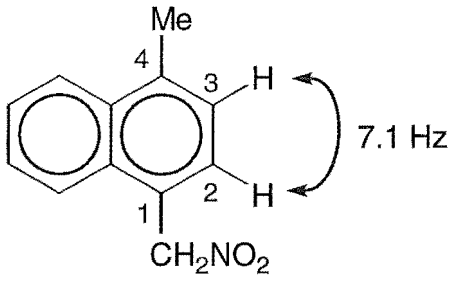

(83)

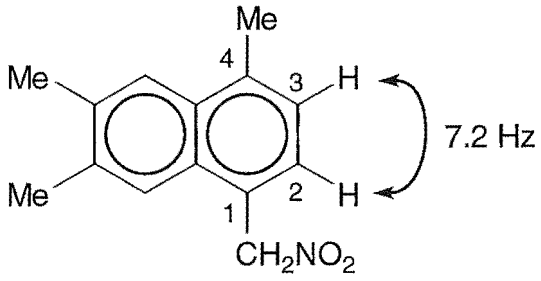

(81)

1-CH_2	5.89	1-CH_2	5.85
H2, H3	7.37, 7.50	H2, H3	7.25, 7.38
4-Me	2.74	4-Me	2.69

Fig. 2.7 Comparison of the characteristic ^1H n.m.r. resonances (in ppm) and coupling constants for the side-chain nitro derivatives (83) and (81).

In particular, the characteristic ^1H n.m.r. resonance at δ 5.85 for the CH_2NO_2 function provided evidence for product (81).

On monitoring both the +20 and -20° reactions in dichloromethane with time, it appeared that the major primary products of the photochemical reaction of the 1,4,6,7-tetramethylnaphthalene (56) / TNM charge-transfer

complex were the nitro/trinitromethyl adducts (75)-(77). Table 2.1 gives an overview of product yields in dichloromethane. At -20° adducts (75) and (76) decreased with time and there was a corresponding increase in the side-chain nitro derivative (81). With an increase in temperature to +20° there was a decrease in adducts (75)-(77) and a corresponding increase in the aromatic compounds (78)-(81), especially noticeable in the case of the 2-nitro aromatic compound (80).

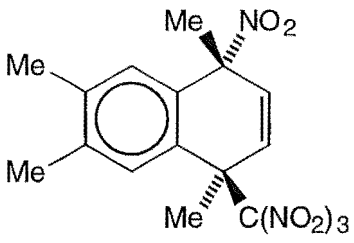

(75)

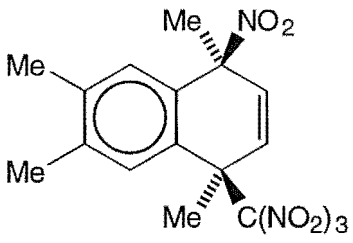

(76)

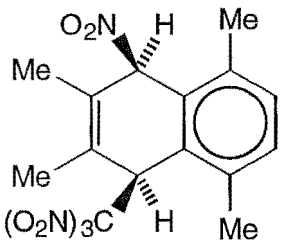

(77)

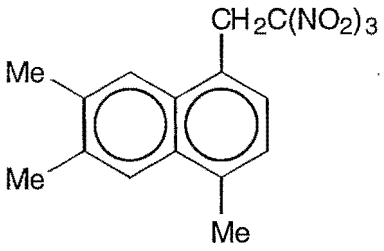

(78)

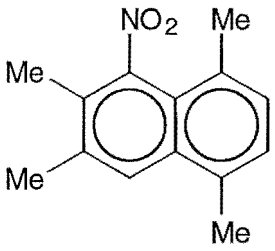

(79)

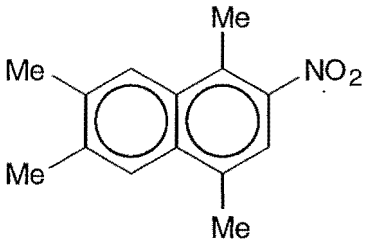

(80)

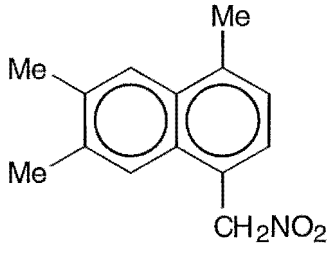

(81)

Table 2.1 Overview of product yields from the photolysis of 1,4,6,7-tetramethylnaphthalene (56) (0.34 mol L^{-1}) and TNM (0.68 mol L^{-1}) in dichloromethane.

		Yield (%)									
	Conversion				Total					Unknown	Total
t (h)	(%)	(75)	(76)	(77)	adducts	(78)	(79)	(80)	(81)	aromatics	aromatics
At +20°											
0.25	16	31.0	3.9	2.0	36.9	2.2	2.3	22.5	28.8	7.3	63.1
0.5	47	34.6	5.8	1.9	42.3	1.7	3.3	21.1	22.7	8.9	57.1
1	86	44.8	3.2	2.7	50.7	1.7	3.8	17.0	20.8	6.0	49.3
2	100	11.3	2.9	2.4	16.6	8.4	5.8	38.2	30.5	0.5	83.4
At -20°											
0.25	13	69.6	5.6	3.9	79.1	1.1	2.1	3.3	10.9	3.5	20.9
0.5	26	60.7	5.4	2.9	69.0	1.9	2.6	4.1	20.4	2.0	31.0
1	58	54.7	4.8	3.1	62.6	3.0	3.2	4.2	25.6	1.4	37.4
2	100	57.7	1.9	3.2	62.8	2.1	4.0	3.3	26.8	1.0	37.2

2.4 Rearrangement of 1,4,6,7-Tetramethyl-*r*-1-nitro-*t*-4-trinitromethyl-1,4-dihydronaphthalene (75) on Silica Gel

The nitro/trinitromethyl adduct (75) was adsorbed onto a silica gel Chromatotron plate, which was then eluted using first pentane and then pentane/ether mixtures. The first material eluted was unreacted nitro/trinitro-methyl adduct (75), identified from its spectroscopic characteristics. Subsequently, three closely related adducts (84)-(86) were eluted.

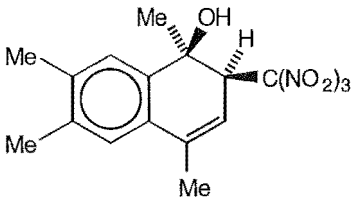

(84)

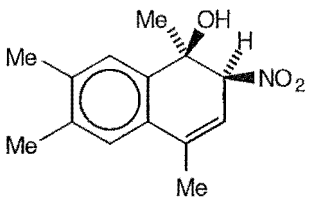

(85)

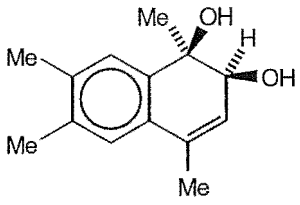

(86)

The second compound eluted, 1,4,6,7-tetramethyl-2-trinitromethyl-1,2-dihydronaphthalen-1-ol (84), was isolated only in low yield and failed to give a molecular ion in the mass spectrum under a variety of operating conditions. However, the substituents present in the structure and its connectivity were established from n.O.e. and HMBC experiments, which allowed the complete assignment of the ^{1}H and ^{13}C n.m.r. spectra. In particular, irradiation at δ 4.38 (H2) gave enhancements at δ 1.69 (1-Me) and at δ 5.63 (H3), while irradiation at δ 5.63 (H3) gave enhancements at δ 2.11 (4-Me) and at δ 4.38 (H2), as depicted in Fig. 2.8. Furthermore, the locations of the hydroxy and trinitromethyl functions were defined by the chemical shifts for the 1-Me (^{1}H n.m.r. δ 1.69) and C1 (^{13}C n.m.r. δ 72.8), and H2 (^{1}H n.m.r. δ 4.38) and C2 (^{13}C n.m.r. δ 49.3), respectively, as presented in Fig. 2.12 (see below). A broad singlet resonance in the ^{1}H n.m.r. spectra at δ 2.45 was observed corresponding to the -O**H** function.

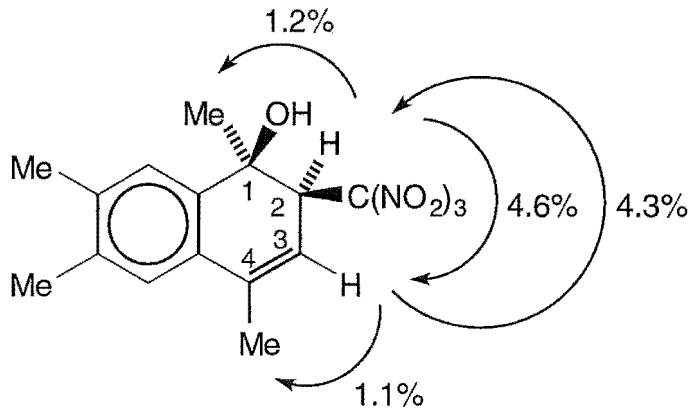

Fig. 2.8 Enhancements (%) from selected n.O.e. experiments for compound (84).

Confirmation of the presence of the two functional groups was provided by the characteristic infrared absorptions observed at 3590 cm^{-1} (-OH) and at 1620 and 1593 cm^{-1} [$-C(NO_2)_3$]. The stereochemistry of this compound (84) remains uncertain, but arguments will be presented below which suggest that it has the *r*-1-hydroxy-*c*-2-trinitromethyl stereochemistry.

The third compound eluted, 1,4,6,7-tetramethyl-2-nitro-1,2-dihydro-naphthalen-1-ol (85), was again isolated only in low yield and also failed to give a parent molecular ion in the mass spectrum under a variety of operating conditions. As for the 1-hydroxy-2-trinitromethyl compound (84), above, the substituents present and the connectivity in the 1-hydroxy-2-nitro compound (85) were established from n.O.e. and HMBC experiments which allowed the complete assignment of the ^1H and ^{13}C n.m.r. spectra. In particular, irradiation at δ 4.99 (H2) gave enhancements at δ 1.52 (1-Me) and at δ 5.88 (H3), while irradiation at δ 5.88 (H3) gave enhancements at δ 2.14 (4-Me) and at δ 4.99 (H2), as seen in Fig. 2.9. Furthermore, the location of the hydroxy function *ipso* to the 1-methyl group was indicated by the ^1H n.m.r. chemical shift for the 1-Me (δ 1.52) and the ^{13}C n.m.r chemical shift for C1 (δ 72.3), while the nitro function located at C2 was indicated by the ^1H

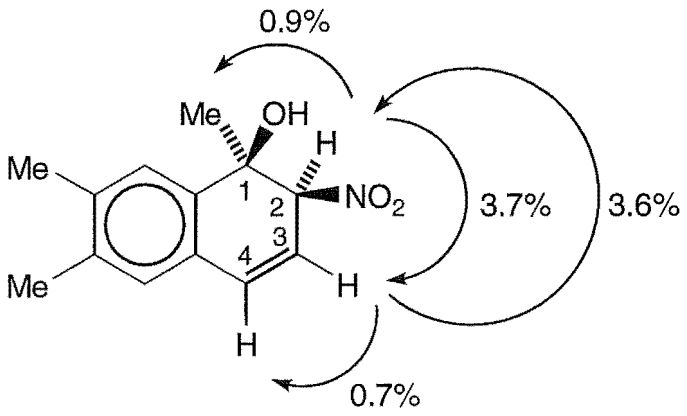

Fig. 2.9 Enhancements (%) from selected n.O.e. experiments for compound (85).

n.m.r. chemical shift for H2 (δ 4.99) and the ^{13}C n.m.r. chemical shift for C2 (δ 89.7), as observed in Fig. 2.12 (see below). The ^{1}H n.m.r. spectra of adduct (85) contained a singlet resonance at δ 2.94 corresponding to the -O**H** function. Further evidence for the two functional groups was provided by the characteristic infrared absorptions at 1548 cm^{-1}, corresponding to the $-NO_2$ function, and a broad absorption at 3378 cm^{-1} corresponding to the -OH function. The stereochemistry of this compound (85) is uncertain, but it seems likely that it has the *r*-1-hydroxy-*c*-2-nitro stereochemistry (see below).

The structure of the final compound eluted was determined by single crystal X-ray analysis. A perspective drawing of 1,4,6,7-tetramethyl-1,2-dihydronaphthalene-*r*-1,*c*-2-diol (86), $C_{14}H_{18}O_2$, m.p. 98-98.5° is presented in Fig. 2.10, and corresponding atomic coordinates are given in Table 5.2 (See Chapter 5, Section 5.5). In the solid state the alicyclic ring of diol (86) exists in a conformation in which the unsaturated systems are twisted from coplanarity [torsional angle: C(3)-C(4)-C(4a)-C(8a) -16.3(2)°] and the conformation of the remainder of that ring is defined by torsional angles: C(4)-C(3)-C(2)-C(1) 37.8(2)°; C(4a)-C(8a)-C(1)-C(2) 35.9(2)°. In that conformation the C(2)-O(2) bond is staggered with respect to the vicinal

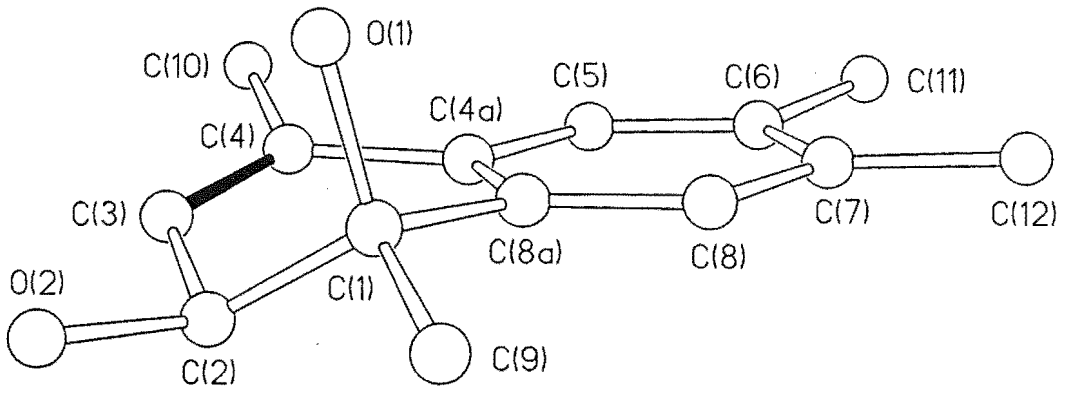

Fig. 2.10 Perspective drawing of compound (86). Double bond shown in black.

C(1)-O(1) and C(1)-C(9) bonds [torsional angles: O(2)-C(2)-C(1)-O(1) -58.9(1)°; O(2)-C(2)-C(1)-C(9) 60.9(2)°], and the *peri* interactions involving the methyl groups on the alicyclic ring are somewhat relieved [torsional angles: C(10)-C(4)-C(4a)-C(5) -15.1(2)°; C(9)-C(1)-C(8a)-C(8) -27.3(2)°]. It is clear that diol (86) exists in a markedly different conformation in solution from that observed in the solid state. In the solid state the torsional angle H(3)-C(3)-C(2)-H(2) 99.2(1)° would be consistent with a vicinal H-H coupling constant close to zero. In solution the observed coupling constant $J_{H3,H2}$ 5.9 Hz would appear more consistent with an alternative twisting of the alicyclic ring in which the C(2)-O(2) and C(1)-C(9) bonds would have orientations close to perpendicular to the mean plane of the molecule, leading to a H(3)-C(3)-C(2)-H(2) torsional angle close to 30°. In this conformation the *peri* interaction between the C1-methyl group and the adjacent aromatic ring would be minimized. The probable origin of this conformational difference in diol (86) in the solid state lies in the hydrogen bond between O(1) and H(2') in a second molecule (Fig. 2.11). The

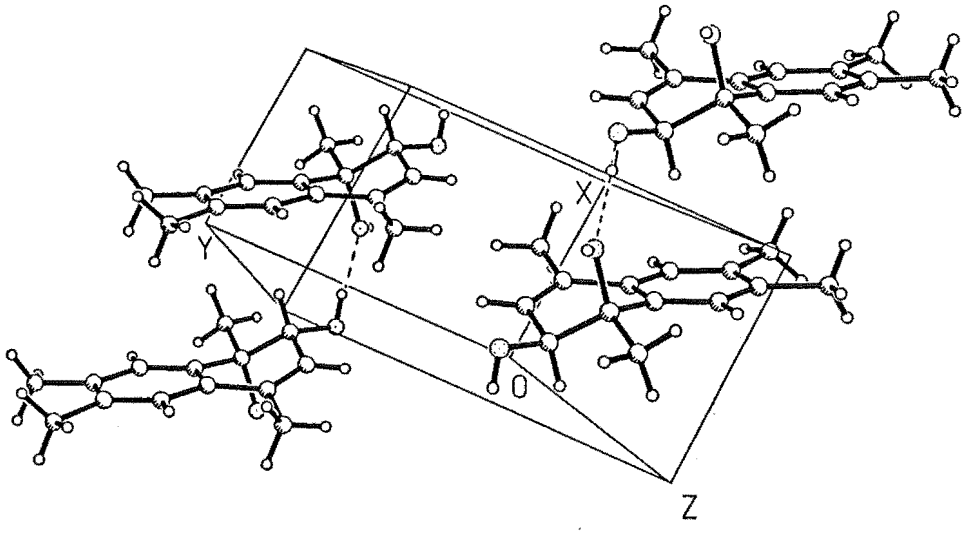

Fig. 2.11 Perspective drawing showing the hydrogen bond between O(1) and H(2') in the solid state for compound (86).

O(1)/O(2') distance is 2.713 Å, and the O(1)-H(2')-O(2') angle is 167.2°, consistent with a strong hydrogen bond. The remaining spectroscopic data for adduct (86) were in accord with the established structure. In particular, the Me-**C**(1)-OH ^{13}C n.m.r. resonance appeared at δ 73.05 while the Me-**C**(2)-OH ^{13}C n.m.r. resonance appeared at δ 71.1, as outlined in Fig. 2.12.

In solution the vicinal coupling constants $J_{H3,H2}$ are closely similar for compounds (84) (5.9 Hz), (85) (6.3 Hz), and (86) (5.9 Hz), as shown in Fig. 2.12. It is clear therefore that the H3-C3-C2-H2 torsional angles for these compounds are similar in solution with the C2-X bond (X = $C(NO_2)_3$, NO_2, and OH, respectively) perpendicular to the mean plane of the molecule in each case. Given the similar ratio of n.O.e. enhancements to H8 and H2 on irradiation of the 1-methyl signal in the ^1H n.m.r. spectra for compounds (84), (85) and (86) (see Fig. 2.13), it appears that the three compounds have the

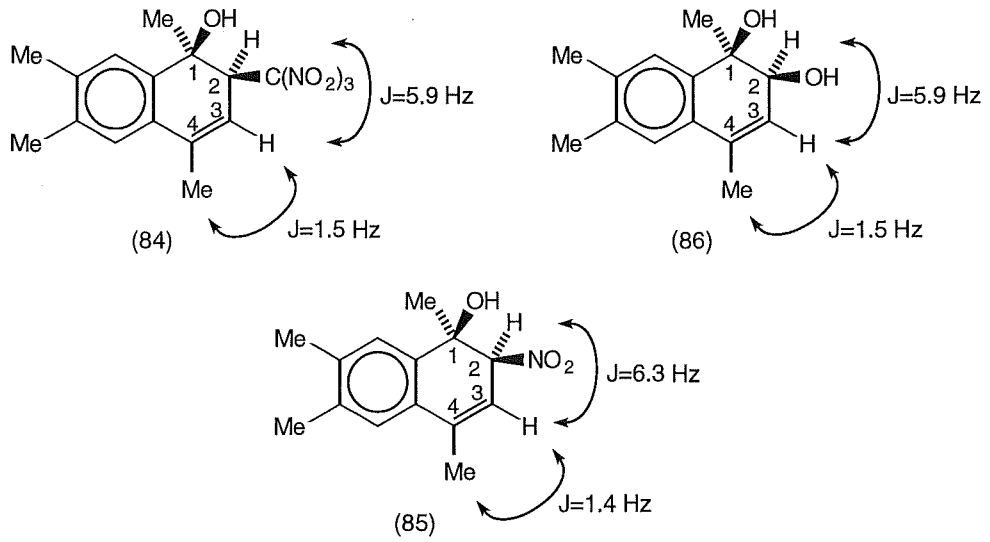

(84)		(85)		(86)	
1-Me	1.69	1-Me	1.52	1-Me	1.38
H2	4.38	H2	4.99	H2	3.84
H3	5.63	H3	5.88	H3	5.93
4-Me	2.11	4-Me	2.14	4-Me	2.08
1-O**H**	2.45	1-O**H**	2.94	1 and 2-O**H**	-
C1	72.8	C1	72.3	C1	73.05
C2	49.3	C2	89.7	C2	71.7
C3	112.65	C3	115.5	C3	123.5
C4	140.6	C4	140.3	C4	129.7

Fig. 2.12 Characteristic ^{1}H and ^{13}C n.m.r. resonances (in ppm) and coupling constants for adducts (84), (85) and (86).

same stereochemistry with the 1-methyl/H8 distance being greater than the 1-methyl/H2 distance. Given that diol (86) has been shown by single crystal X-ray analysis to have the *r*-1-*c*-2-diol stereochemistry, the same

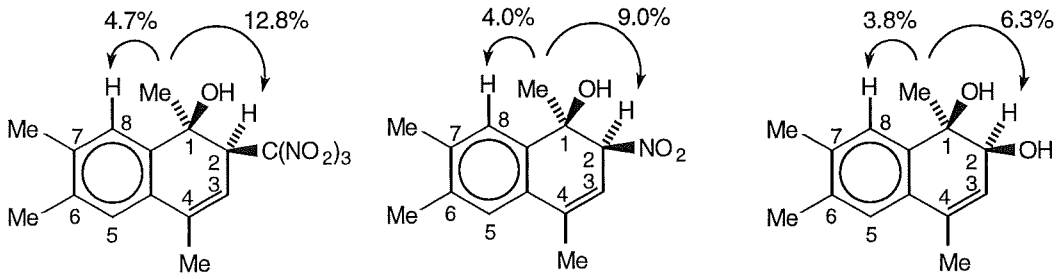

Fig. 2.13 N.O.e. enhancements (%) to H8 and H2 on irradiation of the 1-methyl signal for compounds (84), (85) and (86).

stereochemistry, *r*-hydroxy-*c*-2-X, is assigned tentatively to compounds (84) and (85).

The mode of formation of the three 1,4,6,7-tetramethyl-*c*-2-X-1,2-dihydronapthalen-*r*-1-ols (84), (85) and (86) (X = $C(NO_2)_3$, NO_2, and OH, respectively), on adsorption of the nitro/trinitromethyl adduct (75) onto silica gel Chromatotron plate, remains uncertain. However, at a superficial level it appears that 1,3-migration of a trinitromethyl group, to form (84), occurs under these conditions. In conclusion, these results imply that chromatography of such adducts on silica gel may not give a simple chromatographic outcome.

2.5 The Photochemistry of 1,4,6,7-Tetramethylnaphthalene (56) in Acetonitrile

Reaction of 1,4,6,7-tetramethylnaphthalene (56) (0.34 mol L^{-1}) / TNM (0.68 mol L^{-1}) in acetonitrile at +20°, as above, for 2 h gave a product which was shown by ^1H n.m.r. spectra to be a mixture of adduct (77) (1%), aromatic compounds (78)-(81) (total 92%), and further unidentified aromatic compounds (total 7%). Table 2.2 gives an overview of product yields in

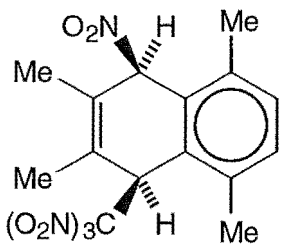

(77)

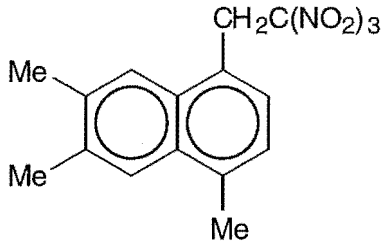

(78)

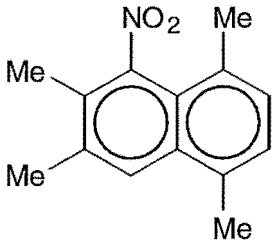

(79)

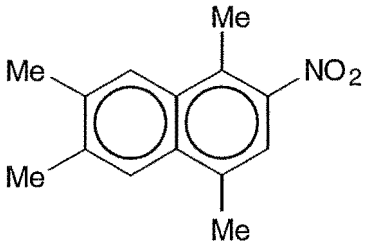

(80)

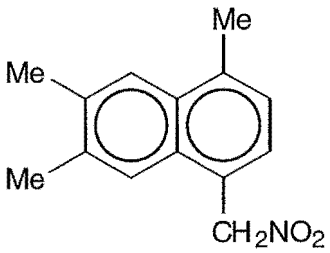

(81)

acetonitrile. After 0.5 h (conversion 33%) the yield of adducts was somewhat higher (total 15%), but compounds (79) and (80) (total 78%) were still predominant among the products detected by ^{1}H n.m.r. spectroscopy.

On comparison of the +20° acetonitrile reaction with the +20° dichloromethane reaction (see Table 2.1, Section 2.3), it can be seen that the adducts were more labile in acetonitrile, with only adduct (77) present after 2 h in acetonitrile. Adducts (84) and (85), which were not observed in dichloromethane, were observed in acetonitrile, but only during the first hour of the reaction. It was also of interest to note the increase in the relative yields of the ring nitro aromatic compounds (79) and (80), and the decrease in the side-chain nitro aromatic (81), in dichloromethane versus acetonitrile. Unfortunately, comparisons with the -20° dichloromethane reaction were not possible due to the low solubility of 1,4,6,7-tetramethylnaphthalene (56) in the more polar acetonitrile at -20°.

Table 2.2 Overview of product yields from the photolysis of 1,4,6,7-tetramethylnaphthalene (56) (0.34 mol L^{-1}) and TNM (0.68 mol L^{-1}) in acetonitrile, at +20°.

		Yield (%)											
	Conversion						Total					Unknown	Total
t (h)	(%)	(75)	(76)	(77)	(84)	(85)	adducts	(78)	(79)	(80)	(81)	aromatics	aromatics
0.5	33	6.7	2.2	4.8	0.6	0.5	14.8	0.6	28.9	48.8	2.8	4.1	85.2
1	68	3.3	1.0	3.4	0.6	0.2	8.5	0.9	33.6	51.7	2.7	2.6	91.5
2	100	-	-	1.3	-	-	1.3	1.3	33.0	52.9	4.2	7.3	98.7

2.6 The Photochemistry of 1,4,6,7-Tetramethylnaphthalene (56) in Dichloromethane Containing Trifluoroacetic Acid (TFA)

Reaction of 1,4,6,7-tetramethylnaphthalene (56) (0.34 mol L^{-1}), TNM (0.68 mol L^{-1}), and TFA (0.68 mol L^{-1}) in dichloromethane at +20°, as above, for 2 h (conversion ≈ 69%) gave a product which was shown by ^1H n.m.r. spectra to be a mixture (see Table 2.3) of 2,3,5,8-tetramethyl-1-nitro-

Table 2.3 Overview of product yields from the photolysis of 1,4,6,7-tetramethylnaphthalene (56) (0.34 mol L^{-1}) and TNM (0.68 mol L^{-1}) in dichloromethane containing trifluoroacetic acid (0.68 mol L^{-1}), at +20°.

		Yield (%)			
	Conversion				Unidentified
t (h)	(%)	(79)	(80)	(81)	material
0.5	16	28.8	44.4	10.0	16.8
1	33	29.5	48.0	8.5	14.0
2	69	32.1	48.2	5.9	13.8

naphthalene (79) (32%), 1,4,6,7-tetramethyl-2-nitronaphthalene (80) (48%), 4,6,7-trimethyl-1-nitromethylnaphthalene (81) (6%) and some unidentified material (14%). Notably, neither nitro/trinitromethyl adducts (75)-(77) nor 4,6,7-trimethyl-1-(2',2',2'-trinitromethyl)-naphthalene (78) were detected in this reaction mixture, indicating that the TFA effectively protonated the nucleophilic $(O_2N)_3C^-$. Formation of the nitro aromatic compounds (79)-(81) were seen as the products of the remaining $^{\bullet}NO_2$ with the radical cation of 1,4,6,7-tetramethylnaphthalene (56).

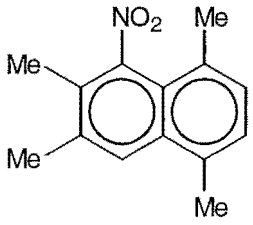

(79)

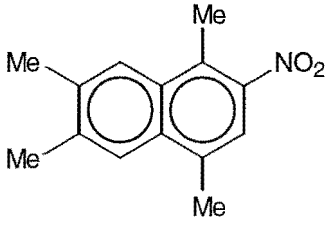

(80)

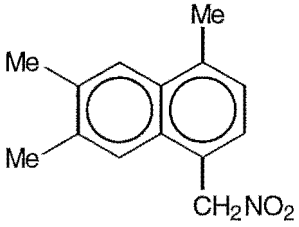

(81)

2.7 Rearrangement of 1,4,6,7-Tetramethyl-*r*-1-nitro-*t*-4-trinitromethyl-1,4-dihydronaphthalene (75) in (D)Chloroform

A solution of the nitro/trinitromethyl adduct (75) in (D)chloroform was stored at +20° in the dark and its ^1H n.m.r. spectrum monitored at appropriate time intervals. Table 2.4 summarises the changes in the composition which occurred during the rearrangement of adduct (75). The

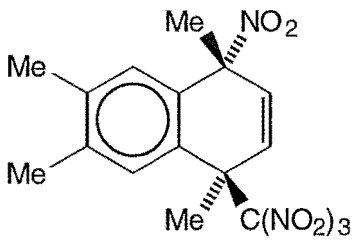

(75)

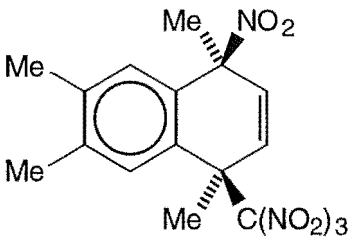

(76)

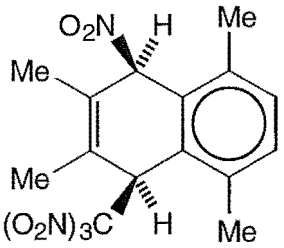

(77)

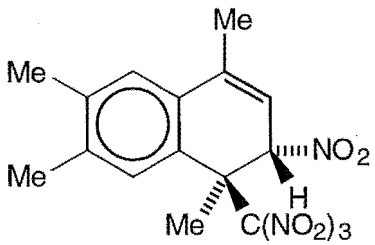

(87)

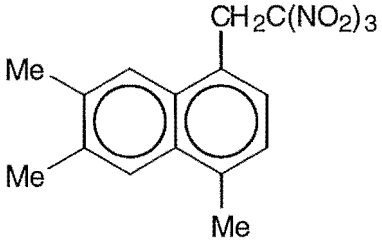

(78)

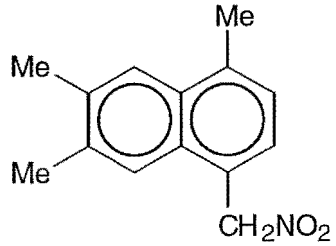

(81)

Table 2.4 Rearrangement of 1,4,6,7-tetramethyl-*r*-1-nitro-*t*-4-trinitromethyl-1,4-dihydronaphthalene (75) in (D)chloroform, at +20°.

	Composition (%)								
t (h)	(75)	(76)	(77)	(87)	Total adducts	(78)	(81)	Unknown aromatics	Total aromatics
0	100	-	-	-	100	-	-	-	-
1	96.5	3.5	-	-	100	-	-	-	-
4	90.0	8.9	-	0.5	99.4	-	0.6	-	0.6
8	84.2	12.7	-	2.0	98.9	-	1.1	-	1.1
24	75.6	14.0	-	6.7	96.3	0.4	3.1	0.2	3.7
48	52.6	10.0	-	13.3	79.7	11.5	7.3	1.5	20.3
120	6.7	1.2	0.5	17.4	26.4	51.5	14.9	7.2	73.6
168	-	-	0.7	10.4	11.1	65.0	12.9	11.0	88.9
216	-	-	0.4	3.9	4.3	72.7	7.5	13.6	95.7

major products after 12 days were identified from their ^{1}H n.m.r. spectra as 4,6,7-trimethyl-1-(2',2',2'-trinitroethyl)-naphthalene (78) (73%) and 4,6,7-trimethyl-1-nitro-methylnaphthalene (81) (7%). In the early stages of the rearrangement, epimerization of adduct (75) occurred to give 1,4,6,7-tetramethyl-*r*-1-nitro-*c*-4-trinitromethyl-1,4-dihydronaphthalene (76), equilibrium apparently being attained some time between 8 h and 24 h [(75):(76) ratio *c.* 5:1]. After some 4 h, the concentration of a third adduct increased, reaching a maximum level (17%) after 5 days. This adduct was tentatively identified as 1,4,6,7-tetramethyl-*t*-2-nitro-*r*-1-trinitromethyl-1,2-dihydronaphthalene (87) on the basis of a comparison of its ^{1}H n.m.r. spectrum with that for *trans*-4-methyl-2-nitro-1-trinitromethyl-1,2-dihydronaphthalene (88), the structure of which was determined by single crystal X-ray analysis,[6] as outlined in Fig. 2.14. Given the closely similar coupling constant $J_{H2,H3}$, for

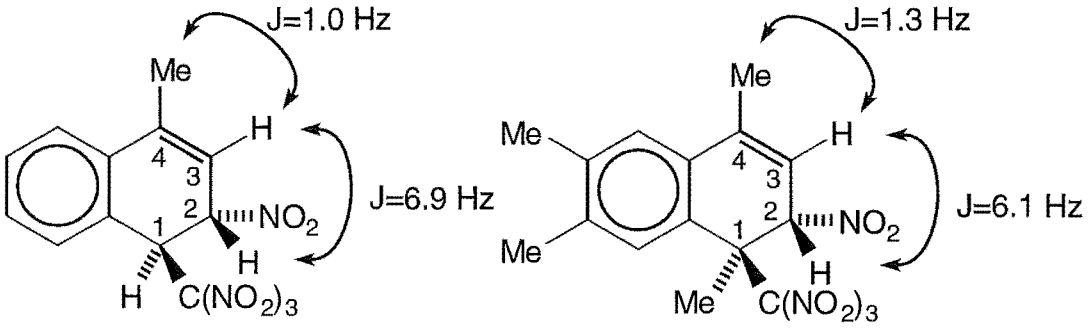

(88) (87)

H1	5.73	1-Me	2.08
H2	5.63	H2	5.61
H3	5.85	H3	5.72
4-Me	2.20	4-Me	2.09

Fig. 2.14 Comparison of the characteristic ^{1}H n.m.r. resonances (in ppm) and coupling constants for adducts (88) and (87).

the two adducts (88) and (87), it is assumed that the two compounds have the same 1,2-stereochemistry. Furthermore, in this structure the bulky 1-trinitromethyl group would be expected to adopt a conformation such that the C1-$C(NO_2)_3$ bond was nearly perpendicular to the plane of the aromatic ring. Given the magnitude of the coupling constant $J_{H2,H3}$ 6.1 Hz, it appears that the C2-NO_2 bond was close to *anti*-coplanar with the C1-$C(NO_2)_3$ bond, and that adduct (87) therefore had the *t*-2-nitro-*r*-1-trinitromethyl configuration.

2.8 The Rearrangement of 1,4,6,7-Tetramethyl-*r*-1-nitro-*t*-4-trinitromethyl-1,4-dihydronaphthalene (75) in Acetonitrile

A quantitative study of the rearrangement of the nitro/trinitromethyl adduct (75) in acetonitrile was limited by the low solubility of adduct (75) in that solvent. However, epimerization of adduct (75) to give the *r*-1-nitro-*c*-4-trinitromethyl adduct (76) was clearly a rapid reaction with the concurrent formation of the rearrangement product 4,6,7-trimethyl-1-nitromethyl-naphthalene (81). These observations parallel closely the analogous rearrangement of 1,4-dimethyl-*r*-1-nitro-*t*-4-trinitromethylnaphthalene (13) reported by Eberson *et al.*[4] (See Chapter 1, Section 1.11). In the early

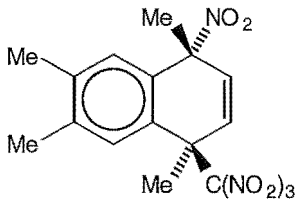

(75)

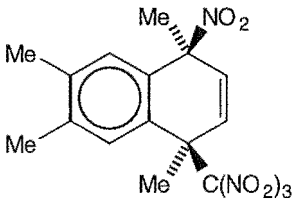

(76)

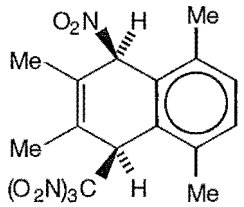

(77)

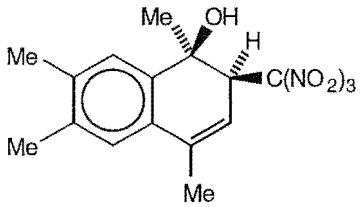

(84)

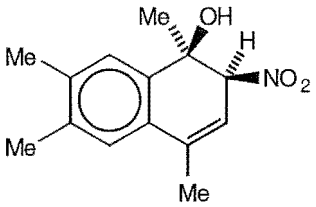

(85)

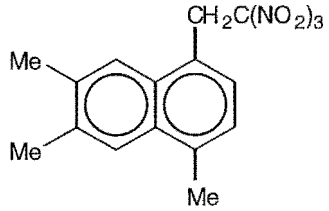

(78)

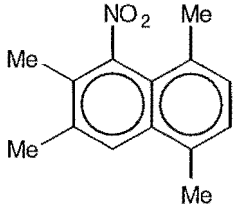

(79)

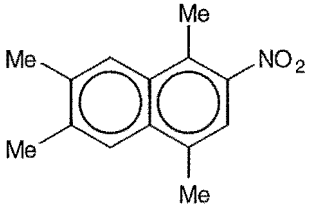

(80)

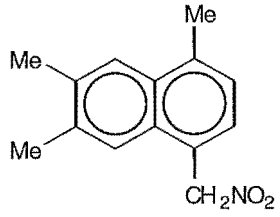

(81)

stages of the rearrangement (1-5 min.) two further adducts were present, 1,4,6,7-tetramethyl-*c*-2-trinitromethyl-1,2-dihydronaphthalen-*r*-1-ol (84) and 1,4,6,7-tetramethyl-*c*-2-nitro-1,2-dihydronaphthalen-*r*-1-ol (85). A further adduct, *cis*-2,3,5,8-tetramethyl-1-nitro-4-trinitromethyl-1,4-dihydro-naphthalene (77), was present at low levels (maximum 3%) at reaction times between 3 min. and 2 h. During the course of the rearrangement (over 4 h) the concentration of adducts (75), (76), (84) and (85) decreased steadily with the formation of increasing amounts of the nitro aromatic compounds giving finally 4,6,7-trimethyl-1-(2',2',2'-trinitroethyl)-naphthalene (78) (1%), 2,3,5,8-tetramethyl-1-nitronaphthalene (79) (14%), 1,4,6,7-tetramethyl-2-nitro-naphthalene (80) (52%), 4,6,7-trimethyl-1-nitromethylnaphthalene (81) (27%) and unidentified aromatic products (total 6%).

2.9 Overview of the Photonitration of 1,4,6,7-Tetramethyl-naphthalene (56)

In the photolysis of the 1,4,6,7-tetramethylnaphthalene (56) / TNM charge-transfer complex it appears that the nitro/trinitromethyl adducts (75)-(77) were the major primary products. For the reaction in dichloromethane

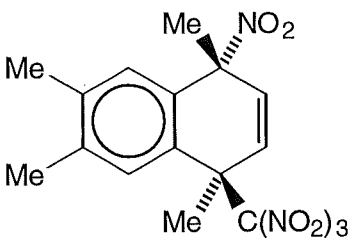

(75)

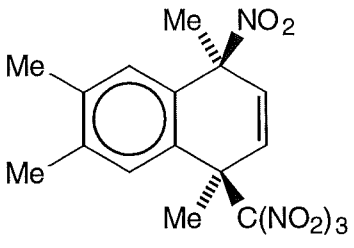

(76)

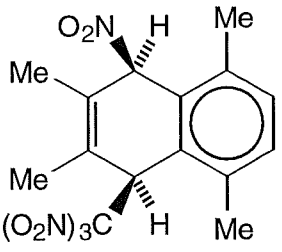

(77)

at -20° (see Table 2.1, Section 2.3) adduct formation dominates and of the total adducts identified (63%), the majority (60% out of 63%) were formed by

attack of $(O_2N)_3C^-$ at C1 of the 1,4,6,7-tetramethylnaphthalene radical cation, the remainder (3%) arose by attack of $(O_2N)_3C^-$ at C5 on that radical cation (See Fig. 2.15).

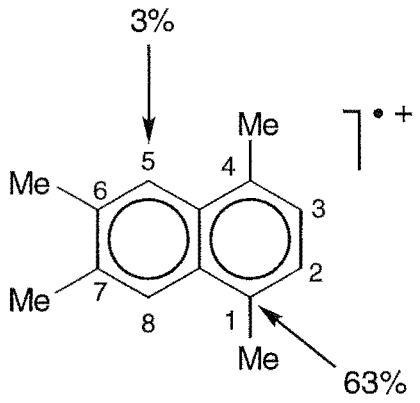

Fig. 2.15 Adducts (%) identified corresponding to attack of $(O_2N)_3C^-$ on the 1,4,6,7-tetramethylnaphthalene radical cation.

It therefore appears that the first chemical step leading to adduct formation disfavours the formation of the benzylic radicals (61) and (62),

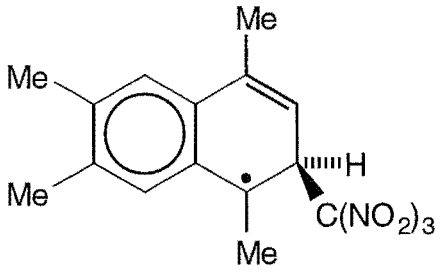

(61)

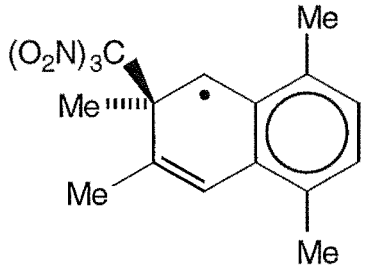

(62)

formed *via* attack of $(O_2N)_3C^-$ at C2 or C6, respectively, on the radical cation of 1,4,6,7-tetramethylnaphthalene. Instead the favoured pathway is *via* formation of the phenylallylic radical (59), but also with some of the phenylallylic radical (60). These radicals were formed by attack of the $(O_2N)_3C^-$ at C1 and C5, respectively, on the 1,4,6,7-tetramethylnaphthalene radical cation.

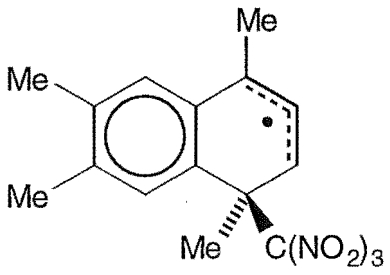

(59)

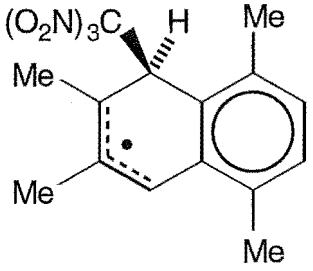

(60)

Although the identification of adduct (77) is somewhat uncertain, it is interesting that this adduct was formed by $(O_2N)_3C^-$ attack at C5, the ring position hindered by the *vicinal* and *peri*-methyl substituents. Steric interactions were predicted to favour attack of $(O_2N)_3C^-$ at C1 over C5, with attack of $(O_2N)_3C^-$ at C1 only having to overcome the *ipso* interaction with the methyl group.

Attack of $(O_2N)_3C^-$ on the 1,4,6,7-tetramethylnaphthalene radical cation was indeed found to give mainly the delocalized carbon radical (59) but also some of the isomeric radical (60), as illustrated in Scheme 2.11. The final adduct-forming steps involved coupling of the delocalized carbon

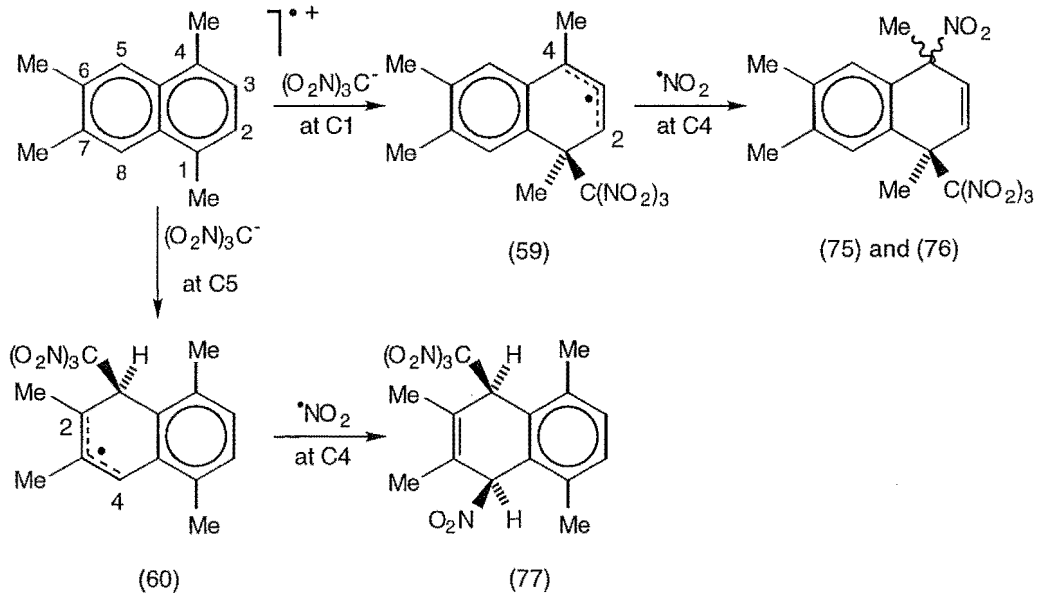

Scheme 2.11

radicals with $^{\bullet}NO_2$. Coupling with C-N bond formation occurred with the phenylallylic radical (59) at C4 to give the epimeric nitro/trinitromethyl adducts (75) and (76), and with the phenylallylic radical (60) at C4 to give the *cis*-1-nitro-4-trinitromethyl adduct (77).

Reactions in dichloromethane and acetonitrile at +20° (see Tables 2.1 and 2.2, Sections 2.3 and 2.5, respectively) were characterized by low adduct yields and clear indications of adduct instability were observed, especially in acetonitrile. Subsequently, it was found that many of the observed products were formed by rearrangement of adduct (75).

The rearrangement study of adduct (75) in (D)chloroform (see Table 2.4, Section 2.7) proved to be invaluable in understanding many of the observed results. In the early stages of the rearrangement it was clear that epimerization occurred to give adduct (76), presumably *via* the intermediate nitrocyclohexadienyl cation/trinitromethanide ion pair (89), as summarized in Scheme 2.12. This was accompanied by formation of the side-chain nitro

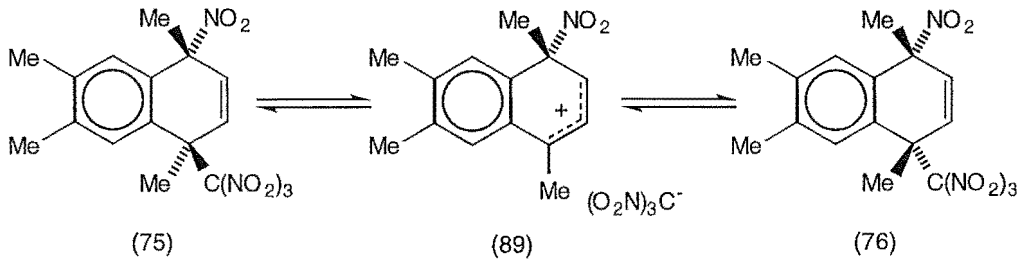

Scheme 2.12

compound (81). Initially, loss of nitroform from the intermediate nitrocyclohexadienyl cation/trinitromethanide ion pair (89), would occur by abstraction of an acidic proton from the methyl group by $(O_2N)_3C^-$, as shown in Scheme 2.13. This would be followed by homolytic cleavage of the C-NO_2 bond in diene (90). Subsequent coupling of $^{\bullet}NO_2$ with the resulting radical (91) would lead to the formation of the side-chain nitro compound (81). This

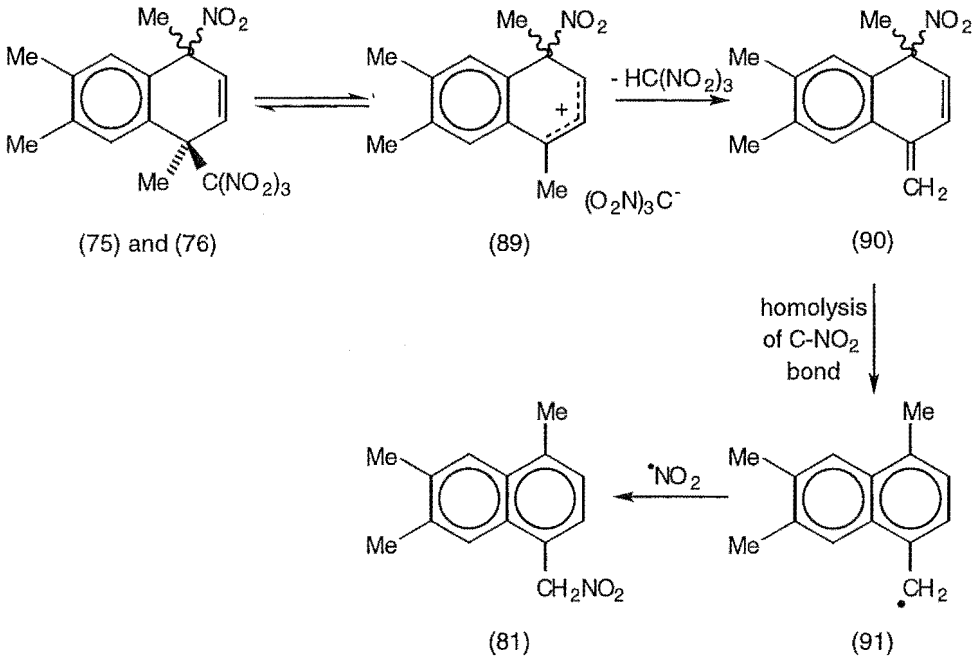

Scheme 2.13

behaviour mirrors closely the rearrangement of 1,4-dimethyl-*r*-1-nitro-*t*-4-trinitromethyl-1,4-dihydronaphthalene (13)[4] (See Chapter 1, Section 1.11). Early in the rearrangement a further adduct, 1,4,6,7-tetramethyl-*t*-2-nitro-*r*-1-trinitromethyl-1,2-dihydronaphthalene (87), was detected. Adduct (87) was seen as arising by homolytic cleavage of the C-NO_2 bond in either adduct (75) or adduct (76), with recombination of the radical species occurring on the less hindered face of the delocalized carbon radical (59) at C2, *anti* to the bulky trinitromethyl group, as depicted in Scheme 2.14. The detection, at

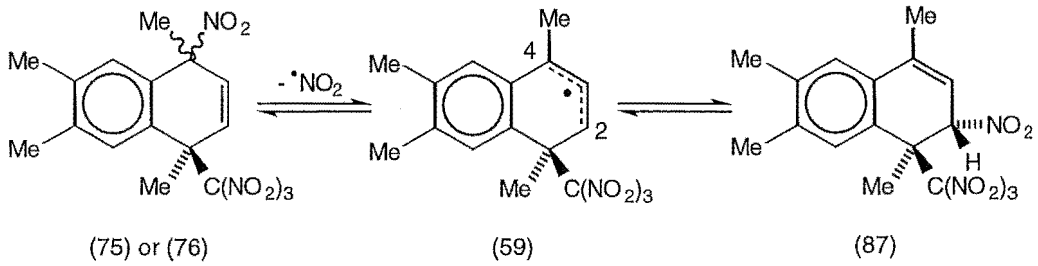

Scheme 2.14

low levels, of *cis*-2,3,5,8-tetramethyl-1-nitro-4-trinitromethyl-1,4-dihydro-naphthalene (77) was a clear indication that one or more of the adducts present in the rearrangement mixture was capable of reverting to some equivalent of the triad [$ArH^{\bullet+}$ $(O_2N)_3C^-$ $^{\bullet}NO_2$] in the original photochemical reaction. In the latter stages of the rearrangement the amount of adduct (77) remained at a low level, but adduct (87) clearly reacted further under the prevailing reaction conditions. Indeed, adduct (87) was seen as the precursor of the major final product, the side-chain trinitromethyl aromatic (78). A possible mechanism for this transformation is given in Scheme 2.15. Loss of nitrous acid from adduct (87) would yield the trinitromethyl diene (92), which might be expected to rearrange *via* the ion pair (93) to give the side-chain trinitromethyl compound (78).

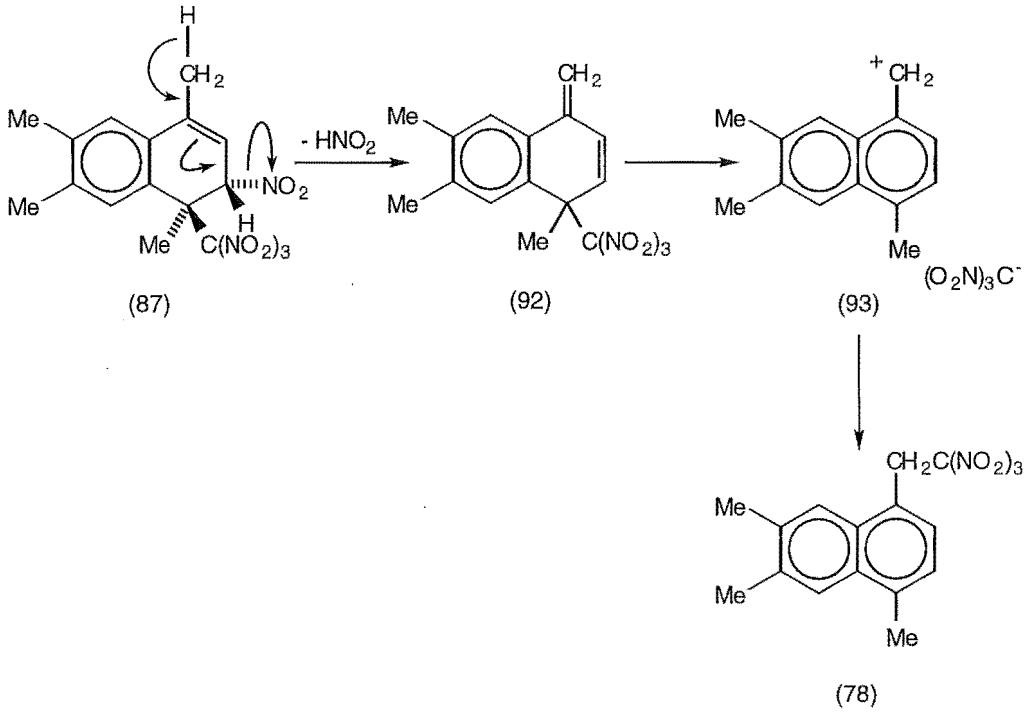

Scheme 2.15

The rearrangement of adduct (75) in acetonitrile at +20° (see Section 2.8) gave rise predominantly to the nitro aromatic compounds (79)-(81) (total

93%), while the remainder of the products (7%) were unidentified aromatics. Based on a comparison of the relative yields of aromatic products from the photochemical reaction in acetonitrile (see Table 2.2, Section 2.5) and the products of the rearrangement of the nitro/trinitromethyl adduct (75) in acetonitrile (see Section 2.8), it appears that most of the nitro aromatics (79) and (80) may arise by direct coupling of $^{\bullet}NO_2$ with the radical cation of 1,4,6,7-tetramethylnaphthalene. Comparison of the photochemical reactions in acetonitrile (see Table 2.2, Section 2.5) and in dichloromethane containing TFA (see Table 2.3, Section 2.6) showed that the relative yields of aromatic products (79) and (80) were very similar. In the presence of TFA $(O_2N)_3C^-$ was protonated leaving only the radical coupling reaction. Therefore the photolysis reaction in dichloromethane containing TFA provided further evidence for direct coupling of $^{\bullet}NO_2$ with the radical cation of 1,4,6,7-tetramethylnaphthalene to form products (79) and (80).

In conclusion, it appears that the phenylallylic type radicals were favoured over the benzylic type radicals and that steric effects further directed the attack of $(O_2N)_3C^-$ towards less hindered ring positions.

2.10 The Photolysis of 2,6-Dimethylnaphthalene (57)

General procedure for the photonitration of 2,6-dimethylnaphthalene (57) *with TNM.*

A solution of 2,6-dimethylnaphthalene (57) (500 mg, 0.4 mol L^{-1}) and TNM (0.8 mol L^{-1}) in dichloromethane or acetonitrile was irradiated at +20 or -20° with filtered light ($\lambda_{cut\text{-}off}$<435 nm) and small samples were withdrawn for analysis at suitable intervals. The work-up procedure, involving evaporation of solvent and TNM, was conducted at ≤0°. The crude product mixtures were stored at -20° and were analysed by ^1H n.m.r. spectroscopy

as soon as possible (For complete experimental details see Chapter 5, Section 5.2.2).

2.11 The Photochemistry of 2,6-Dimethylnaphthalene (57) in Dichloromethane

2.11.1 Photochemistry in dichloromethane at +20° and identification of adducts.

A solution of 2,6-dimethylnaphthalene (57) (0.4 mol L^{-1}) and TNM (0.8 mol L^{-1}) in dichloromethane was irradiated at +20° until the deep red/brown colour of the charge-transfer band was bleached. The composition of the reaction mixture was monitored by withdrawing samples for ^1H n.m.r. spectral analysis. After work-up, the final solution (after 2 h, conversion ≈ 95%) was shown to contain a mixture of adducts (94)-(104) (total 77%), aromatic compounds (105)-(107) (total 19%), and other unidentified compounds (total 4%). The adducts were separated partially by h.p.l.c. on a cyanopropyl column using hexane/dichloromethane mixtures as the eluting solvents. In the following discussion the identification of the adducts will be

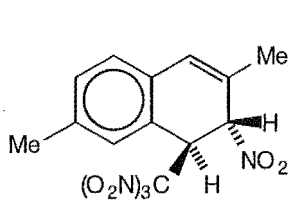

(94)

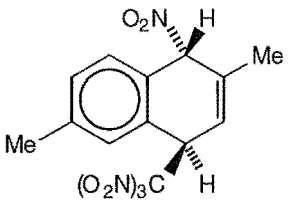

(95)

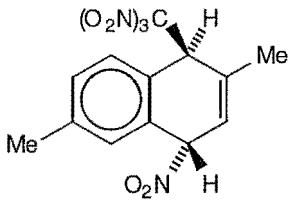

(96)

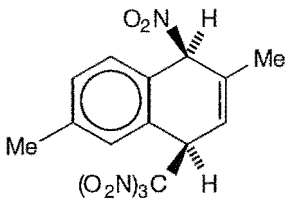

(97)

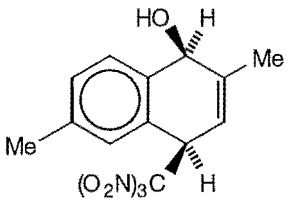

(98)

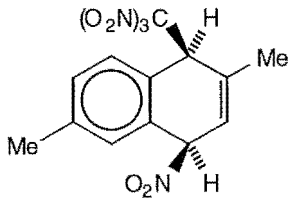

(99)

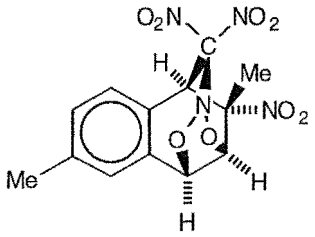

(100)

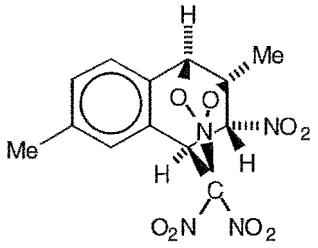

(101)

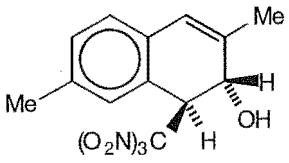

(102)

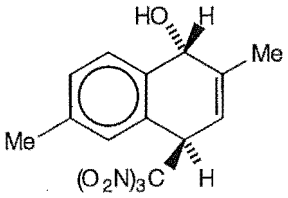

(103)

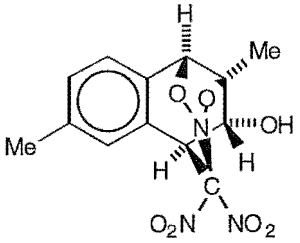

(104)

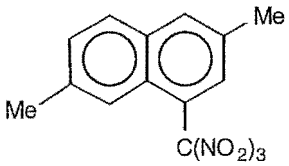

(105)

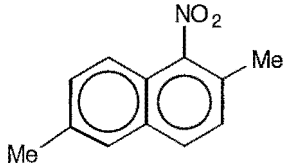

(106)

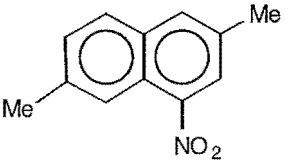

(107)

described for groups of compounds, rather than in the order of elution given in the Experimental section (See Chapter 5, Section 5.2.2).

Adducts (94) *and* (101).

Adduct (94) was only isolated in admixture with adduct (95), the structure of which was determined by single crystal X-ray analysis. Adduct (94), identified as *trans*-3,7-dimethyl-2-nitro-1-trinitromethyl-1,2-dihydro-naphthalene, was unstable in solution and underwent thermal cycloaddition of a nitro group of the trinitromethyl group with the C3/C4 alkene function to give the nitro cycloadduct (101), the structure of which was determined by single crystal X-ray analysis. The structure of adduct (94) was therefore assigned on the basis of (i) a comparison of its ^{1}H n.m.r. spectrum with the spectral features for *trans*-4-methyl-2-nitro-1-trinitromethyl-1,2-dihydro-

naphthalene (88), the structure of which was determined by single crystal X-ray analysis,[6] as seen in Fig. 2.16; and (ii) the cycloaddition reaction to give the nitro cycloadduct (101), as discussed below and in Section 2.13. The

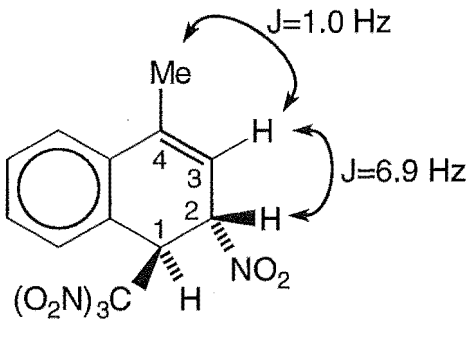

(88)

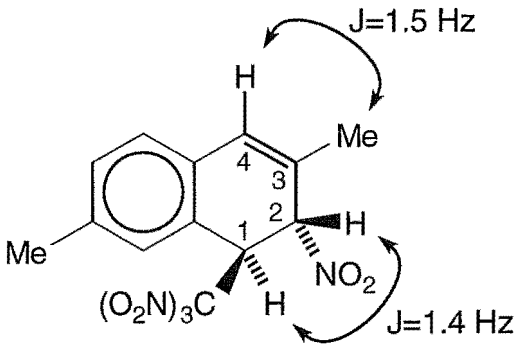

(94)

H1	5.73	H1	5.67
H2	5.63	H2	5.41
H3	5.85	3-Me	2.05
4-Me	2.70	H4	6.53

Fig. 2.16 Comparison of the characteristic ^{1}H n.m.r. resonances (in ppm) and coupling constants for adducts (88) and (94).

characteristic ^{1}H n.m.r. signals due to the C**H**C$(NO_2)_3$ (δ 5.67) appeared as a broad singlet and the C**H**NO_2 (δ 5.41) appeared as a doublet ($J_{H2,H1}$ 1.4 Hz). The *vicinal* coupling constant $J_{H2,H1}$ 1.4 Hz suggests that the dihedral angle between H2 and H1 is ≈ 70°. This implies that the bonds to the trinitromethyl and nitro groups must be close to perpendicular to the plane of the ring. If the trinitromethyl and nitro groups were to lie in the plane of the ring the expected coupling constant would be much larger as the angle between H1 and H2 would be ≈ 180° and by the Karplus equation this would correspond to $J_{H2,H1}$ 12 Hz.

The structure of the nitro cycloadduct (101) was determined by single crystal X-ray analysis. A perspective drawing of the nitro cycloadduct (101), $C_{13}H_{12}N_4O_8$, m.p. 169° (dec.) is presented in Fig. 2.17, and the

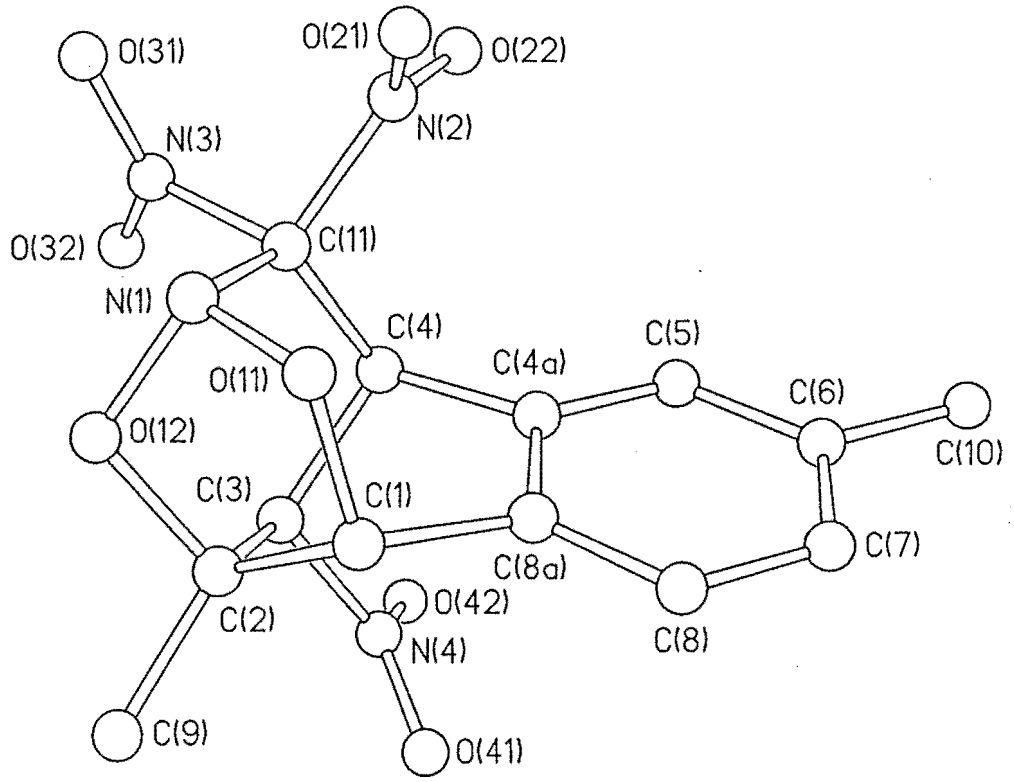

Fig. 2.17 Perspective drawing of the nitro cycloadduct (101).

corresponding atomic coordinates are given in Table 5.5 (See Chapter 5, Section 5.5). In the formation of the heterocyclic cage structure it is clear that the nitrogen atom N(1) of the planar nitro group involved in the cycloaddition reaction assumes a trigonal pyramidal geometry in the nitro cycloadduct (101), accounting for some of the changes observed in the bond lengths of the nitro cycloadduct (101). Some of the bond lengths of interest are shown in Table 2.5. In particular, there is a substantial lengthening of the N(1)-O(11) and N(1)-O(12) bonds (which is the nitro group involved in the cycloaddition), increasing from the typical nitro N-O bond length of ≈ 1.214(3) to ≈ 1.409(2) Å. Similarly, the C(11)-N(1) bond length is shortened in

Table 2.5 Selected bond lengths of the nitro cycloadduct (101).

Bonds	Bond Lengths (Å)	Bonds	Bond Lengths (Å)
N(1)-O(11)	1.403(2)	N(4)-O(42)	1.211(3)
N(1)-O(12)	1.414(2)	C(11)-N(1)	1.485(3)
N(2)-O(21)	1.209(3)	C(11)-N(2)	1.520(3)
N(2)-O(22)	1.216(3)	C(11)-N(3)	1.534(3)
N(3)-O(31)	1.209(3)	C(3)-N(4)	1.505(3)
N(3)-O(32)	1.212(3)	C(1)-O(11)	1.470(3)
N(4)-O(41)	1.217(3)	C(2)-O(12)	1.466(3)

comparison with the normal C-NO_2 bond length. For example the C(11)-N(1) bond length was 1.485(3) Å whereas the typical C-NO_2 bond length can be compared to C(11)-N(2) 1.520(3) Å, C(11)-N(3) 1.534(3) Å and C(3)-N(4) 1.505(3) Å. The shortening of this bond points to an increased bond order due to some donation of the N(1) lone pair towards the carbon C(11) in an attempt to stabilise the electron withdrawing effect of the two nitro groups on C(11) involving N(2) and N(3). The bond lengths from the C(1)-O(11) and C(2)-O(12) of 1.470(3) Å and 1.466(3) Å, respectively, are typical for a C-O bond. Similar results have been observed for analogous heterocyclic cage structures formed *via* photolyses of substituted naphthalene and benzene compounds with TNM.[5-10]

In the context of confirming the structure of the nitro/trinitromethyl adduct (94), the C(4)-C(11) bond in the nitro cycloadduct (101) was close to *anti* to the C(3)-N(4) bond, pointing to a *trans*-2-nitro-1-trinitromethyl stereochemistry for adduct (94) [torsional angle: N(4)-C(3)-C(4)-C(11) -173.0(2)°].

The spectroscopic data for the nitro cycloadduct (101) were consistent with the established structure. The characteristic ^1H and ^{13}C n.m.r. data are presented in Fig. 2.18. N.O.e. experiments confirmed the assignments of

the chemical shifts for the protons. In particular, irradiation at δ 2.07 (2-Me) gave enhancements at δ 5.19 (H1) and at δ 5.64 (H3), while irradiation at δ 5.64 (H3) gave enhancements at δ 2.07 (2-Me) and at δ 5.17 (H4), as shown in Fig. 2.18. Furthermore, the nitro function was indicated by the ^{13}C chemical shift for C3 (δ 84.1) and the cyclized trinitromethyl function by the ^{13}C n.m.r. chemical shift for C4 (δ 46.2). These assignments were confirmed by an HMBC experiment. The observed coupling constant $J_{H3,H4}$ 4.0 Hz was consistent with the existence of the molecule in the same confirmation in the solid state and in solution.

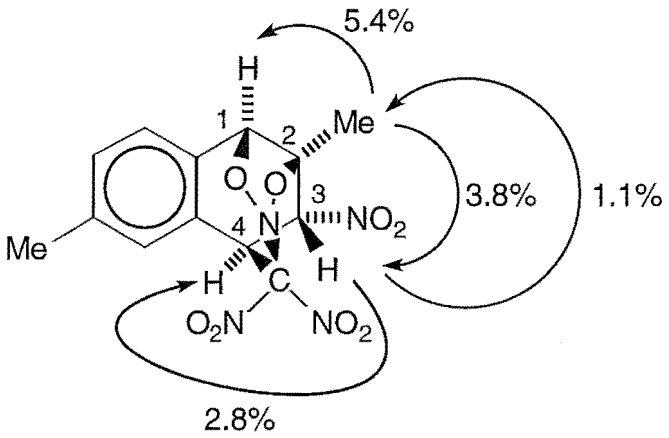

(101)

H1	5.19, s	C1	85.7
2-Me	2.07, s	C2	86.3
H3	5.64, d, J=4.0 Hz	C3	84.1
H4	5.17, d, J=4.0 Hz	C4	46.2

Fig. 2.18 Characteristic ^{1}H and ^{13}C n.m.r. resonances (in ppm) and enhancements (%) from selected n.O.e. experiments for the nitro cycloadduct (101).

Adducts (102) *and* (104).

The *trans*-3,7-dimethyl-1-trinitromethyl-1,2-dihydronaphthalen-2-ol (102), obtained from h.p.l.c., always contained significant amounts of the hydroxy cycloadduct (104), the structure of which was determined by single crystal X-ray analysis. Presumably this was due to cycloaddition of the hydroxy/trinitromethyl adduct (102) in the h.p.l.c. solvents after separation and prior to their removal under reduced pressure. The structure of adduct (102) was assigned on the basis of (i) a comparison of its ^{1}H n.m.r. spectra with the spectroscopic data for adduct (94), as seen in Fig. 2.19; and (ii) the cycloaddition reaction to give the hydroxy cycloadduct (104), as discussed below and in Section 2.14. In particular, the ^{1}H n.m.r. signals due to adduct (102) were all shifted upfield relative to adduct (94), due to the presence of the -OH function.

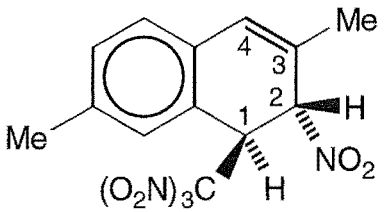

(94)

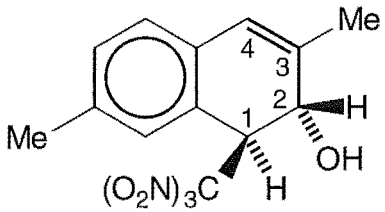

(102)

H1	5.67	H1	4.58
H2	5.41	H2	4.78
3-Me	2.05	3-Me	1.91
H4	6.53	H4	6.23

Fig. 2.19 Comparison of the characteristic ^{1}H n.m.r. resonances (in ppm) for adducts (94) and (102).

The structure of the hydroxy cycloadduct (104), $C_{13}H_{13}N_3O_7$, m.p. 183-184°, was determined by single crystal X-ray analysis. A perspective drawing of the hydroxy cycloadduct (104) is presented in Fig. 2.20, and

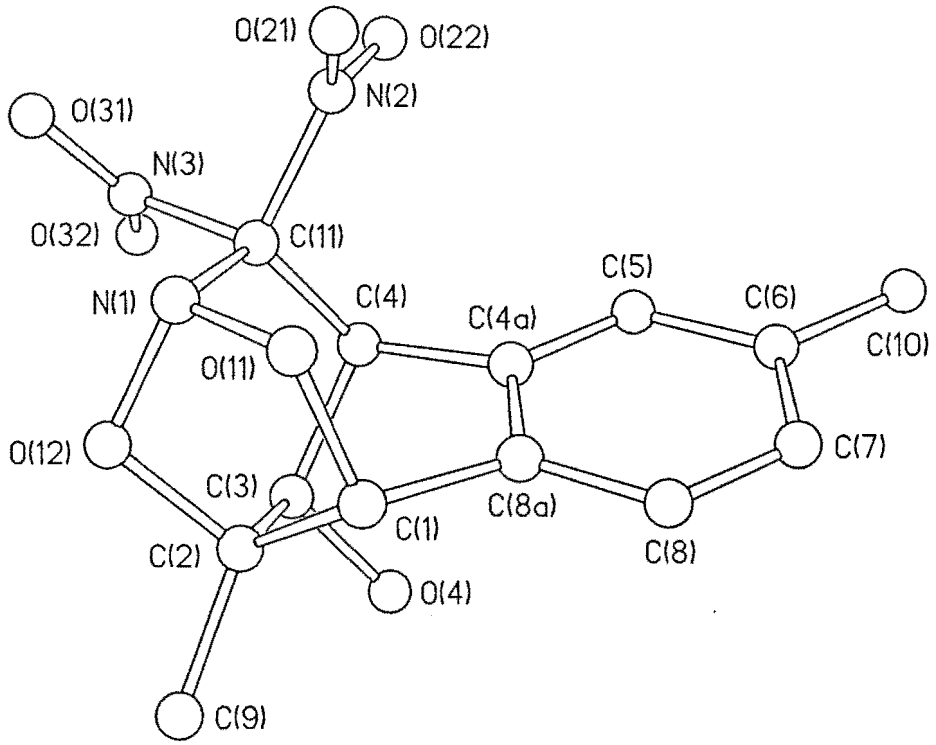

Fig. 2.20 Perspective drawing of the hydroxy cycloadduct (104).

corresponding atomic coordinates are given in Table 5.6 (See Chapter 5, Section 5.5). The structure is closely similar to that of the nitro cycloadduct (101), including even the conformations of the geminal nitro groups. Similar to the nitro cycloadduct (101), the bond length of the C(11)-N(1) bond [1.477(7) Å] is significantly shorter than the C(11)-N(2) [1.526(7) Å] and the C(11)-N(3) [1.543(7) Å] bond lengths, reflecting the structure of the heterocyclic cage. The C(4)-C(11) bond in the hydroxy cycloadduct (104) is close to *anti* to the C(3)-O(4) bond [torsional angle: O(4)-C(3)-C(4)-C(11) -169.0(4)°], thus indicating the *trans*-2-hydroxy-1-trinitromethyl structure for the hydroxy/trinitromethyl adduct (102).

The spectroscopic data for the hydroxy cycloadduct (104) were in accord with the established structure. An infrared absorption was observed at 3415 cm^{-1}, which is characteristic for an -OH function. N.O.e. experiments confirmed the assignments of the chemical shifts for the protons. In particular, irradiation at δ 1.75 (2-Me) gave enhancements at δ 4.75 (H3) and at δ 4.93 (H1), as presented in Fig. 2.21. The characteristic ^{1}H and ^{13}C n.m.r. data are also presented in Fig. 2.21. In particular, ^{13}C n.m.r. resonances for the hydroxy function attached to C3 appeared at δ 70.6, while the cyclized trinitromethyl function attached to C4 appeared at δ 48.8. These assignments were confirmed by an HMBC experiment.

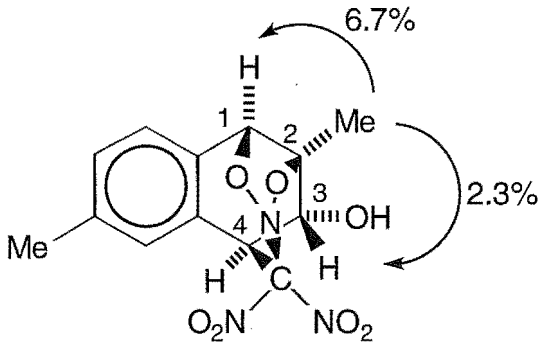

(104)

H1	4.93, s	C1	84.7
2-Me	1.75, s	C2	87.7
H3	4.75, d, $J_{H3,OH}$=3.9 Hz	C3	70.6
H4	4.73, s	C4	48.8

Fig. 2.21 Characteristic ^{1}H and ^{13}C n.m.r. resonances (in ppm) and enhancements (%) from a selected n.O.e. experiment for the hydroxy cycloadduct (104).

Adducts (95), (97), (98), *and* (103).

The structure of adduct (95) was determined by single crystal X-ray analysis. A perspective drawing of the *trans*-2,6-dimethyl-1-nitro-4-trinitro-methyl-1,4-dihydronaphthalene (95), $C_{13}H_{12}N_4O_8$, m.p. 104° (dec.), is presented in Fig. 2.22, and the corresponding atomic coordinates are

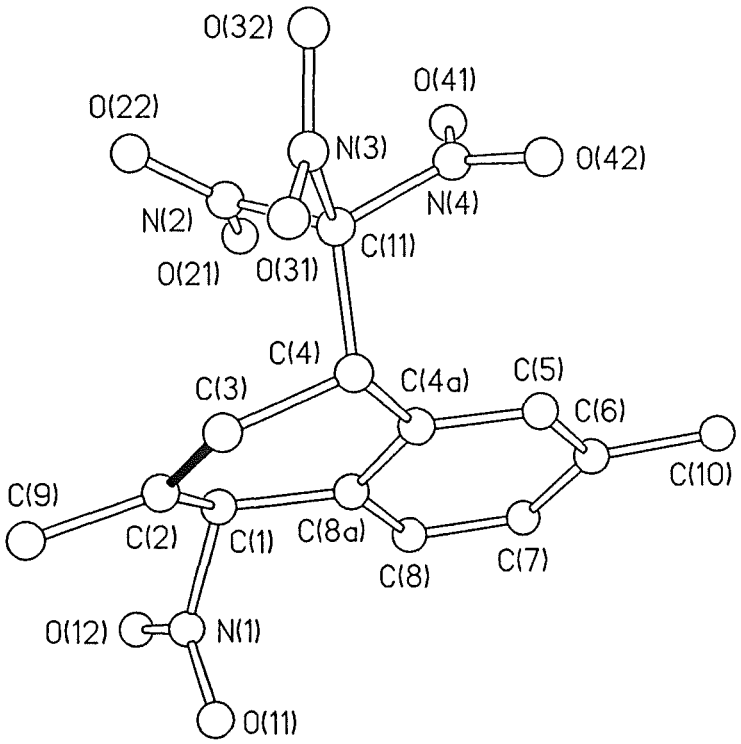

Fig. 2.22 Perspective drawing of adduct (95). Double bond shown in black.

presented in Table 5.3 (See Chapter 5, Section 5.5). In the solid state the alicyclic ring exists in a somewhat distorted boat conformation [torsional angles: C(2)-C(1)-C(8a)-C(4a) 21.7(3)°, C(3)-C(4)-C(4a)-C(8a) -15.6(3)°]. This indicates that the trinitromethyl group adopts an orientation such that the C(4)-C(11) bond is close to perpendicular to the plane of the aromatic ring [torsional angle: C(5)-C(4a)-C(4)-C(11) -75.5(2)°]. The *trans* orientation of the nitro group is indicated by the C(1)-N(1) bond orientation [torsional angle: N(1)-C(1)-C(8a)-C(8) -38.3(2)°].

The spectroscopic data for adduct (95) were in accord with the established structure. In particular, the **C**H-C$(NO_2)_3$ resonance appeared at δ 45.4, while the **C**H-NO_2 resonance appeared at δ 87.0. These assignments were confirmed by an HMBC experiment (See summary in Fig. 2.23). N.O.e. experiments confirmed the assignments of the chemical shifts

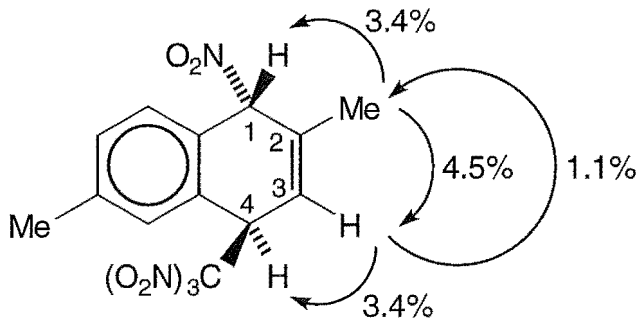

(95)

H1	6.13, br s	C1	87.0
2-Me	1.97, d, J=1.5 Hz	C2	138.1
H3	6.29, dq, J=3.0 Hz, J'=1.5 Hz	C3	119.2
H4	5.35, br s	C4	45.4

Fig. 2.23 Characteristic ^1H and ^{13}C n.m.r. resonances (in ppm) and enhancements (%) from selected n.O.e. experiments for adduct (95).

for the protons. Specifically, irradiation at δ 1.97 (2-Me) gave enhancements at δ 6.13 (H1) and at δ 6.29 (H3), while irradiation at δ 6.29 (H3) gave enhancements at δ 1.97 (2-Me) and at δ 5.35 (H4), as observed in Fig. 2.23. The ^1H n.m.r. coupling constants for adduct (95) were as expected for the established structure and consistent with the existence of the molecule in the same conformation in the solid state and in solution, also seen in Fig. 2.23.

The structure of the epimeric adduct (97) was also determined by single crystal X-ray analysis. A perspective drawing of the *cis*-2,6-dimethyl-1-nitro-4-trinitromethyl-1,4-dihydronaphthalene (97), $C_{13}H_{12}N_4O_8$, m.p. 134-136°, is presented in Fig. 2.24, and the corresponding atomic coordinates are

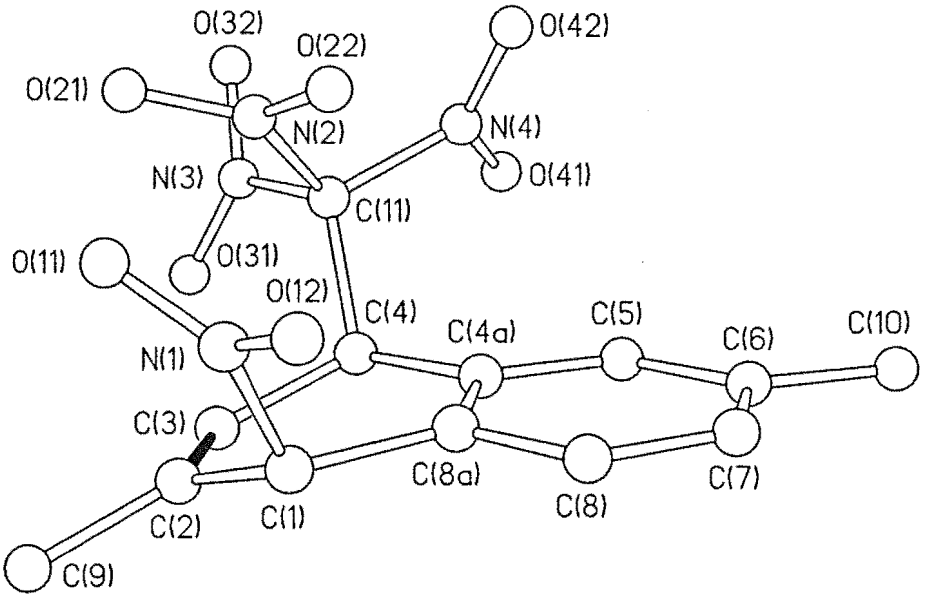

Fig. 2.24 Perspective drawing of adduct (97). Double bond shown in black.

presented Table 5.4 (See Chapter 5, Section 5.5). In the solid state the ring conformation of adduct (97) is closely similar to its epimer (95), with the alicyclic ring also in a somewhat distorted boat conformation [torsional angles: C(2)-C(1)-C(8a)-C(4a) 14.0(4)°, C(3)-C(4)-C(4a)-C(8a) -17.0(4)°]. Once again, the trinitromethyl group clearly adopts an orientation such that the C(4)-C(1) bond is close to perpendicular to the plane of the aromatic ring [torsional angle: C(5)-C(4a)-C(4)-C(11) -76.8°]. However, the orientation of the C(1)-N(1) bond differs significantly due to the *cis*-stereochemistry [torsional angle: N(1)-C(1)-C(8a)-C(8) 73.1(3)°].

The spectroscopic data for adduct (97) were in accord with the established structure. The ^{1}H and ^{13}C n.m.r. data were confirmed by n.O.e. and HMBC experiments, and from comparison with the spectroscopic data for its epimer (95). A summary of some of the characteristic data is outlined in Fig. 2.25, and is consistent with their assignment as epimers.

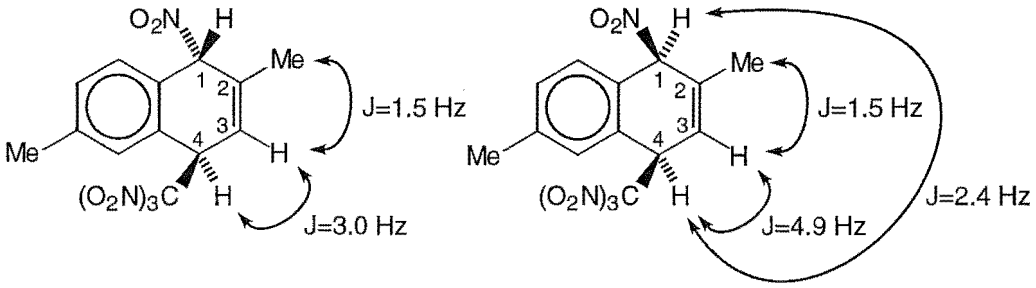

(95) (97)

H1	6.13	H1	5.78
2-Me	1.97	2-Me	2.08
H3	6.29	H3	6.47
H4	5.35	H4	5.30
C1	87.0	C1	85.3
C2	138.1	C2	137.2
C3	119.2	C3	121.4
C4	45.2	C4	44.9

Fig. 2.25 Comparison of the characteristic ^{1}H and ^{13}C n.m.r. resonances (in ppm) and coupling constants for adducts (95) and (97).

It is interesting to note that the elution order on h.p.l.c. of compounds (95) and (97) is consistent with the pattern observed in earlier studies of substituted naphthalenes where, *r*-1-nitro-*t*-4-trinitromethyl-1,4-dihydro-

THE LIBRARY
UNIVERSITY OF CANTERBURY
CHRISTCHURCH, N.Z.

naphthalenes were eluted ahead of their corresponding *r*-1-nitro-*c*-4-trinitro-methyl epimers.[5,6,9]

Adduct (98) could not be induced to give crystals of adequate quality for single crystal X-ray analysis and hence its identification as *cis*-2,6-dimethyl-4-trinitromethyl-1,4-dihydronaphthalen-1-ol (98) was based on a comparison of its ^{1}H n.m.r. spectroscopic data with the stereochemically related nitro adduct (97), the structure of which was determined by single crystal X-ray analysis, as illustrated in Fig. 2.26. The chemical shifts of the aromatic

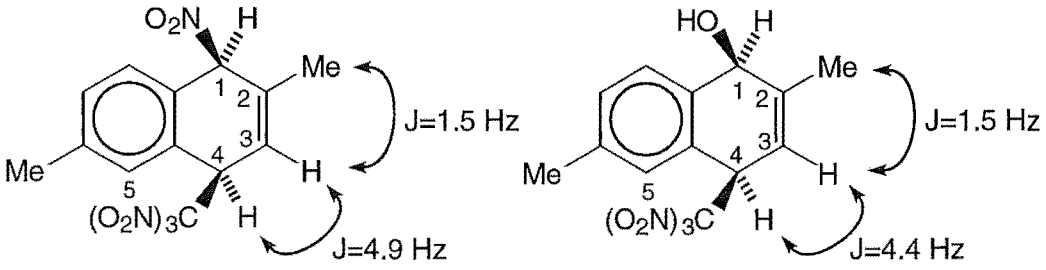

(97) (98)

H1	5.78	H1	4.79
2-Me	2.08	2-Me	2.02
H3	6.47	H3	6.02
H4	5.30	H4	5.16
H5	6.97	H5	6.95

Fig. 2.26 Comparison of the characteristic ^{1}H n.m.r. resonances (in ppm) and coupling constants for adducts (97) and (98).

protons H5 [(97), δ 6.97; (98), δ 6.95], upfield of the normal range for aromatic protons, are characteristic of compounds with an aromatic proton *peri* to a 4-trinitromethyl function. Given the closely similar coupling constant $J_{H3,H4}$ for the two adducts (97) and (98), as seen in Fig. 2.26, it is

assumed that the two compounds have the same 1,4-stereochemistry and that the difference between the two compounds lies only in the nature of the C1-substituent. An infrared absorption was observed at 3416 cm^{-1} for the hydroxy adduct (98), indicating the presence of an -OH function. In the nitro adduct (97) the ^1H n.m.r. signal for H1 appears at δ 5.78, but in the hydroxy adduct (98) H1 is located upfield at δ 4.79, consistent with the difference in the substituent at C1.

Crystals of adduct (103) were of inadequate quality for single crystal X-ray analysis and therefore its identification as *trans*-2,6-dimethyl-4-trinitro-methyl-1,4-dihydronaphthalen-1-ol (103) was based on a comparison of its ^1H n.m.r. spectroscopic data with its epimer (98). The close similarity between the spectroscopic data for compounds (98) and (103) is depicted in Fig. 2.27, and was consistent with their assignment as epimers.

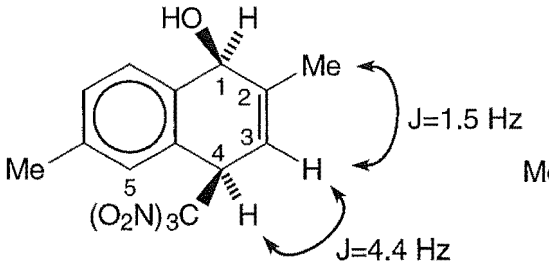

(98)

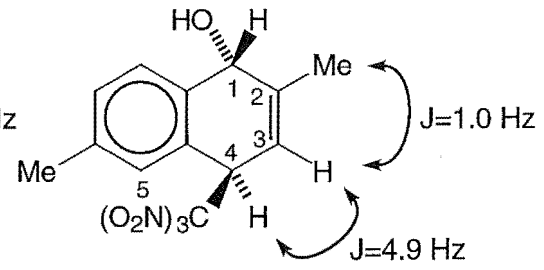

(103)

H1	4.79	H1	4.96
2-Me	2.02	2-Me	2.04
H3	6.02	H3	6.00
H4	5.16	H4	5.19
H5	6.95	H5	7.02

Fig. 2.27 Comparison of the characteristic ^1H n.m.r. resonances (in ppm) and coupling constants for adducts (98) and (103).

Furthermore, the presence of the -OH function was indicated by an infrared absorption at 3452 cm^{-1} in adduct (103).

The relatively early elution of the *cis*-1-hydroxy-4-trinitromethyl compound (98) is of interest in the context of the more usual elution order (see above) for analogous 1-nitro-4-trinitromethyl adducts. This unusual elution order for the 1-hydroxy-4-trinitromethyl adducts is ascribed to the inherently more hindered environment of the hydroxy group in the *cis*-1-hydroxy-4-trinitromethyl compound (98) compared with that of the *trans*-1-hydroxy-4-trinitromethyl epimer (103). Given the apparent conformational control exerted by the trinitromethyl group in the 1-nitro-4-trinitromethyl adducts (95) and (97), it is reasonable to assume that the conformation of the *cis*-1-hydroxy-4-trinitromethyl adduct would be similar to that found for the *cis*-1-nitro-4-trinitromethyl adduct (97) (see Fig. 2.24) except for the obvious replacement of the nitro by a hydroxy group. In such a conformation, the hydroxy group in the *cis*-1-hydroxy-4-trinitromethyl epimer (98) would be significantly more hindered than that for the *trans*-1-hydroxy-4-trinitromethyl epimer (103), which would resemble the *trans*-1-nitro-4-trinitromethyl adduct (95) (see Fig. 2.22) in conformation. The hydroxy group in the *trans*-1-hydroxy-4-trinitromethyl adduct (103) would therefore be more exposed for adsorption to a chromatographic substrate leading to a longer retention time on h.p.l.c.

Adducts (96), (99), *and* (100).

Adduct (96) gave crystals of inadequate quality for single crystal X-ray analysis and its identification as *trans*-3,7-dimethyl-1-nitro-4-trinitromethyl-1,4-dihydronaphthalene (96) was based on its spectroscopic data. N.O.e. experiments confirmed the assignments of the chemical shifts for the protons. Specifically, irradiation at δ 2.11 (3-Me) gave enhancements at δ 5.33 (H4) and at δ 6.29 (H2), while irradiation at δ 6.29 (H2) gave

enhancements at δ 2.11 (3-Me) and at δ 6.18 (H1), as represented in Fig. 2.28. HMBC experiments allowed the complete assignment of the ^{13}C

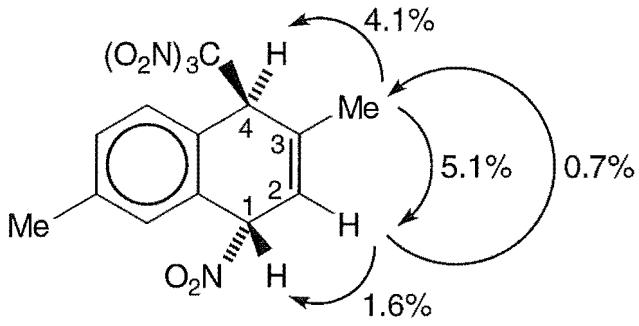

(96)

H1	6.18, m	C1	83.6
H2	6.29, m	C2	128.7
3-Me	2.11, m	C3	132.1
H4	5.33, br s	C4	49.5

Fig. 2.28 Characteristic ^{1}H and ^{13}C n.m.r. resonances (in ppm) and n.O.e. enhancements (%) for adduct (96).

n.m.r. spectra. In particular, the locations of the nitro and the trinitromethyl functions were defined by the chemical shifts for C1 (δ 83.6) and C4 (δ 49.5), respectively. The *trans*-1-nitro-4-trinitromethyl stereochemistry was assigned to adduct (96) on the basis of its elution earlier than its *cis*-1-nitro-4-trinitromethyl stereoisomer (99), and the known h.p.l.c. elution order for such pairs of stereoisomers as seen earlier for adducts (95) and (97) and in previous examples.[5,6,9]

Adduct (99) was isolated in low yield and then only as an impure oil. The identification of *cis*-3,7-dimethyl-1-nitro-4-trinitromethyl-1,4-dihydronaphthalene (99) was based on comparison of its ^{1}H n.m.r. spectra with its

epimeric adduct (96). The two sets of spectroscopic data for adducts (96) and (99) were closely similar and consistent with their assignment as epimers, as illustrated in Fig. 2.29. The signal assigned to H5 appeared as

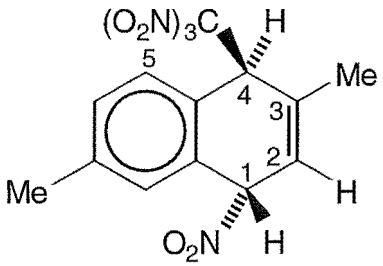

(96)

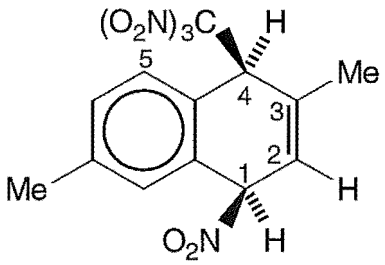

(99)

H1	6.18	H1	5.82
H2	6.29	H2	6.48
3-Me	2.11	3-Me	2.10
H4	5.33	H4	5.40
H5	7.21-7.22	H5	7.07

Fig. 2.29 Comparison of the characteristic ^{1}H n.m.r. resonances (in ppm) for adducts (96) and (99).

a doublet ($J_{H5,H6}$ 7.9 Hz) at δ 7.07, pointing to the presence of the trinitromethyl group at C4 on the 3,7-dimethylnaphthalene skeleton. Furthermore, a change in coupling constant was observed between adduct (99) and the similar *cis*-1-nitro-4-trinitromethyl adduct (97), lacking the 3-methyl-4-trinitromethyl interaction (See Fig. 2.30). The increase in coupling constant, from $J_{H3,H4}$ 4.9 Hz for adduct (97) to $J_{H1,H2}$ 6.3 Hz for adduct (99), is presumably due to conformational changes in adduct (99) induced by steric interactions between the 4-trinitromethyl group and the adjacent 3-methyl group. These changes would be expected to lead to a more

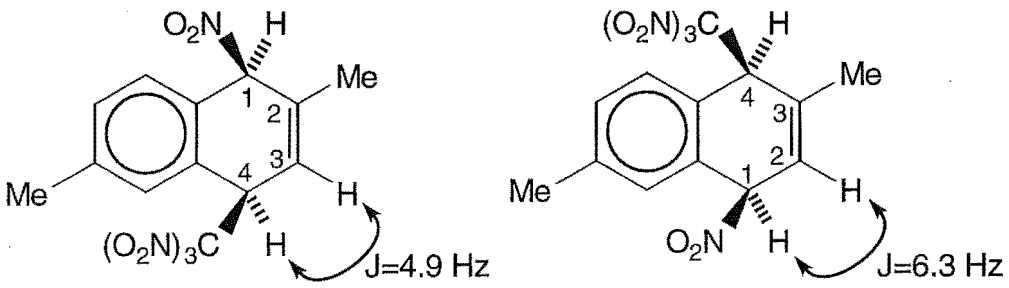

(97) (99)

Fig. 2.30 Comparison of a characteristic coupling constant for adducts (97) and (99).

extreme boat conformation in adduct (99), leading to some reduction in the H1-C1-C2-H2 torsional angle and hence a somewhat larger coupling constant.

The nitro cycloadduct (100) was isolated in small quantities and then only in admixture with its structural isomeric nitro cycloadduct (101), the structure of which was determined by single crystal X-ray analysis. N.O.e. experiments confirmed the assignments of the chemical shifts for the protons. Specifically, irradiation at δ 1.94 (3-Me) gave enhancements at δ 5.29 (H4) and at δ 5.66 (H2), while irradiation at δ 5.64 (H2)/(H1) gave enhancements at δ 1.94 (3-Me) and at δ 7.07 (H8), as depicted in Fig. 2.31. ^{13}C n.m.r. data were confirmed by an HMBC experiment, also seen Fig. 2.31. In particular, the nitro function attached to C3 appeared at δ 87.1, while the cyclized trinitromethyl function attached to C4 appeared at δ 48.1. The stereochemistry of the nitro cycloadduct (100) was assigned on comparison with the related nitro cycloadduct (108),[5] as observed in Fig. 2.32. The coupling constants, $J_{H1,H2}$ and $J_{H2,H4}$, between the two nitro cycloadducts (109) and (100) agreed very closely, implying that the conformations of the two adducts were closely similar.

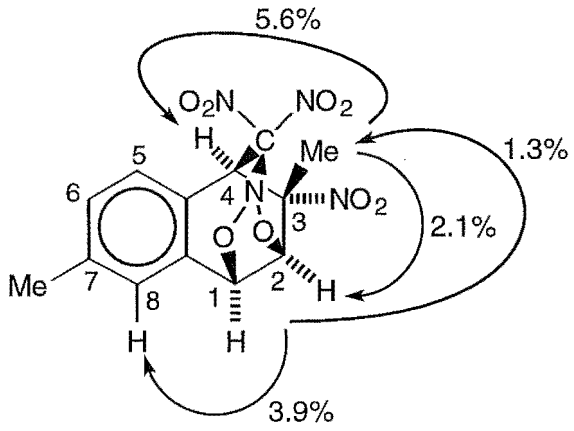

(100)

H1	5.62	C1	82.3
H2	5.66	C2	79.1
3-Me	1.94	C3	87.1
H4	5.29	C4	48.1

Fig. 2.31 Characteristic ^{1}H and ^{13}C n.m.r. resonances (in ppm) and enhancements (%) from selected n.O.e. experiments for adduct (100).

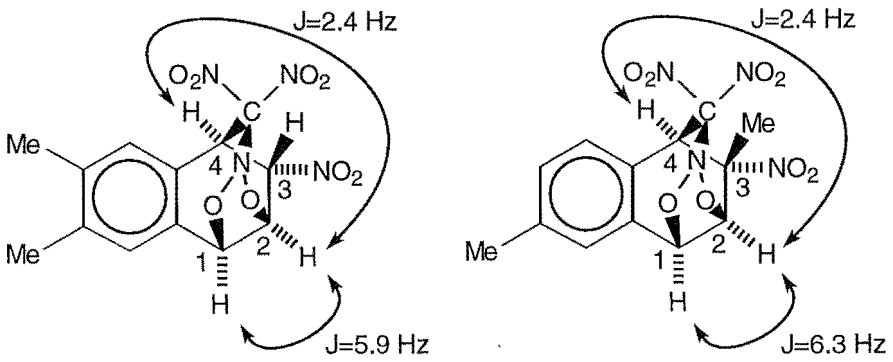

(108) (100)

Fig. 2.32 Comparison of the characteristic coupling constants for nitro cycloadducts (108) and (100).

2.11.2 Photochemistry in dichloromethane at -20° and identification of some of the nitro aromatic products.

A solution of 2,6-dimethylnaphthalene (57) (0.4 mol L^{-1}) and TNM (0.8 mol L^{-1}) in dichloromethane was irradiated at -20° for 3 h and gave a product which was shown by ^1H n.m.r. to be a mixture of adducts (total 15%), aromatic compounds (105)-(107) (total 65%), and a mixture of other unidentified nitroaromatic products (total 20%). Chromatography of this mixture on a silica gel Chromatotron plate gave pure samples of the compounds (105)-(107).

The first compound eluted was identified as 3,7-dimethyl-1-trinitro-methylnaphthalene (105). The trinitromethyl aromatic (105) gave a satisfactory parent molecular ion in the mass spectrum, indicating the molecular formula $C_{13}H_{11}N_3O_6$. N.O.e. experiments confirmed the assignments of the chemical shifts for the protons. In particular, irradiation at δ 2.47 (7-Me) gave enhancements at δ 7.02 (H8) and at δ 7.42 (H6), irradiation at δ 7.80 (H5) gave enhancements at δ 7.42 (H6) and at δ 7.93 (H4), and irradiation at δ 2.54 (3-Me) gave enhancements at δ 7.36 (H2) and at δ 7.93 (H4), as observed in Fig. 2.33. Furthermore, the presence of very strong infrared absorptions at 1617, 1593 and 1576 cm^{-1} provided evidence

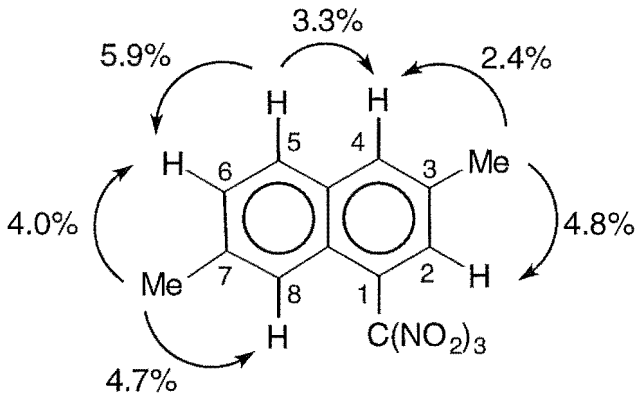

Fig. 2.33 Enhancements (%) from selected n.O.e. experiments for the trinitromethyl aromatic (105).

for the -$C(NO_2)_3$ substituent.

The second compound eluted was identified as 2,6-dimethyl-1-nitro-naphthalene (106) and the structure was confirmed by comparing its melting point and n.m.r. data with literature data.[11,12]

The final compound eluted was identified as 3,7-dimethyl-1-nitro-naphthalene (107) and the structure was confirmed by comparing its melting point and n.m.r. data with literature data.[11,13]

On monitoring the +20 and -20° reactions in dichloromethane with time, it was noted that the adduct yields increased with time and temperature. Table 2.6 gives an overview of product yields from the photochemical reaction between 2,6-dimethylnaphthalene (57) and TNM. At -20° the total adduct yield was 15% and this increased to 79% at +20°. Correspondingly, the yields of the aromatic compounds increased at low temperatures, particularly 2,6-dimethyl-1-nitronaphthalene (106). The absence (or near absence) of the nitro and hydroxy cycloadducts (100), (101) and (104) was noted early on in the -20° reaction. However, in the +20° reaction the cycloadducts were observed to increase with time and this provides further support for the observations discussed below involving the thermal nitro/ alkene cycloaddition reactions which occurred *via* their precursor 1,2-adducts (See Sections 2.13 and 2.14).

2.12 The Photochemistry of 2,6-Dimethylnaphthalene (57) in Acetonitrile

A solution of 2,6-dimethylnaphthalene (57) (0.4 mol L^{-1}) and TNM (0.8 mol L^{-1}) in acetonitrile was irradiated at +20° for 3 h to give a mixture of adducts (total 46%) and aromatic compounds (total 54%). The composition of the reaction mixture was monitored with time and an overview of product

Table 2.6 Overview of product yields from the photolysis of 2,6-dimethylnaphthalene (57) (0.4 mol L^{-1}) and TNM (0.8 mol L^{-1}) in dichloromethane.

		Yield (%)																
	Conversion												Unknown	Total				Unknown
t (h)	(%)	(94)	(95)	(96)	(97)	(98)	(99)	(100)	(101)	(102)	(103)	(104)	adducts	adducts	(105)	(106)	(107)	aromatics
At +20°																		
1	75	9.9	10.2	8.7	12.5	3.5	1.6	0.4	0.4	5.3	2.4	0.5	1.1	56.5	1.8	16.4	3.3	22.0
2	95	14.5	13.6	11.1	16.0	4.6	3.1	1.2	1.1	6.9	3.7	1.1	1.7	78.6	trace	16.0	2.8	2.6
At -20°																		
1	30	1.2	2.2	0.9	2.1	0.9	0.6	-	-	1.0	0.7	0.1	0.2	9.9	3.8	41.8	6.1	38.4
2	71	1.5	3.1	1.6	2.9	1.2	1.0	0.1	-	1.3	0.7	0.1	0.4	13.9	3.1	63.3	8.6	11.1
3	100	1.8	3.3	1.9	3.2	1.1	1.0	0.3	-	1.3	0.7	-	0.5	15.1	2.4	54.7	7.9	19.9

yields is shown in Table 2.7. Comparison of the +20° acetonitrile reaction with the +20° dichloromethane reaction (see Table 2.6, Section 2.11) showed a decrease in yield across all of the adducts in acetonitrile, with a corresponding increase in all of the aromatic compounds. Similar to both of

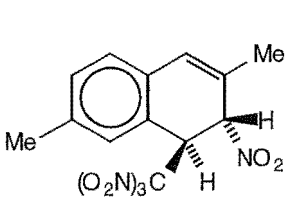

(94)

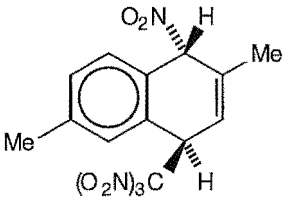

(95)

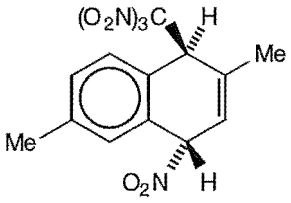

(96)

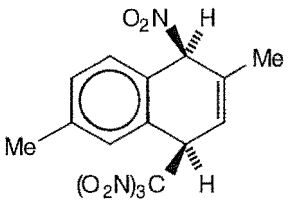

(97)

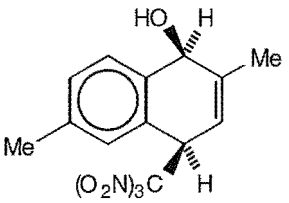

(98)

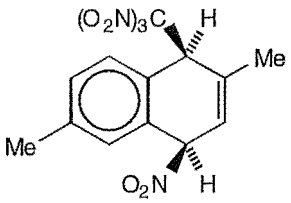

(99)

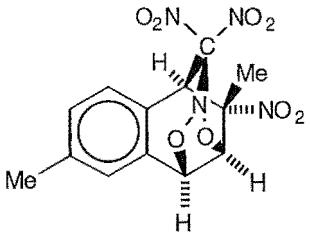

(100)

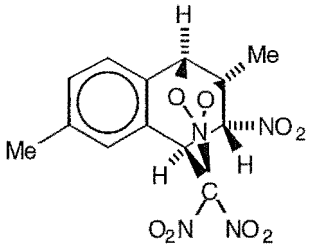

(101)

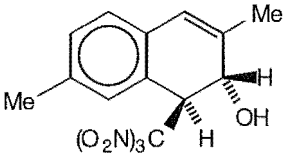

(102)

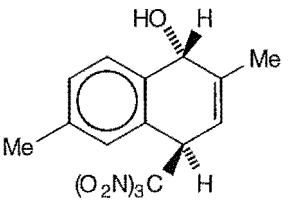

(103)

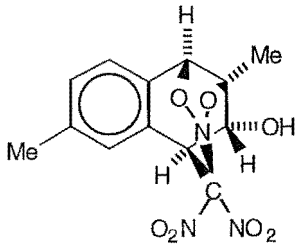

(104)

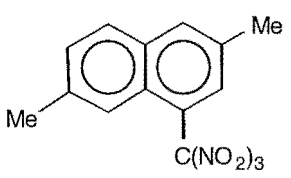

(105)

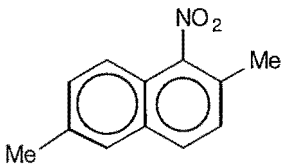

(106)

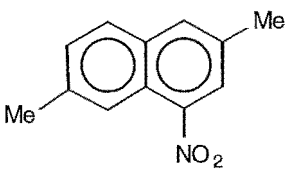

(107)

Table 2.7 Overview of product yields from the photolysis of 2,6-dimethylnaphthalene (57) (0.4 mol L^{-1}) and TNM (0.8 mol L^{-1}) in acetonitrile, at +20°.

		Yield (%)															
	Conversion												Unknown	Total				Unknown
t (h)	(%)	(94)	(95)	(96)	(97)	(98)	(99)	(100)	(101)	(102)	(103)	(104)	adducts	adducts	(105)	(106)	(107)	aromatics
0.5	19	2.0	2.8	1.4	3.6	1.0	0.4	-	-	1.6	0.6	0.2	0.8	14.4	1.0	51.8	9.0	23.8
1	50	4.4	6.1	2.6	7.8	1.6	1.0	0.2	-	3.1	1.6	0.7	1.1	30.2	4.1	41.0	9.0	15.7
2	74	6.8	8.8	3.6	10.0	2.3	1.6	0.3	0.4	3.6	2.2	1.4	1.1	42.1	2.7	45.4	9.8	-
3	84	6.9	9.3	4.5	12.0	1.5	1.9	0.7	0.8	3.5	1.3	2.0	1.9	46.3	3.6	42.0	8.1	-

the dichloromethane reactions, the 1-nitro aromatic compound (106) was the major product formed in acetonitrile (42%). Once again the yields of cycloadducts (100), (101) and (104) were observed to increase with time and in the latter half of the reaction, formation of the precursor adducts (94) and (102) slowed, presumably due to the cycloaddition reactions taking place. Due to the limited solubility of 2,6-dimethylnaphthalene in the more polar acetonitrile, even at +20°, reactions were not possible at -20°.

2.13 Thermal Cycloaddition of *trans*-3,7-Dimethyl-2-nitro-1-trinitromethyl-1,2-dihydronaphthalene (94) to give the Nitro Cycloadduct (101)

The isolation of *trans*-3,7-dimethyl-2-nitro-1-trinitromethyl-1,2-dihydronaphthalene (94), albeit in a mixture containing *c.* 71% *trans*-2,6-dimethyl-1-nitro-4-trinitromethyl-1,4-dihydronaphthalene (95), afforded the opportunity to study its cycloaddition reaction. A mixture of adducts (94) and (95) in (D)chloroform was stored at +22°, in the dark, and the ^{1}H n.m.r. spectra monitored at appropriate time intervals. Under these conditions adduct (95) was unchanged during the period of observation, but the precursor adduct (94) was slowly transformed into the nitro cycloadduct (101), as represented

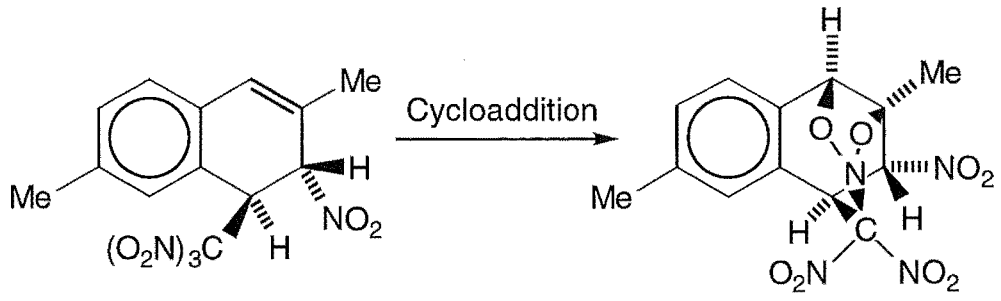

(94) (101)

Scheme 2.16

in Scheme 2.16 and Fig. 2.34. The half-life for the cycloaddition of adduct (94) into the nitro cycloadduct (101) was *c.* 96 h. This observation established that the cycloaddition was thermal rather than photochemical in character. Similar thermal rearrangements of adducts have been observed in a variety of substituted naphthalenes.[5-9]

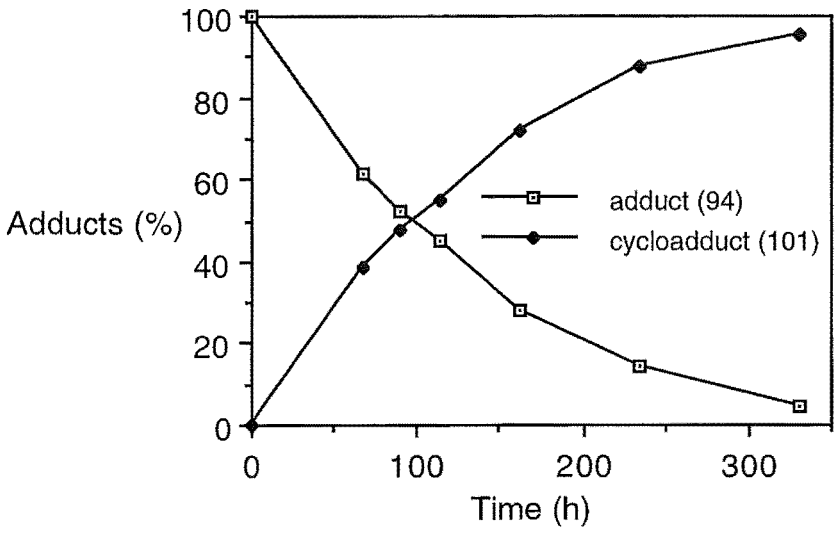

Fig. 2.34 Kinetics of cycloaddition of adduct (94) to nitro cycloadduct (101) in (D)chloroform, at +22°.

2.14 Thermal Cycloaddition of *trans*-3,7-Dimethyl-1-trinitromethyl-1,2-dihydronaphthalen-2-ol (102) to give the Hydroxy Cycloadduct (104)

The isolation of a mixture of *trans*-3,7-dimethyl-1-trinitromethyl-1,2-dihydronaphthalen-2-ol (102) (80%) and the hydroxy cycloadduct (104) (20%), afforded the opportunity to study the precursor's cycloaddition reaction. A mixture of adduct (102) and the cycloadduct (104) in (D)chloroform was stored at +22°, in the dark, and the ^{1}H n.m.r. spectra monitored at

appropriate time intervals. The precursor adduct (102) was completely transformed into the hydroxy cycloadduct (104) after 170 h, as summarized in Scheme 2.17 and Fig. 2.35. The half-life for the cycloaddition of adduct

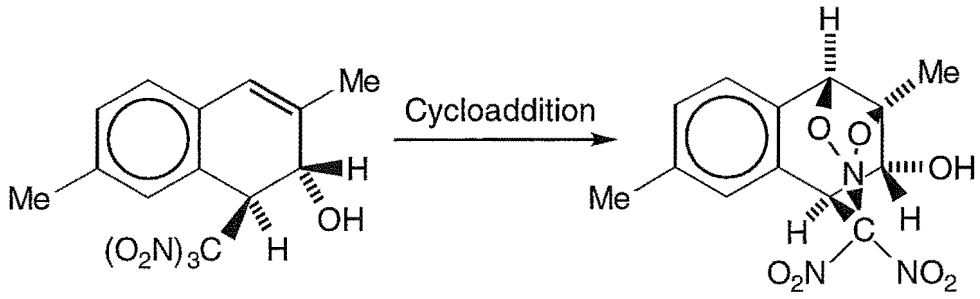

(102) (104)

Scheme 2.17

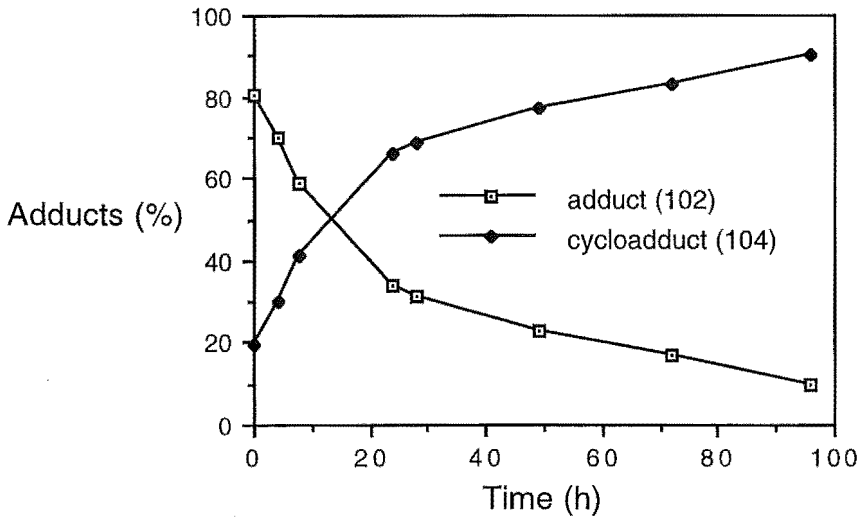

Fig. 2.35 Kinetics of cycloaddition of adduct (102) to hydroxy cycloadduct (104) in (D)chloroform at, +22°.

(102) into the hydroxy cycloadduct (104) was *c.* 13 h. The estimation of the half-life for this cycloaddition was complicated by precipitation of the hydroxy cycloadduct (104) during the period of observation. Once again this

observation established that the cycloaddition was thermal rather than photochemical in character.

2.15 Overview of the Photonitration of 2,6-Dimethyl-naphthalene (57)

The photochemical reaction of 2,6-dimethylnaphthene (57) with TNM led to a large number of adducts (94)-(104). For the reaction in dichloro-methane at +20°, identified adducts accounted for 77% of the reaction

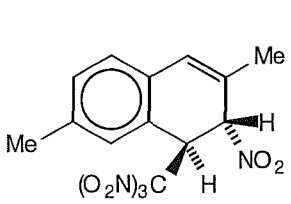

(94)

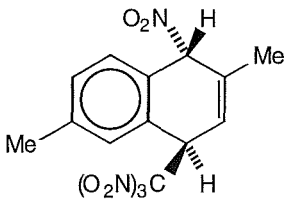

(95)

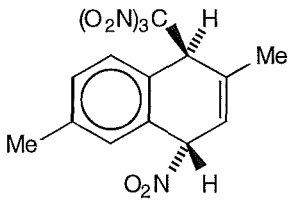

(96)

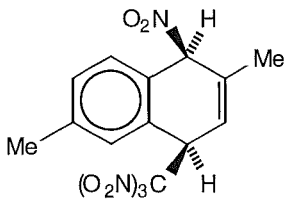

(97)

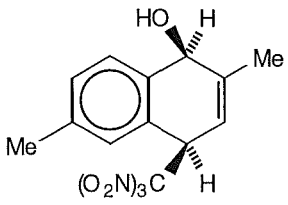

(98)

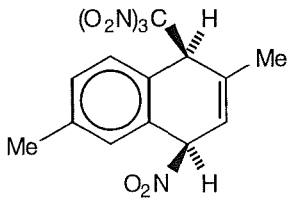

(99)

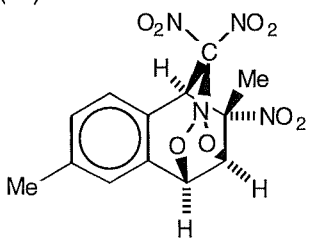

(100)

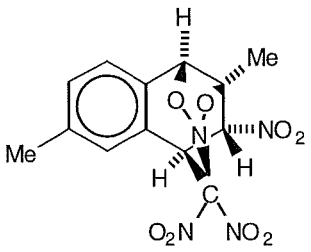

(101)

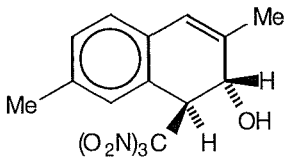

(102)

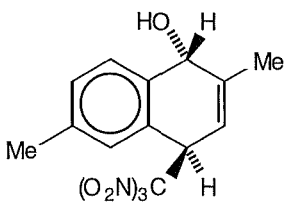

(103)

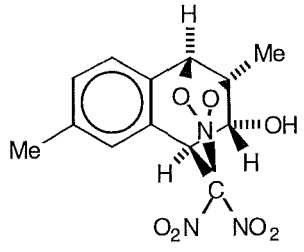

(104)

mixture. There was a clear preference (*c.* 4:1) for $(O_2N)_3C^-$ attack at C4 of the 2,6-dimethylnaphthalene radical cation, compared with reaction at C1, as illustrated in Fig. 2.36.

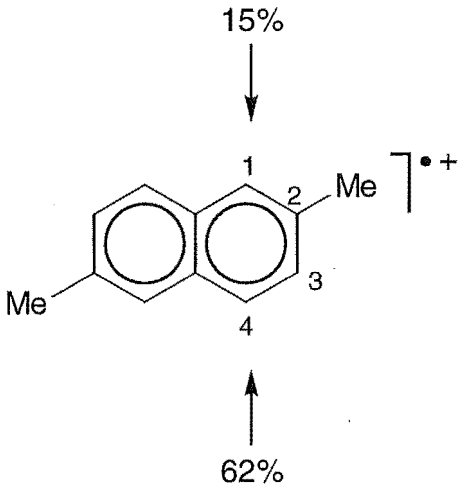

Fig. 2.36 Products (%) identified corresponding to attack of $(O_2N)_3C^-$ on the 2,6-dimethylnaphthalene radical cation.

As in the case of 1,4,6,7-tetramethylnaphthalene, it appears that no adducts were formed *via* benzylic radicals (65) and (66), which arose after

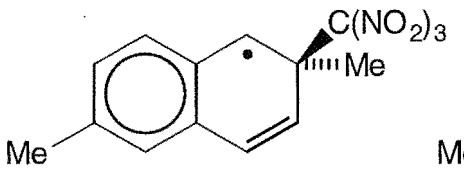

(65)

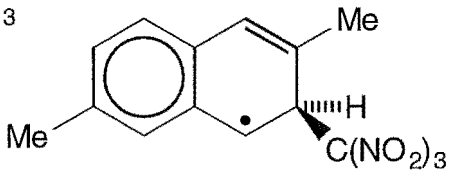

(66)

attack of $(O_2N)_3C^-$ at C2 and C3, respectively, on the radical cation of 2,6-dimethylnaphthalene. The favoured pathway (*c.* 4:1) was *via* formation of the phenylallylic radical (64), on attack of $(O_2N)_3C^-$ at C4 on the radical cation of 2,6-dimethylnaphthalene. The phenylallylic radical (63), which arose *via* attack of $(O_2N)_3C^-$ on the 2,6-dimethylnaphthalene radical cation at C1, was

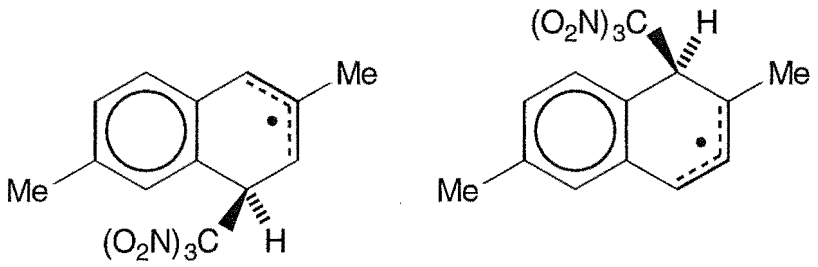

(64) (63)

also formed and led to the formation of adducts (96), (99) and (100), as seen in Scheme 2.18. After the phenylallylic radical (63) was formed, radical coupling with $^{\bullet}NO_2$ occurred either at C4, to give the epimeric 3,7-dimethyl-1-nitro-4-trinitromethyl adducts (96) and (99), or at C2. Radical coupling of

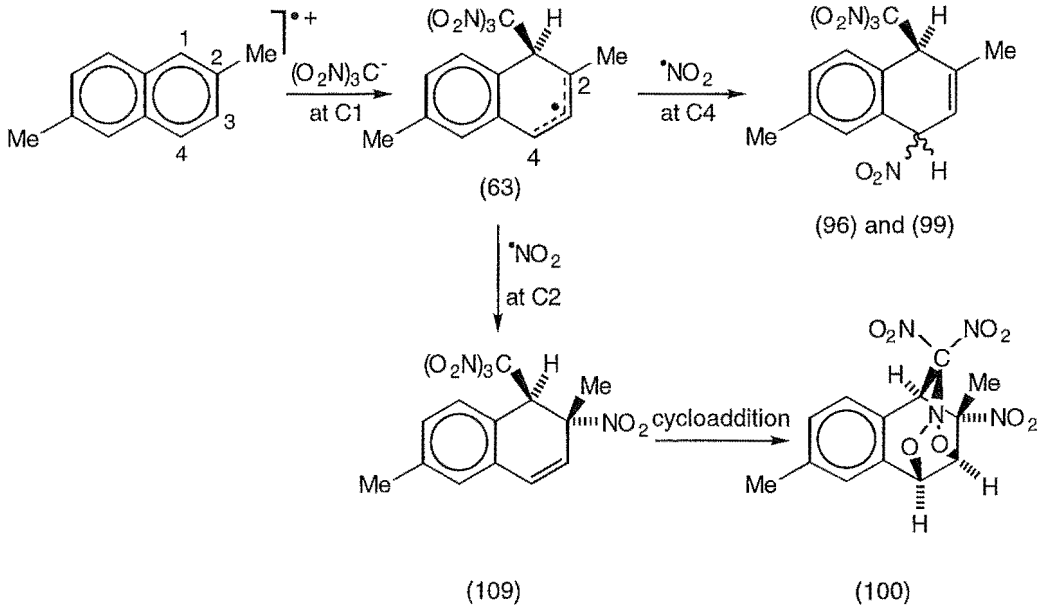

Scheme 2.18

$^{\bullet}NO_2$ at C2 on radical (63) *ipso* to the adjacent methyl group would be expected to occur *anti* to the extremely bulky trinitromethyl group, to yield the *trans*-2,6-dimethyl-2-nitro-1-trinitromethyl adduct (109). Cycloaddition of adduct (109) could then occur to give the nitro cycloadduct (100).

The favoured pathway in the formation of adducts was *via* $(O_2N)_3C^-$

attack at C4 in the 2,6-dimethylnaphthalene radical cation. Radical coupling of $^{\bullet}NO_2$ with the delocalized carbon radical (64) at C4 with C-N bond formation would yield the epimeric 2,6-dimethyl-1-nitro-4-trinitromethyl adducts (95) and (97), as depicted in Scheme 2.19. Alternatively, coupling

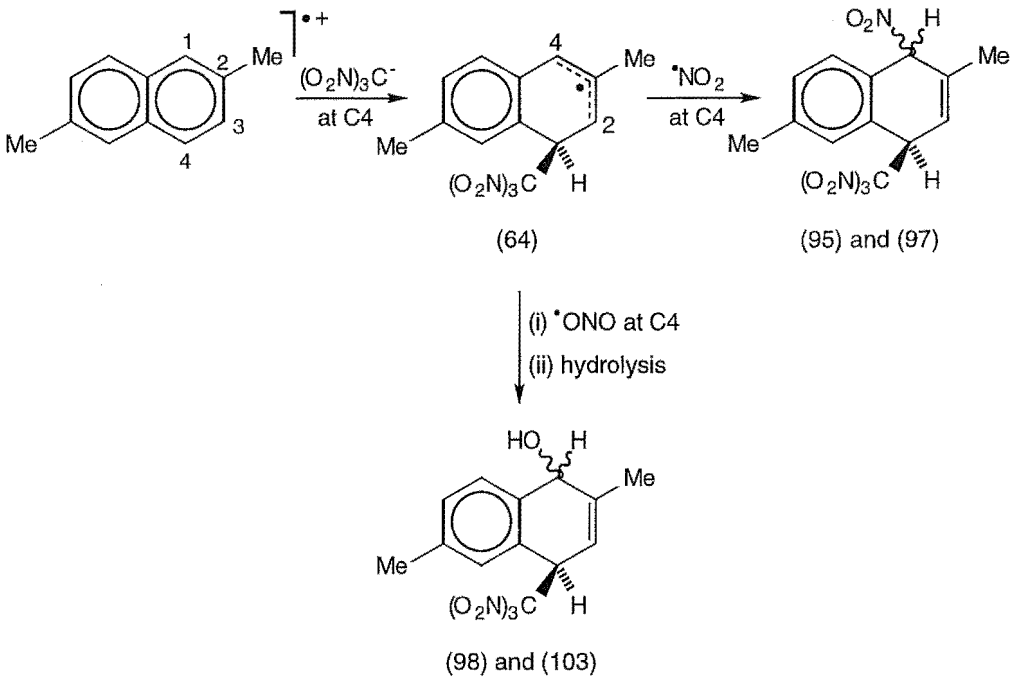

Scheme 2.19

of $^{\bullet}NO_2$ at C4 could occur with C-O bond formation and would give the epimeric nitrito/trinitromethyl adducts, which would be expected to hydrolyse rapidly to the epimeric 2,6-dimethyl-1-hydroxy-4-trinitromethyl adducts (98) and (103) under the prevailing acidic conditions of the reaction and workup procedure, also seen in Scheme 2.19. Similar radical coupling of $^{\bullet}NO_2$ at C2 in the delocalized carbon radical (64) would occur *trans* to the bulky trinitromethyl group at C1, giving the *trans*-2,6-dimethyl-2-nitro-1-trinitro-methyl adduct (94) by C-N bond formation and the *trans*-2,6-dimethyl-2-hydroxy-1-trinitromethyl adduct (102) by C-O bond formation followed by hydrolysis, as shown in Scheme 2.20. Formation of the nitro and hydroxy cycloadducts (101) and (104), respectively, then occurred *via* thermal

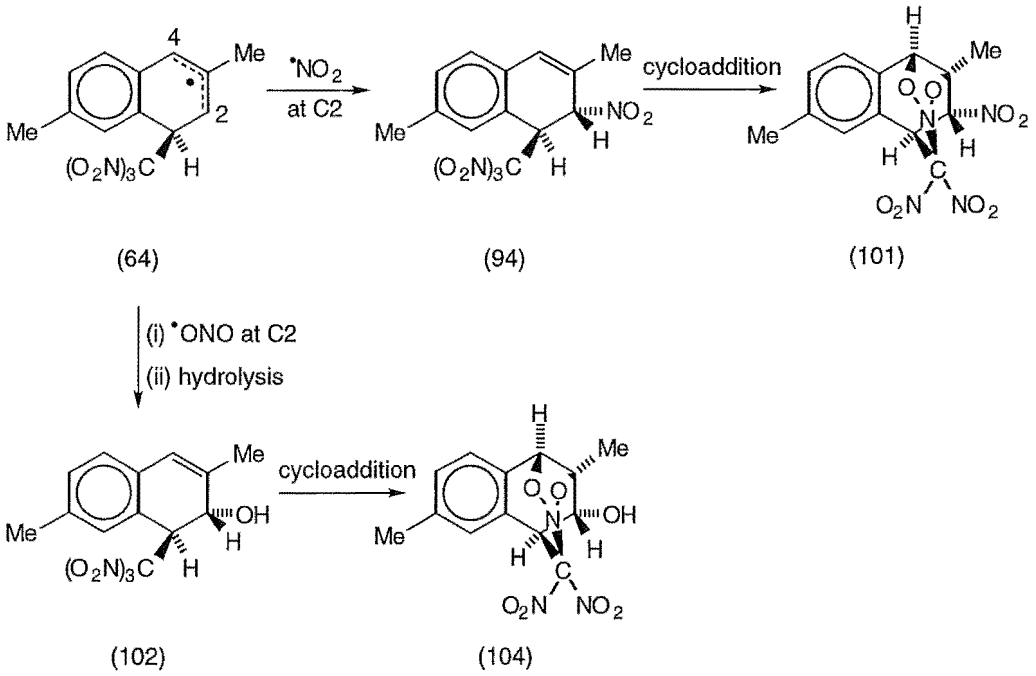

Scheme 2.20

alkene/nitro cycloaddition of their respective precursor adducts (94) and (102), as demonstrated in Sections 2.13 and 2.14 and in Scheme 2.20.

The precise mode of formation of 3,7-dimethyl-1-trinitromethyl-naphthalene (105) from the phenylallylic radical (64) is uncertain. However, one possibility is the loss of nitrous acid from either the epimeric 1,4-nitro/ trinitromethyl adducts (95) and (97), or the postulated intermediate epimeric

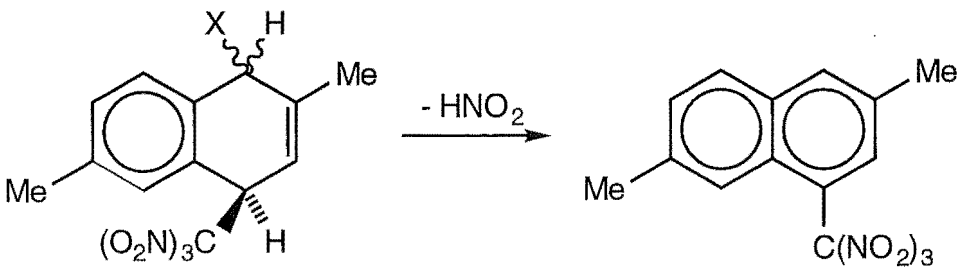

X = NO_2 (95) and (97)
= ONO (98a) and (103a)

(105)

Scheme 2.21

1,4-nitrito/trinitromethyl adducts (98a) and (103a), in competition with hydrolysis to give the 1,4-hydroxy/trinitromethyl adducts (98) and (103), as summarized in Scheme 2.21.

Reactions at -20° in dichloromethane and at +20° in acetonitrile led to an increase in nitro aromatics, particularly 2,6-dimethyl-1-nitronaphthalene (106). In connection with the formation of the 1-nitro aromatic (106) it is notable that C1 is the centre with the highest calculated unpaired electron spin density (+0.43) in the 2,6-dimethylnaphthalene radical cation,[14] and it appears likely that much of the 2,6-dimethyl-1-nitronaphthalene (106) was formed by direct coupling of the radical cation with $^{\bullet}NO_2$.

In conclusion, it appears most probable that in the reaction between the 2,6-dimethylnaphthalene radical cation and $(O_2N)_3C^-$, the secondary benzylic radicals (65) and (66) were unfavourable. It appears likely that the steric hindrance to $(O_2N)_3C^-$ attack at C1, due to interaction with the *vicinal* 2-methyl group, was a contributing factor in the observed regioselectivity, and that this led to the non-stabilized phenylallylic radical (64) being favoured over the methyl stabilized phenylallylic radical (65).

2.16 The Photolysis of 1,3-Dimethylnaphthalene (58)

General procedure for the photonitration of 1,3-dimethylnaphthalene (58) *with TNM.*

A solution of 1,3-dimethylnaphthalene (58) (500 mg, 0.4 mol L^{-1}) and TNM (0.8 mol L^{-1}) in dichloromethane (at +20, 0, or -20°) or acetonitrile (at +20 or -20°) was irradiated with filtered light ($\lambda_{cut\text{-}off}$<435 nm) and small samples were withdrawn for analysis at suitable intervals. The work-up procedure, involving evaporation of solvent and TNM, was conducted at ≤0°. The crude product mixtures were stored at -20° and were analysed by ^1H

n.m.r. spectroscopy as soon as possible (For complete experimental details see Chapter 5, Section 5.2.3).

2.17 The Photochemistry of 1,3-Dimethylnaphthalene (58) in Dichloromethane

2.17.1 Photochemistry in dichloromethane at +20 ° and identification of adducts.

A solution of 1,3-dimethylnaphthalene (0.4 mol L^{-1}) and TNM (0.8 mol L^{-1}) in dichloromethane was irradiated at +20° until the deep red colour of the charge transfer band was bleached. The composition of the reaction mixture was monitored by withdrawing samples for ^1H n.m.r. spectral analysis. After work-up, the final solution (after 2h, conversion ≈ 100%) was shown to contain a mixture of adducts (110)-(116) (total 43%), aromatic compounds (117)-(119) (total 50%), and other unidentified adducts (total 7%). The adducts were separated partially by h.p.l.c. on a cyanopropyl column using hexane/dichloromethane mixtures as the eluting solvents.

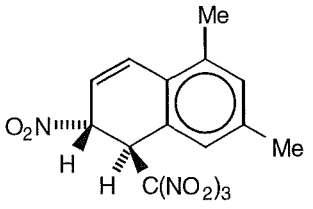

(110)

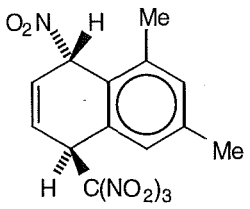

(111)

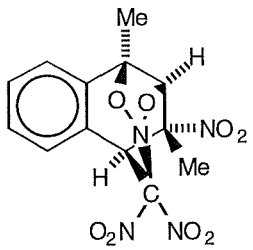

(112)

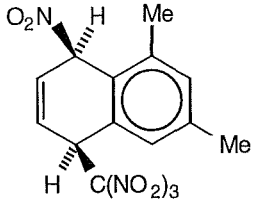

(113)

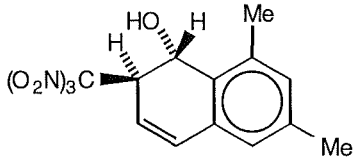

(114)

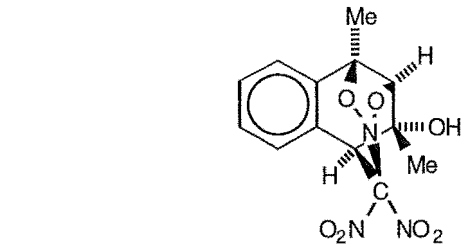

(115)

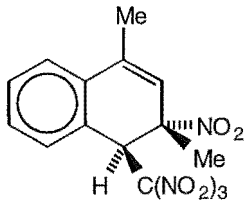

(116)

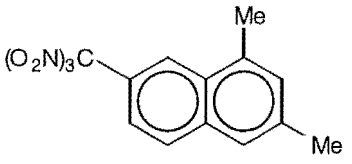

(117)

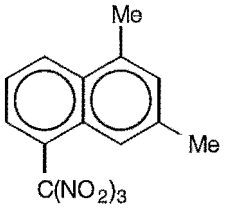

(118)

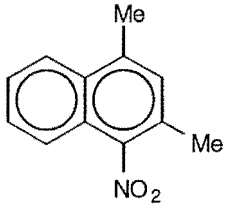

(119)

The first adduct eluted was isolated only as an impure oil and was identified as *trans*-5,7-dimethyl-2-nitro-1-trinitromethyl-1,2-dihydro-naphthalene (110) on the basis of its spectroscopic data and its slow (half-life 178 h) conversion into the nitro cycloadduct (122) (see below and Section 2.18). N.O.e. experiments confirmed the assignment of the chemical shifts for the protons. In particular, irradiation at δ 5.98 (H3) gave enhancements at δ 5.66 (H2) and at δ 7.04 (H4), while irradiation at δ 6.81 (H8) gave enhancements at δ 2.29 (7-Me) and at δ 5.70 (H1), as summarized in Fig. 2.37. The similarities of the characteristic coupling constants and

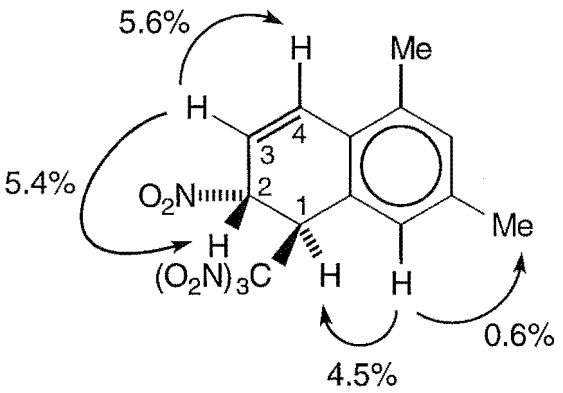

Fig. 2.37 Enhancements (%) from selected n.O.e. experiments for adduct (110).

resonances in the ^1H n.m.r. spectra between the analogous *trans*-6,7-dimethyl-2-nitro-1-trinitromethyl-1,2-dihydronaphthalene (120)[5] and adduct (110) are represented in Fig. 2.38. Given the closely similar coupling

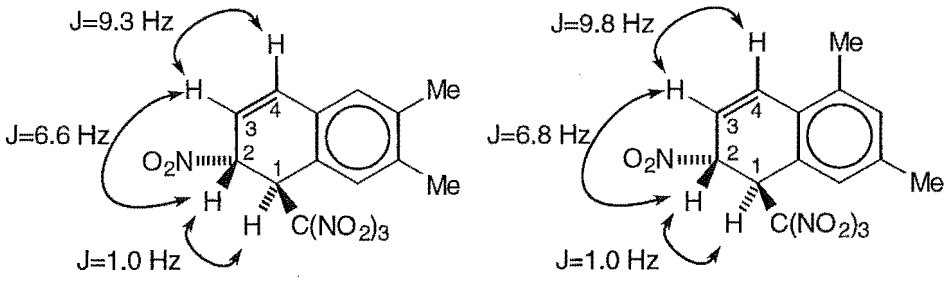

(120) (110)

H1	5.73	H1	5.70
H2	5.65	H2	5.66
H3	5.95	H3	5.98
H4	6.78	H4	7.04

Fig. 2.38 Comparison of the characteristic ^1H n.m.r. resonances (in ppm) and coupling constants for adducts (120) and (110).

constants, $J_{H1,H2}$, $J_{H2,H3}$ and $J_{H3,H4}$, between the two adducts (121) and (110), it was assumed that the two compounds had the same *trans*-1,2-stereochemistry. An HMBC experiment confirmed the assignment of the ^{13}C n.m.r. resonances. In particular, the **C**H-$C(NO_2)_3$ resonance appeared at δ 43.8, while the **C**H-NO_2 resonance appeared at δ 76.1. Subsequently, the structural and stereochemical assignment to adduct (110) was confirmed by the X-ray crystal structure determination for the related nitro cycloadduct (122), reported below.

The structure of the second adduct eluted from the h.p.l.c. column was determined by single crystal X-ray analysis. A perspective drawing of *trans*-

6,8-dimethyl-1-nitro-4-trinitromethyl-1,4-dihydronaphthalene (111), $C_{13}H_{12}N_4O_8$, m.p. 114.5-115.5° is presented in Fig. 2.39, and the

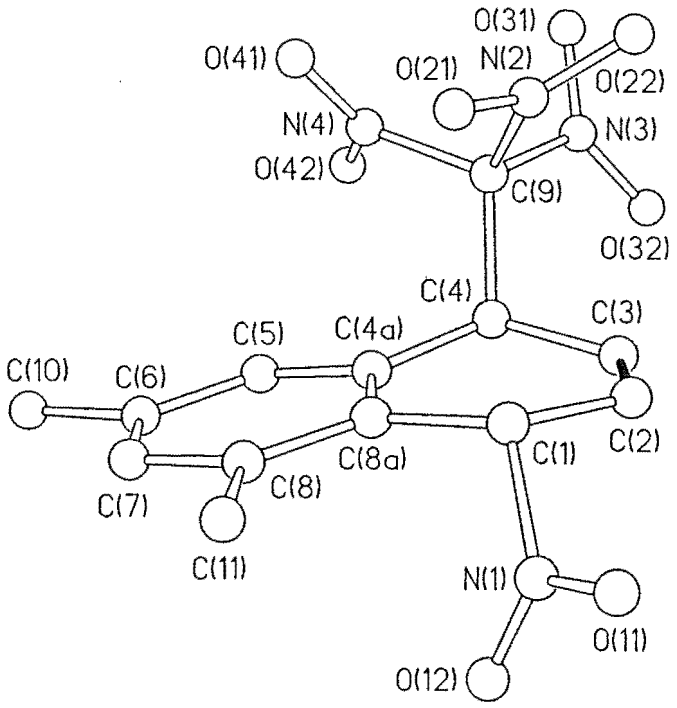

Fig. 2.39 Perspective drawing of adduct (111). Double bond shown in black.

corresponding atomic coordinates are given in Table 5.7 (See Chapter 5, Section 5.5). In the solid state, the alicyclic ring exists in a slightly distorted boat conformation as indicated by the torsional angles: C(3)-C(4)-C(4a)-C(8a) 17.5(3)°; C(2)-C(1)-C(8a)-C(4a) -10.3(4)°. Similar to the analogous adducts (95) and (97), formed in the photolysis of 2,6-dimethylnaphthalene (56) and TNM, the trinitromethyl group adopts an orientation such that the C(4)-C(9) bond is close to perpendicular to the plane of the aromatic ring [torsional angle: C(5)-C(4a)-C(4)-C(9) 74.9(3)°]. The spectroscopic data for adduct (111) were consistent with the established structure and the characteristic ^1H and ^{13}C n.m.r. data are presented in Fig. 2.40. N.O.e.

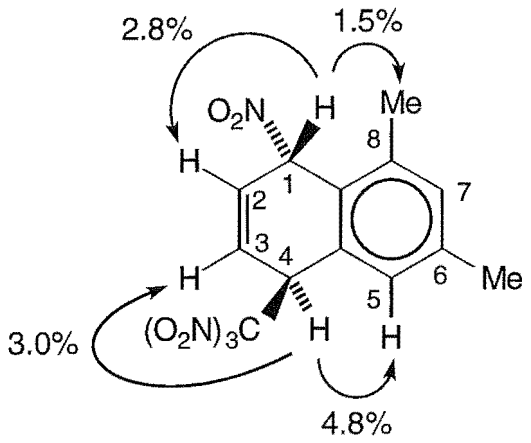

(111)

H1	6.20, br s	C1	82.4
H2	6.57, m	C2	124.5
H3	6.56, m	C3	131.1
H4	5.39, br s	C4	44.7

Fig. 2.40 Characteristic ^{1}H and ^{13}C n.m.r. resonances (in ppm) and enhancements (%) from selected n.O.e. experiments for adduct (111).

experiments confirmed the assignment of the chemical shifts for the protons. In particular, irradiation at δ 5.39 (H4) gave enhancements at δ 6.56 (H3) and at δ 6.98 (H5), while irradiation at δ 6.20 (H1) gave enhancements at δ 2.23 (8-Me) and at δ 6.57 (H2), also seen in Fig. 2.40. Furthermore, the nitro function was indicated by the ^{13}C n.m.r. chemical shift for C1 (δ 82.4) and the trinitromethyl function by the ^{13}C n.m.r. chemical shift for C4 (δ 44.7). These assignments were confirmed by an HMBC experiment.

The structure of the third adduct eluted from the h.p.l.c. column was also determined by single crystal X-ray analysis. A perspective drawing of the nitro cycloadduct (112), $C_{13}H_{12}N_4O_8$, m.p. 179.5-180.5° is presented in

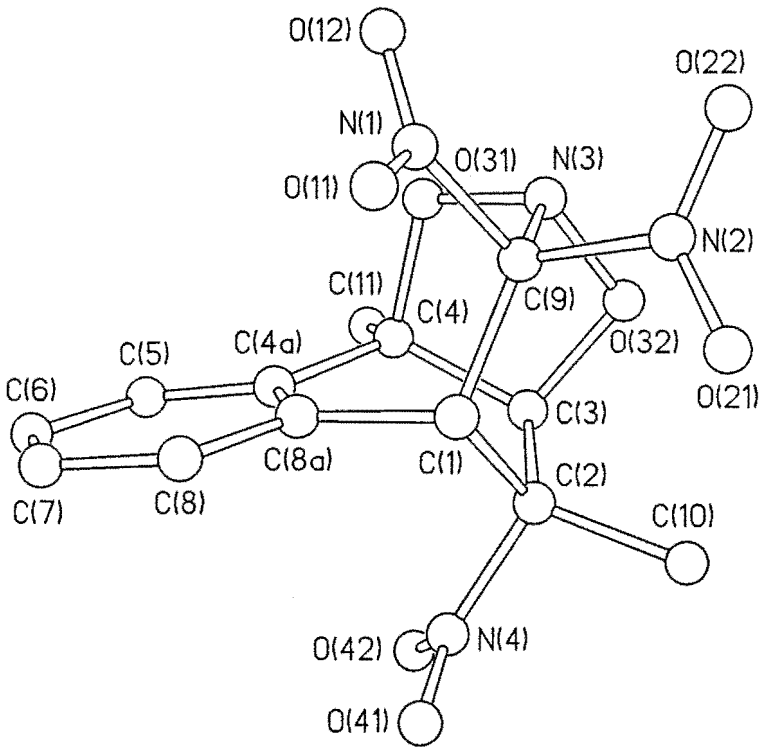

Fig. 2.41 Perspective drawing of the nitro cycloadduct (112).

Fig. 2.41, and corresponding atomic coordinates are given in Table 5.8 (See Chapter 5, Section 5.5). In the nitro cycloadduct (112), N(3) is clearly trigonal pyramidal and bond length differences [C(9)-N(1) 1.546(6) Å, C(9)-N(2) 1.538(6) Å, C(9)-N(3) 1.482(6) Å] are similar to those observed for the analogous heterocyclic cage structures in adducts (101) and (104), formed *via* thermal rearrangement of adducts (94) and (102), respectively, from the photolysis of 2,6-dimethylnaphthalene (57) / TNM. The spectroscopic data for the nitro cycloadduct (112) were in accord with the established structure. N.O.e. experiments confirmed the assignment of the chemical shifts for the protons. Specifically, irradiation at δ 1.90 (3-Me) gave enhancements at δ 5.23 (H2) and at δ 5.32 (H4), while irradiation at δ 5.23 (H2) gave enhancements at δ 1.90 (3-Me) and at δ 2.02 (1-Me), as outlined in Fig. 2.42. The characteristic ^{1}H and ^{13}C n.m.r. data are also presented in

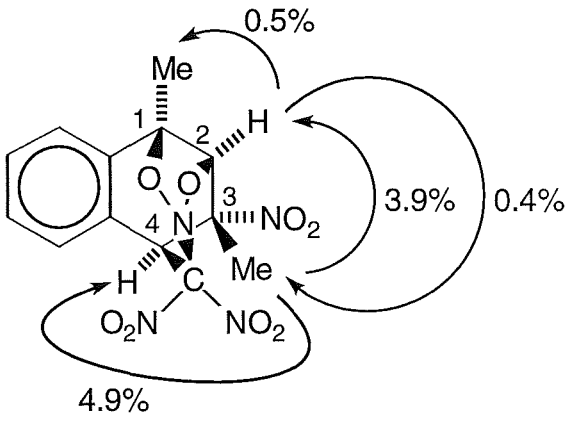

(112)

1-Me	2.02, s	C1	88.0
H2	5.23, d, J=2.5 Hz	C2	84.4
3-Me	1.90, s	C3	88.6
H4	5.32, d, J=2.5 Hz	C4	48.6

Fig. 2.42 Characteristic ^{1}H and ^{13}C n.m.r. resonances (in ppm) and enhancements (%) from selected n.O.e. experiments for adduct (112).

Fig. 2.42. In particular, ^{13}C n.m.r. resonances for the nitro function attached to C3 appeared at δ 88.6, while the cyclized trinitromethyl function attached to C4 appeared at δ 48.6. These assignments were confirmed by an HMBC experiment.

The fourth adduct eluted from the h.p.l.c. column was identified as the epimer of the *trans*-1-nitro-4-trinitromethyl adduct (111) by single crystal X-ray analysis. A perspective drawing of *cis*-6,8-dimethyl-1-nitro-4-trinitro-methyl-1,4-dihydronaphthalene (113), $C_{13}H_{12}N_4O_8$, m.p. 129° (dec.) is presented in Fig. 2.43, and corresponding atomic coordinates are given in Table 5.9 (See Chapter 5, Section 5.5). As with the structure of its epimer

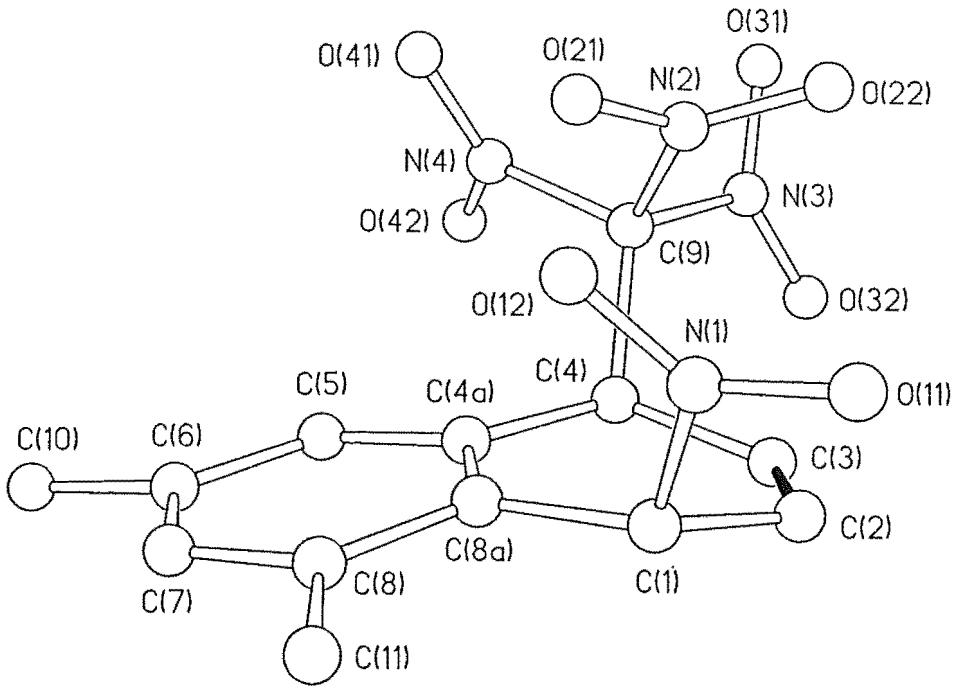

Fig. 2.43 Perspective drawing of adduct (113). Double bond shown in black.

(111), the alicyclic ring of the *cis*-1-nitro-4-trinitromethyl adduct (113) exists in a boat conformation [torsional angles: C(2)-C(1)-C(8a)-C(4a) -14.1(5)°; C(3)-C(4)-C(4a)-C(8a) 14.0(5)°] with the C(4)-C(9) bond close to perpendicular to the plane of the aromatic ring [torsional angle: C(5)-C(4a)-C(4)-C(9) 75.6(4)°]. The spectroscopic data for the nitro/trinitromethyl adduct (113) were consistent with its established structure. The ^{1}H and ^{13}C n.m.r. data were confirmed by n.O.e. and HMBC experiments, and from a comparison with the spectroscopic data for its epimer (111). Some of their characteristic n.m.r. data are summarized in Fig. 2.44, and are consistent with their assignment as epimers.

Adduct (114) was isolated towards the end of the h.p.l.c. chromatogram in low yield and then only as an impure oil. The structural assignment for *trans*-6,8-dimethyl-2-trinitromethyl-1,2-dihydronaphthalen-1-ol (114) is based

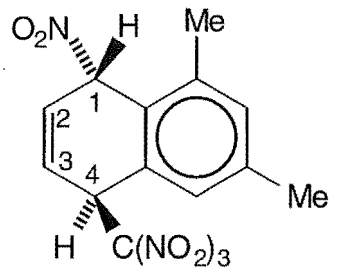

(111)

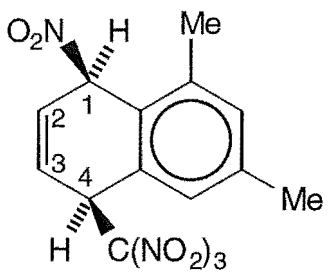

(113)

H1	6.20	H1	6.01
H2	6.57	H2	6.85
H3	6.56	H3	6.62
H4	5.39	H4	5.34
C1	82.4	C1	79.1
C2	124.5	C2	125.7
C3	131.1	C3	130.4
C4	44.7	C4	45.0

Fig. 2.44 Comparison of the characteristic ^{1}H and ^{13}C n.m.r. resonances (in ppm) for adducts (111) and (113).

on comparison of its ^{1}H n.m.r. spectra with that for *trans*-4,8-dimethyl-2-trinitromethyl-1,2-dihydronaphthalen-1-ol (121).[2] N.O.e. experiments confirmed the assignments of the chemical shifts for the protons. Specifically, irradiation at δ 5.20 (H1) gave enhancements at δ 2.34 (8-Me) and at δ 4.46 (H2), while irradiation at δ 5.77 (H3) gave enhancements at δ 4.46 (H2) and at δ 6.85 (H4), as observed in Fig. 2.45. Similarities between the ^{1}H n.m.r. spectra of adducts (121) and (114) are presented in Fig. 2.46. The minor differences in the chemical shift which were observed

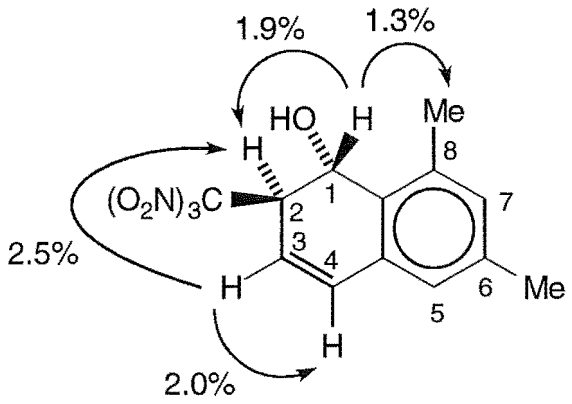

Fig. 2.45 Enhancements (%) from selected n.O.e. experiments for adduct (114).

result from effects arising from the 4-Me group in adduct (121), and the 6-Me group in adduct (114). Given the closely similar coupling constant $J_{H2,H3}$, it is assumed that the two compounds have the same *trans*-1,2-stereochemistry. The observation that *trans*-1-hydroxy-2-trinitromethyl adduct

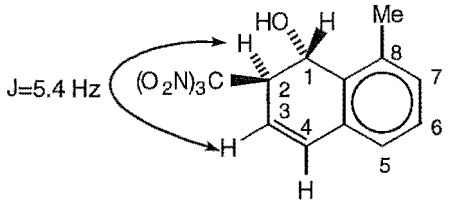

(121)

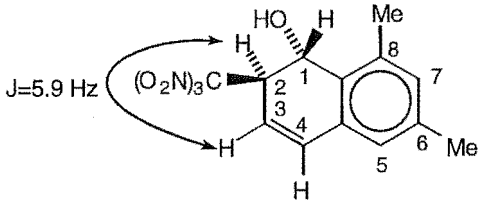

(114)

H1	5.24	H1	5.20
H2	4.44	H2	4.46
H3	5.61	H3	5.77
8-Me	2.40	8-Me	2.34

Fig. 2.46 Comparison of the characteristic ^{1}H n.m.r. resonances (in ppm) and coupling constants for adducts (121) and (114).

(114) failed to undergo intramolecular cycloaddition on storage of a (D)chloroform solution at +22° for 350 h is consistent with its structural assignment. Although *t*-1-trinitromethyl-1,2-dihydronaphthalen-*r*-1-ols undergo intramolecular cycloaddition readily, *t*-2-trinitromethyl-1,2-dihydronaphthalen-*r*-1-ols appear to be inert.[2]

The final adduct eluted from the h.p.l.c. column was identified as the hydroxy cycloadduct (115), but could not be induced to give crystals of adequate quality for single crystal X-ray analysis. Its identification was

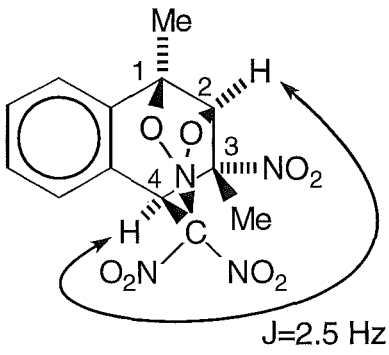

(112)

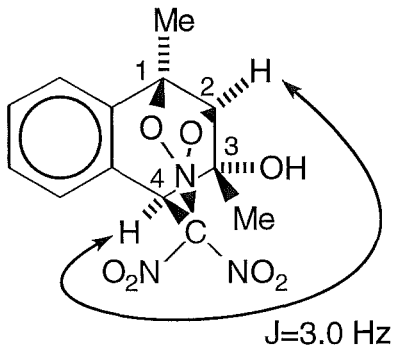

(115)

1-Me	2.02	1-Me	1.92
H2	5.23	H2	4.38
3-Me	1.90	3-Me	1.54
H4	5.32	H4	4.82
C1	88.0	C1	87.1
C2	84.4	C2	87.85
C3	88.6	C3	71.1
C4	48.6	C4	52.85

Fig. 2.47 Comparison of the characteristic ^{1}H and ^{13}C n.m.r. resonances (in ppm) and coupling constants for adducts (112) and (115).

based on a comparison of its spectroscopic data with the stereochemically related nitro adduct (112), the structure of which was determined by single crystal X-ray analysis (see above), as seen in Fig. 2.47. Given the closely similar coupling constant $J_{H2,H4}$ for the two adducts (112) and (115), as seen in Fig. 2.47, it is assumed that the two compounds have the same stereo-chemistry and that the difference between the two compounds lies only in the nature of the C3-substituent. An infrared absorption was observed at 3565 cm^{-1}, indicating the presence of an -OH function. All of the ^1H n.m.r. signals, whose assignments were confirmed by n.O.e. experiments, were shifted upfield in the hydroxy cycloadduct (115), relative to the nitro cycloadduct (112), consistent with the difference in the substituent at C3. An HMBC experiment confirmed the assignment of the ^{13}C n.m.r. resonances. In particular, the locations of the hydroxy and cyclized trinitromethyl functions were defined by the chemical shifts for C3 (δ 71.1) and C4 (δ 52.85),

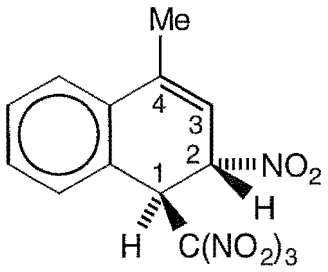

(88)

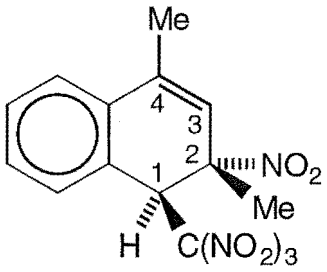

(116)

H1	5.73	H1	5.55
H2	5.63	2-Me	2.09
H3	5.85	H3	6.14
4-Me	2.70	4-Me	2.07

Fig. 2.48 Comparison of the characteristic ^1H n.m.r. resonances (in ppm) for adducts (88) and (116).

respectively.

Finally, although the precursor of the nitro cycloadduct (112) could not be isolated by h.p.l.c., *trans*-2,4-dimethyl-2-nitro-1-trinitromethyl-1,2-dihydro-naphthalene (116) was detected in the ^{1}H n.m.r. spectra of product mixtures as a transient intermediate in the formation of the nitro cycloadduct (112). Furthermore, comparison of the ^{1}H n.m.r. spectra of adduct (116) with the related *trans*-4-methyl-2-nitro-1-trinitromethyl-1,2-dihydro-naphthalene (88), the structure of which was determined by single crystal X-ray analysis,[6] showed that the two sets of spectroscopic data were similar (See summary in Fig. 2.48).

2.17.2 Photochemistry in dichloromethane at -20° and identification of aromatic substitution products (117)-(119).

A solution of 1,3-dimethylnaphthalene (0.4 mol L^{-1}) and TNM (0.8 mol L^{-1}) in dichloromethane was irradiated at -20° for 2 h and gave a product which was shown by ^{1}H n.m.r. to be a mixture of adducts (total 9%) and aromatic compounds (117)-(119) (total 91%). Chromatography of this mixture on a silica gel Chromatotron plate gave pure samples of the compounds (117)-(119).

The first compound eluted was identified as 6,8-dimethyl-2-trinitro-methylnaphthalene (117). The trinitromethyl aromatic (117) gave a satisfactory parent molecular ion in the mass spectrum, indicating the molecular formula $C_{13}H_{11}N_3O_6$. N.O.e. experiments confirmed the assignments of the chemical shifts for the protons. In particular, irradiation at δ 2.68 (8-Me) gave enhancements at δ 7.34 (H7) and at δ 8.26 (H1), irradiation at δ 2.53 (6-Me) gave enhancements at δ 7.34 (H7) and at δ 7.56 (H5), and irradiation at δ 7.92 (H4) gave enhancements at δ 7.50 (H3) and at δ 7.56 (H5), as depicted in Fig. 2.49. Furthermore, strong infrared absorptions at 1602 and 1587 cm^{-1} provided evidence for the $-C(NO_2)_3$

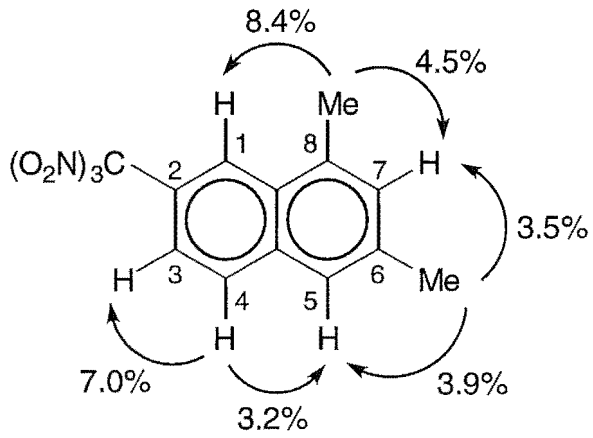

Fig. 2.49 Enhancements (%) from selected n.O.e. experiments for the trinitromethyl aromatic (117).

substituent.

The second compound eluted was identified as 5,7-dimethyl-1-trinitromethylnaphthalene (118). Once again a satisfactory parent molecular ion was obtained in the mass spectrum, indicating the molecular formula $C_{13}H_{11}N_3O_6$, for the trinitromethyl aromatic (118). N.O.e. experiments confirmed the assignments of the chemical shifts for the protons. Specifically, irradiation at δ 6.92 (H8) gave an enhancement at δ 2.44 (7-Me), irradiation at δ 7.31 (H6) gave enhancements at δ 2.44 (7-Me) and at δ 2.73

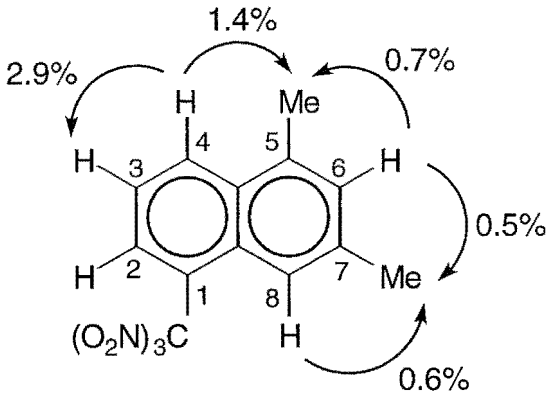

Fig. 2.50 Enhancements (%) from selected n.O.e. experiments for the trinitromethyl aromatic (118).

(5-Me), and irradiation at δ 8.37 (H4) gave enhancements at δ 2.73 (5-Me) and at δ 7.55 (H3), as shown in Fig. 2.50. The presence of the -$C(NO_2)_3$ substituent was supported by the presence of strong infrared absorptions at 1621 and 1590 cm^{-1}.

The final compound eluted was identified as 2,4-dimethyl-1-nitro-naphthalene (119) and the structure was confirmed by comparing its melting point and n.m.r. data with literature data.[11]

On monitoring the photochemical reaction between 1,3-dimethyl-naphthalene (58) and TNM at +20, 0 and -20° in dichloromethane, there was a marked change in the relative yields of the adducts and aromatics. An

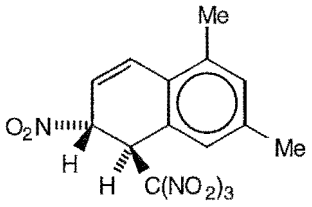

(110)

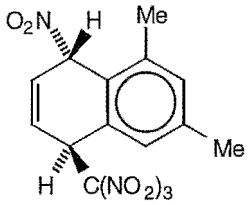

(111)

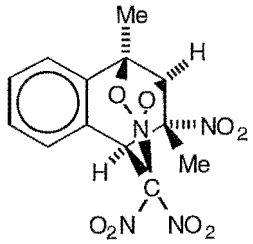

(112)

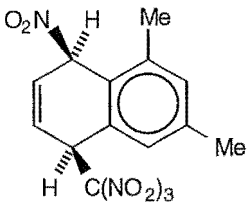

(113)

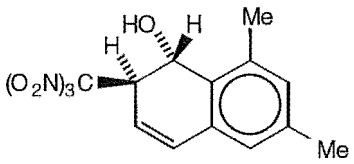

(114)

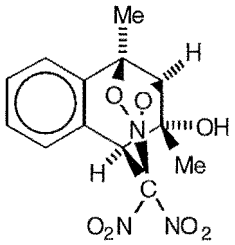

(115)

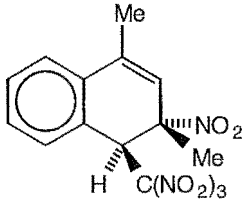

(116)

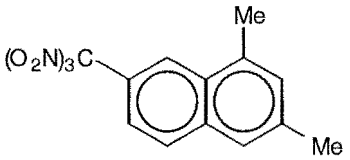

(117)

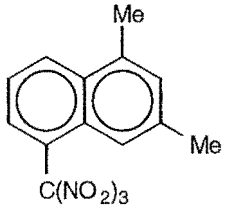

(118)

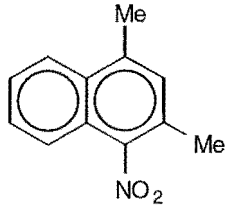

(119)

Table 2.8 Overview of product yields from the photolysis of 1,3-dimethylnaphthalene (58) (0.4 mol L^{-1}) and TNM (0.8 mol L^{-1}) in dichloromethane.

		Yield (%)													
Conversion						Adducts (110,				Adducts (112,	Unknown	Total				Total
t (h)	(%)	(110)	(111)	(113)	(114)	111, 113, 114)	(112)	(115)	(116)	115, 116)	adducts	adducts	(117)	(118)	(119)	aromatics
At +20°																
1	80	8.6	7.6	11.7	1.6	29.5	1.8	1.6	5.9	9.3	6.9	45.7	2.7	3.4	48.2	54.3
1.5	98	9.3	8.1	12.0	1.6	31.0	2.4	1.8	5.9	10.1	6.7	47.8	2.3	6.6	43.3	52.2
2	100	10.1	8.5	10.5	1.4	30.5	4.5	1.8	5.6	11.9	7.3	49.7	2.5	9.9	37.9	50.3
At 0°																
1	71	2.7	2.4	2.1	0.3	7.5	0.6	0.3	2.2	3.1	2.7	13.3	1.9	1.9	82.9	86.7
1.5	90	3.0	2.5	2.4	0.3	8.2	1.3	0.2	2.6	4.1	3.0	15.3	1.6	2.2	80.9	84.7
2	100	4.2	3.7	3.2	0.4	11.5	1.3	0.3	3.5	5.1	1.7	18.3	2.0	2.9	76.8	81.7
At -20°																
1	42	1.4	0.6	0.1	-	2.1	trace	0.1	2.5	2.6	1.7	6.4	1.4	1.6	90.6	93.6
1.5	68	1.2	1.1	1.4	-	3.7	0.3	0.2	2.6	3.1	1.5	8.0	0.8	0.9	90.0	91.7
2	74	1.0	1.3	1.5	-	3.8	0.5	0.2	2.8	3.5	1.7	9.0	1.0	1.0	89.0	91.0

overview of product yields in dichloromethane is given in Table 2.8. At +20° the adduct : aromatic ratio was *c.* 1:1, at 0° it was *c.* 1:4, but at -20° the ratio was *c.* 1:10. Clearly the major change occurred with the nitro aromatic compound (119), which markedly increased in yield at lower reaction temperatures. There was a more consistent change across all of the adducts at lower reaction temperatures. The cycloaddition reaction of adduct (116) into the nitro cycloadduct (112) could be seen occurring as the yield of the nitro cycloadduct (112) increased with time at successive points in the time scans.

2.18 Thermal Cycloaddition of *trans*-5,7-Dimethyl-2-nitro-1-trinitromethyl-1,2-dihydronaphthalene (110) to give the Nitro Cycloadduct (122)

A solution of the impure nitro/trinitromethyl adduct (110) in (D)chloroform was stored at +22°, in the dark, and the ^{1}H n.m.r. spectra of the solution monitored at appropriate time intervals. While the impurities were stable under these conditions, the nitro/trinitromethyl adduct (110) was slowly converted into the nitro cycloadduct (122), as summarized in Scheme 2.22. After 33 days the reaction was essentially complete, as shown in Fig. 2.51.

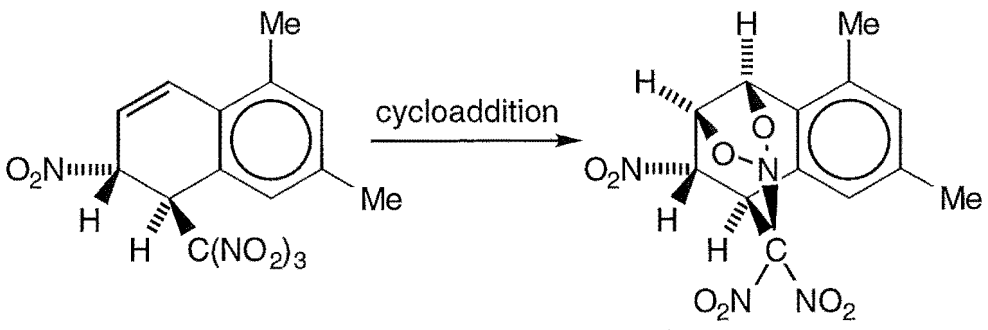

(110) (122)

Scheme 2.22

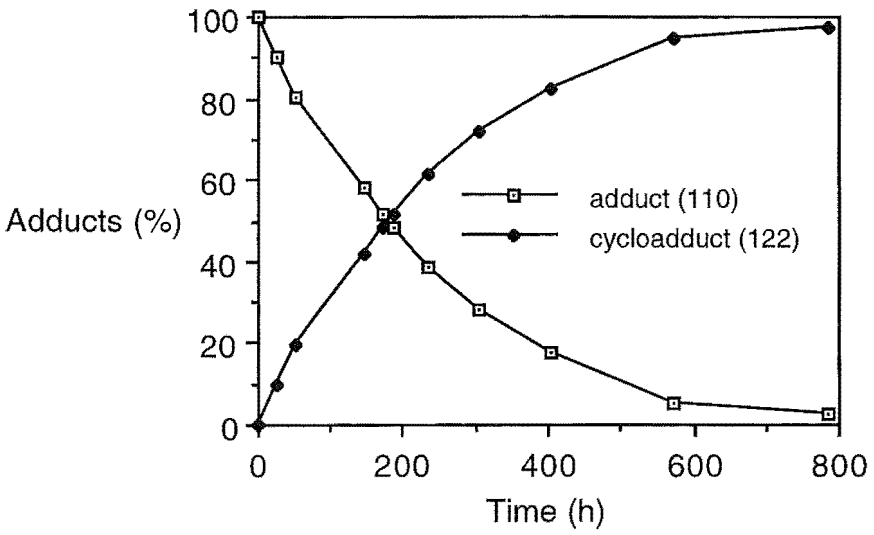

Fig. 2.51 Kinetics of cycloaddition of adduct (110) to nitro cycloadduct (122) in (D)chloroform, at +22°.

The half-life for the cycloaddition of adduct (110) into the nitro cycloadduct (122) was *c.* 178 h. The nitro cycloadduct (122) was isolated by removal of the solvent under reduced pressure and crystallization from dichloromethane/ hexane, and its structure determined by single crystal X-ray analysis. A perspective drawing of the nitro cycloadduct (122), $C_{13}H_{12}N_4O_8$, m.p. 195° (dec.), is presented in Fig. 2.52, and corresponding atomic coordinates are given in Table 5.10 (See Chapter 5, Section 5.5). The structure of nitro cycloadduct (122) was essentially identical with that determined above for nitro cycloadduct (112), except for the positions of attachment of the two methyl groups in the two structures. As for the nitro cycloadduct (112), the nitrogen atom N(3) in the heterocyclic cage structure of the nitro cycloadduct (122) is trigonal pyramidal and the pattern of the bond lengths is similar [C(9)-N(1) 1.520(3) Å, C(9)-N(2) 1.553(3) Å, C(9)-N(3) 1.503(3) Å]. The spectroscopic data for nitro cycloadduct (122) were in accord with the established structure. N.O.e. experiments confirmed the assignments of the

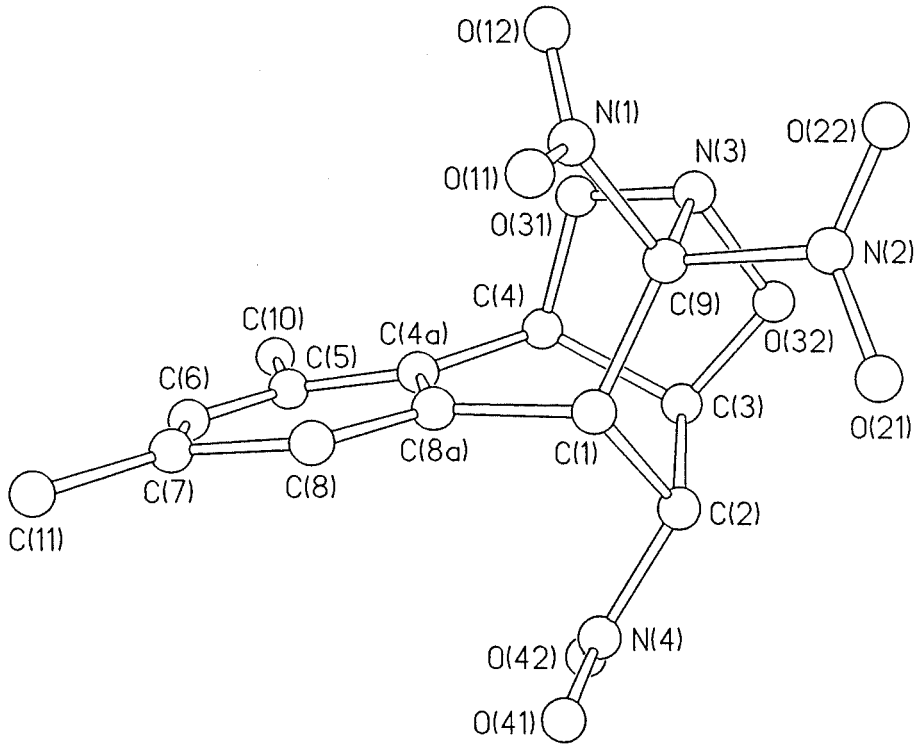

Fig. 2.52 Perspective drawing of the nitro cycloadduct (122).

chemical shifts for the protons. Specifically, irradiation at δ 2.36 (8-Me) gave enhancements at δ 5.96 (H1) and at δ 7.01 (H7), while irradiation at δ 5.70 (H3) gave enhancements at δ 5.16 (H4) and at δ 5.91 (H2), as represented in Fig. 2.53. The characteristic ^{1}H and ^{13}C n.m.r. data is also presented in Fig. 2.53. In particular, the nitro function was indicated by the ^{13}C n.m.r. chemical shift for C3 (δ 78.8) and the cyclized trinitromethyl function by the ^{13}C n.m.r. chemical shift for C4 (δ 45.4). These assignments were confirmed by an HMBC experiment.

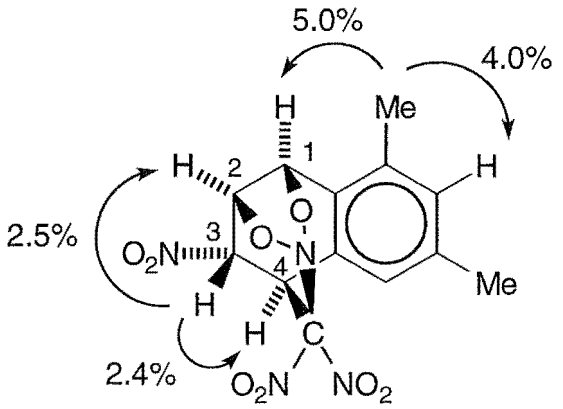

(122)

H1	5.96	C1	77.2
H2	5.91	C2	75.9
H3	5.70	C3	78.8
H4	5.16	C4	45.4

Fig. 2.53 Characteristic ^{1}H and ^{13}C n.m.r. resonances (in ppm) and enhancements (%) from selected n.O.e. experiments for the nitro cycloadduct (122).

2.19 The Photochemistry of 1,3-Dimethylnaphthalene (58) in Acetonitrile

Photolyses of solutions of 1,3-dimethylnaphthalene (58) (0.4 mol L^{-1}) and TNM (0.8 mol L^{-1}) in acetonitrile were carried out at +20 and -20° as for reactions in dichloromethane, above. The results of these reactions, monitored with time, are summarized in Table 2.9. There was a less marked change in the relative yields of the adducts and aromatics as the temperature was lowered in acetonitrile, compared with dichloromethane (See Table 2.8,

Table 2.9 Overview of product yields from the photolysis of 1,3-dimethylnaphthalene (58) (0.4 mol L^{-1}) and TNM (0.8 mol L^{-1}) in acetonitrile.

		Yield (%)													
Conversion						Adducts (110,				Adducts (112,	Unknown	Total				Total
t (h)	(%)	(110)	(111)	(113)	(114)	111, 113, 114)	(112)	(115)	(116)	115, 116)	adducts	adducts	(117)	(118)	(119)	aromatics
At +20°																
1.5	89	3.2	3.5	3.3	0.9	10.9	0.6	0.2	3.7	4.5	3.7	19.1	3.7	4.1	73.1	80.9
2	100	2.8	3.2	2.4	0.5	8.9	1.0	0.2	2.7	3.9	3.2	16.0	3.3	4.5	76.2	84.0
At -20°																
1	57	1.4	1.7	1.5	-	4.6	-	0.1	3.0	3.1	1.9	9.6	1.9	1.4	87.1	90.4
2	89	1.3	1.5	1.6	-	4.4	-	0.1	3.2	3.3	2.5	10.2	1.1	0.7	88.0	89.8

Section 2.17). In acetonitrile at +20° the adduct : aromatic ratio was *c.* 1:5, whereas at -20° the ratio was *c.* 1:9. Once again the product which changed the most upon changing temperatures was the nitro aromatic (119). The reactions at -20° in both dichloromethane and acetonitrile produced very similar results, whereas the +20° acetonitrile reaction was more similar to the 0° dichloromethane reaction than the +20° dichloromethane reaction.

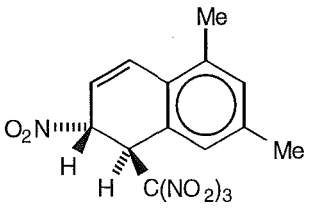

(110)

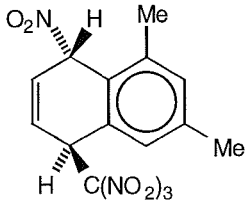

(111)

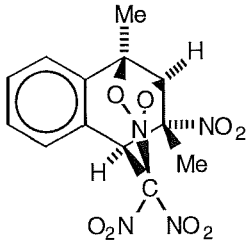

(112)

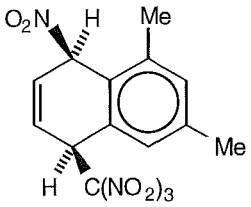

(113)

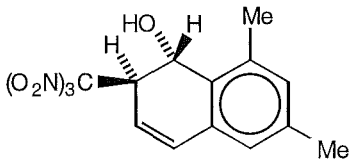

(114)

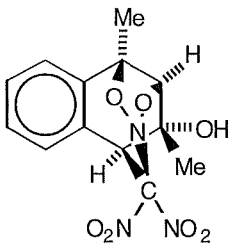

(115)

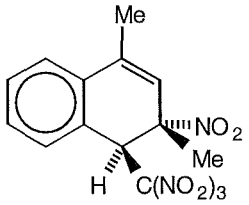

(116)

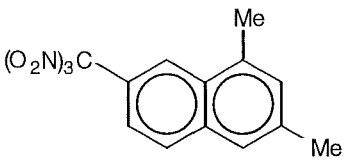

(117)

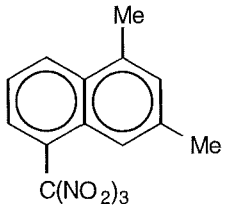

(118)

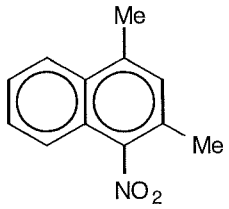

(119)

2.20 The Photochemistry of 1,3-Dimethylnaphthalene (58) in Dichloromethane Containing Trifluoroacetic Acid (TFA)

A solution of 1,3-dimethylnaphthalene (58) (0.4 mol L^{-1}) and TNM (0.8 mol L^{-1}) in dichloromethane containing TFA (0.8 mol L^{-1}) was irradiated at +20° for 30 min. to give a mixture of unreacted 1,3-dimethylnaphthalene (42% conversion), 2,4-dimethyl-1-nitronaphthalene (119) (34%), 2,2',4,4'-tetramethyl-1,1'-binaphthyl (123) (54%), and unidentified aromatics (total 12%). Chromatography of this mixture on a silica gel Chromatotron plate gave pure samples of 1,3-dimethylnaphthalene (58) and compounds (119) and (123).

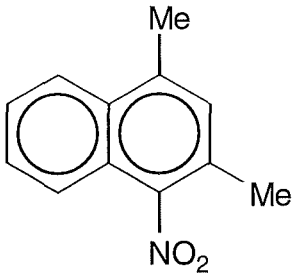

(119)

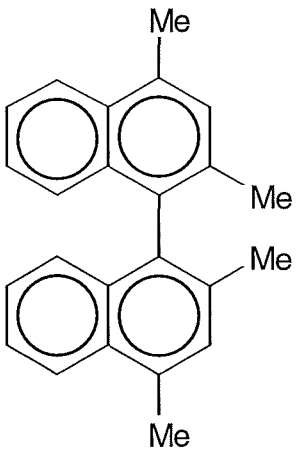

(123)

The first compound eluted was identified as unreacted 1,3-dimethyl-naphthalene (58).

The second compound eluted was identified as 2,2',4,4'-tetramethyl-1,1'-binaphthyl (123) and the structure was confirmed by comparison of its melting point and n.m.r. data with literature data.[15]

The final compound eluted had already been identified as the known[11] 2,4-dimethyl-1-nitronaphthalene (119) (see above).

2.21 Overview of the Photonitration of 1,3-Dimethyl-naphthalene (58)

In terms of the products which were identified for the reaction at +20° in dichloromethane (see Table 2.8, Section 2.17), there was a clear preference (*c.* 4:1) for $(O_2N)_3C^-$ attack on the unsubstituted ring in the radical cation of 1,3-dimethylnaphthalene, as represented in Fig. 2.54. The major point of

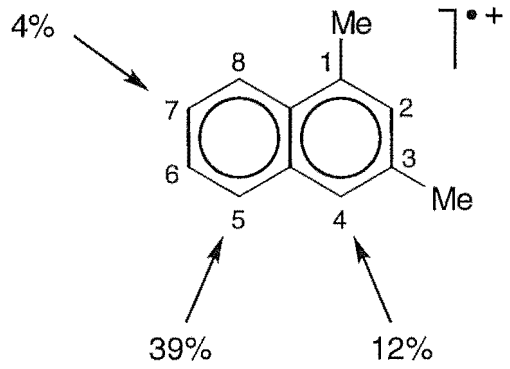

Fig. 2.54 Products (%) identified corresponding to attack of $(O_2N)_3C^-$ on the 1,3-dimethylnaphthalene radical cation.

attack of $(O_2N)_3C^-$ on the 1,3-dimethylnaphthalene radical cation was at C5 (total 39%) and this led to the formation of the phenylallylic radical (73). The formation of adduct (114) and 6,8-dimethyl-2-trinitromethylnaphthalene (117) (total 4%) was particularly interesting, since these apparently formed by initial attack of $(O_2N)_3C^-$ at C7 on the radical cation of 1,3-dimethylnaphthalene. This would result in formation of the less stable secondary benzylic radical (70). Lowering the temperature, in either dichloromethane or acetonitrile, showed that adduct (114) and the trinitromethyl aromatic (117) decreased in yield (See Tables 2.8 and 2.9, Sections 2.17 and 2.19, respectively). Indeed adduct (114) was not detected at -20° in either solvent, supporting the view that the secondary benzylic radical (70) was indeed less stable than the

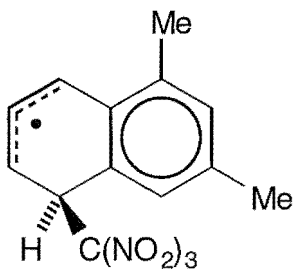

(73)

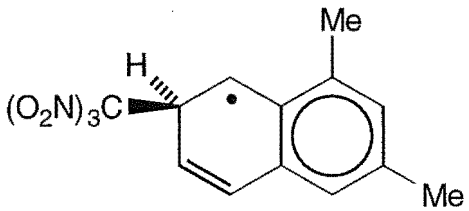

(70)

phenylallylic radical (73). Notably, neither adducts nor 6,8-dimethyl-1-trinitromethylnaphthalene were detected which might result from $(O_2N)_3C^-$ attack at C8. This outcome was clearly a reflection of the steric hindrance to attack by $(O_2N)_3C^-$ at C8 exerted by the *peri* 1-methyl substituent.

The modes of formation of the products arising from attack of $(O_2N)_3C^-$ on the unsubstituted ring of the radical cation of 1,3-dimethylnaphthalene are given in Schemes 2.23 and 2.24. In Scheme 2.23 attack of $(O_2N)_3C^-$ at C5 would give the delocalized phenylallylic radical (73). Subsequently, radical

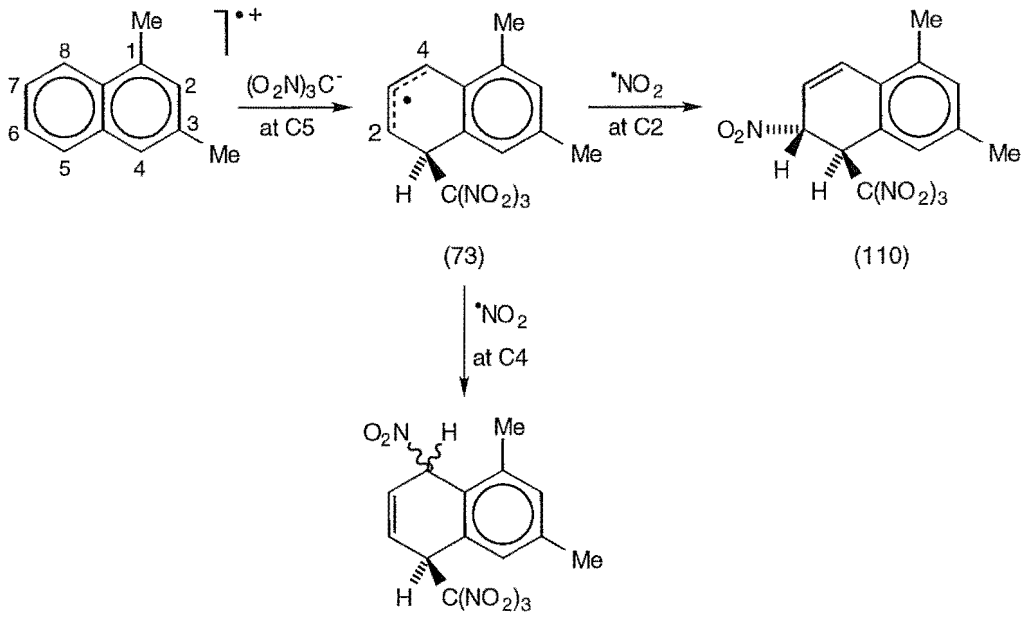

(73) (110)

(111) and (113)

Scheme 2.23

coupling with $^{\bullet}NO_2$ at C2 in (73) would occur *anti* to the bulky trinitromethyl group to give the nitro/trinitromethyl adduct (110), while coupling with $^{\bullet}NO_2$ at C4 would be expected to be non-stereospecific and give the epimeric nitro/trinitromethyl adducts (111) and (113). Alternatively, attack of $(O_2N)_3C^-$ at C7 of the radical cation of 1,3-dimethylnaphthalene would give the benzylic radical (70), as represented in Scheme 2.24. Radical coupling with

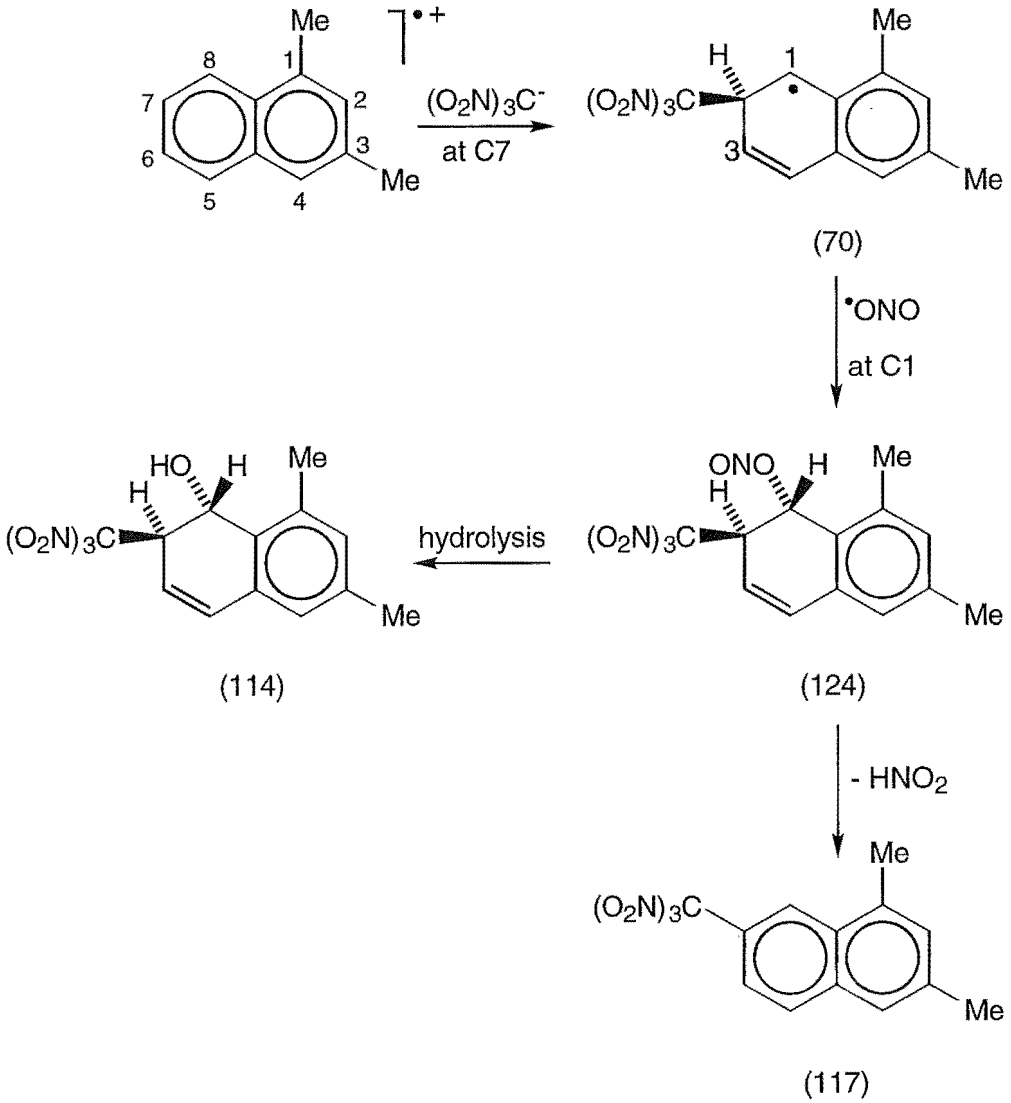

Scheme 2.24

$^{\bullet}NO_2$ at C1 with C-O bond formation would yield the nitrito/trinitromethyl adduct (124), which would be expected to be hydrolysed to give the hydroxy/

trinitromethyl adduct (114), either under the prevailing acidic reaction conditions or during the work-up procedures. The precise mode of formation of 6,8-dimethyl-2-trinitromethylnaphthalene (117) from the benzylic radical (70) is uncertain, but one possibility is the loss of nitrous acid from the postulated intermediate, nitrito/trinitromethyl adduct (124), in competition with hydrolysis to give the hydroxy/trinitromethyl adduct (114), also seen in Scheme 2.24.

Similarly, the precise mode of formation of 5,7-dimethyl-1-trinitromethyl-naphthalene (118) from the phenylallylic radical (73) is uncertain, but one possibility is the loss of nitrous acid from the 1,4-nitro/trinitromethyl adducts (111) and (113), as outlined in Scheme 2.25.

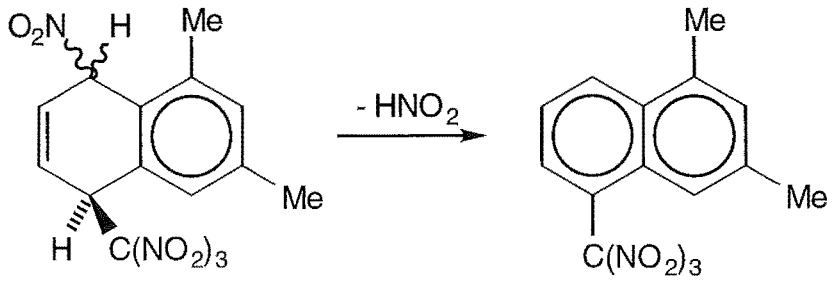

(111) and (113) (118)

Scheme 2.25

In spite of the enhanced stability on the phenylallylic radical (72) due to the position of the two methyl groups, attack of $(O_2N)_3C^-$ at C4 was limited by the steric interaction between the trinitromethyl group and the methyl group at the adjacent C3 position. The mode of formation of adducts arising from $(O_2N)_3C^-$ attack at C4 is given in Scheme 2.26. The delocalized carbon radical (72), formed initially, undergoes radical coupling with $^{\bullet}NO_2$ apparently exclusively at C2 with both C-N and C-O bond formation to give adducts (116) and (125), respectively, the latter after hydrolysis of the corresponding nitrito/trinitromethyl adduct. While the nitro/trinitromethyl

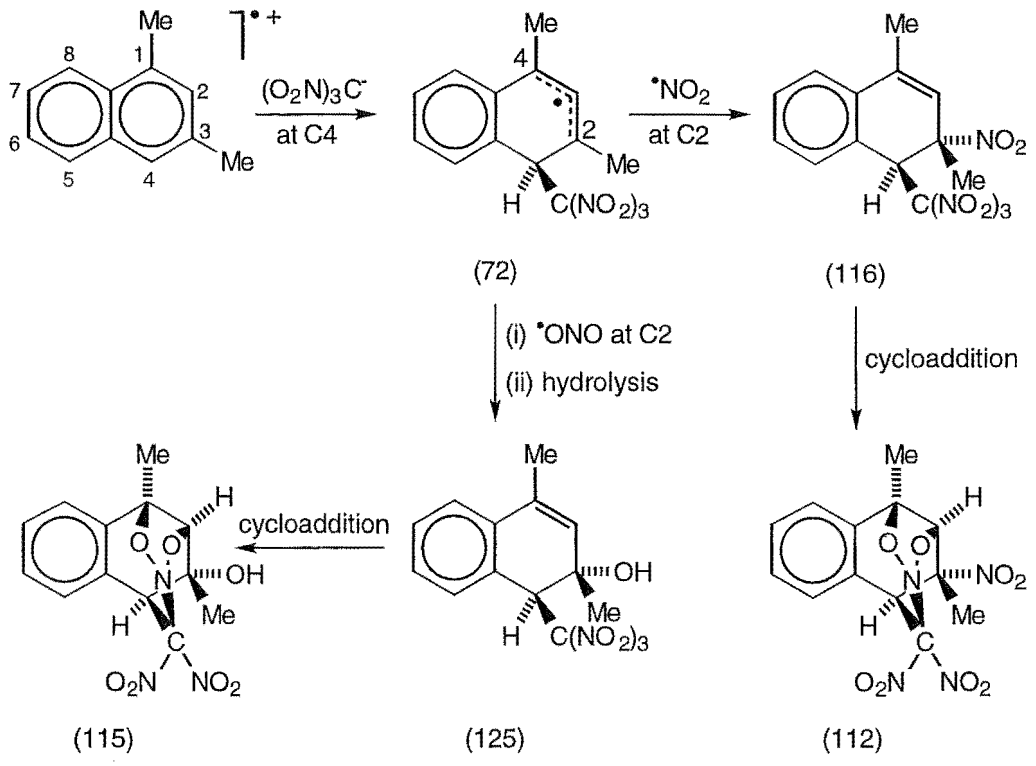

Scheme 2.26

adduct (116) was detected among the reaction products, it was not isolated but yielded the nitro cycloadduct (112), the product of nitro/alkene cycloaddition. Correspondingly, the hydroxy/trinitromethyl precursor (125) of the hydroxy cycloadduct (115) was never apparent in the ^1H n.m.r. spectra of the product mixtures. This is consistent with the earlier observations in the 2,6-dimethylnaphthalene (57) / TNM reactions and others[5] that the hydroxy/trinitromethyl adducts such as compound (125) undergo cycloaddition more rapidly than the corresponding nitro/trinitromethyl adducts, such as compound (116). For example, the half-lives in the 2,6-dimethylnaphthalene (57) / TNM reactions for the hydroxy and nitro cycloadduct precursors were 13 h and 96 h, respectively (See Sections 2.13 and 2.14). No products were detected which could have been derived by coupling of $^{\bullet}NO_2$ at C1 in the delocalized phenylallylic radical (72), but in this context it must be emphasized that of the total adduct yield (50%), some 7% remains

unidentified.

In the photolysis at +20° of 1,3-dimethylnaphthalene (58) / TNM in dichloromethane containing TFA the formation of adducts and the trinitromethyl aromatic derivatives (117) and (118) was suppressed by the protonation of $(O_2N)_3C^-$ in the triad of 1,3-dimethylnaphthalene radical cation, $(O_2N)_3C^-$ and $^{\bullet}NO_2$. In the absence of $(O_2N)_3C^-$, the 1,3-dimethylnaphthalene radical cation undergoes radical coupling with $^{\bullet}NO_2$ to give the 2,4-dimethyl-1-nitronaphthalene (119), or with itself to give the dehydrodimer (123). The formation of the dehydrodimer (123) in photolyses in the presence of TFA parallels dehydrodimer (126) formation in a similar reaction of 1-methoxynaphthalene.[16] Furthermore, it is notable that C4 is the centre

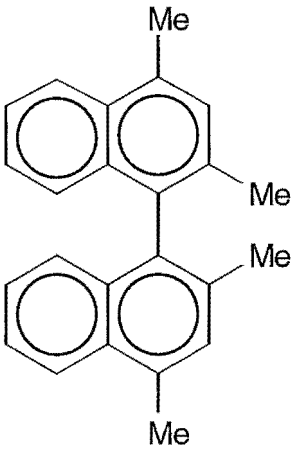

(123)

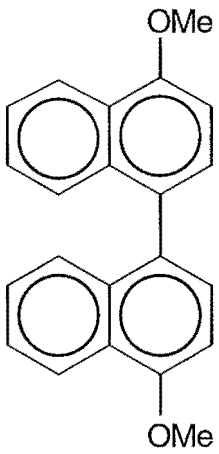

(126)

with the highest calculated unpaired electron spin density (+0.48) in the 1,3-dimethylnaphthalene radical cation.[14]

Reactions at lower temperatures in dichloromethane and acetonitrile led to an increase in the 1-nitro aromatic (119) and it therefore appears likely that much of the 2,4-dimethyl-1-nitronaphthalene (119) was formed by direct coupling of $^{\bullet}NO_2$ with the radical cation.

In conclusion, it appears likely that steric interactions play a major role in the regiochemistry of attack of $(O_2N)_3C^-$ on the 1,3-dimethylnaphthalene

radical cation. Without unfavourable methyl interactions, it appears that even secondary benzylic radicals may form on the pathway to adducts. Clearly however, the phenylallylic radicals, (72) and (73), are more stable than the benzylic radical (70), with the majority of attack of $(O_2N)_3C^-$ *via* these intermediates. Stabilization of the phenylallylic radical (72) by the methyl substituents at C1 and C3 appears to offset some of the steric interactions between the bulky trinitromethyl group and the β-methyl group at C3.

2.22 References for Chapter Two

1 Eberson, L., Hartshorn, M. P., Radner, F., and Svensson, J. O., *J. Chem. Soc., Perkin Trans. 2*, 1994, 1719.

2 Butts, C. P., Eberson, L., Hartshorn, M. P., and Robinson, W. T., *Aust. J. Chem.*, 1995, **48**, 1989.

3 Eberson, L., Hartshorn, M. P., and Radner, F., *J. Chem. Soc., Perkin Trans. 2*, 1992, 1793.

4 Eberson, L., Hartshorn, M. P., and Radner, F., *J. Chem. Soc., Perkin Trans. 2*, 1992, 1799.

5 Butts, C. P., Calvert, J. L., Eberson, L., Hartshorn, M. P., Radner, F., and Robinson, W. T., *J. Chem. Soc., Perkin Trans. 2*, 1994, 1485.

6 Calvert, J. L., Eberson, L., Hartshorn, M. P., Maclagan, R. G. A. R., and Robinson, W. T., *Aust. J. Chem.*, 1994, **47**, 1591.

7 Butts, C. P., Calvert, J. L., Eberson, L., Hartshorn, M. P., and Robinson, W. T., *J. Chem. Soc., Chem. Commun.*, 1993, 1513.

8 Butts, C. P., Calvert, J. L., Eberson, L., Hartshorn, M. P., Maclagan, R. G. A. R., and Robinson, W. T., *Aust. J. Chem.*, 1994, **47**, 1087.

9 Calvert, J. L., Eberson, L., Hartshorn, M. P., Maclagan, R. G. A. R., and Robinson, W. T., *Aust. J. Chem.*, 1994, **47**, 1211.

10 Butts, C. P., Eberson, L., Foulds, G. J., Fulton, K. L., Hartshorn, M. P., and Robinson, W. T., *Acta Chem. Scand.*, 1995, **49**, 76.

11 Davies, A., and Warren, K. D., *J. Chem. Soc. B*, 1969, 873.

12 Wells, P. R., *Aust. J. Chem.*, 1964, **17**, 967.

13 Clark, D. T., and Fairweather, D. J., *Tetrahedron*, 1969, **25**, 5525.

14 Maclagan, R. G. A. R., *Personal communication*.

15 Greenland, H., Pinhey, J. T., and Sternhell, S., *Aust. J. Chem.*, 1987, **40**, 325.

16 Butts, C. P., Eberson, L., Hartshorn, M. P., Persson, O., and Robinson, W. T., *Acta Chem. Scand.*, 1995, **49**, 253.

CHAPTER THREE

PHOTONITRATION OF 1,2,3-TRIMETHYLBENZENE, 1,2,4,5-TETRAMETHYLBENZENE, PENTAMETHYLBENZENE AND HEXAMETHYLBENZENE

3.1 Introduction

The photochemical addition of TNM to naphthalene and various methylated naphthalenes leads predominantly to adducts, which arise *via* nitro/trinitromethyl or nitrito/trinitromethyl addition across 1,2- or 1,4- bonds of the aromatic substrate.[1-8] However, in contrast to this, Masnovi *et al.*[9] reported that the photochemical reactions of 1,3,5-trimethylbenzene, 1,2,4,5-tetramethylbenzene, pentamethylbenzene, or hexamethylbenzene with TNM yield only products of $^{\bullet}NO_2$ or $(O_2N)_3C^-$ side-chain and nuclear substitution, with no indication of the formation of adducts.

Subsequently, Eberson *et al.*[10,11] investigated the photochemical reaction between benzene and TNM. They found that photolysis of benzene and TNM at +20° in dichloromethane, after 48 h, produced a reaction mixture which contained adducts (54%), trinitromethyl substitution products (26%), nitro substitution products (8%), and various phenolic products (12%).

In determining the structure of the adducts formed, the first bond formation involving reaction of $(O_2N)_3C^-$ with the aromatic radical cation is crucial.[8] It was also shown that the relative energies of the various delocalized carbon radicals are important in understanding the regio-chemistry of the photochemical reactions between aromatic compounds and TNM. The relative energies are affected both by steric interactions

between the trinitromethyl group and the remainder of the molecule, and by the extent of stabilization of the discrete carbon radical by any substituents present.

In the photochemical reaction between 1,2,3,4-tetramethylbenzene and TNM,[12,13] adduct formation occurred predominantly by attack of $(O_2N)_3C^-$ at C5 of the 1,2,3,4-tetramethylbenzene radical cation (37% from a total of 44% in dichloromethane at -50°). The remainder of adducts arose *via* attack of $(O_2N)_3C^-$ at C1 of the 1,2,3,4-tetramethylbenzene radical cation. The possible delocalized carbon radicals are outlined in Scheme 3.1. Each of the three possible delocalized carbon radicals (127)-(129)

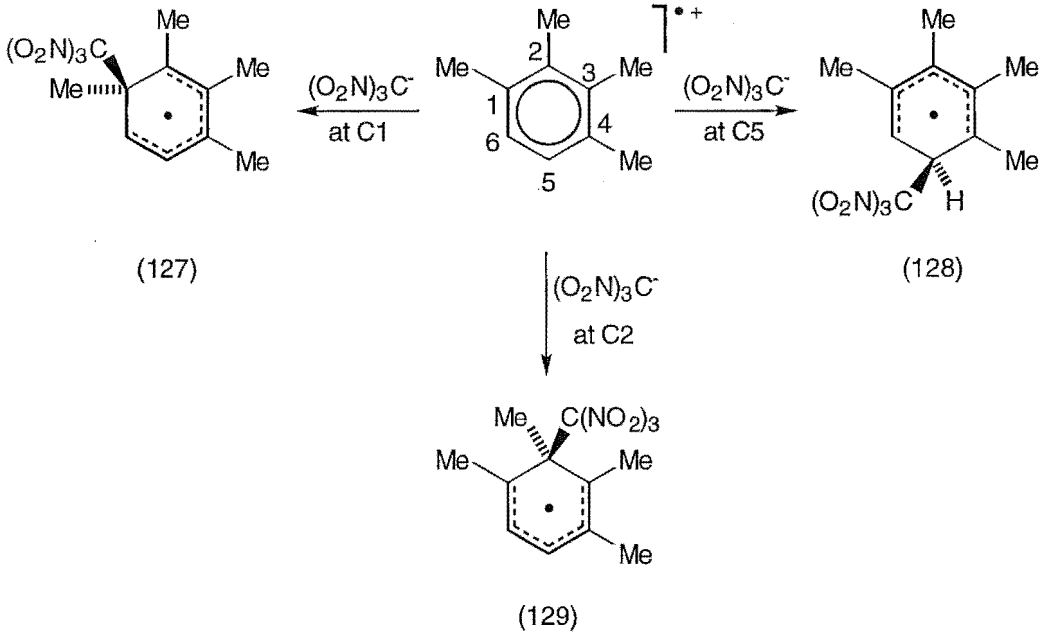

Scheme 3.1

would be stabilized by two methyl groups, hence steric interactions would determine the regiochemistry of attack of $(O_2N)_3C^-$ on the 1,2,3,4-tetramethylbenzene radical cation. Attack at C2 by $(O_2N)_3C^-$ on the 1,2,3,4-tetramethylbenzene radical cation to give radical (129) would be disfavoured due to the two β-methyl interactions with the bulky trinitromethyl

group and the steric compression arising from the *ipso*-methyl group. Radical (127), arising *via* attack of $(O_2N)_3C^-$ at C1 of the 1,2,3,4-tetramethylbenzene radical cation, would also contain some steric compression arising from the *ipso*-attachment of the bulky trinitromethyl group, but would only contain a single β-methyl interaction. It therefore appears that radical (128), arising from attack of $(O_2N)_3C^-$ at the unsubstituted C5 position on the 1,2,3,4-tetramethylbenzene radical cation, would be the most stable delocalized carbon radical with only a single β-methyl interaction.

Photolysis studies on the 1,2,3,5-tetramethylbenzene/TNM system[14] found that adduct formation resulted mainly from addition of $(O_2N)_3C^-$ at C5 on the 1,2,3,5-tetramethylbenzene radical cation (13% of adducts from a total of 15% in dichloromethane at +20°). The remainder of adducts arose *via* attack of $(O_2N)_3C^-$ at C1 on the 1,2,3,5-tetramethylbenzene radical cation. The possible initial modes of attack of $(O_2N)_3C^-$ on the 1,2,3,5-tetramethylbenzene radical cation are depicted in Scheme 3.2. Carbon radicals (130) and (131), which formed *via* attack of $(O_2N)_3C^-$ at C1 and C5

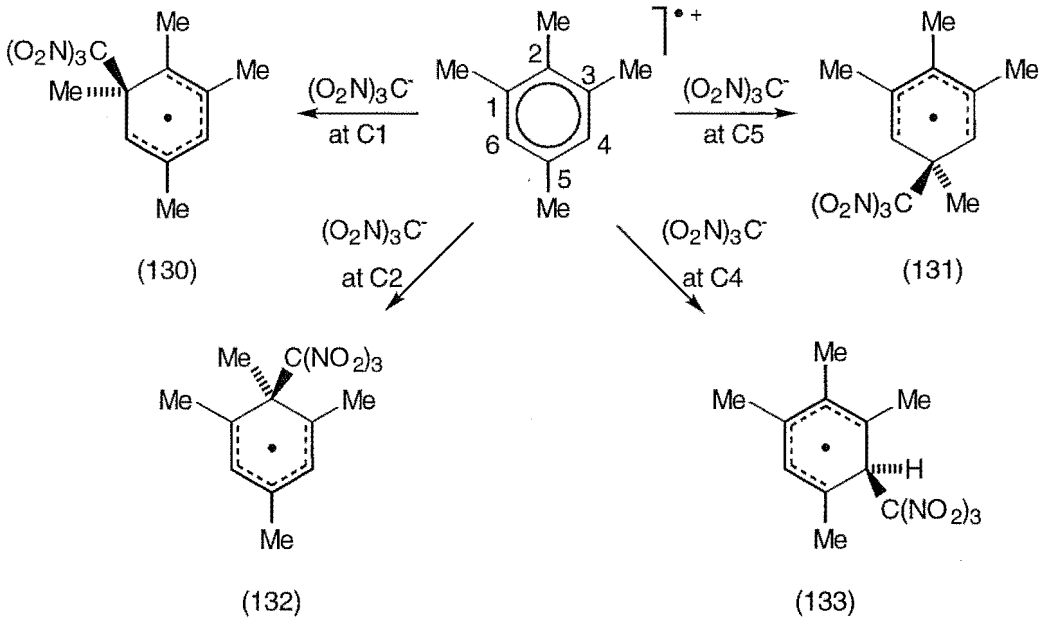

Scheme 3.2

on the 1,2,3,5-tetramethylbenzene radical cation, respectively, would each be stabilized by a single methyl group. Both radicals (130) and (131) would be destabilized by steric compression arising from the *ipso*-methyl interaction with the bulky trinitromethyl group, but radical (130) would be further destabilized due to the β-methyl interaction with the trinitromethyl group. Attack on the 1,2,3,5-tetramethylbenzene radical cation by $(O_2N)_3C^-$ at C2 and C4 would lead to the formation of radicals (132) and (133), respectively. These radicals would be expected to be less stable than radicals (130) and (131) due to the presence in each case of two β-methyl interactions with the bulky trinitromethyl group, even though they would both be stabilized by three methyl groups. Additionally, radical (132) would be further destabilized due to the presence of an *ipso*-methyl interaction with the trinitromethyl group. It therefore appears that radical (131) would be the most stable delocalized carbon radical.

The studies discussed in this Chapter aimed to gain further evidence for adduct formation in the photochemical reactions between polymethyl-substituted benzene derivatives and TNM, and to examine the regio-chemistry of attack of $(O_2N)_3C^-$ on the respective aromatic radical cations. In light of the adducts identified in the photochemical reactions between TNM and 1,2,3,4-tetramethylbenzene[12,13] and 1,2,3,5-tetramethyl-benzene,[14] the photolysis reactions of 1,2,4,5-tetramethylbenzene (134), pentamethylbenzene (135) and hexamethylbenzene (136) were re-examined carefully in anticipation that adducts might also be observed.

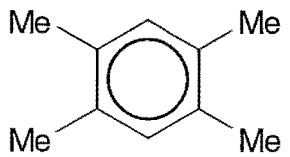

(134)

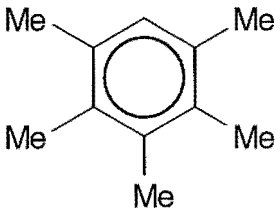

(135)

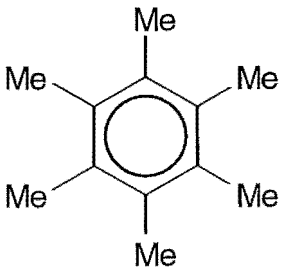

(136)

The photochemical reaction of 1,2,3-trimethylbenzene (137) was also studied in detail, after preliminary work by Young in his B.Sc. Honours III research project[15] had identified products (138) and (139) by single crystal X-ray analysis.

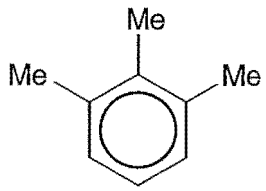

(137)

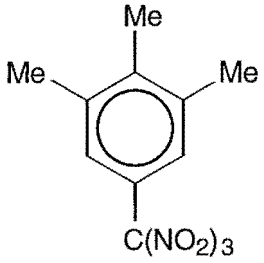

(138)

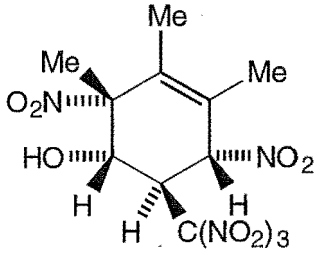

(139)

Attack of $(O_2N)_3C^-$ in the photolysis of 1,2,3-trimethylbenzene (137) with TNM was expected to occur predominantly at the unsubstituted ring position at C5 of the 1,2,3-trimethylbenzene radical cation. The potential radicals are represented in Scheme 3.3. The delocalized carbon radical (140) would form *via* initial attack of $(O_2N)_3C^-$ at C5 on the 1,2,3-trimethyl-benzene radical cation. This radical was expected to be the most likely

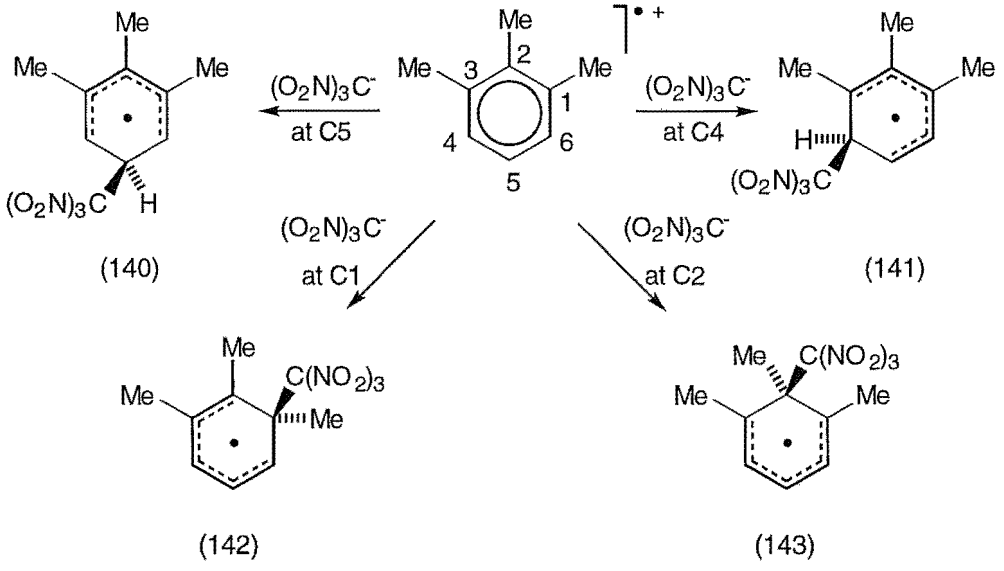

Scheme 3.3

carbon radical to form as steric interactions between the trinitromethyl group and the remainder of the molecule would be minimal, even though stabilization of the radical system would be afforded by only one methyl group. Attack of $(O_2N)_3C^-$ at C4 on the radical cation of 1,2,3-trimethylbenzene would give the delocalized radical (141), which is stabilized by two methyl groups, but its energy would be raised by the interaction between the trinitromethyl group and the neighbouring β-methyl group. Radicals (142) and (143) would be formed *via* $(O_2N)_3C^-$ attack on the 1,2,3-trimethylbenzene radical cation at C1 and C2, respectively. The energies of the delocalized carbon radicals (142) and (143) would be expected to be greater than that of carbon radical (140), as (142) and (143) would be subject to both steric compression arising from the *ipso*-attachment of the trinitromethyl group and interaction between the bulky trinitromethyl group and the β-methyl group(s).

Photolysis of the 1,2,4,5-tetramethylbenzene (134) / TNM system could generate two possible delocalized carbon radicals, (144) and (145), as summarized in Scheme 3.4. Both (144) and (145) would be stabilized

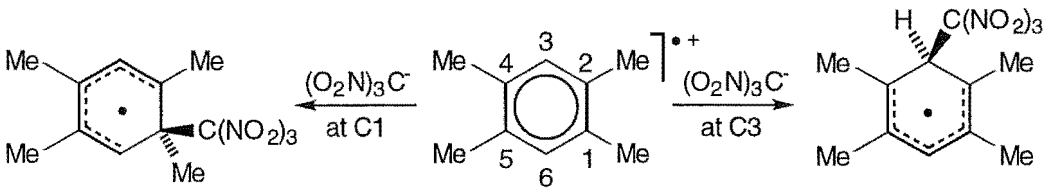

(144) (145)

Scheme 3.4

by two methyl groups and hence steric interactions would determine the radical of lower relative energy. Attack of $(O_2N)_3C^-$ at C1 on the 1,2,4,5-tetramethylbenzene radical cation would lead to the delocalized radical (144). This would be destabilized by the steric interaction between the

bulky trinitromethyl group and the *ipso*- and β-methyl groups. Radical (144) would, however, be expected to be more stable than radical (145), formed *via* attack of $(O_2N)_3C^-$ at C3 on the radical cation of 1,2,4,5-tetramethylbenzene, due to radical (145) being destabilized by two β-methyl/ trinitromethyl steric interactions.

In the photolysis of pentamethylbenzene (135) with TNM, it was expected that the delocalized radical (146), formed *via* initial attack of $(O_2N)_3C^-$ at C1 on the pentamethylbenzene radical cation, would be favoured over radicals (147)-(149) which would form after initial attack of $(O_2N)_3C^-$ at C6, C2 and C3, respectively, on the pentamethylbenzene radical cation (See Scheme 3.5). From the results of photolysis studies on

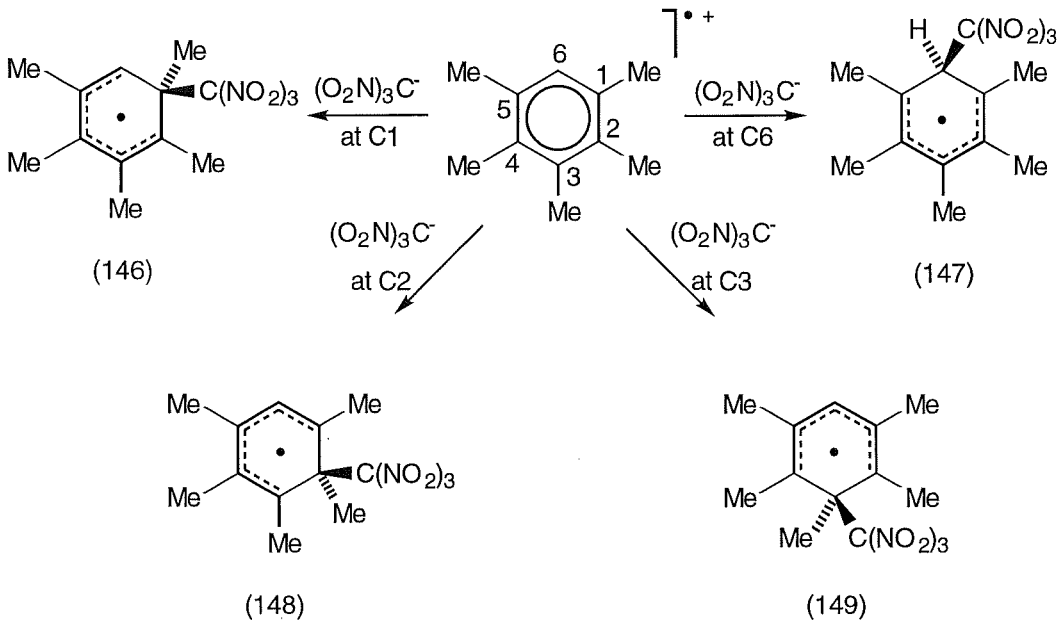

Scheme 3.5

1,2,3,4- and 1,2,3,5-tetramethylbenzene with TNM,[12-14] it appears that the β-methyl steric interactions with the trinitromethyl group are more destabilizing than the *ipso*-methyl steric interactions with the trinitromethyl group and dominate any enhanced stability conferred by suitably

positioned methyl groups. Therefore, radical (146) which would only contain one β-methyl/trinitromethyl steric interaction would be expected to be favoured over radicals (147)-(149), each of which would contain two β-methyl/trinitromethyl steric interactions.

In the photochemical reaction between hexamethylbenzene (136) and TNM, the delocalized radical (150) would be expected to be highly unstable due to severe hindrance by the two β-methyl/trinitromethyl interactions and the steric compression resulting from the *ipso*-methyl interaction with the bulky trinitromethyl group, as illustrated in Scheme 3.6.

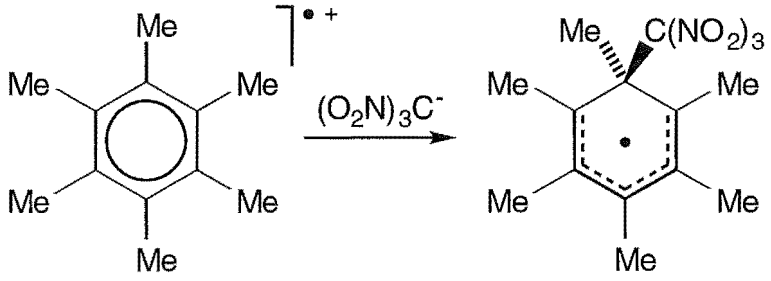

(150)

Scheme 3.6

3.2 The Photolysis of 1,2,3-Trimethylbenzene (137)

General procedure for the photonitration of 1,2,3-trimethylbenzene (137) *with TNM.*

A solution of 1,2,3-trimethylbenzene (137) (500 mg, 0.52 mol L^{-1}) and TNM (1.04 mol L^{-1}) in dichloromethane or acetonitrile (at +20, -20 or -50°) was irradiated with filtered light ($\lambda_{cut\text{-}off}$<435 nm) and small samples were withdrawn for analysis at suitable intervals. The work-up procedure, involving evaporation of solvent and TNM, was conducted at ≤0°. The crude product mixtures were stored at -20 or -78° and were analysed by ^1H

n.m.r. spectroscopy as soon as possible (For complete experimental details see Chapter 5, Section 5.3.1).

3.3 The Photochemistry of 1,2,3-Trimethylbenzene (137) in Dichloromethane

Photochemistry in dichloromethane at +20° and identification of adducts.

A solution of 1,2,3-trimethylbenzene (137) (0.52 mol L^{-1}) and TNM (1.04 mol L^{-1}) in dichloromethane was irradiated at +20° until the yellow colour of the charge-transfer band was bleached. The composition of the reaction mixture was monitored by withdrawing samples for ^1H n.m.r. spectral analysis. After work-up, the final solution (after 8 h) was shown to contain a mixture of "single" adducts (151)-(156) (total 30%), "double" adducts (137) and (157)-(162) (total 26%), nitro dienones (163) and (164) (total 1%), aromatic compounds (138) and (165)-(169) (total 42%), and other unidentified adducts (total 1%). Here the term "single" adducts refers to those products formed by a single addition of the elements of TNM to 1,2,3-trimethylbenzene (137), while the term "double" adducts refers to

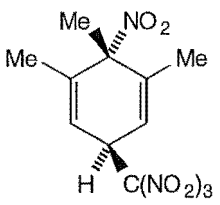

(151)

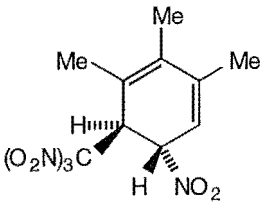

(152)

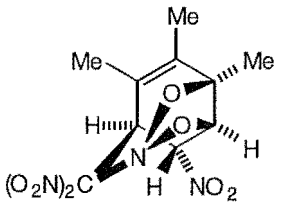

(153)

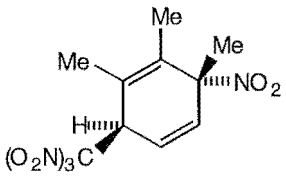

(154)

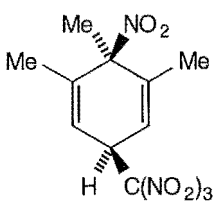

(155)

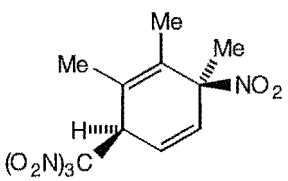

(156)

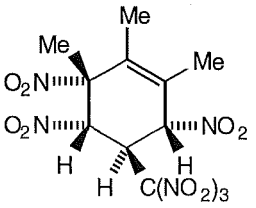

(157)

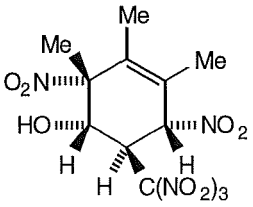

(139)

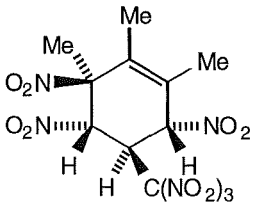

(158)

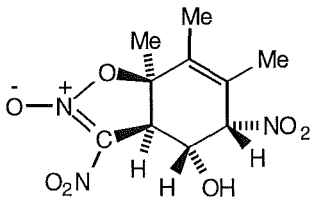

(159)

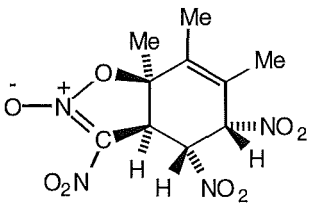

(160)

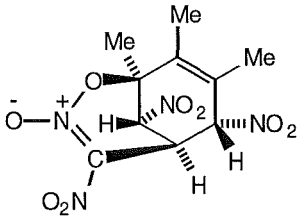

(161)

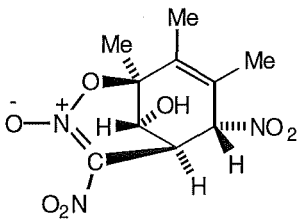

(162)

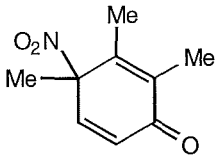

(163)

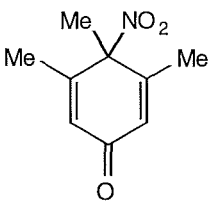

(164)

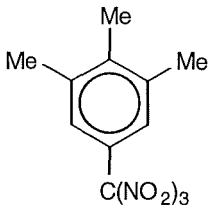

(138)

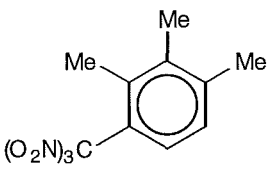

(165)

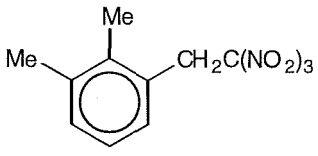

(166)

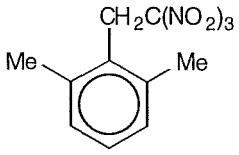

(167)

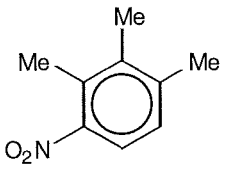

(168)

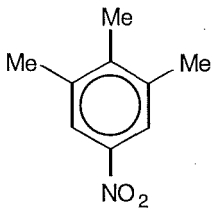

(169)

products derived by some form of extramolecular addition to initially formed "single" adducts. The components of the mixture were partially separated by h.p.l.c. on a cyanopropyl column, cooled to 0°, using hexane/dichloromethane mixtures as the eluting solvents. In the following discussion, adduct identification will be described for groups of compounds, rather than in the order of elution which is given in the Experimental section (See Chapter 5, Section 5.3.1).

"Single" adducts (151) *and* (155).

Adduct (151) was identified as an impure oil and decomposed to give the known[15] 3,4,5-trimethyl-1-trinitromethylbenzene (138) when crystallization was attempted . The identification of adduct (151) as 1,5,6-trimethyl-*t*-6-nitro-*r*-3-trinitromethylcyclohexa-1,4-diene (151) was based on: (i) a comparison of its ^{1}H and ^{13}C n.m.r. spectroscopic data with those for 1,3,5,6-tetramethyl-*t*-6-nitro-*r*-3-trinitromethylcyclohexa-1,4-diene (170), the structure of which was determined by single crystal X-ray analysis,[14] as seen in Fig. 3.1; and (ii) its conversion into 3,4,5-trimethyl-1-trinitromethylbenzene (138) on treatment with 2,6-di-*tert*-butyl-4-methylpyridine in dichloromethane, as discussed in Section 3.6. The ^{13}C n.m.r. spectra were confirmed by short range reverse detected heteronuclear correlation spectra (HMQC) and HMBC experiments. In particular, the location of the trinitromethyl function was defined by the chemical shift for C3 (δ 43.2). Furthermore, the presence of very strong infrared absorptions at 1613, 1586 and 1550 cm^{-1} provided evidence for the $-C(NO_2)_3$ and $-NO_2$ substituents. The *trans*-6-nitro-3-trinitromethyl stereochemistry was assigned to adduct (151) because it eluted from the cyanopropyl h.p.l.c. column with the dichloromethane/hexane solvent system earlier than its *cis*-6-nitro-3-trinitromethyl stereoisomer (155). The h.p.l.c. elution order for such pairs of stereoisomers is known, with *trans*-1,4-nitro/trinitromethyl adducts eluting

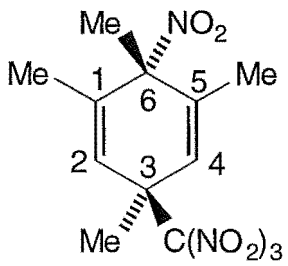

(170)

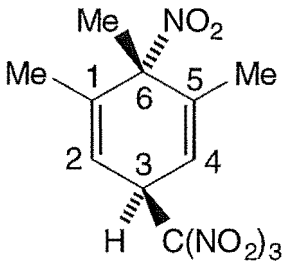

(151)

1-Me, 5-Me	1.79	1-Me, 5-Me	1.82
H2, H4	5.94	H2, H4	5.82
3-Me	1.79	H3	4.74
6-Me	1.79	6-Me	1.77
C1, C5	137.0	C1, C5	140.9
C2, C4	124.1	C2, C4	117.2
C3	47.6	C3	43.2
C6	90.9	C6	not observed

Fig. 3.1 Comparison of the characteristic ^{1}H and ^{13}C n.m.r. resonances (in ppm) for adducts (170) and (151).

ahead of their *cis*-1,4-isomers.[5-7]

Adduct (155) gave crystals of inadequate quality for single crystal X-ray analysis and its identification as 1,5,6-trimethyl-*c*-6-nitro-*r*-3-trinitromethylcyclohexa-1,4-diene (155) was based on its spectroscopic data, and its conversion into 3,4,5-trimethyl-1-trinitromethylbenzene (138) on treatment with 2,6-di-*tert*-butyl-4-methylpyridine in dichloromethane, as discussed in Section 3.6. N.O.e. experiments confirmed the assignments of the chemical shifts for the protons. Specifically, irradiation at δ 5.75 (H2,

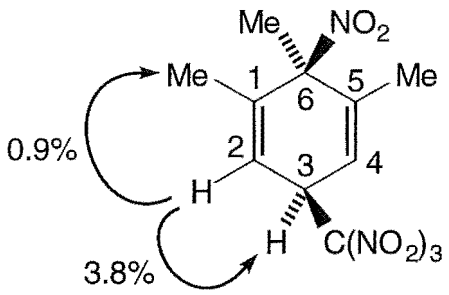

(155)

1-Me, 5-Me	1.83	C1, C5	139.7
H2, H4	5.75	C2, C4	116.8
H3	4.61	C3	42.0
6-Me	1.77	C6	90.0

Fig. 3.2 Characteristic ^{1}H and ^{13}C n.m.r. resonances (in ppm) and enhancements (%) from a selected n.O.e. experiment for adduct (155).

H4) gave enhancements at δ 1.83 (1-Me, 5-Me) and at δ 4.61 (H3), as shown in Fig. 3.2. HMQC and HMBC experiments allowed the complete assignment of the ^{13}C n.m.r. spectra, also seen in Fig. 3.2. In particular, the nitro function attached to C6 appeared at δ 90.0, while the trinitromethyl function attached to C3 appeared at δ 42.0. The closely similar spectroscopic data for compounds (151) and (155) are presented in Fig. 3.3, and were consistent with their assignment as epimers.

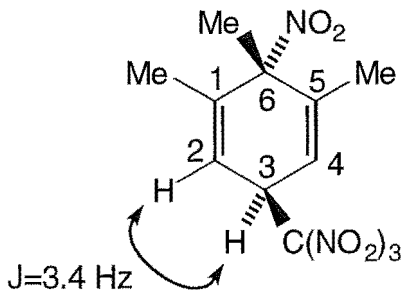

(151)

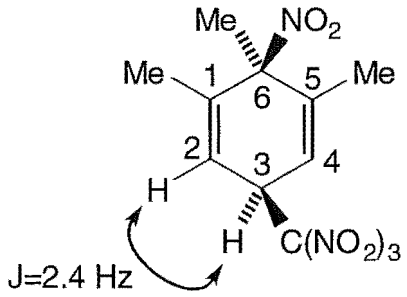

(155)

1-Me, 5-Me	1.82	1-Me, 5-Me	1.83
H2, H4	5.82	H2, H4	5.75
H3	4.74	H3	4.61
6-Me	1.77	6-Me	1.77
C1, C5	140.9	C1, C5	139.7
C2, C4	117.2	C2, C4	116.8
C3	43.2	C3	42.0
C6	not observed	C6	90.0

Fig. 3.3 Comparison of the characteristic ^{1}H and ^{13}C n.m.r. resonances (in ppm) and coupling constants for adducts (151) and (155).

Single adducts (154) *and* (156).

Adduct (154) was isolated only as an oil containing an impurity (*c.* 5%) and was identified as 1,2,3-trimethyl-*r*-3-nitro-*t*-6-trinitromethyl-cyclohexa-1,4-diene (154) on the basis of its spectroscopic data, and its conversion into 2,3,4-trimethyl-1-trinitromethylbenzene (165) on treatment with 2,6-di-*tert*-butyl-4-methylpyridine in dichloromethane, as discussed in Section 3.6. N.O.e. experiments confirmed the assignments of the

chemical shifts for the protons. Specifically, irradiation at δ 4.89 (H6) gave enhancements at δ 1.81 (1-Me) and at δ 6.24 (H5), while irradiation at δ 6.21 (H4) gave an enhancement at δ 1.74 (3-Me), as observed in Fig. 3.4. HMQC and HMBC experiments confirmed the assignments of the ^{13}C n.m.r. resonances, also illustrated in Fig. 3.4. In particular, the **C**H-C$(NO_2)_3$ resonance appeared at δ 47.6, while the **C**Me-NO_2 resonance appeared at δ 88.8. The *trans*-3-nitro-6-trinitromethyl stereochemistry was assigned to adduct (154) because it eluted earlier than its *cis*-3-nitro-6-trinitromethyl stereoisomer (156), and the h.p.l.c. elution order for such pairs of stereoisomers is known from previous examples.[5-7]

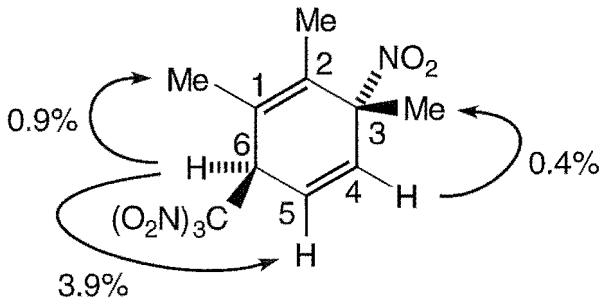

(154)

1-Me	1.81	C1	123.2
2-Me	1.75	C2	135.4
3-Me	1.74	C3	88.8
H4	6.21	C4	121.7
H5	6.24	C5	135.5
H6	4.89	C6	47.6

Fig. 3.4 · Characteristic ^{1}H and ^{13}C n.m.r. resonances (in ppm) and enhancements (%) from selected n.O.e. experiments for adduct (154).

Adduct (156) was identified as 1,2,3-trimethyl-*r*-3-nitro-*c*-6-trinitromethylcyclohexa-1,4-diene (156), but could not be induced to give crystals of adequate quality for single crystal X-ray analysis. Its identification was based on its spectroscopic data, and its conversion into 2,3,4-trimethyl-1-trinitromethylbenzene (165) on treatment with 2,6-di-*tert*-butyl-4-methylpyridine in dichloromethane, as discussed in Section 3.6. N.O.e. experiments confirmed the assignments of the chemical shifts for the protons. In particular, irradiation at δ 4.79 (H6) gave enhancements at δ 1.81 (1-Me) and at δ 6.24 (H5), while irradiation at δ 6.30 (H4) gave enhancement at δ 1.77 (3-Me), as seen in Fig. 3.5. Furthermore, the nitro

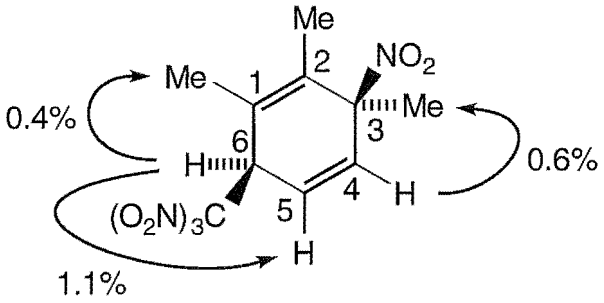

(156)

1-Me	1.81	C1	124.1
2-Me	1.89	C2	134.8
3-Me	1.77	C3	86.7
H4	6.30	C4	134.9
H5	6.24	C5	122.3
H6	4.79	C6	47.0

Fig. 3.5 Characteristic ^{1}H and ^{13}C n.m.r. resonances (in ppm) and enhancements (%) from selected n.O.e. experiments for adduct (156).

function was indicated by the ^{13}C n.m.r. chemical shift for C3 (δ 86.7) and the trinitromethyl function by the ^{13}C n.m.r. chemical shift for C6 (δ 47.0), also shown in Fig. 3.5. These assignments were confirmed by HMQC and HMBC experiments. Comparison of the characteristic spectroscopic data for adducts (156) and (154) is depicted in Fig. 3.6. The closely similar data are consistent with their assignment as epimers.

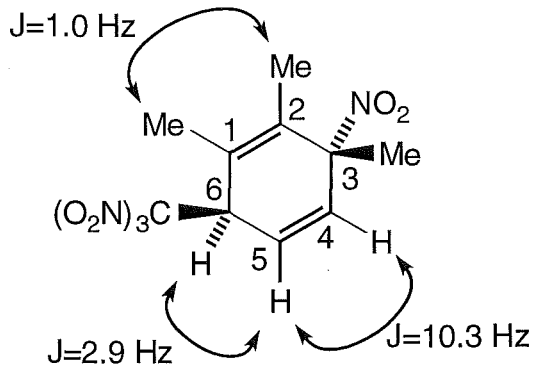

(154)

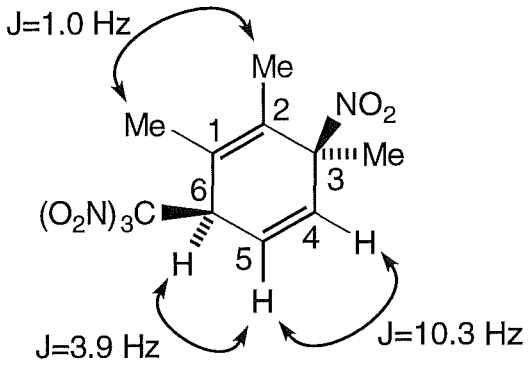

(156)

3-Me	1.74	3-Me	1.77
H4	6.21	H4	6.30
H5	6.24	H5	6.24
H6	4.89	H6	4.79
C3	88.8	C3	86.7
C4	121.7	C4	134.9
C5	135.5	C5	122.3
C6	47.6	C6	47.0

Fig. 3.6 Comparison of the characteristic ^{1}H and ^{13}C n.m.r. resonances (in ppm) and coupling constants for adducts (154) and (156).

"Single" adduct (152) *and its cycloaddition product* (153).

Adduct (152) was isolated only in admixture with adducts (151) and (154), above, and traces of its related nitro cycloadduct (153). The identity of adduct (152) as 1,2,3-trimethyl-*r*-5-nitro-*t*-6-trinitromethylcyclohexa-1,3-diene (152) was assigned on the basis of its spectroscopic data, and its conversion into the nitro cycloadduct (153) (See below and Section 3.7). N.O.e. experiments confirmed the assignments of the chemical shifts for the protons. In particular, irradiation at δ 5.11 (H4) gave enhancements at δ 1.78 (3-Me) and at δ 5.36 (H5), while irradiation at δ 5.60 (H6) gave enhancements at δ 1.90 (1-Me) and at δ 5.36 (H5), as represented in Fig. 3.7.

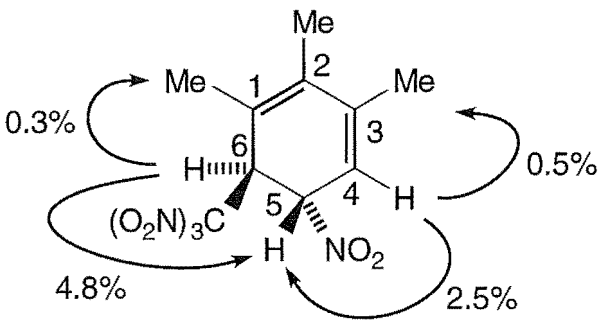

Fig. 3.7 Enhancements (%) from selected n.O.e. experiments for adduct (152).

The structure of the nitro cycloadduct (153) was determined by single crystal X-ray analysis. A perspective drawing of the nitro cycloadduct (153), $C_{10}H_{12}N_4O_8$, m.p. 163° (dec.) is presented in Fig. 3.8, and corresponding atomic coordinates are given in Table 5.11 (See Chapter 5, Section 5.5). In (153), N(3) is clearly trigonal pyramidal and bond length differences [C(7)-N(1) 1.532(4) Å, C(7)-N(2) 1.553(4) Å, C(7)-N(3) 1.490(4) Å] are similar to those observed earlier for analogous heterocyclic cage structures. Specifically, (153) is similar to cycloadducts (101) and (104)

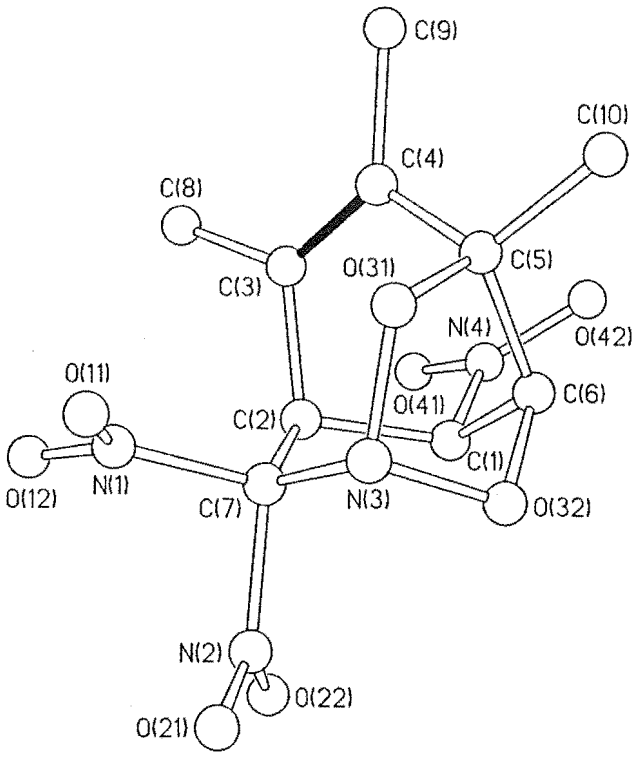

Fig. 3.8 Perspective drawing of nitro cycloadduct (153).

[formed in the photolysis of 2,6-dimethylnaphthalene (57) / TNM], structures (112), (115) and (122) [formed in the photolysis of 1,3-dimethylnaphthalene (58) / TNM], and other examples.[4-7,12] The spectroscopic data for the nitro cycloadduct (153) were in accord with the established structure. N.O.e. experiments confirmed the assignments of the chemical shifts for the protons. In particular, irradiation at δ 4.60 (H6) gave enhancements at δ 1.80 (1-Me) and at δ 5.51 (H5), while irradiation at δ 5.27 (H4) gave enhancements at δ 1.67 (3-Me) and at δ 5.51 (H5), as outlined in Fig. 3.9. The characteristic ^{1}H and ^{13}C n.m.r. data are also seen in Fig. 3.9. Specifically, ^{13}C n.m.r. resonances for the nitro function attached to C5 appeared at δ 79.7, while the cyclized trinitromethyl function attached to C6 appeared at δ 45.2. These assignments were confirmed by HMQC and HMBC experiments. The stereochemistry of the *r*-5-nitro-*t*-6-trinitromethyl system in adduct (152) is established by the observed torsional angle in

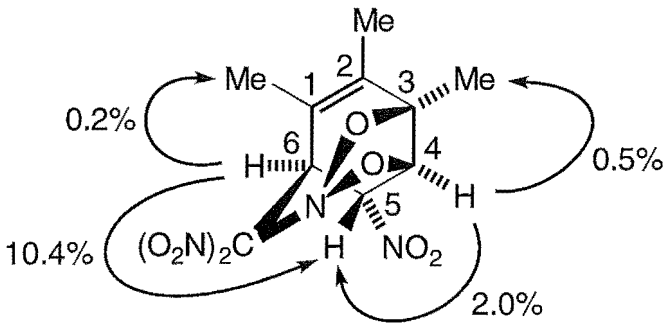

(153)

1-Me	1.80	C1	128.5
2-Me	1.75	C2	140.1
3-Me	1.67	C3	87.4
H4	5.27	C4	81.4
H5	5.51	C5	79.7
H6	4.60	C6	45.2

Fig. 3.9 Characteristic ^{1}H and ^{13}C n.m.r. resonances (in ppm) and enhancements (%) from selected n.O.e. experiments for nitro cycloadduct (153).

nitro cycloadduct (153), C(7)-C(2)-C(1)-N(4) -169.3(2)°. The heterocyclic structure in nitro cycloadduct (153) is clearly formed by thermal cycloaddition of a nitro group of the trinitromethyl group with the C3-C4 alkene system in the nitro/trinitromethyl precursor (152).

"Double" adducts, trinitro/trinitromethyl adducts (157) *and* (158).

The structure of trinitro/trinitromethyl adduct (157) was determined by single crystal X-ray analysis. A perspective drawing of 1,2,3-trimethyl-*r*-3, *c*-4,*c*-6-trinitro-*t*-5-trinitromethylcyclohex-1-ene (157), $C_{10}H_{12}N_6O_{12}$, m.p. 73° (dec.), is presented in Fig. 3.10, and corresponding atomic coordinates

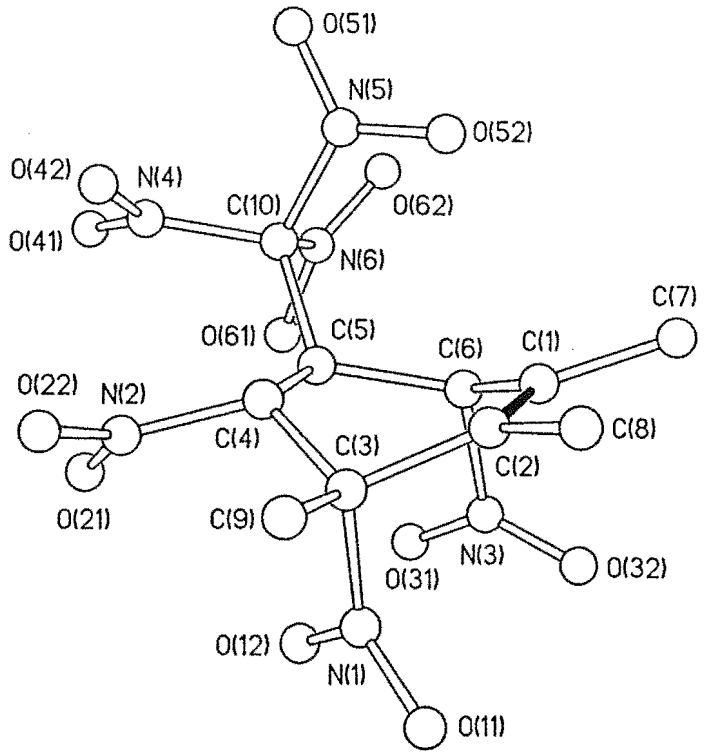

Fig. 3.10 Perspective drawing of "double" adduct (157). Double bond shown in black.

are given in Table 5.12 (See Chapter 5, Section 5.5). In the solid state the alicyclic ring of the trinitro/trinitromethyl compound (157) exists in close to a "pure" boat conformation [torsional angles: C(1)-C(2)-C(3)-C(4) -43.1(4)°; C(2)-C(1)-C(6)-C(5) 34.4(4)°; C(3)-C(4)-C(5)-C(6) -21.8(4)°], with the nitro groups at C(3) and C(6) in the flagpole orientations. The planes of these nitro groups are essentially parallel to each other [torsional angles: C(4)-C(3)-N(1)-O(12) -2.3(4)°; C(5)-C(6)-N(3)-O(31) 31.0(4)°]. The remaining stereochemistry of the trinitro/trinitromethyl adduct (157) is defined by the torsional angles: C(10)-C(5)-C(6)-N(3) -126.0(3)°; C(10)-C(5)-C(4)-N(2) 82.8(3)°; N(1)-C(3)-C(4)-N(2) 62.8(3)°. The spectroscopic data for the trinitro/trinitromethyl adduct (157) were in accord with the established structure. N.O.e. experiments confirmed the assignments of the chemical shifts for the protons. Specifically, irradiation

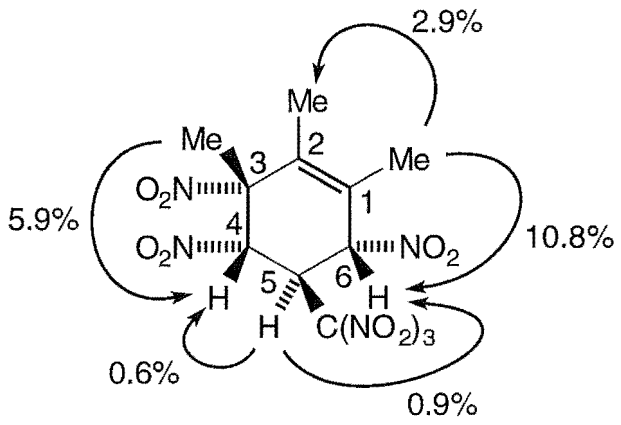

(157)

1-Me	2.185	C1	132.5
2-Me	2.03	C2	130.2
3-Me	2.19	C3	87.8
H4	5.10	C4	82.7
H5	6.62	C5	42.7
H6	5.01	C6	85.5

Fig. 3.11 Characteristic ^{1}H and ^{13}C n.m.r. resonances (in ppm) and enhancements (%) from selected n.O.e. experiments for "double" adduct (157).

at δ 2.19 (1-Me and 3-Me) gave enhancements at δ 2.03 (2-Me), at δ 5.01 (H6) and at δ 5.10 (H4), while irradiation at δ 6.62 (H5) gave enhancements at δ 5.01 (H6) and at δ 5.10 (H4), as presented in Fig. 3.11. Notable among these data was the chemical shift observed for H5 (δ 6.62), remarkably deshielded for a proton *ipso* to a trinitromethyl group. Consideration of the established X-ray structure for the trinitro/trinitromethyl adduct (157) revealed the origin of this marked deshielding, H5 being "sandwiched" between oxygen atoms, O(12), O(21), O(31) and O(61), of four proximate

nitro functions. HMQC and HMBC experiments confirmed the assignments of the ^{13}C n.m.r. resonances (See summary in Fig. 3.11). In particular, the locations of the nitro functions were defined by the chemical shifts for C3 (δ 87.8), C4 (δ 82.7) and C6 (δ 85.5), while the trinitromethyl function was defined by the chemical shift for C5 (δ 42.7).

The second trinitro/trinitromethyl adduct (158) could not be induced to crystallize and was identified as 1,2,3-trimethyl-*r*-3,*t*-4,*t*-6-trinitro-*c*-5-trinitromethylcyclohex-1-ene (158), the epimer of the trinitro/trinitromethyl adduct (157) at C3, on the basis of its ^{1}H and ^{13}C n.m.r. spectra. N.O.e. experiments confirmed the assignments of the chemical shifts for the protons. In particular, irradiation at δ 1.74 (3-Me) gave enhancement at δ 1.93 (2-Me), irradiation at δ 5.92 (H4) gave enhancements at δ 1.74 (3-Me) and at δ 4.88 (H5), and irradiation at δ 5.81 (H6) gave enhancements at δ 1.96 (1-Me) and at δ 4.88 (H5), as observed in Fig. 3.12.

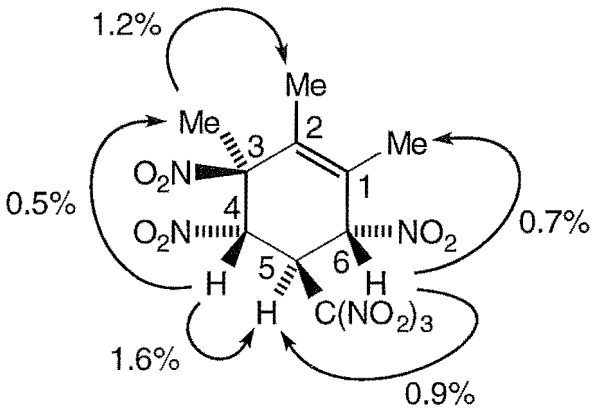

Fig. 3.12 Enhancements (%) from selected n.O.e. experiments for "double" adduct (158).

The assignment of the ^{13}C n.m.r. resonances were confirmed by HMQC and HMBC experiments, which pointed to the presence of nitro groups at C3 (δ 81.1), at C4 (δ 78.6) and at C6 (δ 84.1), in addition to a trinitromethyl group at C5 (δ 46.7), as illustrated in Fig. 3.13. The spectroscopic data

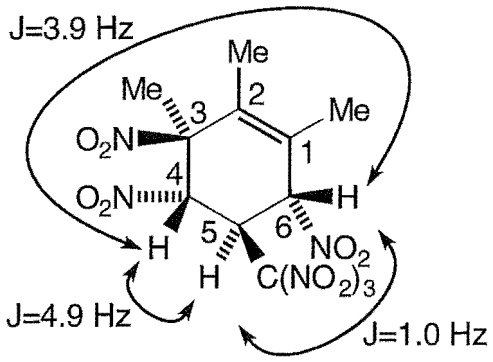

(158)

1-Me	1.96	C1	124.1
2-Me	1.93	C2	132.9
3-Me	1.74	C3	81.1
H4	5.92	C4	78.6
H5	4.88	C5	46.7
H6	5.81	C6	84.1

Fig. 3.13 Characteristic ^1H and ^{13}C n.m.r. resonances (in ppm) and coupling constants for "double" adduct (158).

which were the most informative about the stereochemistry of adduct (158) were the combination of a W-coupling between H4 and H6 ($J_{H4,H6}$ 3.9 Hz), the coupling constants $J_{H4,H5}$ 4.9 Hz and $J_{H5,H6}$ 1.0 Hz (see Fig. 3.13), and the absence of a significant n.O.e. of H4 (δ 5.92) on irradiation of the 3-Me resonance at δ 1.74. These data pointed to a structure for trinitro/trinitro-methyl adduct (158) in which the alicyclic ring existed in a flattened skew boat (C1 and C2, sp^2), with the substituents at C3 and C4 eclipsed. In this conformation the C5-$C(NO_2)_3$ bond was close to *anti*-coplanar with the C4-NO_2 and C6-NO_2 bonds.

"Double" adduct, hydroxy/dinitro/trinitromethyl adduct (139).

Adduct (139) was identified as the known[15] 2,3,4-trimethyl-*c*-2,*c*-5-dinitro-*t*-6-trinitromethylcyclohex-3-en-*r*-1-ol (139), previously identified by single crystal X-ray analysis.

"Double" adducts, nitronic esters (159)-(162).

The structure of the nitronic ester (161) was determined by single crystal X-ray analysis. A perspective drawing of the trinitro nitronic ester (161), $C_{10}H_{12}N_4O_8$, m.p. 131-132.5°, is presented in Fig. 3.14, and corresponding atomic coordinates are given in Table 5.13 (See Chapter 5, Section 5.5). In the solid state, the plane of the N(2)-nitro group is close to eclipsed with the N(1)-C(7) bond [torsional angle: N(1)-C(7)-N(2)-O(21) -20.7(6) °]. The spectroscopic data for adduct (161) were in accord with the

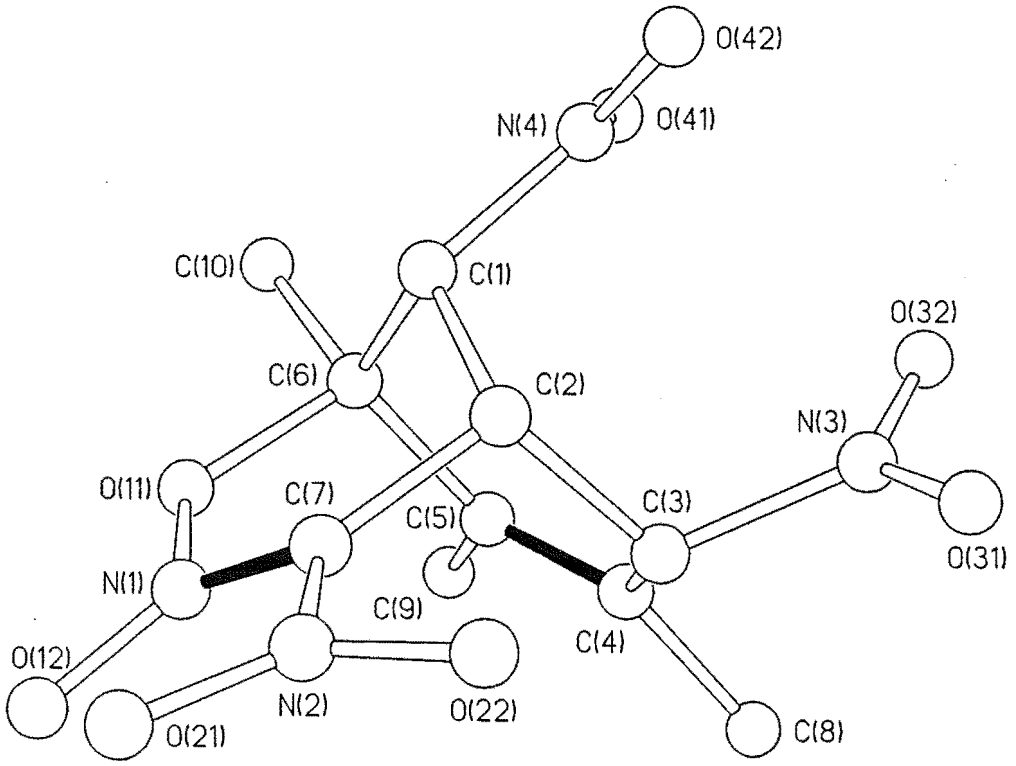

Fig. 3.14 Perspective drawing of "double" adduct (161). Double bonds shown in black.

established structure. The trinitro nitronic ester (161) was highly insoluble in (D)chloroform and hence the ^{1}H and ^{13}C n.m.r. spectra were run in (D_3)acetonitrile and the characteristic data are illustrated in Fig. 3.15. N.O.e. experiments confirmed the assignments of the chemical shifts for the protons. In particular, irradiation at δ 1.88 (3-Me) gave enhancement at δ 5.40 (H4), while irradiation at δ 2.22 (1-Me and 2-Me) gave enhancement at δ 5.34 (H6), also seen in Fig. 3.15. Furthermore, the nitro functions were indicated by the ^{13}C n.m.r. chemical shifts for C4 (δ 78.9) and C6 (δ 83.3), while the cyclized dinitromethyl function was indicated by the ^{13}C n.m.r chemical shift for C5 (δ 38.7). These assignments were confirmed by HMQC and HMBC experiments.

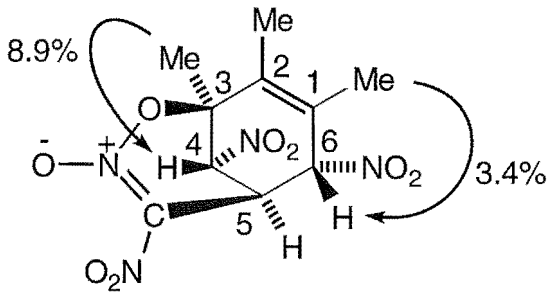

(161)

1-Me	2.22	C1	127.6
2-Me	2.22	C2	133.5
3-Me	1.88	C3	84.0
H4	5.40	C4	78.9
H5	5.29	C5	38.7
H6	5.34	C6	83.3

Fig. 3.15 Characteristic ^{1}H and ^{13}C n.m.r. resonances (in ppm) and enhancements (%) from selected n.O.e. experiments for "double" adduct (161).

The structure of the nitronic ester (162) was also determined by single crystal X-ray analysis. A perspective drawing of the hydroxy dinitro nitronic ester (162), $C_{10}H_{13}N_3O_7$, m.p. 129°, is presented in Fig. 3.16, and corresponding atomic coordinates are given in Table 5.14 (See Chapter 5, Section 5.5). The hydroxy dinitro nitronic ester (162) is closely similar to the trinitro nitronic ester (161) with the most significant difference being in the orientation of the plane of the N(3)-nitro group, which presumably reflects the replacement of the C(1)-NO_2 in the trinitro nitronic ester (161) by the C(1)-OH in the hydroxy dinitro nitronic ester (162). Similar to "double" adduct (161) the plane of the N(2)-nitro group is close to eclipsed with the N(1)-C(7) bond [torsional angle: N(1)-C(7)-N(2)-O(21) -24.4(2) °]. The spectroscopic data for (162) were in accord with the established structure. N.O.e. experiments confirmed the assignments of the chemical shifts for the

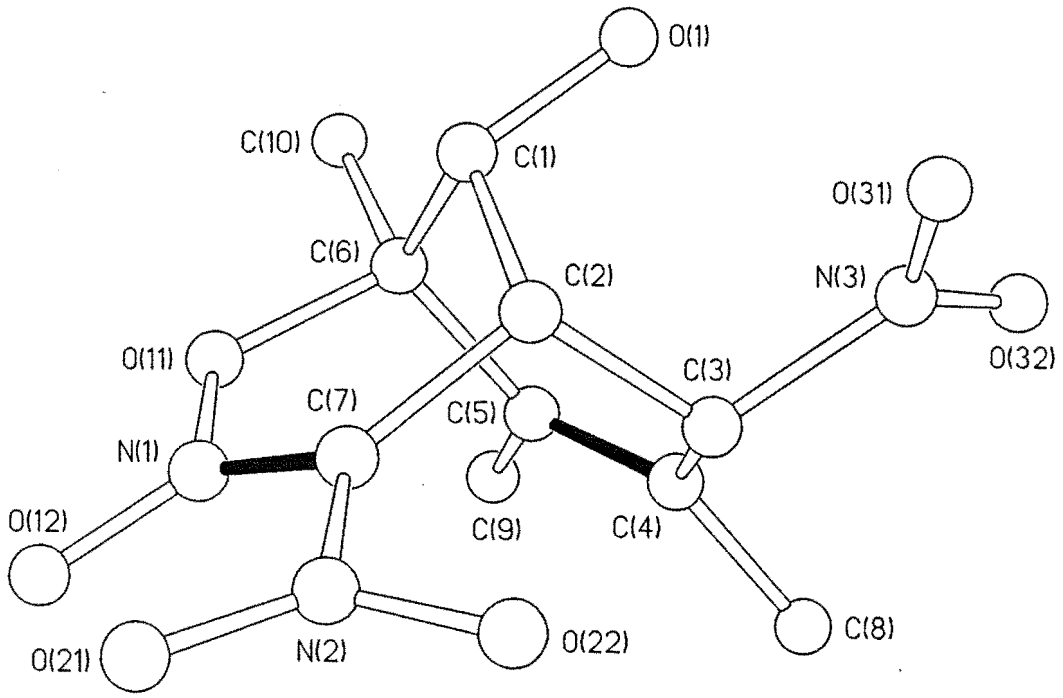

Fig. 3.16 Perspective drawing of "double" adduct (162). Double bonds shown in black.

protons. Specifically, irradiation at δ 1.63 (3-Me) gave enhancements at δ 1.90 (2-Me) and at δ 4.30 (H4), irradiation at δ 4.80 (H5) gave enhancements at δ 4.30 (H4) and at δ 4.91 (H6), and irradiation at δ 2.01 (1-Me) gave enhancement at δ 4.91 (H6), as seen in Fig. 3.16. The characteristic ^{1}H and ^{13}C n.m.r. data are also presented in Fig. 3.16. In particular, ^{13}C n.m.r resonances for the hydroxy function attached to C4 appeared at δ 66.3, the nitro function attached to C6 appeared at δ 82.4, and the cyclized dinitromethyl function attached to C5 appeared at δ 40.1. These assignments were confirmed by HMQC and HMBC experiments.

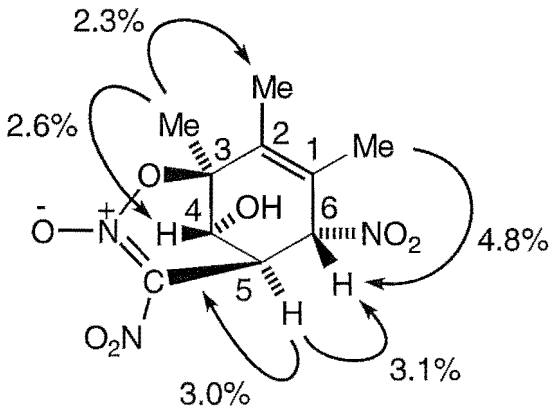

(162)

1-Me	2.01	C1	126.3
2-Me	1.90	C2	131.5
3-Me	1.63	C3	85.4
H4	4.30	C4	66.3
H5	4.80	C5	40.1
H6	4.91	C6	82.4

Fig. 3.17 Characteristic ^{1}H and ^{13}C n.m.r. resonances (in ppm) and enhancements (%) from selected n.O.e. experiments for "double" adduct (162).

The nitronic ester (160) gave a crystal of barely acceptable quality for attempted structure determination by single crystal X-ray analysis. The structure of the trinitro nitronic ester (160) was indicated by the preliminary results of a single crystal X-ray analysis [See Chapter 5, Section 5.5 (a) for the crystal data for a poor quality crystal of trinitro nitronic ester (160)]. Due to apparent disorder in the crystal involving solvent molecules, it was not possible to refine the data to a satisfactory *R*-factor, but the important features of the structure were secured. A perspective drawing of the trinitro nitronic ester (160) is presented in Fig. 3.18. The spectroscopic data for the trinitro nitronic ester (160) were in accord with the established structure. N.O.e. experiments confirmed the assignments of the chemical shifts for the protons. Specifically, irradiation at δ 5.16 (H4) gave enhancement at δ 1.92 (3-Me), while irradiation at δ 5.52 (H6) gave enhancements at δ 2.03 (1-Me)

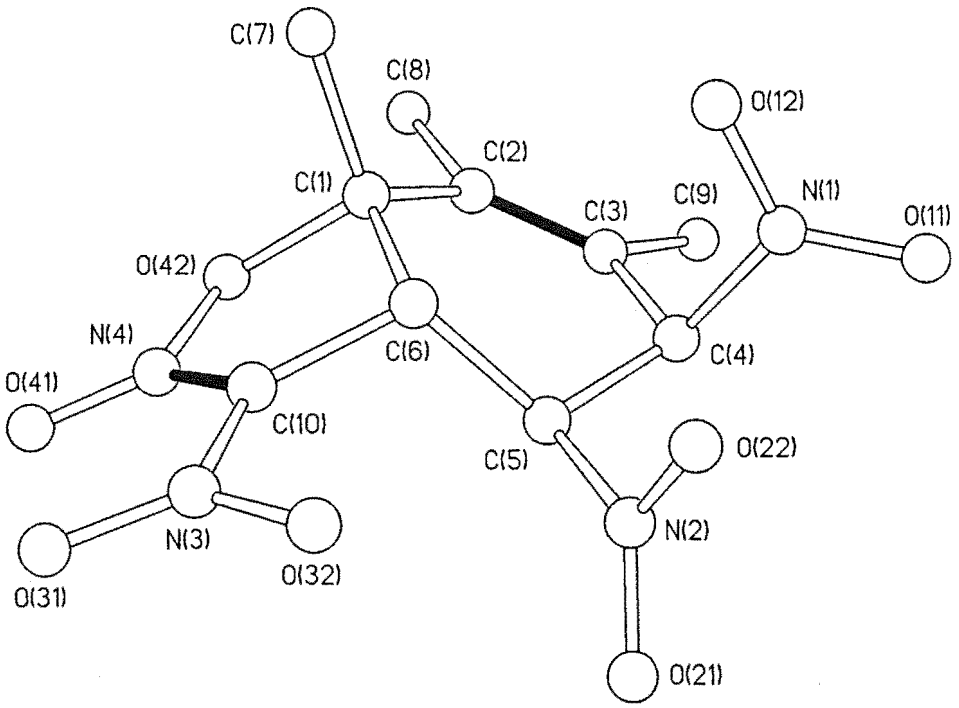

Fig. 3.18 Perspective drawing of "double" adduct (160). Double bonds shown in black.

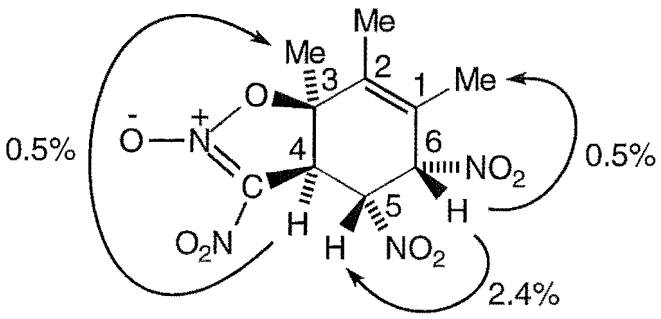

Fig. 3.19 Enhancements (%) from selected n.O.e. experiments for "double" adduct (160).

and at δ 5.12 (H5), as depicted in Fig. 3.19. In the perspective drawing shown in Fig. 3.18, the *anti*-orientation of H(5)-C(5)-C(6)-H(6) was reflected in the coupling constant ($J_{H4,H5}$ 11.7 Hz), and the gauche relationship of H(4) and H(5) in the coupling constant ($J_{H5,H6}$ 3.5 Hz), as shown in Fig. 3.20. Also summarized in Fig. 3.20 are the characteristic ^{13}C n.m.r.

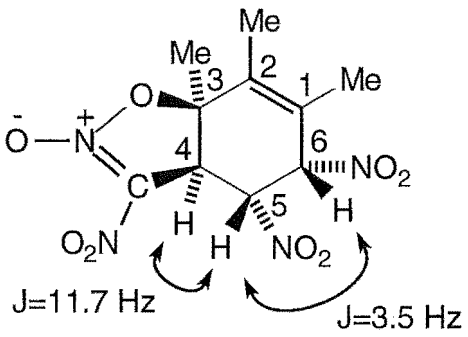

(160)

H4	5.16	C4	44.9
H5	5.12	C5	80.7
H6	5.52	C6	84.2

Fig. 3.20 Characteristic ^{1}H and ^{13}C n.m.r. resonances (in ppm) and coupling constants for "double" adduct (160).

resonances, which were confirmed by an HMQC experiment. In particular, the locations of the nitro functions were defined by the chemical shifts for C5 (δ 80.7) and C6 (δ 84.2), while the cyclized dinitromethyl function was defined by the chemical shift for C4 (δ 44.9).

The "double" adduct (159) was isolated only as an oil, but was identified as the hydroxy dinitro nitronic ester (159) based on a comparison of its spectroscopic data with the stereochemically related trinitro nitronic ester (160). N.O.e. experiments confirmed the assignments of the chemical shifts for the protons. Specifically, irradiation at δ 4.31 (H4) gave enhancement at δ 1.85 (3-Me), while irradiation at δ 5.23 (H6) gave enhancements at δ 1.93 (1-Me) and at δ 4.40 (H5), as represented in Fig. 3.21. Comparisons of the characteristic ^{1}H and ^{13}C n.m.r. data are

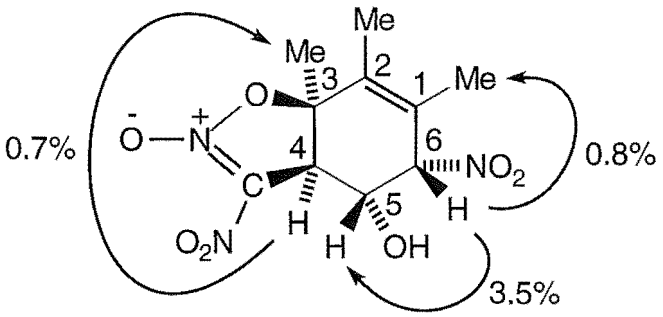

Fig. 3.21 Enhancements (%) from selected n.O.e. experiments for "double" adduct (159).

summarised in Fig. 3.22. In particular, the crucial coupling constants, $J_{H4,H5}$ 10.3 Hz, $J_{H5,H6}$ 4.4 Hz, are closely similar to those for the trinitro nitronic ester (160). The general upfield shift of all resonances in the ^{1}H n.m.r. spectrum of the hydroxy dinitro nitronic ester (159), relative to those for the trinitro nitronic ester (160), are as expected for the replacement of the 5-NO_2 [in (160)] by the 5-OH [in (159)]. The ^{13}C n.m.r. resonances were confirmed by HMQC and HMBC experiments. In particular, the locations of

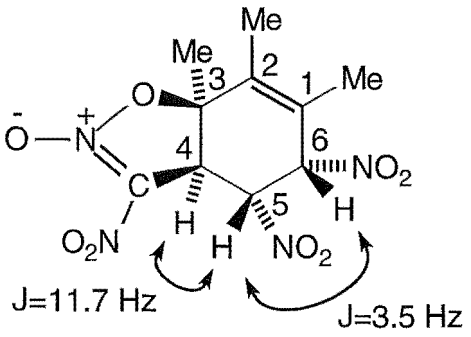

(160)

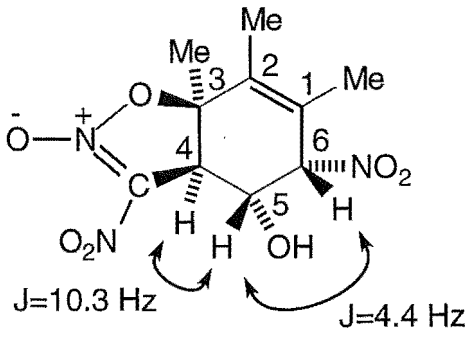

(159)

1-Me	2.03	1-Me	1.93
2-Me	1.91	2-Me	1.87
3-Me	1.92	3-Me	1.85
H4	5.16	H4	4.31
H5	5.12	H5	4.40
H6	5.52	H6	5.23
C4	44.9	C4	48.6
C5	80.7	C5	67.8
C6	84.2	C6	88.8

Fig. 3.22 Comparison of the characteristic ^{1}H and ^{13}C n.m.r. resonances (in ppm) and coupling constants for "double" adducts (160) and (159).

the hydroxy, nitro and cyclized dinitromethyl functions were defined by the chemical shifts for C5 (δ 67.8), C6 (δ 88.8) and C4 (δ 48.6), respectively. Furthermore, a strong infrared absorption at 3511 cm^{-1} provided evidence for the -OH substituent.

Aromatic products.

The ring-substituted trinitromethyl aromatic compound (138) was isolated by chromatography on a silica gel Chromatotron plate after being eluted in the first fraction from h.p.l.c. Compound (138) was identified as the known[15] 3,4,5-trimethyl-1-trinitromethylbenzene (138), previously identified by single crystal X-ray analysis.

The isomeric ring-substituted trinitromethyl aromatic compound (165) was also isolated by chromatography on a silica gel Chromatotron plate after being eluted in the first fraction from h.p.l.c., and was identified as 2,3,4-trimethyl-1-trinitromethylbenzene (165). The trinitromethyl aromatic compound (165) could be isolated only in admixture with the isomeric trinitromethyl compound (138), above, but its structure was established from a consideration of its spectroscopic data and comparison with similar data for its isomer (138). N.O.e. experiments confirmed the assignments of the chemical shifts for the protons. In particular, irradiation at δ 2.04 (2-Me) gave enhancement at δ 2.26 (3-Me), while irradiation at δ 7.19 (H5) gave enhancements at δ 2.40 (4-Me) and at δ 6.99 (H6), as represented in Fig. 3.23. Furthermore, the trinitromethyl function was indicated by the ^{13}C n.m.r. resonance for C1 (δ 119.8), which was closely similar to the isomeric

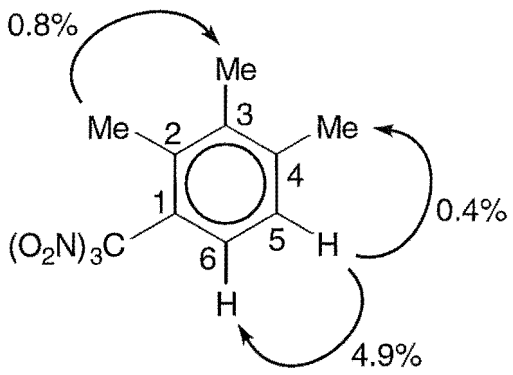

Fig. 3.23 Enhancements (%) from selected n.O.e. experiments for the trinitromethyl aromatic (165).

trinitromethyl compound (138), in which the trinitromethyl function was indicated by the ^{13}C n.m.r. resonance for C1 (δ 119.0), as represented in Fig. 3.24. These assignments were confirmed by HMQC and HMBC experiments. Additionally, compound (165) was formed from the base catalysed decomposition of "single" adducts (154) and (156) after reaction with 2,6-di-*tert*-butyl-4-methylpyridine in dichloromethane (See Section 3.6).

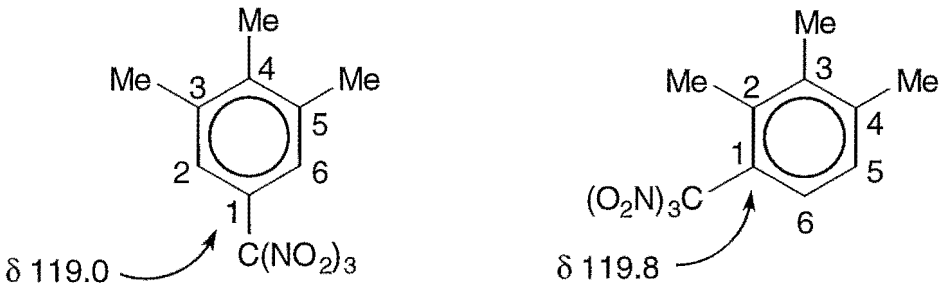

(138) (165)

Fig. 3.24 Comparison of the characteristic ^{13}C n.m.r. resonances (in ppm) for the ring-substituted trinitromethyl aromatic compounds (138) and (165).

The isomeric side-chain trinitromethyl aromatic compound (166) could be isolated only in low yield from the h.p.l.c. separation. The structure of the unsymmetrical 2,3-dimethyl-1-(2',2',2'-trinitroethyl)-benzene (166) rests on an accurately measured mass spectrum which gave the molecular formula $C_{10}H_{11}N_3O_6$, and the ^1H n.m.r. spectrum which revealed two methyl signals at δ 2.29 and δ 2.33, and a signal due to the CH_2-$C(NO_2)_3$ at δ 5.52, as seen in Fig. 3.25.

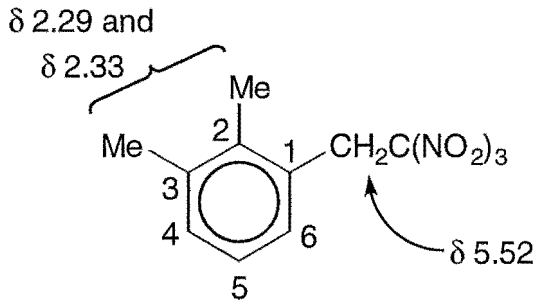

Fig. 3.25 Characteristic ^1H n.m.r. resonances (in ppm) for the side-chain trinitromethyl aromatic compound (166).

The isomeric side-chain trinitromethyl aromatic compound (167) was isolated in low yield in admixture with its isomer (166), above, from the h.p.l.c. separation. As expected for the structure of the symmetrical 2,6-dimethyl-1-(2',2',2'-trinitroethyl)-benzene (167), the ^1H n.m.r. resonances due to the two methyl groups appeared at δ 2.41, while the ^1H n.m.r. resonance due to the CH_2-$C(NO_2)_3$ appeared at δ 5.57, closely similar to the isomeric compound (166), as observed in Fig. 3.26.

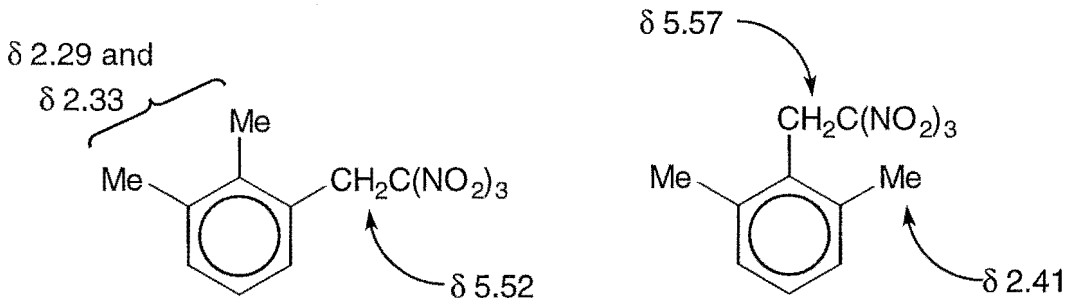

(166) (167)

Fig. 3.26 Comparison of the characteristic ^1H n.m.r. resonances (in ppm) for the side-chain trinitromethyl compounds (166) and (167).

Compound (168) was isolated by chromatography on a silica gel Chromatotron plate after being eluted in the first h.p.l.c. fraction. The structure of 2,3,4-trimethyl-1-nitrobenzene (168) was confirmed by comparison of its ^1H n.m.r. data with literature data.[16]

The isomeric nitrobenzene (169) was also isolated by chromatography on a silica gel Chromatotron plate after being eluted in the first h.p.l.c. fraction. The structure of 3,4,5-trimethyl-1-nitrobenzene (169) was also confirmed by comparison of its ^1H n.m.r. data with literature data.[16]

While the nitro phenol (171) was present in the early stages of the photolysis reaction, it was absent at the end of the reaction. However,

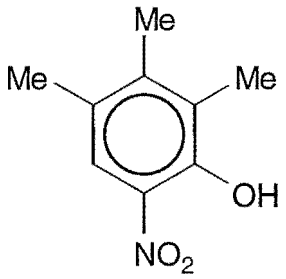

(171)

compound (171) was isolated by chromatography on a silica gel Chromatotron plate after being eluted in the first h.p.l.c. fraction. The structure of 4,5,6-trimethyl-2-nitrophenol (171) was confirmed by comparison of its ^1H n.m.r. data with literature data.[17]

Nitro ketones (163), (164) *and* (172).

Compound (163) was isolated *via* h.p.l.c., but only in admixture with the nitro/trinitromethyl adduct (156). The identification of 2,3,4-trimethyl-4-nitrocyclohexa-2,5-dien-1-one (163) was confirmed by comparing its ^1H n.m.r. data with literature data.[18] Furthermore, the nitro dienone (163) was unstable in (D)chloroform solution and rearranged to give the known[17] 4,5,6-trimethyl-2-nitrophenol (171), above (See Section 3.8).

The isomeric nitro ketone (164) was isolated as an oil *via* h.p.l.c. and its identification as 3,4,5-trimethyl-4-nitrocyclohexa-2,5-dien-1-one (164) was confirmed by comparison of its ^1H n.m.r. data with literature data.[19]

The hydroxy trinitro ketone (172) was not present in the product mixture prior to h.p.l.c. separation, but did appear in low yield among the materials eluted from the cyanopropyl h.p.l.c. column. The structure of the hydroxy trinitro ketone (172) was determined by single crystal X-ray analysis. A perspective drawing of *t*-6-hydroxy-4,5,6-trimethyl-2,*r*-4,*t*-5-trinitrocyclohex-2-enone (172), $C_9H_{11}N_3O_8$, m.p. 121-123°, is presented in Fig. 3.27, and corresponding atomic coordinates are given in Table 5.15 (See Chapter 5, Section 5.5). In the solid state, the alicyclic ring of the hydroxy trinitro ketone (172) exists in a flattened [C(1) sp^2] skew boat form [torsional angles: C(3)-C(2)-C(1)-C(6) 26.9(2); C(2)-C(3)-C(4)-C(5) -8.1(2)°].

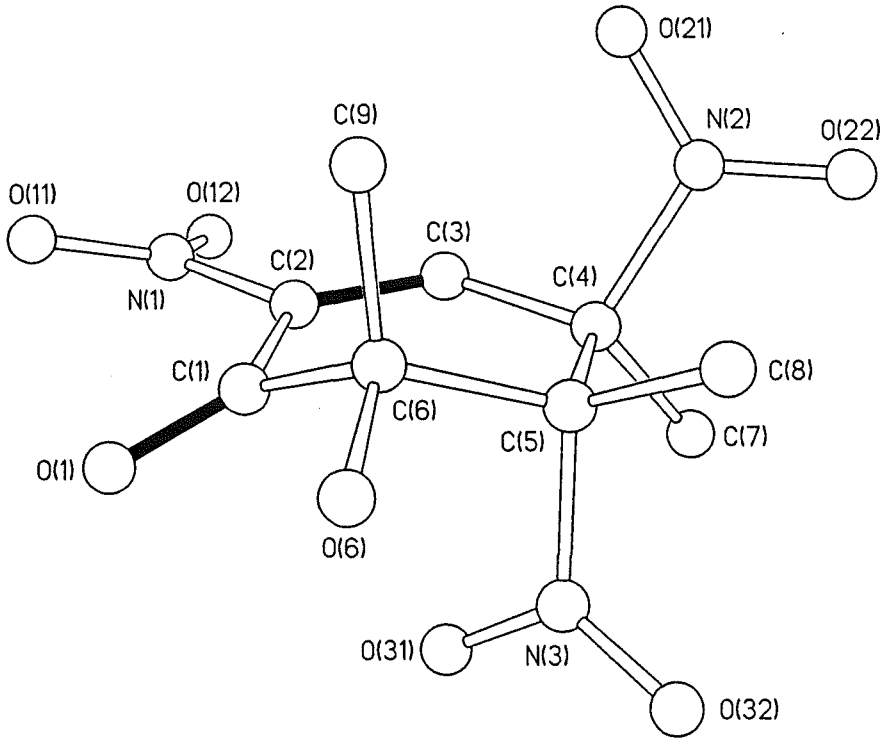

Fig. 3.27 Perspective drawing of the hydroxy trinitro ketone (172). Double bonds shown in black.

The orientations of the planes of the three nitro groups relative to their surroundings are indicated by the following torsional angles: O(12)-N(1)-C(2)-C(3) 19.7(2); O(22)-N(2)-C(4)-C(7) -31.0(2); O(32)-N(3)-C(5)-C(8) -4.4(2)°. The substituents around the C(4)-C(5) bond are imperfectly staggered [torsional angles: C(7)-C(4)-C(5)-C(8) 86.1(2); N(2)-C(4)-C(5)-N(3) -148.5(1)°], and the C(6)-O(6) bond is close to eclipsed with the C(1)-O(1) bond which, coupled with a O(1)·····O(6) distance of 2.697 Å, is probably indicative of intramolecular hydrogen bonding in the solid state. The spectroscopic data for compound (172) were in accord with the established structure. Due to the limited solubility of the hydroxy

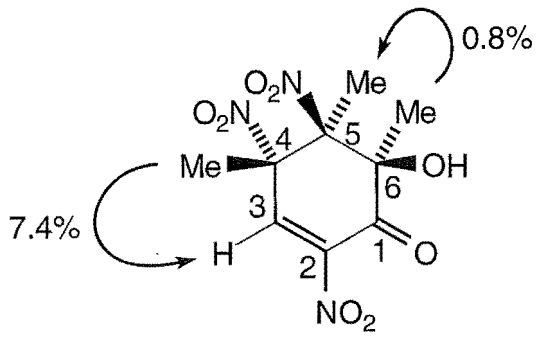

(172)

-	-	C1	188.4
-	-	C2	147.0
H3	7.70	C3	137.5
4-Me	1.91	C4	90.3
5-Me	1.84	C5	99.7
6-Me	1.54	C6	79.2

Fig. 3.28 Characteristic ^{1}H and ^{13}C n.m.r. resonances (in ppm) and enhancements (%) from selected n.O.e. experiments for the hydroxy trinitro ketone (172).

trinitro ketone (172) in (D)chloroform, ^{1}H and ^{13}C n.m.r. spectra were run in (D_3)acetonitrile. N.O.e. experiments confirmed the assignments of the chemical shifts for the protons. Specifically, irradiation at δ 1.91 (4-Me) gave enhancement at δ 7.70 (H3), while irradiation at δ 1.54 (6-Me) gave enhancement at δ 1.84 (5-Me), as outlined in Fig. 3.28. Also presented in Fig. 3.28 are the characteristic ^{1}H and ^{13}C n.m.r. data. In particular, the hydroxy function was indicated by the ^{13}C n.m.r. chemical shift for C6 (δ 79.2), the three nitro functions by the ^{13}C n.m.r. chemical shifts for C2 (δ 147.0), C4 (δ 90.3) and C5 (δ 99.7), and the ketone function by the ^{13}C n.m.r. chemical shift for C1 (δ 188.4). These assignments were confirmed by HMQC and HMBC experiments.

The composition of the photochemical reaction between 1,2,3-trimethylbenzene (137) and TNM was monitored with time at +20, -20 and -50° in dichloromethane. An overview of product yields in dichloromethane is presented in Table 3.1. Notable at lower reaction temperatures was the partial (-20°) or complete (-50°) suppression of the formation of "double" adducts (139) and (157)-(162), and the prevention of the thermal intramolecular cycloaddition of the nitro/trinitromethyl adduct (152) to give the nitro cycloadduct (153). The yields (at 1 h reaction time) of the ring-

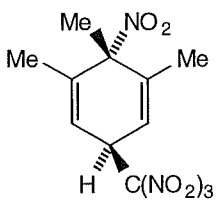

(151)

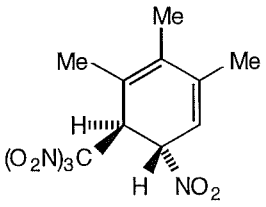

(152)

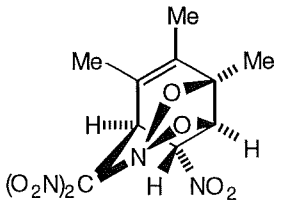

(153)

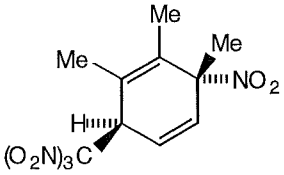

(154)

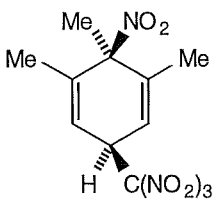

(155)

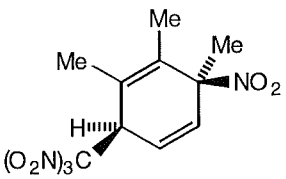

(156)

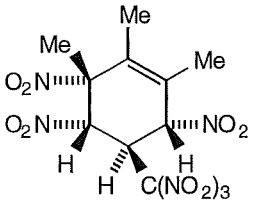

(157)

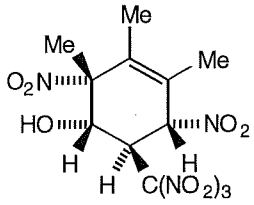

(139)

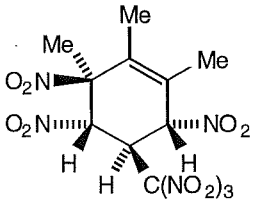

(158)

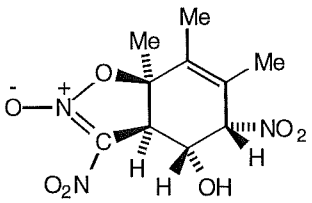

(159)

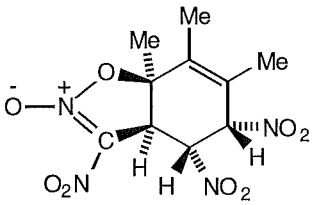

(160)

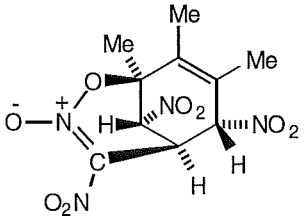

(161)

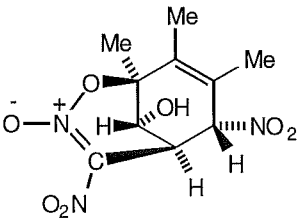

(162)

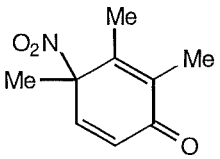

(163)

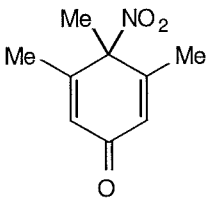

(164)

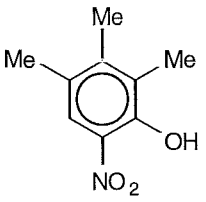

(171)

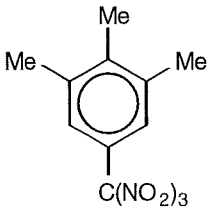

(138)

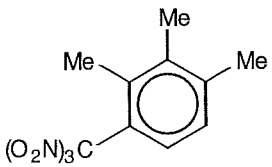

(165)

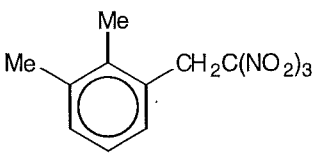

(166)

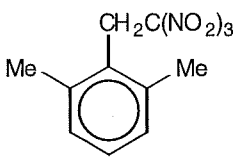

(167)

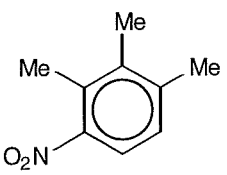

(168)

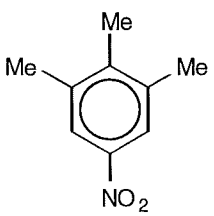

(169)

Table 3.1 Overview of product yields from the photolysis of 1,2,3-trimethylbenzene (137) (0.52 mol L^{-1}) and TNM (1.04 mol L^{-1}) in dichloromethane.

	Yield (%)																					
t (h)	(151)	(154)	(155)	(156)	(152)	(153)	(157)	(139)	(158)	(159)	(160)	(161)	(162)	(163)	(164)	(171)	(138)	(165)	(166)	(167)	(168)	(169)
At +20°																						
1	7.3	3.8	9.3	1.9	5.7	1.7	0.3	3.2	1.0	2.7	1.1	4.5	3.6	1.1	0.3	0.5	31.4	10.2	2.8	2.8	3.3	0.5
4	9.0	5.3	10.0	3.1	4.4	3.2	1.5	4.2	2.7	3.6	1.5	6.7	4.1	0.5	0.6	0.1	23.6	9.5	1.0	0.9	2.4	0.7
8	7.9	3.9	9.7	3.4	2.6	2.8	2.6	3.7	3.1	3.7	1.4	6.6	4.4	trace	0.6	-	26.8	10.8	0.5	0.3	3.2	0.7
At -20°																						
1	3.4	4.2	4.8	3.4	4.4	-	-	-	-	-	-	-	1.3	2.1	0.3	2.8	40.7	4.6	4.7	4.8	3.0	0.9
4	3.1	3.3	3.8	4.2	5.1	-	-	-	-	trace	-	-	1.5	2.0	0.8	0.7	45.8	13.4	1.8	2.1	2.4	1.0
8	3.4	4.6	4.3	4.5	5.4	-	-	-	-	0.7	-	-	1.8	2.0	1.0	0.5	40.8	17.0	0.8	0.9	3.0	1.1
At -50°																						
1	2.8	2.0	4.7	4.2	3.5	-	-	-	-	-	-	-	-	2.2	2.0	2.9	48.8	2.5	6.1	5.7	2.8	0.8
4	5.1	4.6	5.8	7.3	6.4	-	-	-	-	-	-	-	-	2.8	4.2	1.9	31.3	12.0	3.2	3.0	3.2	0.9
8	4.9	4.4	6.7	7.6	6.5	-	-	-	-	-	-	-	-	2.7	9.1	1.0	28.2	12.0	1.9	2.5	3.0	0.9

substituted trinitromethyl aromatic compounds (138) and (165) increased at lower reaction temperatures (total 42% at +20°, total 51% at -50°). Correspondingly, the yields of the side-chain trinitromethyl aromatic compounds (166) and (167) rose at lower reaction temperatures (total 6% at +20°, total 12% at -50°). The two dienones (163) and (164), and rearrangement product (171), were present in higher yields at lower reaction temperatures (total 2% at +20°, total 7% at -50°).

3.4 The Photochemistry of 1,2,3-Trimethylbenzene (137) in Dichloromethane Containing Trifluoroacetic Acid (TFA)

Photochemistry in dichloromethane containing TFA at +20° and the identification of the aromatic compounds (173) *and* (174).

A solution of 1,2,3-trimethylbenzene (137) (0.52 mol L^{-1}) and TNM (1.04 mol L^{-1}) in dichloromethane containing TFA (1.04 mol L^{-1}) was irradiated at +20° for 8 h. The products formed after 8 h were 3,4,5-trimethyl-1-trinitromethylbenzene (138) (62%), 2,3,4-trimethyl-1-trinitromethyl-

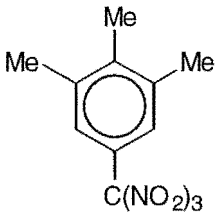

(138)

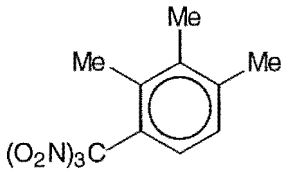

(165)

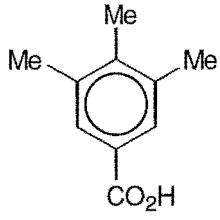

(173)

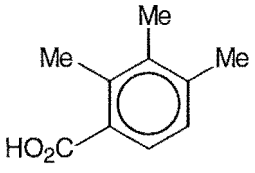

(174)

benzene (165) (11%), 3,4,5-trimethylbenzoic acid (173) (5%), 2,3,4-trimethylbenzoic acid (174) (2%), and some unidentified material (20%).

The carboxylic acid (173) was isolated by h.p.l.c. and its identification as 3,4,5-trimethylbenzoic acid (173) was confirmed by comparing its ^1H n.m.r. data with literature data.[20]

Similarly, the isomeric carboxylic acid (174) was also isolated by h.p.l.c. and its identification as 2,3,4-trimethylbenzoic acid (174) was also confirmed by comparing its ^1H n.m.r. data with literature data.[21]

A similar reaction to the above, but with trifluoroacetic acid (2.08 mol L^{-1}) gave a mixture of 3,4,5-trimethyl-1-trinitromethylbenzene (138) (20%), 2,3,4-trimethyl-1-trinitromethylbenzene (165) (11%), 3,4,5-trimethylbenzoic acid (173) (10%), 2,3,4-trimethylbenzoic acid (174) (5%), 2,3,4-trimethyl-1-nitrobenzene (168) (11%), 3,4,5-trimethyl-1-nitrobenzene (169) (9%) and some unidentified material (34%). An overview of the yields of products in dichloromethane containing trifluoroacetic acid is given in Table 3.2.

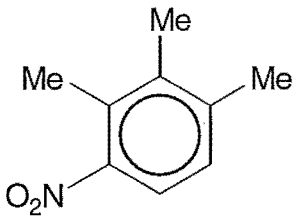

(168)

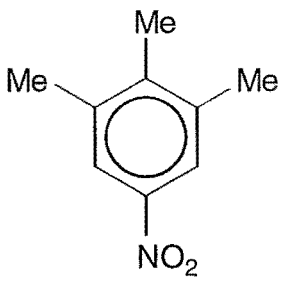

(169)

3.5 The Photochemistry of 1,2,3-Trimethylbenzene (137) in Acetonitrile

Photolyses of solutions of 1,2,3-trimethylbenzene (137) (0.52 mol L^{-1}) and TNM (1.04 mol L^{-1}) in acetonitrile were carried out at +20, -20 and -50° as for reactions in dichloromethane, above. The results of these

Table 3.2 Overview of product yields from the photolysis reaction of 1,2,3-trimethylbenzene (137) (0.52 mol L^{-1}) and TNM (1.04 mol L^{-1}) in dichloromethane containing trifluoroacetic acid, at +20°.

	Yield (%)						
t (h)	(138)	(165)	(173)	(174)	(168)	(169)	Unknown aromatics
Trifluoroacetic acid (1.04 mol L^{-1})							
1	71.4	14.3	-	-	-	-	14.3
4	63.9	12.0	1.9	trace	-	-	22.2
8	62.2	10.5	5.0	2.1	-	-	20.2
Trifluoroacetic acid (2.08 mol L^{-1})							
1	50.0	13.2	-	-	7.9	2.6	26.3
4	28.4	9.7	5.8	5.0	9.1	6.8	35.2
8	20.1	11.3	9.8	4.8	11.2	8.8	34.0

reactions, monitored with time, are summarized in Table 3.3. Interestingly, in acetonitrile "double" adducts (139), (157), (158) and (160) were not seen at any temperature. As was observed when the solvent was dichloromethane (see Table 3.1, Section 3.3), at lower reaction temperatures there was complete suppression of the formation of "double" adducts (161) and (162) and the absence of the nitro cycloadduct (153), formed *via* the thermal intramolecular cycloaddition of the nitro/trinitromethyl adduct (152). Also notable was the formation of the carboxylic acids (173) and (174) at +20°. In contrast to reactions in dichloromethane (see Table 3.1, Section 3.3), where the yields (at 1 h reaction time) of the ring-substituted trinitromethyl aromatic compounds (138) and (165) increased at lower reaction temperature, in acetonitrile compounds (138) and (165) decreased markedly at lower reaction temperatures (total 66% at +20°, total 14% at

Table 3.3 Overview of product yields from the photolysis of 1,2,3-trimethylbenzene (137) (0.52 mol L^{-1}) and TNM (1.04 mol L^{-1}) in acetonitrile.

	Yield (%)																							
t (h)	(151)	(154)	(155)	(156)	(152)	(153)	(157)	(139)	(158)	(159)	(160)	(161)	(162)	(163)	(164)	(171)	(138)	(165)	(166)	(167)	(168)	(169)	(173)	(174)
At +20°																								
1	4.8	1.8	5.2	1.0	2.3	0.8	-	-	-	0.8	-	2.7	2.2	1.4	0.2	0.5	57.5	8.5	1.8	1.6	3.7	1.5	-	-
4	6.1	1.9	5.6	1.7	1.2	1.1	-	-	-	0.7	-	4.1	2.3	1.1	2.1	-	55.1	5.7	0.7	0.7	5.8	1.9	0.6	-
8	4.0	1.5	3.2	1.5	1.0	2.6	-	-	-	1.0	-	5.7	2.4	0.4	1.4	8.9	53.8	6.0	0.6	0.6	2.8	0.9	0.2	0.2
At -20°																								
1	3.2	2.1	5.4	2.7	2.9	-	-	-	-	trace	-	-	1.2	2.6	0.8	3.7	48.0	1.8	4.7	4.5	4.6	2.2	-	-
4	3.1	1.3	4.8	2.3	2.3	-	-	-	-	0.4	-	-	1.3	2.2	1.8	3.3	54.1	7.1	1.6	1.5	4.2	2.0	-	-
8	2.3	1.6	3.1	2.1	2.0	-	-	-	-	0.2	-	-	0.7	2.1	1.7	1.4	62.8	11.6	0.9	0.9	3.6	1.8	-	-
At -50°																								
1	2.8	2.0	5.3	5.9	2.2	-	-	-	-	-	-	-	-	2.6	9.5	7.2	12.3	2.0	14.7	14.1	10.7	3.3	-	-
4	3.4	2.8	5.6	7.4	3.7	-	-	-	-	-	-	-	-	5.3	7.7	7.6	19.5	6.0	5.6	5.3	9.7	4.3	-	-
8	3.6	4.4	5.9	6.2	5.6	-	-	-	-	0.6	-	-	-	4.9	0.7	7.5	26.4	9.6	2.8	2.8	9.7	4.4	-	-

-50°). However, similar to reactions in dichloromethane, the yields of the side-chain trinitromethyl aromatic compounds (166) and (167) rose appreciably in acetonitrile (total 3% at +20°, total 29% at -50°). At lower reaction temperatures in acetonitrile a similar trend to reactions in dichloromethane was seen, with higher yields of the two dienones (163) and (164), and the rearrangement product (171) (total 2% at +20°, total 19% at -50°). The yields of the nitro aromatic compounds (168) and (169) only became appreciable at lower reaction temperatures in acetonitrile (14% at -50°), whereas in dichloromethane they remained constant (total 4% at all temperatures).

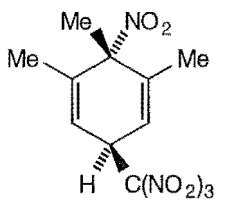

(151)

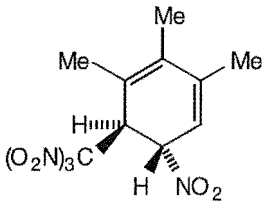

(152)

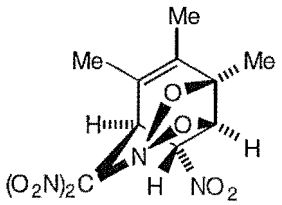

(153)

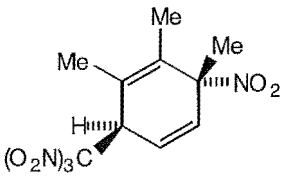

(154)

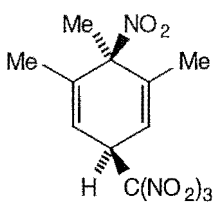

(155)

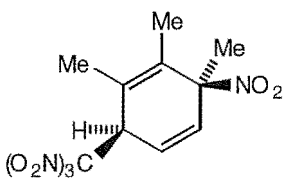

(156)

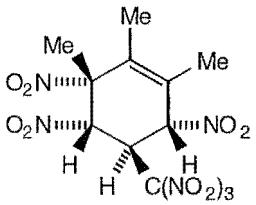

(157)

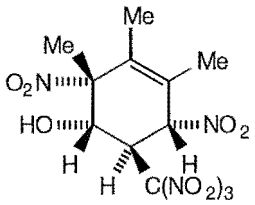

(139)

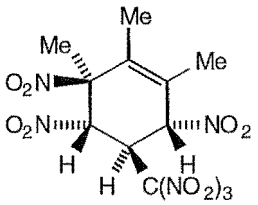

(158)

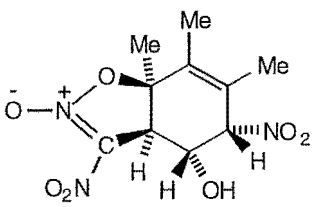

(159)

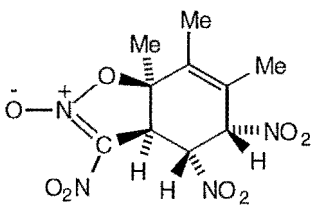

(160)

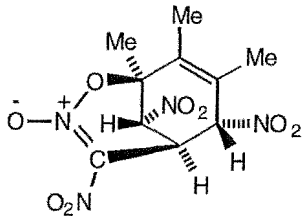

(161)

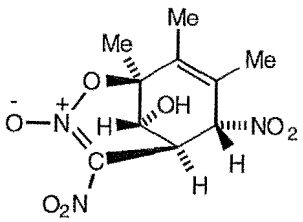

(162)

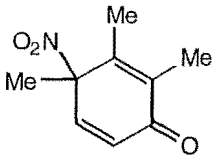

(163)

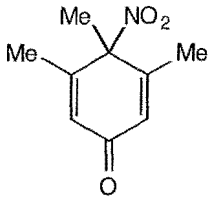

(164)

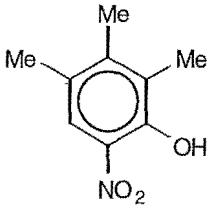

(171)

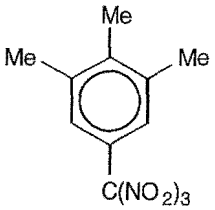

(138)

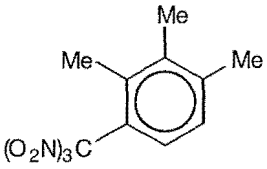

(165)

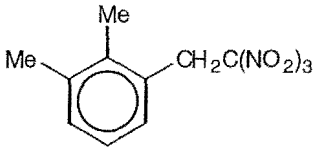

(166)

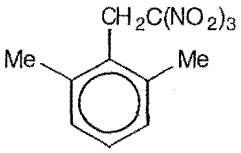

(167)

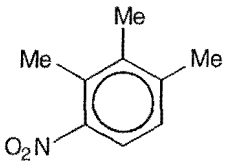

(168)

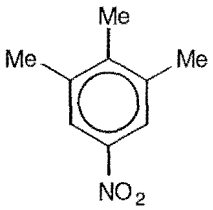

(169)

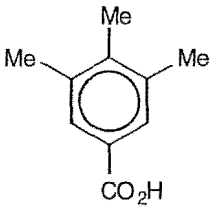

(173)

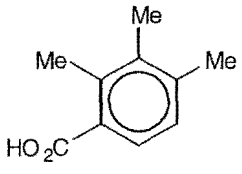

(174)

3.6 Base Catalysed Decomposition of Nitro/Trinitro-methyl Adducts (151), (154)-(156) with 2,6-Di-*tert*-butyl-4-methylpyridine in Dichloromethane

A solution of each of the adducts (151) and (154)-(156) in dichloro-methane was reacted with 2,6-di-*tert*-butyl-4-methylpyridine for 1 h, at +20°, in the dark. After removal of the solvent under reduced pressure, the residue was analysed by ^{1}H n.m.r. spectroscopy. The base catalysed decomposition reactions with adducts (151) and (155) gave 3,4,5-trimethyl-1-trinitromethylbenzene (138), while adducts (154) and (156) gave 2,3,4-tri-methyl-1-trinitromethylbenzene (165), as seen in Scheme 3.7.

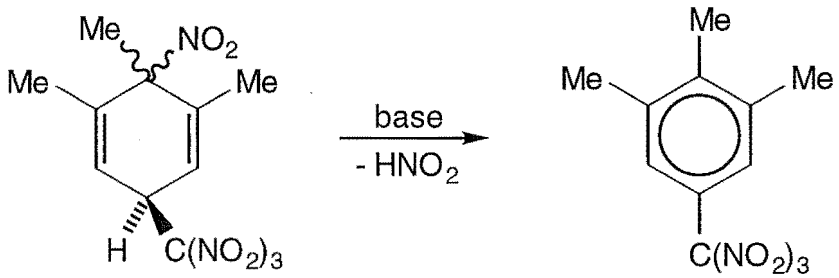

(151) and (155) (138)

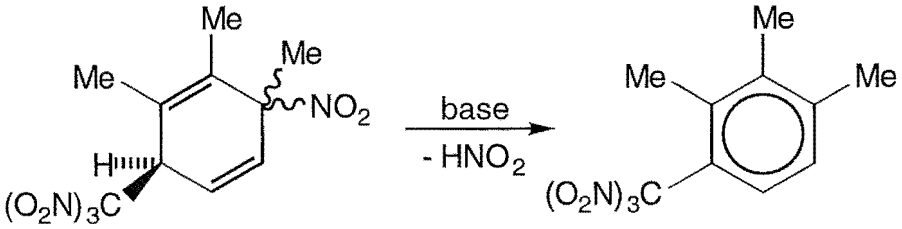

(154) and (156) (165)

Scheme 3.7

3.7 Thermal Cycloaddition of 1,2,3-Trimethyl-*r*-5-nitro-*t*-6-trinitromethylcyclohexa-1,3-diene (152) to give the Nitro Cycloadduct (153)

A solution of a mixture (*c.* 4:1:4:2) of the nitro/trinitromethyl adduct (152), nitro cycloadduct (153) and the nitro/trinitromethyl adducts (151) and (154), respectively, in (D)chloroform was stored at +22°, in the dark, and the

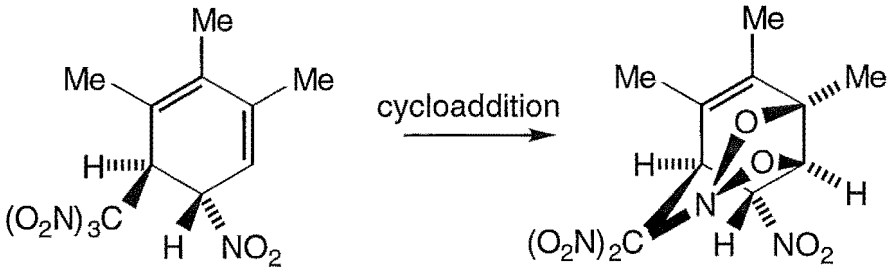

(152) (153)

Scheme 3.8

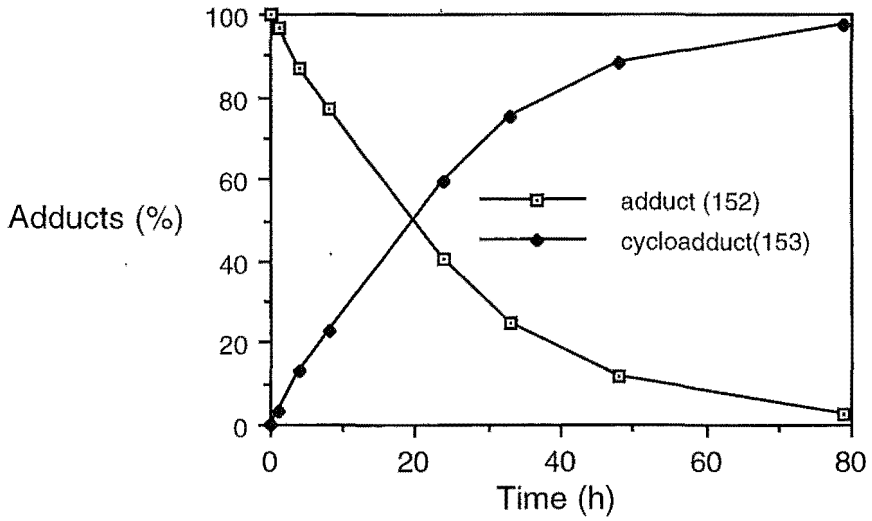

Fig. 3.29 Kinetics of cycloaddition of adduct (152) to nitro cycloadduct (153) in (D)chloroform, at +22°.

^{1}H n.m.r. spectra of the solution monitored at appropriate time intervals. Under these conditions, adducts (151) and (154) were unchanged during the period of observation, but the precursor adduct (152) was slowly transformed into the nitro cycloadduct (153), as depicted in Scheme 3.8 and Fig. 3.29. The half-life for the cycloaddition of adduct (152) into the nitro cycloadduct (153) was *c.* 19.5 h.

3.8 Rearrangement of 2,3,4-Trimethyl-4-nitrocyclohexa-2,5-dien-1-one (163) in (D)Chloroform

A solution of a mixture (*c.* 4:1) of the nitro dienone (163) and the nitro/trinitromethyl adduct (156) in (D)chloroform was stored at +22°, in the dark, and the ^{1}H n.m.r. spectra monitored at appropriate time intervals. Under these conditions, adduct (156) was inert during the period of observation, but the nitro dienone (163) was transformed into 4,5,6-trimethyl-2-nitrophenol (171), as summarized in Scheme 3.9 and Fig. 3.30. The half-life for the rearrangement of the nitro dienone (163) into the nitrophenol (171) was *c.* 6 h.

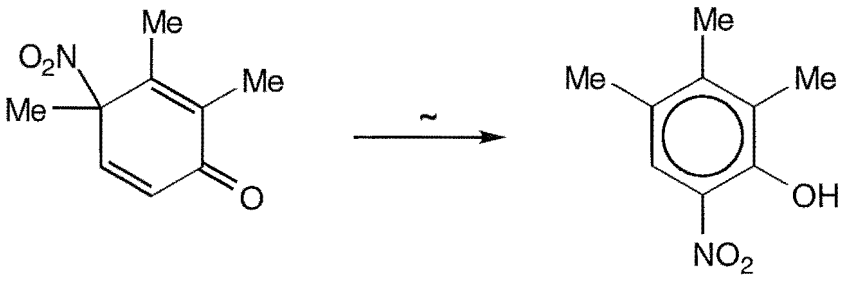

(163) (171)

Scheme 3.9

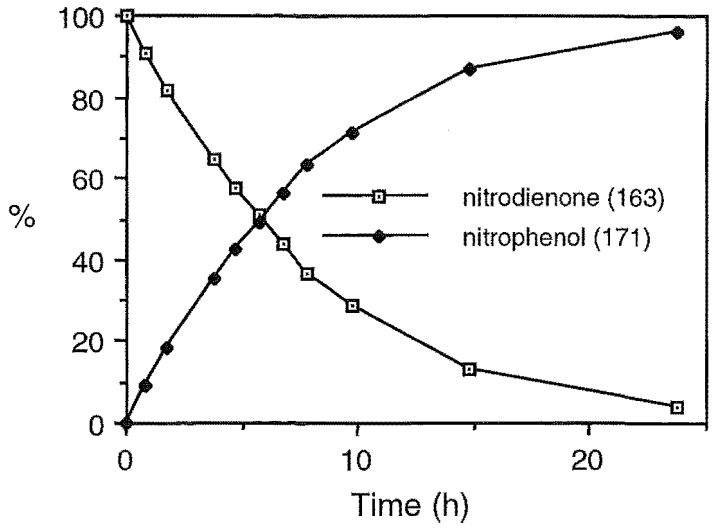

Fig. 3.30 Kinetics of rearrangement of nitro dienone (163) to nitrophenol (171) in (D)chloroform, at +22°.

3.9 Overview of the Photonitration of 1,2,3-Trimethylbenzene (137)

3.9.1 The reactivity of $(O_2N)_3C^-$ with the radical cation of 1,2,3-trimethylbenzene.

In the photolysis of the charge-transfer complex of 1,2,3-trimethylbenzene (137) and TNM, the radical cation of 1,2,3-trimethylbenzene is highly reactive towards $(O_2N)_3C^-$. This can be clearly seen in the photochemical reaction between 1,2,3-trimethylbenzene (137) (0.52 mol L^{-1}) and TNM (1.04 mol L^{-1}) in dichloromethane in the presence of TFA (1.04 mol L^{-1}). In this reaction the trinitromethyl aromatic compounds (138) and (165) were formed in high yield (total *c.* 86% after 1 h; see Table 3.3, Section 3.5) indicating that ionic coupling of $(O_2N)_3C^-$ with the radical cation of 1,2,3-trimethylbenzene was more than competitive with protonation of the trinitro-

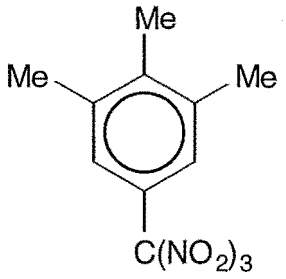

(138)

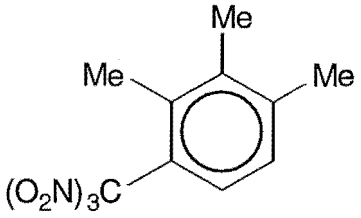

(165)

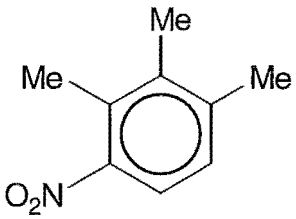

(168)

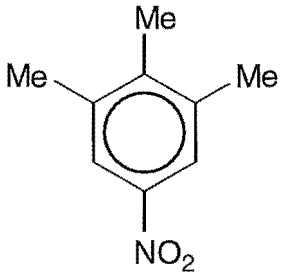

(169)

methyl anion. Even at a higher TFA concentration (2.08 mol L^{-1}) trinitromethyl aromatic products (138) and (165) predominated (total 63% after 1 h) over the nitro aromatic compounds (168) and (169) (total 11%), which were products of the slower radical coupling of the radical cation with $^{\bullet}NO_2$. The preparative results above are consistent with the absence of detectable EPR signals on irradiation at λ>435 nm of 1,2,3-trimethylbenzene in dichloromethane solution in the presence of (i) TNM, (ii) TNM and TFA, and (iii) TFA.[22]

3.9.2 The general pattern of products formed on photolysis of the charge-transfer complex of TNM with 1,2,3-trimethylbenzene (137).

In the photochemical reaction of 1,2,3-trimethylbenzene (137) with TNM it was found that the initial bond formation between $(O_2N)_3C^-$ and the aromatic radical cation occurred at both of the unoccupied ring positions, C4 and C5. For the reaction in dichloromethane at +20° (see Table 3.1,

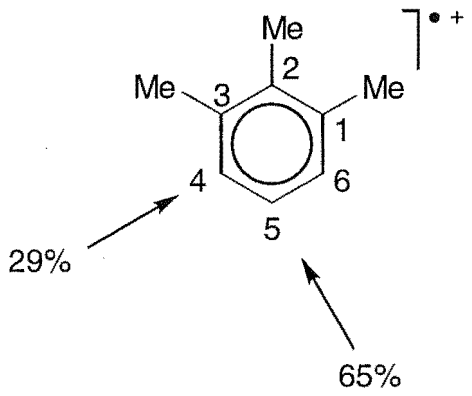

Fig. 3.31 Products (%) identified corresponding to attack of $(O_2N)_3C^-$ on the 1,2,3-trimethylbenzene radical cation.

Section 3.3), there was clear preference (*c.* 2:1) for $(O_2N)_3C^-$ attack at C5 of the 1,2,3-trimethylbenzene radical cation, compared with reaction at C4, as represented in Fig. 3.31. It therefore appears that the first chemical step leading to adduct formation disfavours the formation of the delocalized radicals (142) and (143), formed *via* attack of $(O_2N)_3C^-$ at C1 and C2, respectively, on the radical cation of 1,2,3-trimethylbenzene. The favoured pathway (*c.* 2:1) is *via* formation of radical (140), on attack of $(O_2N)_3C^-$ at C5

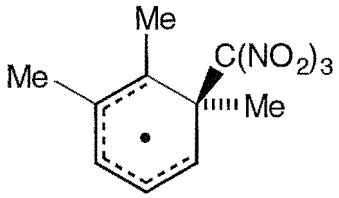

(142)

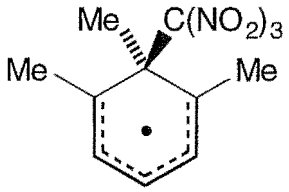

(143)

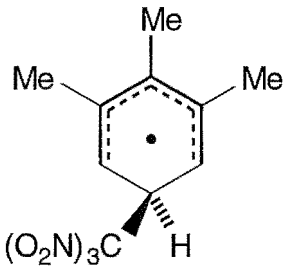

(140)

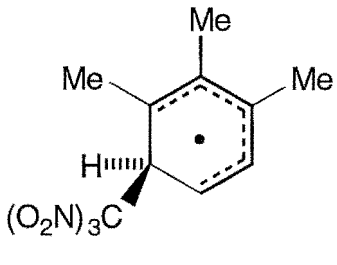

(141)

on the radical cation of 1,2,3-trimethylbenzene. The remaining adducts arose *via* radical (141), formed on attack of $(O_2N)_3C^-$ at C4 on the 1,2,3-trimethylbenzene radical cation.

The complete details of yields of reaction products in dichloromethane and acetonitrile solution at +20, -20, and -50° are given in Tables 3.1 and 3.3 (See Sections 3.3 and 3.5, respectively). A summary of these reactions in terms of "product type" is given in Table 3.4. Here the term "single" adducts refers to those products formed by a single addition of the elements of TNM to 1,2,3-trimethylbenzene (137), while the term "double" adducts refers to products derived by some form of extramolecular addition to initially formed "single" adducts. The details of these processes will be discussed below [See Sections 3.9.3 (b), and 3.9.4 (b) and (c)].

Table 3.4 shows clearly that the incidence of the formation of "double" adducts is markedly temperature dependent in both dichloromethane and acetonitrile, implying a thermal addition process subsequent to the initial photochemical addition of the elements of TNM to 1,2,3-trimethylbenzene (137) to form "single" adducts. These thermal additions appear to be initiated by attack, with C-N bond formation, of the somewhat electrophilic $^{\bullet}NO_2$ on the nitro/trinitromethylcyclohexa-1,3-dienes (152) and (175) and on the hydroxy/trinitromethylcyclohexa-1,3-dienes (176) and (177). The observation that the "double" adducts formed at lower reaction temperatures are those derived from the hydroxy/trinitromethylcyclohexa-

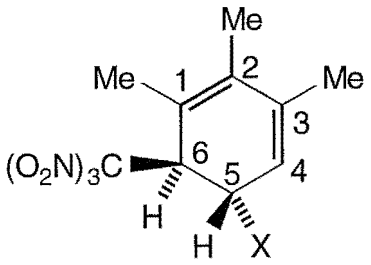

(152) X=NO_2
(176) X=OH

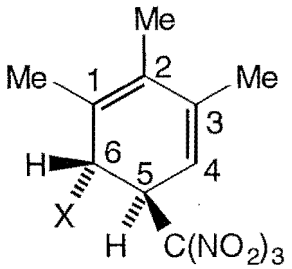

(175) X=NO_2
(177) X=OH

Table 3.4 Yields of product types from the photolysis of 1,2,3-trimethylbenzene (137) (0.52 mol L^{-1}) and TNM (1.04 mol L^{-1}).

	Yield (%)				
t (h)	"Single" adducts	"Double" adducts	Total adducts	Dienones etc[a]	Identified aromatics
Dichloromethane at +20°					
1	29.7	16.4	47.1	1.9	51.0
4	35.0	24.5	60.7	1.2	38.1
8	30.3	25.5	57.1	0.6	39.3
Dichloromethane at -20°					
1	20.2	1.3	36.1	5.2	58.7
4	19.5	1.5	33.0	3.5	63.0
8	22.2	2.5	32.9	3.5	63.6
Dichloromethane at -50°					
1	17.2	-	26.1	7.1	66.8
4	29.2	-	37.5	8.9	53.6
8	30.1	-	38.7	12.8	48.5
Acetonitrile at +20°					
1	15.9	5.7	23.3	2.1	74.6
4	17.6	7.1	26.4	3.2	70.4
8	15.1	10.0	26.6	2.0	71.4
Acetonitrile at -20°					
1	16.3	1.2	27.1	7.1	65.8
4	13.8	1.7	22.2	7.3	70.5
8	11.1	0.9	13.2	5.2	81.6
Acetonitrile at -50°					
1	18.2	-	23.6	19.3	57.1
4	22.9	-	29.0	20.6	50.4
8	25.7	0.6	31.2	13.1	55.7

[a]Including 4,5,6-trimethyl-2-nitrophenol (171).

"Single" Adducts

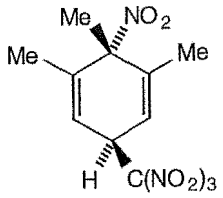

(151)

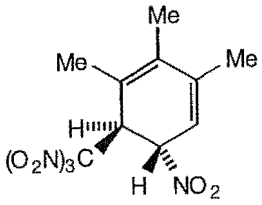

(152)

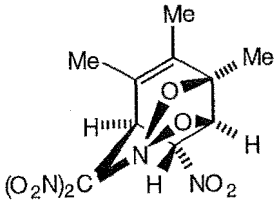

(153)

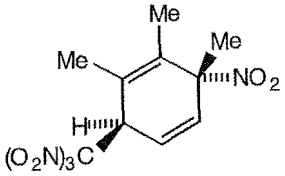

(154)

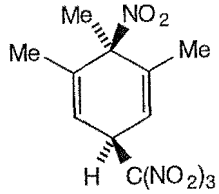

(155)

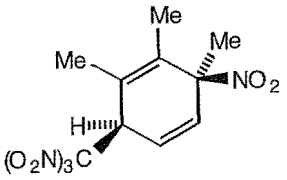

(156)

"Double" Adducts

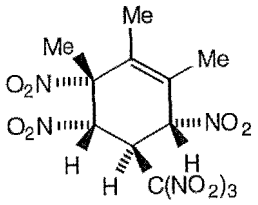

(157)

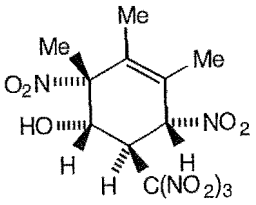

(139)

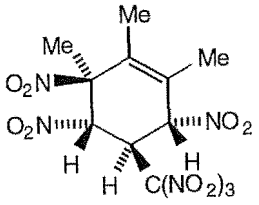

(158)

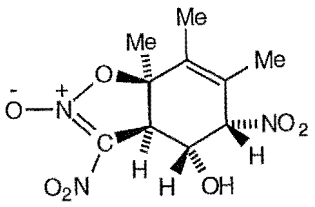

(159)

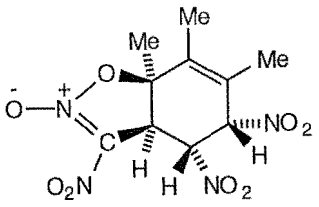

(160)

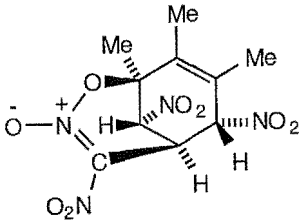

(161)

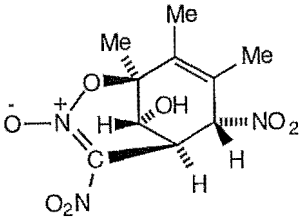

(162)

Dienones etc

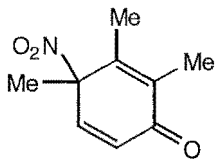

(163)

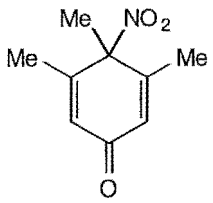

(164)

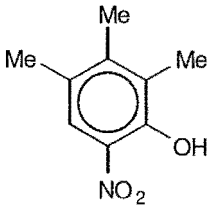

(171)

Aromatics

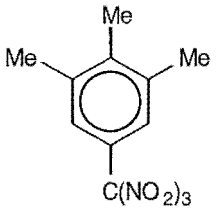

(138)

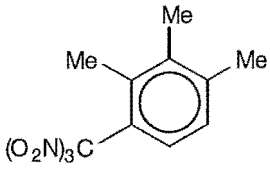

(165)

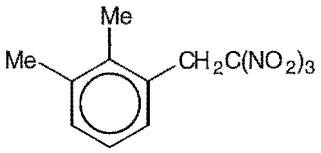

(166)

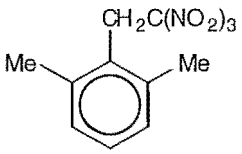

(167)

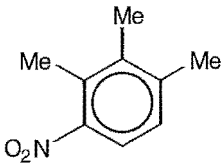

(168)

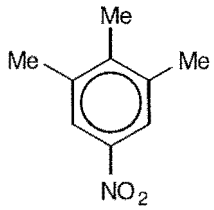

(169)

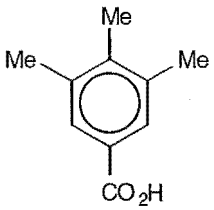

(173)

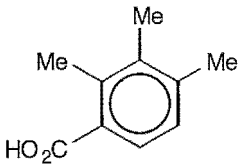

(174)

1,3-dienes (176) and (177) is consistent with this conclusion. Here the electron availability in the diene system might be expected to be higher than in the corresponding nitro/trinitromethylcyclohexa-1,3-dienes (152) and (175).

3.9.3 Some consequences of initial $(O_2N)_3C^-$ attack at C4 of the radical cation of 1,2,3-trimethylbenzene.

(a) The formation of "single" adducts (152), (154) *and* (156), *and nitro cycloadduct* (153).

Attack of $(O_2N)_3C^-$ at C4 of the radical cation of 1,2,3-trimethylbenzene would give the delocalized carbon radical (141), as illustrated in Scheme 3.10. Subsequent coupling of this carbon radical (141) with $^{\bullet}NO_2$ at C4 would yield the epimeric 1,2,3-trimethyl-3-nitro-6-trinitromethylcyclohexa-1,4-dienes (154) and (156), which appear to be relatively stable species. Alternatively, in the radical coupling of $^{\bullet}NO_2$ at C6 in the delocalized carbon radical (141), only the *trans* isomer (152) is formed because of the extensive shielding of the *syn*-face of the system by the bulky trinitromethyl group, itself forced from the plane of the carbon ring system by steric interaction with the adjacent methyl group.

The 5-nitro-6-trinitromethylcyclohexa-1,3-diene (152) underwent

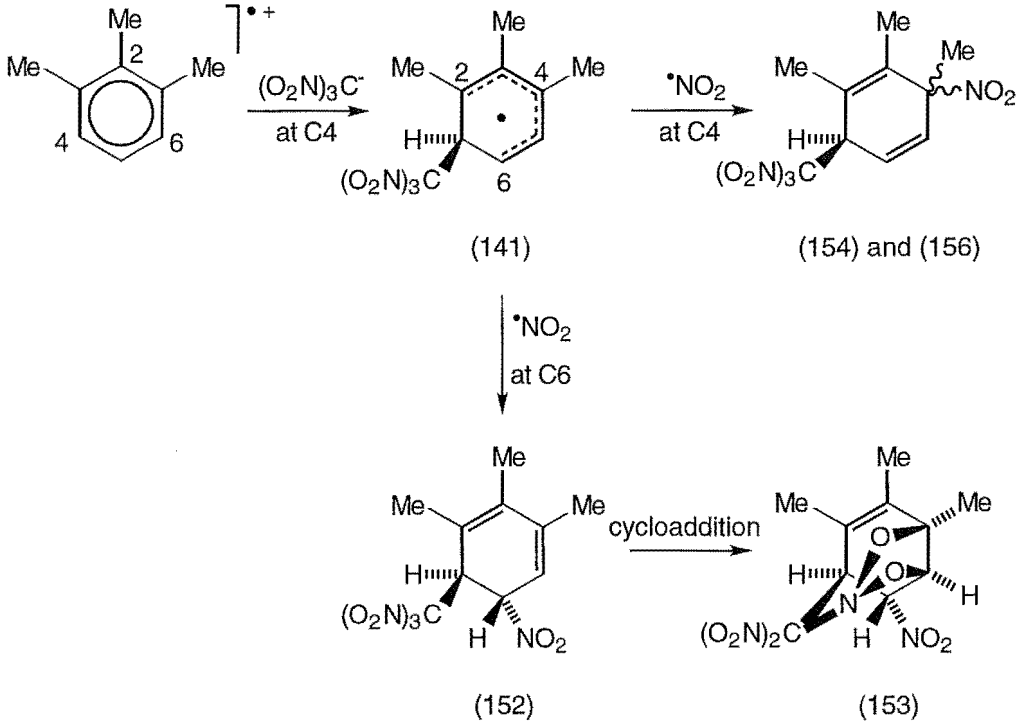

Scheme 3.10

cycloaddition of a nitro group of the trinitromethyl function with the 3,4-alkene system to give the nitro cycloadduct (153), as demonstrated in Section 3.7 and also seen in Scheme 3.10. This intramolecular cyclo-addition is clearly in competition with the formation of the nitronic ester (160), the formation of which is initiated by attack of $^{\bullet}NO_2$ at C4, as discussed below in Section 3.9.3 (b).

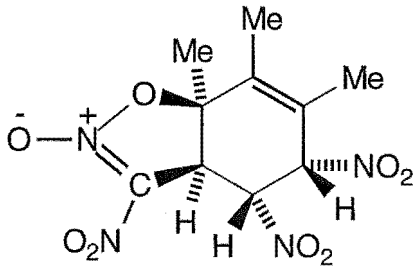

(160)

No products were detected which could be definitively associated with radical coupling of $^{\bullet}NO_2$ at C2 in the delocalized radical (141), but it seems possible that the 2,3,4-trimethyl-1-trinitromethylbenzene (165), isolated from reactions even at -50°, is formed by photochemical decomposition of the highly sterically compressed adduct (178), as observed in Scheme 3.11.

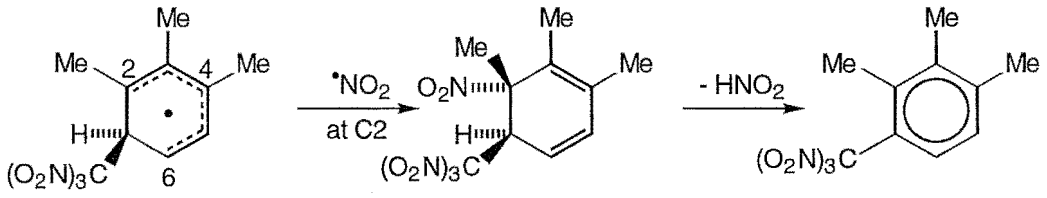

(141) (178) (165)

Scheme 3.11

(b) The formation of nitronic esters (159) *and* (160).

No direct evidence has been obtained on the mode of formation of the nitronic ester (160) from the 5-nitro-6-trinitromethylcyclohexa-1,3-diene (152). However, its formation is closely analogous to the quantitative formation of nitronic ester (179) on the thermal reaction of the hydroxy/trinitromethyl alkene (180) with $^{\bullet}NO_2$ in dichloromethane solution, in the

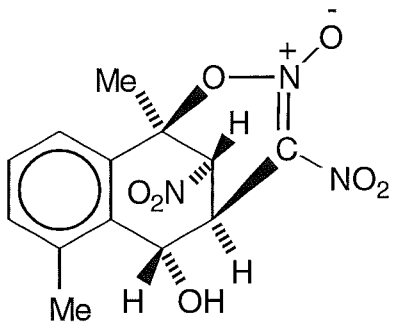

(179)

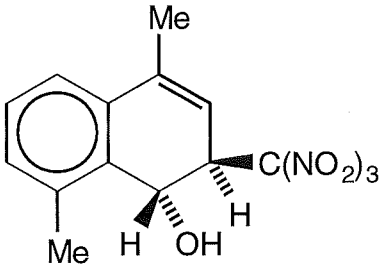

(180)

absence of light.[23] Attack of $^{\bullet}NO_2$ on the alkene system would give carbon radical (181) which interacts with the proximate trinitromethyl group leading to cyclization and loss of a molecule of $^{\bullet}NO_2$ from the former trinitromethyl group, yielding the nitro nitronic ester (179), as shown in Scheme 3.12. Similarly, in the formation of the nitronic ester (160) attack of $^{\bullet}NO_2$ at C4 of the methylated buta-1,3-diene system of the 5-nitro-6-trinitromethyl adduct (152) would give the delocalized carbon radical (182), as depicted in

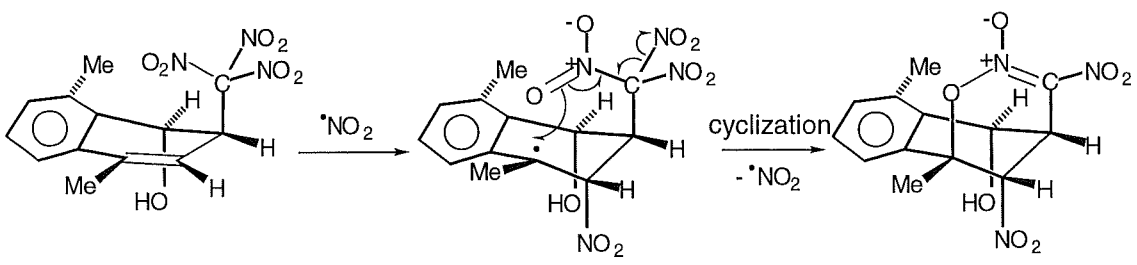

(180) (181) (179)

Scheme 3.12

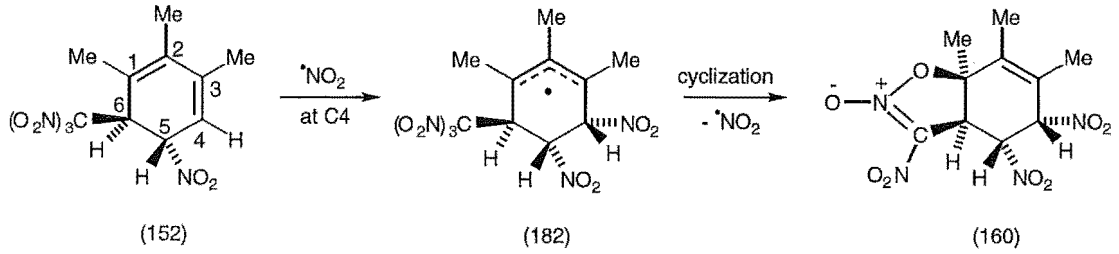

Scheme 3.13

Scheme 3.13. Cyclization and loss of a molecule of $^{\bullet}NO_2$ from this radical (182) would yield the trinitro nitronic ester (160).

Although the 5-hydroxy-6-trinitromethylcyclohexa-1,3-diene (176) was not detected, the hydroxy dinitro nitronic ester (159) is likely to have been formed *via* (183) by the analogous reaction pathway given in Scheme 3.14. The attack by $^{\bullet}NO_2$ *cis* to the hydroxy group is presumably aided by hydrogen bonding.[24] Therefore, $^{\bullet}NO_2$ might be expected to show higher reactivity towards the buta-1,3-diene system in the hydroxy precursor (176), compared with that of the nitro precursor (152). This would account for the observation that the hydroxy dinitro nitronic ester (159) is formed even at low reaction temperatures in both dichloromethane and acetonitrile (See Tables 3.1 and 3.3, Sections 3.3 and 3.5, respectively).

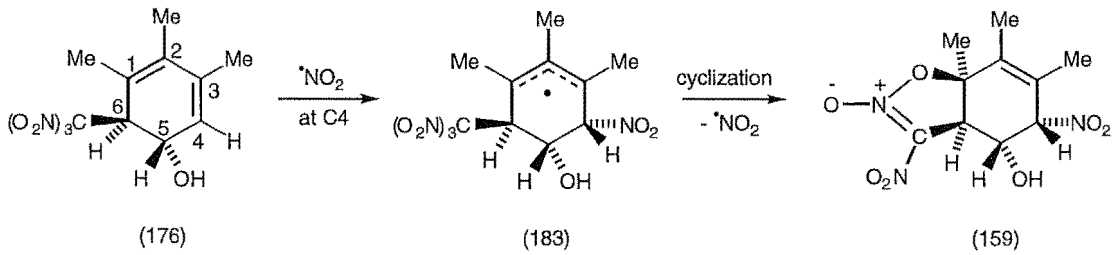

Scheme 3.14

3.9.4 Some consequences of initial $(O_2N)_3C^-$ attack at C5 of the radical cation of 1,2,3-trimethylbenzene.

(a) The formation of "single" adducts (151) *and* (155).

Attack of $(O_2N)_3C^-$ at C5 in the radical cation of 1,2,3-trimethylbenzene would give the delocalized carbon radical (140), as depicted in Scheme 3.15. Subsequent coupling of carbon radical (140) with $^{\bullet}NO_2$ at

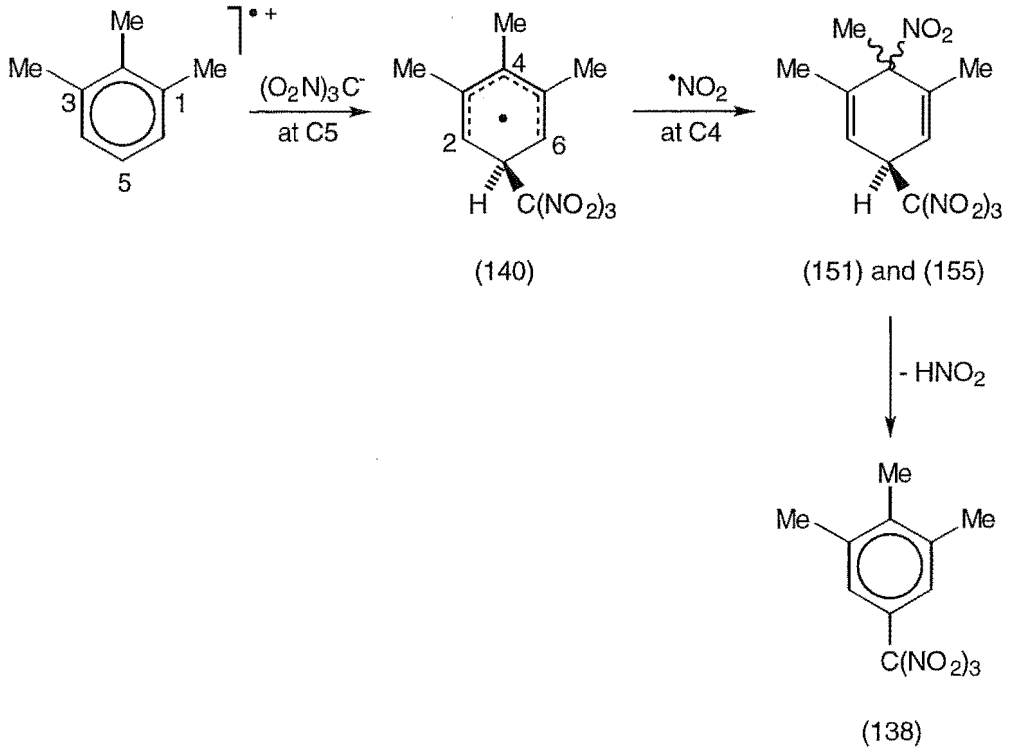

Scheme 3.15

C4 would yield the epimeric 2,3,4-trimethyl-3-nitro-6-trinitromethylcyclohexa-1,4-dienes (151) and (155), which were found to be relatively labile, decomposing to give the 3,4,5-trimethyl-1-trinitromethylbenzene (138) on attempted crystallization.

Similar radical coupling of $^{\bullet}NO_2$ at C2 in the delocalized carbon radical (140) would occur *trans* to the bulky trinitromethyl group at C1, to give adduct (175) by C-N bond formation and adduct (177) by C-O bond

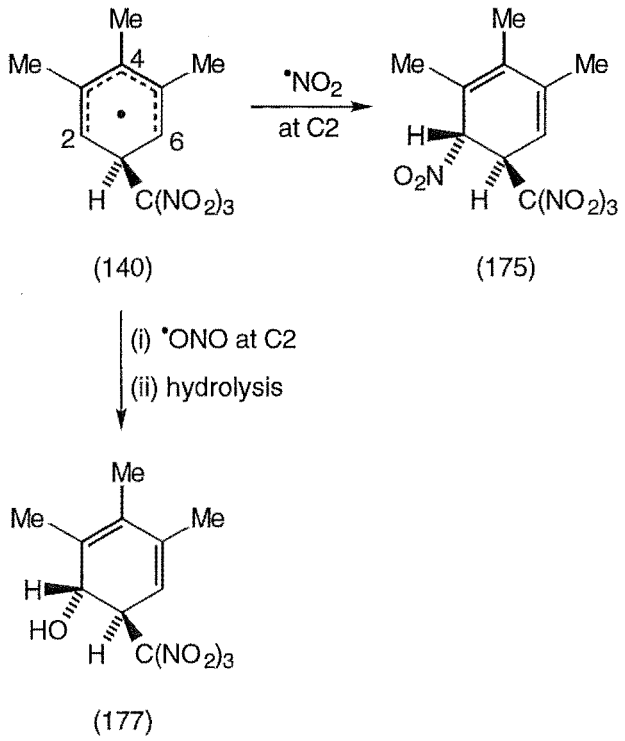

Scheme 3.16

formation followed by hydrolysis, as shown in Scheme 3.16. However, neither adduct (175) nor adduct (177) were isolated from the photolysis reactions. As discussed below in Sections 3.9.4 (b) and (c), these adducts were seen as intermediates in the formation of "double" adducts (157), (139) and (158), and the two nitronic esters (161) and (162).

(b) The formation of "double" adducts (157) *and* (158), *and trinitro nitronic ester* (161).

Reaction of 1,2,3-trimethyl-6-nitro-5-trinitromethylcyclohexa-1,3-diene (175) with $^{\bullet}NO_2$ at C4 would give the delocalized carbon radical (184), the stereochemistry of which is determined by the entry of the $^{\bullet}NO_2$ molecule *anti* to the bulky trinitromethyl group, as represented in Scheme 3.17. Further coupling of this carbon radical with $^{\bullet}NO_2$ at either terminus of the allylic system gives the epimeric trinitro/trinitromethyl adducts (157) and

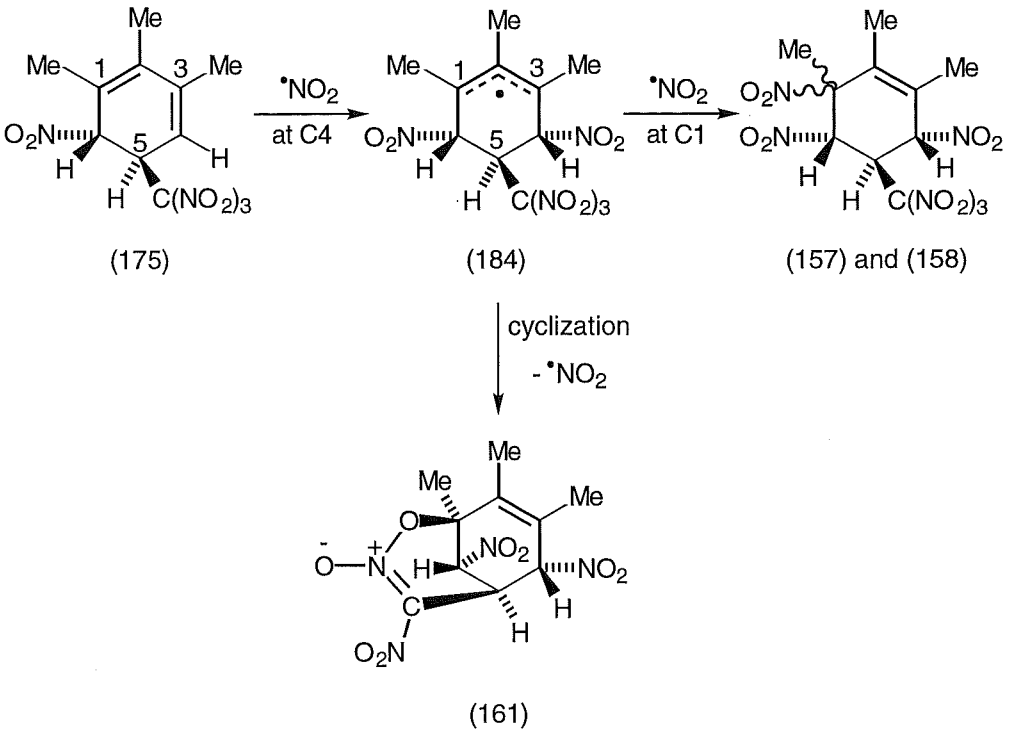

Scheme 3.17

(158). Alternately, cyclization involving the trinitromethyl group can occur with loss of $^{\bullet}NO_2$ to give the trinitro nitronic ester (161), also seen in Scheme 3.17.

(c) The formation of "double" adduct (139) *and hydroxy dinitro nitronic ester* (162).

The modes of formation of "double" adduct (139) and hydroxy dinitro nitronic ester (162) are closely analogous to those for the trinitro/trinitromethyl adducts (157) and (158), and the trinitro nitronic ester (161). As represented in Scheme 3.18, addition of $^{\bullet}NO_2$ at C4 in the hydroxy/trinitromethyl adduct (177) would give the delocalized carbon radical (185), the stereochemistry of this addition being determined as for delocalized radical (184), above. Subsequent attack of $^{\bullet}NO_2$ at C1 in allylic radical (185)

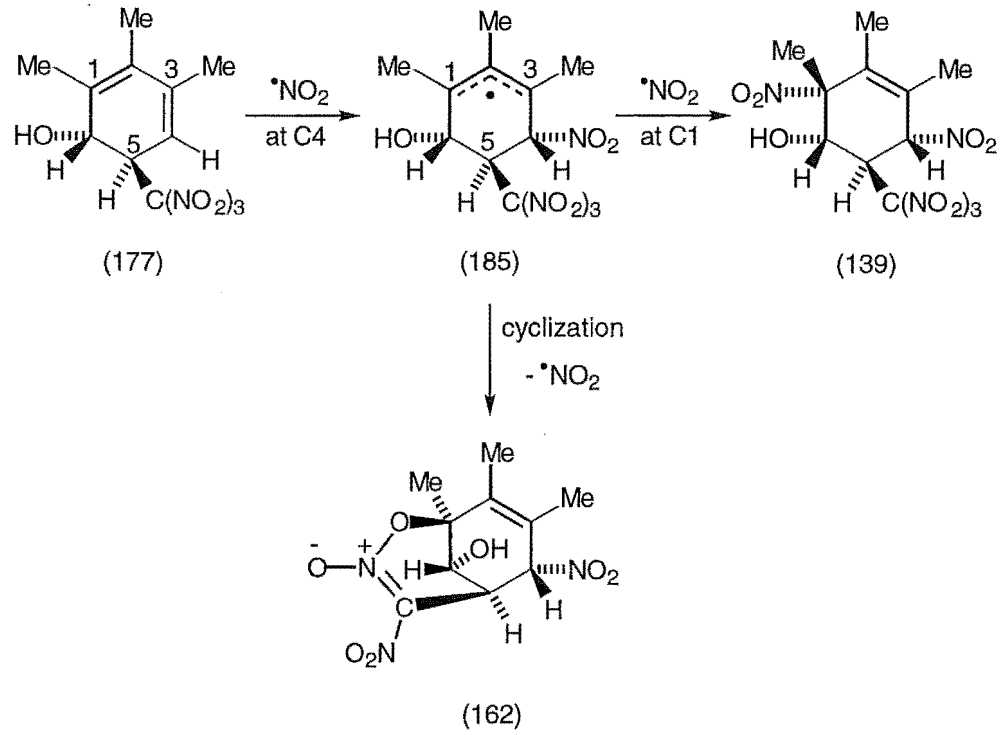

Scheme 3.18

occurs *vicinal* and *syn* to the hydroxyl group in the system, to give the "double" adduct (139). The alternative pathway for further reaction of allylic radical (185) results from cyclization involving the trinitromethyl group and loss of $^{\bullet}NO_2$ from that functional group to give the hydroxy dinitro nitronic ester (162) (See Scheme 3.18).

3.9.5 The formation of aromatic compounds and dienones.

(a) The formation of the side-chain trinitromethyl compounds (166) *and* (167).

The yields of the side-chain trinitromethyl compounds (166) and (167) increased at lower reaction temperatures in both dichloromethane and acetonitrile (See Tables 3.1 and 3.3, Sections 3.3 and 3.5, respectively). This suggests that they are probably derived by photo-chemically promoted decomposition of nitro/trinitromethyl adducts. A

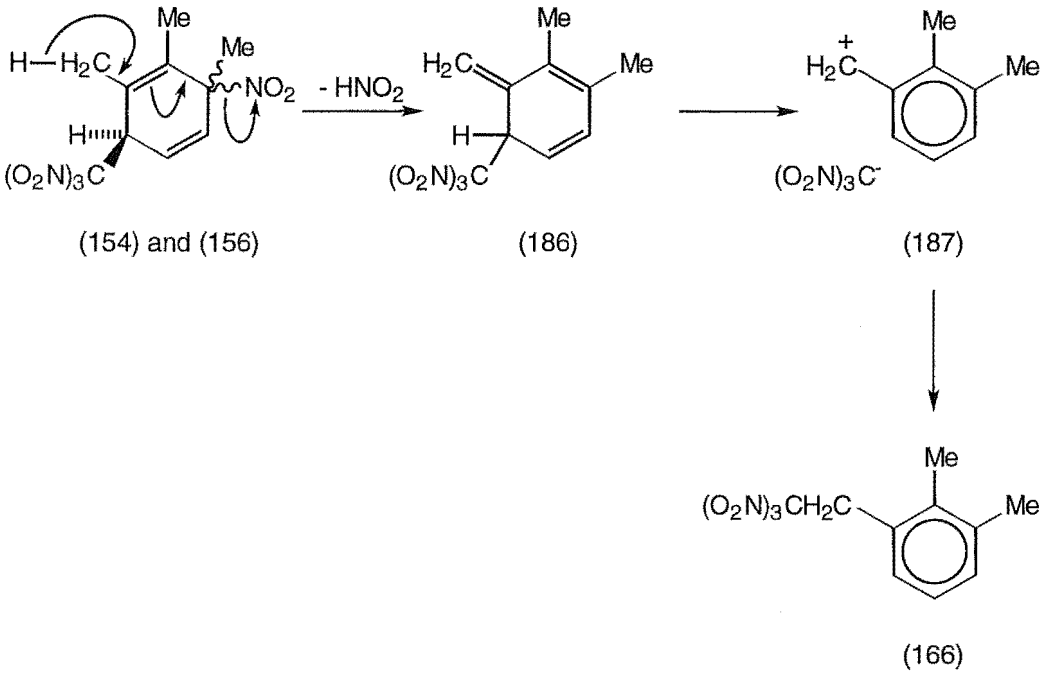

(154) and (156) (186) (187)

(166)

Scheme 3.19

possible mechanism for the formation of compound (166) is summarized in Scheme 3.19. Loss of nitrous acid from adducts (154) or (156) would yield the trinitromethyl diene (186), which might rearrange *via* the ion pair (187) to give the side-chain trinitromethyl aromatic (166).

A similar mechanism could occur in the formation of compound (167). Initial loss of nitrous acid from adduct (175), the proposed precursor to "double" adducts (157) and (158) and the nitronic ester (161) [see Section 3.9.4 (b)], would yield the trinitromethyl diene (188), as outlined in Scheme 3.20. Subsequently, diene (188) could rearrange *via* the ion pair (189) to give the side-chain trinitromethyl aromatic (167).

(b) The formation of the nitro aromatic compounds (168) *and* (169).

While the yields of the nitro compounds (168) and (169) in dichloromethane remained almost invariant of temperature (see Table 3.1, Section 3.3), in acetonitrile they increased as the temperature was lowered (see

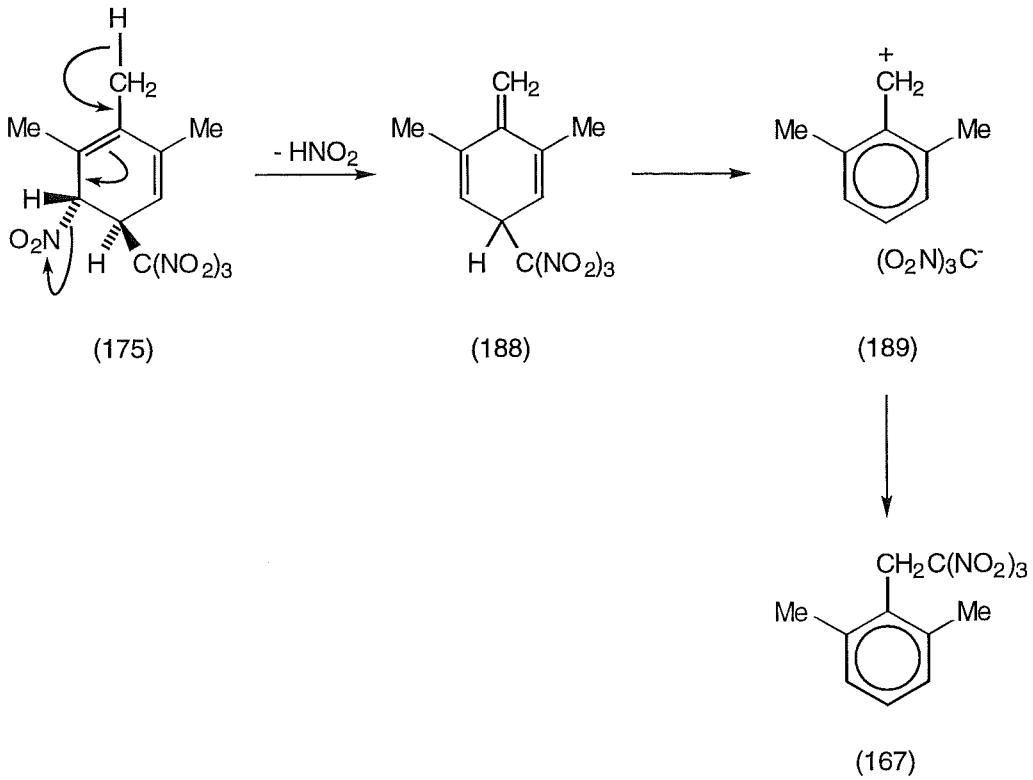

(175) (188) (189) (167)

Scheme 3.20

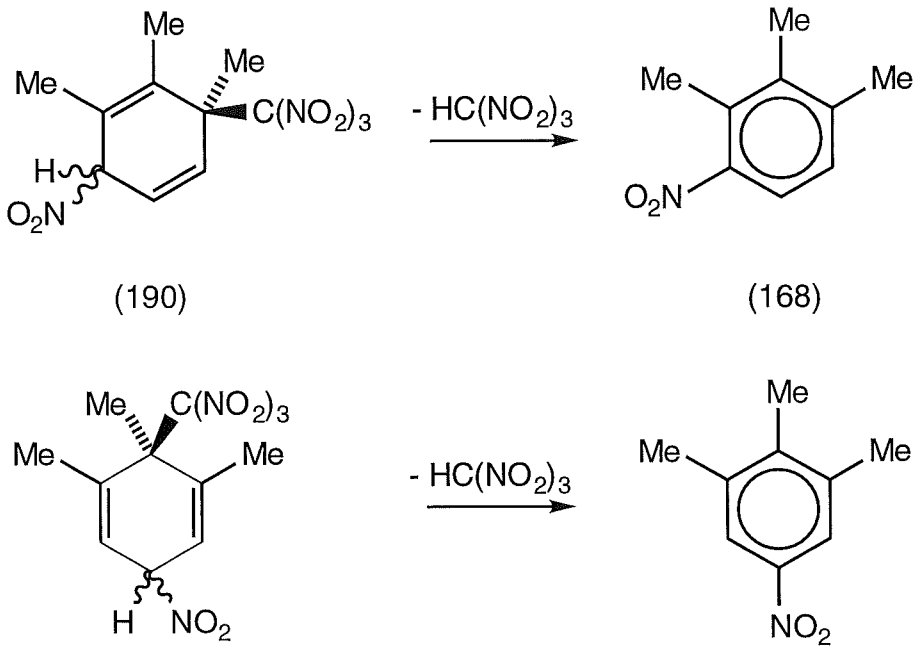

(190) (168)

(191) (169)

Scheme 3.21

Table 3.3, Section 3.5). This suggests that at least some of the nitro compounds are derived from decomposition of nitro/trinitromethyl adducts. Possible mechanisms for the formation of compounds (168) and (169) are presented in Scheme 3.21, and involve loss of nitroform from the proposed highly sterically hindered adducts (190) and (191), respectively.

(c) *The formation of dienones* (163) *and* (164), *nitro phenol* (171) *and hydroxy trinitro ketone* (172).

The mode of formation of nitro dienones (163) and (164) is most likely to be *via* their corresponding phenols (192) and (193), as illustrated in Scheme 3.22. Reaction of $^{\bullet}NO_2$ with the labile phenolic hydrogen in phenols (192) and (193) leads to loss of nitrous acid and the generation of the phenoxy radicals (194) and (195), respectively. Radical coupling between $^{\bullet}NO_2$ and the phenoxy radicals (194) and (195) then occurs to give the 4-nitrocyclohexa-2,5-dienones (163) and (164), respectively. The mechanisms proposed above are analogous to that proposed by Brunton *et al.*[25] for reactions of 2,6-disubstituted-4-methyl phenols (196) and (197)

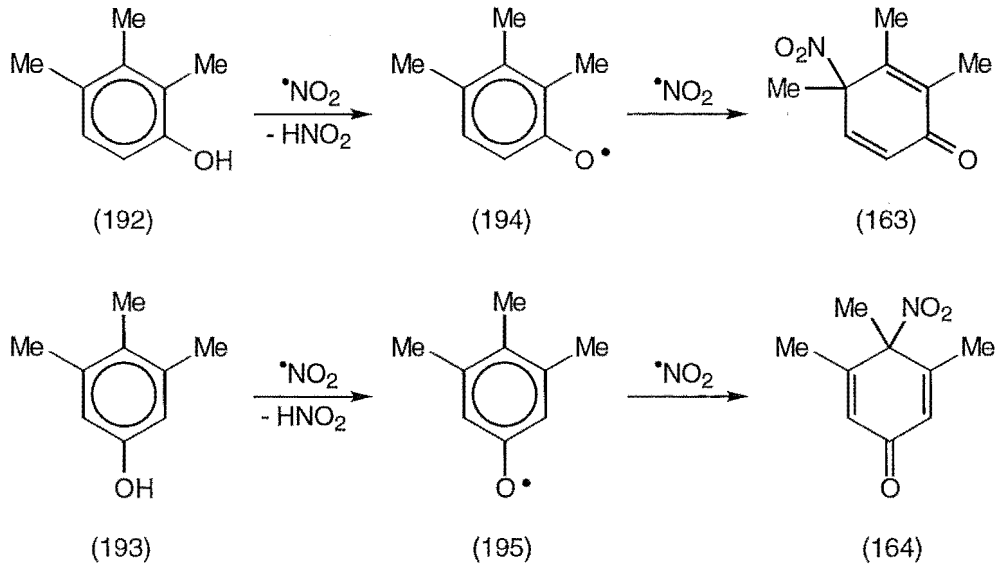

Scheme 3.22

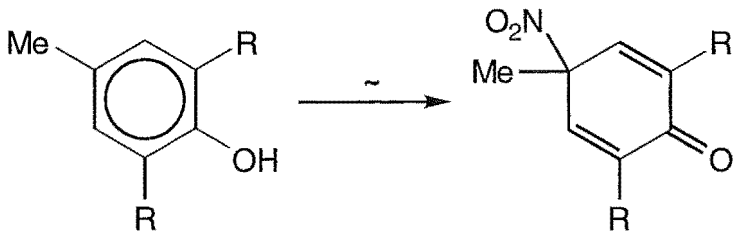

(196) R=Me
(197) R=Bu^t

(198) R=Me
(199) R=Bu^t

Scheme 3.23

with $^{\bullet}NO_2$ to give the 4-nitrocyclohexa-2,5-dienones (198) and (199), respectively, as observed in Scheme 3.23.

The rearrangement of dienone (163) in (D)chloroform was shown to yield the nitro phenol (171) (See Section 3.8). This rearrangement was envisaged as occurring *via* homolysis of the C4-NO_2 bond to form the

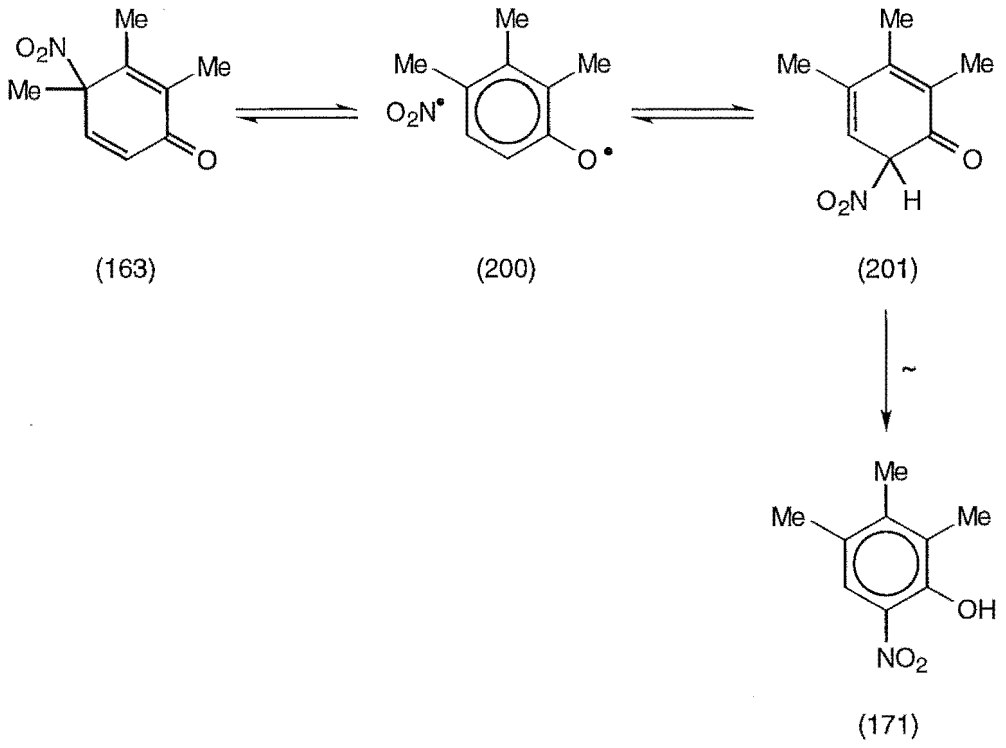

(163) (200) (201)

(171)

Scheme 3.24

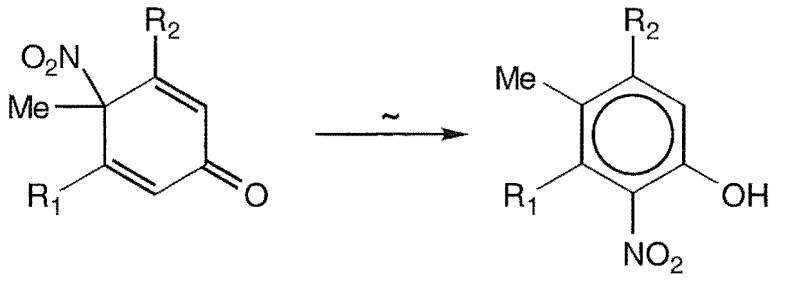

(202) R_1=H, R_2=H
(203) R_1=Me, R_2=H
(204) R_1=Me, R_2=Me

(205) R_1=H, R_2=H
(206) R_1=Me, R_2=H
(207) R_1=Me, R_2=Me

Scheme 3.25

solvent caged species (200), as depicted in Scheme 3.24. Subsequently, a 1,3-nitro group migration occurs to form the dienone (201), which then undergoes enolization to yield the nitro phenol (171). The mechanism proposed above is analogous to that proposed by Barnes and Myhre[26] in the rearrangement of substituted 4-nitrocyclohexa-2,5-dienones (202)-(204) to give the corresponding 2-nitro phenols (205)-(207), as seen in Scheme 3.25.

A possible mechanism for the formation of the hydroxy trinitro ketone (172) is shown in Schemes 3.26 and 3.27. Initially, reaction of $^{\bullet}NO_2$ with the nitro phenol (171) leads to loss of nitrous acid and the formation of the phenoxy radical (208), as summarized in Scheme 3.26. Radical coupling

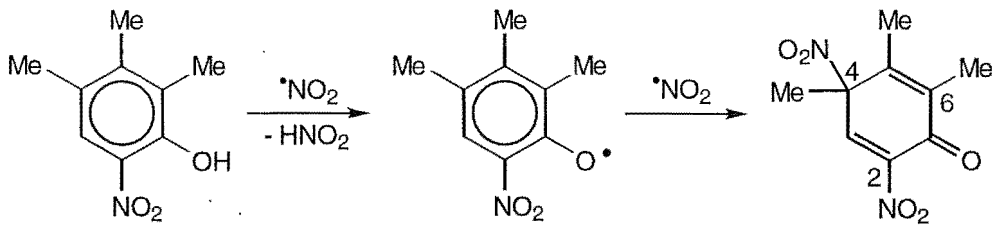

(171) (208) (209)

Scheme 3.26

between the phenoxy radical and $^{\bullet}NO_2$ then occurs to give the 2,4-dinitro-cyclohexa-2,5-dienone (209), in a similar manner to that proposed above in the formation of nitro dienones (163) and (164) (See Scheme 3.22). Subsequently, homolysis of the C4-NO_2 bond would form the solvent caged species (210), as represented in Scheme 3.27. A 1,3-nitro group migration

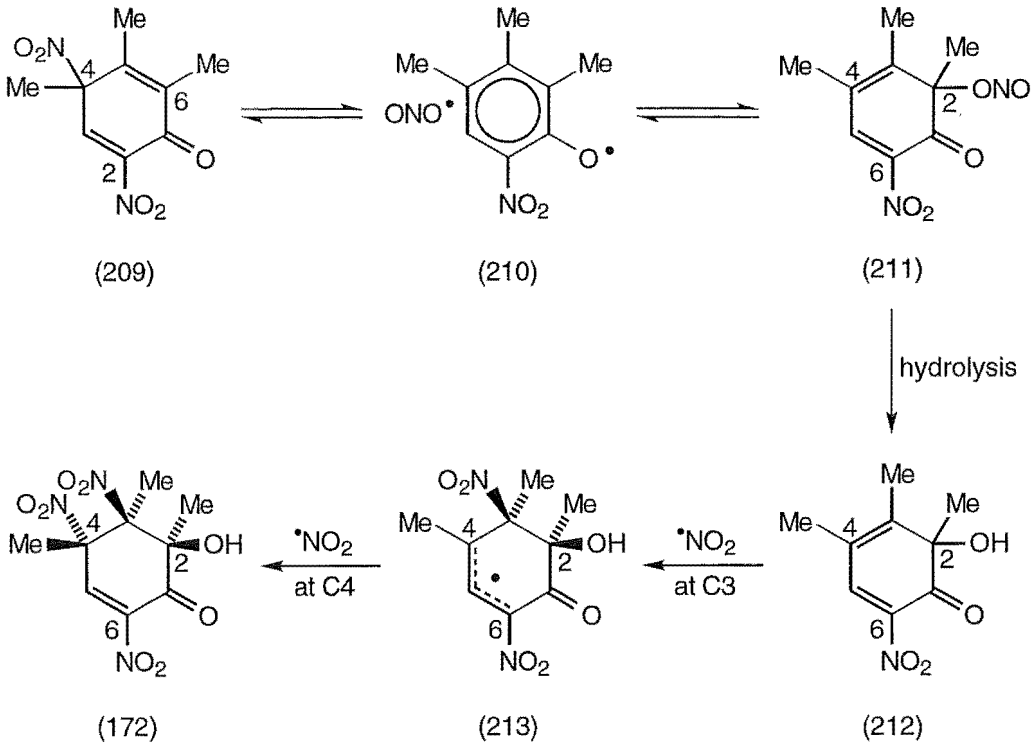

Scheme 3.27

could then occur with C-O bond formation to form the 2-nitrito-6-nitro dienone (211), which then could undergo hydrolysis to form the 2-hydroxy-6-nitro dienone (212). Subsequent 3,4-addition of $^{\bullet}NO_2$ to dienone (212) would yield the hydroxy dinitro ketone (172). This was envisaged as occurring *via* the delocalized radical (213), which might be expected to undergo radical coupling with $^{\bullet}NO_2$ preferentially at the less hindered C4 position. The mechanism proposed in Scheme 3.27 is analogous to that reported by Coombes *et al.*[27] for the formation of 2,6-di-*tert*-butyl-*c*-6-hydroxy-4-methyl-*r*-4,*c*-5-dinitrocyclohexa-2-enone (214) from 2,6-di-*tert*-

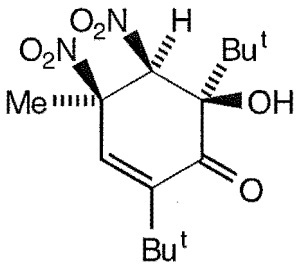

(214)

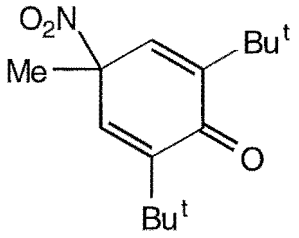

(215)

butyl-4-methyl-4-nitrocyclohexa-2,5-dienone (215).

(d) The formation of carboxylic acids (173) *and* (174).

While the formation of the carboxylic acids (173) and (174) remains uncertain, it appears likely that they arise *via* the trinitromethyl aromatic compounds (138) and (165), respectively, as discussed by Eberson and Radner.[28]

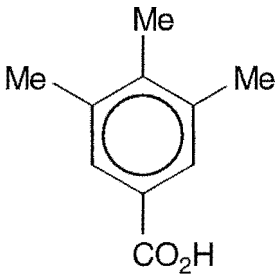

(173)

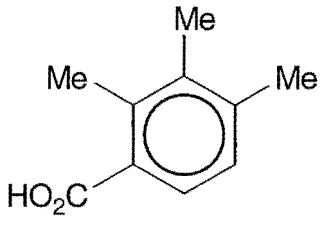

(174)

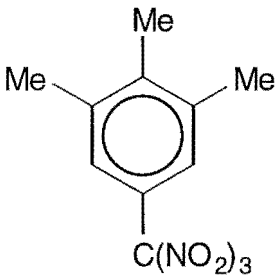

(138)

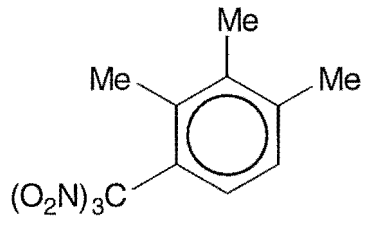

(165)

In conclusion, it appears likely that reaction of $(O_2N)_3C^-$ at the methyl substituted positions C1 and C2 of the 1,2,3-trimethylbenzene radical cation

are disfavoured due to the steric interactions between the bulky trinitromethyl group and the *β*- and *ipso*-methyl interactions. With the majority of attack of $(O_2N)_3C^-$ occurring at C5, the least sterically hindered position on the 1,2,3-trimethylbenzene radical cation, it would appear that delocalized carbon radical (140) is more stable than delocalized radical (141), formed after attack of $(O_2N)_3C^-$ on the 1,2,3-trimethylbenzene radical cation at C4.

3.10 The Photolysis of 1,2,4,5-Tetramethylbenzene (134)

General procedure for the photonitration of 1,2,4,5-tetramethylbenzene (134) *with TNM.*

A solution of 1,2,4,5-tetramethylbenzene (134) (500 mg, 0.47 mol L^{-1}) and TNM (0.94 mol L^{-1}) in dichloromethane (at +20, -20 or -50°) or acetonitrile (at +20 or -20°) was irradiated with filtered light ($\lambda_{cut\text{-}off}$<435 nm) and small samples were withdrawn for analysis at suitable intervals. The work-up procedure, involving evaporation of solvent and TNM, was conducted at ≤0°. The crude product mixtures were stored at -78° and were analysed by ^1H n.m.r. spectroscopy as soon as possible (For complete experimental details see Chapter 5, Section 5.3.2).

3.11 The Photochemistry of 1,2,4,5-Tetramethylbenzene (134) in Dichloromethane

Photochemistry in dichloromethane at -50° and the identification of adducts (216) *and* (217) *and aromatic compound* (225).

A solution of 1,2,4,5-tetramethylbenzene (134) (0.47 mol L^{-1}) and

TNM (0.94 mol L^{-1}) in dichloromethane was irradiated at -50° until the orange colour of the charge-transfer band was bleached. The composition of the reaction mixture was monitored by withdrawing samples for ^1H n.m.r. spectral analysis. After work-up, the final solution (after 4 h, conversion 71%) contained the epimeric 1,3,4,6-tetramethyl-3-nitro-6-trinitromethyl-cyclohexa-1,4-dienes (216) (46%) and (217) (7%), aromatic compounds (218)-(225) (total 41%) and unidentified aromatic compounds (total 6%).

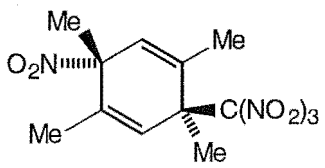

(216)

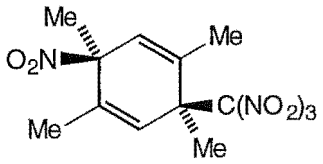

(217)

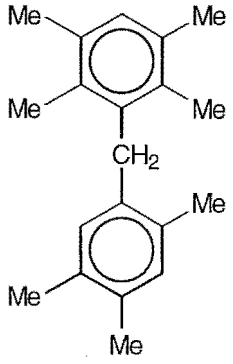

(218)

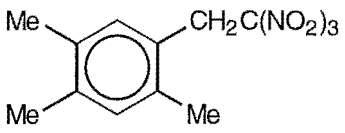

(219)

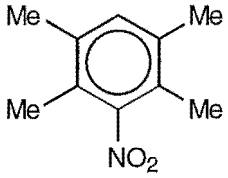

(220)

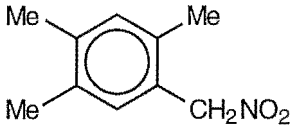

(221)

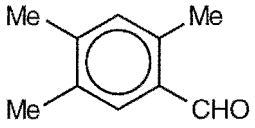

(222)

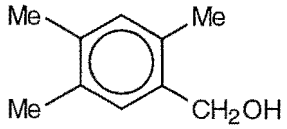

(223)

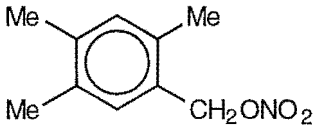

(224)

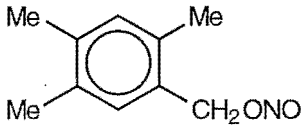

(225)

The adducts (216) and (217) were separated partially by h.p.l.c. on a cyanopropyl column, cooled to 0°, using hexane/dichloromethane mixtures as the eluting solvents. The first material eluted was a mixture of aromatic compounds, the separation and identification of which is given below.

The major adduct (216) was isolated as an unstable oil and was

identified as 1,3,4,6-tetramethyl-*r*-3-nitro-*t*-6-trinitromethylcyclohexa-1,4-diene (216) on the basis of its spectroscopic data and a comparison of its characteristic ^{1}H and ^{13}C n.m.r. resonances with the spectral features for 1,3,5,6-tetramethyl-*t*-6-nitro-*r*-3-trinitromethylcyclohexa-1,4-diene (170), the structure of which was determined by single crystal X-ray analysis.[14] N.O.e. experiments confirmed the assignments of the chemical shifts for the protons. In particular, irradiation at δ 5.82 (H2) gave enhancements at δ 1.74 (3-Me) and at δ 1.87 (1-Me), while irradiation at δ 6.20 (H5) gave enhancements at δ 1.80 (4-Me) and at δ 1.96 (6-Me), as outlined in Fig.

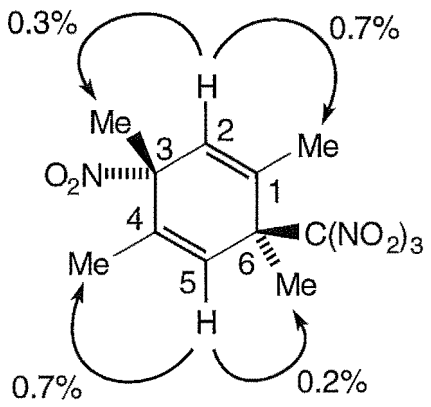

(216)

1-Me	1.87	C1	134.1
H2	5.82	C2	130.2
3-Me	1.74	C3	88.3
4-Me	1.80	C4	136.2
H5	6.20	C5	126.0
6-Me	1.96	C6	51.2

Fig. 3.32 Characteristic ^{1}H and ^{13}C n.m.r. resonances (in ppm) and enhancements (%) from selected n.O.e. experiments for adduct (216).

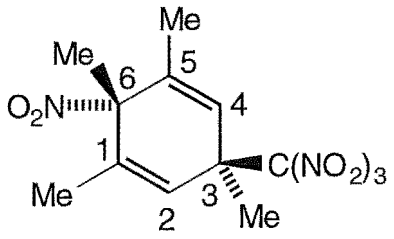

(170)

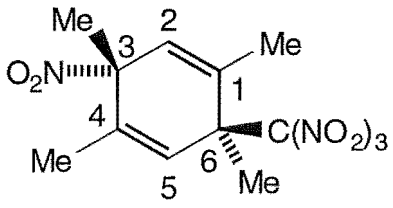

(216)

6-Me	1.79	3-Me	1.74
1-Me	1.79	4-Me	1.80
H2	5.94	H5	6.20
3-Me	1.79	6-Me	1.96
C6	90.9	C3	88.3
C1	137.0	C4	136.2
C2	124.1	C5	126.0
C3	47.6	C6	51.2

Fig. 3.33 Comparison of the characteristic ^{1}H and ^{13}C n.m.r. resonances (in ppm) for adducts (170) and (216).

3.32. The assignment of the ^{13}C n.m.r. resonances, also shown in Fig. 3.32, was confirmed by HMQC and HMBC experiments. Specifically, the nitro function was indicated by the ^{13}C n.m.r. chemical shift for C3 (δ 88.3) and the trinitromethyl function by the ^{13}C n.m.r. chemical shift for C6 (δ 51.2). Furthermore, comparisons of the characteristic ^{1}H and ^{13}C n.m.r. resonances between the closely related adducts (170) and (216) are illustrated in Fig. 3.32, further supporting the identification of adduct (216). The *trans*-3-nitro-6-trinitromethyl stereochemistry was assigned to adduct (216) because it eluted from the cyanopropyl h.p.l.c. column with the

dichloromethane/hexane solvent system earlier than its *cis*-3-nitro-6-trinitromethyl stereoisomer (217). The h.p.l.c. elution order for such pairs of stereoisomers is known, with *trans*-1,4-nitro/trinitromethyl adducts eluting ahead of their *cis*-1,4-isomers.[5-7]

The minor adduct (217) was obtained only in admixture containing *c.* 5% of adduct (216). The identification of adduct (217) as 1,3,4,6-tetramethyl-*r*-3-nitro-*c*-6-trinitromethylcyclohexa-1,4-diene (217) was based on a comparison of its spectroscopic data with (216), its epimer. N.O.e. experiments confirmed the assignments of the chemical shifts for the

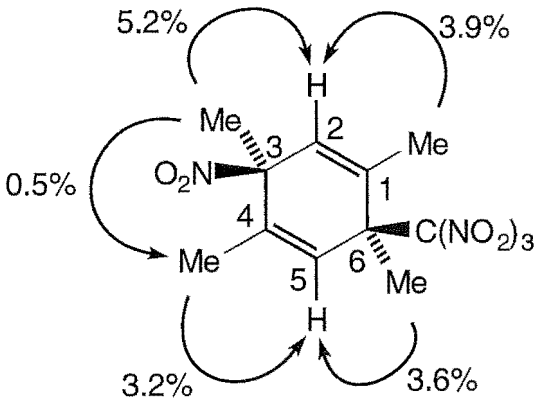

(217)

1-Me	1.87	C1	134.4
H2	5.98	C2	130.3
3-Me	1.74	C3	85.4
4-Me	1.94	C4	136.3
H5	6.28	C5	126.4
6-Me	1.85	C6	50.6

Fig. 3.34 Characteristic ^{1}H and ^{13}C n.m.r. resonances (in ppm) and enhancements (%) from selected n.O.e. experiments for adduct (217).

protons. In particular, irradiation at δ 1.87 (1-Me) gave an enhancement at δ 5.98 (H2), irradiation at δ 1.74 (3-Me) gave enhancements at δ 1.94

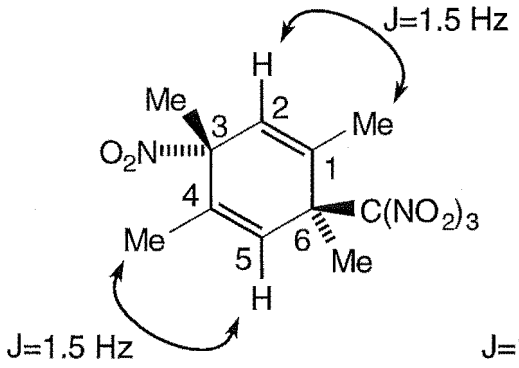

(216)

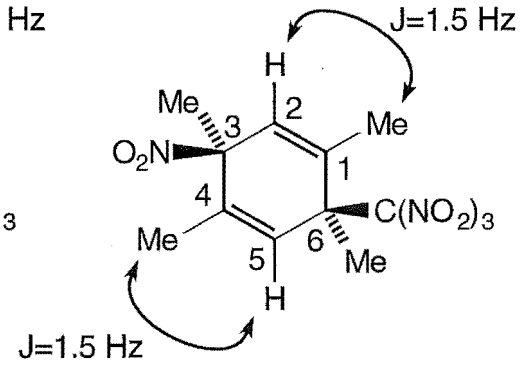

(217)

1-Me	1.87	1-Me	1.87
H2	5.82	H2	5.98
3-Me	1.74	3-Me	1.74
4-Me	1.80	4-Me	1.94
H5	6.20	H5	6.28
6-Me	1.96	6-Me	1.85
C1	134.1	C1	134.4
C2	130.2	C2	130.3
C3	88.3	C3	85.4
C4	136.2	C4	136.3
C5	126.0	C5	126.4
C6	51.2	C6	50.6

Fig. 3.35 Comparison of the characteristic ^{1}H and ^{13}C n.m.r. resonances (in ppm) for adducts (216) and (217).

(4-Me) and at δ 5.98 (H2), irradiation at δ 1.94 (4-Me) gave an enhancement at δ 6.28 (H5), and irradiation at δ 1.85 (6-Me) gave an enhancement at δ 6.28 (H5), as seen in Fig. 3.34. The characteristic ^{1}H and ^{13}C n.m.r. data are also presented in Fig. 3.34. In particular, ^{13}C n.m.r. resonances for the nitro function attached to C3 appeared at δ 85.4, while the trinitromethyl function attached to C6 appeared at δ 50.6. These assignments were confirmed by HMQC and HMBC experiments and comparison with data for the epimeric adduct (216). A comparison of the characteristic spectroscopic data for adducts (216) and (217) is summarized in Fig. 3.35, and was consistent with their assignment as epimers.

Compound (225) could not be isolated from the h.p.l.c. column. However, the presence of the known[9] 2,4,5-trimethylbenzyl nitrite (225) in the reaction mixture was inferred from the ^{1}H n.m.r. signal due to the -C**H$_2$**-ONO group. Specifically, the -C**H$_2$**-ONO resonance appeared as a broad singlet at δ 5.64.

The composition of the photochemical reaction between 1,2,4,5-tetramethylbenzene (134) and TNM was monitored with time at +20, -20, and -50° in dichloromethane. An overview of product yields in dichloromethane is presented in Table 3.5. The most notable feature was the increase in the yields of the epimeric adducts (216) and (217) at lower reaction temperatures. After 4 h, at +20°, the total adduct yield was 7%. This increased to 53% at -50°. Correspondingly, yields of the side-chain trinitromethyl compound (219), ring nitro compound (220), benzaldehyde (222) and side-chain nitrate compound (224) all decreased at lower reaction temperatures (total 69% at +20°, total 21% at -50°).

Table 3.5 Overview of product yields from the photolysis of 1,2,4,5-tetramethylbenzene (134) (0.47 mol L^{-1}) and TNM (0.94 mol L^{-1}) in dichloromethane.

		Yield (%)										
	Conversion											Unknown
t (h)	(%)	(216)	(217)	(218)	(219)	(220)	(221)	(222)	(223)	(224)	(225)	aromatics
At +20°												
1	42	11.8	3.5	1.2	26.1	9.9	10.8	13.0	0.8	14.7	3.0	5.2
2	69	9.8	3.5	0.8	24.5	9.4	12.7	6.6	0.5	24.0	2.9	5.3
4	87	4.8	2.1	0.5	27.4	5.4	15.4	5.3	0.5	30.7	2.7	5.2
At -20°												
4	87	24.0	4.4	1.0	9.5	1.8	27.7	1.5	1.0	19.5	4.0	5.6
At -50°												
2	46	50.3	7.9	2.2	6.3	0.6	13.0	1.2	0.8	9.3	1.3	7.1
4	71	46.1	7.1	1.1	6.0	0.9	17.7	0.6	1.2	13.0	2.8	5.9

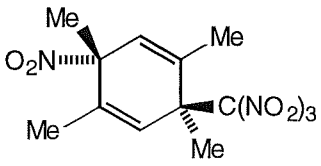

(216)

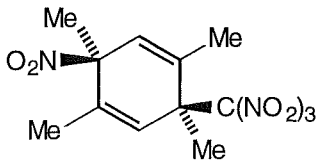

(217)

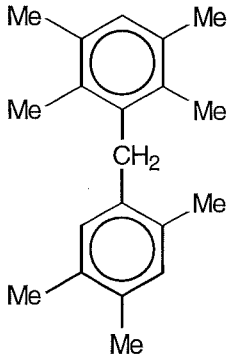

(218)

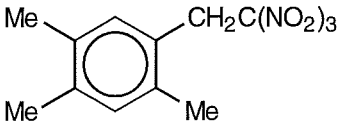

(219)

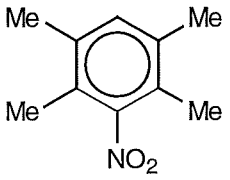

(220)

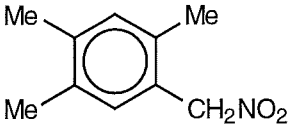

(221)

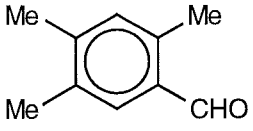

(222)

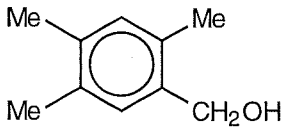

(223)

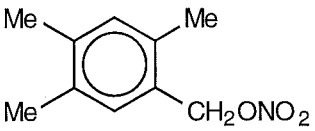

(224)

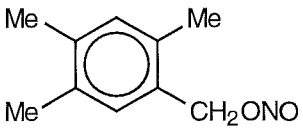

(225)

3.12 The Photochemistry of 1,2,4,5-Tetramethylbenzene (134) in 1,1,1,3,3,3-Hexafluoropropan-2-ol (HFP)

Photochemistry in HFP at +20° and the identification of the aromatic products (218)-(224) *and* (226).

Photolysis of the charge-transfer complex of 1,2,4,5-tetramethylbenzene (134) (0.47 mol L^{-1}) / TNM (0.94 mol L^{-1}) in HFP at +20° for 20 h (conversion 87%) gave a product which was shown by ^1H n.m.r. spectral analysis to be a mixture of the aromatic compounds (218)-(224) and (226) (total 86%) and further unidentified aromatic compounds (total 14%).

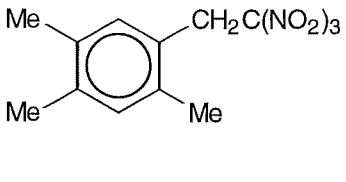

(219)

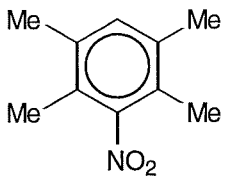

(220)

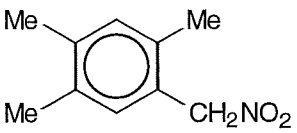

(221)

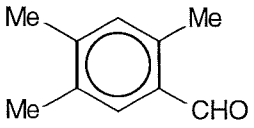

(222)

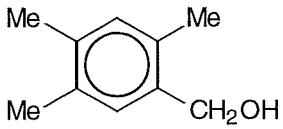

(223)

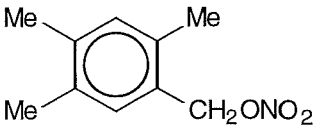

(224)

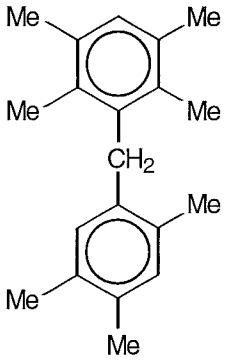

(218)

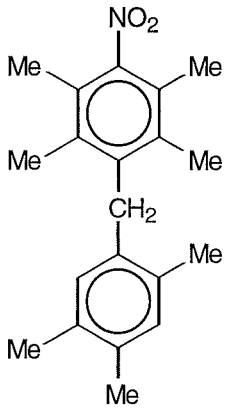

(226)

Chromatography of this mixture on a silica gel Chromatotron plate gave the following in elution order.

The first compound eluted was identified as 2,2',3,4',5,5',6-hepta-methyldiphenylmethane (218) and the structure was confirmed by comparison with literature data.[29]

The second compound eluted was identified as 2,4,5-trimethyl-1-(2',2',2'-trinitromethyl)-benzene (219). The side-chain trinitromethyl aromatic (219) gave a satisfactory parent molecular ion in the mass spectrum, indicating the molecular formula $C_{11}H_{13}N_3O_6$. N.O.e. experiments confirmed the assignments of the chemical shifts for the protons. In particular, irradiation at δ 2.18 (5-Me) gave an enhancement at δ 6.82 (H6), irradiation at δ 4.38 (C**H**$_2$) gave enhancements at δ 2.17 (2-Me)

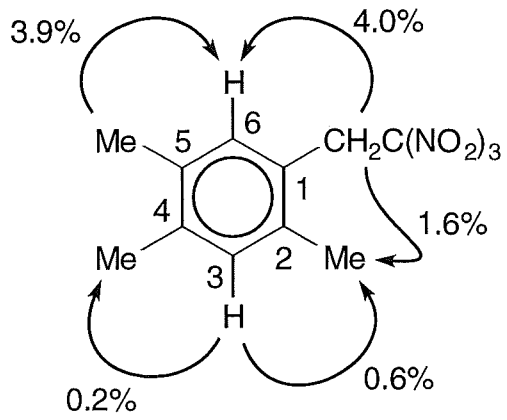

Fig. 3.36 Enhancements (%) from selected n.O.e. experiments for the side-chain trinitromethyl aromatic (219).

and at δ 6.82 (H6), and irradiation at δ 7.00 (H3) gave enhancements at δ 2.17 (2-Me) and at δ 2.21 (4-Me), as shown in Fig. 3.36. Furthermore, the presence of very strong infrared absorptions at 1605 and 1578 cm^{-1} provided evidence for the $-C(NO_2)_3$ substituent.

The third compound eluted was identified as 2,3,5,6-tetramethyl-1-nitrobenzene (220) and the structure was confirmed by comparing its melting point and spectroscopic data with literature data.[21]

The fourth compound eluted was identified as 2,4,5-trimethylphenyl-nitromethane (221) and the structure was confirmed by comparing its spectroscopic data with literature data.[9]

The fifth compound eluted was identified as 2,2',3,4',5,5',6-hepta-methyl-4-nitrodiphenylmethane (226). Compound (226) gave a satisfactory parent molecular ion in the mass spectrum, indicating the molecular formula $C_{20}H_{25}NO_2$. N.O.e. experiments confirmed the assignments of the chemical shifts for the protons. Specifically, irradiation at δ 2.08 (5'-Me) gave an enhancement at δ 6.20 (H6'), irradiation at δ 3.88 (CH_2) gave enhancements at δ 2.11 (2-Me), δ 2.36 (2'-Me) and at δ 6.20 (H6'), and irradiation at δ 6.99 (H3') gave enhancements at δ 2.19 (4'-Me)

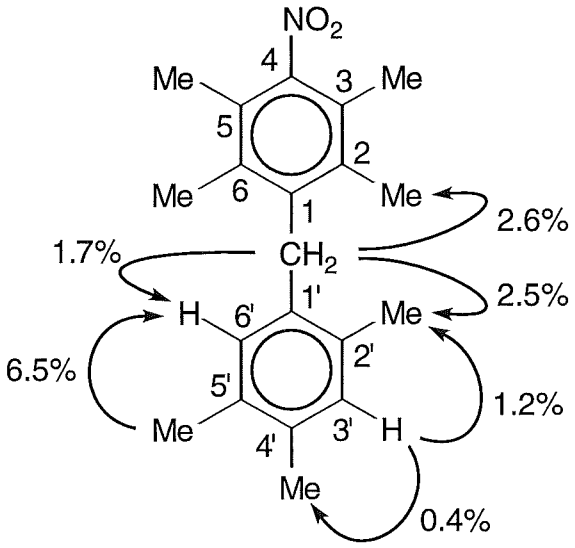

Fig. 3.37 Enhancements (%) from selected n.O.e. experiments for compound (226).

and at δ 2.36 (2'-Me), as presented in Fig. 3.37. Furthermore, the presence of a very strong infrared absorption at 1524 cm^{-1} provided evidence for the $-NO_2$ substituent.

The sixth compound eluted was identified as 2,4,5-trimethylbenzaldehyde (222) and the structure was confirmed by comparing its spectroscopic data with literature data[9].

The final compound eluted was identified as 2,4,5-trimethylbenzyl alcohol (223) and the structure was confirmed by comparing its spectroscopic data with an authentic sample.

Compound (224) could not be isolated from the silica gel Chromatotron plate. However, the presence of the known[9] 2,4,5-trimethylbenzyl nitrate (224) in the reaction mixture was inferred from the ^1H n.m.r. signal due to the $-CH_2-ONO_2$ function. Specifically, the $-CH_2-ONO_2$ resonance appeared as a singlet at δ 5.39.

On monitoring the photolysis of the charge-transfer complex of TNM with 1,2,4,5-tetramethylbenzene (134) in HFP at +20° with time, it was noted

that adducts (216) and (217) were absent (See Table 3.6). Comparison of the +20° HFP reaction with the +20° dichloromethane reaction (see Table 3.5, Section 3.11) showed that the reaction in HFP was slow. After 4 h, the conversion in dichloromethane was 87%, while in HFP conversion was 21% and only reached 87% after 20 h. The major product of reaction in HFP was 2,3,5,6-tetramethylnitrobenzene (220) (*c.* 60%). The limited yield of the side-chain trinitromethyl derivative (219) was also notable. Formation of the nitro dimer (226), which was not observed in the +20° dichloromethane reaction, increased between 4 h and 20 h (3% at 4 h, 8% at 20 h), with a corresponding decrease in the dimer (218) (9% at 4 h, 3% at 20 h).

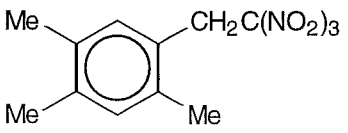

(219)

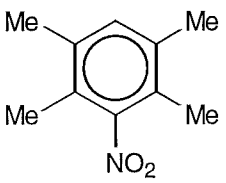

(220)

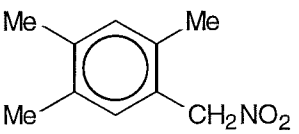

(221)

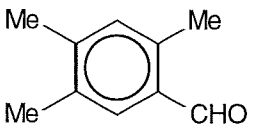

(222)

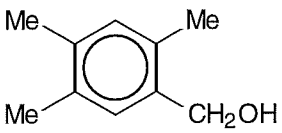

(223)

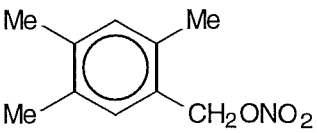

(224)

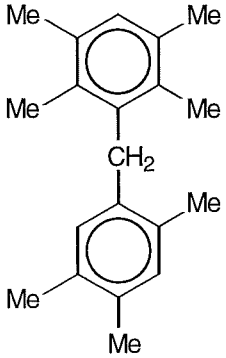

(218)

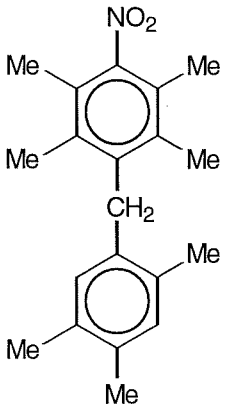

(226)

Table 3.6 Overview of product yields from the photolysis of 1,2,4,5-tetramethylbenzene (134) (0.47 mol L^{-1}) and TNM (0.94 mol L^{-1}) in 1,1,1,3,3,3-hexafluoropropan-2-ol, at +20°.

		Yield (%)								
	Conversion									Unknown
t (h)	(%)	(218)	(219)	(220)	(221)	(222)	(223)	(224)	(226)	aromatics
0.5	3	4.5	0.8	60.0	1.7	8.8	10.2	3.2	trace	10.8
1	7	5.2	1.6	57.0	2.2	4.6	9.5	4.5	1.5	13.9
2	13	7.3	2.0	62.4	2.5	3.1	5.8	4.8	3.1	9.0
4	21	8.5	4.0	61.5	3.0	1.4	6.1	3.9	2.8	8.8
20	87	2.5	8.8	53.3	6.8	2.0	1.5	3.0	7.8	14.3

3.13 The Photochemistry of 1,2,4,5-Tetramethylbenzene (134) in Acetonitrile

Photochemistry in acetonitrile at +20° and the identification of the N-*nitroso acetamide* (227).

Photolysis of the charge-transfer complex of 1,2,4,5-tetramethylbenzene (134) (0.47 mol L^{-1}) / TNM (0.94 mol L^{-1}) in acetonitrile at +20° for 4 h (conversion 52%) gave a product which was shown by ^1H n.m.r. spectral analysis (see Table 3.7, below) to be a mixture of the epimeric nitro/trinitromethyl adducts (216) and (217) (trace amounts), aromatic compounds (218)-(224) and (226) (total 86%), the *N*-nitroso acetamide (227) (9%) and further unidentified aromatic compounds (total 5%). Chromatography of this mixture on a silica gel Chromatotron plate gave a small amount of compound (227) in a fraction eluted immediately before the aldehyde (222).

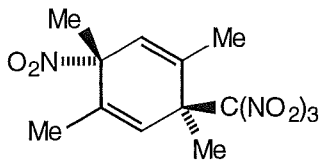

(216)

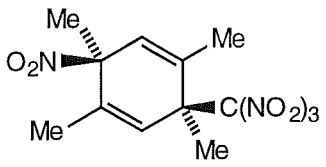

(217)

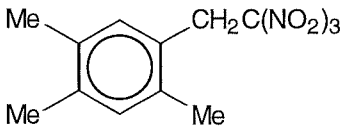

(219)

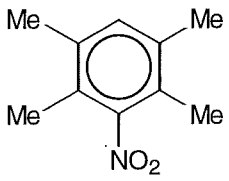

(220)

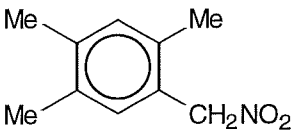

(221)

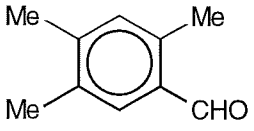

(222)

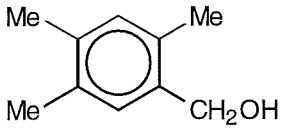

(223)

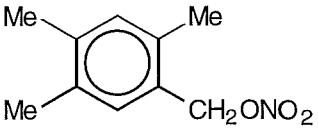

(224)

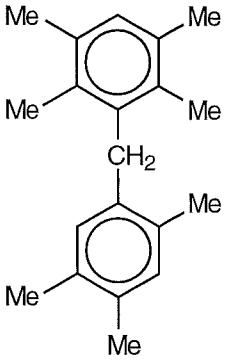

(218)

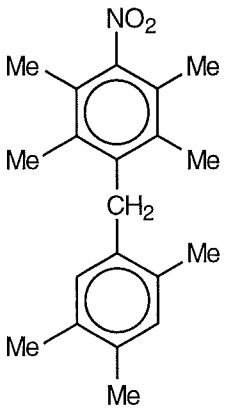

(226)

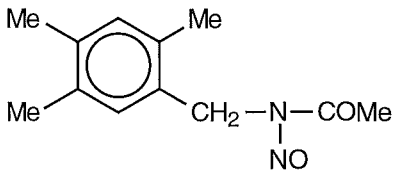

(227)

Compound (227) was identified as *N*-(2,4,5-trimethylbenzyl)-*N*-nitroso acetamide (227) by comparing its spectroscopic data with the related *N*-nitroso-*N*-(pentamethylbenzyl)-acetamide (228), which was identified in the corresponding photochemical reaction involving hexamethylbenzene (136), TNM and acetonitrile at +20° (See later in Section 3.30). The *N*-nitroso acetamide (227) gave a satisfactory parent molecular ion in the mass spectrum, indicating the molecular formula $C_{12}H_{16}N_2O_2$. N.O.e. experiments confirmed the assignments of the chemical shifts for the

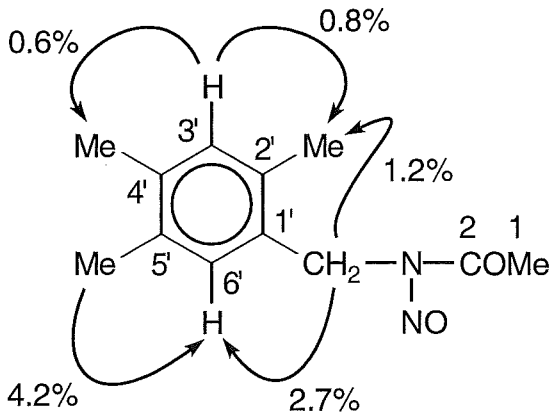

Fig. 3.38 Enhancements (%) from selected n.O.e. experiments for the *N*-nitroso acetamide (227).

protons. In particular, irradiation at δ 2.13 (5'-Me) gave an enhancement at δ 6.50 (H6'), irradiation at δ 4.86 (C**H**$_2$) gave enhancements at δ 2.31 (2'-Me) and at δ 6.50 (H6'), and irradiation at δ 6.90 (H3') gave enhancements at δ 2.16 (4'-Me) and at δ 2.31 (2'-Me), as seen in Fig. 3.38. HMQC and HMBC experiments confirmed the assignments of the ^{13}C n.m.r. resonances and the characteristic ^{1}H and ^{13}C n.m.r. and infrared absorptions for the closely related compounds (228) and (227) are compared in Fig. 3.39. Specifically, ^{13}C n.m.r. resonances for the amide carbonyl carbon appeared at δ 174.6, the **C**H$_3$-CO function appeared at δ 22.8, and the **C**H$_2$ function appeared at δ 39.5. Furthermore, the presence of a strong carbonyl stretching frequency at 1726 cm^{-1} was observed, reflecting the effect of the electron-withdrawing substituent in the *N*-nitroso-disubstituted amide functionality.[30] Finally, a structure such as (227) would be expected to readily lose NO, a fragment of mass 30 in the mass spectrum, as was observed.

Photolyses of solutions of 1,2,4,5-tetramethylbenzene (134) and TNM in acetonitrile were carried out at +20 and -20°. The results of these reactions, monitored with time, are summarized in Table 3.7. Similar to

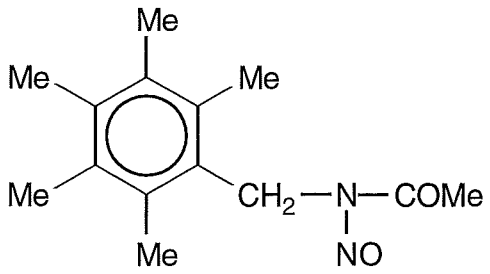

(228)

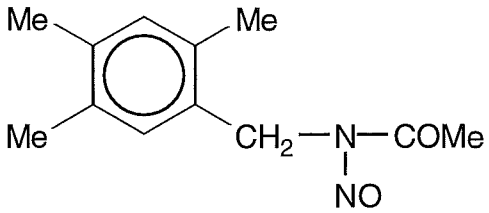

(227)

CH_3-CO	2.73	CH_3-CO	2.85
CH_2	4.99	CH_2	4.86
CH_3-CO	20.3	CH_3-CO	22.8
CH_2	39.7	CH_2	39.5
C=O	174.5	C=O	174.6
ν_{max} 1719, 1504, 1121		ν_{max} 1726, 1499, 1128	

Fig. 3.39 Comparison of the characteristic ^1H and ^{13}C n.m.r. resonances (in ppm) and infrared absorptions (in cm^{-1}) for compounds (228) and (227).

reactions in dichloromethane (see Table 3.5, Section 3.11), the yields of adducts (216) and (217) increased at lower reaction temperature in acetonitrile (trace amounts at +20°, total 15% at -20°). However, the yields of adducts (216) and (217) were lower in acetonitrile than in dichloromethane (trace amounts at +20° and total 15% at -20° in acetonitrile c.f. total 7% at +20° and total 28% at -20° in dichloromethane). Interestingly, the yield of the side-chain nitro compound (221) also decreased at lower reaction temperature (after 4 h, 48% at +20°, 19% at -20°). There was also

Table 3.7 Overview of product yields from the photolysis of 1,2,4,5-tetramethylbenzene (134) (0.47 mol L^{-1}) and TNM (0.94 mol L^{-1}) in acetonitrile.

		Yield (%)											
	Conversion												Unknown
t (h)	(%)	(216)	(217)	(218)	(219)	(220)	(221)	(222)	(223)	(224)	(226)	(227)	aromatics
At +20°													
2	30	trace	trace	3.8	5.5	2.0	44.6	1.6	4.2	22.8	1.0	9.6	4.9
4	52	trace	trace	1.7	4.5	2.9	47.5	1.9	2.5	23.5	1.1	9.4	5.0
At -20°													
2	31	10.5	4.7	4.0	21.7	1.5	15.5	4.6	4.8	23.8	-	1.6	7.3
4	49	9.6	4.9	2.4	6.2	3.9	19.0	3.2	1.8	25.1	-	4.2	19.7

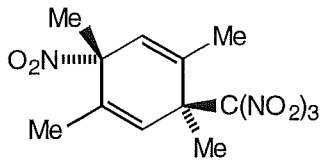

(216)

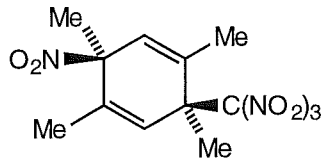

(217)

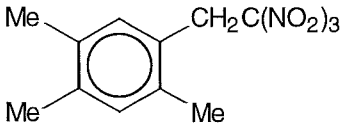

(219)

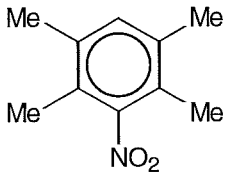

(220)

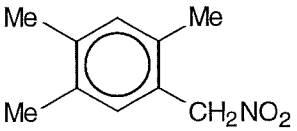

(221)

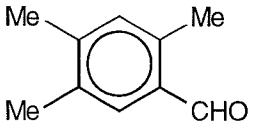

(222)

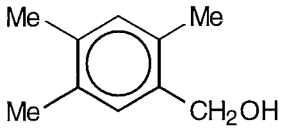

(223)

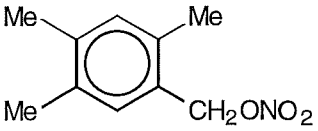

(224)

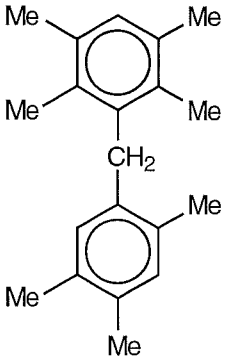

(218)

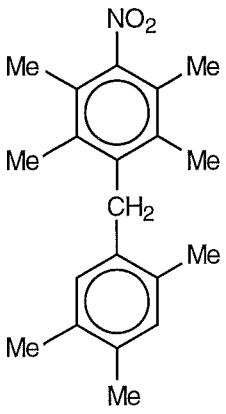

(226)

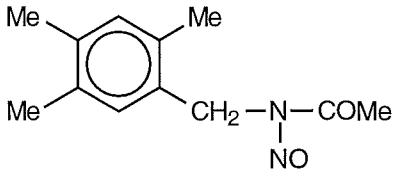

(227)

a reduced yield of the *N*-nitroso acetamide (227) not observed in reactions in dichloromethane or HFP at lower reaction temperature (after 4 h, 9% at +20°, 4% at -20°). Unfortunately, comparisons with the -50° dichloromethane reaction were not possible due to the limited solubility of 1,2,4,5-tetramethylbenzene (134) in the more polar acetonitrile at -50°.

3.14 The Photochemistry of 1,2,4,5-Tetramethylbenzene (134) in Dichloromethane Containing Trifluoroacetic Acid (TFA)

Photolysis of the charge-transfer complex of 1,2,4,5-tetramethylbenzene (134) (0.47 mol L^{-1}) / TNM (0.94 mol L^{-1}) in dichloromethane containing TFA (0.71 mol L^{-1}) at +20° for 4 h (conversion 38%) gave a product which was shown by ^1H n.m.r. spectral analysis (see Table 3.8) to be a mixture of the aromatic compounds (218)-(222), (224) and (226) (total 80%), and unidentified aromatic products (20%).

Notable among these products is the formation of the trinitromethyl derivative (219), initially (30 min.) 22% yield, but declining during the reaction to a yield of 8% after 4 h. It was also of interest to note that the +20° reaction in dichloromethane with TFA was slower than the corresponding reaction without added acid [after 4 h, 38% conversion with TFA, 87% conversion without added acid (See Table 3.5, Section 3.11)].

Table 3.8 Overview of product yields from the photolysis of 1,2,4,5-tetramethylbenzene (134) (0.47 mol L^{-1}) and TNM (0.94 mol L^{-1}) in dichloromethane containing trifluoroacetic acid (0.71 mol L^{-1}), at +20°

		Yield (%)							
	Conversion								Unknown
t (h)	(%)	(218)	(219)	(220)	(221)	(222)	(224)	(226)	aromatics
0.5	9	31.0	22.3	4.3	6.0	5.8	17.0	0.4	13.2
1	16	32.7	18.5	4.0	7.4	3.2	20.0	0.9	13.3
2	22	31.9	12.8	4.5	9.2	4.5	21.9	1.6	13.6
4	38	22.2	8.1	7.6	9.7	7.4	22.1	2.7	20.2

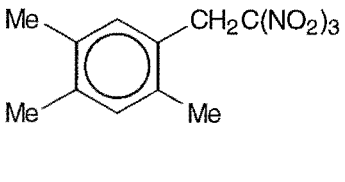

(219)

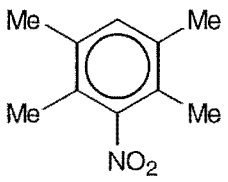

(220)

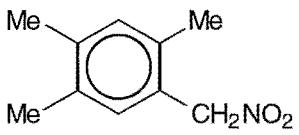

(221)

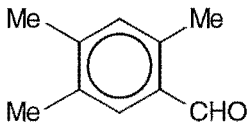

(222)

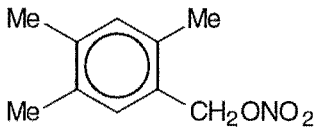

(224)

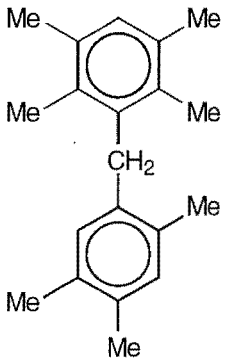

(218)

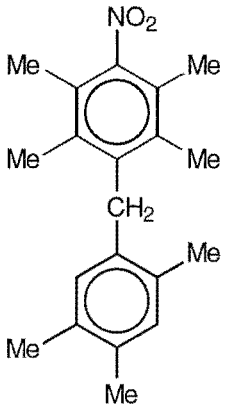

(226)

3.15 Rearrangement of 1,3,4,6-Tetramethyl-*r*-3-nitro-*t*-6-trinitromethylcyclohexa-1,4-diene (216) in Acetonitrile

Rearrangement of adduct (216) *in acetonitrile at +20° and identification of adducts* (231) *and* (232).

A solution of adduct (216) in acetonitrile was stored in the dark at +20°. Aliquots were removed at appropriate time intervals and the solvent was removed under reduced pressure at ≤0°. The composition of the residues were determined by ^{1}H n.m.r. spectral analysis. Within 5 min. adduct (216) underwent epimerization to give adduct (217), and also nitro-

nitrito rearrangement to give the epimeric trinitromethyl/nitrite adducts (229) and (230). During the work-up procedure the trinitromethyl/nitrite adducts (229) and (230) were hydrolysed to give the corresponding hydroxy/trinitromethyl adducts (231) and (232), as identified below. Subsequently (over *c.* 2 h) the mixture of (216), (217), (229) and (230) was converted into a mixture of 2,4,5-trimethyl-1-(2',2',2'-trinitroethyl)-benzene (219) (15%), 2,3,5,6-tetramethylnitrobenzene (220) (19%), 2,4,5-trimethylphenylnitromethane (221) (16%), 2,4,5-trimethylbenzyl alcohol (223) (24%), 2,4,5-trimethylbenzyl nitrate (224) (3%), and unidentified aromatic products (total 23%).

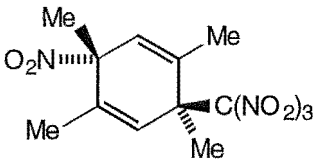

(216)

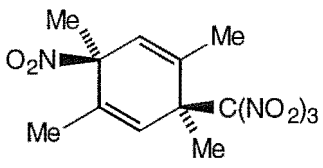

(217)

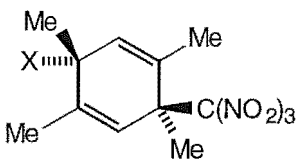

(229) X=ONO
(231) X=NO_2

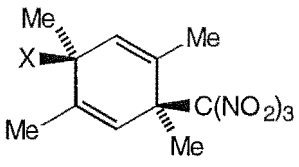

(230) X=ONO
(232) X=NO_2

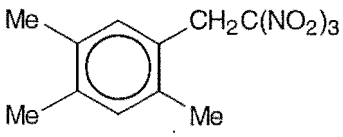

(219)

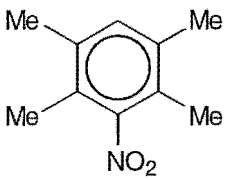

(220)

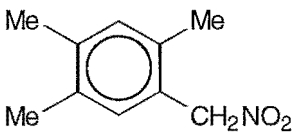

(221)

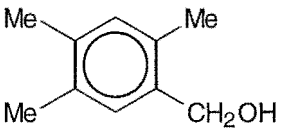

(223)

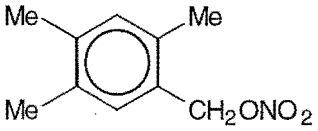

(224)

The major hydroxy/trinitromethyl adduct (231) was identified as 1,2,4,5-tetramethyl-*t*-4-trinitromethylcyclohexa-2,5-dien-*r*-1-ol (231) based on comparison of its ^{1}H n.m.r. spectroscopic data with that for the stereochemically related major nitro adduct (216), as depicted in Fig. 3.40. In particular, the ^{1}H n.m.r. signals due to adduct (231) were all shifted upfield relative to adduct (216), due to the presence of the -OH function.

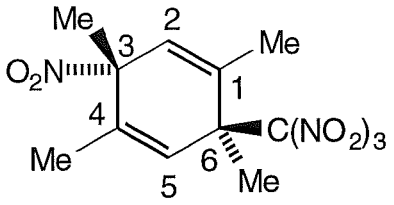

(216)

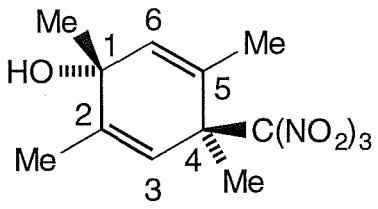

(231)

3-Me	1.74	1-Me	1.42
4-Me	1.80	2-Me	1.78
H5	6.20	H3	5.88
6-Me	1.96	4-Me	1.75
1-Me	1.87	5-Me	1.92
H2	5.82	H6	5.54

Fig. 3.40 Comparison of the characteristic ^{1}H resonances (in ppm) for adducts (216) and (231).

The epimeric hydroxy/trinitromethyl adduct (232) was identified as 1,2,4,5-tetramethyl-*c*-4-trinitromethylcyclohexa-2,5-dien-*r*-1-ol (232) based on comparison of its ^{1}H n.m.r. spectroscopic data with its epimer (231). The closely similar spectroscopic data for compounds (231) and (232) are

summarized in Fig. 3.41, and were consistent with their assignment as epimers.

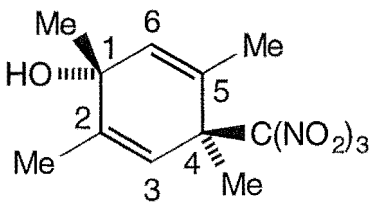

(231)

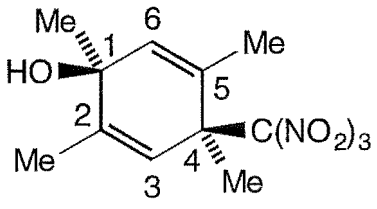

(232)

1-Me	1.42	1-Me	1.32
2-Me	1.78	2-Me	1.76
H3	5.88	H3	5.84
4-Me	1.75	4-Me	1.69
5-Me	1.92	5-Me	1.90
H6	5.54	H6	5.53

Fig. 3.41 Comparison of the characteristic ^1H resonances (in ppm) for adducts (231) and (232).

3.16 Rearrangement of 1,3,4,6-Tetramethyl-*r*-3-nitro-*t*-6-trinitromethylcyclohexa-1,4-diene (216) in (D)Chloroform

A solution of adduct (216) in (D)chloroform was stored in the dark at +20° and its ^1H n.m.r. spectrum monitored at appropriate time intervals. Adduct (216) epimerized only slowly. Equilibrium with its epimer (217) was established only after 90 h. The hydroxy/trinitromethyl adducts (231) and (232) were not observed in this rearrangement. The epimeric adducts

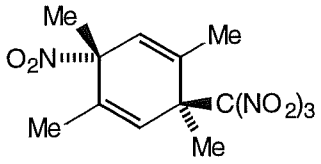

(216)

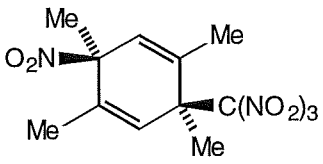

(217)

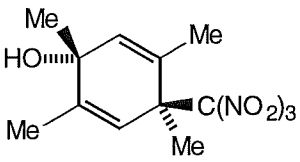

(231)

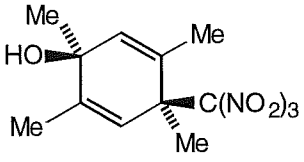

(232)

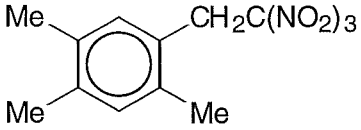

(219)

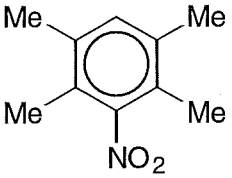

(220)

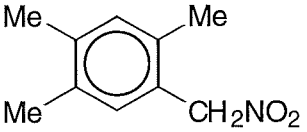

(221)

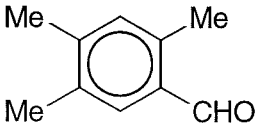

(222)

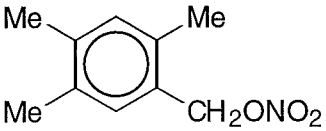

(224)

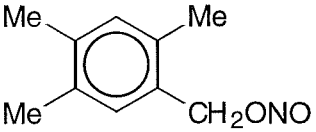

(225)

(216) and (217) were slowly converted (25 days) into a mixture of 2,4,5-trimethyl-1-(2',2',2'-trinitroethyl)-benzene (219) (52%), 2,3,5,6-tetramethyl-nitrobenzene (220) (1%), 2,4,5-trimethylphenylnitromethane (221) (18%), 2,4,5-trimethylbenzaldehyde (222) (6%), 2,4,5-trimethylbenzyl nitrate (224) (10%), 2,4,5-trimethylbenzyl nitrite (225) (trace) and some unidentified aromatic compounds (13%).

3.17 Reactions of 1,2,4,5-Tetramethylbenzene (134) with Nitrogen Dioxide in Dichloromethane

A solution of 1,2,4,5-tetramethylbenzene (134) (0.47 mol L^{-1}) in dichloromethane saturated with $^{\bullet}NO_2$ was irradiated with filtered light ($\lambda_{cut\text{-}off}$ <435 nm) at +20°. A similar mixture was stored in the dark at +20°. Aliquots were removed at appropriate time intervals and the excess $^{\bullet}NO_2$ and solvent were removed under reduced pressure at ≤0°. The product compositions were determined by ^1H n.m.r. spectral analysis and are given in Table 3.9. After reaction for 4 h the two product compositions were

Table 3.9 Overview of product yields from the reaction of 1,2,4,5-tetramethylbenzene (134) (0.47 mol L^{-1}) in dichloromethane saturated with $^{\bullet}NO_2$, at +20°.

		Yield (%)					
	Conversion						Unknown
t (h)	(%)	(218)	(221)	(222)	(223)	(224)	aromatics
In the dark							
0.5	16	1.0	21.8	4.9	2.6	67.6	2.1
1	24	1.1	23.0	4.3	2.5	67.0	2.1
2	32	1.0	21.6	7.5	1.7	66.1	2.1
4	60	1.1	22.7	5.6	1.2	67.6	1.8
Irradiation with filtered light ($\lambda_{cut\text{-}off}$<435 nm)							
0.5	18	1.0	22.2	5.3	3.3	67.0	1.2
1	28	1.3	22.8	3.3	2.6	69.2	0.8
2	45	0.9	20.7	5.8	1.2	69.7	1.7
4	68	0.7	19.9	7.0	0.5	69.5	2.4

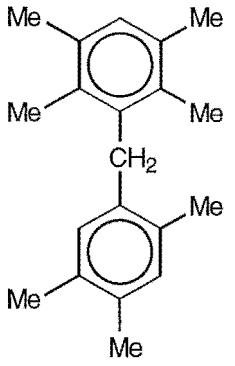

(218)

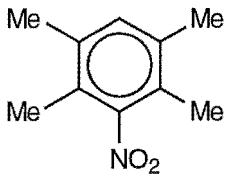

(220)

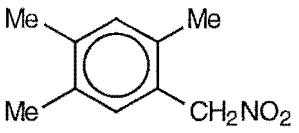

(221)

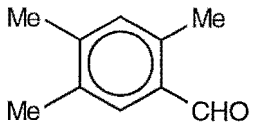

(222)

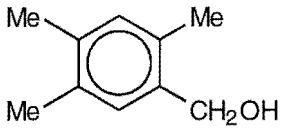

(223)

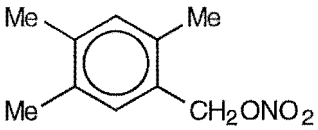

(224)

similar, *viz.* 2,4,5-trimethylbenzyl nitrate (224) (*c.* 70%), 2,4,5-trimethylphenylnitromethane (221) (*c.* 20%), with small amounts of aromatic compounds (218), (222) and (223) (total 8%), and unidentified aromatic compounds (total 2%). These results are comparable with those reported by Bosch and Kochi,[31] except that they also observed a low yield of the nuclear nitration product (220).

3.18 Reactions of 1,2,4,5-Tetramethylbenzene (134) with Nitrogen Dioxide in 1,1,1,3,3,3-Hexafluoropropan-2-ol (HFP)

Reaction in HFP at +20° and the identification of the aromatic compounds (233) *and* (234).

A solution of 1,2,4,5-tetramethylbenzene (134) (0.47 mol L^{-1}) in HFP saturated with $^{\bullet}NO_2$ was irradiated with filtered light ($\lambda_{cut\text{-}off}$<435 nm) at +20°. A similar mixture was stored in the dark at +20°. After 0.5 h, at which

time the 1,2,4,5-tetramethylbenzene (134) in both reactions was consumed, the excess $^{\bullet}NO_2$ and solvent were removed under reduced pressure at ≤0°. The product compositions, determined by ^1H n.m.r. spectral analysis, were similar, *viz.* 2,3,5,6-tetramethylnitrobenzene (220) (*c.* 71%), 2,4,5-trimethylbenzoic acid (233) (18%), 2,3,5,6-tetramethyl-1,4-dinitrobenzene (234) (4%), with small amounts of aromatic compounds (221) and (222), and unidentified aromatic compounds (*c.* 6%).

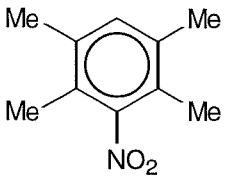

(220)

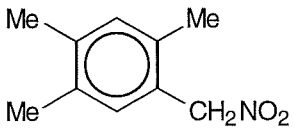

(221)

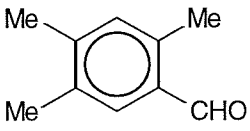

(222)

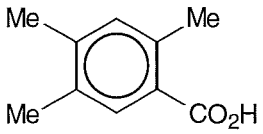

(233)

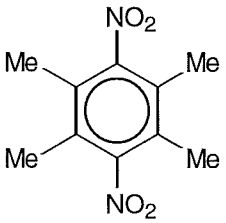

(234)

Chromatography of the "dark" reaction mixture on a silica gel Chromatotron plate gave compound (233) in a fraction eluted immediately after the aldehyde (222). The structure of 2,4,5-trimethylbenzoic acid (233) was confirmed by comparison of its spectroscopic data with an authentic sample.

Compound (234) was not isolated from the silica gel Chromatotron plate. However, the presence of 2,3,5,6-trimethyl-1,4-dinitrobenzene (234) in the reaction mixture was inferred by comparing its ^1H n.m.r. signal with an authentic sample. Specifically, the methyl resonance appeared as a singlet at δ 2.32.

3.19 Overview of the Photonitration of 1,2,4,5-Tetramethylbenzene (134)

In the photolysis of the 1,2,4,5-tetramethylbenzene (134) / TNM charge-transfer complex adduct formation was observed exclusively by attack of $(O_2N)_3C^-$ at C1 on the radical cation of 1,2,4,5-tetramethylbenzene (See Fig. 3.42). No adducts were observed arising from the alternative

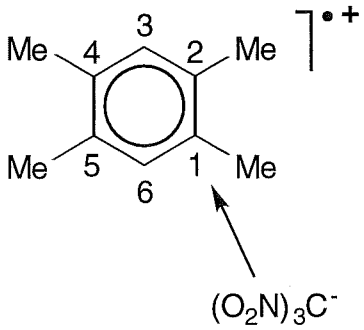

Fig. 3.42 Adducts identified correspond only to attack of $(O_2N)_3C^-$ at C1 of the 1,2,4,5-tetramethylbenzene radical cation.

attack of $(O_2N)_3C^-$ at C3 on the 1,2,4,5-tetramethylbenzene radical cation, presumably due to the instability of the delocalized carbon radical (145) which would be required to form.

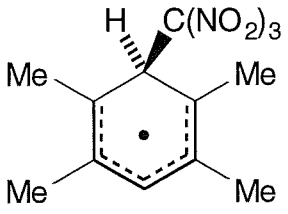

(145)

Attack of $(O_2N)_3C^-$ on the 1,2,4,5-tetramethylbenzene radical cation at C1 would lead to the formation of the delocalized carbon radical (144), as shown in Scheme 3.25. Subsequently, radical coupling with $^{\bullet}NO_2$ at C4

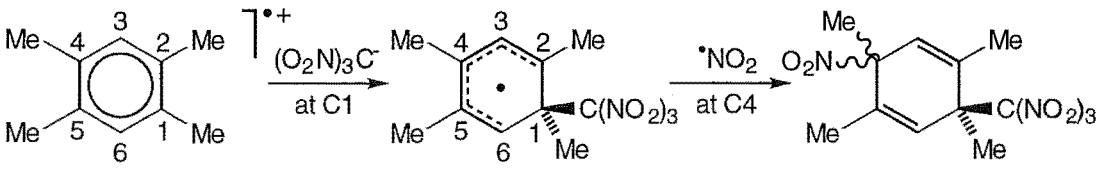

(144) (216) and (217)

Scheme 3.25

would give the epimeric 1,3,4,6-tetramethyl-3-nitro-6-trinitromethyl adducts (216) and (217).

The yields of adducts (216) and (217) were found to be temperature dependent and increased at lower reaction temperatures in both dichloromethane and acetonitrile (See Tables 3.5 and 3.7, Sections 3.11 and 3.13, respectively). The pattern of adduct yields found for photolyses in dichloromethane or acetonitrile solution is understandable in the light of the rearrangement of the nitro/trinitromethyl adduct (216) in acetonitrile and (D)chloroform at +20°. The rearrangement of nitro/trinitromethyl adduct (216) was complete in 2 h in acetonitrile but considerably slower in (D)chloroform (half-life *c.* 72 h). The rearrangement of adduct (216) to aromatic products proceeded *via* initial equilibration to its epimer (217), and in the rearrangement in acetonitrile also *via* nitrates (229) and (230).

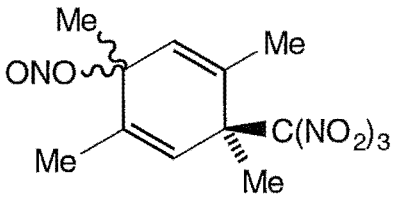

(229) and (230)

These rearrangements were seen as being analogous to the rearrangement of the 1,4-nitro/trinitromethyl adduct (75) of 1,4,6,7-tetramethylnaphthalene (56) (see Chapter 2, Sections 2.7-2.9) and the

rearrangement of the 1,4-nitro/trinitromethyl adduct (13)[2] of 1,4-dimethyl-naphthalene (see Chapter 1, Section 1.11).

In the early stages of the rearrangement, epimerization occurred to give adduct (217), presumably *via* the intermediate nitrocyclohexadienyl cation/trinitromethanide ion pair (235), as observed in Scheme 3.26.

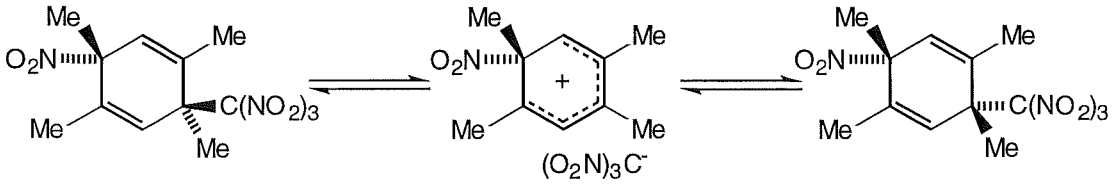

Scheme 3.26

The nitro-nitrito rearrangement would probably occur in a radical mechanism involving loss of $^{\bullet}NO_2$ from the nitro/trinitromethyl adducts (216) and (217), to form the radical pair (236), as seen in Scheme 3.27.

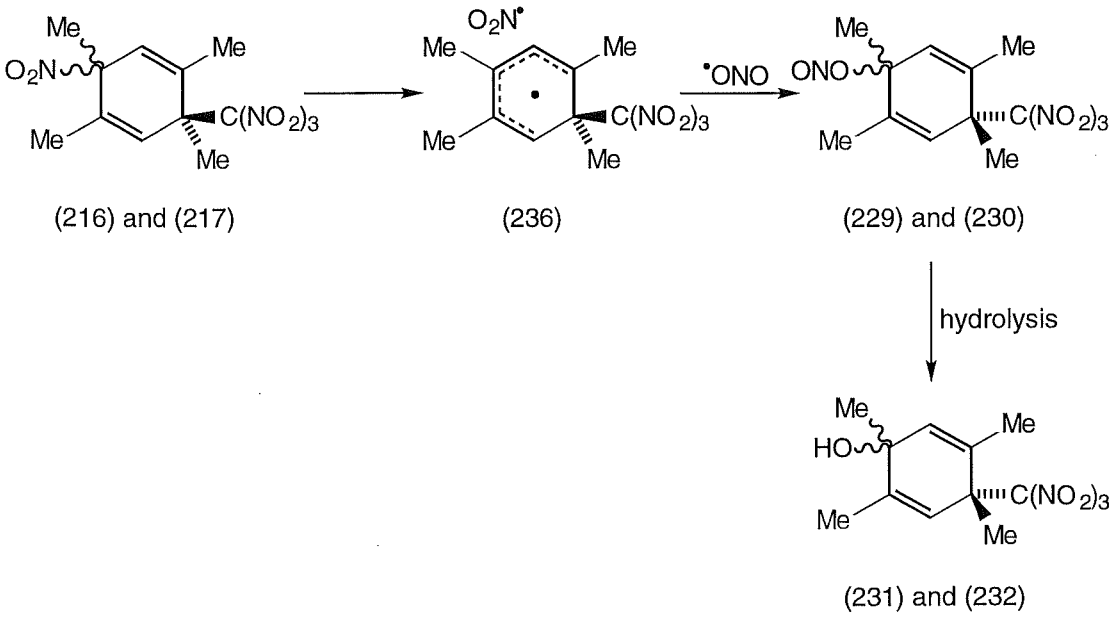

Scheme 3.27

Subsequent recombination of $^{\bullet}NO_2$, *via* C-O bond formation, would form the nitrito/trinitromethyl adducts (229) and (230). Hydrolysis of the nitrito/trinitromethyl adducts would then give rise to the labile hydroxy/trinitromethyl adducts (231) and (232). Similar to the nitro/trinitromethyl adducts (216) and (217), the nitrito/trinitromethyl adducts (229) and (230) and the hydroxy/trinitromethyl adducts (231) and (232) could undergo epimization *via* the intermediate nitrocyclohexadienyl cation/trinitromethanide ion pair (235).

The intermediate nitrocyclohexadienyl cation/trinitromethanide ion pair (235) affords a possible route to the aromatic side-chain compounds (221)-(225), all proceeding *via* the 2,4,5-trimethylbenzyl radical (238), as illustrated in Scheme 3.28. Initially, loss of nitroform from the intermediate nitrocyclohexadienyl cation/trinitromethanide ion pair (235) would occur by abstraction of an acidic proton from the methyl group by $(O_2N)_3C^-$, forming the diene (237). This would be followed by homolytic cleavage of the C-X bond in diene (237) to give radical (238). Subsequent coupling of $^{\bullet}NO_2$

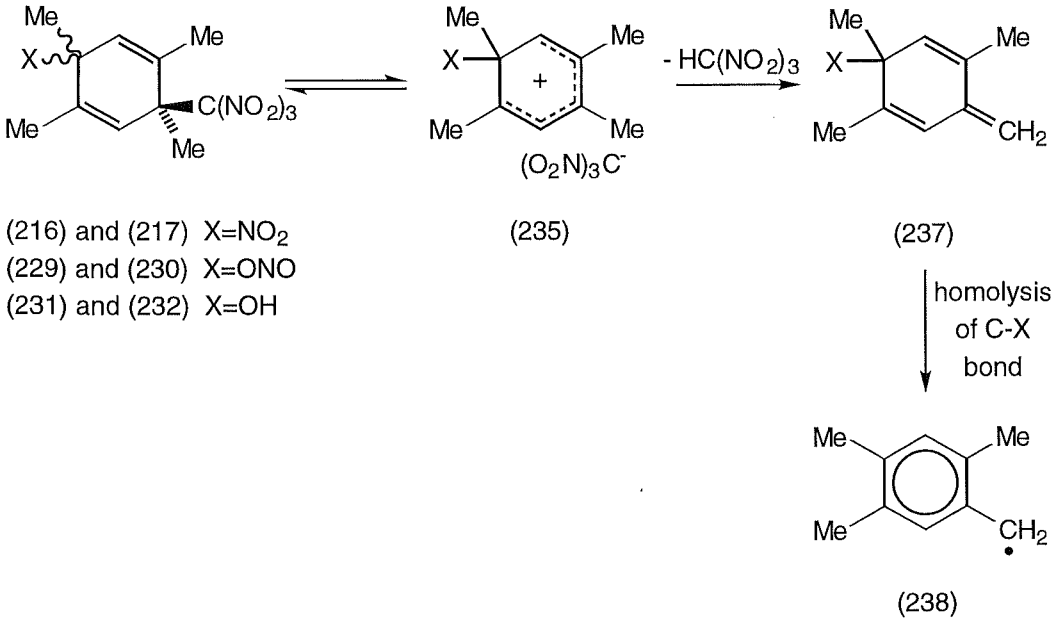

Scheme 3.28

with the resulting 2,4,5-trimethylbenzyl radical (238) with C-N bond formation would lead to the formation of the side-chain nitro compound (221), as seen in Scheme 3.29. Alternatively, coupling of $^{\bullet}NO_2$ could occur with C-O bond formation and would give the side-chain nitrite (225). The side-chain nitrite (225) can then undergo either hydrolysis to yield the side-chain alcohol (223) or oxidation to yield the side-chain nitrate (224). The oxidation of the nitrite (225) to produce the nitrate (224) was shown to be a rapid reaction.[31] Formation of the benzaldehyde (222) could arise either by oxidation of the nitrite (225), as was observed by Masnovi *et al.*,[9] or by oxidation of the alcohol (223).

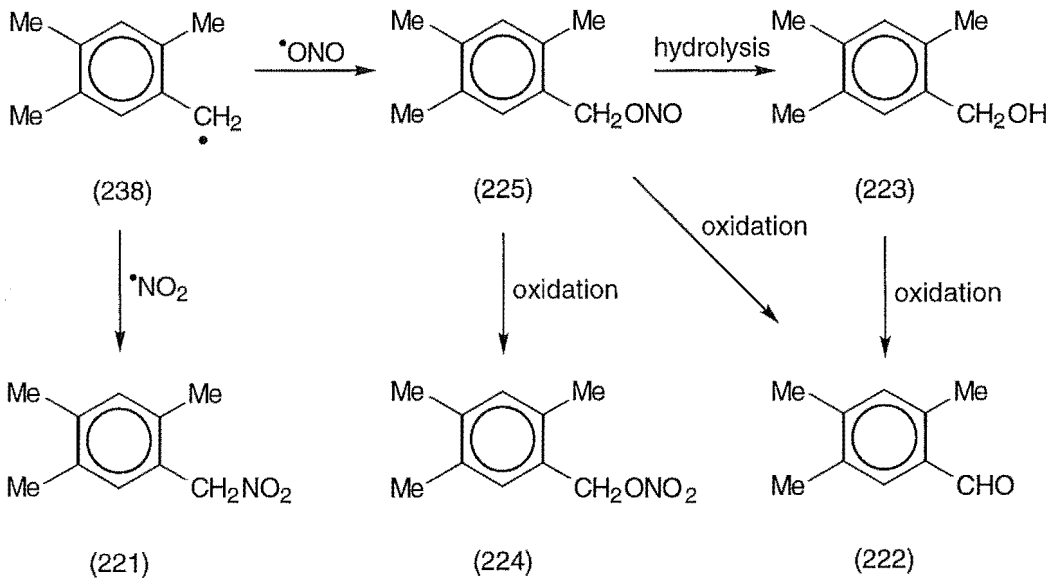

Scheme 3.29

The formation of the side-chain trinitromethyl aromatic (219) could occur *via* loss of nitrous acid from the nitro/trinitromethyl adducts (216) and (217) to form the trinitromethyl diene (239), as depicted in Scheme 3.30. Subsequent rearrangement *via* the ion pair (240) would give the side-chain trinitromethyl compound (219).

A possible mode of formation for dimer (218) is shown in Scheme

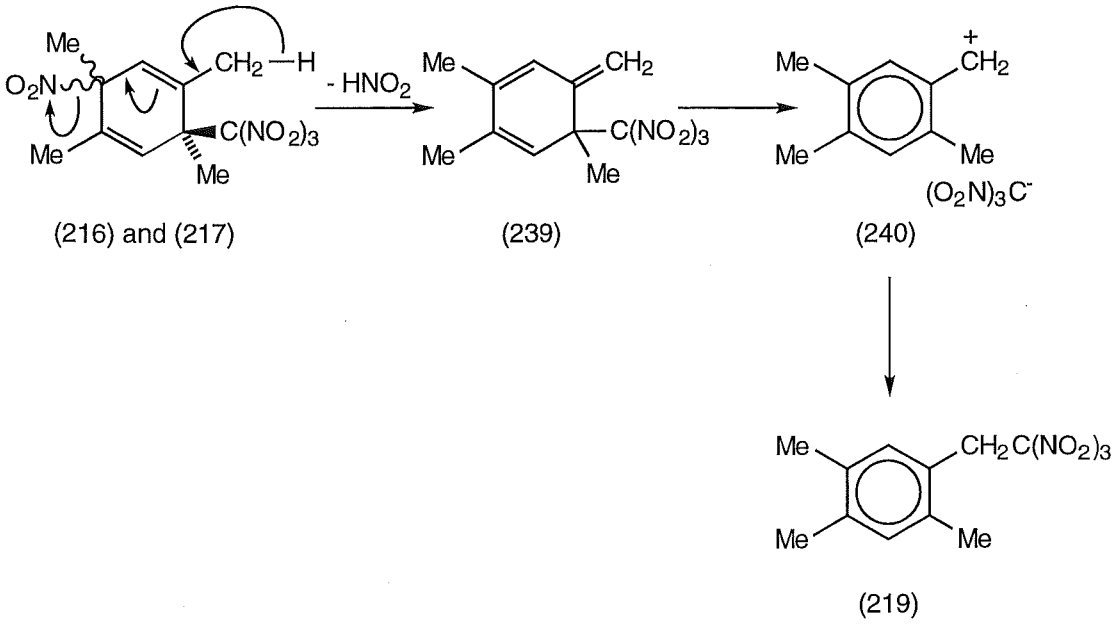

Scheme 3.30

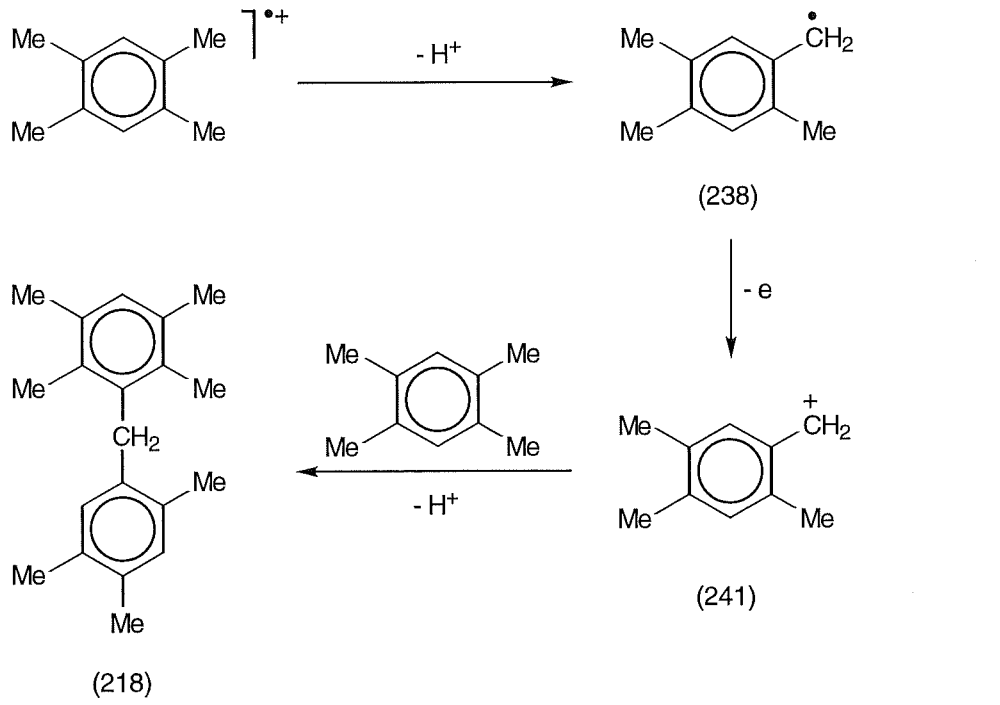

Scheme 3.31

3.31 and follows the oxidative dimerization proposed by Eberson *et al.*[32] The radical cation of 1,2,4,5-tetramethylbenzene can undergo α-deprotonation to yield the 2,4,5-trimethylbenzyl radical (238). Subsequently, loss of an electron from radical (238) would produce the 2,4,5-trimethylbenzyl cation (241). Cation (241) can then couple with 1,2,4,5-tetramethylbenzene (134), and after loss of a proton, would form dimer (218). The formation of dimer (218) affords a pathway to the formation of the nitro dimer (226) by radical coupling of $^{\bullet}NO_2$ with the dimer radical cation, as seen in Scheme 3.32.

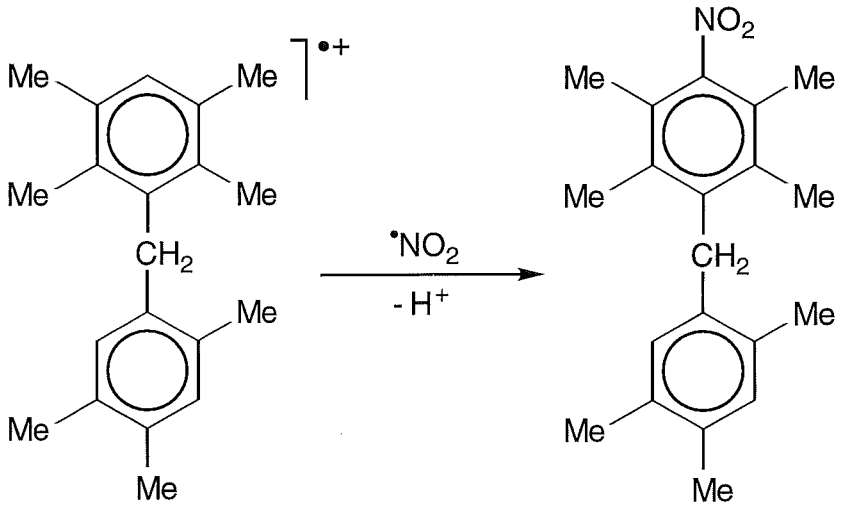

(218) (226)

Scheme 3.32

It has been shown[33,34] that when charge-transfer complexes of aromatic molecules with TNM undergo photolyses in the presence of TFA, $(O_2N)_3C^-$, one component of the triad [$ArH^{\bullet+}$ $(O_2N)_3C^-$ $^{\bullet}NO_2$], is converted into the less nucleophilic nitroform. This results in the predominant recombination process $ArH^{\bullet+}$ / $^{\bullet}NO_2$ being observed. The photolysis of the charge-transfer complex of 1,2,4,5-tetramethylbenzene (134) in dichloromethane containing TFA (0.71 mol L^{-1}) at +20° proceeded more slowly than

the reaction without added acid (see Tables 3.5 and 3.6, Sections 3.11 and 3.13, respectively) and gave aromatic compounds (218)-(222), (224) and (226). Interestingly, 2,4,5-trimethyl-1-(2',2',2'-trinitroethyl)-benzene (219)

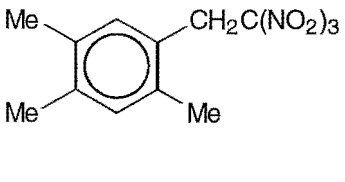

(219)

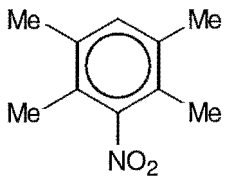

(220)

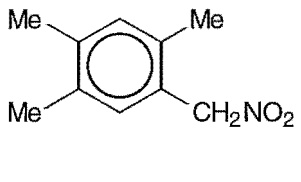

(221)

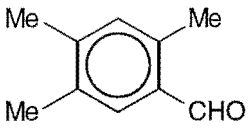

(222)

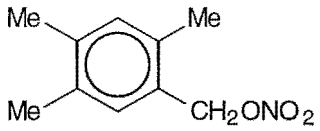

(224)

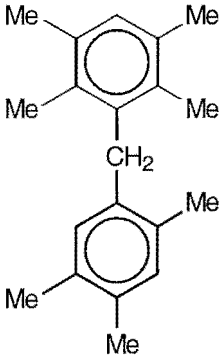

(218)

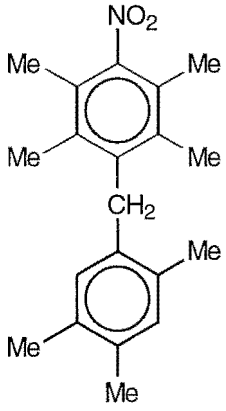

(226)

was still formed in reasonable yield, even though adducts (216) and (217) were not detected. Since compounds (218) and (226) must be derived from the 2,4,5-trimethylbenzyl cation (241) (see Schemes 3.31 and 3.32,

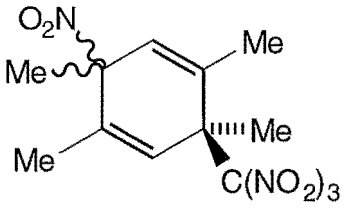

(216) and (217)

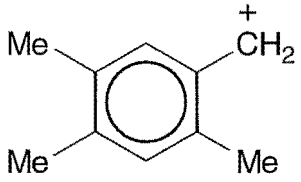

(241)

above), it appears reasonable to assume that nitroform can react as a nucleophile with carbocation (241) with its higher charge density at a single carbon, compared to the situation in the 1,2,4,5-tetramethylbenzene radical cation.

HFP was found strongly to stabilize radical cations,[35-40] partly by rendering any nucleophilic species present exceedingly unreactive.[39] It was therefore anticipated that HFP would inhibit the attack of $(O_2N)_3C^-$ on the 1,2,4,5-tetramethylbenzene radical cation, favouring the $ArH^{\bullet+}$ / $^{\bullet}NO_2$ coupling process instead. The experiments involving photolysis of the charge-transfer complex of TNM with 1,2,4,5-tetramethylbenzene (134) in HFP at +20° was slow. While neither adducts (216) nor (217) were seen, a small amount (4% after 4 h) of the side-chain trinitromethyl derivative (219) was observed. The major product was 2,3,5,6-tetramethylnitrobenzene (220) (*c.* 60%) (See Table 3.6, Section 3.12). Reaction of 1,2,4,5-tetra-

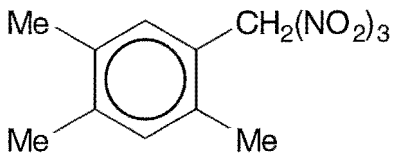

(219)

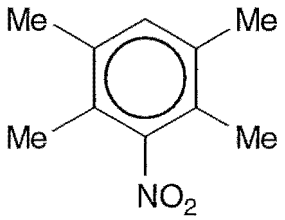

(220)

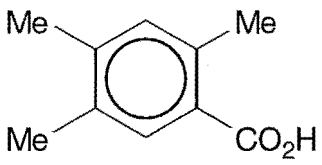

(233)

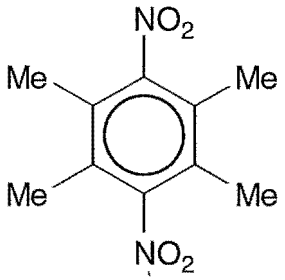

(234)

methylbenzene (134) with a saturated solution of $^{\bullet}NO_2$ in HFP, either on irradiation with filtered light ($\lambda_{cut\text{-}off}$<435 nm) or in the dark at +20°, was

complete in <0.5 h. The major product was 2,3,5,6-tetramethylnitrobenzene (220) (*c.* 74%) with 2,3,5,6-tetramethyl-1,4-dinitrobenzene (234) (4%) as a minor product (See Section 3.18). The trimethylbenzoic acid (223) was also formed in both the "light" and "dark" reactions of 1,2,4,5-tetramethylbenzene (134) with $^{\bullet}NO_2$ in HFP (18% in both reactions).

This result is in marked contrast to the outcome of the analogous reactions of 1,2,4,5-tetramethylbenzene (134) with a saturated solution of $^{\bullet}NO_2$ in dichloromethane at +20°, either on irradiation with filtered light ($\lambda_{cut\text{-}off}$<435 nm) or in the dark. Here the significant products were 2,4,5-trimethylbenzyl nitrate (224) (*c.* 70%) and 2,4,5-trimethylphenylnitromethane (221) (*c.* 20%) (See Table 3.9, Section 3.17). It appears that both

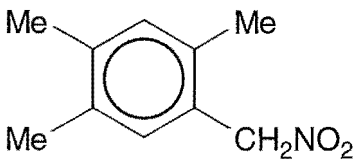

(221)

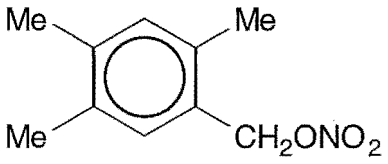

(224)

the "light" and "dark" reaction conditions in the reactions of 1,2,4,5-tetramethylbenzene (134) with $^{\bullet}NO_2$ in dichloromethane resulted in thermal nitration. The product compositions were generally in agreement with product ratios for thermal nitration of 1,2,4,5-tetramethylbenzene (134) with $^{\bullet}NO_2$ in dichloromethane in the dark reported by Bosch and Kochi.[31]

In contrast, the formation of ring-substituted nitration products (222) and (234) in the reactions of 1,2,4,5-tetramethylbenzene (134) with $^{\bullet}NO_2$ in HFP was consistent with the reaction sequence of nitrosation, by NO^+, followed by oxidation of the nitrosoarene to the nitroarene, as represented in Scheme 3.33. Nitrosation of 1,2,4,5-tetramethylbenzene (134) would lead to the formation of the nitrosoarene (242). Subsequent oxidation of (242) would give compound (220), while further nitrosation of (242) would

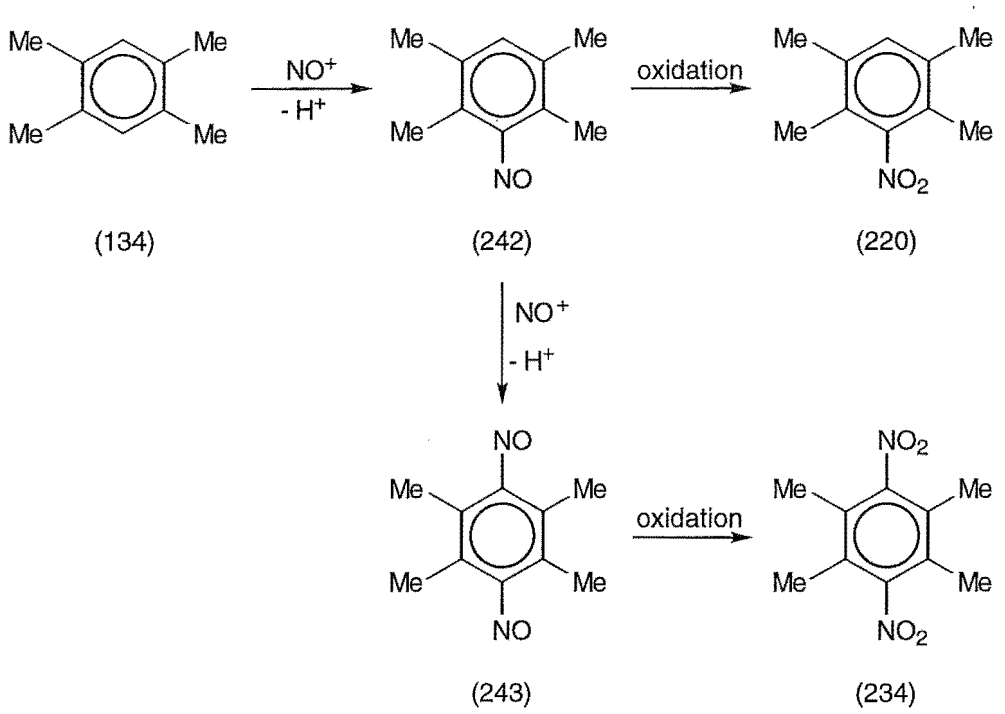

Scheme 3.33

produce the 1,4-dinitroso compound (243). Oxidation of (243) would result in the formation of the 1,4-dinitro compound (234). The formation of the carboxylic acid (233) in the reactions of 1,2,4,5-tetramethylbenzene (134) with $^{\bullet}NO_2$ in HFP was seen as arising *via* the oxidation of the aldehyde (223), present in trace amounts in the reaction.

What then is the role of HFP in promoting the nitrosation of 1,2,4,5-tetramethylbenzene (134)? Bosch and Kochi[31] proposed the following equilibrium arising *via* the interaction between the "head-to-tail" coupled form of $^{\bullet}NO_2$ and an aromatic molecule (See Scheme 3.34). Given that HFP renders any nucleophilic species present very unreactive,[39] it appears likely that the effect of HFP in promoting aromatic nitrosation arises because

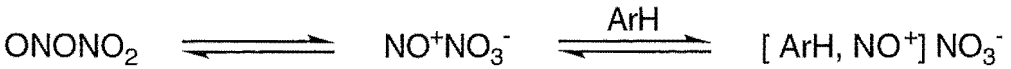

Scheme 3.34

it disturbs the equilibrium in Scheme 3.34. Therefore, the [ArH, NO^+] species would be formed as the nitrate counter-ion would be deactivated by interaction with the solvent. Hence, in the reaction of 1,2,4,5-tetramethylbenzene (134) in the presence of excess $^\bullet NO_2$ in HFP it appears likely that nitrosation occurred.

The photolysis of the charge-transfer complex of 1,2,4,5-tetramethylbenzene (134) with TNM in HFP resulted in extensive ring nitration. Hence, HFP appears to markedly reduce the nucleophilic reactivity of $(O_2N)_3C^-$ and to promote nitrosation of ArH by $^\bullet NO_2$, as outlined above (Scheme 3.34).

It remains unclear how the *N*-nitroso acetamide (227) formed. However, in a later reaction study of hexamethylbenzene (136) in acetonitrile saturated with of $^\bullet NO_2$ at +20° in the dark, the analogous *N*-nitroso acetamide (228) formed (See Section 3.33). Hence, it appears that neither TNM nor irradiation is necessary for the formation of compound (227).

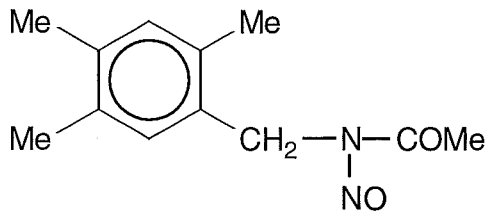

(227)

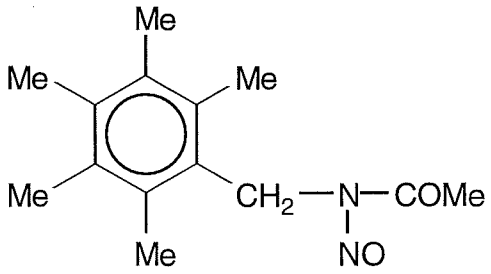

(228)

In conclusion, in the reaction between the 1,2,4,5-tetramethylbenzene radical cation and $(O_2N)_3C^-$ it appears that radical (145) was unfavourable. It is likely that steric hindrance to $(O_2N)_3C^-$ attack at C3, due to interaction with the β-methyl groups at C2 and C4, resulted in the more stable carbon radical (144) being formed.

3.20 The Photolysis of Pentamethylbenzene (135)

General procedure for the photonitration of pentamethylbenzene (135) *with TNM.*

A solution of pentamethylbenzene (135) (500 mg, 0.42 mol L^{-1}) and TNM (0.84 mol L^{-1}) in dichloromethane (at +20, -20, -50 or -78°) or acetonitrile (at +20 or -20°) was irradiated with filtered light ($\lambda_{cut\text{-}off}$<435 nm) and small samples were withdrawn for analysis at suitable intervals. The work-up procedure, involving evaporation of solvent and TNM, was conducted at ≤0°. The crude product mixtures were stored at -78° and were analysed by ^1H n.m.r. spectroscopy as soon as possible (For complete experimental details see Chapter 5, Section 5.3.3).

3.21 The Photochemistry of Pentamethylbenzene (135) in Dichloromethane

3.21.1 Photochemistry in dichloromethane at -78° and the identification of adducts (244) *and* (245).

A solution of pentamethylbenzene (135) (0.42 mol L^{-1}) and TNM (0.84 mol L^{-1}) in dichloromethane was irradiated at -78° until the orange/ brown colour of the charge-transfer band was bleached. The composition of the reaction mixture was monitored by withdrawing samples for ^1H n.m.r. spectral analysis. After work-up, the final solution (after 3 h, conversion 76%) contained the epimeric 1,2,3,4,6-pentamethyl-3-nitro-6-trinitromethyl-cyclohexa-1,4-dienes (244) (15%) and (245) (1%), aromatic compounds (246)-(260) (total 79%) and unidentified aromatic compounds (total 5%). The adduct (244) was partially separated by h.p.l.c. on a cyanopropyl column, cooled to 0°, using hexane/dichloromethane mixtures as the

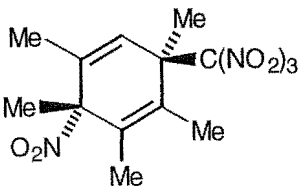

(244)

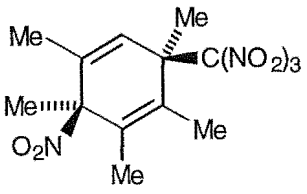

(245)

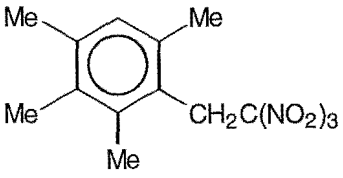

(246)

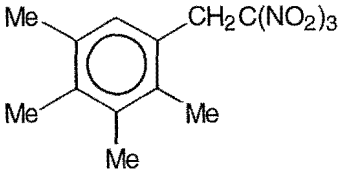

(247)

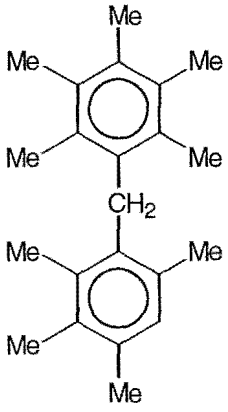

(248)

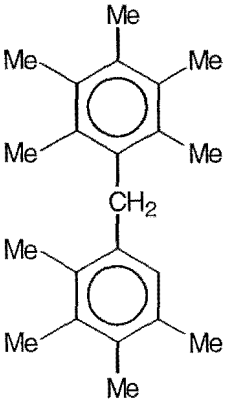

(249)

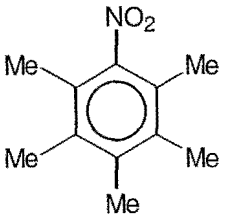

(250)

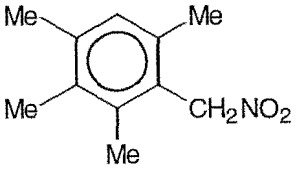

(251)

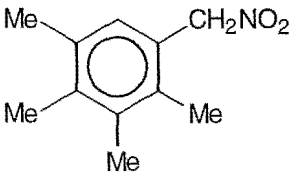

(252)

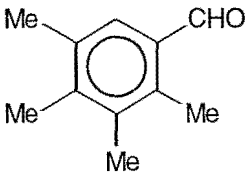

(253)

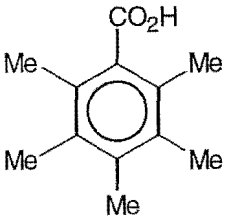

(254)

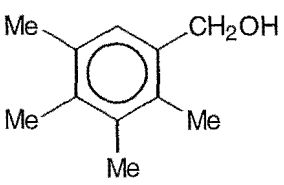

(255)

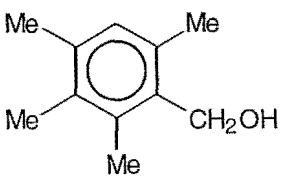

(256)

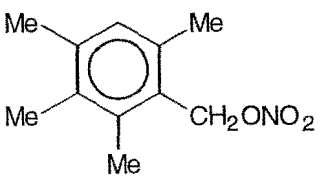

(257)

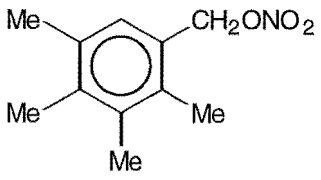

(258)

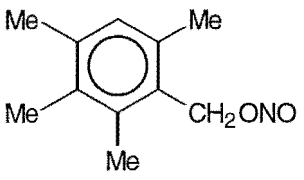

(259)

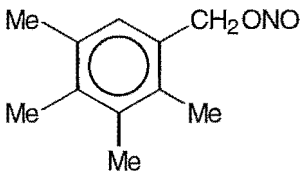

(260)

eluting solvents. The first material eluted was a mixture of aromatic compounds, whose separation and identification is given below.

The major adduct (244) was isolated as unstable oil and was identified as 1,2,3,4,6-pentamethyl-*r*-3-nitro-*t*-6-trinitromethylcyclohexa-1,4-diene (244) on the basis of its spectroscopic data and comparison of its characteristic ^{1}H n.m.r. resonances with the spectral features for 1,3,4,6-tetramethyl-*r*-3-nitro-*t*-6-trinitromethylcyclohexa-1,4-diene (216). N.O.e. experiments confirmed the assignments of the chemical shifts for the protons. In particular, irradiation at δ 1.74 (1-Me, 3-Me and 4-Me) gave enhancements at δ 1.97 (6-Me) and at δ 6.21 (H5), while irradiation at δ 1.97 (6-Me) gave enhancements at δ 1.69 (2-Me), δ 1.74 (1-Me) and δ 6.21 (H5), as represented in Fig. 3.43. The characteristic ^{1}H n.m.r. resonances for the closely related adducts (216) and (244) are compared in Fig. 3.44 and further support the identification of adduct (244). Furthermore, the presence of very strong infrared absorptions at 1616,

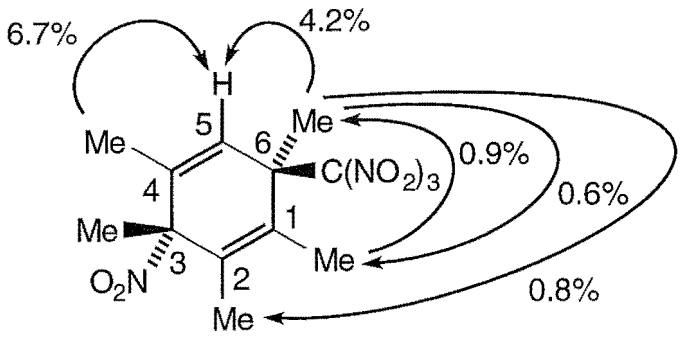

Fig. 3.43 Enhancements (%) from selected n.O.e. experiments for adduct (244).

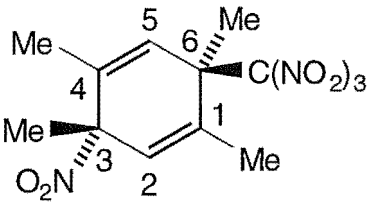

(216)

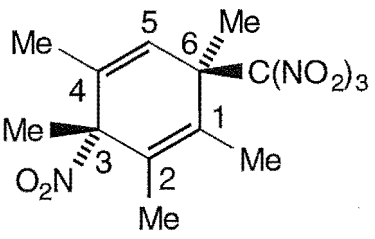

(244)

1-Me	1.87	1-Me	1.74
H2	5.82	2-Me	1.69
3-Me	1.74	3-Me	1.74
4-Me	1.80	4-Me	1.74
H5	6.20	H5	6.21
6-Me	1.96	6-Me	1.97

Fig. 3.44 Comparison of the characteristic ^{1}H n.m.r. resonances (in ppm) for adducts (216) and (244).

1596, 1576 and 1550 cm^{-1} provided evidence for the -C(NO$_2$)$_3$ and -NO$_2$ substituents. The assignment of adduct (244) as the *trans*-isomer was made by comparing its ^{1}H n.m.r. data and the chemical shift of the olefinic proton (the only signal clearly identifiable in the reaction mixture) for the *cis*-isomer (245), with the ^{1}H n.m.r. data for the epimeric adducts (216) and (217) derived from 1,2,4,5-tetramethylbenzene (134), as illustrated in Fig. 3.45. Specifically, the characteristic H5 resonance appeared upfield in each of the major *trans*-isomers, (244) and (216), relative to their minor *cis*-epimers, (245) and (217).

The minor adduct (245) could not be isolated from the h.p.l.c. column. However, identification of adduct (245) as 1,2,3,4,6-pentamethyl-*r*-3-nitro-*c*-6-trinitromethylcyclohexa-1,4-diene (245) was based on the chemical shift

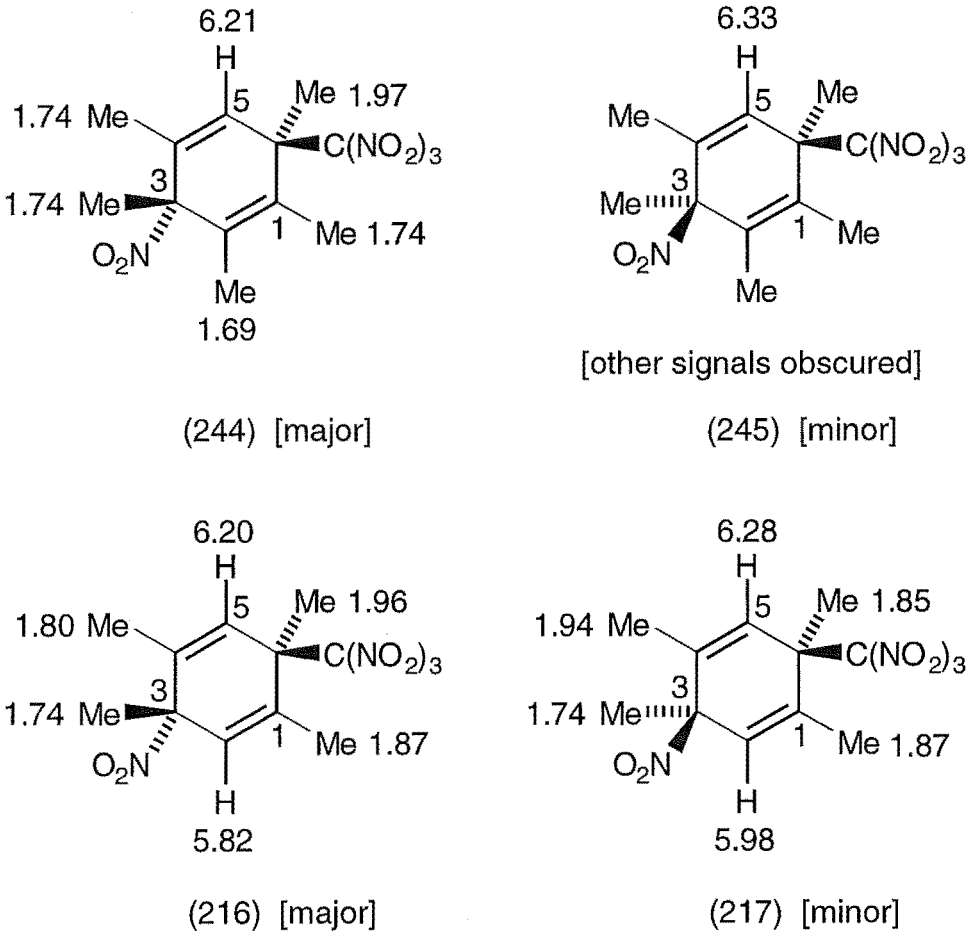

Fig. 3.45 Comparison of the characteristic ^{1}H n.m.r. resonances (in ppm) for adducts (244), (245), (216) and (217).

of its olefinic proton (the only signal clearly identifiable in the reaction mixture), as seen in Fig. 3.45 above. Specifically, the ^{1}H n.m.r. resonance for H5 appeared as a quartet at δ 6.33.

3.21.2 Photochemistry in dichloromethane at +20° and the identification of the aromatic products (246)-(260).

Photolysis of the charge-transfer complex of pentamethylbenzene (135) (0.42 mol L^{-1}) / TNM (0.84 mol L^{-1}) in dichloromethane at +20° for 3 h (conversion 89%) gave a product which was shown by ^{1}H n.m.r. spectral analysis to be a mixture of the aromatic compounds (246)-(260) (total 98%)

and unidentified aromatic compounds (total 2%). Chromatography of this mixture on a silica gel Chromatotron plate gave the following in elution order.

The first compound eluted was identified as 2,3,4,6-tetramethyl-1-(2',2',2'-trinitroethyl)-benzene (246). The side-chain trinitromethyl aromatic (246) gave a satisfactory parent molecular ion in the mass spectrum, indicating the molecular formula $C_{12}H_{15}N_3O_6$. N.O.e. experiments confirmed the assignments of the chemical shifts for the protons. In particular, irradiation at δ 4.74 (CH_2) gave enhancements at δ 2.10 (2-Me) and at δ 2.16 (6-Me), while irradiation at δ 6.88 (H5) gave enhancements at δ 2.16 (6-Me) and at δ 2.25 (4-Me), as depicted in Fig. 3.46. Furthermore,

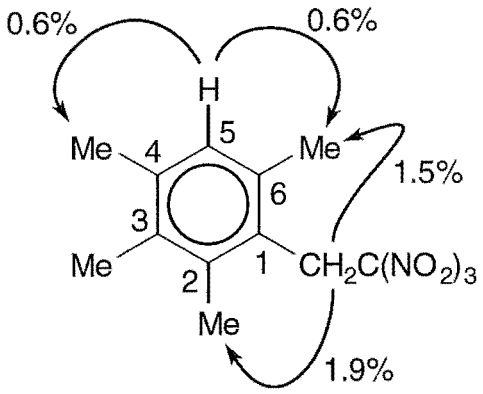

Fig. 3.46 Enhancements (%) from selected n.O.e. experiments for compound (246).

the presence of very strong infrared absorptions at 1616, 1601 and 1580 cm^{-1} provided evidence for the $-C(NO_2)_3$ substituent.

The second compound eluted was identified as 2,3,4,5-tetramethyl-1-(2',2',2'-trinitroethyl)-benzene (247). The isomeric side-chain trinitromethyl aromatic (247) also gave a satisfactory parent molecular ion in the mass spectrum, indicating the molecular formula $C_{12}H_{15}N_3O_6$. N.O.e. experiments confirmed the assignments of the chemical shifts for the

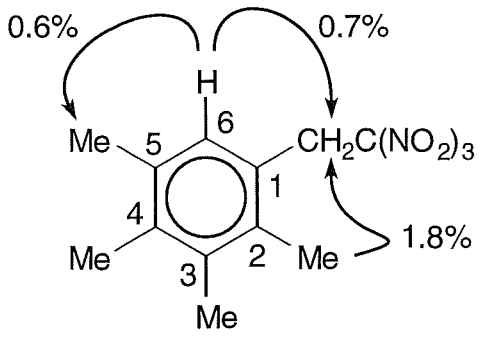

Fig. 3.47 Enhancements (%) from selected n.O.e. experiments for compound (247).

protons. Specifically, irradiation at δ 2.09 (2-Me) gave enhancement at δ 4.45 (CH_2), while irradiation at δ 6.74 (H6) gave enhancements at δ 2.23 (5-Me) and at δ 4.45 (CH_2), as shown in Fig. 3.47. Furthermore, the presence of very strong infrared absorptions at 1609 and 1576 cm^{-1} provided evidence for the $-C(NO_2)_3$ substituent.

The third compound eluted was identified as 2,2',3,3',4,4',5,6,6'-nona-methyldiphenylmethane (248) and the structure was confirmed by comparing its spectroscopic data with literature data.[41]

The fourth compound eluted was identified as 2,2',3,3',4,4',5,5',6-nonamethyldiphenylmethane (249), the isomer of compound (248) above, and the structure was also confirmed by comparing its spectroscopic data with literature data.[41]

The fifth compound eluted was identified as 2,3,4,5,6-pentamethyl-nitrobenzene (250) and the structure was confirmed by comparing its spectroscopic data with literature data.[42]

The sixth compound eluted was identified as 2,3,4,6-tetramethyl-phenylnitromethane (251). The side-chain nitro aromatic (251) gave a satisfactory parent molecular ion in the mass spectrum, indicating the molecular formula $C_{11}H_{15}NO_2$. N.O.e. experiments confirmed the

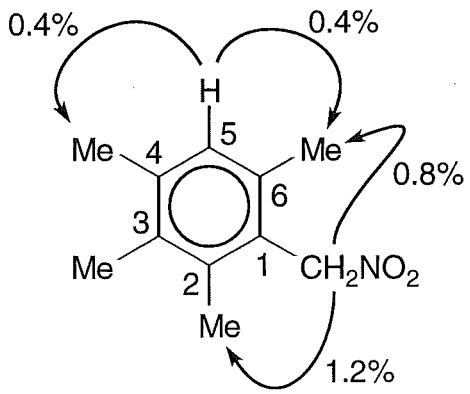

Fig. 3.48 Enhancements (%) from selected n.O.e. experiments for compound (251).

assignments of the chemical shifts for the protons. In particular, irradiation at δ 5.61 (CH_2) gave enhancements at δ 2.30 (2-Me) and at δ 2.35 (6-Me), while irradiation at δ 6.95 (H5) gave enhancements at δ 2.28 (4-Me) and at δ 2.35 (6-Me), as summarized in Fig. 3.48. Furthermore, the presence of a very strong infrared absorption at 1541 cm^{-1} provided evidence for the $-NO_2$ substituent.

The seventh compound eluted was identified as 2,3,4,5-tetramethylphenylnitromethane (252), the isomer of compound (251) above, and the structure was confirmed by comparing its spectroscopic data with literature data.[9]

The eighth compound eluted was identified as 2,3,4,5-tetramethylbenzaldehyde (253) and the structure was confirmed by comparing its spectroscopic data with literature data.[43]

The ninth compound eluted was identified as 2,3,4,5,6-pentamethylbenzoic acid (254) and the structure was confirmed by comparing its spectroscopic data with an authentic sample.

The tenth compound eluted was identified as 2,3,4,5-tetramethylbenzyl alcohol (255) and the structure was confirmed by comparing its spectroscopic data with literature data.[43]

The final compound eluted could only be isolated in admixture with its isomer (255) and was identified as 2,3,4,6-tetramethylbenzyl alcohol (256). N.O.e. experiments confirmed the assignments of the chemical shifts for the protons. In particular, irradiation at δ 4.76 (C**H**$_2$) gave enhancements at δ 2.39 (2-Me) and at δ 2.41 (6-Me), while irradiation at δ 6.92 (H5) gave enhancements at δ 2.31 (4-Me) and at δ 2.41 (6-Me), as

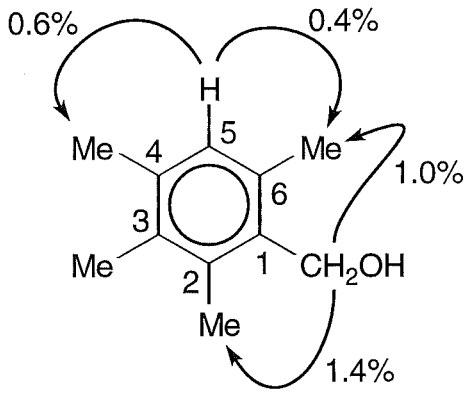

Fig. 3.49 Enhancements (%) from selected n.O.e. experiments for compound (256).

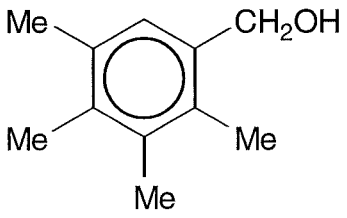

(255)

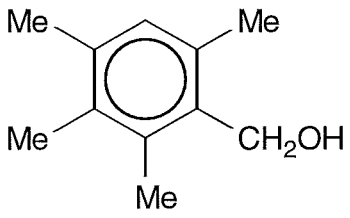

(256)

C**H**$_2$OH	4.64	4.76
CH$_2$OH	64.5	59.6

Fig. 3.50 Comparison of the characteristic ^{1}H and ^{13}C n.m.r. resonances (in ppm) for compounds (255) and (256).

represented in Fig. 3.49. Furthermore, the characteristic ^{1}H and ^{13}C n.m.r. resonances for the CH_2OH function were closely similar to the isomeric side-chain alcohol (255) above, as outlined in Fig. 3.50. Specifically, the ^{1}H n.m.r. resonance for the $C\mathbf{H_2}$ function appeared at δ 4.76, while the ^{13}C n.m.r. resonance for the $\mathbf{C}H_2$ function appeared at δ 59.6.

The labile isomeric benzyl nitrates (257) and (258), and benzyl nitrites (259) and (260), were apparently hydrolysed on the silica gel Chromatotron plate and augmented the yields of the isomeric benzyl alcohols (255) and (256).

The known[43] 2,3,4,6-tetramethylbenzyl nitrate (257) was identified in the reaction mixture from its characteristic ^{1}H n.m.r. resonance due to the $C\mathbf{H_2}ONO_2$ function. Specifically, the $C\mathbf{H_2}ONO_2$ resonance appeared as a singlet at δ 5.56.

Similarly, the known[43] isomeric 2,3,4,5-tetramethylbenzyl nitrate (258) was also identified in the reaction mixture from its characteristic ^{1}H n.m.r. resonance due to the $C\mathbf{H_2}ONO_2$ function. In particular, the $C\mathbf{H_2}ONO_2$ resonance appeared as a singlet at δ 5.42.

The presence of 2,3,4,6-tetramethylbenzyl nitrite (259) in the reaction mixture was determined from its characteristic ^{1}H n.m.r. resonance due to the $C\mathbf{H_2}ONO$ function on comparison with trends seen for the known[9] side-chain compounds (261)-(263) from hexamethylbenzene and the related 2,3,4,5-tetramethylbenzyl side-chain compounds (252), (258) and (260), as observed in Fig. 3.51. Specifically, the $C\mathbf{H_2}ONO$ resonance appeared as a broad singlet at δ 5.73.

The presence of 2,3,4,5-tetramethylbenzyl nitrite (260) in the reaction mixture was determined from its characteristic ^{1}H n.m.r. resonance due to the $C\mathbf{H_2}ONO$ function on comparison with trends seen for the known[9] side-chain compounds (261)-(263) from hexamethylbenzene and the related 2,3,4,6-tetramethylbenzyl side-chain compounds (251), (257) and (259), as

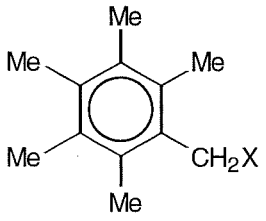

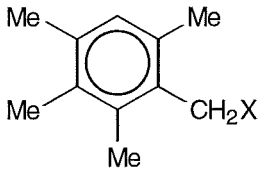

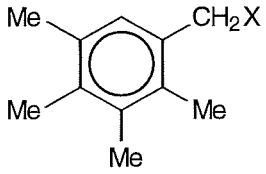

$X=NO_2$	(261)	5.67, s	(251)	5.61, s	(252)	5.43, s
$X=ONO_2$	(262)	5.63, s	(257)	5.56, s	(258)	5.42, s
X=ONO	(263)	5.76, br s	(259)	5.73, br s	(260)	5.65, br s

Fig. 3.51 Comparison of the characteristic ^1H n.m.r. resonances for the related compounds (261), (251) and (252); (262), (257) and (258); and (263), (259) and (260).

seen in Fig. 3.51. In particular, the CH_2ONO resonance appeared as a broad singlet at δ 5.65.

Monitoring the +20, -20, -50 and -78° reactions in dichloromethane with time showed that the adduct yield was highly temperature dependent. Table 3.10 gives an overview of product yields from the photochemical reaction between pentamethylbenzene (135) and TNM. At +20° adducts were not detected. However, at lower reaction temperatures adducts were observed and reached a maximum yield after 1 h at -78° (total 48%). Even at -78°, the adducts decomposed during the reaction (total 48% after 1 h, total 16% after 3 h). At lower reaction temperatures the side-chain trinitromethyl compounds (246) and (247), side-chain nitro (252) and the side-chain nitrate (258) all decreased in yield (after 3h, total 84% at +20°, total 42% at -78°). In contrast, dimer (249), side-chain nitro (251), side-chain nitrate (257) and the side-chain nitrites (259) and (260) all increased in

Table 3.10 Overview of product yields from the photolysis of pentamethylbenzene (135) (0.42 mol L^{-1}) and TNM (0.84 mol L^{-1}) in dichloromethane.

		Yield (%)																
	Conversion			Total														Total
t (h)	(%)	(244)	(245)	adducts	(246)	(247)	(248)	(249)	(251)	(252)	(253)	(255)	(256)	(257)	(258)	(259)	(260)	aromatics[a]
At +20°																		
0.5	30	-	-	-	23.5	5.2	trace	1.9	1.0	39.9	-	0.7	0.3	5.0	20.4	0.1	0.3	100
1	49	-	-	-	17.3	3.7	trace	1.0	0.9	52.0	0.2	0.4	0.5	4.7	16.9	0.5	0.6	100
2	78	-	-	-	11.9	3.6	0.1	1.1	1.9	40.3	0.6	0.1	0.1	6.3	28.9	0.7	2.0	100
3	89	-	-	-	9.7	3.5	0.1	0.5	1.9	40.7	1.1	0.3	0.2	6.5	29.9	0.9	2.8	100
At -20°																		
0.5	56	8.4	-	8.4	10.4	2.4	-	1.7	1.3	22.9	-	0.4	trace	8.9	40.9	-	-	91.6
1	78	-	-	-	9.4	3.7	-	3.6	2.3	36.1	0.1	1.1	trace	8.6	29.6	0.4	3.6	100
2	96	-	-	-	9.0	3.1	-	0.5	3.1	47.3	0.2	0.4	0.2	7.5	24.5	0.6	2.3	100
3	99	-	-	-	8.8	3.2	-	0.1	2.7	45.7	0.2	0.3	0.2	7.6	27.3	0.6	1.6	100

[a] The yields of compounds (250) and (254) could not be assessed individually from the ^1H n.m.r. spectra because of overlapping signals, but these are included within the column "Total aromatics".

Table 3.10 cont.

		Yield (%)																
	Conversion			Total														Total
t (h)	(%)	(244)	(245)	adducts	(246)	(247)	(248)	(249)	(251)	(252)	(253)	(255)	(256)	(257)	(258)	(259)	(260)	aromatics[a]
At -50°																		
0.5	26	25.2	1.4	26.6	6.7	1.1	-	9.4	6.0	14.9	0.4	0.4	0.4	12.9	14.5	0.7	0.5	73.4
1	41	33.0	2.2	35.2	8.4	1.3	0.3	3.9	8.0	14.7	0.2	0.2	0.2	8.4	11.2	2.2	1.9	64.8
2	69	2.1	-	2.1	9.2	4.5	0.2	11.3	10.8	23.6	0.6	0.2	0.1	6.7	15.2	4.9	6.3	97.9
3	79	-	-	-	7.7	3.4	0.1	7.4	10.0	25.6	0.6	0.3	0.1	8.3	21.1	3.9	8.7	100
At -78°																		
0.5	36	31.8	1.8	33.6	6.1	1.6	0.3	14.6	4.3	9.5	-	0.3	trace	14.6	8.7	0.5	1.2	66.4
1	48	46.2	2.1	48.3	5.1	1.6	0.3	7.0	5.3	8.9	trace	0.1	0.1	10.8	7.1	1.0	1.9	51.7
2	64	37.2	2.2	39.4	6.0	1.9	0.4	4.3	6.1	13.5	trace	0.1	0.1	11.6	8.4	1.8	2.3	60.6
3	76	14.9	0.8	15.7	6.2	3.2	0.4	8.3	6.6	18.5	0.2	trace	0.4	12.4	13.7	2.5	6.9	84.3

[a] The yields of compounds (250) and (254) could not be assessed individually from the ^{1}H n.m.r. spectra because of overlapping signals, but these are included within the column "Total aromatics".

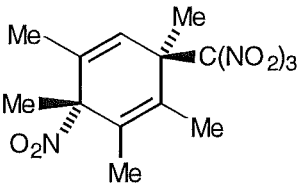

(244)

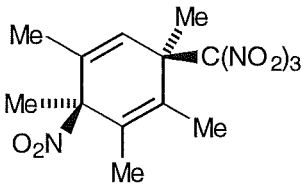

(245)

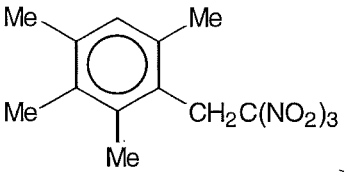

(246)

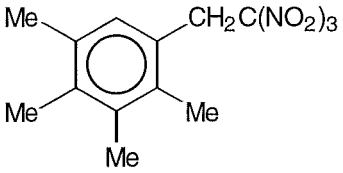

(247)

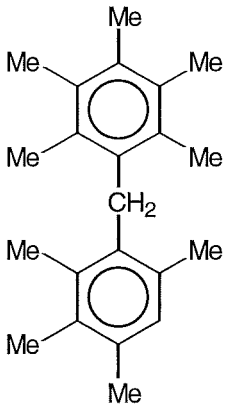

(248)

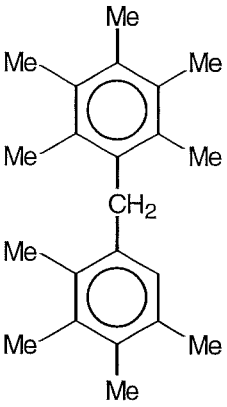

(249)

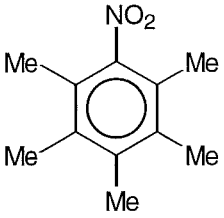

(250)

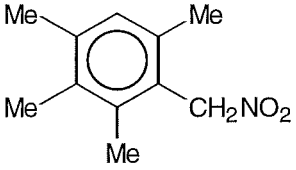

(251)

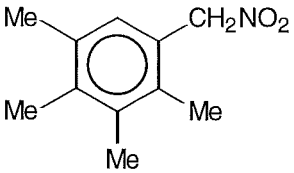

(252)

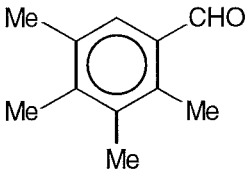

(253)

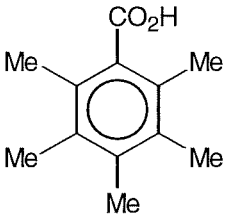

(254)

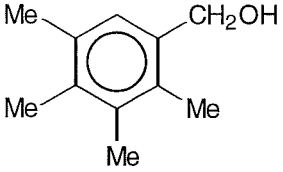

(255)

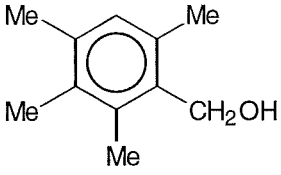

(256)

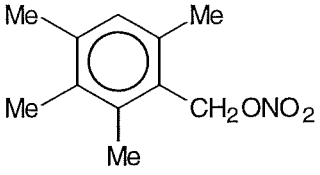

(257)

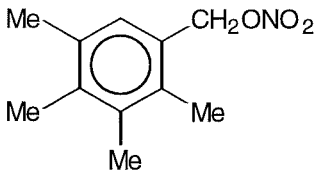

(258)

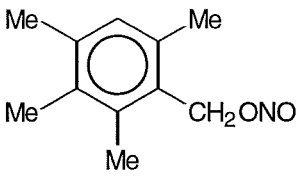

(259)

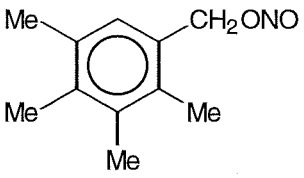

(260)

yield at lower reaction temperatures (after 3 h, total 13% at +20°, total 37% at -78°).

3.22 The Photochemistry of Pentamethylbenzene (135) in Acetonitrile

Photolyses of solutions of pentamethylbenzene (135) (0.42 mol L^{-1}) and TNM (0.84 mol L^{-1}) in acetonitrile were carried out at +20 and -20° as for reactions in dichloromethane, above. The results of these reactions, monitored with time, are summarized in Table 3.11. Interestingly, neither adducts (244) nor (245) were observed in photolysis reactions in acetonitrile. However, only adduct (244) was observed in the corresponding reactions in dichloromethane and then only at -20° after 0.5 h (8%) (See Table 3.10, Section 3.21). Unfortunately, comparisons with the -50 and -78° dichloromethane reactions were not possible due to the limited solubility of pentamethylbenzene (135) in the more polar acetonitrile at -50 and -78°. Similar to reactions in dichloromethane, the yields in acetonitrile of the side-chain trinitromethyl (247) and the side-chain nitrate (252) both decreased at lower reaction temperature (after 2 h, total 82% at +20°, total 58% at -20°). Also similar to the reactions in dichloro-methane, dimer (249), the side-chain nitro (251) and the side-chain nitrates (257) and (258) increased in yield in acetonitrile at lower reaction temperature (after 2 h, total 9% at +20°, total 29% at -20°). Also notable in

Table 3.11 Overview of product yields from the photolysis of pentamethylbenzene (135) (0.42 mol L^{-1}) and TNM (0.84 mol L^{-1}) in acetonitrile.

		Yield (%)											
	Conversion												Total
t (h)	(%)	(246)	(247)	(248)	(249)	(251)	(252)	(253)	(255)	(256)	(257)	(258)	aromatics
At +20°													
0.5	28	3.1	1.3	-	6.3	2.9	75.6	-	1.6	0.7	3.4	1.1	100
1	54	2.7	1.1	-	2.8	3.1	78.7	0.1	1.2	0.4	3.3	1.3	100
2	69	2.2	1.0	trace	1.4	3.1	81.4	0.1	0.9	0.5	3.1	1.7	100
3	83	1.9	1.3	0.1	1.0	2.8	68.7	0.2	0.8	0.4	2.8	13.2	100
At -20°													
1	21	5.0	1.5	-	14.8	3.7	46.9	-	0.7	1.2	7.0	10.4	100
2	36	2.8	0.4	0.1	6.1	6.1	58.0	-	0.4	0.8	8.0	9.1	100
3	45	2.4	0.2	0.1	3.4	7.2	67.4	0.3	0.2	0.3	7.9	5.0	100

acetonitrile was the absence of the side-chain nitrites (259) and (260) which were observed in reactions in dichloromethane.

3.23 The Photochemistry of Pentamethylbenzene (135) in 1,1,1,3,3,3-Hexafluoropropan-2-ol (HFP)

The photolysis of the charge-transfer complex of pentamethylbenzene (135) (0.42 mol L^{-1}) and TNM (0.84 mol L^{-1}) in HFP at +20° was a slow process, resulting in only a low conversion (*c.* 17%) after 3 h. After 24 h (conversion 98%) the product was shown to consist of a mixture of predominantly 2,3,4,5,6-pentamethylnitrobenzene (250) (68%), 2,3,4,5-tetramethyl-1-(2',2',2'-trinitroethyl)-benzene (247) (8%), 2,3,4,5-tetramethylphenylnitromethane (252) (11%), minor amounts of compounds (246), (249), (251), (253), (255) and (256) (total 8%) and unidentified aromatic compounds (total 5%).

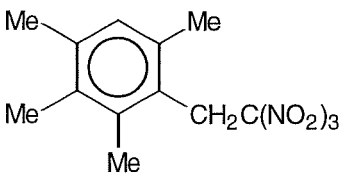

(246)

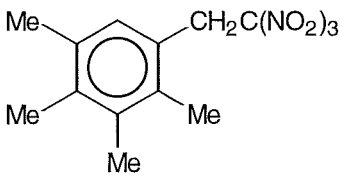

(247)

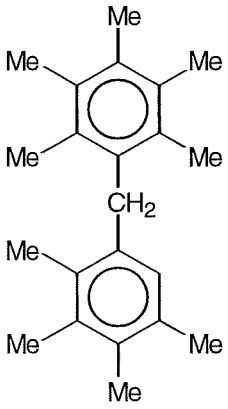

(249)

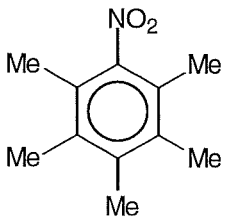

(250)

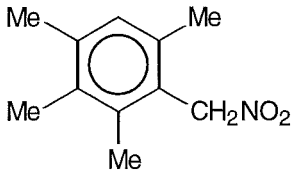

(251)

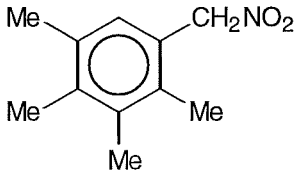

(252)

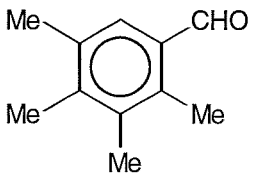

(253)

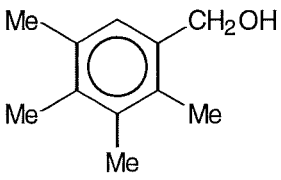

(255)

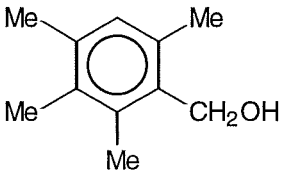

(256)

3.24 The Photochemistry of Pentamethylbenzene (135) in Dichloromethane Containing Trifluoroacetic Acid (TFA)

The photolysis of the charge-transfer complex of pentamethylbenzene (135) (0.42 mol L^{-1}) / TNM (0.84 mol L^{-1}) in dichloromethane containing TFA (0.71 mol L^{-1}) at +20° for 3 h (conversion 26%) gave a product which was shown by ^1H n.m.r. spectral analysis (see Table 3.12) to be a mixture of the 2',2',2'-trinitroethyl compounds (246) (20%) and (247) (5%), nonamethyldiphenylmethanes (248) (9%) and (249) (31%), 2,3,4,5-tetramethylphenylnitromethane (252) (18%), minor amounts of compounds (251), (253), (255)-(258) (total 7%) and unidentified aromatic compounds (total 10%).

While neither adduct (244) nor (245) were observed in the photolysis reaction in dichloromethane containing TFA, it was notable that there were significant amounts of the side-chain trinitromethyl compounds (246) and (247), reaching a maximum yield of 32% after 0.5 h. Similar to the reaction in dichloromethane without added acid (see Table 3.10, Section 3.21), compounds (246) and (247) decreased in yield as the reaction proceeded (total 32% after 0.5 h, total 24% after 3 h). The yield of dimers (248) and (249) in dichloromethane containing TFA greatly increased relative to a similar reaction without acid present (after 3 h, 40% with TFA, 1% without added acid). Correspondingly, there was a large decrease in the side-

Table 3.12 Overview of product yields from the photolysis of pentamethylbenzene (135) (0.42 mol L^{-1}) and TNM (0.84 mol L^{-1}) in dichloromethane containing trifluoroacetic acid (0.71 mol L^{-1}), at +20°.

		Yield (%)											
t (h)	Conversion (%)	(246)	(247)	(248)	(249)	(251)	(252)	(253)	(255)	(256)	(257)	(258)	Total aromatics
0.5	7	26.0	6.2	5.1	24.3	0.7	21.8	-	0.5	0.5	0.6	1.4	100
1	11	24.0	5.7	8.0	28.4	0.6	21.6	-	0.7	0.8	0.7	1.2	100
2	17	20.9	5.0	10.2	30.0	0.6	19.0	0.6	0.8	1.2	0.9	1.8	100
3	26	19.6	4.7	8.9	31.4	0.6	18.3	1.4	1.0	1.1	1.2	1.7	100

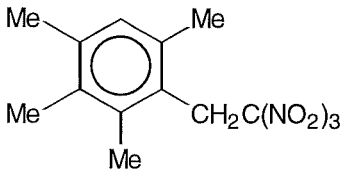

(246)

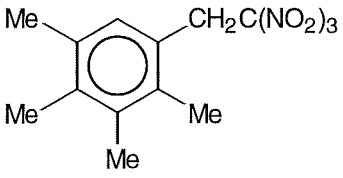

(247)

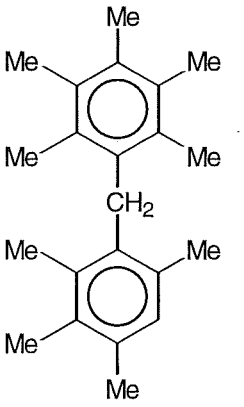

(248)

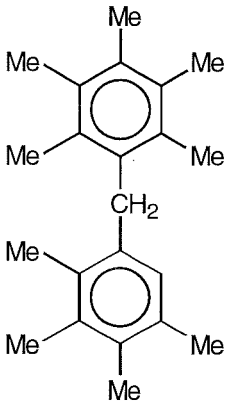

(249)

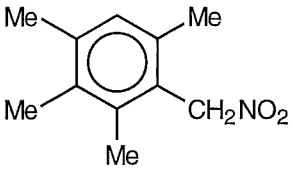

(251)

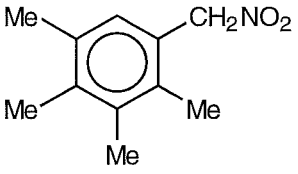

(252)

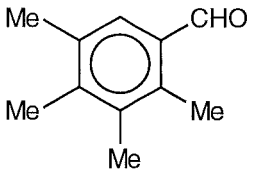

(253)

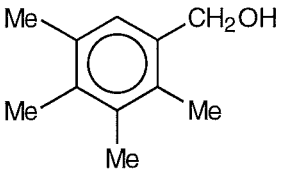

(255)

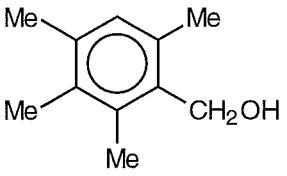

(256)

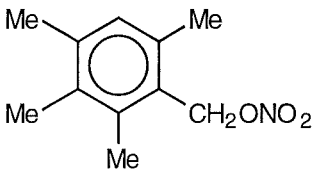

(257)

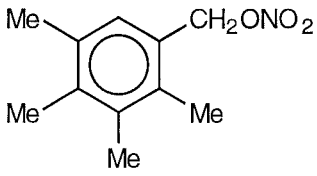

(258)

chain nitrates (257) and (258) in dichloromethane containing TFA when compared with the reaction without added acid (after 3 h, total 3% with TFA, total 36% without added acid). Interestingly, the +20° reaction in dichloromethane with TFA was slower than the corresponding reaction without added acid (after 3 h, 26% conversion with TFA, 89% conversion without TFA).

3.25 Reactions of Pentamethylbenzene (135) with Nitrogen Dioxide in Dichloromethane

A solution of pentamethylbenzene (135) (0.42 mol L^{-1}) in dichloromethane saturated with $^{\bullet}NO_2$ was stored in the dark at +20°. A similar solution was irradiated with filtered light ($\lambda_{cut\text{-}off}$<435 nm), also at +20°. Aliquots were removed at appropriate time intervals. After work-up, under reduced pressure at ≤0°, the product compositions were determined by ^1H n.m.r. spectral analysis (See Table 3.13). The two product compositions were similar after reaction for 3 h, *viz.* 2,3,4,5-tetramethylphenylnitromethane (252) (*c.* 35%), the benzyl nitrates (257) (*c.* 13%) and (258) (*c.* 43%), small amounts of compounds (248), (249), (251), (253), (255) and (256) (total *c.* 7%), and unidentified aromatic compounds (total *c.* 2%). These results were comparable with those reported by Bosch and Kochi,[31] except that they also observed a low yield of the nuclear nitration product (250).

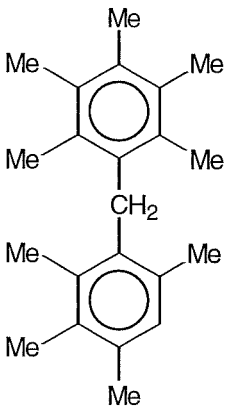

(248)

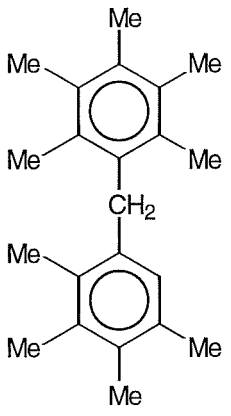

(249)

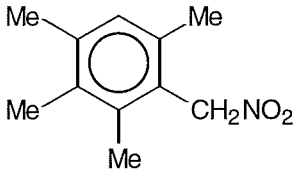

(251)

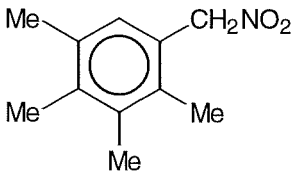

(252)

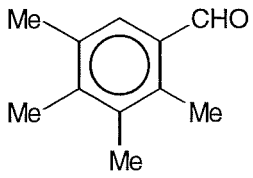

(253)

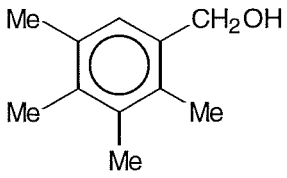

(255)

Table 3.13 Overview of product yields from the reaction of pentamethylbenzene (135) (0.42 mol L^{-1}) in dichloromethane saturated with nitrogen dioxide, at +20°.

		Yield (%)									
	Conversion										Total
t (h)	(%)	(248)	(249)	(251)	(252)	(253)	(255)	(256)	(257)	(258)	aromatics
In the dark											
0.5	31	-	1.1	2.2	33.9	1.5	0.3	0.1	14.4	44.5	100
1	42	-	1.2	2.6	34.6	1.6	0.4	0.2	13.7	43.9	100
2	47	trace	0.8	2.0	36.5	2.2	0.8	0.4	13.7	41.3	100
3	53	0.1	0.9	2.2	38.6	2.3	1.2	0.6	13.6	39.1	100
Irradiation with filtered light ($\lambda_{cut\text{-}off}$<435 nm)											
0.5	38	-	1.0	1.9	27.3	1.5	0.6	0.2	14.3	50.0	100
1	51	-	0.9	2.1	28.4	1.6	0.7	0.3	14.2	50.3	100
2	68	trace	0.7	1.7	31.4	1.7	0.4	0.2	13.7	48.3	100
3	76	0.1	0.6	1.9	31.9	2.0	0.7	0.3	13.0	47.5	100

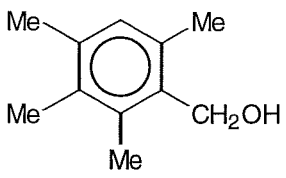

(256)

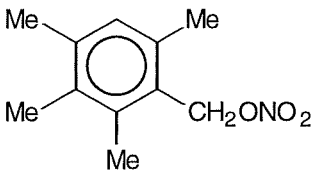

(257)

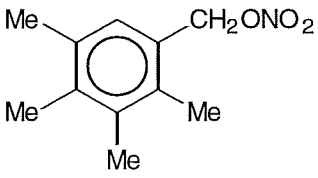

(258)

3.26 Rearrangement of 1,2,3,4,6-Pentamethyl-*r*-3-nitro-*t*-6-trinitromethylcyclohexa-1,4-diene (244) in (D_2)-Dichloromethane

A solution of adduct (244) in (D_2)dichloromethane was stored in the dark at +22° and its ^1H n.m.r. spectrum monitored at appropriate time intervals. The rearrangement of the adduct (244) was rapid (*c.* 26% after 2 min.), including the establishment of equilibrium between the epimeric adducts (244) and (245) during that period. The rearrangement was complete in 1 h (see Fig. 3.52) and gave 2,3,4,6-tetramethyl-1-(2',2',2'-trinitroethyl)-benzene (246) (11%), 2,3,4,5-tetramethylphenylnitromethane (252) (48%), 2,3,4,5-tetramethylbenzyl nitrate (258) (9%), 2,3,4,5-tetramethylbenzyl nitrite (260) (26%) and unidentified aromatics (total 6%).

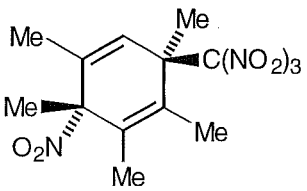

(244)

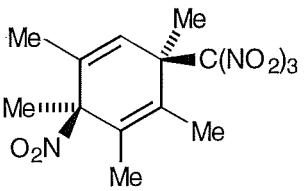

(245)

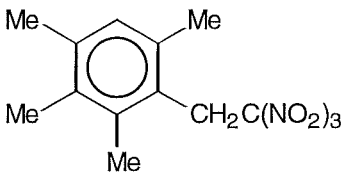

(246)

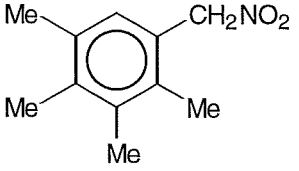

(252)

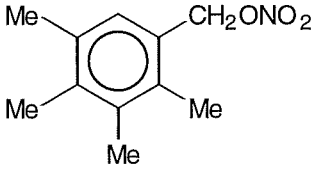

(258)

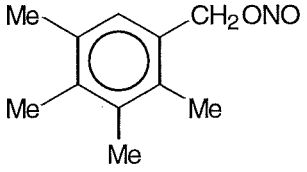

(260)

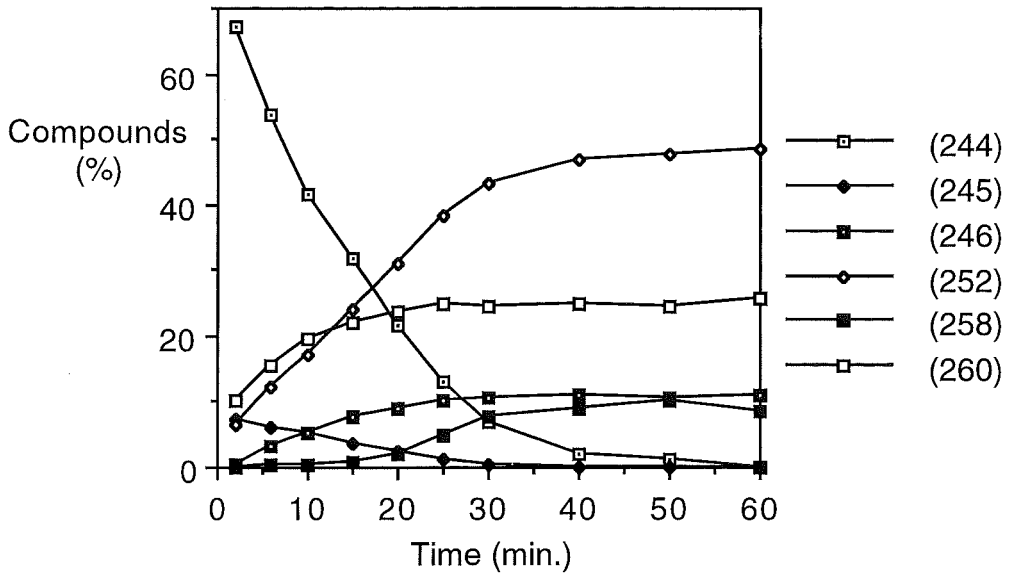

Fig. 3.52 Kinetics of the rearrangement of nitro/trinitromethyl adduct (244) in (D_2)dichloromethane, at +22°.

3.27 Overview of the Photonitration of Pentamethylbenzene (135)

Similar to the photolysis reaction of 1,2,4,5-tetramethylbenzene (134) in TNM (see Section 3.19), the photochemical reaction of pentamethylbenzene (135) with TNM led to adduct formation apparently exclusively by

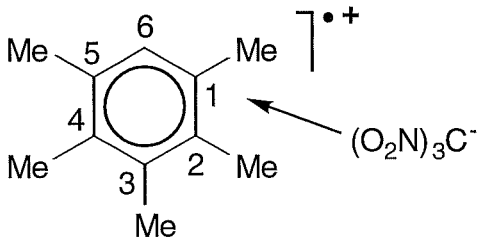

Fig. 3.53 Adducts identified corresponded only to attack of $(O_2N)_3C^-$ at C1 of the pentamethylbenzene radical cation.

attack of $(O_2N)_3C^-$ at C1 on the pentamethylbenzene radical cation, as observed in Fig. 3.53. No adducts were observed arising *via* alternative attack of $(O_2N)_3C^-$ at either C2 or C3 or C6 on the radical cation of penta-methylbenzene. This was probably due to the instability of the delocalized carbon radicals (148), (149) and (147), respectively. However, the

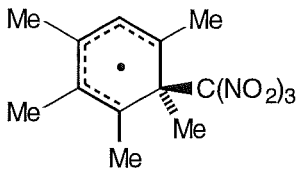

(148)

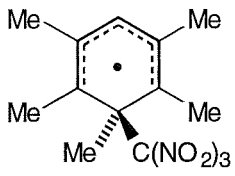

(149)

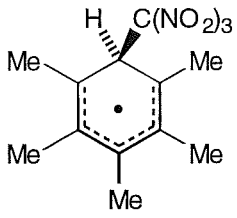

(147)

absence of adducts containing the trinitromethyl function at either C2 or C3 or C6 could also be due to the resulting adducts being highly unstable due to severe steric hindrance from the two β-methyl interactions with the trinitromethyl group. If formed, such adducts might decompose rapidly to further products.

The nitro/trinitromethyl adducts (244) and (245) formed in the photolysis of the charge-transfer complex of pentamethylbenzene (135) and TNM arose by initial attack of $(O_2N)_3C^-$ *ipso* to one of the flanking methyl groups at C1 in the pentamethylbenzene radical cation to give the delocalized carbon radical (146), as outlined in Scheme 3.35. Radical coupling of the delocalized carbon radical (146) with $^{\bullet}NO_2$ at C4 with C-N

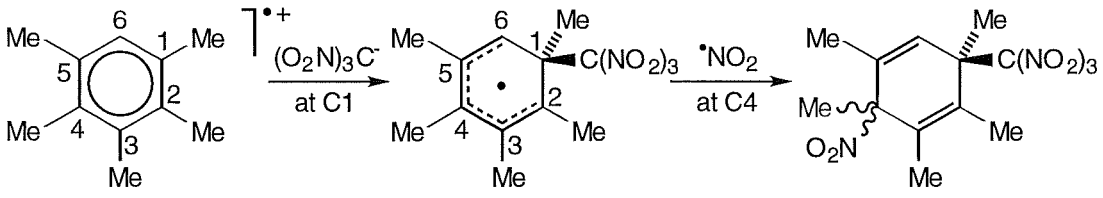

(146) (244) and (245)

Scheme 3.35

bond formation would then give the nitro/trinitromethyl adducts (244) and (245). Adducts (244) and (245) were notably unstable, being undetectable in photolysis reactions in dichloromethane solution of the charge-transfer complex of pentamethylbenzene (135) and TNM at +20°, transiently detectable at -20°, and still clearly labile during photolyses even at -50 or -78°. These observations indicated that the pentamethyl adducts (244) and (245) were much more labile than the tetramethyl adducts (216) and (217) seen in the 1,2,4,5-tetramethylbenzene (134) series (See Section 3.11).

The nitro/trinitromethyl adduct (244) rearranged rapidly in (D_2)dichloromethane at +22° to give 2,3,4,6-tetramethyl-1-(2',2',2'-trinitroethyl)-benzene (246), 2,3,4,5-tetramethylphenylnitromethane (252), 2,3,4,5-tetramethylbenzyl nitrate (258) and 2,3,4,5-tetramethylbenzyl nitrite (260). These were all products isolated from the photolysis reactions of the charge-transfer complex of pentamethylbenzene (135) and TNM. It appears likely that on dissolution in (D_2)dichloromethane the *trans*-adduct (244) epimerized to give an equilibrium mixture with the *cis*-adduct (245) within 2 min. Subsequently, this equilibrium mixture of adducts (244) and (245) rearranged to yield the products, above. The epimerization of (244) in (D_2)dichloromethane was much more rapid than a similar epimerization seen for nitro/trinitromethyl adducts (216) and (217) in the 1,2,4,5-tetramethylbenzene (134) series (See Sections 3.15 and 3.16). A possible mechanism for this rearrangement is presented in Scheme 3.36 and

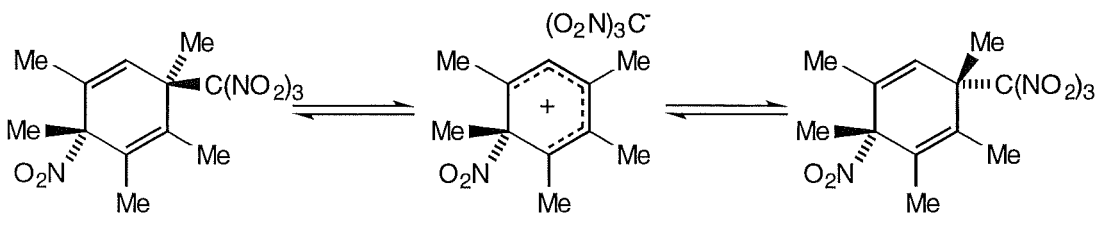

(244) (264) (245)

Scheme 3.36

presumably involves the intermediate nitrocyclohexadienyl cation/trinitromethanide ion pair (264).

What are the implications of this marked lability of nitro/trinitromethyl adducts (244) and (245) for the mode of formation of the non-adduct products from the photolysis of the charge-transfer complex of pentamethylbenzene (135) and TNM? This question is addressed by inspecting the yields in the photolysis reactions at -50 and -78° in dichloromethane, after 1 h and 3 h, of adducts (244) and (245) and the non-adduct products (246), (252), (258) and (260) (See Table 3.10, Section 3.21). These non-adduct products appear to have formed largely, if not exclusively, by rearrangement of nitro/trinitromethyl adducts (244) and (245).

The intermediate nitrocyclohexadienyl cation/trinitromethanide ion pair (264) affords a possible route to the aromatic side-chain compounds (252), (253), (255), (258) and (260), all proceeding *via* the 2,4,5-trimethylbenzyl radical (266), as illustrated in Scheme 3.37. Initially, loss of

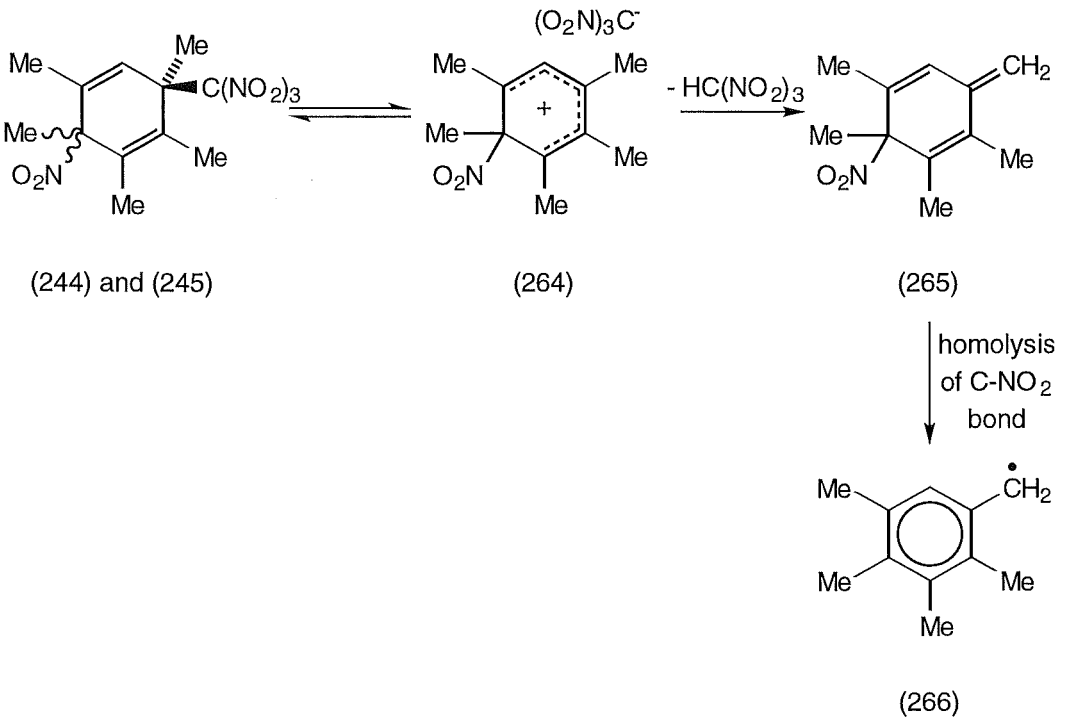

(244) and (245) (264) (265) (266)

Scheme 3.37

nitroform from the intermediate nitrocyclohexadienyl cation/trinitro-methanide ion pair (264) would occur by abstraction of an acidic proton from the methyl group by $(O_2N)_3C^-$, forming diene (265). This would be followed by homolytic cleavage of the C-NO_2 bond in diene (265) to give radical (266). Subsequent coupling of $^{\bullet}NO_2$ with the resulting 2,3,4,5-tetra-methylbenzyl radical (266) with C-N bond formation would lead to the formation of the side-chain nitro compound (252), as seen in Scheme 3.38.

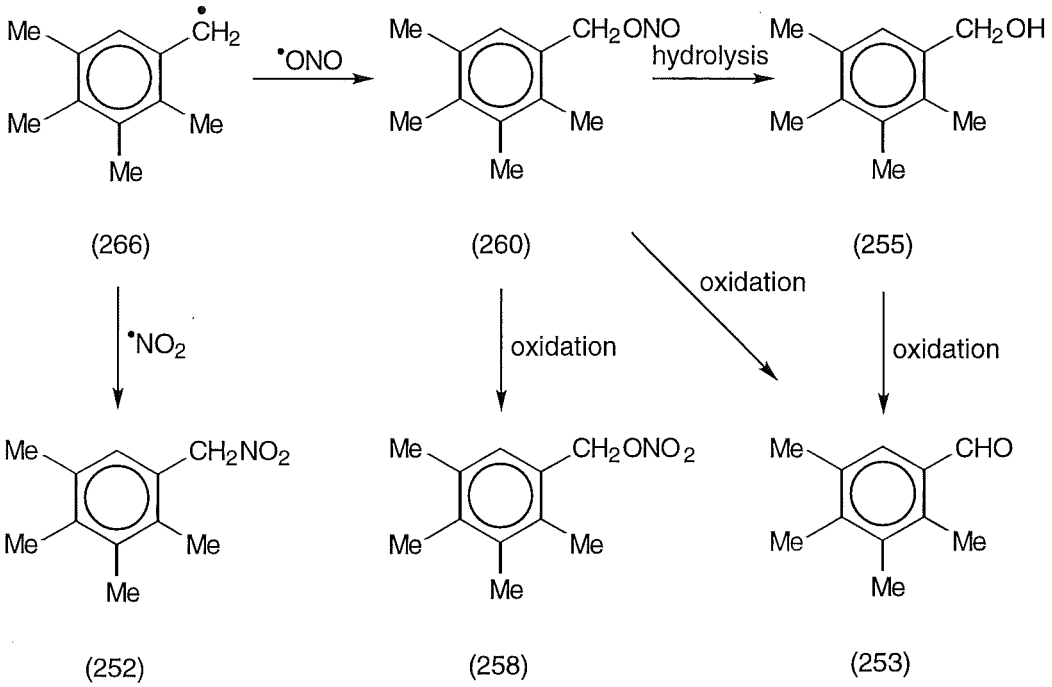

Scheme 3.38

Alternatively, coupling of $^{\bullet}NO_2$ could occur with C-O bond formation and would give the side-chain nitrite (260). The side-chain nitrite (260) can then undergo either hydrolysis to yield the side-chain alcohol (255) or oxidation to yield the side-chain nitrate (258). The oxidation of the nitrite (260) to produce the nitrate (258) was shown to be a rapid reaction.[31] Formation of the benzaldehyde (253) could arise either by oxidation of the nitrite (260) or by oxidation of the alcohol (255).

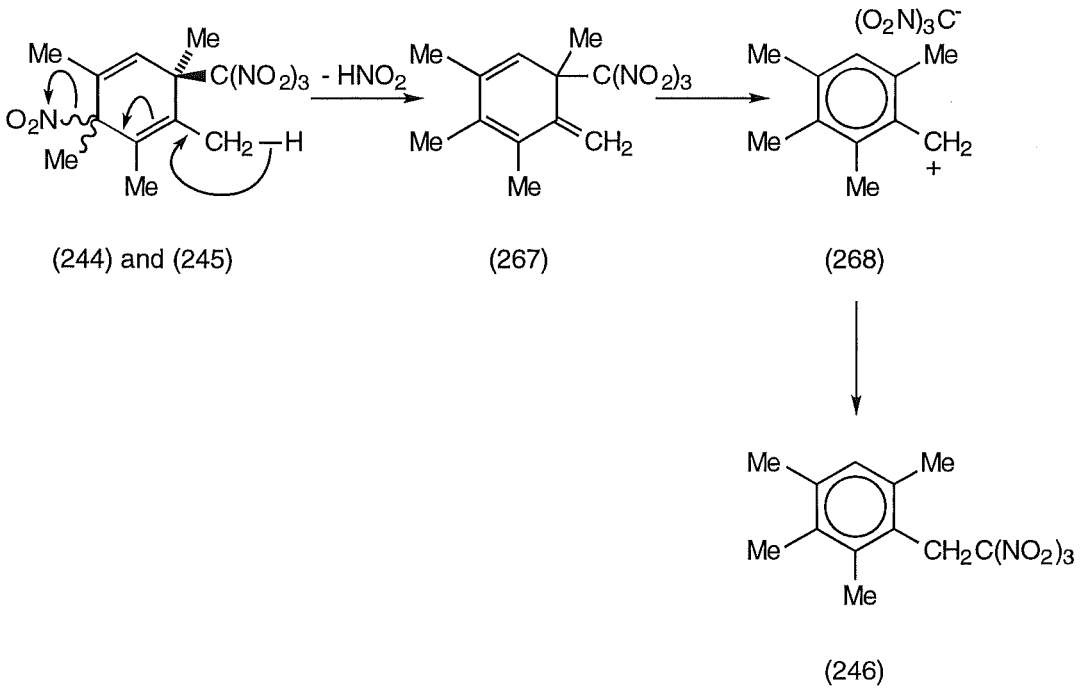

Scheme 3.39

The formation of the side-chain trinitromethyl aromatic (246) could occur *via* loss of nitrous acid from the nitro/trinitromethyl adducts (244) and (245) to form the trinitromethyl diene (267), as depicted in Scheme 3.39. Subsequent rearrangement *via* the ion pair (268) would give the side-chain trinitromethyl compound (246).

Possible modes of formation for dimers (248) and (249) are shown in Scheme 3.40 and follow the oxidative dimerization proposed by Eberson *et al.*[32] The radical cation of pentamethylbenzene can undergo α-deprotonation to yield the 2,3,4,5-tetramethylbenzyl radical (266). Subsequently, loss of an electron from radical (266) would produce the 2,3,4,5-trimethylbenzyl cation (269). Cation (269) can then couple with pentamethylbenzene (135) and, after loss of a proton, would form dimer (249). Alternately, loss of a proton at 2-Me would produce the 2,3,4,6-tetramethylbenzyl radical (270). Loss of an electron from radical (270) gives the 2,3,4,6-tetramethylbenzyl cation (271) which, after coupling with penta-

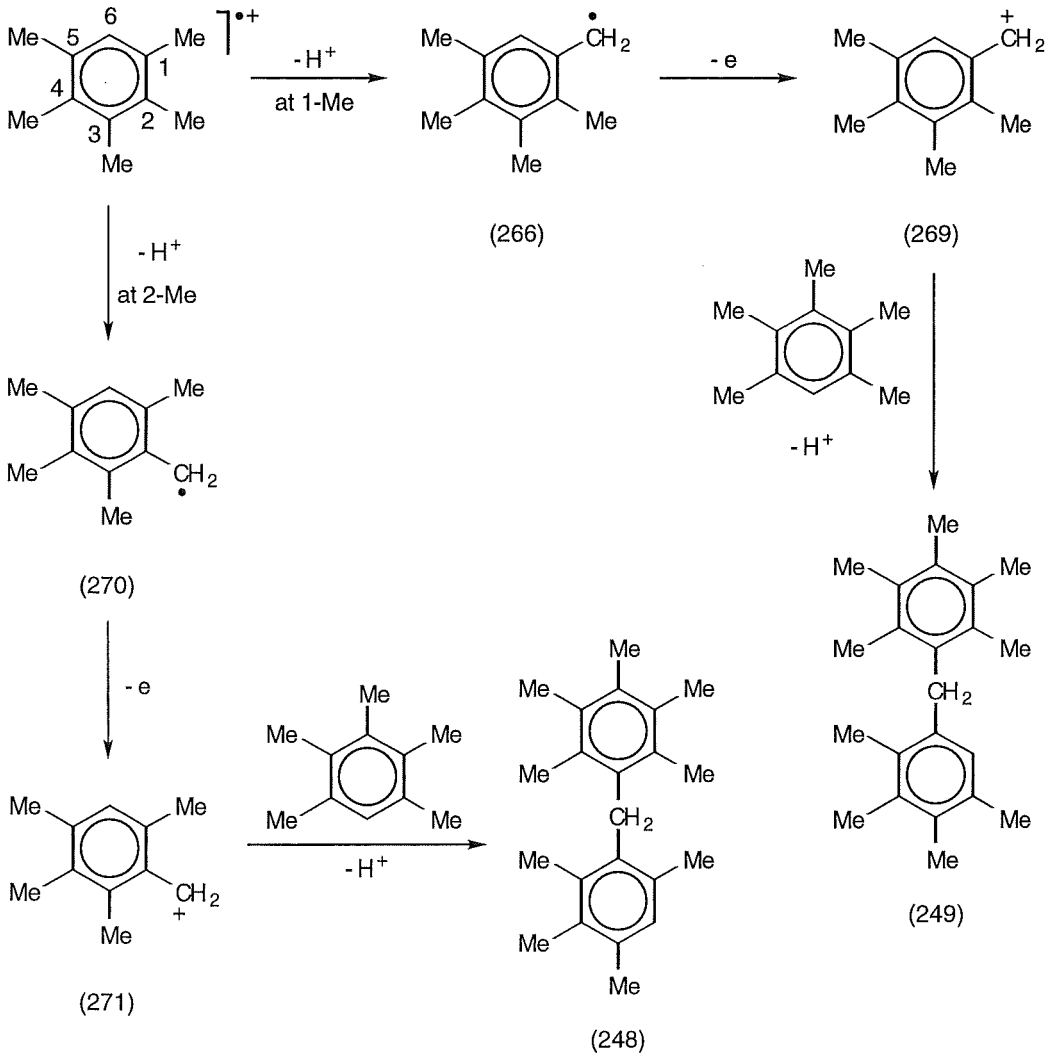

Scheme 3.40

methylbenzene (135) and subsequent loss of a proton, would form dimer (248).

Since the 2,3,4,5-tetramethylbenzyl derivatives (246), (252), (258) and (260) appear to be formed by rearrangement of adducts (244) and (245) during the photolysis of the charge-transfer complex of pentamethylbenzene (135) and TNM, how do the 2,3,4,6-tetramethylbenzyl derivatives (247), (251), (257) and (259) form? Analogous rearrangements of the 1,2,3,4,6-pentamethyl-3-nitro-6-trinitromethylcyclohexa-1,4-dienes (272) and (273) is an attractive postulate. The steric compression in the region of

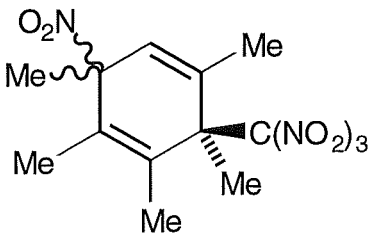

(272) and (273)

the trinitromethyl group would certainly be expected to render the nitro/trinitromethyl adducts (172) and (173) highly susceptible to rearrangement, which would be initiated by cleavage of the C-$C(NO_2)_3$ bond.

Adducts (272) and (273) would be formed *via* initial attack of $(O_2N)_3C^-$ at C2 on the pentamethylbenzene radical cation, as shown in Scheme 3.41. Subsequent radical coupling of $^{\bullet}NO_2$ at C4 on the resulting

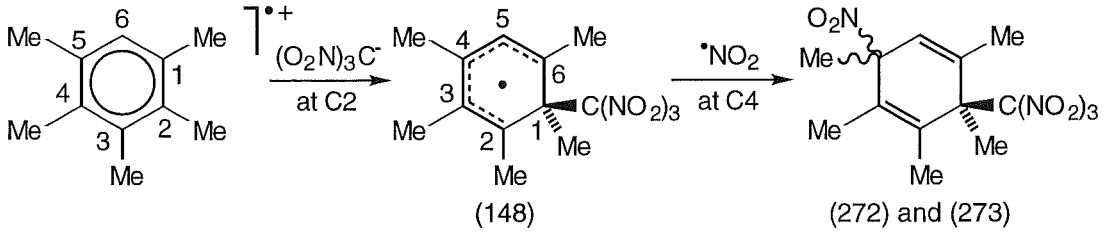

Scheme 3.41

delocalized carbon radical (148) with C-N bond formation would give adducts (272) and (273). Similarly to adducts (244) and (245), the proposed adducts (272) and (273) could undergo epimerization *via* the intermediate nitrocyclohexadienyl cation/trinitromethyl ion pair (274). However, subsequent loss of nitroform from the ion pair (274) appeared to be favoured, leading to the side-chain compounds (251), (256), (257) and (259) being formed, as summarized in Schemes 3.42 and 3.43. Initially, loss of nitroform from the intermediate nitrocyclohexadienyl cation/trinitromethanide ion pair (274) would occur by abstraction of an acidic proton

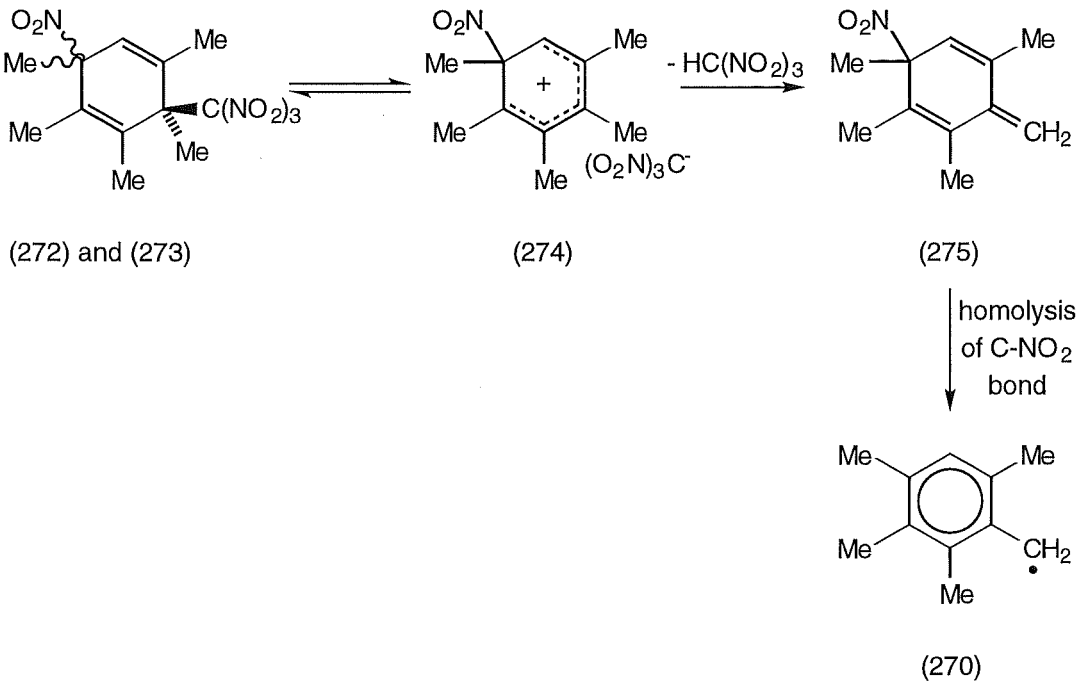

Scheme 3.42

from the methyl group by $(O_2N)_3C^-$, forming diene (275). This would be followed by homolytic cleavage of the C-NO_2 bond in diene (275) to give radical (270), as represented in Scheme 3.42. Subsequent coupling of $^{\bullet}NO_2$ with the resulting 2,3,4,6-tetramethylbenzyl radical (270) with C-N bond formation would lead to the formation of the side-chain nitro compound (251), as seen in Scheme 3.43. Alternately, coupling of $^{\bullet}NO_2$ could occur with C-O bond formation to give the side-chain nitrite (259). The side-chain nitrite (259) can then undergo either hydrolysis to yield the side-chain alcohol (256) or oxidation to yield the side-chain nitrate (257). The oxidation of the nitrite (259) to produce the nitrate (257) was shown to be a rapid reaction.[31]

The side-chain trinitromethyl aromatic (247) could be formed *via* loss of nitrous acid from the nitro/trinitromethyl adducts (272) and (273) to form the trinitromethyl diene (276), as depicted in Scheme 3.44. Subsequent rearrangement *via* the ion pair (277) would give the side-chain trinitro-

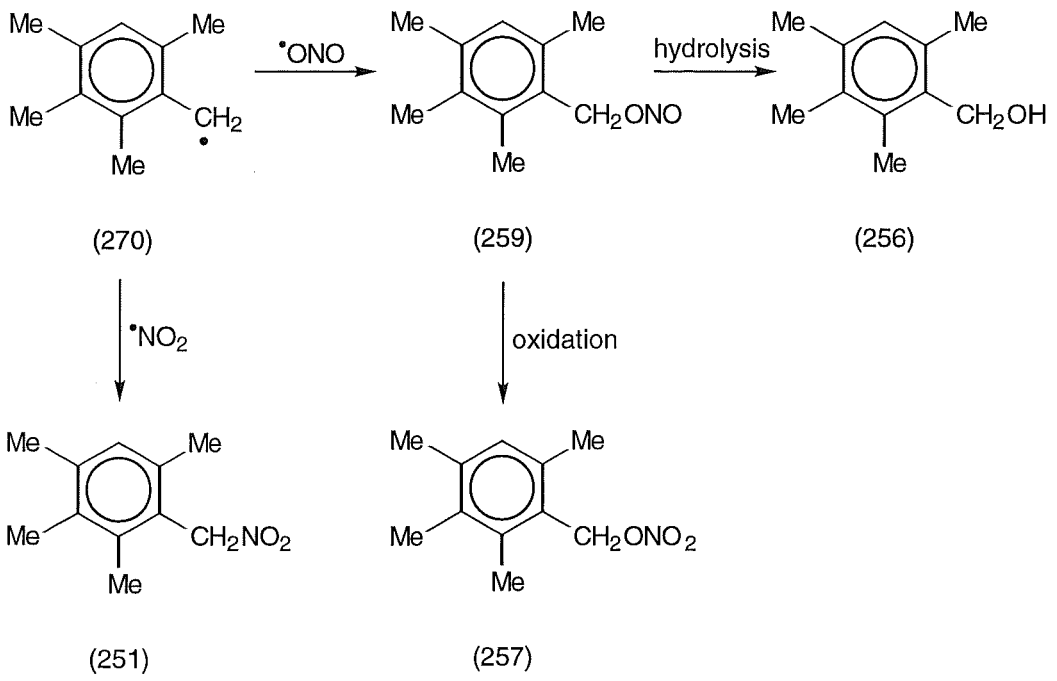

Scheme 3.43

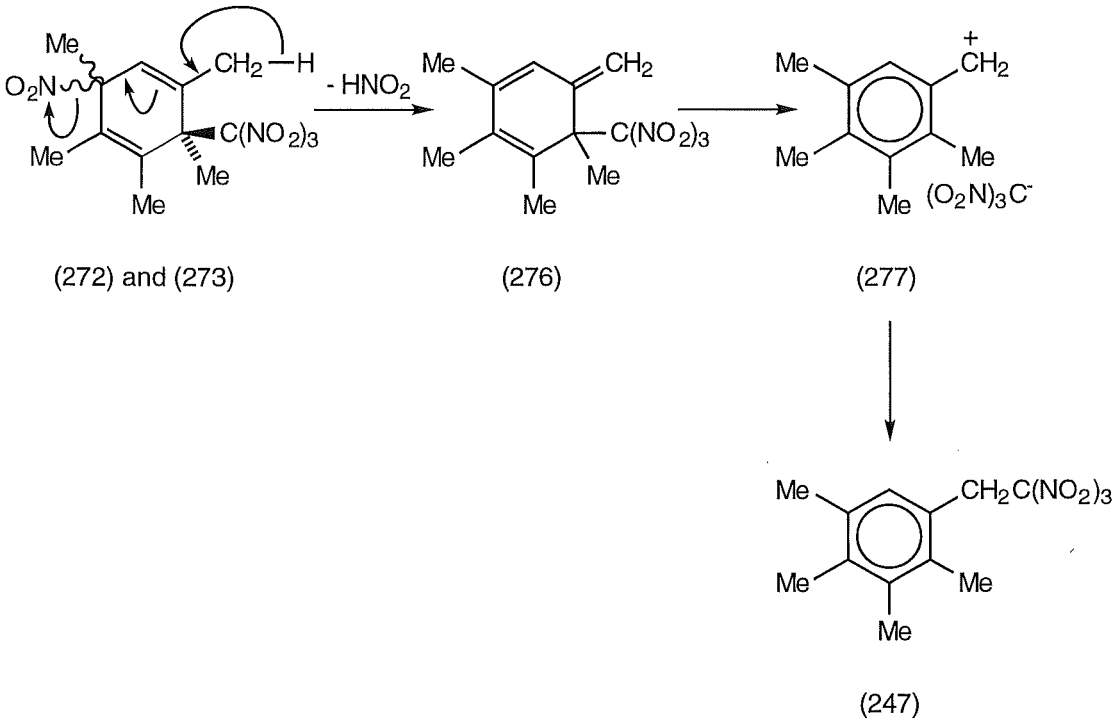

Scheme 3.44

methyl compound (247).

The photolysis of the charge-transfer complex of pentamethylbenzene (135) and TNM either in HFP or in dichloromethane containing TFA (0.71 mol L^{-1}) was slow. Both reactions resulted in low conversion of substrate into products after the normal reaction time of 3 h (17% in HFP, 26% in TFA) (See Sections 3.23 and 3.24, respectively). Under these reaction conditions, the reaction of $(O_2N)_3C^-$ with the radical cation of pentamethylbenzene would be expected to be at least partially suppressed by the solvent, HFP,[35-40] or by protonation by TFA.[33]

The formation of a significant yield of 2,3,4,5,6-pentamethylnitrobenzene (250) (68%) was notable in the photolysis reaction in HFP. This was analogous to the formation of 2,3,5,6-tetramethylnitrobenzene (220) on photolysis of the charge-transfer complex of 1,2,4,5-tetramethylbenzene (134) and TNM in HFP (See Section 3.12). The formation of compound (250) was seen as occurring *via* HFP-promoted nitrosation of pentamethylbenzene (135), as presented in Scheme 3.45 and discussed earlier in Section 3.19. Subsequent oxidation of the nitroso compound (278) would lead to formation of the ring nitro compound (250).

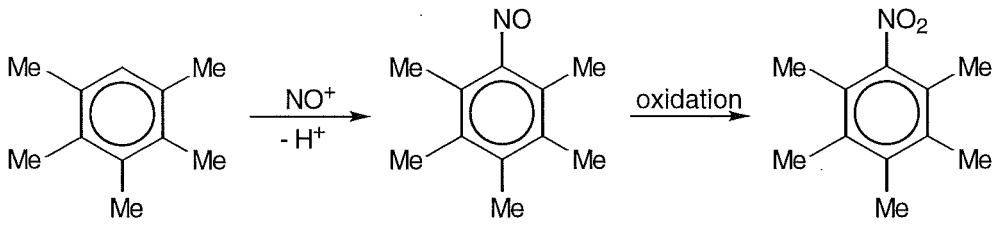

(135) (278) (250)

Scheme 3.45

The reactions either in the dark or on irradiation with filtered light ($\lambda_{cut\text{-}off}$<435 nm) of pentamethylbenzene (135) with excess $^{\bullet}NO_2$ in dichloromethane at +20° gave essentially the same product composition.

The significant products were 2,3,4,5-tetramethylphenylnitromethane (252) (*c.* 35%) and two isomeric benzyl nitrates (257) and (258) (total *c.* 56%) (See Table 3.13, Section 3.25). It appears that both the "light" and "dark"

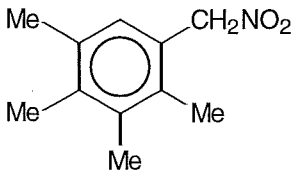

(252)

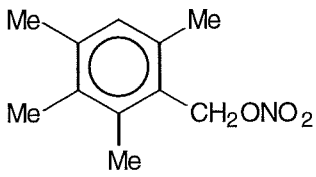

(257)

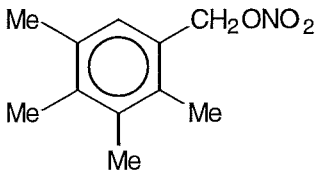

(258)

conditions in the reactions of pentamethylbenzene (135) with $^{\bullet}NO_2$ in dichloromethane resulted in thermal nitration. The product compositions were generally in agreement with product ratios for thermal nitration of pentamethylbenzene (135) with $^{\bullet}NO_2$ in dichloromethane in the dark reported by Bosch and Kochi.[31]

In conclusion, in the photolysis of pentamethylbenzene (135) and TNM, radical (146) appeared to be the most stable delocalized carbon radical. Direct evidence for the attachment of the trinitromethyl function at C2 could not be obtained. However, the 2,3,4,6-tetramethylbenzyl compounds and the trinitromethyl compound (247) were probably formed *via* rearrangement of unstable adducts containing the trinitromethyl function at C2. These adducts would have formed *via* the less stable delocalized carbon radical (148). No products were seen as arising from either radical (147) or radical (149), presumably due to their instability.

3.28 The Photolysis of Hexamethylbenzene (136)

General procedure for the photonitration of hexamethylbenzene (136) *with TNM.*

A solution of hexamethylbenzene (136) (500 mg, 0.39 mol L^{-1}) and TNM (0.78 mol L^{-1}) in dichloromethane (at +20 or -20°) or acetonitrile (at +20°) was irradiated with filtered light ($\lambda_{cut\text{-}off}$<435 nm) and small samples were withdrawn for analysis at suitable intervals. The work-up procedure, involving evaporation of solvent and TNM, was conducted at ≤0°. The crude product mixtures were stored at -78° and were analysed by ^1H n.m.r. spectroscopy as soon as possible (For complete experimental details see Chapter 5, Section 5.3.4).

3.29 The Photochemistry of Hexamethylbenzene (136) in Dichloromethane

3.29.1 Photochemistry in dichloromethane at -78° and the identification of aromatic products (279)-(287).

A solution of hexamethylbenzene (136) (0.39 mol L^{-1}) and TNM (0.78 mol L^{-1}) in dichloromethane was irradiated at -20° until the blood red colour of the charge-transfer band was bleached. The composition of the reaction mixture was monitored by withdrawing samples for ^1H n.m.r. spectral analysis. After work-up, the final solution (after 3 h) contained pentamethyl-(2',2',2'-trinitroethyl)-benzene (279) (10%), pentamethylbenzyl nitrite (280) (6%), pentamethylbenzyl nitrate (281) (42%), pentamethylphenylnitro-methane (282) (40%), and small amounts of compounds (283)-(287). The components of this mixture were separated by h.p.l.c. on a cyanopropyl column using hexane/dichloromethane mixtures as the eluting solvents.

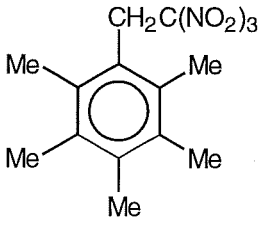

(279)

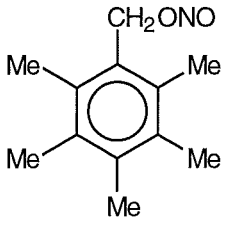

(280)

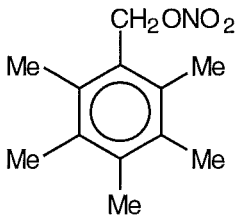

(281)

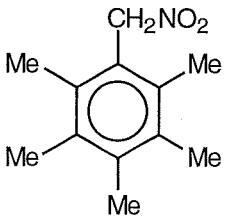

(282)

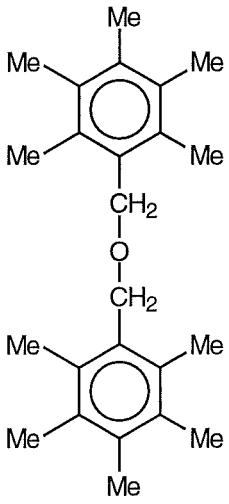

(283)

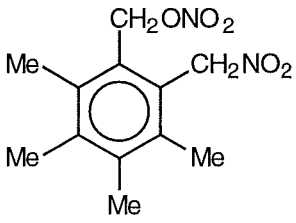

(284)

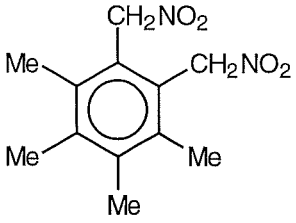

(285)

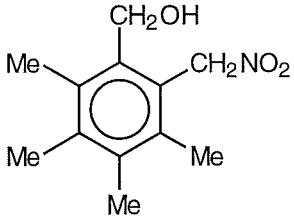

(286)

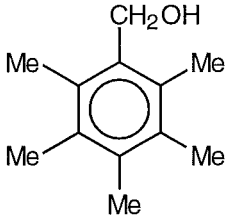

(287)

The first compound eluted was identified as pentamethyl-(2',2',2'-trinitroethyl)-benzene (279) and the structure was confirmed by comparing its spectroscopic data with literature data.[9]

The second compound eluted was identified as pentamethylbenzyl nitrite (280) and the structure was confirmed by comparing its spectroscopic data with literature data.[9]

The third compound eluted was identified as pentamethylbenzyl nitrate (281) and the structure was confirmed by comparing its spectroscopic data with literature data.[9]

The fourth compound eluted was identified as pentamethylphenyl-nitromethane (282) and the structure was confirmed by comparing its spectroscopic data with literature data.[44]

The fifth compound eluted was identified as di-(pentamethylbenzyl) ether (283) and the structure was confirmed by comparing its spectroscopic data with literature data.[45]

The sixth compound eluted was identified as 3,4,5,6-tetramethyl-2-nitromethylbenzyl nitrate (284). Compound (284) gave a satisfactory parent molecular ion in the mass spectrum, indicating the molecular formula $C_{12}H_{16}N_2O_5$. N.O.e. experiments confirmed the assignments of the chemical shifts for the protons. In particular, irradiation at δ 2.36 (6-Me) gave an enhancement at δ 5.70 ($C\mathbf{H_2}ONO_2$), while irradiation at δ 5.72 ($C\mathbf{H_2}NO_2$) gave an enhancement at δ 2.34 (3-Me), as observed in Fig. 3.54.

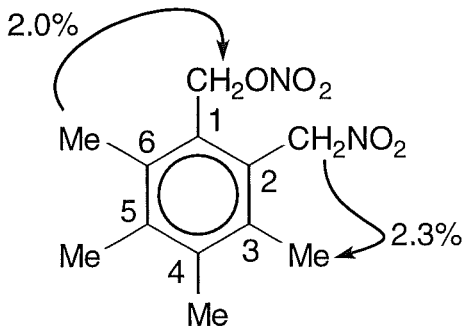

Fig. 3.54 Enhancements (%) from selected n.O.e. experiments for compound (284).

The assignment of the characteristic ^1H and ^{13}C n.m.r. resonances for the $-CH_2X$ functions ($X=ONO_2$ and NO_2) were based on comparison with the known[9,44] monosubstituted compounds (281) and (282), as presented in Fig. 3.55. HMQC and HMBC experiments confirmed the assignment of the ^{13}C n.m.r. resonances. Specifically, the ^{13}C n.m.r. resonance due to the $\mathbf{C}H_2ONO_2$ function appeared at δ 70.1, while the ^{13}C n.m.r. resonance due

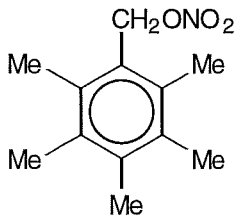

(281)

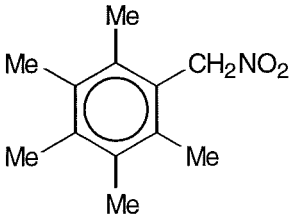

(282)

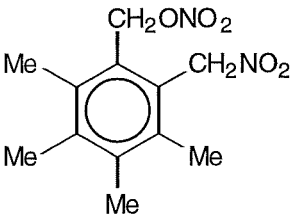

(284)

CH_2ONO_2	5.63, s	-	5.70, s
CH_2NO_2	-	5.67, s	5.72, s
CH_2ONO_2	71.5	-	70.1
CH_2NO_2	-	74.8	74.1

Fig. 3.55 Comparison of the characteristic ^1H and ^{13}C n.m.r. resonances (in ppm) for compounds (281), (282) and (284).

to CH_2NO_2 function appeared at δ 74.1. Furthermore, the presence of very strong infrared absorptions at 1628, 1279 and 858 cm^{-1} provided evidence for the $-ONO_2$ function, while the absorption at 1541 cm^{-1} provided evidence for the $-NO_2$ function.

The seventh compound eluted was identified as 1,2-bis(nitromethyl)-3,4,5,6-tetramethylbenzene (285) and the structure was confirmed by comparing its spectroscopic data with literature data.[9]

The eighth compound eluted was identified as 3,4,5,6-tetramethyl-2-nitromethylbenzyl alcohol (286). Compound (286) gave a satisfactory parent molecular ion in the mass spectrum, indicating the molecular formula $C_{12}H_{17}NO_3$. N.O.e. experiments confirmed the assignments of the chemical shifts for the protons. Specifically, irradiation at δ 5.80 (CH_2NO_2) gave enhancements at δ 2.30 (3-Me) and at δ 4.84 (CH_2OH), while

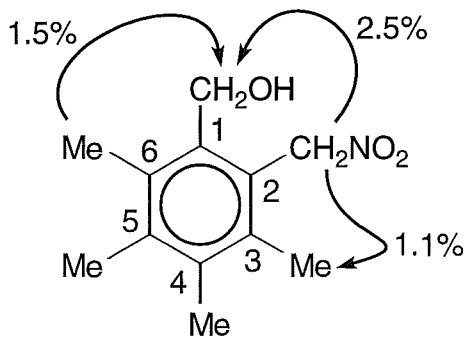

Fig. 3.56 Enhancements (%) from selected n.O.e. experiments for compound (286).

irradiation at δ 2.39 (6-Me) gave an enhancement at δ 4.84 (C**H$_2$**OH), as illustrated in Fig. 3.56. The assignments of the characteristic ^{1}H and ^{13}C n.m.r. resonances for the -CH_2X functions (X=OH and NO_2) were based on comparison with the known[9,44] monosubstituted compounds (287) and

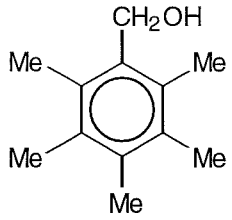

(287)

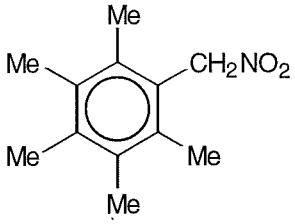

(282)

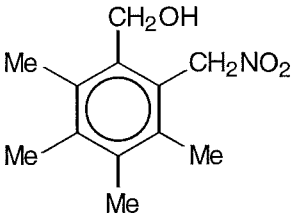

(286)

C**H$_2$**OH	4.78, s	-	4.84, s
C**H$_2$**NO_2	-	5.67, s	5.80, s
CH_2OH	60.0	-	59.8
CH_2NO_2	-	74.8	74.5

Fig. 3.57 Comparison of the characteristic ^{1}H and ^{13}C n.m.r. resonances (in ppm) for compounds (287), (282) and (286).

(282), respectively, as presented in Fig. 3.57. HMQC and HMBC experiments confirmed the assignment of the ^{13}C n.m.r. resonances. In particular, the ^{13}C n.m.r. resonance due to the **C**H_2OH function appeared at δ 59.8, while the ^{13}C n.m.r. resonance due to **C**H_2NO_2 function appeared at δ 74.5. Furthermore, the presence of a broad infrared absorption at 3383 cm^{-1} provided evidence for the -OH function, while a very strong absorption at 1551 cm^{-1} provided evidence for the -NO_2 function.

The final compound eluted from the h.p.l.c. column was identified as pentamethylbenzyl alcohol (287) and the structure was confirmed by comparing its spectroscopic data with literature data.[9]

3.29.2 Photochemistry in dichloromethane at +20° and the identification of pentamethylbenzaldehyde (288).

Photolysis of the charge-transfer complex of hexamethylbenzene (136) (0.39 mol L^{-1}) and TNM (0.78 mol L^{-1}) in dichloromethane at +20°, for 5 h gave a product which was shown by ^1H n.m.r. spectral analysis to be a mixture of the aromatic compounds (279)-(288). Chromatography of this mixture on a silica gel Chromatotron plate gave a small amount of compound (288) in a fraction eluted immediately after the di-(pentamethyl-benzyl) ether (283).

Compound (288) was identified as pentamethylbenzaldehyde (288) and the structure was confirmed by comparing its spectroscopic data with literature data.[42]

The change in composition of the photochemical reaction between hexamethylbenzene (136) and TNM was monitored with time at +20 and -20° in dichloromethane. An overview of product yields in dichloromethane is presented in Table 3.14. Most notable was the absence of any adducts in dichloromethane either at +20 or -20°, unlike all of the other substrates studied and discussed earlier in this thesis. However, the side-chain

trinitromethyl compound (279) was formed, reaching a maximum yield of 19% after 1 h at +20°. At lower temperature, the yields of the side-chain trinitromethyl (279) and the side-chain nitrite (280) decreased (after 5 h,

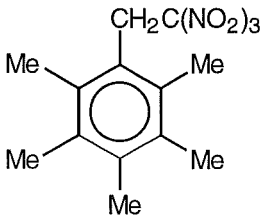

(279)

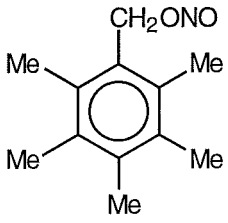

(280)

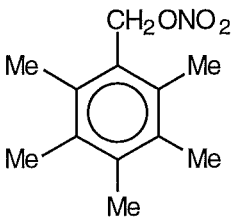

(281)

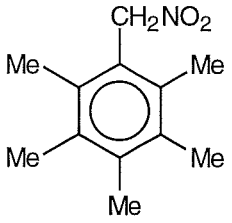

(282)

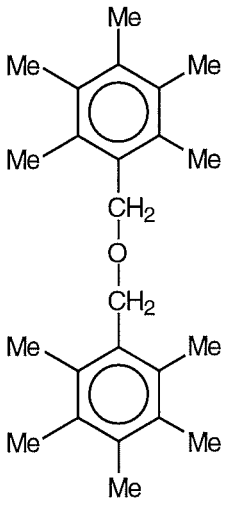

(283)

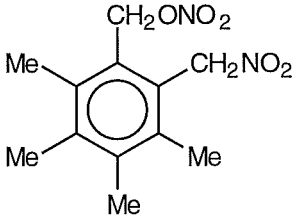

(284)

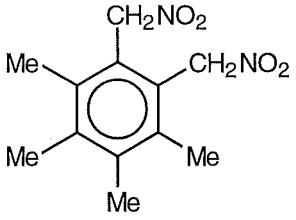

(285)

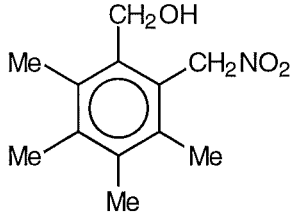

(286)

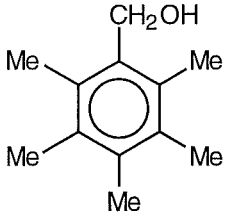

(287)

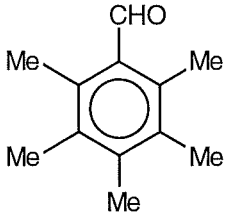

(288)

Table 3.14 Overview of product yields from the reaction of hexamethylbenzene (136) (0.39 mol L^{-1}) and TNM (0.78 mol L^{-1}) in dichloromethane.

	Yield (%)										
t (h)	(279)	(280)	(281)	(282)	(283)	(284)	(285)	(286)	(287)	(288)	Total aromatics
At +20°											
1	18.6	3.3	33.4	32.0	-	-	trace	-	-	trace	12.7
3	17.1	9.7	34.3	32.7	-	0.4	0.9	-	-	0.8	4.1
5	15.7	8.1	31.3	32.1	trace	1.6	2.5	trace	trace	1.9	6.8
At -20° [a]											
1	12.6	1.4	25.0	51.7	-	trace	0.1	-	-	-	9.2
3	12.4	4.5	25.0	56.4	-	0.2	0.8	-	-	-	0.7
5	10.4	5.7	37.0	44.5	trace	0.4	0.9	-	-	-	1.1
8	9.8	5.9	41.8	39.6	0.2	0.8	1.5	trace	trace	-	0.4

[a] Some substrate remained undissolved throughout the reaction.

total 24% at +20°, total 16% at -20°). In contrast, the side-chain nitro compound (282) increased in yield at the lower reaction temperature (after 5 h, 32% at +20°, 45% at -20°). Aldehyde (288), which was present at +20° (7% after 5 h), was not observed at -20°.

3.30 The Photochemistry of Hexamethylbenzene (136) in Acetonitrile

Photochemistry in acetonitrile at +20° and the identification of aromatic products (228), (289) *and* (290).

A solution of hexamethylbenzene (136) (0.39 mol L^{-1}) and TNM (0.78 mol L^{-1}) in acetonitrile was irradiated at +20° for 8 h and gave a mixture of pentamethyl-(2',2',2'-trinitroethyl)-benzene (279) (9%), pentamethylbenzyl

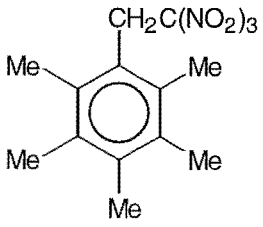

(279)

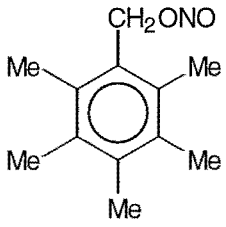

(280)

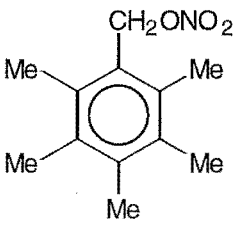

(281)

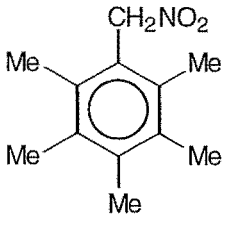

(282)

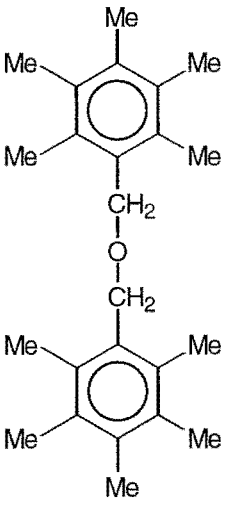

(283)

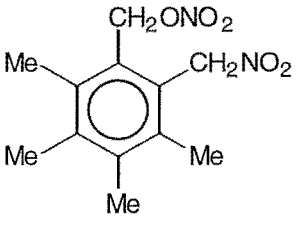

(284)

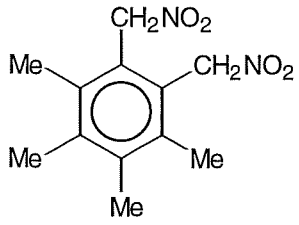

(285)

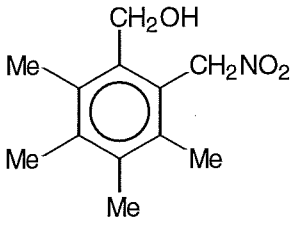

(286)

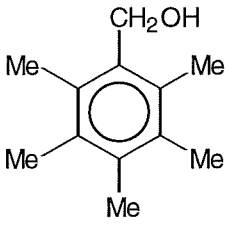

(287)

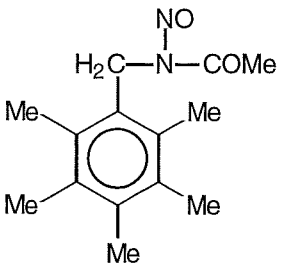

(228)

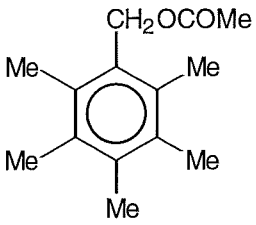

(289)

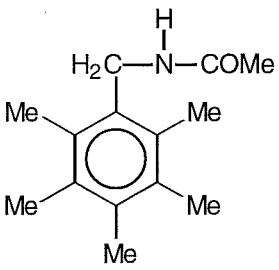

(290)

nitrate (281) (21%), pentamethylphenylnitromethane (282) (40%), 1,2-bis-(nitromethyl)-3,4,5,6-tetramethylbenzene (285) (10%), and small amounts of compounds (228), (280), (283), (284), (286), (287), (289) and (290). This mixture was separated into its components by h.p.l.c. and gave the additional compounds (228), (289) and (290) in elution order.

Compound (228) was identified as *N*-nitroso-*N*-(pentamethylbenzyl)-acetamide (228) on the basis of a comparison of its spectroscopic data with the known[46] parent compound *N*-(pentamethylbenzyl)-acetamide (290), below. Compound (228) gave a satisfactory parent molecular ion in the mass spectrum, indicating the molecular formula $C_{14}H_{20}N_2O_2$. The mass spectrum also included an M^+-NO fragment. N.O.e. experiments confirmed the assignments of the chemical shifts for the protons. In particular, irradiation at δ 2.73 (1-Me) gave an enhancement at 2.17 (2'-Me and 6'-Me), while irradiation at δ 4.99 (**CH_2**) gave an enhancement at δ 2.17 (2'-Me and 6'-Me), as depicted in Fig. 3.58. HMQC and HMBC experiments confirmed the assignments of the ^{13}C n.m.r. resonances and a comparison of the characteristic ^1H and ^{13}C n.m.r. data and infrared

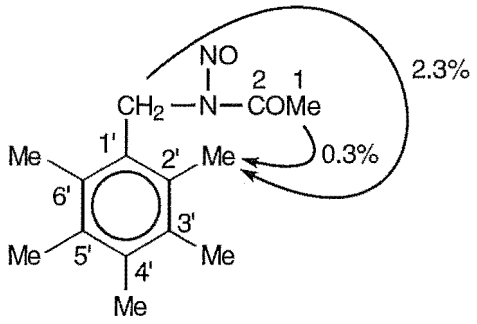

Fig. 3.58 Enhancements (%) from selected n.O.e. experiments for compound (228).

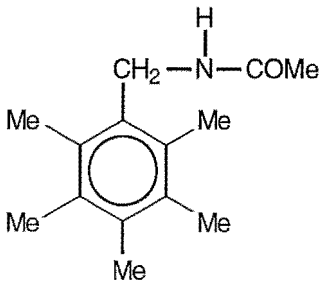

(290)

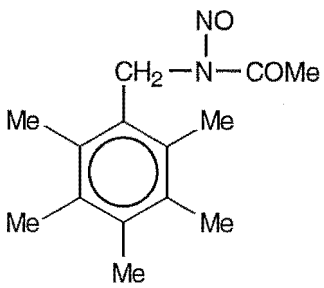

(228)

CH_3-CO	2.00	CH_3-CO	2.73
CH_2	4.46	CH_2	4.99
CH_3-CO	22.4	CH_3-CO	20.3
CH_2	39.6	CH_2	39.7
C=O	170.8	C=O	174.5
ν_{max}	3304, 1643, 1537, 1385	ν_{max}	1719, 1504, 1121

Fig. 3.59 Comparison of the characteristic ^1H and ^{13}C n.m.r. resonances (in ppm) and infrared absorptions (in cm^{-1}) for compounds (290) and (228).

absorptions between compounds (290) and (228) is given in Fig. 3.59. Specifically, ^{13}C n.m.r. resonances for the amide carbonyl carbon appeared at δ 174.5, the **C**H_3-CO function appeared at δ 20.3, and the **C**H_2 function appeared at δ 39.7. Furthermore, the presence of the *N*-nitroso-disubstituted amide functionality followed from its infrared spectrum, which lacked the absorptions at 3304 and 1643 cm^{-1} found for the *N*-mono-substituted amide (290), but exhibited a very strong absorption at 1719 cm^{-1}. Such a shift from 1643 to 1719 cm^{-1} is characteristic for the carbonyl stretching frequency on the introduction of an electron-withdrawing substituent into a *N*-monosubstituted amide.[30]

Compound (289) was identified as pentamethylbenzyl acetate (289) and the structure was confirmed by comparing its spectroscopic data with literature data.[47]

Compound (290) was identified as *N*-(pentamethylbenzyl)-acetamide (290) and the structure was also confirmed by comparing its spectroscopic data with literature data.[46]

The change in composition of the photolysis reaction of hexamethyl-benzene (136) / TNM in acetonitrile was monitored with time and an overview of product yields is shown in Table 3.15. Reactions were only possible at +20° due to the limited solubility of hexamethylbenzene (136) in the more polar acetonitrile. Formation of the related acetamides (228) and (290), and the acetate (289) was one notable difference from the corresponding reaction in dichloromethane (see Table 3.14, Section 3.29). While the yield of *N*-(pentamethylbenzyl)-acetamide (290) remained at *c.* 4% throughout the reaction, the *N*-nitroso acetamide (228) increased in yield (trace after 1 h, 3% after 8h). The yields of the side-chain trinitro-methyl (279) and the side-chain nitrite (280) were both lower in acetonitrile than in dichloromethane (after 5 h, total 9% in acetonitrile, total 24% in dichloromethane). In acetonitrile, the yields of the side-chain nitrite (281)

Table 3.15 Overview of product yields from the photolysis of hexamethylbenzene (136) (0.39 mol L^{-1}) and TNM (0.78 mol L^{-1}) in acetonitrile, at +20°.[a]

	Yield (%)												
t (h)	(279)	(280)	(281)	(282)	(283)	(284)	(285)	(286)	(287)	(228)	(289)	(290)	Unknown aromatics
1	9.1	trace	30.6	52.9	0.4	0.8	0.8	0.5	-	trace	-	3.8	1.1
3	6.5	0.4	28.1	51.4	0.3	1.0	3.4	0.2	-	0.5	trace	4.0	4.2
5	8.6	0.1	28.0	47.0	0.7	1.8	4.0	0.9	-	0.9	0.1	3.3	4.6
8	8.7	1.0	20.9	40.4	0.5	3.0	10.4	0.7	trace	2.7	0.4	4.0	7.4

[a] Some substrate remained undissolved until a reaction time of 7 h.

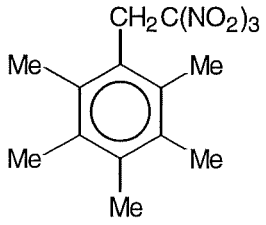

(279)

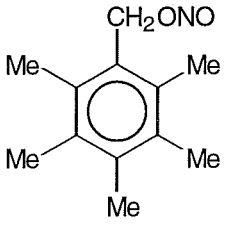

(280)

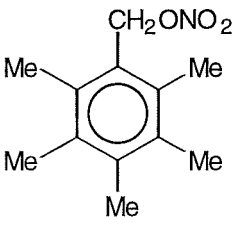

(281)

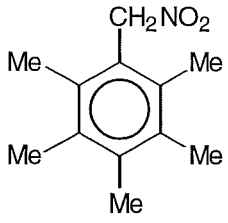

(282)

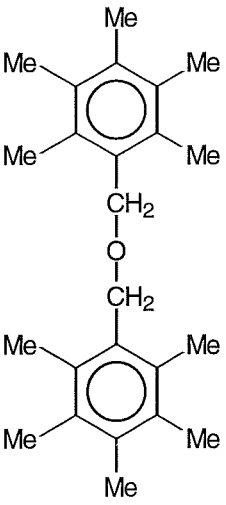

(283)

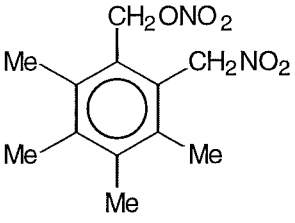

(284)

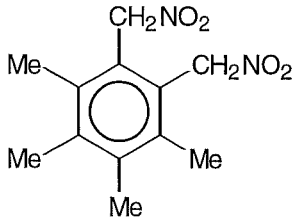

(285)

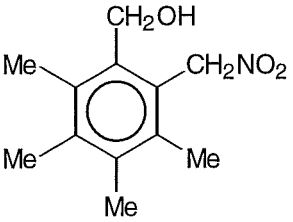

(286)

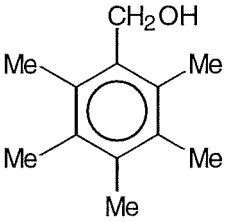

(287)

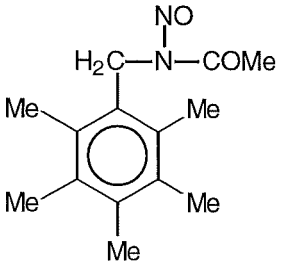

(228)

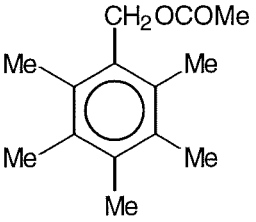

(289)

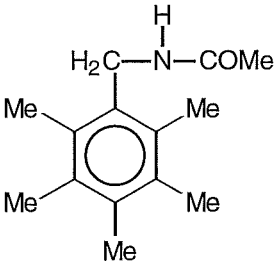

(290)

and the side-chain nitro (282) decreased as the reaction proceeded (total 84% after 1 h, total 61% after 8 h), with a corresponding increase in the yields of the disubstituted side-chain compounds (284) and (285) (total 2%

after 1 h, total 13% after 8 h). In acetonitrile the yield of the side-chain nitro (282) decreased slowly in the first 5 h (53% after 1 h, 47% after 5 h), while in dichloromethane it remained at *c.* 32% throughout the reaction.

3.31 The Photochemistry of Hexamethylbenzene (136) in 1,1,1,3,3,3-Hexafluoropropan-2-ol (HFP)

The photolysis of the charge-transfer complex of hexamethylbenzene (136) (0.39 mol L^{-1}) and TNM (0.78 mol L^{-1}) in HFP at +20°, as above, was a slow process. The product compositions were determined by ^1H n.m.r. spectral analysis and are given in Table 3.16. After 24 h the product consisted of a mixture of predominantly 2,3,4,5,6-pentamethyl-1-(2',2',2'-trinitroethyl)-benzene (279) (67%), and 2,3,4,5,6-pentamethylphenylnitromethane (282) (11%), with minor amounts of compounds (283) (3%) and

Table 3.16 Overview of product yields from the photolysis of hexamethylbenzene (136) (0.39 mol L^{-1}) and TNM (0.78 mol L^{-1}) in 1,1,1,3,3,3-hexafluoropropan-2-ol, at +20°.[a]

	Yield (%)					
t (h)	(279)	(281)	(282)	(283)	(287)	Unidentified aromatics
1	47.6	11.4	21.6	-	8.7	10.7
3	49.9	7.9	20.6	-	8.3	13.3
5	51.8	6.2	19.8	-	7.5	14.7
8	55.9	5.5	19.7	trace	5.9	13.0
24	67.0	-	11.4	2.7	4.8	14.1

[a] Some substrate remained undissolved for the first 1 h of the reaction.

2,3,4,5,6-pentamethylbenzyl alcohol (287) (5%), and unidentified aromatic compounds (total 14%).

3.32 Reactions of Hexamethylbenzene (136) with Nitrogen Dioxide in Dichloromethane

A solution of hexamethylbenzene (136) (0.39 mol L^{-1}) in dichloromethane saturated with $^{\bullet}NO_2$ was stored in the dark at +20°. A similar

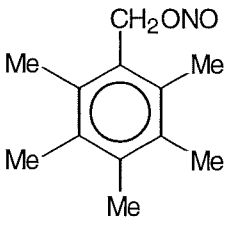

(280)

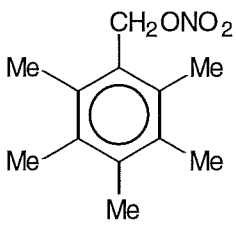

(281)

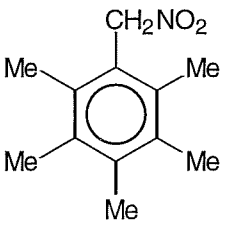

(282)

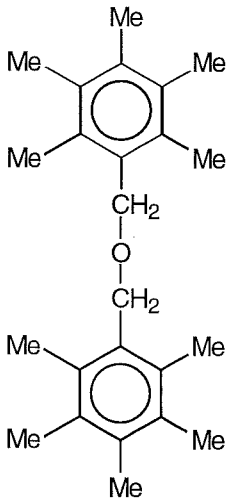

(283)

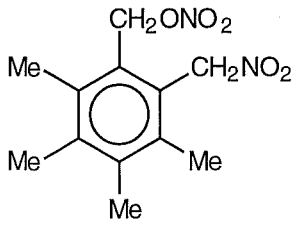

(284)

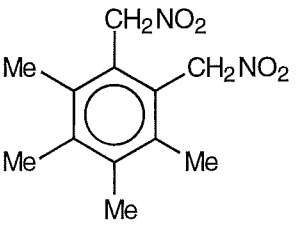

(285)

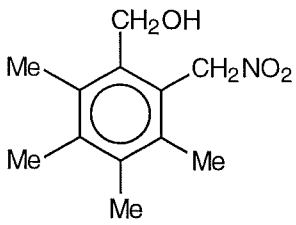

(286)

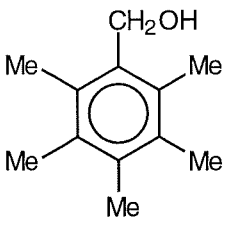

(287)

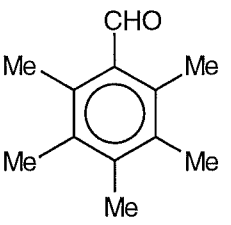

(288)

Table 3.17 Overview of product yields from the reaction of hexamethylbenzene (136) (0.39 mol L^{-1}) in dichloromethane saturated with nitrogen dioxide, at +20°.

	Yield (%)									
t (h)	(280)	(281)	(282)	(283)	(284)	(285)	(286)	(287)	(288)	Unidentified aromatics
In the dark										
1	3.9	53.9	41.0	-	-	0.1	-	0.6	0.3	0.2
3	4.9	53.3	40.2	trace	trace	0.1	-	0.6	0.6	0.3
5	6.2	51.3	40.3	0.1	0.1	0.1	-	0.9	0.6	0.4
8	6.7	50.0	40.4	0.1	0.1	0.1	-	1.6	0.6	0.4
Irradiation with filtered light ($\lambda_{cut\text{-}off}$<435 nm)										
1	2.9	57.8	38.0	trace	trace	0.1	-	0.4	0.6	0.2
3	3.1	58.1	36.2	0.2	0.1	0.2	-	0.8	0.8	0.5
5	3.3	57.9	35.0	0.5	0.2	0.3	-	0.8	1.6	0.4
8	3.4	56.4	35.3	0.4	0.5	1.0	trace	trace	2.0	1.0

solution was irradiated with filtered light ($\lambda_{cut\text{-}off}$<435 nm) also at +20°. At appropriate time intervals, aliquots were removed and after work-up, under reduced pressure at ≤0°, the product compositions were determined by ^1H n.m.r. spectral analysis (See Table 3.17). After reaction for 8 h, the two product compositions were similar, *viz.* 2,3,4,5,6-pentamethylbenzyl nitrate (281) (*c.* 53%), 2,3,4,5,6-pentamethylphenylnitromethane (282) (*c.* 38%) and a small amount of 2,3,4,5,6-pentamethylbenzyl nitrite (280) (*c.* 6%). These results were comparable with those reported by Bosch and Kochi,[31] except they observed a higher yield of the side-chain nitro (282) than the side-chain nitrite (281).

3.33 Reactions of Hexamethylbenzene (136) with Nitrogen Dioxide in Acetonitrile

A solution of hexamethylbenzene (136) (0.39 mol L^{-1}) in acetonitrile saturated with $^{\bullet}NO_2$ was stored in the dark at +20°. A similar solution was irradiated with filtered light ($\lambda_{cut\text{-}off}$<435 nm) also at +20°. Reaction was

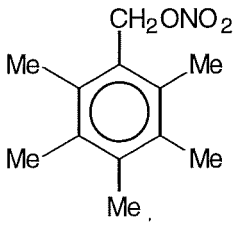

(281)

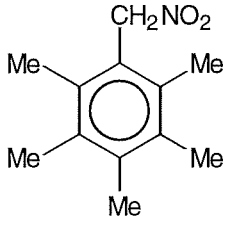

(282)

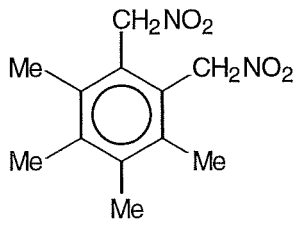

(285)

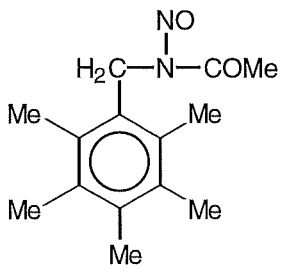

(228)

complete in 1 h, and after work-up the product composition was determined by ^{1}H n.m.r. spectral analysis. The products formed for the two reactions were shown to be similar, *viz.* 2,3,4,5,6-pentamethylbenzyl nitrate (281) (*c.* 16%), 2,3,4,5,6-pentamethylphenylnitromethane (282) (63%), 1,2-bis-(nitromethyl)-3,4,5,6-tetramethylbenzene (285) (*c.* 10%), and *N*-nitroso acetamide (228) (*c.* 3%).

3.34 Overview of the Photonitration of Hexamethylbenzene (136)

The study of the photolysis of the charge-transfer complex of hexamethylbenzene (136) and TNM was hampered considerably by the low solubility of hexamethylbenzene (136), particularly below ambient temperature. Consequently, no serious attempt could be made at detecting labile adducts in the reaction mixtures. The reactions which were possible in dichloromethane or acetonitrile produced substantial amounts of pentamethylbenzyl nitrate (281) and pentamethylphenylnitromethane (282), with lesser amounts of pentamethyl-(2',2',2'-trinitroethyl)-benzene (279) (See Tables 3.14 and 3.15, Sections 3.29 and 3.30, respectively). In HFP, however, the major product of a slow reaction was pentamethyl-(2',2',2'-trinitroethyl)-benzene (279) (67% after 24 h) (See Table 3.16, Section 3.31).

As was discussed for the photochemical reactions of the charge-transfer complex of pentamethylbenzene (135) with TNM (see Section 3.27), the reactions of hexamethylbenzene (136) may also have proceeded *via* labile nitro/trinitromethyl adducts. Attack of $(O_2N)_3C^-$ on the hexamethylbenzene radical cation would lead to the formation of the sterically compressed carbon radical (150), as seen in Scheme 3.46. Subsequent

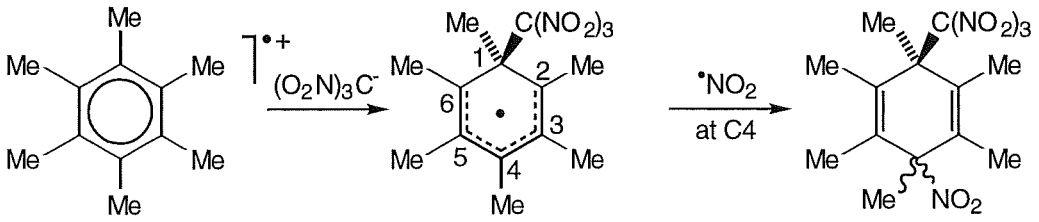

(150) (291) and (292)

Scheme 3.46

coupling of $^{\bullet}NO_2$ at C4 on radical (150) with C-N bond formation would lead to the formation of adducts (291) and (292).

A progressive increase in lability of the nitro/trinitromethyl adducts with increasing methyl substitution was evident in the tetramethyl adducts (216) and (217) (see Sections 3.15 and 3.16), and the pentamethyl adducts (244) and (245) (see Section 3.26). If this extends to adducts from hexamethylbenzene (136), then the adducts formed would be extremely unstable and could afford possible pathways to the observed products (279)-(282) and (284)-(288), as illustrated in Schemes 3.47-3.50.

Rapid epimerization *via* the nitrocyclohexadienyl cation/trinitromethanide ion pair (293) would be expected to occur. Subsequent loss of nitroform from the ion pair (293) appeared to be favoured, however, leading to the side-chain compounds (280)-(282), (287) and (288) being formed, as summarized in Schemes 3.47 and 3.48. Initially, loss of nitroform from the intermediate nitrocyclohexadienyl cation/trinitromethanide ion pair (293) would occur by abstraction of an acidic proton from the methyl group by $(O_2N)_3C^-$, forming diene (294). This would be followed by homolytic cleavage of the C-NO_2 bond in diene (294) to give radical (295), as represented in Scheme 3.47. Subsequent coupling of $^{\bullet}NO_2$ with the resulting pentamethylbenzyl radical (295) with C-N bond formation would lead to the formation of the side-chain nitro compound (282), as seen in

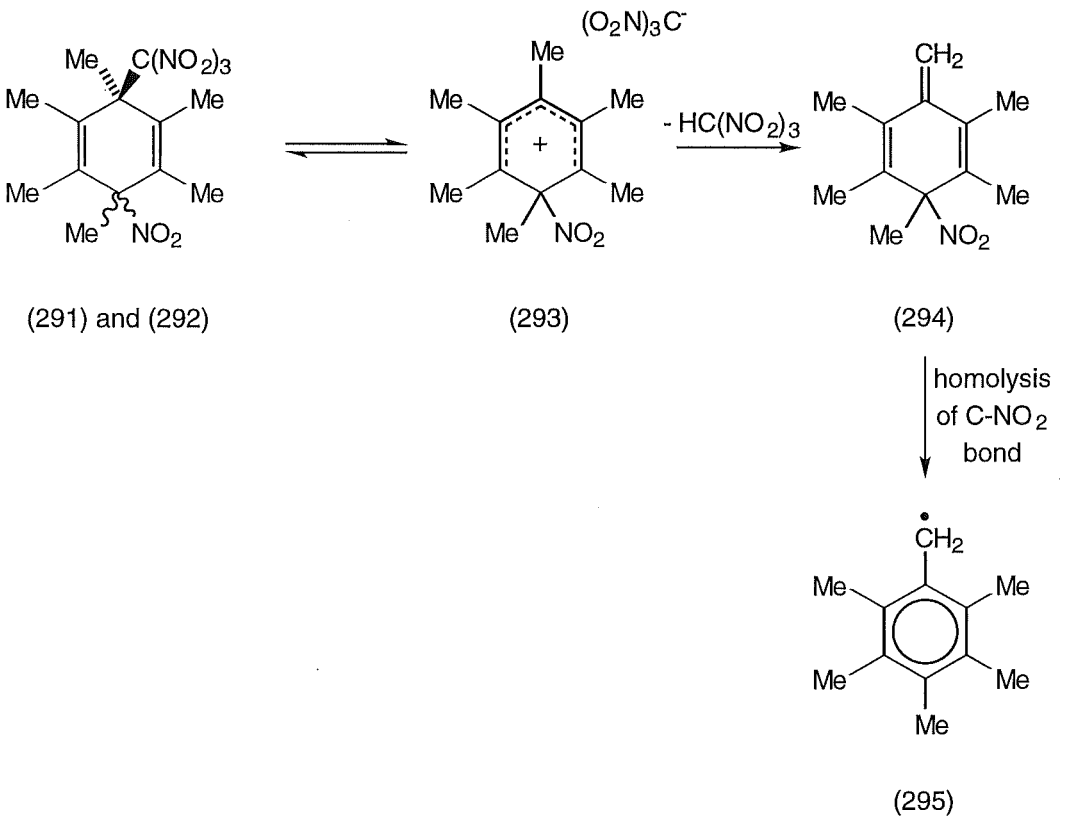

Scheme 3.47

Scheme 3.48. Alternately, coupling of $^{\bullet}NO_2$ could occur with C-O bond formation to give the side-chain nitrite (280). The side-chain nitrite (280) can then undergo either hydrolysis to yield the side-chain alcohol (287), as was observed by Masnovi *et al.*[9], or oxidation to yield the side-chain nitrate (281). Formation of the benzaldehyde (288) could arise by oxidation of either the nitrite (280) or the alcohol (287).

The side-chain trinitromethyl aromatic (279) could form *via* loss of nitrous acid from the nitro/trinitromethyl adducts (291) and (292) to form the trinitromethyl diene (296), as depicted in Scheme 3.49. Subsequent rearrangement *via* the ion pair (297) would give the side-chain trinitro-methyl compound (279).

Unfortunately, this hypothesis cannot be tested directly because of poor solubility of hexamethylbenzene (136). It may be significant, however,

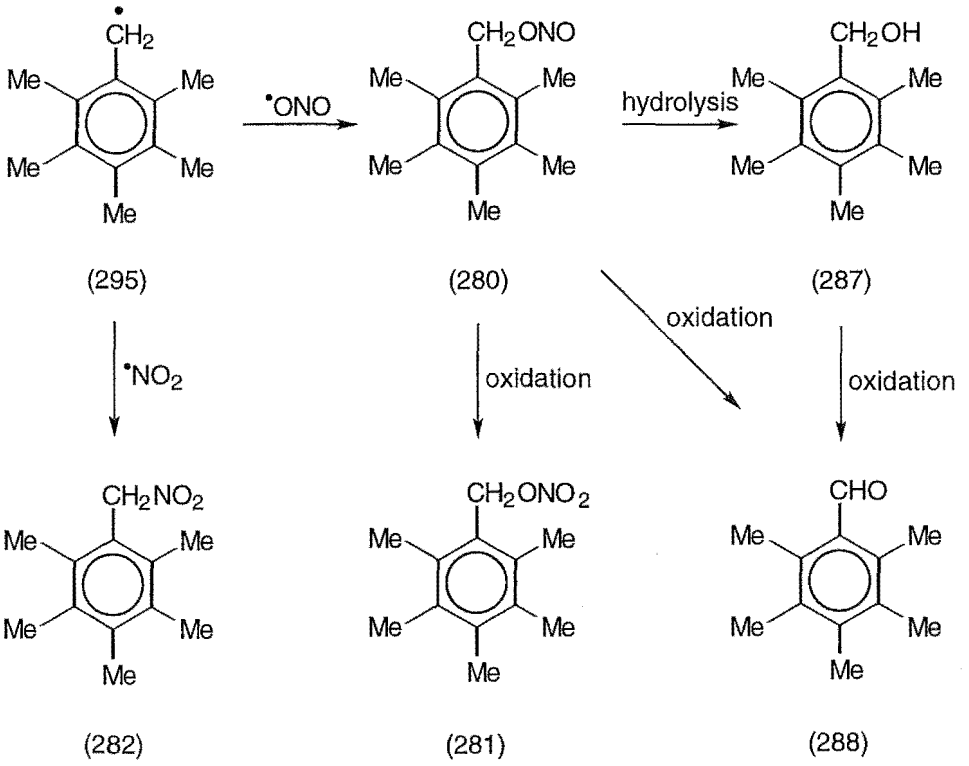

Scheme 3.48

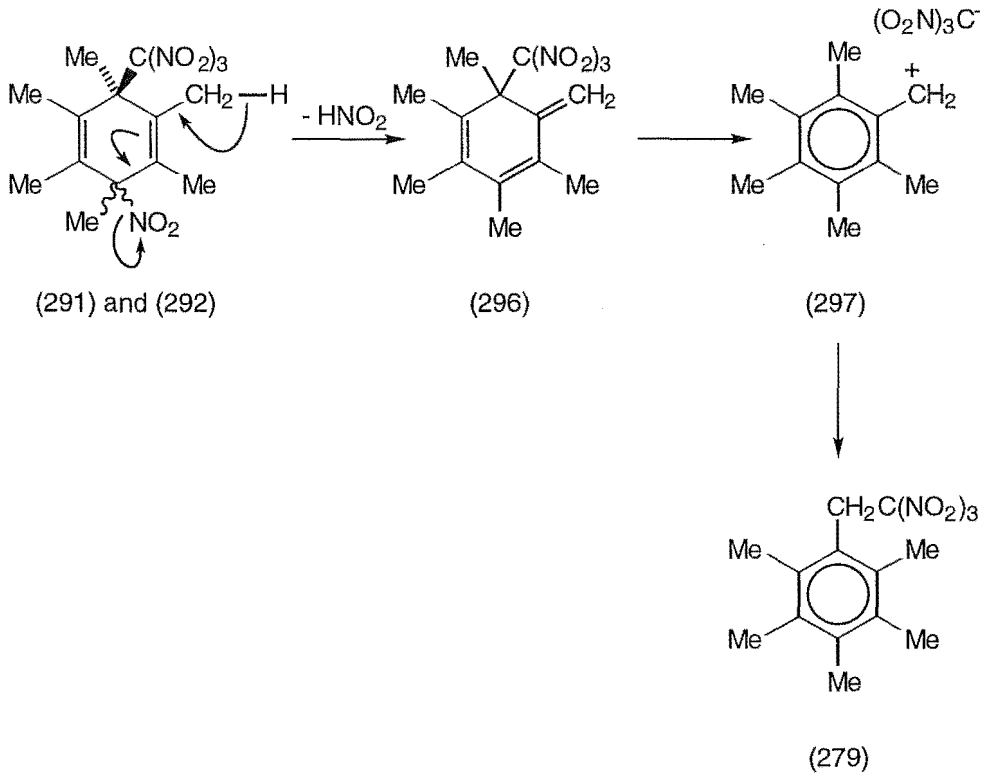

Scheme 3.49

that the trinitromethyl compound (279) was formed in high yield in the photolysis reaction in HFP in contrast to the reactions in dichloromethane or acetonitrile (See Table 3.16, Section 3.31).

During the photochemical reaction of hexamethylbenzene (136) and TNM in acetonitrile, the yield of pentamethylphenylnitromethane (282) decreased as the reaction proceeded (53% after 1 h, 40% after 8 h) (See Table 3.15, Section 3.30). In dichloromethane at +20°, compound (282) remained at *c.* 32% (See Table 3.14, Section 3.29). At -20° in dichloromethane, the yield of compound (282) was almost identical to the +20° reaction in acetonitrile and decreased as the reaction proceeded (52% after 1 h, 40% after 8 h). Correspondingly, the yields of the disubstituted products (284)-(286) increased throughout each of the reactions (In acetonitrile, 2% after 1 h, 14% after 8 h; in dichloromethane both temperatures were similar, trace after 1 h, *c.* 3% after 8 h). It therefore

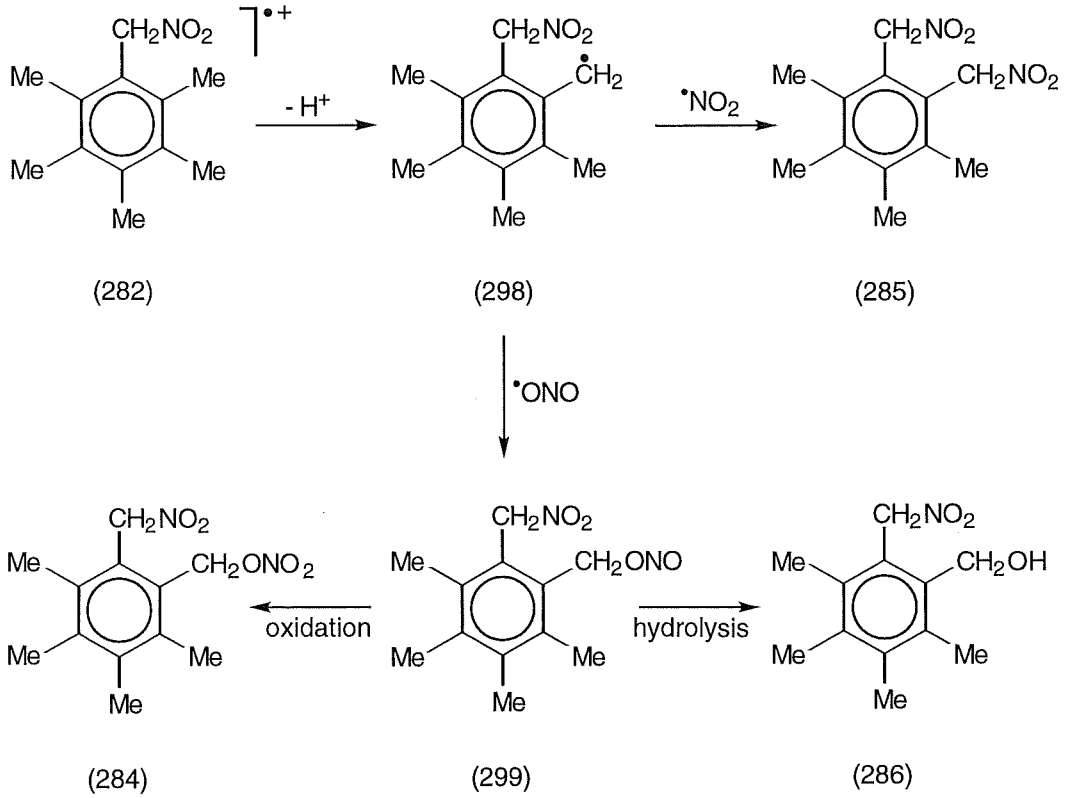

(282) (298) (285)

(284) (299) (286)

Scheme 3.50

appears likely that the pentamethylphenylnitromethane (282) gives rise to the disubstituted products (284)-(286). A possible mechanism for their formation is outlined in Scheme 3.50. Deprotonation of the pentamethylphenylnitromethane radical cation could yield radical (298). Coupling of radical (298) with $^{\bullet}NO_2$ could occur by either C-N bond formation to give the bis-nitromethyl compound (285), or by C-O bond formation to yield the nitromethylbenzyl nitrite (299). Subsequent oxidation of compound (299) would give the nitromethylbenzyl nitrate (284), while hydrolysis of (299) would result in formation of the nitromethylbenzyl alcohol (286).

The reactions in the dark and on irradiation with filtered light ($\lambda_{cut\text{-}off}$<435 nm) of hexamethylbenzene (136) with excess $^{\bullet}NO_2$ in dichloromethane at +20° both gave essentially the same product composition. The significant products were pentamethylbenzyl nitrate (281) (*c.* 54%) and pentamethylphenylnitromethane (282) (*c.* 38%) (See Table 3.17, Section 3.32). Both the "light" and "dark" conditions in the presence of hexamethylbenzene (136) with $^{\bullet}NO_2$ in dichloromethane appear to have resulted in thermal nitration. The products were generally in agreement with those formed in the thermal nitration of hexamethylbenzene (136) with $^{\bullet}NO_2$ in dichloromethane in the dark reported by Bosch and Kochi.[31]

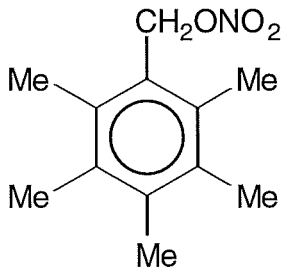

(281)

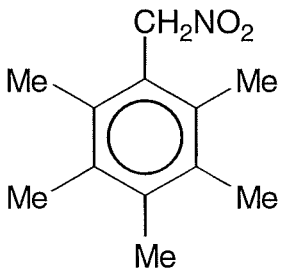

(282)

As in dichloromethane, the reactions of hexamethylbenzene (136) with excess $^{\bullet}NO_2$ in acetonitrile at +20° gave essentially the same product

composition both in the dark and on irradiation with filtered light ($\lambda_{cut\text{-}off}$<435 nm). In addition to pentamethylbenzyl nitrate (281) (*c.* 16%) and the mono- and bis-nitromethyl compounds (282) (*c.* 63%) and (285) (*c.* 10%), the *N*-nitroso acetamide (228) (*c.* 3%) formed (See Section 3.33). While it remains unclear how compound (228) formed, it is clear that neither TNM nor irradiation is necessary for the formation of the *N*-nitroso acetamide (228).

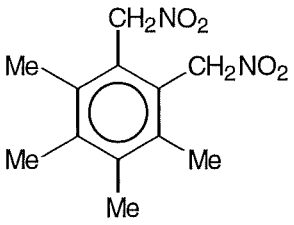

(285)

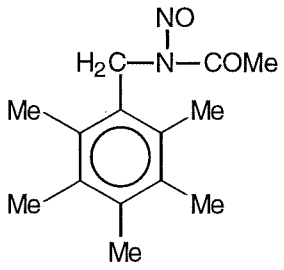

(228)

In conclusion, the photochemical reaction of the charge-transfer complex of hexamethylbenzene (136) and TNM gave no direct evidence for adduct formation. However, following trends in lability of the nitro/trinitro-methyl adducts formed from 1,2,4,5-tetramethylbenzene (134) and penta-methylbenzene (135) (see Sections 3.15 and 3.16, and 3.26, respectively), it appears likely that most of the observed products in hexamethylbenzene (136) arose *via* the highly sterically hindered delocalized carbon radical (150).

3.35 References for Chapter Three

1 Eberson, L., Hartshorn, M. P., and Radner, F., *J. Chem. Soc., Perkin Trans. 2*, 1992, 1793.

2 Eberson, L., Hartshorn, M. P., and Radner, F., *J. Chem. Soc., Perkin Trans. 2*, 1992, 1799.

3 Eberson, L., Calvert, J. L., Hartshorn, M. P., and Robinson, W. T., *Acta Chem. Scand.*, 1993, **47**, 1025.

4 Butts, C. P., Calvert, J. L., Eberson, L., Hartshorn, M. P., Maclagan, R. G. A. R., and Robinson, W. T., *Aust. J. Chem.*, 1994, **47**, 1087.

5 Calvert, J. L., Eberson, L., Hartshorn, M. P., Maclagan, R. G. A. R., and Robinson, W. T., *Aust. J. Chem.*, 1994, **47**, 1211.

6 Butts, C. P., Calvert, J. L., Eberson, L., Hartshorn, M. P., Radner, F., and Robinson, W. T., *J. Chem. Soc., Perkin Trans. 2*, 1994, 1485.

7 Calvert, J. L., Eberson, L., Hartshorn, M. P., Maclagan, R. G. A. R., and Robinson, W. T., *Aust. J. Chem.*, 1994, **47**, 1591.

8 Butts, C. P., Eberson, L., Hartshorn, M. P., and Robinson, W. T., *Aust. J. Chem.*, 1995, **48**, 1989.

9 Masnovi, J. M., Sankararaman, S., and Kochi, J. K., *J. Am. Chem. Soc.*, 1989, **111**, 2263.

10 Eberson, L., and Hartshorn, M. P., *J. Chem. Soc., Chem. Commun.*, 1992, 1563.

11 Eberson, L., Calvert, J. L., Hartshorn, M. P., and Robinson, W. T., *Acta Chem. Scand.*, 1994, **48**, 347.

12 Butts, C. P., Eberson, L., Foulds, G. J., Fulton, K. L., Hartshorn, M. P., and Robinson, W. T., *Acta Chem. Scand.*, 1995, **49**, 76.

13 Butts, C. P., Eberson, L., Fulton, K. L., Hartshorn, M. P., Jamieson, G. B., and Robinson, W. T., *Acta Chem. Scand., in press.*

14 Butts, C. P., Eberson, L., Fulton, K. L., Hartshorn, M. P., Robinson, W. T., and Timmerman-Vaughan, D. J., *Acta Chem. Scand., in press.*

15 Young, D. A. W., *B. Sc. (Hons. III) project*, University of Canterbury, 1994.

16 Banwell, T., Morse, C. S., Myhre, P. C., and Vollmar, A., *J. Am. Chem. Soc.*, 1977, **99**, 3042.

17 Myhre, P. C., *Personal communication.*

18 Barnes, C. E., Fieldman, K. S., Johnson, M. W., Lee, H. W. H., and Myhre, P. C., *J. Org. Chem.*, 1979, **44**, 3925.

19 Hartshorn, M. P., Judd, M. C., Vannoort, R. W., and Wright, G. J., *Aust. J. Chem.*, 1989, **42**, 689; Blackstock, D. J., Hartshorn, M. P., Lewis, A. J., Richards, K. E., Vaughan, J., and Wright, G. J., *J. Chem. Soc. B*, 1971, 1212.

20 Baciocchi, E., Cort, A. D., Eberson, L., Mandolini, L., and Rol, C., *J. Org. Chem.*, 1986, **51**, 4544.

21 Fischer, A., and Leonard, D. R. A., *Can. J. Chem.*, 1976, **54**, 1795.

22 Eberson, L., *Personal communication.*

23 Butts, C. P., Eberson, L., Hartshorn, M. P., and Robinson, W. T., *Acta Chem. Scand.*, 1995, **49**, 389.

24 Hartshorn, M. P., Readman, J. M., Robinson, W. T., Vaughan, J., and Whyte, A. R., *Aust. J. Chem.*, 1985, **38**, 1693, and references cited therein.

25 Brunton, G., Cruse, H. W., Riches, K. M., and Whittle, A., *Tetrahedron Lett.*, 1979, **12**, 1093.

26 Barnes, C. E., and Myhre, P. C., *J. Am. Chem. Soc.*, 1978, **100**, 973.

27 Coombes, R. G., Diggle, A. W., and Kempsell, S. P., *Tetrahedron Lett.*, 1986, **27**, 2037.

28 Eberson, L., and Radner, F., *J. Am. Chem. Soc.*, 1991, **113**, 5825.

29 Nyberg, K., and Wistrand, L. G., *Chem. Scripta*, 1974, **5**, 234.

30 Bellamy, L. J., *Spectrochim. Acta*, 1959, **13**, 60.

31 Bosch, E., and Kochi, J. K., *J. Org. Chem.*, 1994, **59**, 3314.

32 Eberson, L., Hartshorn, M. P., Persson, O., and Svensson, J. O., *J. Chem. Soc. Perkin Trans. 2*, 1995, 1253.

33 Eberson, L., Hartshorn, M. P., Radner, F., and Svensson, J. O., *J. Chem. Soc. Perkin Trans. 2*, 1994, 1719.

34 Eberson, L., Persson, O., Radner, F., and Hartshorn, M. P., *Res. Chem. Intermediat., in press.*

35 Eberson, L., Hartshorn, M.P., and Persson, O., *Angew. Chem. Int. Ed. Engl.*, 1995, **34**, 2268.

36 Eberson, L., Hartshorn, M.P., and Persson, O., *J. Chem. Soc., Chem. Commun.*, 1995, 1131.

37 Eberson, L., Hartshorn, M.P., and Persson, O., *J. Chem. Soc., Perkin Trans. 2* , 1995, 1735.

38 Eberson, L., Hartshorn, M.P., and Persson, O., *Acta Chem. Scand.*, 1995, **49**, 640.

39 Eberson, L., Hartshorn, M.P., and Persson, O., *J. Chem. Soc., Perkin Trans. 2, in press.*

40 Eberson, L., Hartshorn, M.P., and Persson, O., *J. Chem. Soc., Perkin Trans. 2, in press.*

41 Nyberg, K., *Chem. Scripta*, 1974, **5**, 115.

42 Kim, F. K., and Kochi, J. K., *J. Org. Chem.*, 1989, **54**, 1692.

43 Suzuki, H., and Nakamura, K., *Bull. Chem. Soc. Jpn.*, 1970, **43**, 473.

44 Suzuki, H., *Bull. Chem. Soc. Jpn.*, 1970, **43**, 879.

45 Mori, K., Yukitake, K., and Matsui, S., *Japan. Kokai*, 1975, 35123; *Chem. Abs.*, 1975, **83**, 96715z.

46 Suzuki, H., and Hanafusa, T., *Bull. Chem. Soc. Jpn.*, 1973, **46**, 3607.

47 Baciocchi, E., Rol, C., and Mandolini, L., *J. Org. Chem.*, 1977, **42**, 3682.

CHAPTER FOUR

PHOTONITRATION OF 2,3-DIMETHYLANISOLE

4.1 Introduction

Photochemical reactions with TNM and involving naphthalene,[1,2] a series of methylsubstituted naphthalenes,[3-7] benzene[8,9] and a series of methylsubstituted benzenes[10-12] showed that the initial point of attack of $(O_2N)_3C^-$ on the aromatic radical cation is crucial in determining the structures of the adducts formed.[7] While studying the regiochemistry of the photolysis reactions between aromatic compounds and TNM, the importance of the relative energies of the various delocalized carbon radicals was demonstrated.[7] These relative energies can be moderated by steric effects between the attaching $(O_2N)_3C^-$ and methyl substituents on β or *peri* ring positions.[13] The extent of stabilization of the discrete carbon radical by any substituents present will also effect the relative energies of the radicals.[7]

In the above photochemical reactions, there were high yields of adducts.[1-12] In contrast, the photolysis of charge-transfer complexes of substituted anisoles and TNM in dichloromethane gave high yields (60-95%) of products of apparent aromatic substitution, the trinitromethyl-anisoles, while in acetonitrile they gave predominantly nitro substitution products.[14,15] Although adducts were detected, only a small proportion of the nitro or trinitromethyl substitution products could be accounted for by addition-elimination mechanisms.[15]

Butts *et al.*[13] studied the photochemical reaction between 1-methoxy-naphthalene and TNM. The products identified in this study formed exclusively by reaction in the substituted ring. The possible delocalized

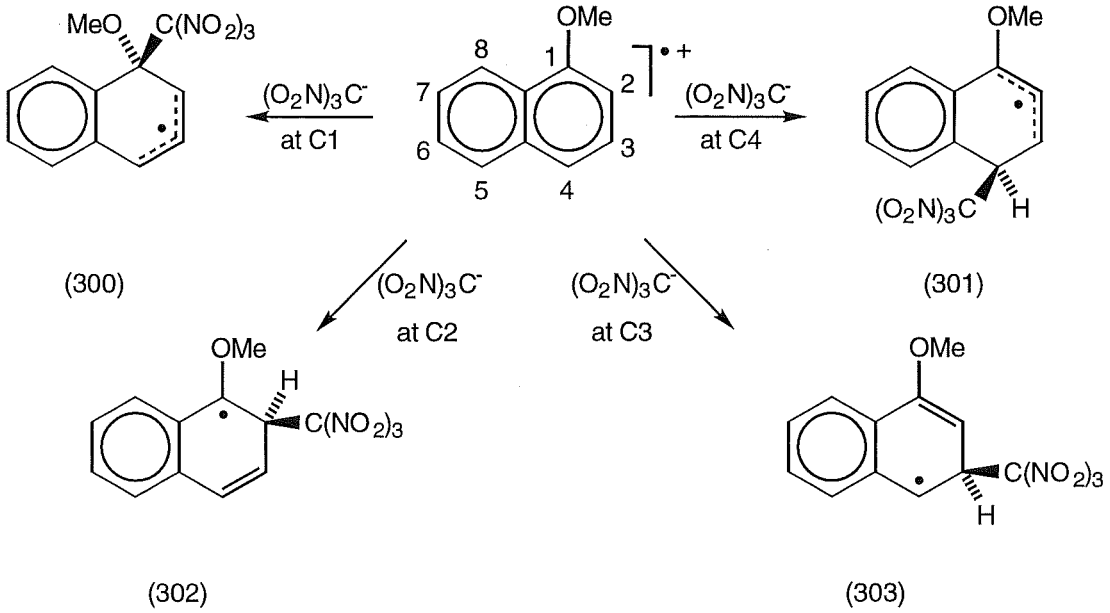

Scheme 4.1

carbon radicals in the substituted ring are illustrated in Scheme 4.1. Attack of $(O_2N)_3C^-$ on the 1-methoxynaphthalene radical cation *ipso* to the methoxy group at C1 would give the phenylallylic radical (300), while attack at C4 would lead to the phenylallylic radical (301). Radical (301) would have enhanced stability over radical (300) due to stabilization by the methoxy group at C1. The less stable benzylic radicals (302) and (303) would be formed *via* attack of $(O_2N)_3C^-$ at C2 and C3, respectively, on the 1-methoxynaphthalene radical cation. Of radicals (302) and (303), the tertiary benzylic radical (302) would have enhanced stability due to the methoxy group at C1. The major adduct (35) contained the trinitromethyl

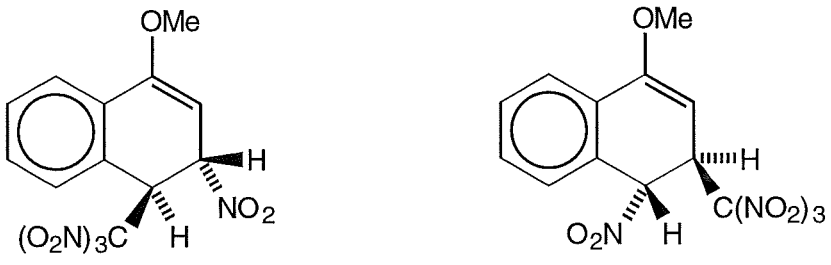

group at C4, the expected favoured position, while the minor adduct (36) contained the trinitromethyl group at C3, the predicted least favoured position. Adduct (36) formation was rationalized as arising *via* attack of $(O_2N)_3C^-$ at C1 on the 1-methoxynaphthalene radical cation, with a subsequent 1,3-allylic rearrangement of the resulting adduct (304), as seen in Scheme 4.2, not *via* an initial attack of $(O_2N)_3C^-$ at C3. Similar allylic

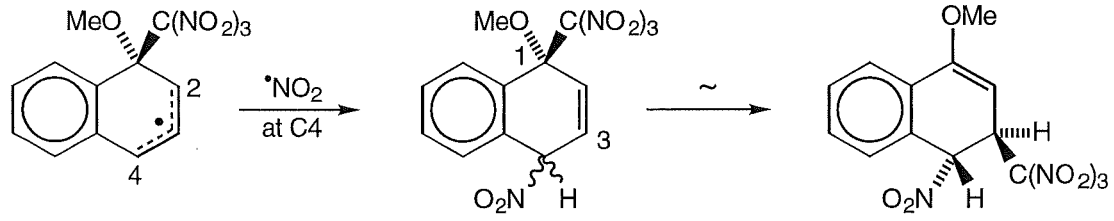

(300) (304) (36)

Scheme 4.2

migration of $(O_2N)_3C^-$ was observed in the rearrangement of 4,8-dimethyl-*r*-1-nitro-*t*-4-trinitromethyl-1,4-dihydronaphthalene (31) into 4,8-dimethyl-*r*-1-nitro-*t*-2-trinitromethyl-1,4-dihydronaphthalene (32),[7] as represented in Scheme 1.32 (See Chapter 1, Section 1.12.2).

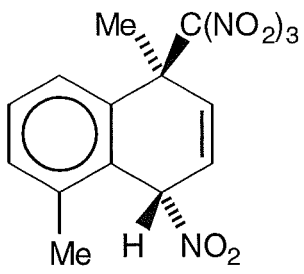

(31)

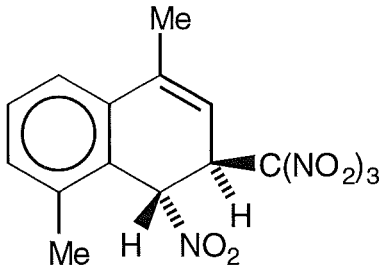

(32)

Sankararaman *et al.*[15] reported the photochemical reactions of 4-methylanisole with TNM in dichloromethane and acetonitrile in the presence and absence of added salts. Reactions in dichloromethane

without added salts gave high yields of 4-methyl-2-trinitromethylanisole (21). However, the addition of salts (either 'common ion' or 'non-common ion') to reactions in dichloromethane gave substantial yields of 4-methyl-2-

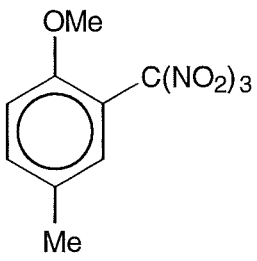

(21)

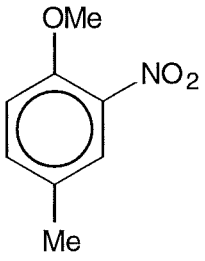

(22)

nitroanisole (22). In acetonitrile, with or without added salts, the major product was 4-methyl-2-nitroanisole (22) (See Chapter 1, Section 1.12.3).

Butts *et al.*[16] studied the reactions of 4-methylanisole and TNM further and identified four unstable isomeric adducts, (23)-(26). The

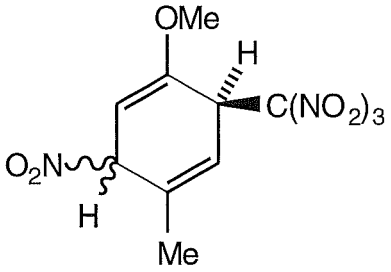

(23) and (24)

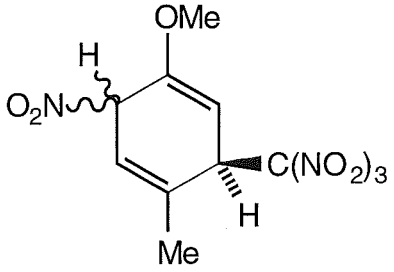

(25) and (26)

possible delocalized carbon radicals are shown in Scheme 4.3. Attack of $(O_2N)_3C^-$ at C1 on the 4-methylanisole radical cation would give the delocalized carbon radical (29), the stability of which would be enhanced by the position of the methyl group at C4. The delocalized radical (27), arising *via* attack of $(O_2N)_3C^-$ at C2 on the 4-methylanisole radical cation, would have enhanced stability due to the position of the methoxy group at C1. Attack of $(O_2N)_3C^-$ on the 4-methylanisole radical cation at C4, forming radical (306), would also be enhanced due to the position of the methoxy

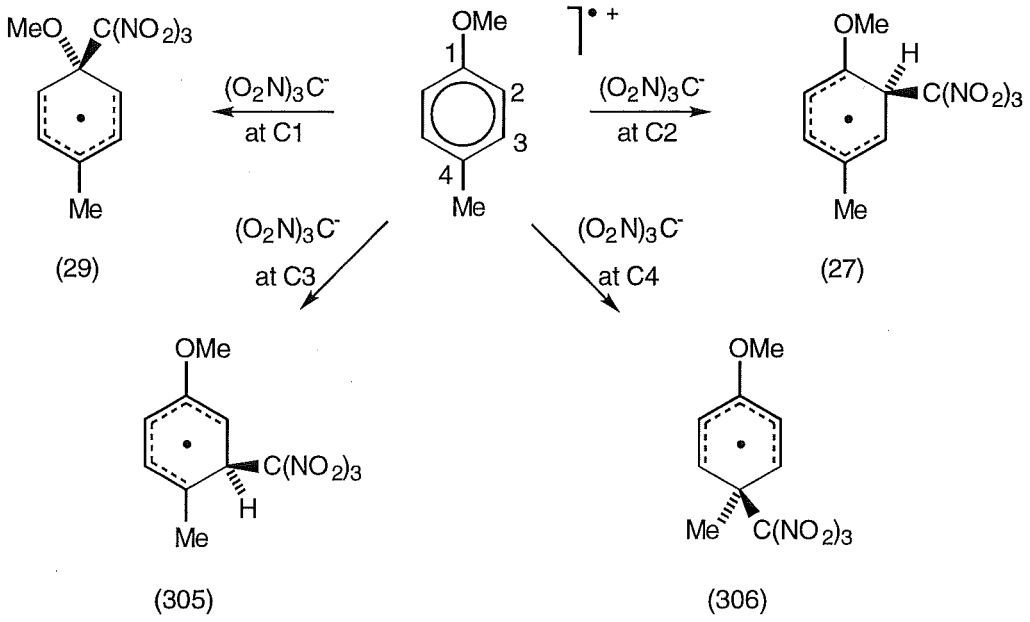

Scheme 4.3

group at C1, but might be hindered due to steric compression arising from interaction between the 4-methyl group and the bulky trinitromethyl group. Delocalized radical (305) would be expected to be the least favoured radical due to the known reluctance of $(O_2N)_3C^-$ to attack a radical cation *vicinal* to a methyl group.[6] The epimeric adducts (23) and (24) were proposed to arise from $^{\bullet}NO_2$ coupling with the delocalized carbon radical (27) at C5, as represented in Scheme 4.4. Alternatively, $^{\bullet}NO_2$ could attack *ipso* to the methoxy group at C1, to give the diene (28). Loss of nitrous acid from either the sterically compressed diene (28) or adducts (23) and (24) would give rise to the 4-methyl-2-trinitromethylanisole (21). In contrast, the epimeric adducts (25) and (26) were seen as arising *via* radical (29), not *via* the least favoured delocalized carbon radical (305), as illustrated in Scheme 4.5. A subsequent 1,3-allylic rearrangement of diene (30), with migration of the trinitromethyl group to C5 would form adducts (25) and (26). Alternately, loss of nitroform from diene (30) would yield 4-methyl-2-nitro-anisole (22). These allylic rearrangements were similar to those seen in

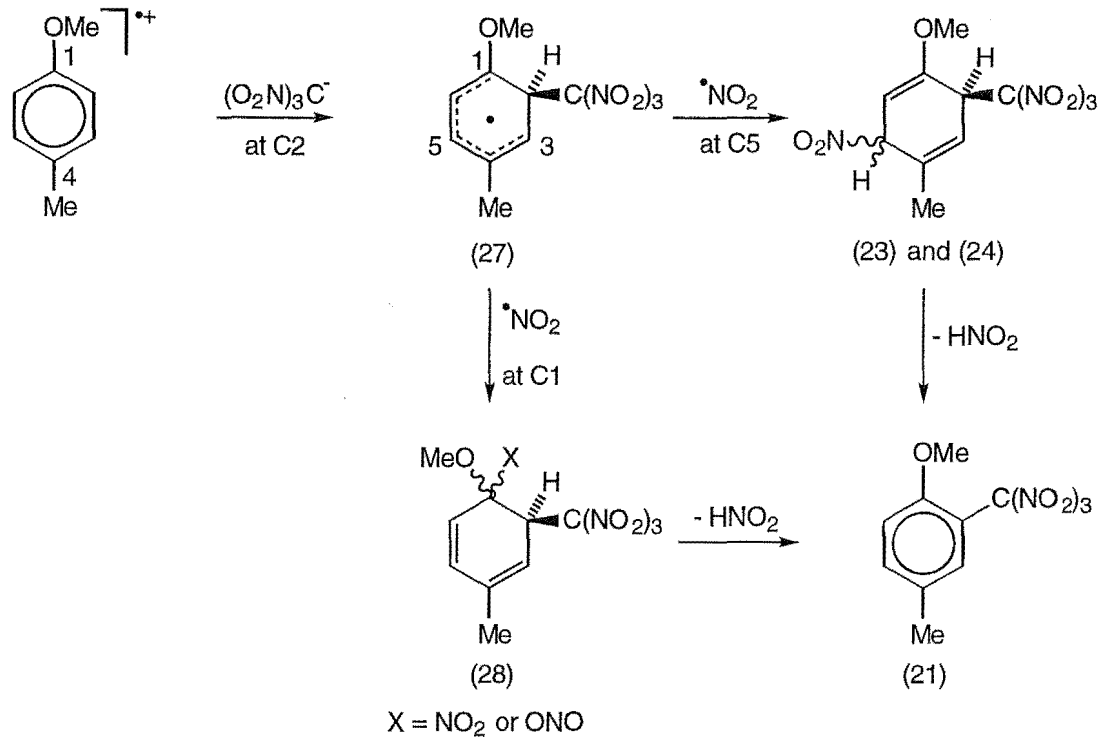

Scheme 4.4

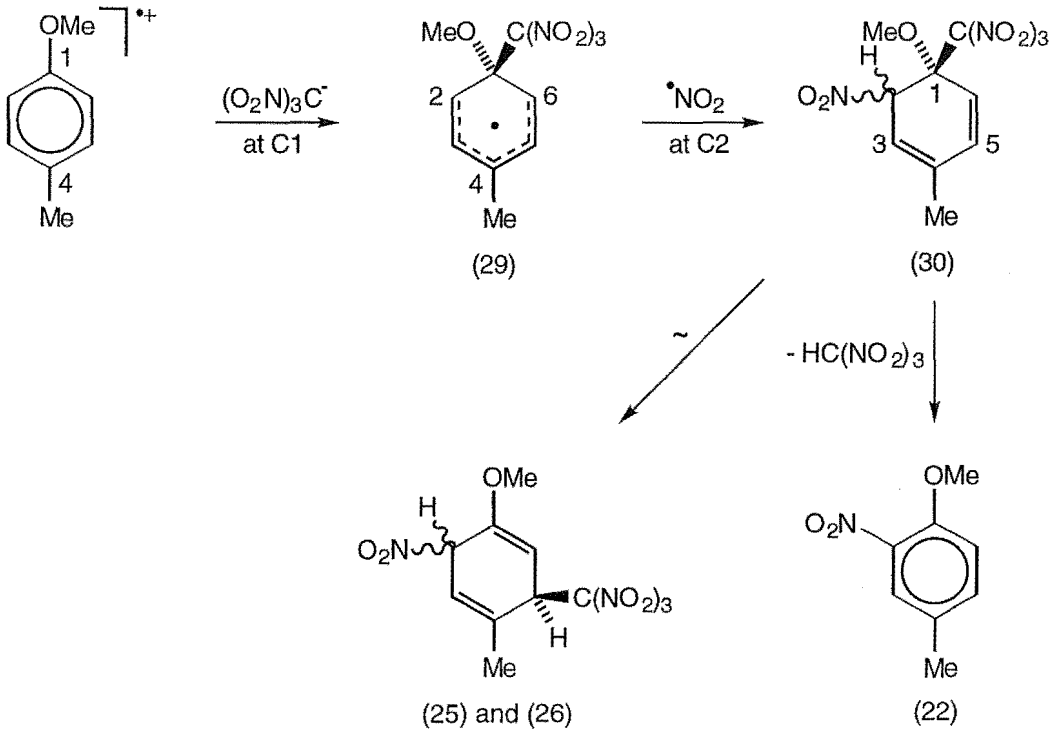

Scheme 4.5

the 1,5-dimethylnaphthalene series[7] and the 1-methoxynaphthalene series,[13] and discussed earlier in this Section and in Chapter 1 (See Section 1.12.1).

The proposed reaction pathways responsible for formation of the labile adducts (23)-(26)[16] also accounted for the observed selective formation of the trinitromethyl and nitro aromatic compounds (21) and (22), respectively, which Sankararaman *et al.*[15] observed earlier. In non-polar dichloromethane, the reaction pathways represented in Scheme 4.4 dominated. In either acetonitrile (with or without added salts) or in dichloromethane with added salts, the solvent polarity was higher than in dichloromethane alone and therefore the reaction pathways in Scheme 4.5 were dominant. It was suggested[16] that the dominance of the pathways in Scheme 4.5 was due to lowering the reactivity of $(O_2N)_3C^-$ towards the radical cation by solvation in the more polar medium.

The study discussed in this Chapter sought to provide further evidence for adduct formation between TNM and methyl-substituted anisoles and to elucidate the mechanism of formation of any observed adducts. In light of the research discussed above, reactions involving 2,3-dimethylanisole (307) were studied in detail in anticipation that similar allylic rearrangements might occur after attack *ipso* to the methoxy group.

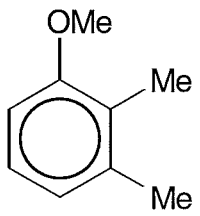

(307)

In the photolysis of 2,3-dimethylanisole (307) with TNM, four of the six possible delocalized carbon radicals would be destabilized by the presence of an unfavourable β-methyl/trinitromethyl interaction, as

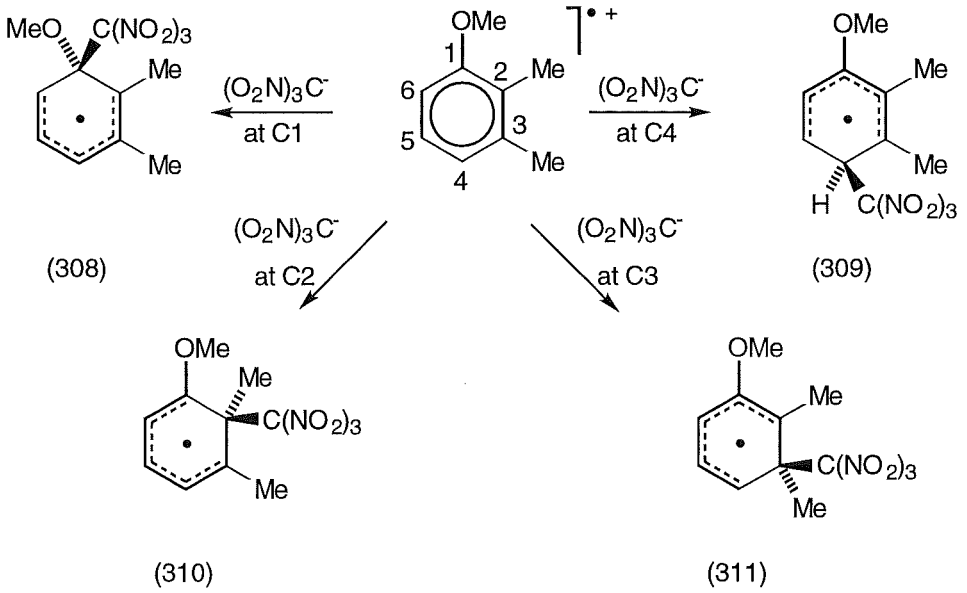

Scheme 4.6

summarized in Scheme 4.6. Radicals (308) and (309), formed *via* attack of $(O_2N)_3C^-$ at C1 and C4, respectively, on the 2,3-dimethylanisole radical cation, both contain stabilization from suitably positioned groups [the 2-methyl group for radical (308), the 1-methoxy and 3-methyl groups for radical (309)]. Radicals (310) and (311), formed after $(O_2N)_3C^-$ attack on the 2,3-dimethylanisole radical cation at C2 and C3, respectively, would be further destabilized relative to radicals (308) and (309), because of steric compression arising from the *ipso* attack of $(O_2N)_3C^-$ at the 2- and 3-methyl positions, respectively. Radical (310) would gain some enhanced stability due to the 1-methoxy and 3-methyl groups, while radical (311) would be less stable with enhanced stability only provided by the 2-methyl group. The remaining possible delocalized carbon radicals (312) and (313) would be formed by attack of $(O_2N)_3C^-$ at C5 and C6, respectively, on the radical cation of 2,3-dimethylanisole (See Scheme 4.7). Radical (312) would gain enhanced stability due to the 2-methyl group, while radical (313) would have its stability enhanced by the 1-methoxy and 3-methyl groups. Hence,

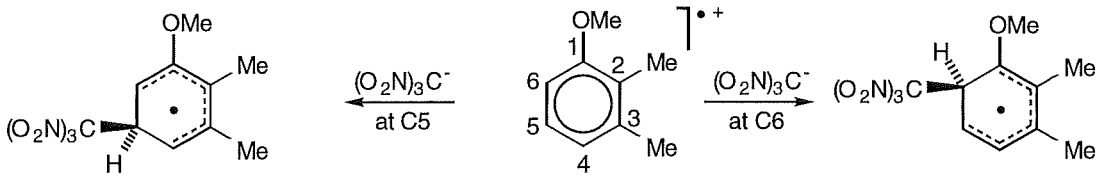

(312) (313)

Scheme 4.7

it appears that attack of $(O_2N)_3C^-$ on the 2,3-dimethylanisole radical cation would probably occur *via* attack at either C5 or C6.

4.2 The Photolysis of 2,3-Dimethylanisole (307)

General procedure for the photonitration of 2,3-dimethylanisole (307) with TNM.

A solution of 2,3-dimethylanisole (307) (500 mg, 0.46 mol L^{-1}) and TNM (0.92 mol L^{-1}) in either dichloromethane or acetonitrile (at +20 or -20°), or in 1,1,1,3,3,3-hexafluoropropan-2-ol (HFP) (at +20°), was irradiated with filtered light ($\lambda_{cut\text{-}off}$<435 nm) and small samples were withdrawn for analysis at suitable intervals. The work-up procedure, involving evaporation of solvent and TNM was conducted at ≤0°. The crude product mixtures were stored at -20° and were analysed by ^1H n.m.r. spectroscopy as soon as possible (For complete experimental details see Chapter 5, Section 5.4).

4.3 The Photochemistry of 2,3-Dimethylanisole (307) in Dichloromethane

Photochemistry in dichloromethane at +20° and the identification of products (314)-(324).

A solution of 2,3-dimethylanisole (307) (0.46 mol L^{-1}) and TNM (0.92 mol L^{-1}) in dichloromethane was irradiated at +20° until the orange/brown colour of the charge-transfer band was bleached. The composition of the mixture was monitored by withdrawing samples for ^1H n.m.r. spectral analysis. After work-up, the final solution (after 8 h, conversion *c.* 100%) was shown to contain the nitro/trinitromethyl adducts (314) (15%) and (315) (9%), hydroxy/trinitromethyl adducts (316) (3%) and (317) (1%), and aromatic compounds (318) (10%), (319) (1%), (320) (7%), (321) (42%), (322) (5%), (323) (1%), and hydroxy dinitro compound (324) (1%). These

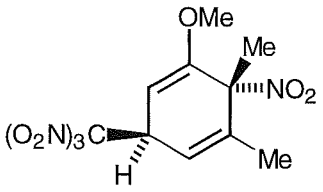

(314)

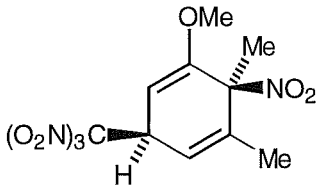

(315)

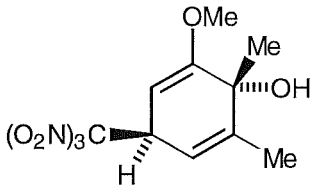

(316)

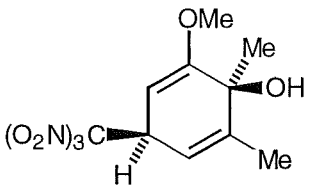

(317)

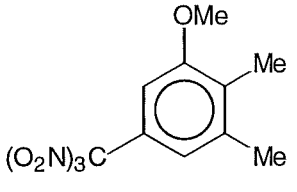

(318)

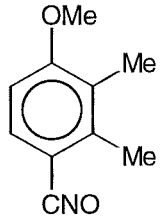

(319)

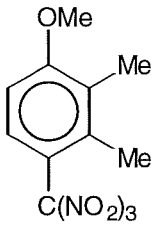

(320)

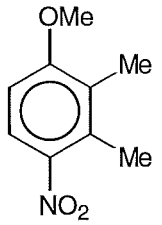

(321)

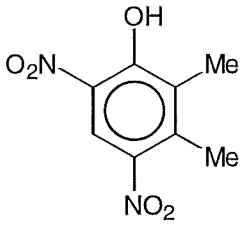

(322)

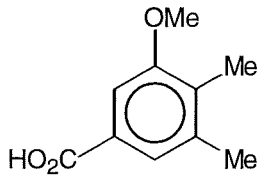

(323)

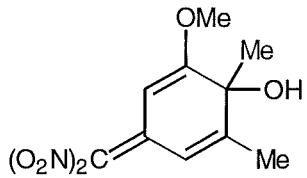

(324)

products were separated partially by h.p.l.c. on a cyanopropyl column, cooled to 0°, using hexane/dichloromethane mixtures as eluting solvents. In the following discussion, product identification will be described for groups of compounds, rather than in the order of elution which is given in the Experimental section (See Chapter 5, Section 5.4.1).

The epimeric nitro/trinitromethyl adducts (314) *and* (315), *the epimeric hydroxy/trinitromethyl adducts* (316) *and* (317), *and the hydroxy dinitro compound* (324).

Adduct (314) was isolated as an oil containing an impurity (*c.* 5%). The identification of adduct (314) as 1-methoxy-5,6-dimethyl-*t*-6-nitro-*r*-3-trinitromethylcyclohexa-1,4-diene (314) was based on its spectroscopic data. N.O.e. experiments confirmed the assignments of the chemical shifts for the protons. Specifically, irradiation at δ 3.64 (OMe) gave an enhancement at δ 5.03 (H2), while irradiation at δ 5.77 (H4) gave enhancements at δ 1.80 (5-Me) and at δ 4.91 (H3), as outlined in Fig. 4.1. HMQC and HMBC experiments allowed the complete assignment of the ^{13}C n.m.r. spectra, also given in Fig. 4.1. In particular, the trinitromethyl function attached to C3 appeared at δ 43.6, while the nitro function attached to C6 appeared at δ 89.1. Furthermore, the presence of very strong infrared absorptions at 1599 and 1558 cm^{-1} provided evidence for the $-C(NO_2)_3$ and $-NO_2$ substituents. The *trans*-6-nitro-3-trinitromethyl stereochemistry was assigned to adduct (314) because it eluted from the cyanopropyl h.p.l.c. column with the dichloromethane/hexane solvent system earlier than its

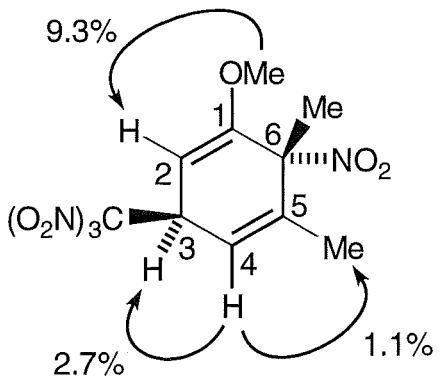

(314)

OCH_3	3.64	OCH_3	55.9
-	-	C1	158.3
H2	5.03	C2	88.5
H3	4.91	C3	43.6
H4	5.77	C4	117.3
5-Me	1.80	C5	140.5
6-Me	1.82	C6	89.1

Fig. 4.1 Characteristic ^{1}H and ^{13}C n.m.r. resonances (in ppm) and enhancements (%) from selected n.O.e. experiments for adduct (314).

cis-6-nitro-3-trinitromethyl stereoisomer (315). The h.p.l.c. elution order for such pairs of stereoisomers is known, with *trans*-1,4-nitro/trinitromethyl adducts eluting ahead of their *cis*-1,4-isomers.[4-7]

Adduct (315) was also isolated as an oil containing an impurity (*c.* 5%). The identification of adduct (315) as 1-methoxy-5,6-dimethyl-*c*-6-nitro-*r*-3-trinitromethylcyclohexa-1,4-diene (315) was based on comparison of its spectroscopic data with 1-methoxy-6-methyl-*c*-6-nitro-*r*-3-trinitro-methylcyclohexa-1,4-diene (325), the structure of which was determined by

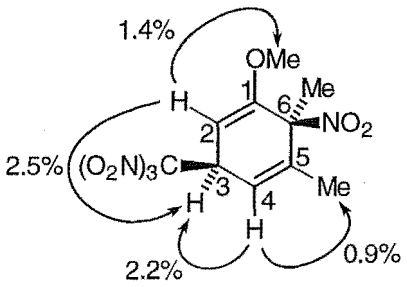

Fig. 4.2 Enhancements (%) from selected n.O.e. experiments for adduct (315).

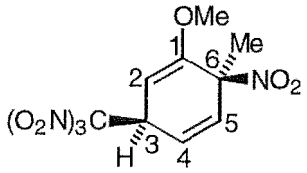

(325)

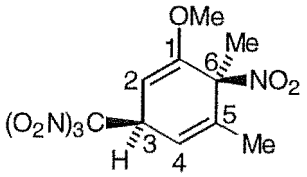

(315)

OCH_3	3.71	OCH_3	3.63
H2	5.03	H2	4.97
H3	4.86	H3	4.81
H4	5.99	H4	5.68
6-Me	1.85	6-Me	1.85
OCH_3	55.8	OCH_3	55.9
C1	157.1	C1	157.7
C2	89.5	C2	88.5
C3	42.6	C3	42.6
C4	121.8	C4	117.2
C6	85.5	C6	88.5

Fig. 4.3 Comparison of the characteristic ^{1}H and ^{13}C n.m.r. resonances (in ppm) for adducts (325) and (315).

single crystal X-ray analysis,[17] as illustrated in Fig. 4.3. N.O.e. experiments confirmed the assignments of the chemical shifts for the protons. In particular, irradiation at δ 4.97 (H2) gave enhancements at δ 3.63 (OMe) and at δ 4.81 (H3), while irradiation at δ 5.68 (H4) gave enhancements at

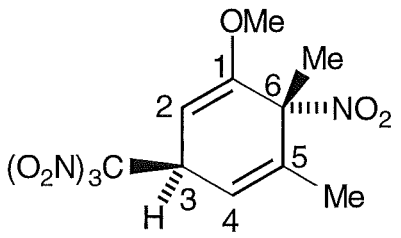

(314)

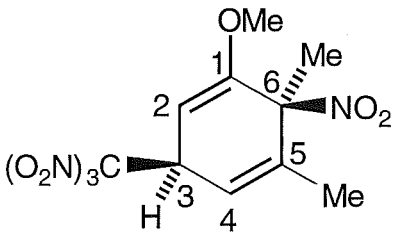

(315)

O**C**H$_3$	3.64	O**C**H$_3$	3.63
H2	5.03	H2	4.97
H3	4.91	H3	4.81
H4	5.77	H4	5.68
5-Me	1.80	5-Me	1.82
6-Me	1.82	6-Me	1.85
O**C**H$_3$	55.9	O**C**H$_3$	55.9
C1	158.3	C1	157.7
C2	88.5	C2	88.5
C3	43.6	C3	42.6
C4	117.3	C4	117.2
C5	140.5	C5	139.3
C6	89.1	C6	88.5

Fig. 4.4 Comparison of the characteristic ^{1}H and ^{13}C n.m.r. resonances (in ppm) for adducts (314) and (315).

δ 1.82 (5-Me) and at δ 4.81 (H3), as presented in Fig. 4.2. The ^{13}C n.m.r. resonances were confirmed by HMQC and HMBC experiments (See Fig. 4.3). Specifically, the **C**H-C$(NO_2)_3$ resonance appeared at δ 42.6, while the **C**Me-NO_2 resonance appeared at δ 88.5. The closely similar spectroscopic data for compounds (314) and (315) are depicted in Fig. 4.4, and were consistent with their assignment as epimers.

Adduct (316) was isolated only in admixture with *c.* 5% of the hydroxy/trinitromethyl adduct (317). The identification of adduct (316) as 2-methoxy-1,6-dimethyl-*t*-4-trinitromethylcyclohexa-2,5-dien-*r*-1-ol (316) was based on comparison of its spectroscopic data with the trans-1,4-nitro/ trinitromethyl adduct (314), as summarized in Fig. 4.6. N.O.e. experiments confirmed the assignments of the chemical shifts for the protons. Specifically, irradiation at δ 1.95 (6-Me) gave enhancements at δ 1.45 (1-Me) and at δ 5.45 (H5), while irradiation at δ 4.71 (H3, H4) gave enhancements at δ 3.66 (OMe) and at δ 5.45 (H5), as shown in Fig. 4.5. The ^1H n.m.r. signals due to adduct (316) were shifted upfield relative to adduct (314), because of the presence of the -OH function (See Fig. 4.6) HMQC and HMBC experiments confirmed the assignments of the ^{13}C n.m.r. resonances. In particular, the location of the hydroxy function was defined

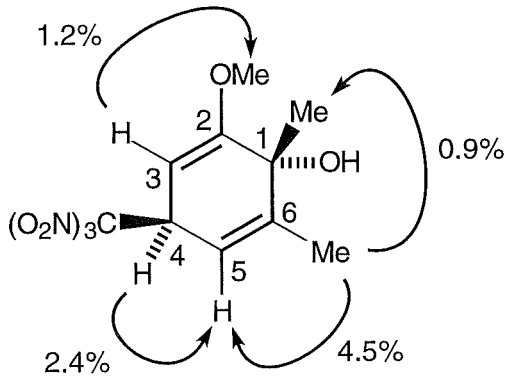

Fig. 4.5 Enhancements (%) from selected n.O.e. experiments for adduct (316).

by the chemical shift for C1 (δ 68.6), while the trinitromethyl function was defined by the chemical shift for C4 (δ 43.9), as represented in Fig. 4.6. Furthermore, the presence of an infrared absorption at 3460 cm^{-1} provided evidence for the -OH substituent.

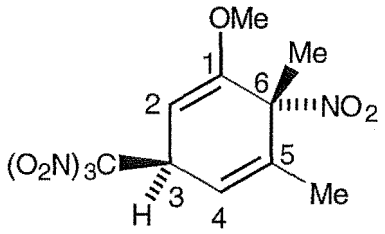

(314)

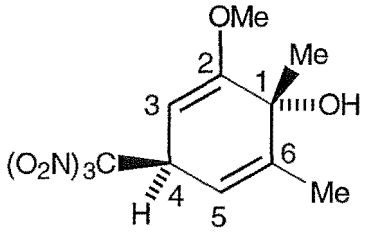

(316)

6-Me	1.82	1-Me	1.45
OCH_3	3.64	OCH_3	3.66
H2	5.03	H3	4.71
H3	4.91	H4	4.71
H4	5.77	H5	5.45
5-Me	1.80	6-Me	1.95
C6	89.1	C1	68.6
OCH_3	55.9	OCH_3	55.4
C1	158.3	C2	163.6
C2	88.5	C3	84.6
C3	43.6	C4	43.9
C4	117.3	C5	112.2
C5	140.5	C6	147.2

Fig. 4.6 Comparison of the characteristic ^{1}H and ^{13}C n.m.r. resonances (in ppm) for adducts (314) and (316).

Adduct (317) was isolated only as a minor component (*c.* 15%) in admixture with the hydroxy/trinitromethyl adduct (316). The identification of adduct (317) as 2-methoxy-1,6-dimethyl-*c*-4-trinitromethylcyclohexa-2,5-dien-*r*-1-ol (317) was based on comparison of its spectroscopic data with its epimer (316). N.O.e. experiments confirmed the assignments of the chemical shifts for the protons. In particular, irradiation at δ 1.94 (6-Me) gave an enhancement at δ 5.40 (H5), while irradiation at δ 3.63 (OMe) gave an enhancement at δ 4.66 (H3), as outlined in Fig. 4.7. The ^{13}C n.m.r.

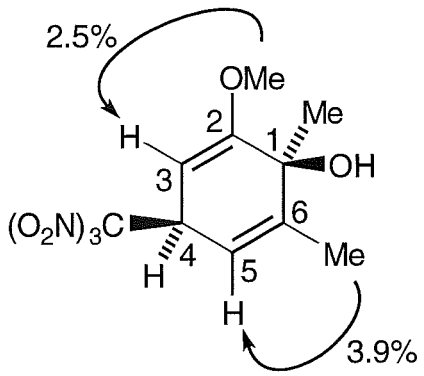

Fig. 4.7 Enhancements (%) from selected n.O.e. experiments for adduct (317).

chemical shifts were confirmed by an HMQC experiment (See Fig. 4.8). Specifically, the trinitromethyl function was indicated by the ^{13}C n.m.r. chemical shift for C4 (δ 42.8). The closely similar spectroscopic data for compounds (316) and (317) are depicted in Fig. 4.8, and were consistent with their assignment as epimers.

The hydroxy dinitro compound (324) was isolated only in low yield as an oil. Compound (324) was identified as 2-(4'-hydroxy-3'-methoxy-4',5'-dimethylcyclohexa-2',5'-dienylidene)-1,1-dinitroethene (324) on the basis of its spectroscopic data. Compound (324) gave a satisfactory parent molecular ion in the mass spectrum, indicating the molecular formula

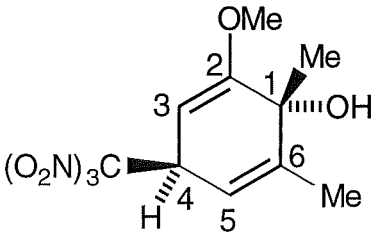

(316)

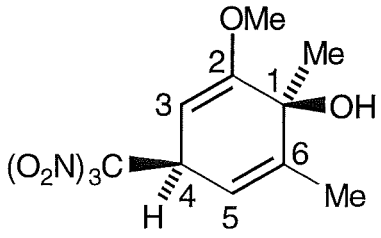

(317)

1-Me	1.45	1-Me	1.45
OCH_3	3.66	OCH_3	3.63
H3	4.71	H3	4.66
H4	4.71	H4	4.61
H5	5.45	H5	5.40
6-Me	1.95	6-Me	1.94
OCH_3	55.4	OCH_3	55.4
C3	84.6	C3	85.2
C4	43.9	C4	42.8
C5	112.2	C5	112.7

Fig. 4.8 Comparison of the characteristic ^{1}H and ^{13}C n.m.r. resonances (in ppm) for adducts (316) and (317).

$C_{10}H_{12}N_2O_6$. N.O.e. experiments confirmed the assignments of the chemical shifts for the protons. Specifically, irradiation at δ 2.16 (5'-Me) gave enhancements at δ 1.55 (4'-Me) and at δ 6.38 (H6'), while irradiation at δ 3.94 (OMe) gave an enhancement at δ 6.44 (H2'), as illustrated in Fig. 4.9. The assignment of the ^{13}C n.m.r. resonances were confirmed by HMQC and HMBC experiments. In particular, the dinitromethyl function attached to C2 appeared at δ 146.6, while the hydroxy function attached to

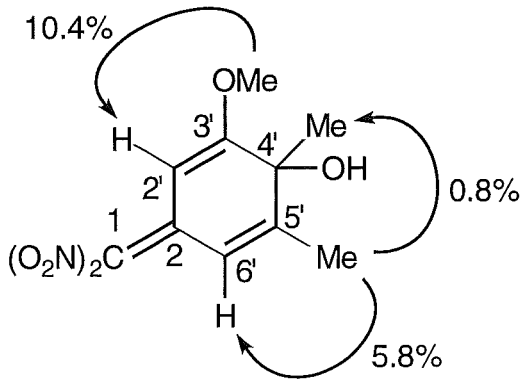

(324)

-	-	C2	146.6
H2'	6.44	C2'	89.9
O**CH$_3$**	3.94	C3'	175.8
4'-Me	1.55	C4'	70.9
5'-Me	2.16	C5'	158.5
H6'	6.38	C6'	114.9
O**H**	2.43	O**C**H$_3$	56.9

Fig. 4.9 Characteristic ^{1}H and ^{13}C n.m.r.1 a bd m o o p M n p l}for SM st gr}{P}{DB}{g enhancements (%) from selected n.O.e. experiments for adduct (324).

C4' appeared at δ 70.9, also seen in Fig. 4.9. Furthermore, the presence of very strong infrared absorptions were observed at 1657 and 1541 cm^{-1} providing evidence for the -C=C(NO$_2$)$_2$ substituent, while a broad infrared absorption at 3427 cm^{-1} provided evidence for the -OH substituent. The ultraviolet absorption with λ_{max} 386 nm (ε 32400) was also consistent with the assigned structure.

The aromatic products (318)-(323).

Compound (318) was identified as 5,6-dimethyl-3-trinitromethyl-anisole (318) on the basis of its spectroscopic data. The trinitromethyl aromatic (318) gave a satisfactory parent molecular ion in the mass spectrum, indicating the molecular formula $C_{10}H_{11}N_3O_7$. N.O.e. experiments confirmed the assignments of the chemical shifts for the protons. In particular, irradiation at δ 2.34 (5-Me) gave an enhancement at δ 6.96 (H4), while irradiation at δ 3.84 (OMe) gave an enhancement at δ 6.87 (H2), as observed in Fig. 4.10. Furthermore, the presence of very strong infrared absorptions at 1614 and 1587 cm^{-1} provided evidence for the $-C(NO_2)_3$ substituent.

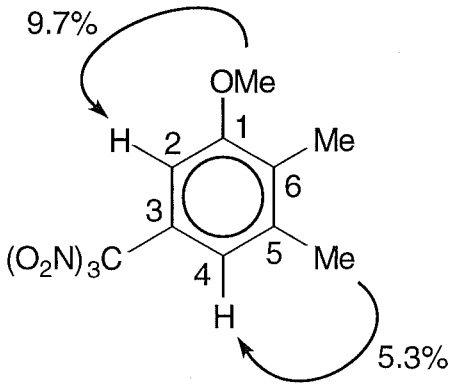

Fig. 4.10 Enhancements (%) from selected n.O.e. experiments for compound (318).

The isomeric trinitromethyl anisole (320) was identified as 2,3-di-methyl-4-trinitromethylanisole (320) by comparison of its spectroscopic data with its isomer (318). Although no parent ion was visible in the mass spectrum of compound (320), a M^+-NO_2 fragment was observed. The ready loss of $^{\bullet}NO_2$ from this 4-trinitromethyl anisole was typical of such structures.[18] HMBC and n.O.e. experiments confirmed the assignments of the chemical shifts for the protons. Specifically, irradiation at δ 2.02 (3-Me)

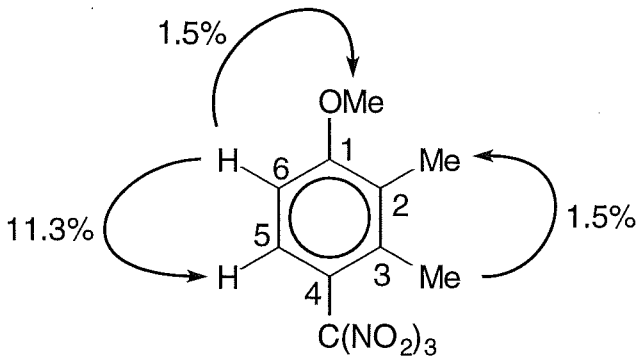

Fig. 4.11 Enhancements (%) from selected n.O.e. experiments for compound (320).

gave an enhancement at δ 2.21 (2-Me), while irradiation at δ 6.83 (H6) gave enhancements at δ 3.91 (OMe) and at δ 7.11 (H5), as illustrated in Fig. 4.11. Furthermore, the trinitromethyl function was indicated by the ^{13}C n.m.r. resonance for C4 (δ 113.7), which was closely similar to the isomeric trinitromethyl compound (318), in which the trinitromethyl function was indicated by the ^{13}C n.m.r. resonance for C3 (δ 119.6), as seen in Fig. 4.12.

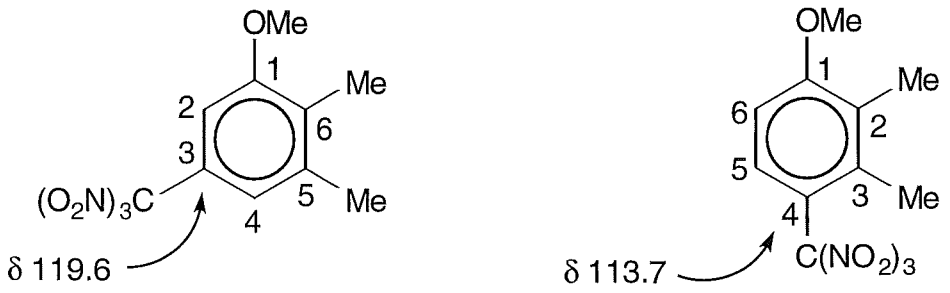

Fig. 4.12 Comparison of the characteristic ^{13}C n.m.r. resonances (in ppm) for the trinitromethyl aromatic compounds (318) and (320).

In addition, the presence of very strong infrared absorptions at 1622 and 1580 cm^{-1} provided evidence for the $-C(NO_2)_3$ substituent.

Compound (319) was identified as 4-methoxy-2,3-dimethylbenzonitrile *N*-oxide (319) on the basis of its spectroscopic data. The nitrile oxide (319) gave a satisfactory parent molecular ion in the mass spectrum, indicating the molecular formula $C_{10}H_{11}NO_2$. HMBC and n.O.e. experiments confirmed the assignments of the chemical shifts for the protons. In particular, irradiation at δ 6.65 (H5) gave enhancements at δ 3.80 (OMe) and at δ 6.92 (H6), as seen in Fig. 4.13. Furthermore, the presence of a very strong infrared absorption at 2280 cm^{-1} provided evidence for the -**CN**O substituent, while the infrared absorption at 1263 cm^{-1} provided evidence for the -C**NO** substituent.

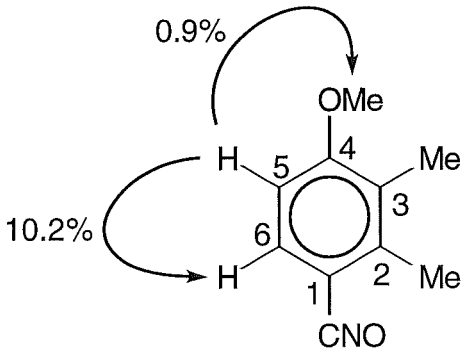

Fig. 4.13 Enhancements (%) from selected n.O.e. experiments for compound (319).

Compound (321) was identified as 2,3-dimethyl-4-nitroanisole (321) and the structure was confirmed by comparing its spectroscopic data with literature data.[19]

Compound (322) was identified as 5,6-dimethyl-2,4-dinitrophenol (322) and the structure was confirmed by comparing its spectroscopic data with literature data.[20]

Compound (323) was identified as 3-methoxy-4,5-dimethylbenzoic acid (323) on the basis of its spectroscopic data. The methoxy benzoic acid (323) gave a satisfactory parent molecular ion in the mass spectrum,

indicating the molecular formula $C_{10}H_{12}O_3$. N.O.e. experiments confirmed the assignments of the chemical shifts for the protons. Specifically, irradiation at δ 2.33 (5-Me) gave enhancements at δ 2.21 (4-Me) and at δ 7.56 (H6), while irradiation at δ 3.88 (OMe) gave an enhancement at δ 7.42 (H2), as depicted in Fig. 4.14. Furthermore, the presence of infrared absorptions at 3421 and 1684 cm^{-1} provided evidence for the $-CO_2H$ substituent.

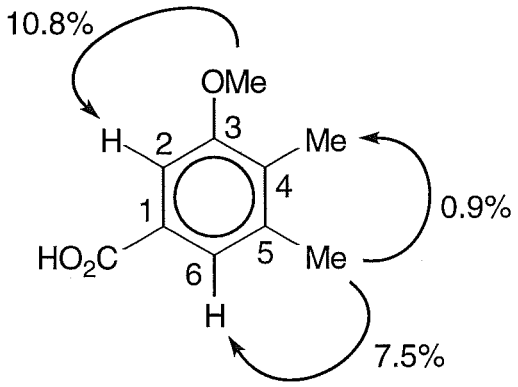

Fig. 4.14 Enhancements (%) from selected n.O.e. experiments for compound (323).

The composition of the photochemical reaction between 2,3-dimethylanisole (307) and TNM was monitored with time at +20 and -20° in dichloromethane. An overview of product yield in dichloromethane is summarized in Table 4.1. At +20° the total adduct yield decreased as the reaction proceeded (total 40% at 1 h, total 29% at 8 h) with a corresponding increase in the total aromatic yield (total 60% at 1 h, total 71% at 8 h). However, at -20° the total adduct yield remained constant (*c.* 23%). At both +20 and -20° the yield of adduct (314) increased throughout the reaction (at +20°, 13% after 1 h, 15% after 8 h; at -20°, 10% after 1 h, 14% after 8 h), while the other identified adducts (315)-(317) all decreased in yield (at +20°, total 24% after 1 h, total 14% after 8 h; at -20°, total 12% after 1 h, total

Table 4.1 Overview of product yields from the photolysis of 2,3-dimethylanisole (307) (0.46 mol L^{-1}) and TNM (0.92 mol L^{-1}) in dichloromethane.

	Yield (%)												
t (h)	(314)	(315)	(316)	(317)	Total adducts[a]	(318)	(319)	(320)	(321)	(322)	(323)	(324)	Total aromatics[b]
at +20°													
1	12.7	14.2	7.1	2.8	39.6	14.6	0.9	11.7	21.1	6.6	-	1.1	60.4
2	13.8	12.5	5.2	2.3	34.5	8.8	0.4	8.4	33.7	6.8	-	2.0	65.5
4	14.0	10.8	4.1	1.8	31.0	9.7	0.4	7.0	39.5	5.7	trace	1.3	69.0
8	15.1	8.8	3.4	1.4	29.0	9.6	1.4	6.9	41.7	5.1	0.6	0.7	71.0
at -20°													
1	9.7	7.0	3.1	1.9	23.6	21.4	5.2	15.7	21.3	5.0	-	-	76.4
2	11.6	7.3	2.7	1.2	24.6	18.5	3.2	13.5	26.7	5.1	-	0.2	75.4
4	11.2	5.8	2.9	1.2	22.4	20.3	3.0	13.2	28.8	4.3	trace	0.5	77.6
8	13.7	5.5	1.5	0.7	22.7	19.5	1.2	10.5	33.8	2.4	0.4	0.4	77.3

[a] Including unidentified adducts. [b] Including unidentified aromatics.

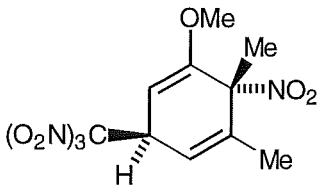

(314)

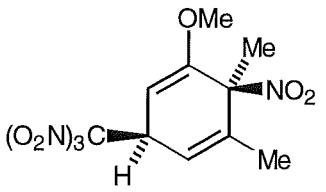

(315)

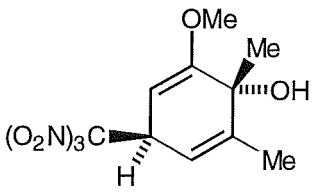

(316)

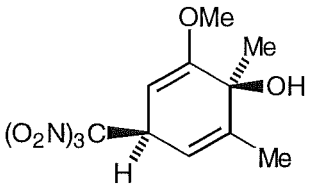

(317)

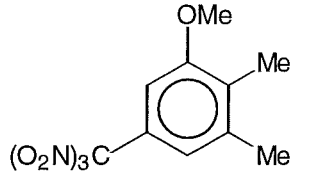

(318)

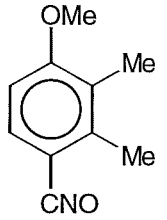

(319)

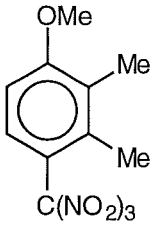

(320)

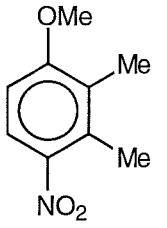

(321)

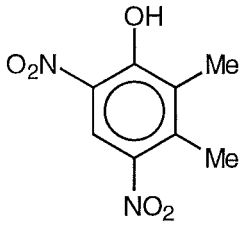

(322)

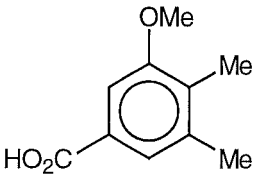

(323)

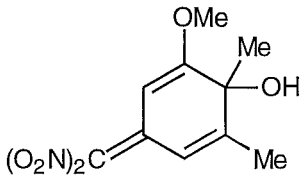

(324)

8% after 8 h). At lower reaction temperature, the yield of the trinitromethyl aromatics (318) and (320) increased (after 8 h, total 17% at +20°, total 30% at -20°). As the reaction proceeded at both +20 and -20° the yield of the major product 2,3-dimethyl-4-nitroanisole (321) increased. However, the increase was less marked at -20° (from 21% after 1 h to 34% after 8 h) c.f. at +20° (from 21% after 1 h to 42% after 8 h). Reaction at -20° also showed that the carboxylic acid (323) and the hydroxy dinitro compound (324) were not present at the early stages of the reaction but formed as the reaction proceeded.

4.4 The Photochemistry of 2,3-Dimethylanisole (307) in Acetonitrile

Photolyses of solutions of 2,3-dimethylanisole (307) (0.46 mol L^{-1}) and TNM (0.92 mol L^{-1}) in acetonitrile were carried out at +20 and -20° as described for reactions in dichloromethane, above. The composition of these reactions, monitored with time, are shown in Table 4.2. The absence of adducts (316) and (317) and the hydroxy dinitro compound (324) was most notable in the reactions in acetonitrile. These three compounds, (316), (317) and (324), were all seen in reactions in dichloromethane (See Table 4.1, Section 4.3). In acetonitrile, the adduct yield was almost constant at +20° (total *c.* 27%), but at -20° it increased with time (total 18% after 1 h, total 28% after 8 h). This was in contrast to reactions in dichloromethane where adduct yield decreased at +20° and was constant at -20°. At lower reaction temperature in acetonitrile, aromatic compounds (320) and (323) were absent. As was observed in dichloromethane, 2,3-dimethyl-4-nitroanisole (321) was the major product in acetonitrile. The yield of compound (321) increased at -20° as the reaction proceeded (35% after 1 h, 52% after 8 h), while at +20° it remained constant (*c.* 53%).

4.5 The Photochemistry of 2,3-Dimethylanisole (307) in 1,1,1,3,3,3-Hexafluoropropan-2-ol (HFP)

Photolysis of the charge-transfer complex of 2,3-dimethylanisole (307) (0.46 mol L^{-1}) and TNM (0.92 mol L^{-1}) in HFP at +20° for 24 h resulted in complete conversion into nitro/trinitromethyl adducts (314) (1%) and (315) (2%), hydroxy/trinitromethyl adducts (316) (0.3%) and (317) (trace), aromatic compounds (318) (19%), (320) (4%), (321) (61%), (322)

Table 4.2 Overview of product yields from the photolysis of 2,3-dimethylanisole (307) (0.46 mol L^{-1}) and TNM (0.92 mol L^{-1}) in acetonitrile.

	Yield (%)									
t (h)	(314)	(315)	Total adducts[a]	(318)	(319)	(320)	(321)	(322)	(323)	Total aromatics[b]
at +20°										
1	22.8	4.4	27.2	1.7	0.4	0.4	53.1	9.1	-	72.8
2	21.6	4.3	25.9	2.6	1.0	0.4	53.0	7.7	-	74.1
4	20.9	4.9	25.8	2.4	1.7	0.4	53.1	6.6	1.4	74.2
8	24.1	5.7	29.8	2.6	1.5	0.4	53.8	3.3	1.0	70.2
at -20°										
1	15.2	2.8	18.0	8.1	17.5	-	34.6	6.0	-	82.0
2	20.1	3.3	23.4	4.4	9.4	-	46.5	6.0	-	76.6
4	22.6	3.8	26.4	7.0	4.6	-	48.5	5.7	-	73.6
8	24.1	4.0	28.1	6.9	2.2	-	52.4	2.9	-	71.9

[a] Including unidentified adducts. [b] Including unidentified aromatics.

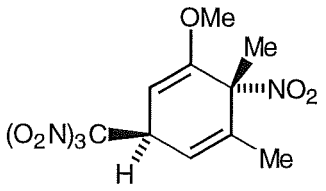

(314)

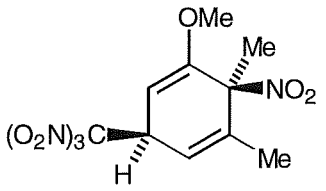

(315)

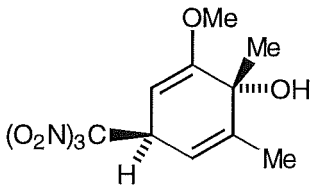

(316)

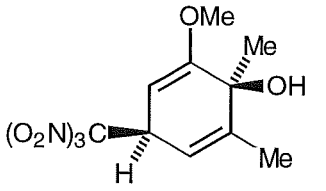

(317)

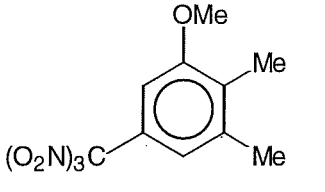

(318)

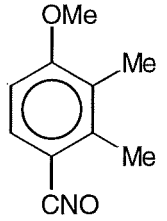

(319)

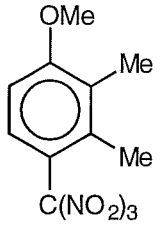

(320)

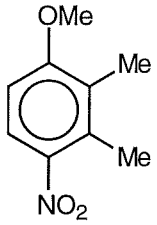

(321)

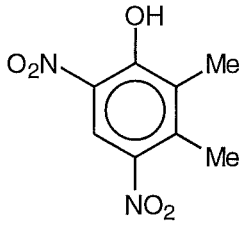

(322)

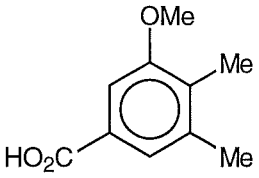

(323)

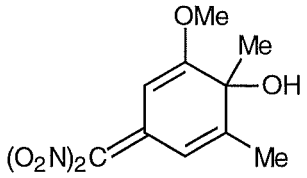

(324)

(0.3%) and unidentified aromatic compounds (total 12%). The reaction was monitored with time and the results are shown in Table 4.3. Reaction in HFP led to a decrease in the yield of adduct (314) with time (15% after 1 h, 1% after 8 h). This was in contrast to reactions in both dichloromethane and acetonitrile where the yield of adduct (314) increased as the reactions proceeded (See Tables 4.1 and 4.2, Sections 4.3 and 4.4, respectively). While the adducts (314)-(317) identified in dichloromethane were all present, the carboxylic acid (323) and the hydroxy dinitro compound (324) were absent. In HFP the conversion of 2,3-dimethyl-

Table 4.3 Overview of product yields from the photolysis of 2,3-dimethylanisole (307) (0.46 mol L^{-1}) and TNM (0.92 mol L^{-1}) in 1,1,1,3,3,3-hexafluoropropan-2-ol at +20°.

	Yield (%)										
t (h)	(314)	(315)	(316)	(317)	Total adducts[a]	(318)	(319)	(320)	(321)	(322)	Total aromatics[b]
1	14.9	4.2	1.3	0.6	21.0	10.7	8.2	5.0	38.4	3.1	79.0
2	14.3	5.0	1.6	0.8	21.7	13.7	1.6	4.4	41.9	3.0	78.3
4	10.6	4.0	2.3	1.1	18.0	25.8	0.8	4.4	40.2	1.2	82.0
8	7.8	4.0	3.1	1.6	16.5	23.3	0.4	4.1	47.0	0.5	83.5
24	1.0	2.2	0.3	trace	3.5	19.2	-	4.0	60.8	0.3	96.5

[a] Including unidentified adducts. [b] Including unidentified aromatics.

anisole (307) into products after a reaction time of 8 h was lower (*c.* 30%) compared with essentially complete conversion in dichloromethane at +20°.

4.6 The Photochemistry of 2,3-Dimethylanisole (307) in Dichloromethane Containing Trifluoroacetic Acid

Photolysis of the charge-transfer complex of 2,3-dimethylanisole (307) (0.46 mol L^{-1}) and TNM (0.92 mol L^{-1}) in dichloromethane containing TFA (0.71 mol L^{-1}) at +20°, as above, for 8 h resulted in a low conversion (*c.* 20%) into a mixture which consisted of nitro/trinitromethyl adducts (314) (3%) and (315) (0.5%), aromatic compounds (318) (42%), (319) (7%), (320) (8%), (321) (23%), (322) (2%) and unidentified aromatic compounds (total 15%). The absence of adducts (316) and (317) and the aromatic compounds (323) and (324) was notable in the reaction in dichloromethane with TFA. These products were observed in the corresponding reaction in

Table 4.4 Overview of product yields from the photolysis of 2,3-dimethylanisole (307) (0.46 mol L^{-1}) and TNM (0.92 mol L^{-1}) in dichloromethane containing trifluoroacetic acid (0.71 mol L^{-1}).

	Yield (%)								
t (h)	(314)	(315)	Total adducts[a]	(318)	(319)	(320)	(321)	(322)	Total aromatics[b]
1	3.3	0.9	4.2	41.6	8.1	5.3	11.0	-	95.8
2	3.3	0.9	4.2	47.1	6.0	8.8	15.3	-	95.8
4	4.3	1.1	5.4	45.9	6.0	4.4	17.4	trace	94.6
8	3.0	0.5	3.5	41.7	6.7	8.0	23.3	1.6	96.5

[a] Including unidentified adducts. [b] Including unidentified aromatics.

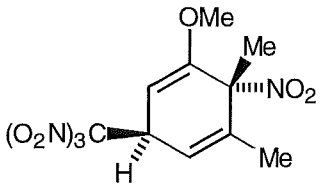

(314)

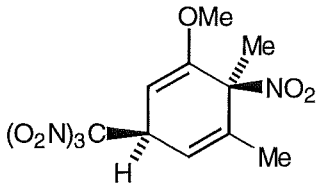

(315)

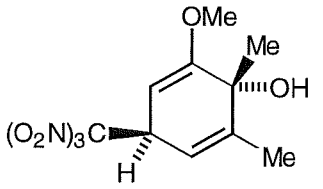

(316)

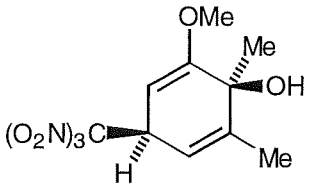

(317)

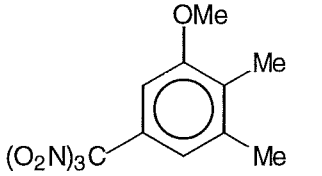

(318)

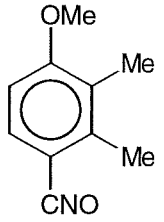

(319)

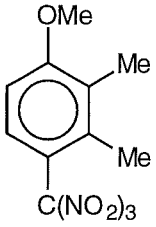

(320)

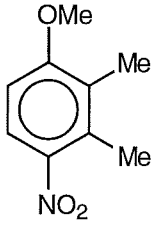

(321)

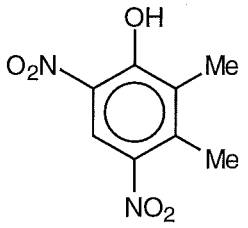

(322)

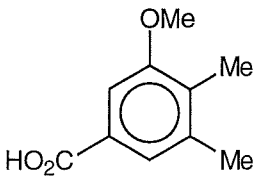

(323)

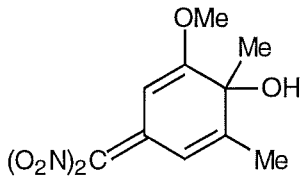

(324)

the absence of TFA (See Table 4.1, Section 4.3). The major product of reaction with TFA present was the 5,6-dimethyl-3-trinitromethylanisole (318) (42% after 8 h). Adduct formation was lower with TFA present (after 8 h, 3.5% with TFA present, 29% without TFA present).

4.7 Overview of the Photonitration of 2,3-Dimethylanisole (307)

In the photolysis of 2,3-dimethylanisole (307) with TNM in dichloromethane, the identified adducts (314)-(317) all contained the trinitromethyl function at the sterically least hindered position. However, the isolation of compounds (321) and (322) indicated that the attack of $(O_2N)_3C^-$ at C1 on

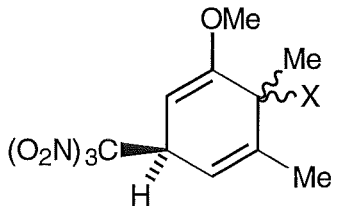

(314) and (315) X=NO_2
(316) and (317) X=OH

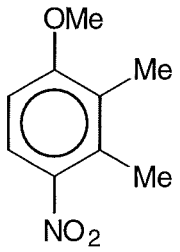

(321)

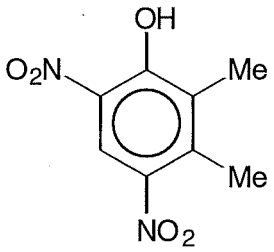

(322)

the 2,3-dimethylanisole radical cation did occur (See Schemes 4.9 and 4.13, 4.14, respectively). Indeed, it appears probable that the formation of adducts (314)-(317) also occurred *via* initial attack of $(O_2N)_3C^-$ at C1 on the radical cation of 2,3-dimethylanisole and proceeded *via* allylic rearrangements of highly labile adducts (326)-(329) (See Scheme 4.8). These allylic rearrangements were similar to those seen in the 1,5-dimethylnaphthalene series[9] and the 1-methoxynaphthalene series.[13]

Attack of $(O_2N)_3C^-$ at C1 of the radical cation of 2,3-dimethylanisole would give the delocalized carbon radical (308), as represented in Scheme 4.8. Coupling of this carbon radical (308) with $^{\bullet}NO_2$ at C2 with C-N bond formation would give the 1,2-nitro/trinitromethyl adducts (326) and (327). Subsequent 1,3-allylic rearrangement of adducts (326) and (327) would yield the 1,4-nitro/trinitromethyl adducts (314) and (315). Alternatively, coupling of $^{\bullet}NO_2$ at C2 could occur with C-O bond formation and would give nitrito/trinitromethyl adducts, which would be expected to hydrolyse rapidly

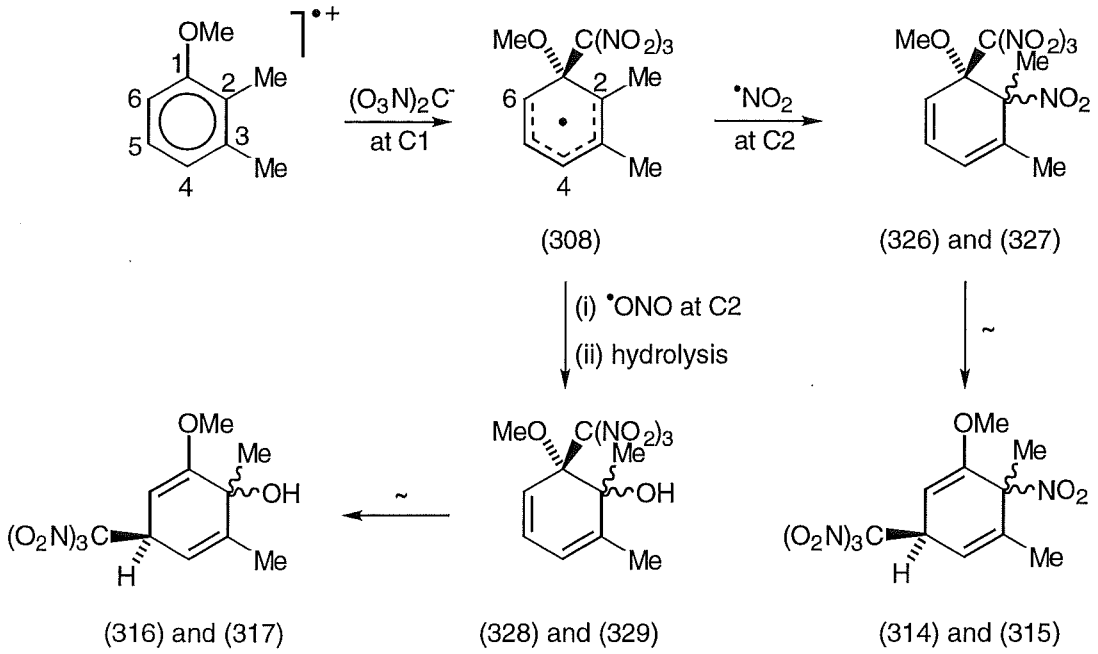

Scheme 4.8

to the epimeric 1,2-hydroxy/trinitromethyl adducts (328) and (329). Subsequent 1,3-allylic rearrangement of adducts (328) and (329) would yield the 1,4-hydroxy/trinitromethyl adducts (316) and (317).

The proposed mechanism for formation of 2,3-dimethyl-4-nitroanisole (321) involves radical coupling of $^{\bullet}NO_2$ with the delocalized carbon radical (308) at C4 with C-N bond formation, as outlined in Scheme 4.9. The resulting sterically hindered epimeric adducts (330) and (331) would then be expected to lose nitroform and form compound (321).

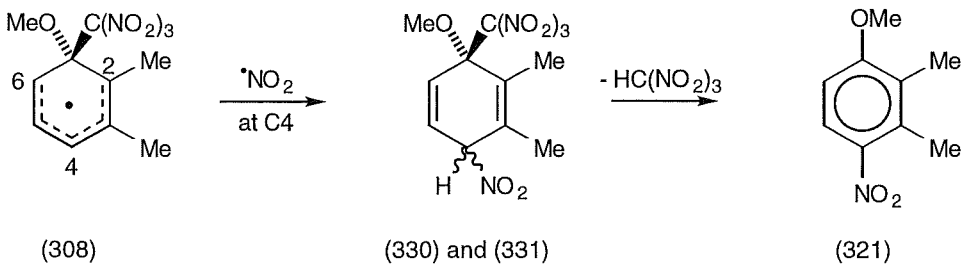

Scheme 4.9

The hydroxy dinitro compound (324) was not observed when the hydroxy/trinitromethyl adducts (316) and (317) were absent (See Tables 4.2 and 4.4, Sections 4.4 and 4.6, respectively). Hence, compound (324) probably arises during the photolysis reaction by loss of nitrous acid from one or both of the hydroxy/trinitromethyl adducts (316) and (317), as observed in Scheme 4.10.

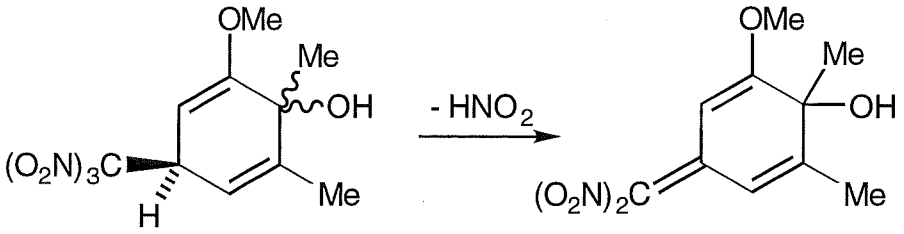

(316) and (317) (324)

Scheme 4.10

The 3-trinitromethyl aromatic (318) was proposed to form *via* loss of nitrous acid from the epimeric nitro/trinitromethyl adducts (314) and (315), as presented in Scheme 4.11. While the mechanism of formation of the carboxylic acid (323) remains uncertain, it appears likely that it arises *via* compound (318) as discussed by Eberson and Radner,[21] and also seen in Scheme 4.11.

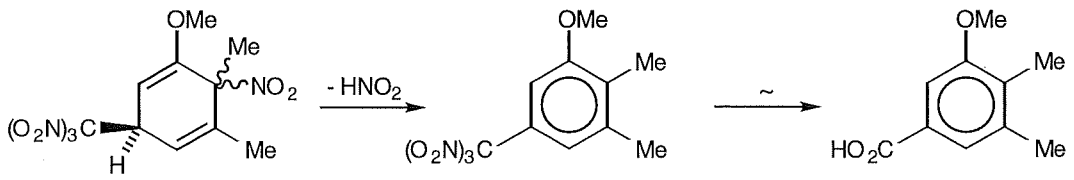

(314) and (315) (318) (323)

Scheme 4.11

Formation of the 4-trinitromethyl aromatic (320) was seen as arising *via* an initial attack of $(O_2N)_3C^-$ at C4 on the radical cation of 2,3-dimethylanisole, as outlined in Scheme 4.12. Subsequent attack of $^{\bullet}NO_2$ at C1 on radical (309), with either C-N or C-O bond formation, would give rise to adducts (332)-(335). Loss of nitrous acid from these adducts would yield compound (320).

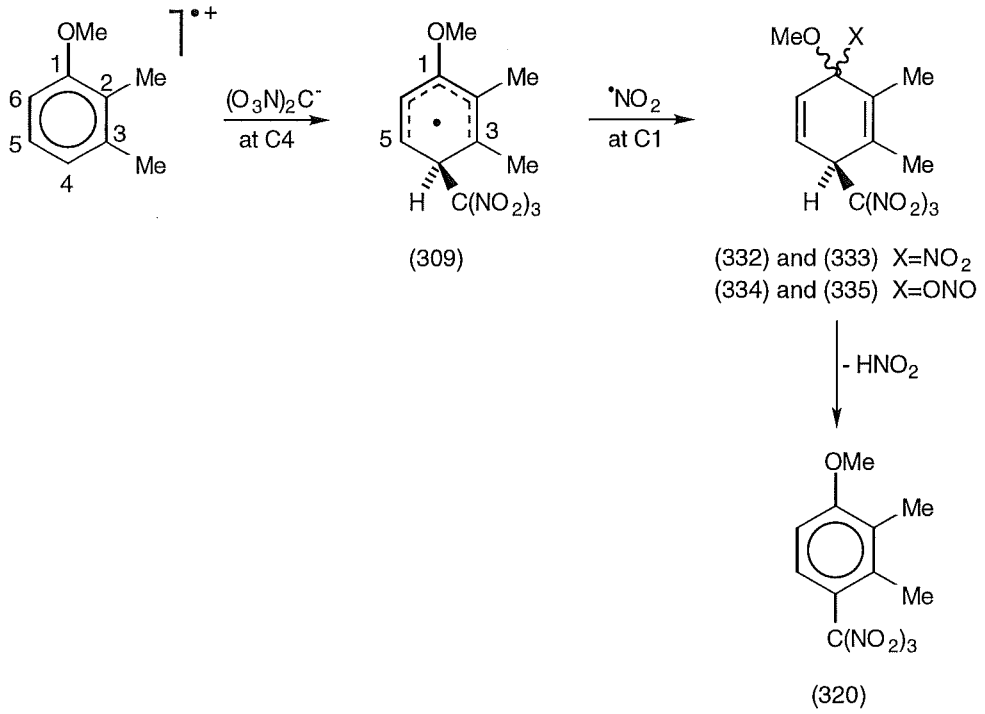

Scheme 4.12

The dinitro phenol (322) was proposed to form *via* the delocalized carbon radical (308), produced after $(O_2N)_3C^-$ attack at C1 on the 2,3-dimethylanisole radical cation, as illustrated in Scheme 4.13. Subsequent attack of $^{\bullet}NO_2$ at C4 in radical (308) would give the nitro/trinitromethyl adducts (330) and (331). Loss of the elements of Me-$C(NO_2)_3$ from adducts (330) and (331) would result in the formation of dienone (336). Dienones such as this have been found[22] to rearrange to nitro phenols [See Chapter 3, Section 3.9.5(c)]. This rearrangement was envisaged as

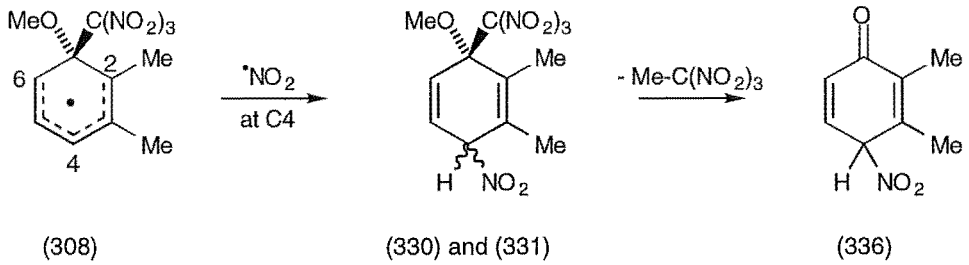

(308) (330) and (331) (336)

Scheme 4.13

occurring *via* homolysis of the C4-NO_2 bond in dienone (336) to form the solvent caged species (337), as seen in Scheme 4.14. Subsequently, a 1,3-nitro group migration could occur to form the diene (388), which would

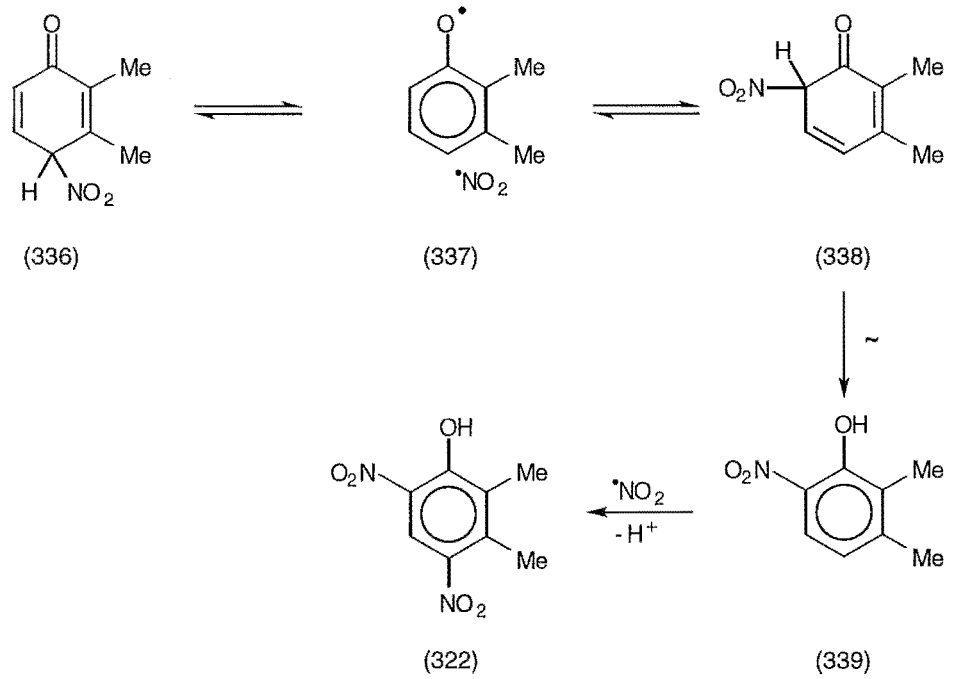

(336) (337) (338) (322) (339)

Scheme 4.14

then undergo enolization to yield the nitro phenol (339). Finally, this nitro phenol (339) could react with $^{\bullet}NO_2$ and, following subsequent loss of a proton, would form the dinitro phenol (322), also depicted in Scheme 4.14.

Conducting the photolysis of the charge-transfer complex of 2,3-dimethylanisole (307) and TNM either in HFP or in dichloromethane containing TFA (0.71 mol L^{-1}) was expected to slow the reaction of $(O_2N)_3C^-$ with the 2,3-dimethylanisole radical cation, either by protonation by TFA[23] or by suppression of the nucleophilic activity of $(O_2N)_3C^-$ through solvation in the HFP solvent.[24-29] This would allow competition from the $^{\bullet}NO_2$ / radical cation coupling process. While the conversion into products was somewhat slowed, product formation involving attack of $(O_2N)_3C^-$ on the 2,3-dimethylanisole radical cation remained significant (See Tables 4.3 and 4.4, Sections 4.5 and 4.6, respectively).

In conclusion, it appears likely that most of the observed products in the photochemical reactions between 2,3-dimethylanisole (307) and TNM arose *via* the sterically hindered delocalized carbon radical (308). While there was no direct evidence for adduct formation involving the trinitromethyl function at C1 , the isolation of aromatic products (321) and (322) suggested that the majority of product formation proceeded *via* initial attack of $(O_2N)_3C^-$ on the 2,3-dimethylanisole radical cation at C1 and subsequent rearrangement of the labile adducts (326)-(329).

4.8 References for Chapter Four

1 Eberson, L., Hartshorn, M. P., Radner, F., and Robinson, W. T., *J. Chem. Soc., Chem. Commun.*, 1992, 566.

2 Eberson, L., Hartshorn, M. P., and Radner, F., *J. Chem. Soc., Perkin Trans. 2*, 1992, 1793.

3 Butts, C. P., Calvert, J. L., Eberson, L., Hartshorn, M. P., Maclagan, R. G. A. R., and Robinson, W. T., *Aust. J. Chem.*, 1994, **47**, 1087.

4 Calvert, J. L., Eberson, L., Hartshorn, M. P., Maclagan, R. G. A. R., and Robinson, W. T., *Aust. J. Chem.*, 1994, **47**, 1211.

5 Butts, C. P., Calvert, J. L., Eberson, L., Hartshorn, M. P., Radner, F., and Robinson, W. T., *J. Chem. Soc., Perkin Trans. 2*, 1994, 1485.

6 Calvert, J. L., Eberson, L., Hartshorn, M. P., Maclagan, R. G. A. R., and Robinson, W. T., *Aust. J. Chem.*, 1994, **47**, 1591.

7 Butts, C. P., Eberson, L., Hartshorn, M. P., and Robinson, W. T., *Aust. J. Chem.*, 1995, **48**, 1989.

8 Eberson, L., and Hartshorn, M. P., *J. Chem. Soc., Chem. Commun.*, 1992, 1563.

9 Eberson, L., Calvert, J. L., Hartshorn, M. P., and Robinson, W. T., *Acta Chem. Scand.*, 1994, **48**, 347.

10 Butts, C. P., Eberson, L., Foulds, G. J., Fulton, K. L., Hartshorn, M. P., and Robinson, W. T., *Acta Chem. Scand.*, 1995, **49**, 76.

11 Butts, C. P., Eberson, L., Fulton, K. L., Hartshorn, M. P., Jamieson, G. B., and Robinson, W. T., *Acta Chem. Scand., in press.*

12 Butts, C. P., Eberson, L., Fulton, K. L., Hartshorn, M. P., Robinson, W. T., and Timmerman-Vaughan, D. J., *Acta Chem. Scand., in press.*

13 Butts, C. P., Eberson, L., Hartshorn, M. P., Persson, O., and Robinson, W. T., *Acta Chem. Scand.*, 1995, **49**, 253.

14 Sankararaman, S, and Kochi, J. K., *Recl. Trav. Chim.*, 1986, **105**,

278.

15 Sankararaman, S., Haney, W. A., and Kochi, J. K., *J. Am. Chem. Soc.*, 1987, **109**, 7824.

16 Butts, C. P., Eberson, L., Hartshorn, M. P., and Robinson, W. T., *Acta Chem. Scand., in press.*

17 Butts, C. P., Eberson, L., Hartshorn, M. P., Robinson, W. T., and Timmerman-Vaughan, D. J., *Acta Chem. Scand., in press.*

18 Butts, C. P., *unpublished data.*

19 Pouchert, C. J., *The Aldrich Library of FT-IR Spectra, Edn. I, vol. 1*, 1985; Pouchert, C. J., *The Aldrich Library of NMR Spectra, Edn. II, vol. 1*, 1983.

20 Holler, A. C., Huggett, C., and Rathmann, F. H., *J. Am. Chem. Soc.*, 1950, **72**, 2034.

21 Eberson, L., and Radner, F., *J. Am. Chem. Soc.*, 1991, **113**, 5825.

22 Barnes, C. E., and Myhre, P. C., *J. Am. Chem. Soc.*, 1978, **100**, 973.

23 Eberson, L., Hartshorn, M. P., Radner, F., and Svensson, J. O., *J. Chem. Soc. Perkin Trans. 2*, 1994, 1719.

24 Eberson, L., Hartshorn, M.P., and Persson, O., *Angew. Chem. Int. Ed. Engl.*, 1995, **34**, 2268.

25 Eberson, L., Hartshorn, M.P., and Persson, O., *J. Chem. Soc., Chem. Commun.*, 1995, 1131.

26 Eberson, L., Hartshorn, M.P., and Persson, O., *J. Chem. Soc., Perkin Trans. 2* , 1995, 1735.

27 Eberson, L., Hartshorn, M.P., and Persson, O., *Acta Chem. Scand.*, 1995, **49**, 640.

28 Eberson, L., Hartshorn, M.P., and Persson, O., *J. Chem. Soc., Perkin Trans. 2, in press.*

29 Eberson, L., Hartshorn, M.P., and Persson, O., *J. Chem. Soc., Perkin Trans. 2, in press.*

CHAPTER FIVE

EXPERIMENTAL AND APPENDIX

5.1 Apparatus, Materials and Instrumentation

Melting points were determined on a microscope slide and remain uncorrected. Infrared spectra were recorded on either a Perkin-Elmer 1600 Series or a Shimadzu 8001PC Series Fourier-transform i.r. spectrometer. ^{1}H and ^{13}C n.m.r. spectra were recorded on either a Varian XL-300 or Unity 300 spectrometer with $SiMe_4$ (TMS) as an internal standard. All chemical shifts are expressed as parts per million (ppm) downfield from TMS and are singlets unless stated. Difference nuclear Overhauser enhancement (n.O.e.) experiments were performed on non-gassed solutions in an arrayed experiment, with the decoupler offset 10000 Hz for the control experiment and then low power cycled over multiplet peaks corresponding to the proton(s) being irradiated in the experiment.[1] An acquisition time (AT) of one second was used , with delay (D_2) of two seconds. The reported percentage enhancements represent the increase in intensity of a particular resonance (independent of the power level used for irradiation or the degree of solvation obtained). All n.O.e. and two-dimensional correlation experiments (HMBC, HMQC) were performed using narrowed spectral windows. Mass spectrometry was carried out on a Kratos MS-80 instrument.

Preparative scale chromatography was routinely carried out using a Chromatotron (a preparative scale, centrifugally accelerated , radial, thin layer chromatograph, Model 7924, Harrison Research Inc.) equipped with rotors using silica gel PF-254 (with $CaSO_4.1/2H_2O$). H.p.l.c. separations were carried out on a Varian 5000 liquid chromatograph equipped with an

Alltech cyanopropyl column, and by using a Varian UV-50 ultraviolet spectrometric detector and hexane/dichloromethane as solvent mixtures.

Tetranitromethane was purchased from Aldrich or synthesised using the procedure described by Poe and Liang in Organic Synthesis Collective, volume 3, pg 803-805. 1,2,3-Trimethylbenzene, 1,2,4,5-tetramethylbenzene, hexamethylbenzene and 2,3-dimethylanisole were purchased from Aldrich, 1,3-dimethylnaphthalene from Janssen Chemicals, 2,6-dimethylnaphthalene from L. Light & Co., 1,4,6,7-tetramethylnaphthalene from Wiley Organics and pentamethylbenzene from Tokyo Kasei Kogyo. Dichloromethane (A.R.) and acetonitrile (HiPerSolv) were from BDH, and 1,1,1,3,3,3-hexafluoropropan-2-ol from Sigma.

WARNING. While no incident was experienced in working with tetranitromethane, it should be noted that its mixtures with hydrocarbons are detonative within certain concentration limits and that due care should be taken in handling mixtures of tetranitromethane and organic compounds.[2]

The photonitration apparatus used for -20, -50 and -78° reactions was set up as illustrated in Fig. 5.1. For reactions at +20 and 0° the same system was employed, except water was used instead of ethanol and ice was used instead of dry ice.

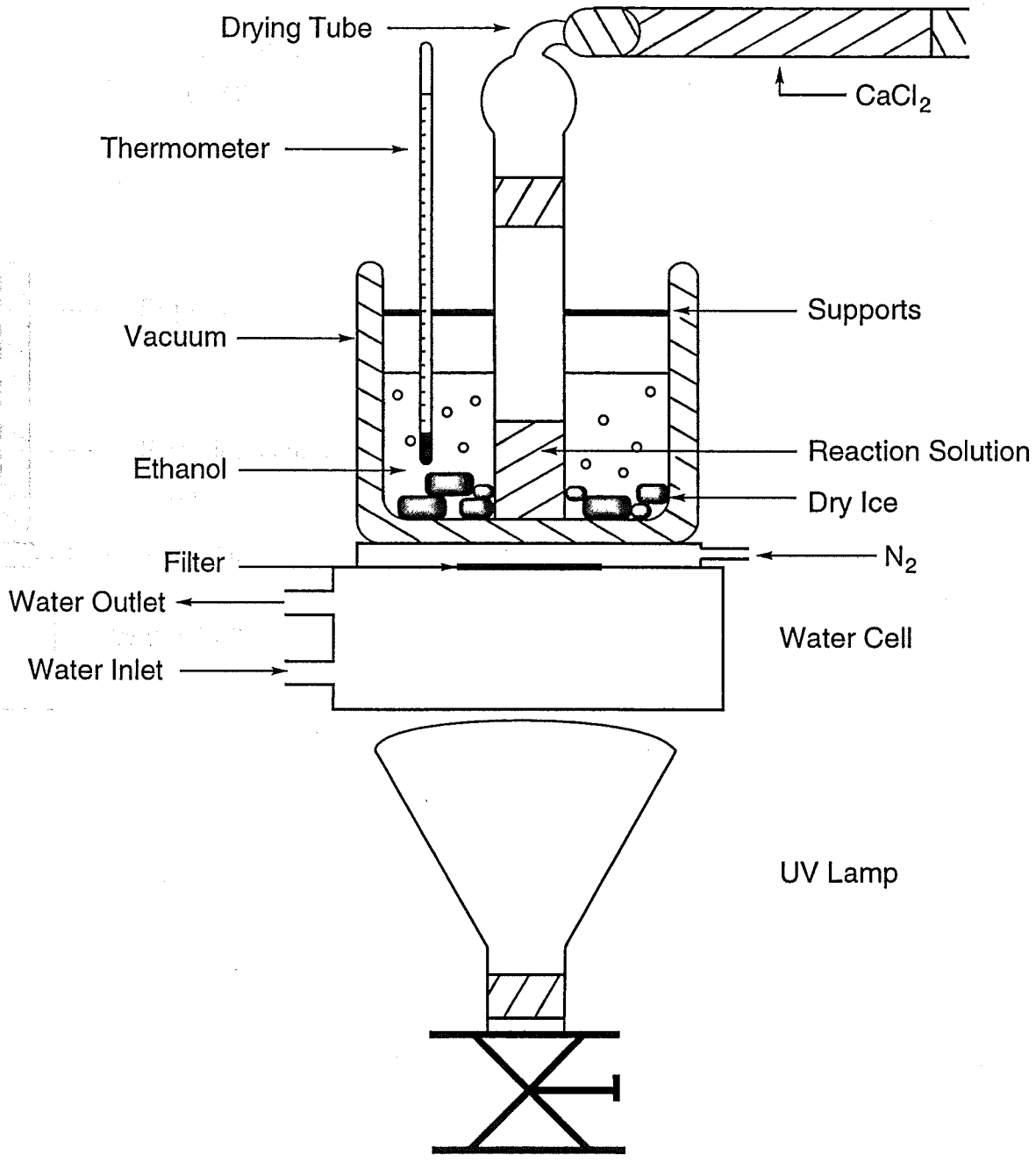

Fig. 5.1 Apparatus used for -20, -50 and -78° photonitrations.

5.2 Experimental Relating to Chapter Two

5.2.1 GENERAL PROCEDURE FOR THE PHOTONITRATION OF 1,4,6,7-TETRAMETHYLNAPHTHALENE (56) WITH TETRANITROMETHANE.

A solution of 1,4,6,7-tetramethylnaphthalene (56) (500 mg, 0.34 mol L^{-1}) and tetranitromethane (0.68 mol L^{-1}) in dichloromethane (at +20 or -20°) or acetonitrile (at +20°) was irradiated with filtered light ($\lambda_{cut\text{-}off}$<435 nm). Aliquots were withdrawn from the reaction mixture at appropriate time intervals, the volatile material removed under reduced pressure at ≤0°, and the product composition determined by ^1H n.m.r. spectral analysis (Tables 2.1-2.3).

5.2.1.1 Photonitration of 1,4,6,7-Tetramethylnaphthalene (56) in Dichloromethane

*Photochemistry in dichloromethane at -20° and the identification of 1,4,6,7-tetramethyl-*r*-1-nitro-*t*-4-trinitromethyl-1,4-dihydronaphthalene* (75) *and adducts* (76) *and* (77).

Reaction of 1,4,6,7-tetramethylnaphthalene (56) / tetranitromethane in dichloromethane at -20°, as above, for 2 h gave a product which was shown by ^1H n.m.r. spectral analysis (Table 2.1) to be a mixture of 1,4,6,7-tetramethyl-*r*-1-nitro-*t*-4-trinitromethyl-1,4-dihydronaphthalene (75) (58%), its epimer (76) (2%), an adduct tentatively identified as 2,3,5,8-tetramethyl-*r*-1-nitro-*c*-4-trinitromethyl-1,4-dihydronaphthalene (77) (3%), 4,6,7-trimethyl-2',2',2'-trinitroethylnaphthalene (78) (2%), 2,3,5,8-tetramethyl-1-nitronaphthalene (79) (4%), 1,4,6,7-tetramethyl-2-nitronaphthalene (80) (3%), 4,6,7-trimethyl-1-nitromethylnaphthalene (81) (27%), and unidentified aromatic products (total 1%). Crystallization of the product mixture from

dichloromethane/pentane gave the major product:

1,4,6,7-Tetramethyl-r-1-nitro-t-4-trinitromethyl-1,4-dihydro-naphthalene (75), m.p. 89° (dec.) (X-ray crystal structure determined, see Section 5.5). ν_{max} (KBr) 1613, 1588, 1544 cm^{-1}. ^1H n.m.r. ($CDCl_3$) δ 2.07, s, 1-Me; 2.19, s, 4-Me; 2.26, s, 6-Me; 2.27, s, 7-Me; 6.22, d, $J_{H2,H3}$ 10.5 Hz, H2; 6.64, d, $J_{H3,H2}$ 10.5 Hz, H3; 7.12, br s, H5; 7.28, br s, H8. N.O.e. experiments gave the following results: irradiation at δ 2.07 gave enhancements at δ 6.22 (4.7%) and at δ 7.28 (8.6%); irradiation at δ 2.19 gave enhancements at δ 6.64 (5.7%) and at δ 7.12 (9.3%); irradiation at δ 6.22 gave enhancements at δ 2.07 (0.4%) and at δ 6.64 (7.2%); irradiation at δ 6.64 gave enhancements at δ 2.19 (0.4%) and at δ 6.22 (7.5%); irradiation at δ 7.12 gave enhancements at δ 2.19 (0.7%) and at δ 2.26 (0.7%); irradiation at δ 7.28 gave enhancements at δ 2.07 (0.6%) and at δ 2.27 (0.6%). ^{13}C n.m.r. ($CDCl_3$) δ 19.6, 19.9, 6-Me, 7-Me; 26.2, 26.8, 1-Me, 4-Me; 48.9, C4; 86.7, C1; 127.05, C8; 127.7, C3; 128.2, C4a; 128.3, C5; 131.3, C8a; 131.6, C2; 139.25, 139.65, C6, C7; resonance for **C**$(NO_2)_3$ not observed. The above assignments were confirmed by long range reverse detected heteronuclear correlation spectra (HMBC).

The minor adducts (76) and (77) were not isolated but were characterized by their ^1H n.m.r. ($CDCl_3$) spectra: 1,4,6,7-Tetramethyl-*r*-1-nitro-*c*-4-trinitromethyl-1,4-dihydronaphthalene (76) – δ 1.99, s, 1-Me; 2.08, s, 4-Me; 2.18 and 2.35, both s, 6-Me, 7-Me; 6.45, d, $J_{H2,H3}$ 10.4 Hz, H2; 6.62, d, $J_{H3,H2}$ 10.4 Hz, H3; 7.06, s, H5; 7.72, s, H8. *cis*-2,3,5,8-Tetra-methyl-1-nitro-4-trinitromethyl-1,4-dihydronaphthalene (77) – δ 1.97 and 2.15, both br s, 2-Me, 3-Me; 2.28 and 2.32, both s, 5-Me, 8-Me; 5.89, br s, H4; 5.91, br s, H1; 7.20 and 7.49, both s, H6, H7.

The aromatic compounds (78), (79), (80) and (81) were isolated by chromatography on a silica gel Chromatotron plate of the product mixture formed in the photolysis of 1,4,6,7-tetramethylnaphthalene (56) / tetranitro-

methane in dichloromethane at +20° (see below).

Photochemistry in dichloromethane at +20° and the identification of some of the nitro aromatic products.

Reaction of 1,4,6,7-tetramethylnaphthalene (56) / tetranitromethane in dichloromethane at +20°, as above, for 2 h gave a product which was shown by ^{1}H n.m.r. spectral analysis (Table 2.1) to be a mixture of adducts (total 17%), 4,6,7-trimethyl-1-(2',2',2'-trinitroethyl)-naphthalene (78) (8%), 2,3,5,8-tetramethyl-1-nitronaphthalene (79) (6%), 1,4,6,7-tetramethyl-2-nitronaphthalene (80) (38%), and 4,6,7-trimethyl-1-nitromethylnaphthalene (81) (31%). Chromatography of this mixture on a silica gel Chromatotron plate gave in elution order:

4,6,7-Trimethyl-1-(2',2',2'-trinitroethyl)-naphthalene (78), m.p. 131-133° (Insufficient for elemental analysis. Found: $M^{+\bullet}$ 333.0961. $C_{15}H_{15}N_3O_6$ requires 333.0962). ν_{max} (KBr) 1605, 1590 cm^{-1}. ^{1}H n.m.r. ($CDCl_3$) δ 2.43, s, 7-Me; 2.45, s, 6-Me; 2.65, s, 4-Me; 4.84, s, C**H$_2$**; 7.16, m, H2, H3; 7.44, s, H8; 7.78, s, H5. N.O.e. experiments gave the following results: irradiation at δ 2.65 gave enhancements at δ 7.16 (5.9%) and at δ 7.78 (8.2%); irradiation at δ 4.84 gave enhancements at δ 7.16 (6.5%) and at δ 7.44 (14.1%); irradiation at δ 7.16 gave enhancements at δ 2.65 (0.8%) and at δ 4.84 (1.0%); irradiation at δ 7.44 gave enhancements at δ 2.43 (1.1%) and at δ 4.84 (3.4%); irradiation at δ 7.78 gave enhancements at δ 2.45 (0.8%) and at δ 2.65 (1.4%). ^{13}C n.m.r. ($CDCl_3$) δ 19.0, 4-Me; 20.3, 20.5, 6-Me, 7-Me; 35.7, **C**H$_2$; 119.85, C1; 121.45, C8; 125.2, C3; 125.4, C5; 127.5, C2; 130.9, C4a; 131.9, C8a; 136.0, C6; 136.2, C4; 136.9, C7; resonance for **C**$(NO_2)_3$ not observed. The above assignments were confirmed by long range reverse detected heteronuclear correlation spectra (HMBC).

2,3,5,8-Tetramethyl-1-nitronaphthalene (79), m.p. 155.5-156.5°

(Insufficient for elemental analysis. Found: $M^{+\bullet}$ 229.1103. $C_{14}H_{15}NO_2$ requires 229.1103). ν_{max} (KBr) 1531 cm^{-1}. ^1H n.m.r. ($CDCl_3$) δ 2.31, s, 2-Me; 2.50, s, 3-Me; 2.53, s, 8-Me; 2.64, s, 5-Me; 7.20, m, H6, H7; 7.88, s, H4. N.O.e. experiments gave the following results: irradiation at δ 2.31 gave an enhancement at δ 2.50 (0.2%); irradiation at δ 2.64 gave enhancements at δ 7.19 (1.7%) and at δ 7.88 (6.1%); irradiation at δ 7.20 gave enhancements at δ 2.53 (0.7%) and at δ 2.64 (0.5%); irradiation at δ 7.88 gave enhancements at δ 2.50 (0.7%) and at δ 2.64 (1.0%). ^{13}C n.m.r. ($CDCl_3$) δ 14.7, 2-Me; 18.9, 5-Me; 19.9, 8-Me; 20.9, 3-Me; 121.95, C8a; 126.6, C4; 127.15, C6; 127.2, C2; 128.9, C8; 130.2, C7; 132.20, C5; 132.23, C4a; 134.3, C3; 148.35, C1. The above assignments were confirmed by long range reverse detected heteronuclear correlation spectra (HMBC).

1,4,6,7-Tetramethyl-2-nitronaphthalene (80), m.p. 100-101° (Found: C, 73.5; H, 6.8; N, 6.0%. $C_{14}H_{15}NO_2$ requires C, 73.3; H, 6.6; N, 6.1%). ν_{max} (KBr) 1586 cm^{-1}. ^1H n.m.r. ($CDCl_3$) δ 2.49, s, 6-Me and 7-Me; 2.66, s, 4-Me; 2.77, s, 1-Me; 7.57, s, H3; 7.76, s, H5; 7.93, s, H8. N.O.e. experiments gave the following results: irradiation at δ 2.49 gave enhancements at δ 7.76 (4.1%) and at δ 7.93 (4.0%); irradiation at δ 2.66 gave enhancements at δ 7.57 (5.0%) and at δ 7.76 (6.4%); irradiation at δ 2.77 gave an enhancement at δ 7.93 (6.5%); irradiation at δ 7.57 gave an enhancement at δ 2.66 (0.5%); irradiation at δ 7.93 gave enhancements at δ 2.49 (1.1%) and at δ 2.77 (2.0%). ^{13}C n.m.r. ($CDCl_3$) δ 14.2, 1-Me; 19.1, 4-Me; 20.3, 6-Me and 7-Me; 119.6, C3; 124.4, C8; 125.9, C5; 127.0, C1; 131.0, C8a; 132.5, C4a; 133.1, C4; 136.95, C6; 138.2, C7; 146.6, C2. The above assignments were confirmed by long range reverse detected heteronuclear correlation spectra (HMBC).

4,6,7-Trimethyl-1-nitromethylnaphthalene (81), was unstable on silica gel and was obtained only in admixture with other materials. ^1H

n.m.r. ($CDCl_3$) δ 2.47 and 2.49, both s, 6-Me, 7-Me; 2.69, s, 4-Me; 5.85, s, C**H$_2$**; 7.25 and 7.38, both d, $J_{H,H}$ 7.2 Hz, H2, H3; 7.72 and 7.80, both s, H5, H8.

5.2.1.2 Rearrangement of 1,4,6,7-Tetramethyl-*r*-1-nitro-*t*-4-trinitromethyl-1,4-dihydronaphthalene (75) on Silica Gel

The adduct (75) (30 mg) was adsorbed onto a silica gel Chromatotron plate and then eluted with first pentane and then pentane/ether mixtures. The identified materials eluted were in elution order:

Recovered adduct (75) (7 mg), identical with authentic material, above.

1,4,6,7-Tetramethyl-2-trinitromethyl-1,2-dihydronaphthalen-1-ol (84) (3.3 mg), m.p. 102° (dec.) (Insufficient for elemental analysis; Found: $M^{+\bullet}$ 351.10611. $C_{15}H_{17}N_3O_7$ requires 351.10665). ν_{max} (KBr) 3590, 1620, 1593 cm^{-1}. ^1H n.m.r. ($CDCl_3$) δ 1.69, s, 1-Me; 2.11, d, $J_{4\text{-Me},H3}$ 1.5 Hz, 4-Me; 2.26, s, 6-Me; 2.29, s, 7-Me; 2.45, br s, OH; 4.38, d, $J_{H2,H3}$ 5.9 Hz, H2; 5.63, dq, $J_{H3,H2}$ 5.9 Hz, $J_{H3,4\text{-Me}}$ 1.5 Hz, H3; 7.03, s, H5; 7.25, s, H8. N.O.e. experiments gave the following results: irradiation at δ 1.69 gave enhancements at δ 4.38 (12.8%) and at δ 7.25 (4.7%); irradiation at δ 2.11 gave enhancements at δ 5.63 (6.4%) and at δ 7.03 (9.5%); irradiation at δ 4.38 gave enhancements at δ 1.69 (1.2%) and at δ 5.63 (4.6%); irradiation at δ 5.63 gave enhancements at δ 2.11 (1.1%) and at δ 4.38 (4.3%); irradiation at δ 7.03 gave enhancements at δ 2.11 (1.7%) and at δ 2.26 (1.2%); irradiation at δ 7.25 gave enhancements at δ 1.69 (0.4%) and at δ 2.29 (1.2%). ^{13}C n.m.r. ($CDCl_3$) δ 19.6, 6-Me; 19.9, 7-Me; 20.0, 4-Me; 34.45, 1-Me; 49.3, C2; 72.8, C1; 112.65, C3; 124.7, C8; 125.6, C5; 128.0, C4a; 136.1, C7; 136.3, C8a; 138.6, C6; 140.6, C4; resonance for **C**$(NO_2)_3$ not observed. The above assignments were confirmed by long range

reverse detected heteronuclear correlation spectra (HMBC).

1,4,6,7-Tetramethyl-2-nitro-1,2-dihydronaphthalen-1-ol (85) (2.3 mg), m.p. 54° (dec.) (Insufficient for elemental analysis; Found: parent ion not visible, $M^{+\bullet}-H_2O$ 229.11054. $C_{14}H_{15}NO_2$ requires 229.11028). ν_{max} (KBr) 3378, 1548 cm^{-1}. ^1H n.m.r. ($CDCl_3$) δ 1.52, s, 1-Me; 2.14, br s, 4-Me; 2.28, s, 6-Me; 2.30, s, 7-Me; 2.94, s, OH; 4.99, d, $J_{H2,H3}$ 6.3 Hz, H2; 5.88, dq, $J_{H3,H2}$ 6.3 Hz, $J_{H3,4\text{-}Me}$ 1.4 Hz, H3; 7.09, s, H5; 7.41, s, H8. N.O.e. experiments gave the following results: irradiation at δ 1.52 gave enhancements at δ 4.99 (9.0%) and at δ 7.41 (4.0%); irradiation at δ 2.14 gave enhancements at δ 5.88 (5.4%) and at δ 7.09 (8.0%); irradiation at δ 4.99 gave enhancements at δ 1.52 (0.9%) and at δ 5.88 (3.7%); irradiation at δ 5.88 gave enhancements at δ 2.14 (0.7%) and at δ 4.99 (3.6%); irradiation at δ 7.09 gave enhancements at δ 2.14 (1.2%) and at δ 2.28 (0.9%); irradiation at δ 7.41 gave enhancements at δ 1.52 (0.5%) and at δ 2.30 (0.9%). ^{13}C n.m.r. ($CDCl_3$) δ 19.5, 4-Me; 19.55, 6-Me; 19.8, 7-Me; 28.7, 1-Me; 72.3, C1; 89.7, C2; 115.5, C3; 124.7, C8; 126.1, C5; 128.8, C4a; 135.9, C7; 138.1, C8a; 138.3, C6; 140.3, C4. The above assignments were confirmed by long range reverse detected heteronuclear correlation spectra (HMBC).

1,4,6,7-Tetramethyl-1,2-dihydronaphthalene-r-*1*,c-*2-diol* (86) (6.7 mg), m.p. 98-98.5° (X-ray crystal structure determined, see Section 5.5). ν_{max} (KBr) 3291 cm^{-1}. ^1H n.m.r. ($CDCl_3$) δ 1.38, s, 1-Me; 2.08, d, $J_{4\text{-}Me,\ H3}$ 1.5 Hz, 4-Me; 2.26, s, 6-Me; 2.29, s, 7-Me; 3.84, d, $J_{H2,H3}$ 5.9 Hz, H2; 5.93, dq, $J_{H3,H2}$ 5.9 Hz, $J_{H3,\ 4\text{-}Me}$ 1.5 Hz, H3; 7.04, s, H5; 7.49, s, H8. N.O.e. experiments gave the following results: irradiation at δ 1.38 gave enhancements at δ 3.84 (6.3%) and at δ 7.49 (3.8%); irradiation at δ 2.08 gave enhancements at δ 5.93 (5.2%) and at δ 7.04 (8.9%); irradiation at δ 3.84 gave enhancements at δ 1.38 (0.9%) and at δ 5.93 (4.0%); irradiation at δ 5.93 gave enhancements at δ 2.08 (0.9%) and at δ 3.84

(2.6%); irradiation at δ 7.04 gave enhancements at δ 2.08 (1.2%) and at δ 2.26 (0.9%); irradiation at δ 7.49 gave enhancements at δ 1.38 (0.5%) and at δ 2.29 (0.9%). ^{13}C n.m.r. ($CDCl_3$) δ 19.3, 4-Me; 19.55, 6-Me; 19.7, 7-Me; 26.4, 1-Me; 71.7, C2; 73.05, C1; 123.5, C3; 125.3, C5; 126.8, C8; 129.7, C4; 135.3, C7; 135.4, C4a; 137.2, C6; 139.0, C8a. The above assignments were confirmed by long range reverse detected heteronuclear correlation spectra (HMBC).

5.2.1.3 Photonitration of 1,4,6,7-Tetramethylnaphthalene (56) in Dichloromethane Containing Trifluoroacetic Acid

Reaction of 1,4,6,7-tetramethylnaphthalene (56) (0.34 mol L^{-1}) and tetranitromethane (0.68 mol L^{-1}) in dichloromethane containing trifluoroacetic acid (0.68 mol L^{-1}) at +20°, as above, for 2 h gave a product which was shown by ^1H n.m.r. spectral analysis (Table 2.3) to be a mixture of 2,3,5,8-tetramethyl-1-nitronaphthalene (79) (32%), 1,4,6,7-tetramethyl-2-nitronaphthalene (80) (48%) and 4,6,7-trimethyl-1-nitromethylnaphthalene (81) (6%).

5.2.1.4 Rearrangement of 1,4,6,7-Tetramethyl-*r*-1-nitro-*t*-4-trinitromethyl-1,4-dihydronaphthalene (75) in (D)Chloroform

A solution of the adduct (75) (20 mg) in (D)chloroform (0.6 mL) was stored at +20° in the dark and the ^1H n.m.r. spectrum monitored at appropriate time intervals (Table 2.4). The major products of the rearrangement after 12 days were identified from comparison of their ^1H n.m.r. spectra as 4,6,7-trimethyl-1-(2',2',2'-trinitroethyl)-naphthalene (78) (73%) and 4,6,7-trimethyl-1-nitromethylnaphthalene (81) (7%). In the early stages of the rearrangement it was clear that epimerization of adduct (75)

was occurring to give 1,4,6,7-tetramethyl-*r*-1-nitro-*c*-4-trinitromethyl-1,4-dihydronaphthalene (76), equilibrium being approached after 8 h [(75):(76) ratio *c.* 5:1]. Subsequently two further adducts were formed tentatively identified from their ^{1}H n.m.r. spectra as 2,3,5,8-tetramethyl-*r*-1-nitro-*c*-4-trinitromethyl-1,4-dihydronaphthalene (77) (after 5 days), above, and 1,4,6,7-tetramethyl-*t*-2-nitro-*r*-1-trinitromethyl-1,2-dihydronaphthalene (87) (after 4 h): ^{1}H n.m.r. ($CDCl_3$) δ 2.08, s, 1-Me; 2.09, d, $J_{4\text{-Me, H3}}$ 1.3 Hz, 4-Me; 2.33 and 2.35, both s, 6-Me, 7-Me; 5.61, d, $J_{H2,H3}$ 6.1 Hz, H2; 5.72, dq, $J_{H3,H2}$ 6.1 Hz, $J_{H3,4\text{-Me}}$ 1.3 Hz, H3; 7.13 and 7.21, both s, H5, H8.

5.2.1.5 Rearrangement of 1,4,6,7-Tetramethyl-*r*-1-nitro-*t*-4-trinitromethyl-1,4-dihydronaphthalene (75) in Acetonitrile

A quantitative study of the progess of this reaction was not possible because of the limited solubility of the adduct (75) in acetonitrile. Initially a slurry of the adduct (75) (110 mg) in acetonitrile (11 mL) was stirred at +20° in the dark and aliquots of the solution were removed at appropriate time intervals. The solvent was removed rapidly (<30 s) from each sample under reduced pressure at ≤0°, and the composition of the residue determined from ^{1}H n.m.r. spectra. The reaction of adduct (75) in acetonitrile was rapid, being essentially complete in 4 h [c.f. 9 days in (D)chloroform] and gave predominantly different products. In acetonitrile after 4 h the rearrangment of (75) yielded mainly the nitro aromatic compounds 2,3,5,8-tetramethyl-1-nitronaphthalene (79) (14%), 1,4,6,7-tetramethyl-2-nitronaphthalene (80) (52%) and 4,6,7-trimethyl-1-nitromethylnaphthalene (81) (27%), these compounds being identified by comparison with the ^{1}H n.m.r. spectra of authentic samples; the 4,6,7-trimethyl-1-(2',2',2'-trinitroethyl)-naphthalene (78) (1%) was only a minor product in this rearrangement, with unidentified aromatic products (total 6%)

accounting for the remainder of the rearrangement products. Apart from rapid (after 1 min.) epimerization of adduct (75) to give (76), adducts (84), (85), and two unidentified adducts could be detected in the ^{1}H n.m.r. spectrum at that time, and 2,3,5,8-tetramethyl-*r*-1-nitro-*c*-4-trinitromethyl-1,4-dihydronaphthalene (77) was detectable at reaction times between 3 min. and 2 h, reaching a maximum level (3%) after 40 min.

5.2.2 GENERAL PROCEDURE FOR THE PHOTONITRATION OF 2,6-DIMETHYLNAPHTHALENE (57) WITH TETRANITROMETHANE.

A solution of 2,6-dimethylnaphthalene (57) (500 mg, 0.4 mol L^{-1}) and tetranitromethane (0.8 mol L^{-1}) in dichloromethane or acetonitrile was irradiated at +20 or -20° with filtered light ($\lambda_{cut\text{-}off}$<435 nm). Aliquots were withdrawn from the reaction mixture at appropriate time intervals, the volatile material removed under reduced pressure at ≤0°, and the product composition determined by ^{1}H n.m.r. spectral analysis (Tables 2.6 and 2.7).

5.2.2.1 Photonitration of 2,6-Dimethylnaphthalene (57) in Dichloromethane

Photochemistry in dichloromethane at +20° and the identification of the adducts (94)-(104).

Reaction of 2,6-dimethylnaphthalene (57) / tetranitromethane in dichloromethane at +20°, as above, for 2 h gave a product which was shown by ^{1}H n.m.r. spectral analysis (Table 2.6) to be a mixture of adducts (total 79%), 2,6-dimethyl-1-nitronaphthalene (106) (16%) and other minor nitro aromatic compounds (total 3%). The adducts were partially separated by h.p.l.c. and gave in elution order:

trans-3,7-Dimethyl-2-nitro-1-trinitromethyl-1,2-dihydronaphthalene (94) , isolated only in admixture with adduct (95) below. ^{1}H n.m.r. ($CDCl_3$) δ 2.05, d, $J_{Me,H4}$ 1.5 Hz, 3-Me; 2.32, s, 7-Me; 5.41, d, $J_{H2,H1}$ 1.4 Hz, H2; 5.67, br s, H1; 6.53, d, $J_{H4,Me}$ 1.5 Hz, H4; 6.95, br s, H8; 7.05, d, $J_{H5,H6}$ 7.8 Hz, H5; 7.21, br d, $J_{H6,H5}$ 7.8 Hz, H6. The structure and stereochemistry of this adduct is confirmed by its coversion into the nitro cycloadduct, the structure of which is determined below by X-ray crystallography.

trans-*2,6-Dimethyl-1-nitro-4-trinitromethyl-1,4-dihydronaphthalene* (95), m.p. 104° (dec.) (X-ray crystal structure determined, see Section 5.5). ν_{max} (KBr) 1620, 1592, 1568 cm^{-1}. ^{1}H n.m.r. ($CDCl_3$) δ 1.97, d, $J_{Me,H3}$ 1.5 Hz, 2-Me; 2.36, s, 6-Me; 5.35, br s, H4; 6.13, br s, H1; 6.29, dq, $J_{H3,H4}$ 3.0 Hz, $J_{H3,Me}$ 1.5 Hz, H3; 7.11, br s, H5; 7.30-7.31, m, H7, H8. N.O.e. experiments gave the following results: irradiation at δ 1.97 gave enhancements at δ 6.13 (3.4%) and at δ 6.29 (4.5%); irradiation at δ 5.35 gave enhancements at δ 6.29 (5.1%) and at δ 7.11 (3.7%); irradiation at δ 6.29 gave enhancements at δ 1.97 (1.1%) and at δ 5.35 (3.4%). ^{13}C n.m.r. ($CDCl_3$) δ 20.1, 2-Me; 21.2, 6-Me; 45.4, C4; 87.0, C1; 119.2, C3; 124.2, C4a; 126.9, C8; 128.4, C5; 129.1, C8a; 131.5, C7; 138.1, C2; 140.9, C6; resonance for **C**$(NO_2)_3$ not observed. The above assignments were confirmed by long range reverse detected heteronuclear correlation spectra (HMBC).

trans-3,7-Dimethyl-1-nitro-4-trinitromethyl-1,4-dihydronaphthalene (96) , m.p. 185° (dec.) (crystals of inadequate quality for single crystal X-ray analysis; insufficient for elemental analysis; parent ion not visible in mass spectrum). ν_{max} (KBr) 1620, 1590 cm^{-1}. ^{1}H n.m.r. ($CDCl_3$) δ 2.11, m, 3-Me; 2.37, s, 7-Me; 5.33, br s, H4; 6.18, m, H1; 6.29, m, H2; 7.21-7.22, m, H5, H6, H8. N.O.e. experiments gave the following results: irradiation at δ 2.11 gave enhancements at δ 5.33 (4.1%) and at δ 6.29 (5.1%); irradiation at δ 5.33 gave enhancements at δ 2.11 (0.7%) and at δ 7.21 (1.6%);

irradiation at δ 6.29 gave enhancements at δ 2.11 (0.7%) and at δ 6.18 (1.6%). ^{13}C n.m.r. ($CDCl_3$) δ 21.2, 7-Me; 23.8, 3-Me; 49.5, C4; 83.6, C1; 122.4, C4a; 126.6, C6; 128.7, C2; 129.1, C5; 131.0, C8; 131.2, C8a; 132.1, C3; 141.0, C7; resonance for **C**$(NO_2)_3$ not observed. The above assignments were confirmed by long range reverse detected heteronuclear correlation spectra (HMBC).

cis-*2,6-Dimethyl-1-nitro-4-trinitromethyl-1,4-dihydronaphthalene* (97), m.p. 134-136° (X-ray crystal structure determined, see Section 5.5). ν_{max} (KBr) 1647, 1599, 1578, 1554 cm^{-1}. ^1H n.m.r. ($CDCl_3$) δ 2.08, br s, 2-Me; 2.37, s, 6-Me; 5.30, br s, H4; 5.78, d, $J_{H1,H4}$ 2.4 Hz, H1; 6.47, dq, $J_{H3,H4}$ 4.9 Hz, $J_{H3,Me}$ 1.5 Hz, H3; 6.97, br s, H5; 7.34, br d, $J_{H7,H8}$ 7.8 Hz, H7; 7.70, d, $J_{H8,H7}$ 7.8 Hz, H8. N.O.e. experiments gave the following results: irradiation at δ 2.08 gave enhancements at δ 5.78 (4.3%) and at δ 6.47 (5.5%); irradiation at δ 5.30 gave enhancements at δ 6.47 (3.7%) and at δ 6.97 (3.4%); irradiation at δ 5.78 gave enhancements at δ 2.08 (0.7%) and at δ 7.70 (3.1%); irradiation at δ 6.47 gave enhancements at δ 2.08 (0.6%) and at δ 5.30 (2.9%). ^{13}C n.m.r. ($CDCl_3$) δ 21.4, 6-Me; 22.5, 2-Me; 44.9, C4; 85.3, C1; 121.4, C3; 126.2, C8a; 127.4, C4a; 128.0, C7; 131.0, C5; 131.5, C8; 137.2, C2; 141.2, C6; resonance for **C**$(NO_2)_3$ not observed. The above assignments were confirmed by long range reverse detected heteronuclear correlation spectra (HMBC).

cis-2,6-Dimethyl-4-trinitromethyl-1,4-dihydronaphthalen-1-ol (98), m.p. 108-110° (crystals of inadequate quality for single crystal X-ray analysis; insufficient for elemental analysis; parent ion not visible in mass spectrum). ν_{max} (KBr) 3416, 1618, 1598 cm^{-1}. ^1H n.m.r. ($CDCl_3$) δ 2.02, br s, 2-Me; 2.34, s, 6-Me; 4.79, br d, $J_{H1,OH}$ 9.7 Hz, H1; 5.16, br s, H4; 6.02, dq, $J_{H3,H4}$ 4.4 Hz, $J_{H3,Me}$ 1.5 Hz, H3; 6.95, br s, H5; 7.29, br d, $J_{H7,H8}$ 7.8 Hz, H7; 7.48, d, $J_{H8,H7}$ 7.8 Hz, H8.

cis-3,7-Dimethyl-1-nitro-4-trinitromethyl-1,4-dihydronaphthalene (99),

an impure oil isolated only in small quantity. ^{1}H n.m.r. ($CDCl_3$) δ 2.10, s, 3-Me; 2.43, s, 7-Me; 5.40, br s, H4; 5.82, d, $J_{H1,H2}$ 6.3 Hz, H1; 6.48, dq, $J_{H2,H1}$ 6.3 Hz, $J_{H2,Me}$ 1.5 Hz, H2; 7.07, d, $J_{H5,H6}$ 7.9 Hz, H5; 7.24, br d, $J_{H6,H5}$ 7.9 Hz, H6; 7.46, br s, H8.

Nitro Cycloadduct (100), isolated only in small quantity and in admixture with the major nitro cycloadduct (101). ^{1}H n.m.r. ($CDCl_3$) δ 1.94, s, 3-Me; 2.33, s, 7-Me; 5.29, d, $J_{H4,H2}$ 2.4 Hz, H4; 5.62, d, $J_{H1,H2}$ 6.3 Hz, H1; 5.66, dd, $J_{H2,H1}$ 6.3 Hz, $J_{H2,H4}$ 2.4 Hz, H2; 7.07, br s, H8; 7.17, br d, $J_{H6,H5}$ 7.8 Hz, H6; 7.25, d, $J_{H5,H6}$ 7.8 Hz, H5. N.O.e. experiments gave the following results: irradiation at δ 1.94 gave enhancements at δ 5.29 (5.6%) and at δ 5.66 (2.1%); irradiation at δ 2.33 gave enhancements at δ 7.07 (3.8%) and at δ 7.25 (2.5%); irradiation at δ 5.64 gave enhancements at δ 1.94 (1.3%) and at δ 7.07 (3.9%). ^{13}C n.m.r. ($CDCl_3$) δ 21.3, 7-Me; 23.5, 3-Me; 48.1, C4; 79.1, C2; 82.3, C1; 87.1, C3; 127.9, C8a; 128.5, C8; 131.41, 131.44, C5, C6; 133.3, C4a; 141.0, C7; resonance for **C**$(NO_2)_3$ not observed. The above assignments were confirmed by long range reverse detected heteronuclear correlation spectra (HMBC).

Nitro Cycloadduct (101), m.p. 169° (dec.) (X-ray crystal structure determined, see Section 5.5). ν_{max} (KBr) 1588, 1556 cm^{-1}. ^{1}H n.m.r. ($CDCl_3$) δ 2.07, s, 2-Me; 2.33, s, 6-Me; 5.17, d, $J_{H4,H3}$ 4.0 Hz, H4; 5.19, s, H1; 5.64, d, $J_{H3,H4}$ 4.0 Hz, H3; 7.06, br s, H5; 7.19, br d, $J_{H7,H8}$ 7.8 Hz, H7; 7.22, d, $J_{H8,H7}$ 7.8 Hz, H8. N.O.e. experiments gave the following results: irradiation at δ 2.07 gave enhancements at δ 5.19 (5.4%) and at δ 5.64 (3.8%); irradiation at δ 2.33 gave enhancements at δ 7.06 (4.0%) and at δ 7.19 (1.9%), irradiation at δ 5.18 gave enhancements at δ 2.07 (1.6%), at δ 5.64 (5.3%), at δ 7.06 (4.6%), and at δ 7.22 (2.6%); irradiation at δ 5.64 gave enhancements at δ 2.07 (1.1%) and at δ 5.17 (2.8%). ^{13}C n.m.r. ($CDCl_3$) δ 19.3, 2-Me; 21.3, 6-Me; 46.2, C4; 84.1, C3; 85.7, C1; 86.3, C2; 125.9, C8a; 127.9, C8; 131.61, C5; 131.64, C7; 132.5, C4a; 141.6, C6;

resonance for **C**$(NO_2)_2$ not observed. The above assignments were confirmed by long range reverse detected heteronuclear correlation spectra (HMBC).

trans-3,7-Dimethyl-1-trinitromethyl-1,2-dihydronaphthalen-2-ol (102), an oil isolated only in admixture with the hydroxy cycloadduct (104), below. ^{1}H n.m.r. ($CDCl_3$) δ 1.91, d, $J_{Me,H4}$ 1.5 Hz, 3-Me; 2.31, s, 7-Me; 4.58, br s, H1; 4.78, br s, H2; 6.23, d, $J_{H4,Me}$ 1.5 Hz, H4; 6.94, br s, H8; 7.02, d, $J_{H5,H6}$ 7.8 Hz, H5; 7.19, br d, $J_{H6,H5}$ 7.8 Hz, H6.

trans-2,6-Dimethyl-4-trinitromethyl-1,4-dihydronaphthalen-1-ol (103), m.p. 75° (dec.), isolated in small quantity with crystals of inadequate quality for single crystal X-ray analysis, parent ion not visible in mass spectrum. ν_{max} (KBr) 3452, 1599 cm^{-1}. ^{1}H n.m.r. ($CDCl_3$) δ 2.04, m, 2-Me; 2.34, s, 6-Me; 4.96, br s, H1; 5.19, br s, H4; 6.00, dq, $J_{H3,H4}$ 4.9 Hz, $J_{H3,Me}$ 1.0 Hz, H3; 7.02, br s, H5; 7.30, br d, $J_{H7,H8}$ 7.8 Hz, H7; 7.68, d, $J_{H8,H7}$ 7.8 Hz, H8.

Hydroxy cycloadduct (104), m.p. 183-184° (X-ray crystal structure determined, see Section 5.5). ν_{max} (KBr) 3415, 1618, 1580 cm^{-1}. ^{1}H n.m.r. ($CDCl_3$) δ 1.75, s, 2-Me; 2.38, s, 6-Me; 4.73, s, H4; 4.75, d, $J_{H3,OH}$ 3.9 Hz, H3; 4.93, s, H1; 7.18, br s, H5; 7.21-7.26, m, H7, H8. N.O.e. experiments gave the following results: irradiation at δ 1.75 gave enhancements at δ 4.75 (2.3%) and at δ 4.93 (6.7%); irradiation at δ 2.38 gave enhancements at δ 7.18 (3.7%) and at δ 7.21 (2.7%); irradiation at δ 4.93 gave enhancements at δ 1.75 (0.9%) and at δ 7.23 (2.9%). ^{13}C n.m.r. ($CDCl_3$) δ 16.9, 2-Me; 21.4, 6-Me; 48.8, C4; 70.6, C3; 84.7, C1; 87.7, C2; 127.9, C8; 128.5, C8a; 130.6, C5; 132.2, C4a; 132.7, C7; 141.2, C6; resonance for **C**$(NO_2)_2$ not observed. The above assignments were confirmed by long range reverse detected heteronuclear correlation spectra (HMBC).

Photochemistry in dichloromethane at -20° and the identification of some of the aromatic products (105)-(107).

Reaction of 2,6-dimethylnaphthalene (57) / tetranitromethane in dichloromethane at -20°, as above, for 3 h gave a product which was shown by ^{1}H n.m.r. spectra to be a mixture (Table 2.6) of adducts (total 15%), 3,7-dimethyl-1-trinitromethylnaphthalene (105) (2%), 2,6-dimethyl-1-nitro-naphthalene (106) (55%), 3,7-dimethyl-1-nitronaphthalene (107) (8%),and other unidentified nitro aromatic compounds (20%). Chromatography of this mixture on a silica gel Chromatotron plate gave, in order of elution:

3,7-Dimethyl-1-trinitromethylnaphthalene (105), m.p. 108° (dec.) (Insufficient for elemental analysis, Found: $M^{+\bullet}$ 305.0652. $C_{13}H_{11}N_3O_6$ requires 305.0648). ν_{max} (KBr) 1617, 1593, and 1576 cm^{-1}. ^{1}H n.m.r. ($CDCl_3$) δ 2.47, s, 7-Me; 2.54, s, 3-Me; 7.02, br s, H8; 7.36, d, $J_{H2,H4}$ 1.5 Hz, H2; 7.42, dd, $J_{H6,H5}$ 8.3 Hz, $J_{H6,H8}$ 1.5 Hz, H6; 7.80, d, $J_{H5,H6}$ 8.3 Hz, H5; 7.93, br s, H4. N.O.e. experiments gave the following results: irradiation at δ 2.47 gave enhancements at δ 7.02 (4.7%) and at δ 7.42 (4.0%); irradiation at δ 2.54 gave enhancements at δ 7.36 (4.8%) and at δ 7.93 (2.4%); irradiation at δ 7.02 gave an enhancement at δ 2.47 (0.5%); irradiation at δ 7.39 gave enhancements at δ 2.47 (0.5%), at δ 2.54 (0.5%) and at δ 7.80 (5.3%); irradiation at δ 7.80 gave enhancements at δ 7.42 (5.9%) and at δ 7.93 (3.3%); irradiation at δ 7.93 gave enhancements at δ 2.54 (0.5%) and at δ 7.80 (2.5%).

2,6-Dimethyl-1-nitronaphthalene (106), m.p. 66.5-67° (Lit.[3] 67-67.5°). ν_{max} (KBr) 1612, 1518 cm^{-1}. ^{1}H n.m.r. ($CDCl_3$) δ 2.47, s, 2-Me; 2.50, s, 6-Me; 7.29, d, $J_{H3,H4}$ 8.3 Hz, H3; 7.41, dd, $J_{H7,H8}$ 8.8 Hz, $J_{H7,H5}$ 2.0 Hz, H7; 7.61, br s, H5; 7.61, d, $J_{H8,H7}$ 8.8 Hz, H8; 7.76, d, $J_{H4,H3}$ 8.3 Hz, H4. N.O.e. experiments gave the following results: irradiation at δ 7.29 gave enhancements at δ 7.76 (5.4%) and at δ 2.47 (0.7%); irradiation at δ 7.41 gave enhancements at δ 7.61 (4.6%) and at δ 2.50 (0.5%); irradiation at

δ 7.61 gave enhancements at δ 7.76 (1.8%), at δ 7.41 (7.9%), and at δ 2.50 (0.8%); irradiation at δ 7.76 gave enhancements at δ 7.61 (1.5%) and at δ 7.29 (7.0%).

3,7-Dimethyl-1-nitronaphthalene (107), m.p. 80-81° (Lit.[3] 83-84°). ν_{max} (KBr) 1615, 1518 cm^{-1}. ^1H n.m.r. ($CDCl_3$) δ 2.55, s, 3-Me; 2.56, s, 7-Me; 7.41, dd, $J_{H6,H5}$ 8.3 Hz, $J_{H6,H8}$ 1.4 Hz, H6; 7.75, d, $J_{H5,H6}$ 8.3 Hz, H5; 7.84, br s, H4; 8.05, d, $J_{H8,H6}$ 1.4 Hz, H8; 8.29, d, $J_{H4,H2}$ 1.0 Hz, H2. N.O.e. experiments gave the following results: irradiation at δ 7.41 gave enhancements at δ 7.75 (3.9%) and at δ 2.56 (0.2%); irradiation at δ 7.75 gave enhancements at δ 7.84 (1.6%) and at δ 7.41 (5.1%); irradiation at δ 7.84 gave enhancements at δ 7.75 (1.5%), and at δ 2.55 (0.1%); irradiation at δ 8.05 gave an enhancement at δ 2.56 (0.1%); irradiation at δ 8.29 gave an enhancement at δ 2.55 (0.2%).

5.2.2.2 Thermal Cycloaddition of *trans*-3,7-Dimethyl-2-nitro-1-trinitromethyl-1,2-dihydronaphthalene (94) in (D)Chloroform

A solution of a mixture of the nitro trinitromethyl adduct [(94); 29%] and *trans*-2,6-dimethyl-1-nitro-4-trinitromethyl-1,4-dihydronaphthalene [(95); 71%] in (D)chloroform was stored at +22° in the dark and the ^1H n.m.r. spectrum monitored at appropriate time intervals. The nitro trinitromethyl adduct (94) was slowly transformed (half-life 96 h) into the nitro cycloadduct (101). The *trans*-2,6-dimethyl-1-nitro-4-trinitromethyl-1,4-dihydronaphthalene (95) was unchanged during the duration of the experiment. The nitro cycloadduct (101), isolated by h.p.l.c., was identical with an authentic sample, see above.

5.2.2.3 Thermal Cycloaddition of *trans*-3,7-Dimethyl-1-trinitromethyl-1,2-dihydronaphthalen-2-ol (102) in (D)Chloroform

A solution of a mixture of the hydroxy trinitromethyl adduct [(102); 80%] and the hydroxy cycloadduct [(104); 20%] in (D)chloroform was stored at +22° in the dark and the ^{1}H n.m.r. spectrum monitored at appropriate time intervals. The hydroxy trinitromethyladduct (102) was transformed into the hydroxy cycloadduct (104) with a half-life estimated to be *c.* 13 h, the measurements being complicated by the precipitation of the hydroxy cycloadduct (104) during the period of the observations. After 170 h the ^{1}H n.m.r. spectrum obtained was essentially that of the pure hydroxy cycloadduct (104), above.

5.2.3 GENERAL PROCEDURE FOR THE PHOTONITRATION OF 1,3-DIMETHYLNAPHTHALENE (58) WITH TETRANITROMETHANE.

A solution of 1,3-dimethylnaphthalene (58) (500 mg, 0.4 mol L^{-1}) and tetranitromethane (0.8 mol L^{-1}) in dichloromethane (at +20, 0, or -20°) or acetonitrile (+20 or -20°) was irradiated with filtered light ($\lambda_{cut\text{-}off}$<435 nm). Aliquots were withdrawn from the reaction mixture at appropriate time intervals, the volatile material removed under reduced pressure at ≤0°, and the product composition determined by ^{1}H n.m.r. spectral analysis (Tables 2.8 and 2.9).

5.2.3.1 Photonitration of 1,3-Dimethylnaphthalene (58) in Dichloromethane

Photochemistry in dichloromethane at +20° and the identification of adducts (110)-(116).

Reaction of 1,3-dimethylnaphthalene (58) / tetranitromethane in dichloromethane at +20°, as above, for 2 h gave a product which was shown by ^{1}H n.m.r. spectral analysis (Table 2.8) to be a mixture of *trans*-5,7-dimethyl-2-nitro-1-trinitromethyl-1,2-dihydronaphthalene (110) (10%), *trans*-6,8-dimethyl-1-nitro-4-trinitromethyl-1,4-dihydronaphthalene (111) (8.5%), the nitro cycloadduct (112) (4.5%), *cis*-6,8-dimethyl-1-nitro-4-trinitromethyl-1,4-dihydronaphthalene (113) (10.5%), and three further adducts (114) (1%), (115) (2%) and (116) (6%) which were identified tentatively from their ^{1}H n.m.r. spectra, 6,8-dimethyl-2-trinitromethylnaphthalene (117) (2.5%), 5,7-dimethyl-1-trinitromethylnaphthalene (118) (10%), and 2,4-dimethyl-1-nitronaphthalene (119) (38%). The adducts were partially separated by h.p.l.c. and gave the following in elution order:

trans-5,7-Dimethyl-2-nitro-1-trinitromethyl-1,2-dihydronaphthalene (110) as an impure oil. ^{1}H n.m.r. ($CDCl_3$) δ 2.29, s, 7-Me; 2.34, s, 5-Me; 5.66, dd, $J_{H2,H3}$ 6.8 Hz, $J_{H2,H1}$ 1.0 Hz, H2; 5.70, br s, H1; 5.98, ddd, $J_{H3,H4}$ 9.8 Hz, $J_{H3,H2}$ 6.8 Hz, $J_{H3,H1}$ 1.0 Hz, H3; 6.81, br s, H8; 7.04, d, $J_{H4,H3}$ 9.8 Hz, H4; 7.08, br s, H6. N.O.e. experiments gave the following results: irradiation at δ 2.29 gave enhancements at δ 6.81 (3.5%) and at δ 7.08 (3.7%); irradiation at δ 2.34 gave enhancements at δ 7.04 (8.0%) and at δ 7.08 (5.3%); irradiation at δ 5.66 gave enhancements at δ 5.98 (5.7%) and at δ 6.81 (4.7%); irradiation at δ 5.98 gave enhancements at δ 5.66 (5.4%) and at δ 7.04 (5.6%); irradiation at δ 6.81 gave enhancements at δ 2.29 (0.6%) and at δ 5.70 (4.5%). ^{13}C n.m.r. ($CDCl_3$) δ 18.8, 5-Me; 21.2, 7-Me; 43.8, C1; 76.1, C2; 114.9, C3; 120.1, C8a; 127.7, C4a; 128.4, C8;

131.6, C4; 134.3, C6; 136.0, C5; 140.5, C7; resonance for **C**$(NO_2)_3$ not observed. The above assignments were confirmed by long range reverse detected heteronuclear correlation spectra (HMBC). The structure of the nitro trinitromethyl adduct (110) was further confirmed by its thermal cycloaddition in (D)chloroform to give the nitro cycloadduct (122), the structure of which is established below.

trans-*6,8-Dimethyl-1-nitro-4-trinitromethyl-1,4-dihydronaphthalene* (111), m.p. 114.5-115.5° (X-ray crystal structure determined, see Section 5.5). ν_{max} (KBr) 1615, 1594, 1576, 1558 cm^{-1}. ^1H n.m.r. ($CDCl_3$) δ 2.23, s, 8-Me; 2.34, s, 6-Me; 5.39, br s, H4; 6.20, br s, H1; 6.56, m, H3: 6.57, m, H2; 6.98, s, H5; 7.17, s, H7. N.O.e. experiments gave the following results: irradiation at δ 2.23 gave enhancements at δ 6.20 (7.2%) and at δ 7.17 (6.6%); irradiation at δ 2.34 gave enhancements at δ 6.98 (5.3%) and at δ 7.17 (5.0%); irradiation at δ 5.39 gave enhancements at δ 6.56 (3.0%) and at δ 6.98 (4.8%); irradiation at δ 6.20 gave enhancements at δ 2.23 (1.5%) and at δ 6.57 (2.8%); irradiation at δ 6.98 gave enhancements at δ 2.34 (1.4%) and at δ 5.39 (4.7%). ^{13}C n.m.r. ($CDCl_3$) δ 19.2, 8-Me; 21.15, 6-Me; 44.7, C4; 82.4, C1; 124.5, C2; 125.2, C4a; 125.55, C8a; 126.3, C5; 131.1, C3; 133.7, C7; 138.9, C8; 140.7, C6; resonance for **C**$(NO_2)_3$ not observed. The above assignments were confirmed by long range reverse detected heteronuclear correlation spectra (HMBC).

Nitro cycloadduct (112), m.p. 179.5-180.5° (X-ray crystal structure determined, see Section 5.5). ν_{max} (KBr) 1595, 1552 cm^{-1}. ^1H n.m.r. ($CDCl_3$) δ 1.90, s, 3-Me; 2.02, s, 1-Me; 5.23, d, $J_{H2,H4}$ 2.5 Hz, H2; 5.32, d, $J_{H4,H2}$ 2.5 Hz, H4; 7.31-7.41, m, H5-H8. N.O.e. experiments gave the following results: irradiation at δ 1.90 gave enhancements at δ 5.23 (3.9%) and at δ 5.32 (4.9%); irradiation at δ 2.02 gave enhancements at δ 5.23 (7.5%) and at δ 7.35 (3.8%); irradiation at δ 5.23 gave enhancements at δ 1.90 (0.4%) and at δ 2.02 (0.5%); irradiation at δ 5.32 gave

enhancements at δ 1.90 (0.4%) and at δ 7.37 (1.1%). ^{13}C n.m.r. ($CDCl_3$) δ 20.7, 1-Me; 23.2, 3-Me; 48.6, C4; 84.4, C2; 88.0, C1; 88.6, C3; 129.3, C4a; 136.9, C8a; 124.05, 130.2, 130.5, 131.7, C5, C6, C7, C8; resonance for **C**$(NO_2)_3$ not observed. The above assignments were confirmed by long range reverse detected heteronuclear correlation spectra (HMBC).

cis-*6,8-Dimethyl-1-nitro-4-trinitromethyl-1,4-dihydronaphthalene* (113), m.p. 129.0° (dec.) (X-ray crystal structure determined, see Section 5.5). ν_{max} (KBr) 1616, 1601, 1572, 1547 cm^{-1}. ^1H n.m.r. ($CDCl_3$) δ 2.32, s, 8-Me; 2.35, s, 6-Me; 5.34, br s, H4; 6.01, dd, $J_{H1,H2}$ 5.9 Hz, $J_{H1,H4}$ 2.7 Hz, H1; 6.62, ddd, $J_{H3,H2}$ 10.2 Hz, $J_{H3,H4}$ 4.8 Hz, $J_{H3,H1}$ 1.0 Hz, H3; 6.85, ddd, $J_{H2,H3}$ 10.2 Hz, $J_{H2,H1}$ 5.9 Hz, $J_{H2,H4}$ 1.0 Hz, H2; 6.90, s, H5; 7.23, s, H7. N.O.e. experiments gave the following results: irradiation at δ 2.33 gave enhancements at δ 6.01 (7.2%), at δ 6.90 (4.8%) and at δ 7.23 (8.7%); irradiation at δ 5.34 gave enhancements at δ 6.62 (4.7%) and at δ 6.90 (4.5%); irradiation at δ 6.01 gave enhancements at δ 2.32 (1.8%) and at δ 6.85 (4.6%); irradiation at δ 6.62 gave enhancements at δ 5.34 (4.4%) and at δ 6.85 (7.8%); irradiation at δ 7.23 gave enhancements at δ 2.32 (1.2%) and at δ 2.35 (0.9%). ^{13}C n.m.r. ($CDCl_3$) δ 19.4, 8-Me; 21.2, 6-Me; 45.0, C4; 79.1, C1; 124.6, C8a; 125.7, C2; 126.8, C5; 127.1, C4a; 130.4, C3; 133.6, C7; 140.7, C8; 141.2, C6; resonance for **C**$(NO_2)_3$ not observed. The above assignments were confirmed by long range reverse detected heteronuclear correlation spectra (HMBC).

trans-6,8-Dimethyl-2-trinitromethyl-1,2-dihydronaphthalen-1-ol (114), isolated only in low yield as an impure oil. ^1H n.m.r. ($CDCl_3$) δ 2.31, s, 6-Me; 2.34, s, 8-Me; 4.46, d, $J_{H2,H3}$ 5.9 Hz, H2; 5.20, br s, H1; 5.77, ddd, $J_{H3,H4}$ 9.8 Hz, $J_{H3,H2}$ 5.9 Hz, $J_{H3,H1}$ 2.0 Hz, H3; 6.85, dd, $J_{H4,H3}$ 9.8 Hz, $J_{H4,H2}$ 1.5 Hz, H4; 6.85, s, H5; 7.02, s, H7. N.O.e. experiments gave the following results: irradiation at δ 4.46 gave enhancements at δ 5.20 (1.7%) and at δ 5.77 (1.9%); irradiation at δ 5.20 gave enhancements at δ 2.34

(1.3%) and at δ 4.46 (1.9%); irradiation at δ 5.77 gave enhancements at δ 4.46 (2.5%) and at δ 6.85 (2.0%); irradiation at δ 6.85 gave enhancements at δ 2.31 (0.8%) and at δ 5.77 (3.6%); irradiation at δ 7.02 gave enhancements at δ 2.31 (0.8%) and at δ 2.34 (0.8%).

Hydroxy cycloadduct (115), m.p. 151-153° (insufficient for elemental analysis; parent ion not visible in mass spectrum; crystals were obtained by crystallization but were of inadequate quality for single crystal X-ray analysis). ν_{max} (KBr) 3565, 1603 cm^{-1}. ^1H n.m.r. ($CDCl_3$) δ 1.54, s, 3-Me; 1.92, s, 1-Me; 4.38, d, $J_{H2,H4}$ 3.0 Hz, H2; 4.82, d, $J_{H4,H2}$ 3.0 Hz, H4; 7.40-7.49, m, H5, H6, H7, H8. N.O.e. experiments gave the following results: irradiation at δ 1.54 gave enhancements at δ 4.38 (4.7%) and at δ 4.82 (5.7%); irradiation at δ 1.92 gave enhancements at δ 4.38 (7.9%) and at δ 7.43 (3.4%); irradiation at δ 4.38 gave enhancements at δ 1.54 (0.4%) and at δ 1.92 (0.6%); irradiation at δ 4.82 gave enhancements at δ 1.54 (0.6%) and at δ 7.46 (2.4%). ^{13}C n.m.r. ($CDCl_3$) δ 21.1, 1-Me; 24.1, 3-Me; 52.85, C4; 71.1, C3; 87.1, C1; 87.85, C2; 123.9, C6; 129.7, C5; 130.0, C7; 131.1, C4a; 132.2, C8; 137.5, C8a; resonance for **C**$(NO_2)_3$ not observed. The above assignments were confirmed by long range reverse detected heteronuclear correlation spectra (HMBC).

Finally, although *trans*-2,4-dimethyl-2-nitro-1-trinitromethyl-1,2-dihydronaphthalene (116) could not be isolated, it was detected through its ^1H n.m.r. spectrum in product mixtures. ^1H n.m.r. ($CDCl_3$) δ 2.07, d, $J_{4\text{-}Me,H3}$ 1.4 Hz, 4-Me; 2.09, s, 2-Me; 5.55, s, H1; 6.14, d, $J_{H3,4\text{-}Me}$ 1.4 Hz, H3; the remainder of the spectrum was obscured by other signals of the reaction mixture.

Photochemistry in dichloromethane at -20°and the identification of the aromatic products (117)-(119).

Reaction of 1,3-dimethylnaphthalene (58) / tetranitromethane in

dichloromethane at -20°, as above, for 2 h gave a product which was shown by ^{1}H n.m.r. spectral analysis (Table 2.8) to be a mixture of adducts (110) (1%), (111) (1.3%), (112) (0.5%), (113) (1.5%), (115) (0.2%) and (116) (3%) together with the aromatic compounds 6,8-dimethyl-2-trinitromethyl-naphthalene (117) (1%), 5,7-dimethyl-1-trinitromethylnaphthalene (118) (1%), and 2,4-dimethyl-1-nitronaphthalene (119) (89%). Chromatography of this mixture on a silica gel Chromatotron plate gave in elution order:

6,8-Dimethyl-2-trinitromethylnaphthalene (117), m.p. 73-74.5° (Insufficient for elemental analysis. Found: $M^{+\bullet}$ 305.06478. $C_{13}H_{11}N_3O_6$ requires 305.06478). ν_{max} (KBr) 1602, 1587 cm^{-1}. ^{1}H n.m.r. ($CDCl_3$) δ 2.53, s, 6-Me; 2.68, s, 8-Me; 7.34, br s, H7; 7.50, dd, $J_{H3,H4}$ 8.8 Hz, $J_{H3,H1}$ 1.9 Hz, H3; 7.56, br s, H5; 7.92, d, $J_{H4,H3}$ 8.8 Hz, H4; 8.26, d, $J_{H1,H3}$ 1.9 Hz, H1. N.O.e. experiments gave the following results: irradiation at δ 2.53 gave enhancements at δ 7.34 (3.5%) and at δ 7.56 (3.9%); irradiation at δ 2.68 gave enhancements at δ 7.34 (4.5%) and at δ 8.26 (8.4%); irradiation at δ 7.34 gave enhancements at δ 2.53 (0.3%) and at δ 2.68 (0.6%); irradiation at δ 7.53 gave enhancements at δ 2.53 (0.5%) and at δ 7.92 (9.5%); irradiation at δ 7.92 gave enhancements at δ 7.50 (7.0%) and at δ 7.56 (3.2%); irradiation at δ 8.26 gave an enhancement at δ 2.68 (1.0%).

5,7-Dimethyl-1-trinitromethylnaphthalene (118), m.p. 99.0° (dec.) (Insufficient for elemental analysis. Found: $M^{+\bullet}$ 305.06478. $C_{13}H_{11}N_3O_6$ requires 305.06478). ν_{max} (KBr) 1621, 1590 cm^{-1}. ^{1}H n.m.r. ($CDCl_3$) δ 2.44, s, 7-Me; 2.73, s, 5-Me; 6.92, br s, H8; 7.31, br s, H6; 7.55, dd, $J_{H3,H2}$ 7.0 Hz, $J_{H3,H4}$ 6.5 Hz, H3; 7.55, dd, $J_{H2,H3}$ 7.0 Hz, $J_{H2,H4}$ 1.8 Hz, H2; 8.37, dd, $J_{H4,H3}$ 6.5 Hz, $J_{H4,H2}$ 1.8 Hz, H4. N.O.e. experiments gave the following results: irradiation at δ 2.44 gave enhancements at δ 6.92 (4.8%) and at δ 7.31 (3.4%); irradiation at δ 2.73 gave enhancements at δ 7.31 (4.6%) and at δ 8.37 (7.8%); irradiation at δ 6.92 gave an enhancement at

δ 2.44 (0.6%); irradiation at δ 7.31 gave enhancements at δ 2.44 (0.5%) and at δ 2.73 (0.7%); irradiation at δ 7.55 gave an enhancement at δ 8.37 (4.0%); irradiation at δ 8.37 gave enhancements at δ 7.55 (2.9%) and at δ 2.73 (1.4%).

2,4-Dimethyl-1-nitronaphthalene (119), m.p. 84-85° (Lit.[3] 83-83.5°). ν_{max} (KBr) 1513 cm^{-1}. ^1H n.m.r. ($CDCl_3$) δ 2.47, s, 2-Me; 2.70, s, 4-Me; 7.21, s, H3; 7.59, m, H6, H7; 7.74, m, H8; 8.00, m, H5. N.O.e. experiments gave the following results: irradiation at δ 2.47 gave an enhancement at δ 7.21 (2.8%); irradiation at δ 2.70 gave enhancements at δ 8.00 (5.1%) and at δ 7.21 (4.0%); irradiation at δ 7.21 gave enhancements at δ 2.47 (0.8%) and at δ 2.70 (0.7%); irradiation at δ 7.74 gave an enhancement at δ 7.59 (1.5%); irradiation at δ 8.00 gave enhancements at δ 7.59 (4.2%) and at δ 2.70 (1.1%).

5.2.3.2 Thermal Cycloaddition of *trans*-5,7-Dimethyl-2-nitro-1-trinitromethyl-1,2-dihydronaphthalene (110) in (D)Chloroform

A solution of the nitro trinitromethyl adduct (110) in (D)chloroform was stored at +22° in the dark and the ^1H n.m.r. spectrum monitored at appropriate time intervals. The nitro trinitromethyl adduct (110) was slowly transformed (half-life 178 h) into the nitro cycloadduct (122). Removal of the solvent under reduced pressure after 33 days and crystallization of the residue from dichloromethane/hexane gave:

Nitro cycloadduct (122), m.p. 195° (dec.) (X-ray crystal structure determined, see Section 5.5). ν_{max} (KBr) 1600, 1560 cm^{-1}. ^1H n.m.r. ($CDCl_3$) δ 2.28, s, 6-Me; 2.36, s, 8-Me; 5.16, dd, $J_{H4,H3}$ 4.1 Hz, $J_{H4,H2}$ 2.4 Hz, H4; 5.70, dd, $J_{H3,H4}$ 4.1 Hz, $J_{H3,H2}$ 2.0 Hz, H3; 5.91, ddd, $J_{H2,H1}$ 6.1 Hz, $J_{H2,H4}$ 2.4 Hz, $J_{H2,H3}$ 2.0 Hz, H2; 5.96, d, $J_{H1,H2}$ 6.1 Hz, H1; 6.91, s, H5; 7.01, s, H7. N.O.e. experiments gave the following results: irradiation at

δ 2.28 gave enhancements at δ 6.91 (3.4%) and at δ 7.01 (3.3%); irradiation at δ 2.36 gave enhancements at δ 5.96 (5.0%) and at δ 7.01 (4.0%); irradiation at δ 5.16 gave enhancements at δ 5.70 (4.1%) and at δ 6.91 (3.7%); irradiation at δ 5.70 gave enhancements at δ 5.16 (2.4%) and at δ 5.91 (2.5%); irradiation at δ 6.91 gave enhancements at δ 2.28 (0.8%) and at δ 5.16 (4.1%); irradiation at δ 7.01 gave enhancements at δ 2.28 (0.4%) and at δ 2.36 (0.3%). ^{13}C n.m.r. ($CDCl_3$) δ 17.9, 8-Me; 21.15, 6-Me; 45.4, C4; 75.9, C2; 77.2, C1; 78.8, C3; 127.1, C4a; 128.9, C8; 129.8, C5; 133.6, C7; 136.5, C8a; 141.1, C6; resonance for **C**$(NO_2)_3$ not observed. The above assignments were confirmed by reverse detected heteronuclear correlation spectra (HMQC, HMBC).

5.2.3.3 Photonitration of 1,3-Dimethylnaphthalene (58) in Dichloromethane Containing Trifluoroacetic Acid

Photochemistry in dichloromethane containing trifluoroacetic acid at +20° and identification of the tetramethylbinaphthyl (123).

Reaction of 1,3-dimethylnaphthalene (58) / tetranitromethane in dichloromethane at +20°, as above, for 30 min. except for the addition of trifluoroacetic acid (0.8 mol L^{-1}) gave a product which was shown by ^1H n.m.r. spectral analysis to be a mixture of unreacted 1,3-dimethylnaphthalene (58) (42% conversion), 2,4-dimethyl-1-nitronaphthalene (119) (34%), 2,2',4,4'-tetramethyl-1,1'-binaphthyl (123) (54%), and unidentified aromatics (total 12%). Chromatography of this mixture on a silica gel Chromatotron plate gave the binaphthyl (123) in a fraction eluted immediately before 2,4-dimethyl-1-nitronaphthalene (119).

2,2',4,4'-tetramethyl-1,1'-binaphthyl (123), m.p. 176-177° (Lit.[4] 171.5-173°). ^1H n.m.r. ($CDCl_3$) δ 1.99, s, 2-Me, 2'-Me; 2.77, br s , 4-Me, 4'-Me; 7.08, dd, $J_{H8,H7} = J_{H8',H7'} = 8.3$ Hz, $J_{H8,H6} = J_{H8',H6'} = 1.0$ Hz, H8/H8'; 7.19,

ddd, $J_{H7,H8} = J_{H7',H8'}$ = 8.3 Hz, $J_{H7,H6} = J_{H7',H6'}$ = 6.8 Hz, $J_{H7,H5} = J_{H7',H5'}$ = 1.0 Hz, H7/H7'; 7.35, s, H3/H3'; 7.41, ddd, $J_{H6,H5} = J_{H6',H5'}$ = 8.3 Hz, $J_{H6,H7} = J_{H6',H7'}$ = 6.8 Hz, $J_{H6,H8} = J_{H6',H8'}$ = 1.5 Hz, H6/H6'; 8.03, d, $J_{H5,H6} = J_{H5',H6'}$ = 8.3 Hz, H5/H5'. N.O.e. experiments gave the following results: irradiation at δ 1.99 gave enhancements at δ 7.08 (1.9%) and at δ 7.35 (7.2%); irradiation at δ 2.77 gave enhancements at δ 7.35 (8.2%) and at δ 8.03 (10.6%); irradiation at δ 7.08 gave enhancements at δ 1.99 (0.4%) and at δ 7.19 (6.6%); irradiation at δ 7.19 gave enhancements at δ 7.08 (14.3%) and at δ 7.41 (8.5%); irradiation at δ 7.39 gave enhancements at δ 1.99 (1.3%), at δ 2.77 (1.2%), at δ 7.19 (5.9%) and at δ 8.03 (6.9%); irradiation at δ 8.03 gave enhancements at δ 2.77 (1.7%) and at δ 7.41 (6.0%). ^{13}C n.m.r. ($CDCl_3$) δ 19.4, 4-Me, 4'-Me; 20.0, 2-Me, 2'-Me; 124.1, C5, C5'; 124.6, C6, C6'; 125.7, C7, C7'; 126.3, C8, C8'; 129.6, C3, C3'; 131.3, C4a, C4a'; 133.0, C8a, C8a'; 133.4, C4, C4'; 133.5, C2, C2'; 134.0, C1, C1'. The above assignments were confirmed by reverse detected heteronuclear correlation spectra (HMQC, HMBC).

5.3 Experimental Relating to Chapter Three

5.3.1 GENERAL PROCEDURE FOR THE PHOTONITRATION OF 1,2,3-TRIMETHYLBENZENE (137) WITH TETRANITROMETHANE.

A solution of 1,2,3-trimethylbenzene (137) (500 mg, 0.52 mol L^{-1}) and tetranitromethane (1.04 mol L^{-1}) in dichloromethane or acetonitrile was irradiated at +20, -20 or -50° with filtered light ($\lambda_{cut\text{-}off}$<435 nm). Aliquots were withdrawn from the reaction mixture at appropriate time intervals, the volatile material removed under reduced pressure at ≤0°, and the product composition determined by ^1H n.m.r. spectral analysis (Tables 3.1 and 3.2).

5.3.1.1 Photonitration of 1,2,3-Trimethylbenzene (137) in Dichloromethane

Photochemistry in dichloromethane at +20° and the identification of the products (138), (139), (151)-(169), (171) *and* (172).

Reaction of 1,2,3-trimethylbenzene (137) / tetranitromethane in dichloromethane at +20°, as above, for 8 h gave a product which was shown by ^{1}H n.m.r. spectral analysis (Table 3.1) to be a mixture of adducts (139) and (151)-(162) (total 56%), nitro dienones (163) and (164) (total 1%), 3,4,5-trimethyl-1-trinitromethylbenzene (138) (27%), 2,3,4-trimethyl-1-trinitromethylbenzene (165) (11%), minor amounts of the 2',2',2'-trinitroethyl compounds (166) and (167) (total 1%), 2,3,4-trimethyl-1-nitrobenzene (168) (3%), 3,4,5-trimethyl-1-nitrobenzene (169) (1%). The mixture was partially separated into its components by h.p.l.c. and gave the following in elution order:

The first material eluted was a mixture of the aromatic compounds (138), (165), (168), (169) and 4,5,6-trimethyl-2-nitrophenol (171), which was separated into its components by chromatography on a silica gel Chromatotron plate (see below).

1,5,6-Trimethyl-*t*-6-nitro-*r*-3-trinitromethylcyclohexa-1,4-diene (151), as an impure oil [Decomposed to give 3,4,5-trimethyl-1-trinitromethylbenzene (138) on attempted crystallization]. ν_{max} (liquid film) 1613, 1586, 1550 cm^{-1}. ^{1}H n.m.r. ($CDCl_3$) δ 1.77, s, 6-Me; 1.82, br s, 1-Me, 5-Me; 4.74, br s, H3; 5.82, d, $J_{H2,H3} = J_{H4,H3}$ 3.4 Hz, H2, H4. ^{13}C n.m.r. ($CDCl_3$) δ 18.5, 1-Me, 5-Me; 22.5, 6-Me; 43.2, C3; 117.2, C2, C4; 140.9, C1, C5; resonances for **C**$(NO_2)_3$ and C3 not observed in a weak spectrum. The above assignments were confirmed by reverse detected heteronuclear correlation spectra (HMQC, HMBC).

1,2,3-Trimethyl-*r*-5-nitro-*t*-6-trinitromethylcyclohexa-1,3-diene (152), isolated only in admixture with adducts (151) and (154), and traces of nitro

cycloadduct (153). ^{1}H n.m.r. ($CDCl_3$) δ 1.78, br s, 3-Me; 1.82, br s, 2-Me; 1.90, br s, 1-Me; 5.11, br s, H4; 5.36, d, $J_{H5,H6}$ 6.8 Hz, H5; 5.60, d, $J_{H6,H5}$ 6.8 Hz, H6. N.O.e. experiments gave the following results: irradiation at δ 1.78 gave an enhancement at δ 5.11 (5.0%); irradiation at δ 1.90 gave an enhancement at δ 5.60 (5.3%); irradiation at δ 5.11 gave enhancements at δ 1.78 (0.5%) and at δ 5.36 (2.5%); irradiation at δ 5.36 gave enhancements at δ 5.11 (1.3%) and at δ 5.60 (2.6%); irradiation at δ 5.60 gave enhancements at δ 1.90 (0.3%) and at δ 5.36 (4.8%). The structure of the nitro trinitromethyl adduct (152) was further confirmed by its thermal cycloaddition in (D)chloroform to give the nitro cycloadduct (153), the structure of which is established below.

1,2,3-Trimethyl-*r*-3-nitro-*t*-6-trinitromethylcyclohexa-1,4-diene (154), isolated as an oil containing an impurity (*c.* 5%). ν_{max} (liquid film) 1615, 1603, 1575, 1551 cm^{-1}. ^{1}H n.m.r. ($CDCl_3$) δ 1.74, s, 3-Me; 1.75, q, $J_{2\text{-Me},1\text{-Me}}$ 1.0 Hz, 2-Me; 1.81, q, $J_{1\text{-Me},2\text{-Me}}$ 1.0 Hz, 1-Me; 4.89, br s, H6; 6.21, d, $J_{H4,H5}$ 10.3 Hz, H4; 6.24, dd, $J_{H5,H4}$ 10.3 Hz, $J_{H5,H6}$ 2.9 Hz, H5. N.O.e. experiments gave the following results: irradiation at δ1.74 gave an enhancement at δ 6.21 (2.0%); irradiation at δ 1.81 gave an enhancement at δ 4.89 (2.9%); irradiation at δ 4.89 gave enhancements at δ 1.81 (0.9%) and at δ 6.24 (3.9%); irradiation at δ 6.21 gave an enhancement at δ 1.74 (0.4%); irradiation at δ 6.24 gave an enhancement at δ 4.89 (5.4%). ^{13}C n.m.r. ($CDCl_3$) δ 15.3, 2-Me; 17.2, 1-Me; 25.4, 3-Me; 47.6, C6; 88.8, C3; 121.7, C4; 123.2, C1; 135.4, C2; 135.5, C5; the resonance for **C**$(NO_2)_3$ was not observed. The above assignments were confirmed by reverse detected heteronuclear correlation spectra (HMQC, HMBC).

2,3-Dimethyl-1-(2',2',2'-trinitroethyl)-benzene (166), isolated as an oil (Insufficient for elemental analysis. Found: $M^{+\bullet}$ 269.06463. $C_{10}H_{11}N_3O_6$ requires 269.06479). ^{1}H n.m.r. ($CDCl_3$) δ 2.29 and 2.33, both s, 2-Me, 3-Me; 5.52, s, C**H$_2$**; 7.13-7.24, m, H4, H5, H6.

2,6-Dimethyl-1-(2',2',2'-trinitroethyl)-benzene (167), isolated only in admixture with its isomer (166). ^{1}H n.m.r. ($CDCl_3$) (by subtraction) δ 2.41, s, 2-Me and 6-Me; 5.57, s, C**H$_2$**; 7.06-7.37, m, H4, H5, H6.

1,5,6-Trimethyl-*c*-6-nitro-*r*-3-trinitromethylcyclohexa-1,4-diene (155), m.p. 45° (dec.) (Insufficient for elemental analysis; parent ion not visible in the mass spectrum under a variety of experimental conditions). ν_{max} (liquid film) 1595, 1544 cm^{-1}. ^{1}H n.m.r. ($CDCl_3$) δ 1.77, s, 6-Me; 1.83, br s, 1-Me, 5-Me; 4.61, br s, H3; 5.75, d, $J_{H2,H3} = J_{H4,H3}$ 2.4 Hz, H2, H4. N.O.e. experiments gave the following results: irradiation at δ 4.61 gave an enhancement at δ 5.75 (1.6%); irradiation at δ 5.75 gave enhancements at δ 1.83 (0.9%) and at δ 4.61 (3.8%). ^{13}C n.m.r. ($CDCl_3$) δ 18.4, 1-Me, 5-Me; 21.9, 6-Me; 42.0, C3; 90.0, C6; 116.8, C2, C4; 139.7, C1, C5; the resonance for **C**$(NO_2)_3$ was not observed. The above assignments were confirmed by reverse detected heteronuclear correlation spectra (HMQC, HMBC).

1,2,3-Trimethyl-*r*-3-nitro-*c*-6-trinitromethylcyclohexa-1,4-diene (156), m.p. 72° (dec.) (Insufficient for elemental analysis; parent ion not visible in mass spectrum under a variety of experimental conditions). ν_{max} (KBr) 1604, 1575, 1546 cm^{-1}. ^{1}H n.m.r. ($CDCl_3$) δ 1.77, s, 3-Me; 1.81, q, $J_{1\text{-Me},2\text{-Me}}$ 1.0 Hz, 1-Me; 1.89, q, $J_{2\text{-Me},1\text{-Me}}$ 1.0 Hz, 2-Me; 4.79, br s, H6; 6.24, dd, $J_{H5,H4}$ 10.3 Hz, $J_{H5,H6}$ 3.9 Hz, H5; 6.30, dd, $J_{H4,H5}$ 10.3 Hz, $J_{H4,H6}$ 1.0 Hz, H4. N.O.e. experiments gave the following results: irradiation at δ 1.77 gave an enhancement at δ 6.30 (3.9%); irradiation at δ 1.81 gave an enhancement at δ 4.79 (3.4%); irradiation at δ 4.79 gave enhancements at δ 1.81 (0.4%) and at δ 6.24 (1.1%); irradiation at δ 6.24 gave an enhancement at δ 4.79 (1.8%); irradiation at δ 6.30 gave an enhancement at δ 1.77 (0.6%). ^{13}C n.m.r. ($CDCl_3$) δ 16.2, 2-Me; 17.6, 1-Me; 25.6, 3-Me; 47.0, C6; 86.7, C3; 122.3, C5; 124.1, C1; 134.8, C2; 134.9, C4; the resonance for **C**$(NO_2)_3$ was not observed. The above assignments were confirmed by reverse detected heteronuclear correlation spectra (HMQC,

HMBC).

2,3,4-Trimethyl-4-nitrocyclohexa-2,5-dien-1-one (163),[5] isolated only in admixture with adduct (156). ^{1}H n.m.r. ($CDCl_3$) δ 1.88, s, 4-Me; 1.95, br s, 2-Me, 3-Me; 6.41, d, $J_{H6,H5}$ 9.8 Hz, H6; 6.81, d, $J_{H5,H6}$ 9.8 Hz, H5. A n.O.e. experiment gave the following result: irradiation at δ 1.88 gave an enhancement at δ 6.81 (3.2%). The nitro dienone (163) was unstable in (D)chloroform solution and rearranged (half life *c.* 6 h) to give 4,5,6-trimethyl-2-nitrophenol (171) (See below).

Nitro cycloadduct (153), m.p. 163° (dec.) (X-ray crystal structure determined, see Section 5.5). ν_{max} (KBr) 1590, 1556 cm^{-1}. ^{1}H n.m.r. ($CDCl_3$) δ 1.67, s, 3-Me; 1.75, q, $J_{2\text{-Me},1\text{-Me}}$ 1.4 Hz, 2-Me; 1.80, q, $J_{1\text{-Me},2\text{-Me}}$ 1.4 Hz, 1-Me; 4.60, dd, $J_{H6,H5}$ 4.4 Hz, $J_{H6,H4}$ 2.5 Hz, H6; 5.27, dd, $J_{H4,H6}$ 2.5 Hz, $J_{H4,H5}$ 2.0 Hz, H4; 5.51, dd, $J_{H5,H6}$ 4.4 Hz, $J_{H5,H4}$ 2.0 Hz, H5. N.O.e. experiments gave the following results: irradiation at δ 1.67 gave an enhancement at δ 5.27 (7.1%); irradiation at δ 1.80 gave an enhancement at δ 4.60 (3.2%); irradiation at δ 4.60 gave enhancements at δ 1.80 (0.2%) and at δ 5.51 (10.4%); irradiation at δ 5.27 gave enhancements at δ 1.67 (0.5%) and at δ 5.51 (2.0%); irradiation at δ 5.51 gave enhancements at δ 4.60 (2.3%) and at δ 5.27 (1.0%). ^{13}C n.m.r. ($CDCl_3$) δ 14.1, 2-Me; 20.0, 1-Me; 21.7, 3-Me; 45.2, C6; 79.7, C5; 81.4, C4; 87.4, C3; 128.5, C1; 140.1, C2. The above assignments were confirmed by reverse detected heteronuclear correlation spectra (HMQC, HMBC).

3,4,5-Trimethyl-4-nitrocyclohexa-2,5-dien-1-one (164),[6] isolated as an oil. ν_{max} (liquid film) 1677, 1638, 1598, 1551 cm^{-1}. ^{1}H n.m.r. ($CDCl_3$) δ 1.88, s, 4-Me; 1.99, d, $J_{3\text{-Me},H2} = J_{5\text{-Me},H6}$ 1.5 Hz, 3-Me, 5-Me; 6.23, br s, H2, H6.

*1,2,3-Trimethyl-*r*-3,*c*-4,*c*-6-trinitro-*t*-5-trinitromethylcyclohex-1-ene* (157), m.p. 73° (dec.) (X-ray crystal structure determined, see Section 5.5). ν_{max} (KBr) 1605, 1566, 1529 cm^{-1}. ^{1}H n.m.r. ($CDCl_3$) δ 2.03, br s, 2-Me;

2.185, br s, 1-Me; 2.19, s, 3-Me; 5.01, d, $J_{H6,H5}$ 6.8 Hz, H6; 5.10, br s, H4; 6.62, br d, $J_{H5,H6}$ 6.8 Hz, H5. N.O.e. experiments gave the following results: irradiation at δ 2.03 gave an enhancement at δ 2.19 (0.5%); irradiation at δ 2.19 gave enhancements at δ 2.03 (2.9%), at δ 5.01 (10.8%), and at δ 5.10 (5.9%); irradiation at δ 5.01 gave enhancements at δ 2.19 (0.5%) and at δ 6.62 (3.2%); irradiation at δ 5.10 gave an enhancement at δ 2.19 (0.3%); irradiation at δ 6.62 gave enhancements at δ 5.01 (0.9%) and at δ 5.10 (0.6%). ^{13}C n.m.r. ($CDCl_3$) δ 15.6, 2-Me; 23.0, 1-Me; 24.3, 3-Me; 42.7, C5; 82.7, C4; 85.5, C6; 87.8, C3; 130.2, C2; 132.5, C1; the resonance for **C**$(NO_2)_3$ was not observed. The above assignments were confirmed by reverse detected heteronuclear correlation spectra (HMQC, HMBC).

t-*6-Hydroxy-4,5,6-trimethyl-2,*r-*4,*t-*5-trinitrocyclohex-2-enone* (172), m.p. 121-123° (X-ray crystal structure determined, see Section 5.5). ν_{max} (KBr) 3423, 1740, 1560, 1541 cm^{-1}. ^1H n.m.r. ($CDCl_3$) δ 1.52, s, 6-Me; 1.85, s, 5-Me; 1.88, s, 4-Me; 3.97, br s, OH; 7.44, s, H3. N.O.e experiments gave the following results: irradiation at δ 1.52 gave an enhancement at δ 1.85 (0.8%); irradiation at δ 7.44 gave an enhancement at δ 1.88 (0.3%). ^1H n.m.r. (CD_3CN) δ 1.54, s, 6-Me; 1.84, s, 5-Me; 1.91, s, 4-Me; 4.92, br s, OH; 7.70, s, H3. N.O.e. experiments gave the following results: irradiation at δ 1.54 gave an enhancement at δ 1.84 (0.8%); irradiation at δ 1.84 gave an enhancement at δ 1.54 (1.2%); irradiation at δ 1.91 gave an enhancement at δ 7.70 (7.4%); irradiation at δ 7.70 gave an enhancement at δ 1.91 (0.2%). ^{13}C n.m.r. (CD_3CN) δ 15.9, 5-Me; 23.5, 6-Me; 23.6, 4-Me; 79.2, C6; 90.3, C4; 99.7, C5; 137.5, C3; 147.0, C2; 188.4, C1. The above assignments were confirmed by reverse detected heteronuclear correlation spectra (HMQC, HMBC).

2,3,4-Trimethyl-*c*-2,*c*-5-dinitro-*t*-6-trinitromethylcyclohex-3-en-*r*-1-ol (139), m.p. 65° (dec.) [Lit.[7] 65° (dec.)]. ν_{max} (KBr) 3502, 1610, 1571, 1545

cm^{-1}. ^1H n.m.r. ($CDCl_3$) δ 1.94, s, 2-Me; 1.97. br s, 4-Me; 2.05, br s, 3-Me; 3.86, d, $J_{OH,H1}$ 12.7 Hz, 1-OH; 4.09, dd, $J_{H1,OH}$ 12.7 Hz, $J_{H1,H6}$ 10.8 Hz, H1; 4.99, dd, $J_{H6,H1}$ 10.8 Hz, $J_{H6,H5}$ 6.3 Hz, H6; 5.25, d, $J_{H5,H6}$ 6.3 Hz, H5. N.O.e. experiments gave the following results: irradiation at δ 1.97 gave an enhancement at δ 5.25 (4.2%); irradiation at δ 4.09 gave enhancements at δ 1.94 (0.8%) and at δ 5.25 (1.1%); irradiation at δ 5.25 gave an enhancement at δ 1.97 (0.5%). ^{13}C n.m.r. ($CDCl_3$) δ 16.6, 3-Me; 18.7, 4-Me; 22.2, 2-Me; 45.4, C6; 71.4, C1; 87.8, C5; 88.4, C2; 127.0, C4; 134.9, C3; the resonance for **C**$(NO_2)_3$ was not observed. The above assignments were confirmed by reverse detected heteronuclear correlation spectra (HMQC, HMBC).

1,2,3-Trimethyl-*r*-3,*t*-4,*t*-6-trinitro-*c*-5-trinitromethylcyclohex-1-ene (158), isolated only as an oil (Insufficient for elemental analysis, parent ion not visible in mass spectrum under a variety of experimental conditions). ν_{max} (liquid film) 1647, 1570 cm^{-1}. ^1H n.m.r. ($CDCl_3$) δ 1.74, s, 3-Me; 1.93, br s, 2-Me; 1.96, br s, 1-Me; 4.88, dd, $J_{H5,H4}$ 4.9 Hz, $J_{H5,H6}$ 1.0 Hz, H5; 5.81, dd, $J_{H6,H4}$ 3.9 Hz, $J_{H6,H5}$ 1.0 Hz, H6; 5.92, dd, $J_{H4,H5}$ 4.9 Hz, $J_{H4,H6}$ 3.9 Hz, H4. N.O.e. experiments gave the following results: irradiation at δ 1.74 gave an enhancement at δ 1.93 (1.2%); irradiation at δ 1.93 gave an enhancement at δ 1.74 (1.3%); irradiation at δ 1.96 gave an enhancement at δ 5.81 (3.3%); irradiation at δ 4.88 gave enhancements at δ 5.81 (1.3%) and at δ 5.92 (3.6%); irradiation at δ 5.81 gave enhancements at δ 1.96 (0.7%) and at δ 4.88 (0.9%); irradiation at δ 5.92 gave enhancements at δ 1.74 (0.5%) and at δ 4.88 (1.6%). ^{13}C n.m.r. ($CDCl_3$) δ 14.5, 2-Me; 17.7, 1-Me; 24.7, 3-Me; 46.7, C5; 78.6, C4; 81.1, C3; 84.1, C6; 124.1, C1; 132.9, C2; the resonance for **C**$(NO_2)_3$ was not observed. The above assignments were confirmed by reverse detected heteronuclear correlation spectra (HMQC, HMBC).

Hydroxy dinitro nitronic ester (159), isolated only as an oil

(Insufficient for elemental analysis, parent ion not visible in mass spectrum under a variety of experimental conditions). ν_{max} (liquid film) 3511, 1637, 1560 cm^{-1}. ^1H n.m.r. ($CDCl_3$) δ 1.85, s, 3-Me; 1.87, br s, 2-Me; 1.93, br s, 1-Me; 3.92, br, O**H**; 4.31, d, $J_{H4,H5}$ 10.3 Hz, H4; 4.40, dd, $J_{H5,H4}$ 10.3 Hz, $J_{H5,H6}$ 4.4 Hz, H5; 5.23, d, $J_{H6,H5}$ 4.4 Hz, H6. N.O.e. experiments gave the following results: irradiation at δ 1.85 gave an enhancement at δ 4.31 (5.8%); irradiation at δ 1.93 gave an enhancement at δ 5.23 (3.2%); irradiation at δ 4.31 gave an enhancement at δ 1.85 (0.7%); irradiation at δ 4.40 gave an enhancement at δ 5.23 (5.8%); irradiation at δ 5.23 gave enhancements at δ 1.93 (0.8%) and at δ 4.40 (3.5%). ^{13}C n.m.r. ($CDCl_3$) δ 14.1, 2-Me; 18.3, 1-Me; 24.8, 3-Me; 48.6, C4; 67.8, C5; 85.3, C3; 88.8, C6; 124.8, C1; 132.8, C2; the resonance for =**C**-NO_2 was not observed. The above assignments were confirmed by reverse detected heteronuclear correlation spectra (HMQC, HMBC).

Trinitro nitronic ester (160), m.p. 127° (dec.) (Preliminary X-ray crystal structure reported in Section 5.5). ν_{max} (KBr) 1639, 1564, 1512 cm^{-1}. ^1H n.m.r. ($CDCl_3$) δ 1.91, br s, 2-Me; 1.92, s, 3-Me; 2.03, br s, 1-Me; 5.12, dd, $J_{H5,H4}$ 11.7 Hz, $J_{H5,H6}$ 3.5 Hz, H5; 5.16, d, $J_{H4,H5}$ 11.7 Hz, H4; 5.52, d, $J_{H6,H5}$ 3.5 Hz, H6. N.O.e. experiments gave the following results: irradiation at δ 1.92 gave an enhancement at δ 5.16 (5.3%); irradiation at δ 2.03 gave an enhancement at δ 5.52 (4.4%); irradiation at δ 5.12 gave an enhancement at δ 5.52 (3.1%); irradiation at δ 5.16 gave an enhancement at δ 1.92 (0.5%); irradiation at δ 5.52 gave enhancements at δ 2.03 (0.5%) and at δ 5.12 (2.4%). ^{13}C n.m.r. ($CDCl_3$) δ 15.2, 2-Me; 18.3, 1-Me; 25.0, 3-Me; 44.9, C4; 80.7, C5; 84.2, C6; these assignments were confirmed by short range reverse detected heteronuclear correlation spectra (HMQC), but the remainder of the resonances were not detected in a weak spectrum.

Trinitro nitronic ester (161), m.p. 131-132.5° (X-ray crystal structure determined, see Section 5.5). ν_{max} (KBr) 1608, 1565, 1525 cm^{-1}. ^1H

n.m.r. ($CDCl_3$) δ 1.83, s, 3-Me; 2.01, br s, 2-Me; 2.09, br s, 1-Me; 5.04, br s, H6; 5.08 d, $J_{H4,H5}$ 3.4 Hz, H4; 5.42, dd, $J_{H5,H4}$ 3.4 Hz, $J_{H5,H6}$ 1.4 Hz, H5. ^1H n.m.r. (CD_3CN) δ 1.88, s, 3-Me; 2.22, br s, 1-Me, 2-Me; 5.29, dd, $J_{H5,H4}$ 4.0 Hz, $J_{H5,H6}$ 1.4 Hz, H5; 5.34, br s, H6; 5.40, d, $J_{H4,H5}$ 4.0 Hz, H4. N.O.e. experiments gave the following results: (in $CDCl_3$) irradiation at δ 1.83 gave an enhancement at δ 5.08 (5.9%). (in CD_3CN) irradiation at δ 1.88 gave an enhancement at δ 5.40 (8.9%); irradiation at δ 2.22 gave an enhancement at δ 5.34 (3.4%); irradiation at δ 5.34 gave an enhancement at δ 2.22 (0.4%), irradiation at δ 5.40 gave an enhancement at δ 1.88 (0.3%). ^{13}C n.m.r. (CD_3CN) δ 14.1, 2-Me; 19.3, 1-Me; 21.3, 3-Me; 38.7, C5; 78.9, C4; 83.3, C6; 84.0, C3; 127.6, C1; 133.5, C2. The above assignments were confirmed by reverse detected heteronuclear correlation spectra (HMQC, HMBC).

Hydroxy dinitro nitronic ester (162), m.p. 129° (X-ray crystal structure determined, see Section 5.5). ν_{max} (KBr) 3463, 1604, 1556, 1295 cm^{-1}. ^1H n.m.r. ($CDCl_3$) δ 1.63, s, 3-Me; 1.90, br s, 2-Me; 2.01, br s, 1-Me; 4.30, d, $J_{H4,H5}$ 3.9 Hz, H4; 4.80, dd, $J_{H5,H4}$ 3.9 Hz, $J_{H5,H6}$ 2.4 Hz, H5; 4.91, br s, H6. N.O.e. experiments gave the following results: irradiation at δ 1.63 gave enhancements at δ 1.90 (2.3%) and at δ 4.30 (2.6%); irradiation at δ 1.90 gave an enhancement at δ 1.63 (1.0%); irradiation at δ 2.01 gave an enhancement at δ 4.91 (4.8%); irradiation at δ 4.30 gave enhancements at δ 1.63 (1.1%) and at δ 4.80 (3.2%); irradiation at δ 4.80 gave enhancements at δ 4.30 (3.0%) and at δ 4.91 (3.1%); irradiation at δ 4.91 gave an enhancement at δ 2.01 (1.1%). ^{13}C n.m.r. ($CDCl_3$) δ 13.9. 2-Me; 19.5, 1-Me; 19.7, 3-Me; 40.1, C5; 66.3, C4; 82.4, C6; 85.4, C3; 126.3, C1; 131.5, C2. The above assignments were confirmed by reverse detected heteronuclear correlation spectra (HMQC, HMBC).

Chromatography on a silical gel Chromatotron plate of the mixture of compounds (138), (165), (168) and (169), first eluted from the h.p.l.c.

column, gave the following compounds in elution order:

3,4,5-Trimethyl-1-trinitromethylbenzene (138), m.p. 91° (dec.) [Lit.[7] 91° (dec.)]. ν_{max} (KBr) 1617, 1585 cm $^{-1}$. ^{1}H n.m.r. ($CDCl_3$) δ 2.27, s, 4-Me; 2.36, s, 3-Me, 5-Me; 7.20, s, H2, H6. ^{13}C n.m.r. ($CDCl_3$) δ 15.9, 4-Me; 20.8, 3-Me, 5-Me; 119.0, C1; 128.1, C2, C6; 138.1, C3, C5; 143.2, C4; the resonance for **C**$(NO_2)_3$ was not observed. The above assignments were confirmed by reverse detected heteronuclear correlation spectra (HMQC, HMBC).

2,3,4-Trimethyl-1-trinitromethylbenzene (165), obtained only in admixture with 3,4,5-trimethyl-1-trinitromethylbenzene (138). ^{1}H n.m.r. ($CDCl_3$) δ 2.04, s, 2-Me; 2.26, s, 3-Me; 2.40, s, 4-Me; 6.99, d, $J_{H6,H5}$ 8.3 Hz, H6; 7.19, d, $J_{H5,H6}$ 8.3 Hz, H5. N.O.e. experiments gave the following results: irradiation at δ 2.04 gave an enhancement at δ 2.26 (0.8%); irradiation at δ 2.26 gave an enhancement at δ 2.04 (0.5%); irradiation at δ 2.40 gave an enhancement at δ 7.19 (2.7%); irradiation at δ 6.99 gave an enhancement at δ 7.19 (5.3%); irradiation at δ 7.19 gave enhancements at δ 2.40 (0.4%) and at δ 6.99 (4.9%). ^{13}C n.m.r. ($CDCl_3$) δ 16.0, 3-Me; 18.5, 2-Me; 21.4, 4-Me; 119.8, C1; 126.8, C6; 128.2, C5; 138.0, C2; 138.7, C3; 143.7, C4; the resonance for **C**$(NO_2)_3$ was not observed. The above assignments were confirmed by reverse detected heteronuclear correlation spectra (HMQC, HMBC).

4,5,6-Trimethyl-2-nitrophenol (171),[8] isolated as an oil (*c.* 95% pure). ν_{max} (liquid film) 3442, 1612, 1593, 1537 cm^{-1}. ^{1}H n.m.r. ($CDCl_3$) δ 2.25, s, 6-Me; 2.26, s, 5-Me; 2.27, s, 4-Me; 7.75, s, H3; 10.98, s, OH. ^{13}C n.m.r. ($CDCl_3$) δ 12.1, 6-Me; 17.0, 5-Me; 20.1, 4-Me; 121.9, C3; 126.8, C6; 128.5, C4; 131.0, C1; 147.0, C5; 152.0, C2. The above assignments were confirmed by reverse detected heteronuclear correlation spectra (HMQC, HMBC).

2,3,4-Trimethylnitrobenzene (168),[9] isolated as an oil (*c.* 95% pure)

(Found: $M^{+\bullet}$ 165.07890. $C_9H_{11}NO_2$ requires 165.07898). ν_{max} (liquid film) 1518 cm^{-1}. ^1H n.m.r. ($CDCl_3$) δ 2.26, s, 3-Me; 2.35, s, 4-Me; 2.39, s, 2-Me; 7.09, d, $J_{H5,H6}$ 8.4 Hz, H5; 7.51, d, $J_{H6,H5}$ 8.4 Hz, H6. N.O.e. experiments gave the following results: irradiation at δ 2.35 gave an enhancement at δ 7.09 (2.0%); irradiation at δ 7.09 gave enhancements at δ 2.35 (0.2%) and δ 7.51 (5.3%); irradiation at δ 7.51 gave an enhancement at δ 7.09 (2.4%). ^{13}C n.m.r. ($CDCl_3$) δ 15.8, 2-Me; 16.0, 3-Me; 21.2, 4-Me; 121.1, C6; 127.6, C5; 130.4, C2; 137.6, C3; 141.5, C4; 149.4, C1.

3,4,5-Trimethylnitrobenzene (169),[9] isolated as an oil (*c.* 90% pure) (Found: $M^{+\bullet}$ 165.07886. $C_9H_{11}NO_2$ requires 165.07898). ν_{max} (liquid film) 1517 cm^{-1}. ^1H n.m.r. ($CDCl_3$) δ 2.26, s, 4-Me; 2.37, s, 3-Me, 5-Me; 7.87, s, H2, H6.

5.3.1.2 Photonitration of 1,2,3-Trimethylbenzene (137) in Dichloromethane Containing Trifluoroacetic Acid

Reaction of 1,2,3-trimethylbenzene (137) / tetranitromethane in dichloromethane at +20°, as above, for 8 h except for the addition of trifluoroacetic acid (1.04 mol L^{-1}) gave 3,4,5-trimethyl-1-trinitromethyl-benzene (138) (62%), 2,3,4-trimethyl-1-trinitromethylbenzene (165) (10.5%), 3,4,5-trimethylbenzoic acid (172) (5%), 2,3,4-trimethylbenzoic acid (173) (2%), and unidentified material (20%). The carboxylic acids (172) and (173) were isolated by h.p.l.c. and were identified by comparison with literature data.[10,11] A similar reaction to the above, but with trifluoroacetic acid (2.08 mol L^{-1}) gave a mixture of 3,4,5-trimethyl-1-trinitromethylbenzene (138) (20%), 2,3,4-trimethyl-1-trinitromethylbenzene (165) (11.5%), 3,4,5-trimethylbenzoic acid (172) (10%), 2,3,4-trimethylbenzoic acid (173) (4.5%), 2,3,4-trimethylnitro-benzene (168) (11%), 3,4,5-trimethylnitrobenzene (169)

(9%), and unidentified material (34%). Full time/yield data are given in Table 3.3.

5.3.1.3 Reaction of Nitro Trinitromethyl Adducts (151) and (154)-(156) with 2,6-Di-*tert*-butyl-4-methylpyridine in Dichloromethane

A solution of each of the adducts (151) and (154)-(156) in dichloromethane was treated with 2,6-di-*tert*-butyl-4-methylpyridine (1.1 molar ratio) for 1 h at +20° in the dark. Removal of the solvent under reduced pressure gave a residue, the ^{1}H n.m.r. spectrum of which was determined. Adducts (151) and (155) gave 3,4,5-trimethyl-1-trinitromethylbenzene (138), while adducts (154) and (156) gave 2,3,4-trimethyl-1-trinitromethylbenzene (165).

5.3.1.4 Thermal Cycloaddition of 1,2,3-Trimethyl-*r*-5-nitro-*t*-6-trinitromethylcyclohexa-1,3-diene (152) in (D)Chloroform

A solution of a mixture (*c.* 4:1:4:2) of the trinitromethyl diene (152), nitro cycloadduct (153), and the 1,2,3-trimethyl-3-nitro-6-trinitromethylcyclohexa-1,4-dienes (151) and (154), respectively in (D)chloroform was stored at +22° in the dark and the ^{1}H n.m.r. spectrum monitored at appropriate time intervals. The adducts (151) and (154) were inert under these reaction conditions for the time-scale of the reaction of compound (152), but the trinitromethyl diene (152) was transformed (half-life 19.5 h) into the nitro cycloadduct (153).

5.3.1.5 Rearrangement of 2,3,4-Trimethyl-4-nitrocyclohexa-2,5-dien-1-one (163) in (D)Chloroform

A solution of a mixture (*c.* 4:1) of the nitro dienone (163) and 1,2,3-trimethyl-*r*-3-nitro-*c*-6-trinitromethylcyclohexa-1,4-diene (156) in (D)chloroform was stored at +22° in the dark and the ^{1}H n.m.r. spectrum monitored at appropriate time intervals. The adduct (156) was inert under these reaction conditions but the nitro dienone (163) was transformed (half-life 6 h) into 4,5,6-trimethyl-2-nitrophenol (171).

5.3.2 GENERAL PROCEDURE FOR THE PHOTONITRATION OF 1,2,4,5-TETRAMETHYLBENZENE (134) WITH TETRANITROMETHANE.

A solution of 1,2,4,5-tetramethylbenzene (134) (500 mg, 0.47 mol L^{-1}) and tetranitromethane (0.94 mol L^{-1}) in dichloromethane (at +20, -20 or -50°), acetonitrile (+20 or -20°), or 1,1,1,3,3,3-hexafluoropropan-2-ol (+20°) was irradiated with filtered light ($\lambda_{cut\text{-}off}$<435 nm). Aliquots were withdrawn from the reaction mixture at appropriate time intervals, the volatile material removed under reduced pressure at ≤0°, and the product composition determined by ^{1}H n.m.r. spectral analysis (Tables 3.5-3.9).

5.3.2.1 Photonitration of 1,2,4,5-Tetramethylbenzene (134) in Dichloromethane

Photochemistry of 1,2,4,5-tetramethylbenzene (134) *in dichloromethane at* -50° *and the identification of adducts* (216) *and* (217) *and compound* (225).

Reaction of 1,2,4,5-tetramethylbenzene (134) / tetranitromethane in dichloromethane at -50°, as above, for 4 h gave a product which was shown

by ^{1}H n.m.r. spectral analysis (Table 3.5) to be a mixture of adduct (216) (46%), adduct (217) (7%), aromatic compounds (218)-(225) (total 41%), and unidentified aromatic products (6%). The mixture was partially separated into its components by h.p.l.c. and gave the following in elution order:

The first material eluted was a mixture of aromatic compounds.

1,3,4,6-Tetramethyl-*r*-3-nitro-*t*-6-trinitromethylcyclohexa-1,4-diene (216), as an unstable oil (elemental analysis not possible because of instability; parent ion not visible in mass spectrum). ν_{max} (liquid film) 1599, 1583, 1549 cm^{-1}. ^{1}H n.m.r. ($CDCl_3$) δ 1.74, s, 3-Me; 1.80, d, $J_{4\text{-Me,H5}}$ 1.5 Hz, 4-Me; 1.87, d, $J_{1\text{-Me,H2}}$ 1.5 Hz, 1-Me; 1.96, s, 6-Me; 5.82, q, $J_{\text{H2,1-Me}}$ 1.5 Hz, H2; 6.20, q, $J_{\text{H5,4-Me}}$ 1.5 Hz, H5. N.O.e. experiments gave the following results: irradiation at δ 1.74 gave an enhancement at δ 5.82 (4.0%); irradiation at δ 1.80 gave an enhancement at δ 6.20 (4.4%); irradiation at δ 1.87 gave an enhancement at δ 5.82 (4.9%); irradiation at δ 1.96 gave an enhancement at δ 6.20 (4.1%); irradiation at δ 5.82 gave enhancements at δ 1.74 (0.3%) and at δ 1.87 (0.7%); irradiation at δ 6.20 gave enhancements at δ 1.80 (0.7%) and at δ 1.96 (0.2%). ^{13}C n.m.r. ($CDCl_3$) δ 18.3, 4-Me; 19.1, 1-Me; 23.3, 3-Me, 6-Me; 51.2, C6; 88.3, C3; 126.0, C5; 130.2, C2; 134.1, C1; 136.2, C4; resonance for **C**$(NO_2)_3$ not observed. The above assignments were confirmed by reverse detected heteronuclear correlation spectra (HMQC, HMBC).

1,3,4,6-Tetramethyl-*r*-3-nitro-*c*-6-trinitromethylcyclohexa-1,4-diene (217), as an oil in admixture with adduct (216) (*c.* 5%). ^{1}H n.m.r. ($CDCl_3$) δ 1.74, s, 3-Me; 1.85, s, 6-Me; 1.87, d, $J_{1\text{-Me, H2}}$ 1.5 Hz, 1-Me; 1.94, d, $J_{4\text{-Me,H5}}$ 1.5 Hz, 4-Me; 5.98, q, $J_{\text{H2,1-Me}}$ 1.5 Hz, H2; 6.28, q, $J_{\text{H5,4-Me}}$ 1.5 Hz, H5. N.O.e. experiments gave the following results: irradiation at δ 1.74 gave enhancements at δ 1.94 (0.5%) and at δ 5.98 (5.2%); irradiation at δ 1.85 gave an enhancement at δ 6.28 (3.6%); irradiation at δ 1.87 gave an

enhancement at δ 5.98 (3.9%); irradiation at δ 1.94 gave an enhancement at δ 6.28 (3.2%); irradiation at δ 5.98 gave enhancements at δ 1.74 (0.6%) and at δ 1.87 (0.9%); irradiation at δ 6.28 gave an enhancement at δ 1.94 (1.3%). ^{13}C n.m.r. ($CDCl_3$) δ 18.7, 4-Me; 18.9, 23.7, 1-Me, 6-Me; 25.6, 3-Me; 50.6, C6; 85.4, C3; 126.4, C5; 130.3, C2; 134.4, C1; 136.3, C4; resonance for $\mathbf{C}(NO_2)_3$ not observed. The above assignments were confirmed by reverse detected heteronuclear correlation spectra (HMQC, HMBC), and comparison with data for the epimeric adduct (216).

2,4,5-Trimethylbenzyl nitrite (225) was not eluted by h.p.l.c. on the cyanopropyl column, being presumably decomposed to the 2,4,5-trimethyl-benzaldehyde (222) or hydrolysed to 2,4,5-trimethylbenzyl alcohol (223). The presence of the known 2,4,5-trimethylbenzyl nitrite (225) in the crude reaction mixture was inferred from the ^1H n.m.r. signal due to the $-C\mathbf{H_2}-ONO_2$ group at δ 5.64.[12]

5.3.2.2 Photonitration of 1,2,4,5-Tetramethylbenzene (134) in 1,1,1,3,3,3,-Hexafluoropropan-2-ol (HFP)

Photochemistry in HFP at +20° and identification of the aromatic products (218)-(224) *and* (226).

A solution of 1,2,4,5-tetramethylbenzene (134) (250 mg, 0.47 mol L^{-1}) and tetranitromethane (0.94 mol L^{-1}) in HFP at +20° was irradiated with filtered light ($\lambda_{cut\text{-}off}$<435 nm) for 20 h. After workup the product composition was determined by ^1H n.m.r. spectral analysis (Table 3.6) and shown to be a mixture of the aromatic compounds (218)-(224) and (226). Chromatography of the crude product on a silica gel Chromatotron plate allowed the separation of aromatic compounds (218)-(223) and (226), compound (224) not being eluted from the plate, in elution order:

2,2',3,4',5,5',6-Heptamethyldiphenylmethane (218), m.p. 139° (dec.)

(Found: $M^{+\bullet}$ 266.2034. $C_{20}H_{26}$ requires 266.20345). ^1H n.m.r. ($CDCl_3$) δ 2.04, s, 5'-Me; 2.06, s, 2-Me, 6-Me; 2.18, s, 4'-Me; 2.27, s, 3-Me, 5-Me; 2.36, s, 2'-Me; 3.87, s, CH_2; 6.28, s, H6'; 6.94, s, H4; 6.97, s, H3'; identical with an authentic sample.[13] N.O.e. experiments gave the following results: irradiation at δ 2.04 gave an enhancement at δ 6.28 (7.2%); irradiation at δ 2.06 gave enhancements at δ 2.27 (1.1%) and at δ 3.87 (6.4%); irradiation at δ 2.18 gave an enhancement at δ 6.97 (5.0%); irradiation at δ 2.27 gave enhancements at δ 2.06 (1.4%) and at δ 6.94 (9.0%); Irradiation at δ 2.36 gave enhancements at δ 3.87 (3.4%) and at δ 6.97 (5.5%); irradiation at δ 3.87 gave enhancements at δ 2.06 (2.6%) and at δ 2.36 (2.9%); irradiation at δ 6.28 gave an enhancement at δ 2.04 (1.0%); irradiation at δ 6.94 gave an enhancement at δ 2.27 (1.7%); irradiation at δ 6.97 gave enhancements at δ 2.18 (1.0%) and at δ 2.36 (1.2%). ^{13}C n.m.r. ($CDCl_3$) δ 15.7, 2-Me, 6-Me; 19.1, 19.2, 2'-Me, 4'-Me; 19.3, 5'-Me; 20.6, 3-Me, 5-Me; 32.7, CH_2; 127.9, C6; 129.8, C4; 131.2, C3'; 133.2, 133.5, C2, C3, C5, C5', C6; 133.8, C4'; 135.3, C2'; 136.7, C1. The above assignments were confirmed by reverse detected heteronuclear correlation spectra (HMQC, HMBC).

2,4,5-Trimethyl-1-(2',2',2'-trinitroethyl)-benzene (219), m.p. 70-73° (Found: $M^{+\bullet}$ 283.0804. $C_{11}H_{13}N_3O_6$ requires 283.0804). ν_{max} (KBr) 1605, 1578 cm^{-1}. ^1H n.m.r. ($CDCl_3$) δ 2.17, s, 2-Me; 2.18, s, 5-Me; 2.21, s, 4-Me; 4.38, br s, CH_2; 6.82, s, H6; 7.00, s, H3. N.O.e. experiments gave the following results: irradiation at δ 2.17 gave enhancements at δ 4.38 (1.3%) and at δ 7.00 (4.1%); irradiation at δ 2.18 gave an enhancement at δ 6.82 (3.9%); irradiation at δ 2.21 gave an enhancement at δ 7.00 (3.8%); irradiation at δ 4.38 gave enhancements at δ 2.17 (1.6%) and at δ 6.82 (4.0%); irradiation at δ 6.82 gave enhancements at δ 2.18 (0.6%) and at δ 4.38 (0.6%); irradiation at δ 7.00 gave enhancements at δ 2.17 (0.6%) and at δ 2.21 (0.2%). ^{13}C n.m.r. ($CDCl_3$) δ 18.6, 5-Me; 19.2, 4-Me; 19.4,

2-Me; 36.3, **C**H_2; 122.4, C1 or C2; 130.4, C6; 132.7, C3; 135.4, C2 or C1, and C4 or C5; 138.3, C5 or C4; resonance for **C**$(NO_2)_3$ not observed. The above assignments were confirmed by reverse detected heteronuclear correlation spectra (HMQC, HMBC).

2,3,5,6-Tetramethylnitrobenzene (220), m.p. 109-114°, identical with an authentic sample.[11] ν_{max} (KBr) 1520 cm^{-1}. ^1H n.m.r. ($CDCl_3$) δ 2.12, s, 2-Me, 6-Me; 2.25, s, 3-Me, 5-Me; 7.04, s, H4. N.O.e. experiments gave the following results: irradiation at δ 2.25 gave an enhancement at δ 7.04 (4.4%); irradiation at δ 7.04 gave an enhancement at δ 2.25 (0.3%).

2,4,5-Trimethylphenylnitromethane (221),[12] isolated as an oil (Found: $M^{+\bullet}$ 179.0944. $C_{10}H_{13}NO_2$ requires 179.0946). ν_{max} (liquid film) 1543, 1369 cm^{-1}. ^1H n.m.r. ($CDCl_3$) δ 2.23, s, 4-Me, 5-Me; 2.31, s, 2-Me; 5.41, s, C**H**$_2$; 7.02, s, H3; 7.10, s, H6. N.O.e. experiments gave the following results: irradiation at δ 2.23 gave enhancements at δ 7.02 (2.3%) and at δ 7.10 (2.7%); irradiation at δ 2.31 gave enhancements at δ 5.41 (0.8%) and at δ 7.02 (2.5%); irradiation at δ 5.41 gave enhancements at δ 2.31 (0.5%) and at δ 7.10 (3.6%); irradiation at δ 7.02 gave enhancements at δ 2.23 (0.2%) and at δ 2.31 (0.5%); irradiation at δ 7.10 gave enhancements at δ 5.41 (0.7%).

2,2',3,4',5,5'6-Heptamethyl-4-nitrodiphenylmethane (226), m.p. 157° (dec.) (Insufficient for elemental analysis. Found: $M^{+\bullet}$ 311.1885. $C_{20}H_{25}NO_2$ requires 311.1885). ν_{max} (KBr) 1524 cm^{-1}. ^1H n.m.r. ($CDCl_3$) δ 2.08, s, 5'-Me; 2.11, s, 2-Me, 6-Me; 2.19, s, 3-Me, 4'-Me, 5-Me; 2.36, s, 2'-Me; 3.88, s, C**H**$_2$; 6.20, s, H6'; 6.99, s, H3'. N.O.e. experiments gave the following results: irradiation at δ 2.08 gave an enhancement at δ 6.20 (6.5%); irradiation at δ 2.11 gave an enhancement at δ 3.88 (4.1%); irradiation at δ 2.19 gave an enhancement at δ 6.99 (5.0%); irradiation at δ 2.36 gave enhancements at δ 3.88 (2.1%) and at δ 6.99 (5.9%); irradiation at δ 3.88 gave enhancements at δ 2.11 (2.6%), at δ 2.36 (2.5%),

and at δ 6.20 (1.7%); irradiation at δ 6.20 gave an enhancement at δ 2.08 (1.2%); irradiation at δ 6.99 gave enhancements at δ 2.19 (0.4%) and at δ 2.36 (1.2%). ^{13}C n.m.r. ($CDCl_3$) δ 15.0, 3-Me or 4'-Me; 16.2, 2-Me; 19.1, 2'-Me and 4'-Me or 3-Me; 19.3, 5'-Me; 33.1, **C**H_2; 127.5, C6'; 131.4, C3'; 133.2, 133.9, C1', C2'; 135.1, C2; 138.9, C1; signals due to C3, C4, C4' and C5' could not be assigned. The above assignments were confirmed by reverse detected heteronuclear correlation spectra (HMQC, HMBC).

2,4,5-Trimethylbenzaldehyde (222),[12] isolated as an oil (Found: $M^{+\bullet}$ 148.0886. $C_{10}H_{12}O$ requires 148.0888. Fragmentation pattern identical with an authentic sample). ν_{max} (liquid film) 2754, 1697 cm^{-1}. ^1H n.m.r. ($CDCl_3$) δ 2.29, s, 4-Me, 5-Me; 2.60, s, 2-Me; 7.03, s, H3; 7.55, s, H6; 10.19, s, C**H**O. N.O.e. experiments gave the following results: irradiation at δ 2.29 gave enhancements at δ 7.03 (2.3%) and at δ 7.55 (2.3%); irradaiation at δ 2.60 gave enhancements at δ 7.03 (2.3%) and at δ 10.19 (1.7%); irradiation at δ 7.03 gave enhancements at δ 2.29 (0.1%) and at δ 2.60 (0.3%); irradiation at δ 7.55 gave enhancements at δ 2.29 (0.2%) and at δ 10.19 (2.0%); irradiation at δ 10.19 gave enhancements at δ 2.60 (0.2%) and at δ 7.55 (1.4%).

2,4,5-Trimethylbenzyl alcohol (223), isolated as an oil (Found: $M^{+\bullet}$ 150.1040. $C_{10}H_{14}O$ requires 150.1045. Fragmentation pattern identical with an authentic sample). ν_{max} (liquid film) 3379 cm^{-1}. ^1H n.m.r. ($CDCl_3$) δ 2.22, s, 4-Me, 5-Me; 2.28, s, 2-Me; 4.61, s, C**H**$_2$; 6.95, s, H3; 7.08, s, H6. N.O.e. experiments gave the following results: irradiation at δ 2.22 gave enhancements at δ 6.95 (2.5%) and at δ 7.08 (2.3%); irradiation at δ 2.28 gave enhancements at δ 4.61 (0.6%) and at δ 6.95 (2.2%); irradiation at δ 4.61 gave enhancements at δ 2.28 (0.3%) and at δ 7.08 (2.1%); irradiation at δ 6.95 gave enhancements at δ 2.22 (0.4%) and at δ 2.28 (0.4%); irradiation at δ 7.08 gave enhancements at δ 2.22 (0.1%) and at δ 4.61 (0.4%).

2,4,5-Trimethylbenzyl nitrate (224) was not eluted from the silica gel Chromatotron plate, being presumably hydrolysed to the corresponding 2,4,5-trimethylbenzyl alcohol (223). The presence of the known 2,4,5-trimethylbenzyl nitrate (224) in the crude reaction mixture was inferred from the ^{1}H n.m.r. signal due to the -C**H$_2$**-ONO$_2$ group at δ 5.39.[12]

5.3.2.3 Photonitration of 1,2,4,5-Tetramethylbenzene (134) in Acetonitrile

Photochemistry in acetonitrile at +20° and the identification of the N*-nitroso acetamide* (227).

Reaction of 1,2,4,5-tetramethylbenzene (134) / tetranitromethane in acetonitrile at +20°, as above, for 4 h gave a product which was shown by ^{1}H n.m.r. spectral analysis (Table 3.7) to be a mixture of aromatic compounds (218)-(224) and (226) (total 86%), the dioxadiazole (227) (9%) and unidentified aromatic products (5%). Chromatography of the reaction mixture on a silica gel Chromatotron plate gave the N-nitroso acetamide (227) in a fraction eluted immediately before 2,4,5-trimethylbenzaldehyde (222):

N-(*2,4,5-trimethylbenzyl*)-N-*nitroso acetamide* (227), isolated as an oil (Insufficient for elemental analysis. Found: $M^{+\bullet}$ 220.12105. $C_{12}H_{16}N_2O_2$ requires 220.1212. M^+-NO 190.1227. $C_{12}H_{16}NO$ requires 190.1232). ν_{max} (liquid film) 1726, 1499, 1128 cm^{-1}. ^{1}H n.m.r. ($CDCl_3$) δ 2.13, s, 5'-Me; 2.16, s, 4'-Me; 2.31, s, 2'-Me; 2.85, s, 1-Me; 4.86, s, C**H$_2$**; 6.50, s, H6'; 6.90, s, H3'. N.O.e. experiments gave the following results: irradiation at δ 2.13 gave an enhancement at δ 6.50 (4.2%); irradiation at δ 2.16 gave an enhancement at δ 6.90 (3.5%); irradiation at δ 2.31 gave enhancements at δ 4.86 (1.3%) and at δ 6.90 (3.7%); irradiation at δ 4.86 gave enhancements at δ 2.31 (1.2%) and at δ 6.50 (2.7%); irradiation at δ 6.50 gave enhancements at δ 2.13 (0.9%) and at δ 4.86 (0.5%);

irradiation at δ 6.90 gave enhancements at δ 2.16 (0.6%) and at δ 2.31 (0.8%). ^{13}C n.m.r. ($CDCl_3$) δ 18.7, 2'-Me; 19.2, 19.3, 4'-Me, 5'-Me; 22.8, 1-Me; 39.5, **C**H_2; 127.9, C6'; 129.4, C2'; 131.8, C3'; 133.0, C1'; 134.1, C4'; 135.8, C5'; 174.6, C2. The above assignments were confirmed by reverse detected heteronuclear correlation spectra (HMQC, HMBC).

5.3.2.4 Photonitration of 1,2,4,5-Tetramethylbenzene (134) in Dichloromethane Containing Trifluoroacetic Acid

Reaction of 1,2,4,5-tetramethylbenzene (134) / tetranitromethane in dichloromethane containing trifluoroacetic acid (0.71 mol L^{-1}) at +20°, as above, for 4 h gave a product which was shown by ^1H n.m.r. spectral analysis (Table 3.8) to be a mixture of aromatic compounds (218)-(222), (224) and (226) (total 80%), and unidentified aromatic products (20%).

5.3.2.5 Rearrangement of 1,3,4,6-Tetramethyl-*r*-3-nitro-*t*-6-trinitromethylcyclohexa-1,4-diene (216) in Acetonitrile

A solution of the adduct (216) (11 mg) in acetonitrile (11 mL) was stored in the dark at +20°. Aliquots were withdrawn from the reaction mixture at appropriate time intervals, the solvent removed under reduced pressure at ≤0°, and the composition of each residue determined by ^1H n.m.r. spectral analysis. Within the first 5 min. adduct (216) underwent epimerization to give adduct (217), and also nitro-nitrito rearrangement to give the epimeric trinitromethyl nitrites (229) and (230), equilibrium (8:9:22a:23a ~ 3:1:4:1) between these species being reached after a reaction time of 3-5 min. During the workup procedure the trinitromethyl nitrites (229) and (230) were converted into the corresponding 1,2,4,5-tetramethyl-*t*-4-trinitromethylcyclohexa-2,5-dien-*r*-1-ol (231), ^1H n.m.r.

($CDCl_3$) δ 1.42, s, 1-Me; 1.75, s, 4-Me; 1.78, d, $J_{2\text{-Me,H3}}$ 1.5 Hz, 2-Me; 1.92, d, $J_{5\text{-Me,H6}}$ 1.5 Hz, 5-Me; 5.54, q, $J_{H6,5\text{-Me}}$ 1.5 Hz, H6; 5.88, q, $J_{H3,2\text{-Me}}$ 1.5 Hz, H3; and 1,2,4,5-tetramethyl-*c*-4-trinitromethylcyclohexa-2,5-dien-*r*-1-ol (232), ^1H n.m.r. ($CDCl_3$) δ 1.32, s, 1-Me; 1.69, s, 4-Me; 1.76, br s, 2-Me; 1.90, br s, 5-Me; 5.53, q, $J_{H6,5\text{-Me}}$ 1.5 Hz, H6; 5.84, q, $J_{H3,2\text{-Me}}$ 1.5 Hz, H3. Subsequently over *c.* 2 h this equilibrium mixture of adducts (216), (217), (229) and (230) was converted into a mixture of 2,4,5-trimethyl-1-(2',2',2'-trinitroethyl)-benzene (219) (15%), 2,3,5,6-tetramethylnitrobenzene (220) (19%), 2,4,5-trimethylphenylnitromethane (221) (13%), 2,4,5-trimethylbenzyl alcohol (223) (24%), 2,4,5-trimethylbenzyl nitrate (224) (3%), and unidentified aromatic products (total 23%).

5.3.2.6 Rearrangement of 1,3,4,6-Tetramethyl-*r*-3-nitro-*t*-6-trinitromethylcyclohexa-1,4-diene (216) in (D)Chloroform

A solution of the adduct (216) in (D)chloroform was stored in the dark at +20°, and the ^1H n.m.r. spectrum of the solution was monitored at appropriate time intervals. In comparison with the rearrangement of adduct (216) in acetonitrile, above, the transformations of adduct (216) in (D)chloroform occurred sluggishly, equilibrium with the epimeric adduct (217) (8:9 ~ 6:1) being established only after *c.* 90 h, and the formation of products from the adduct mixture being complete after >14 days. In contrast to the rearrangement in acetonitrile, the hydroxy/trinitromethyl adducts (231) and (232) were not detected in the rearrangement in (D)chloroform. The products present after 25 days were 1-(2',2',2'-trinitroethyl)-2,4,5-trimethylbenzene (219) (52%), 2,3,5,6-tetramethyl-1-nitrobenzene (220) (1%) 2,4,5-trimethylphenylnitromethane (221) (18%), 2,4,5-trimethylbenzaldehyde (222) (6%), 2,4,5-trimethylbenzyl nitrate (224) (10%), 2,4,5-trimethylbenzyl nitrite (225) (trace) and unidentified aromatic

compounds (total 13%).

5.3.2.7 Nitration of 1,2,4,5-Tetramethylbenzene (134) with Nitrogen Dioxide in Dichloromethane

A solution of 1,2,4,5-tetramethylbenzene (134) (0.47 mol L^{-1}) in dichloromethane saturated with nitrogen dioxide was stored at +20° in the dark. Aliquots were removed at appropriate time intervals, the excess nitrogen dioxide and solvent were removed under reduced pressure at ≤0°, and the product composition determined by ^1H n.m.r. spectral analysis (Table 3.9). After 4 h the products formed were shown to be predominantly 2,4,5-trimethylbenzyl nitrate (224) (68%), and 2,4,5-trimethylphenylnitromethane (221) (23%), with small amounts of aromatic compounds (218), (222) and (223) and unidentified aromatic compounds.

5.3.2.8 Photonitration of 1,2,4,5-Tetramethylbenzene (134) with Nitrogen Dioxide in Dichloromethane

A solution of 1,2,4,5-tetramethylbenzene (134) (0.47 mol L^{-1}) in dichloromethane saturated with nitrogen dioxide was irradiated with filtered light ($\lambda_{cut\text{-}off}$<435 nm) at +20°. Aliquots were removed at appropriate time intervals, the excess nitrogen dioxide and solvent were removed under reduced pressure at ≤0°, and the product composition determined by ^1H n.m.r. spectral analysis (Table 3.9). After 4 h the products formed were shown to be similar to those of the "dark" reaction, above, i.e. predominantly 2,4,5-trimethylbenzyl nitrate (224) (70%), and 2,4,5-trimethylphenylnitromethane (221) (20%), with small amounts of aromatic compounds (218), (222) and (223) and unidentified aromatic compounds.

5.3.2.9 Nitration of 1,2,4,5-Tetramethylbenzene (134) with Nitrogen Dioxide in 1,1,1,3,3,3-Hexafluoropropan-2-ol (HFP)

A solution of 1,2,4,5-tetramethylbenzene (134) (0.47 mol L^{-1}) in HFP saturated with nitrogen dioxide was stored at +20° in the dark. Aliquots were removed at appropriate time intervals, the excess nitrogen dioxide and solvent were removed under reduced pressure at ≤0°, and the product composition determined by ^1H n.m.r. spectral analysis. Complete reaction of 1,2,4,5-tetramethylbenzene (134) had occurred after <0.5 h and the products formed were shown to be predominantly 2,3,5,6-tetramethylnitrobenzene (220) (72%), 2,4,5-trimethylbenzoic acid (233) (18%), 2,3,5,6-tetramethyl-1,4-dinitrobenzene (234) (4%), with small amounts of aromatic compounds (221) (1%) and (222) (trace) and unidentified aromatic compounds (total 5%).

Chromatography of the reaction mixture on a silica gel Chromatotron plate gave the carboxylic acid (233) in a fraction eluted immediately after 2,4,5-trimethylbenzaldehyde (222):

2,4,5-Trimethylbenzoic acid (233), m.p. 148-149°, (Found: $M^{+\bullet}$ 164.0838. $C_{10}H_{12}O_2$ requires 164.0837 Fragmentation pattern identical with an authentic sample). ν_{max} (KBr) 2966, 2928, 1690 cm^{-1}. ^1H n.m.r. ($CDCl_3$) δ 2.25, s, 5-Me; 2.26, s, 4-Me; 2.58, s, 2-Me; 7.02, s, H3; 7.85, s, H6. N.O.e. experiments gave the following results: irradiation at δ 2.25 gave an enhancement at δ 7.85 (7.7%); irradiation at δ 2.26 gave an enhancement at δ 7.02 (5.8%); irradiation at δ 2.58 gave an enhancement at δ 7.02 (7.0%); irradiation at δ 7.02 gave enhancements at δ 2.26 (0.5%) and at δ 2.58 (1.7%); irradiation at δ 7.85 gave an enhancement at δ 2.25 (1.4%). ^{13}C n.m.r. ($CDCl_3$) δ 19.0, 5-Me; 19.7, 4-Me; 21.6, 2-Me; 125.5, C1; 132.7, C6; 133.3, C3; 134.0, C5; 138.8, C2; 142.4, C4; 173.7, $\mathbf{C}O_2H$. The above assignments were confirmed by reverse detected heteronuclear correlation

spectra (HMQC, HMBC).

2,3,5,6-Tetramethyl-1,4-dinitrobenzene (234) was not eluted from the silica gel Chromatotron plate. However, the presence of 2,3,5,6-tetramethyl-1,4-dinitrobenzene (234) in the crude mixture was inferred by comparing the ^{1}H n.m.r. signal due to the methyl groups, δ 2.32, with an authentic sample.

5.3.2.10 Photonitration of 1,2,4,5-Tetramethylbenzene (134) with Nitrogen Dioxide in 1,1,1,3,3,3-Hexafluoropropan-2-ol (HFP)

A solution of 1,2,4,5-tetramethylbenzene (134) (0.47 mol L^{-1}) in HFP saturated with nitrogen dioxide was irradiated with filtered light ($\lambda_{cut\text{-}off}$<435 nm) at +20°. Aliquots were removed at appropriate time intervals, the excess nitrogen dioxide and solvent were removed under reduced pressure at ≤0°, and the product composition determined by ^{1}H n.m.r. spectral analysis. Complete reaction of 1,2,4,5-tetramethylbenzene (134) had occurred after <0.5 h and the products formed were shown to be similar to those of the "dark" reaction, above, i.e. predominantly 2,3,5,6-tetramethylnitrobenzene (220) (70%), 2,4,5-trimethylbenzoic acid (233) (18%), 2,3,5,6-tetramethyl-1,4-dinitrobenzene (234) (4%), with small amounts of aromatic compounds (221) (1%) and (222) (trace), and unidentified aromatic compounds (total 7%).

5.3.3 GENERAL PROCEDURE FOR THE PHOTONITRATION OF PENTAMETHYLBENZENE (135) WITH TETRANITROMETHANE.

A solution of pentamethylbenzene (135) (500 mg, 0.42 mol L^{-1}) and tetranitromethane (0.84 mol L^{-1}) in dichloromethane (at +20, -20, -50, or -78°) or acetonitrile (at +20 or -20°) was irradiated with filtered light ($\lambda_{cut\text{-}off}$<435 nm). Aliquots were withdrawn from the reaction mixture at appropriate time intervals, the volatile material removed under reduced pressure at ≤0°, and the product composition determined by ^1H n.m.r. spectral analysis (Tables 3.10 and 3.11).

5.3.3.1 Photonitration of Pentamethylbenzene (135) in Dichloromethane

Photochemistry in dichloromethane at -78° and the identification of adducts (244) *and* (245).

Reaction of pentamethylbenzene (135) / tetranitromethane in dichloromethane at -78°, as above, for 3 h gave a product which was shown by ^1H n.m.r. spectral analysis (Table 3.10) to be a mixture of adduct (244) (15%), adduct (245) (1%), aromatic compounds (246)-(260) (total 79%), and unidentified aromatic products (5%). H.p.l.c. allowed the separation of the unstable adduct (244), but adduct (245) was not isolated by this means and its identification is only tentative.

1,2,3,4,6-Pentamethyl-*r*-3-nitro-*t*-6-trinitromethylcyclohexa-1,4-diene (244), isolated as an impure (*c.* 95%) oil. ν_{max} (liquid film) 1616, 1596, 1576, 1550 cm^{-1}. ^1H n.m.r. ($CDCl_3$) δ 1.69, q, $J_{2\text{-}Me,1\text{-}Me}$ 1.5 Hz, 2-Me; 1.74, br s, 1-Me, 3-Me and 4-Me; 1.97, s, 6-Me; 6.21, q, $J_{H5,4\text{-}Me}$ 1.5 Hz, H5. N.O.e. experiments gave the following results: irradiation at δ 1.69 gave an enhancement at δ 1.97 (0.4%); irradiation at δ 1.74 gave enhancements at δ 1.97 (0.9%), and at δ 6.21 (6.7%); irradiation at δ 1.97 gave

enhancements at δ 1.69 (0.8%), at δ 1.74 (0.6%), and at δ 6.21 (4.2%); irradiation at δ 6.21 gave enhancements at δ 1.74 (0.6%) and at δ 1.97 (0.7%). ^{13}C n.m.r. not obtainable because of the instability of adduct (244) in solution.

1,2,3,4,6-Pentamethyl-*r*-3-nitro-*c*-6-trinitromethylcyclohexa-1,4-diene (245), only seen as a minor component in complex mixtures. ^1H n.m.r. ($CDCl_3$) δ 6.33, q, $J_{H5,4\text{-}Me}$ 1.5 Hz, H5; the remainder of the spectrum was obscured by signals due to other compounds.

Photochemistry in dichloromethane at +20° and the identification of aromatic products (246)-(260).

Reaction of pentamethylbenzene (135) / tetranitromethane in dichloromethane at +20°, as above, for 3 h gave a product which was shown by ^1H n.m.r. spectral analysis (Table 3.10) to be a mixture of aromatic compounds (246)-(260) (in Table 3.10, the yields of compounds (250) and (254) could not be assessed individually from ^1H n.m.r. spectra because of signal coincidences). Chromatography on a silica gel Chromatotron plate allowed the separation of compounds (246)-(256) in the order of elution below, the benzyl nitrates (257) and (258) and benzyl nitrites (259) and (260) being presumably hydrolysed to give the related benzyl alcohols (256) and (255), respectively.

2,3,4,6-Tetramethyl-1-(2',2',2'-trinitroethyl)-benzene (246) as an oil, which could not be induced to crystallize (Insufficient for elemental analysis. Found: $M^{+\bullet}$ 297.0959. $C_{12}H_{15}N_3O_6$ requires 297.0961). ν_{max} (liquid film) 1616, 1601, 1580 cm^{-1}. ^1H n.m.r. ($CDCl_3$) δ 2.10, s, 2-Me; 2.14, s, 3-Me; 2.16, s, 6-Me; 2.25, s, 4-Me; 4.74, br s, CH_2; 6.88, s, H5. N.O.e. experiments gave the following results: irradiation at δ 2.10 gave an enhancement at δ 4.74 (1.9%); irradiation at δ 2.16 gave enhancements at δ 4.74 (1.5%) and at δ 6.88 (3.8%); irradiation at δ 2.25 gave an

enhancement at δ 6.88 (3.8%); irradiation at δ 4.74 gave enhancements at δ 2.10 (1.9%) and at δ 2.16 (1.5%); irradiation at δ 6.88 gave enhancements at δ 2.16 (0.6%) and at δ 2.25 (0.6%). ^{13}C n.m.r. ($CDCl_3$) δ 16.1, 3-Me; 16.7, 2-Me; 20.1, 6-Me; 20.7, 4-Me; 34.8, **C**H_2; 123.5, C1; 130.6, C5; 134.2, C3; 135.1, C6; 136.9, C2; 137.8, C4; resonance for **C**$(NO_2)_3$ not observed. The above assignments were confirmed by reverse detected heteronuclear correlation spectra (HMQC, HMBC).

2,3,4,5-Tetramethyl-1-(2',2',2'-trinitroethyl)-benzene (247) as an oil, which could not be induced to crystallize (Insufficient for elemental analysis. Found: $M^{+\bullet}$ 297.0960. $C_{12}H_{15}N_3O_6$ requires 297.0961). ν_{max} (liquid film) 1609, 1576 cm^{-1}. ^1H n.m.r. ($CDCl_3$) δ 2.09, s, 2-Me; 2.19 and 2.20, both s, 3-Me, 4-Me; 2.23, s, 5-Me; 4.45, br s, C**H$_2$**; 6.74, s, H6. N.O.e. experiments gave the following results: irradiation at δ 2.09 gave an enhancement at δ 4.45 (1.8%); irradiation at δ 2.23 gave an enhancement at δ 6.74 (4.2%); irradiation at δ 4.45 gave enhancements at δ 2.09 (1.6%) and at δ 6.74 (5.4%); irradiation at δ 6.74 gave enhancements at δ 2.23 (0.6%) and at δ 4.45 (0.7%). ^{13}C n.m.r. ($CDCl_3$) δ 16.1, 2-Me; 16.2 and 16.7, 3-Me, 4-Me; 20.7, 5-Me; 37.2, **C**H_2; 121.9, C1; 128.6, C6; 134.2, C2; 134.8, C5; 136.6, C3; 136.9, C4; resonance for **C**$(NO_2)_3$ not observed. The above assignments were confirmed by reverse detected heteronuclear correlation spectra (HMQC, HMBC).

2,3,4,5,6,2',3',4',6'-Nonamethyldiphenylmethane (248),[14] (Found: $M^{+\bullet}$ 294.2349. $C_{22}H_{30}$ requires 294.23475). ^1H n.m.r. ($CDCl_3$) δ 2.00, s, 2'-Me; 2.04, s, 6'-Me; 2.07, s, 2-Me, 6-Me; 2.13, s, 3'-Me; 2.19, s, 3-Me, 5-Me; 2.23, s, 4-Me, 4'-Me; 4.12, s, C**H$_2$**; 6.77, s, H5'. N.O.e. experiments gave the following results: irradiation at δ 2.00 gave enhancements at δ 2.13 (1.3%) and at δ 4.12 (1.9%); irradiation at δ 2.04 gave enhancements at δ 4.12 (1.9%) and at δ 6.77 (5.7%); irradiation at δ 2.07 gave enhancements at δ 2.19 (1.0%) and at δ 4.12 (3.2%); irradiation at

δ 2.13 gave an enhancement at δ 2.00 (1.8%); irradiation at δ 2.19 gave an enhancement at δ 2.07 (1.5%); irradiation at δ 2.23 gave an enhancement at δ 6.77 (5.2%); irradiation at δ 4.12 gave enhancements at δ 2.00 (2.1%), δ 2.04 (1.7%) and at δ 2.07 (1.9%); irradiation at δ 6.77 gave enhancements at δ 2.04 (1.3%) and at δ 2.23 (0.7%). ^{13}C n.m.r. ($CDCl_3$) δ 16.0, 3'-Me; 16.6, 2'-Me; 16.9, 3-Me, 5-Me; 17.0, 4-Me; 17.2, 2-Me, 6-Me; 20.6, 4'-Me; 21.0, 6'-Me; 33.3, **C**H_2; 130.1, C5'; 132.3, C3, C4, C5; 132.4, C2, C6; 132.8, C3'; 133.3, C4'; 133.5, C6'; 135.2, C2'; 136.2, C1, C1'. The above assignments were confirmed by reverse detected heteronuclear correlation spectra (HMQC, HMBC).

2,3,4,5,6,2',3',4',5'-Nonamethyldiphenylmethane (249),[14] m.p. 148° (sublimed) (Found: $M^{+\bullet}$ 294.2350. $C_{22}H_{30}$ requires 294.23475). ^1H n.m.r. ($CDCl_3$) δ 2.08, s, 5'-Me; 2.09, s, 2-Me, 6-Me; 2.16, 2.26, 2.28, all s, 3'-Me, 4-Me, 4'-Me; 2.24, s, 3-Me, 5-Me; 2.34, s, 2'-Me; 3.92, br s, C**H$_2$**; 6.25, s, H6'. N.O.e. experiments gave the following results: irradiation at δ 2.08 gave an enhancement at δ 6.25 (9.5%); irradiation at δ 2.09 gave enhancements at δ 2.24 (1.8%), δ 3.92 (4.4%) and at δ 6.25 (7.9%); irradiation at δ 2.24 gave an enhancement at δ 2.09 (1.5%); irradiation at δ 2.34 gave an enhancement at δ 3.92 (2.9%); irradiation at δ 3.92 gave enhancements at δ 2.09 (2.8%), δ 2.34 (3.8%) and at δ 6.25 (2.1%); irradiation at δ 6.25 gave enhancements at δ 2.08 (1.1%), δ 2.09 (0.3%) and at δ 3.92 (0.6%). ^{13}C n.m.r. ($CDCl_3$) δ 15.4, 2'-Me; 16.0, 16.4, 16.9, 3'-Me, 4-Me, 4'-Me; 16.8, 2-Me, 3-Me, 5-Me, 6-Me; 20.8, 5'-Me; 34.4, **C**H_2; 125.9, C6'; 131.8, C1'; 132.2, C3, C5; 132.7, 133.3, C4, C4', C5'; 133.0, C2, C6; 134.0, C1; 134.6, C3'; 134.9, C2'. The above assignments were confirmed by reverse detected heteronuclear correlation spectra (HMQC, HMBC).

2,3,4,5,6-Pentamethylnitrobenzene (250),[15] (Found: $M^{+\bullet}$ 193.1102. $C_{11}H_{15}NO_2$ requires 193.1103). ν_{max} (KBr) 1524 cm^{-1}. ^1H n.m.r. ($CDCl_3$) δ 2.15, 2.22, both s, 2-Me, 3-Me, 5-Me, 6-Me; 2.24, s, 4-Me.

2,3,4,6-Tetramethylphenylnitromethane (251), as an oil which could not be induced to crystallize (Insufficient for elemental analysis. Found: $M^{+\bullet}$ 193.1102. $C_{11}H_{15}NO_2$ requires 193.1103). ν_{max} (liquid film) 1541 cm^{-1}. ^1H n.m.r. ($CDCl_3$) δ 2.19, s, 3-Me; 2.28, s, 4-Me; 2.30, s, 2-Me; 2.35, s, 6-Me; 5.61, s, C**H**$_2$; 6.95, s, H5. N.O.e. experiments gave the following results: irradiation at δ 2.28 gave an enhancement at δ 6.95 (2.9%); irradiation at δ 2.30 gave an enhancement at δ 5.61 (1.4%); irradiation at δ 2.35 gave enhancements at δ 5.61 (1.3%) and at δ 6.95 (2.7%); irradiation at δ 5.61 gave enhancements at δ 2.30 (1.2%) and at δ 2.35 (0.8%); irradiation at δ 6.95 gave enhancements at δ 2.28 (0.4%) and at δ 2.35 (0.4%). ^{13}C n.m.r. ($CDCl_3$) δ 16.0, 3-Me; 16.2, 2-Me; 19.8, 6-Me; 20.9, 4-Me; 74.4, **C**H_2; 124.8, C1; 130.0, C5; 133.6, C3; 135.5, C6; 137.2, C2; 138.6, C4. The above assignments were confirmed by reverse detected heteronuclear correlation spectra (HMQC, HMBC).

2,3,4,5-Tetramethylphenylnitromethane (252),[12] (Found: $M^{+\bullet}$ 193.11025. $C_{11}H_{15}NO_2$ requires 193.1103). ν_{max} (KBr) 1549 cm^{-1}. ^1H n.m.r. ($CDCl_3$) δ 2.20, s, 4-Me; 2.22, s, 3-Me; 2.24, s, 2-Me; 2.27, s, 5-Me; 5.43, s, C**H**$_2$; 6.98, s, H5. N.O.e. experiments gave the following results: irradiation at δ 2.24 gave an enhancement at δ 5.43 (1.2%); irradiation at δ 2.27 gave an enhancement at δ 6.98 (3.0%); irradiation at δ 5.43 gave enhancements at δ 2.24 (1.0%) and at δ 6.98 (4.2%); irradiation at δ 6.98 gave enhancements at δ 2.27 (0.4%) and at δ 5.43 (0.8%). ^{13}C n.m.r. ($CDCl_3$) δ 15.9, 2-Me; 16.3, 3-Me, 4-Me; 20.5, 5-Me; 78.5, **C**H_2; 125.4, C1; 130.6, C6; 133.9, C2; 134.2, C5; 136.2, C3. The above assignments were confirmed by reverse detected heteronuclear correlation spectra (HMQC, HMBC).

2,3,4,5-Tetramethylbenzaldehyde (253),[16] (Found: $M^{+\bullet}$ 162.1041. $C_{11}H_{14}O$ requires 162.1045). ν_{max} (KBr) 1693, 1383 cm^{-1}. ^1H n.m.r. ($CDCl_3$) δ 2.24, s, 3-Me; 2.26, s, 4-Me; 2.33, s, 5-Me; 2.57, s, 2-Me; 7.45, s,

H6; 10.24, s, C**H**O. N.O.e. experiments gave the following results: irradiation at δ 2.24 gave an enhancement at δ 2.57 (0.8%); irradiation at δ 2.33 gave an enhancement at δ 7.45 (2.5%); irradiation at δ 2.57 gave enhancements at δ 2.24 (1.0%) and at δ 10.24 (2.1%); irradiation at δ 7.45 gave enhancements at δ 2.33 (0.4%) and at δ 10.24 (1.9%); irradiation at δ 10.24 gave enhancements at δ 2.57 (0.5%) and at δ 7.45 (1.9%). ^{13}C n.m.r. ($CDCl_3$) δ 14.6, 2-Me; 15.6, 3-Me; 16.8, 4-Me; 20.5, 5-Me; 130.6, C6; 131.8, C1; 134.0, C5; 136.4, 136.6, C2, C3; 141.9, C4; 193.1, **C**HO. The above assignments were confirmed by reverse detected heteronuclear correlation spectra (HMQC, HMBC).

2,3,4,5,6-Pentamethylbenzoic acid (254), as an oil containing an impurity (*c.* 5%), identical with an authentic sample, (Found: $M^{+\bullet}$ 192.1151. $C_{12}H_{16}O_2$ requires 192.1150). ν_{max} (liquid film) 1697, 1383, 1279 cm^{-1}. ^1H n.m.r. ($CDCl_3$) δ 2.21, 2.29, both s, 2-Me, 3-Me, 5-Me, 6-Me; 2.24, s, 4-Me.

2,3,4,5-Tetramethylbenzyl alcohol (255),[16] (Found: $M^{+\bullet}$ 164.1199. $C_{11}H_{16}O$ requires 164.1201). ν_{max} (KBr) 3373, 3298 cm^{-1}. ^1H n.m.r. ($CDCl_3$) δ 2.20, s, 4-Me; 2.22, s, 3-Me; 2.27, s, 2-Me, 5-Me; 4.64, s, C**H$_2$**; 6.98, s, H6. N.O.e. experiments gave the following results: irradiation at δ 2.27 gave enhancements at δ 4.64 (1.0%) and at δ 6.98 (2.2%); irradiation at δ 4.64 gave enhancements at δ 2.27 (0.3%) and at δ 6.98 (2.6%); irradiation at δ 6.98 gave enhancements at δ 2.27 (0.3%) and at δ 4.64 (0.7%). ^{13}C n.m.r. ($CDCl_3$) δ 15.3, 2-Me; 16.1, 3-Me, 4-Me; 20.6, 5-Me; 64.5, **C**H_2; 127.5, C6; 132.3, C2; 133.6, C5; 134.8, C4; 135.5, C1; 135.7, C3. The above assignments were confirmed by reverse detected heteronuclear correlation spectra (HMQC, HMBC).

2,3,4,6-Tetramethylbenzyl alcohol (256), isolated only in admixture with 2,3,4,5-tetramethylbenzyl alcohol (255). ^1H n.m.r. ($CDCl_3$) δ 2.23, s, 3-Me; 2.31, s, 4-Me; 2.39, s, 2-Me; 2.41, s, 6-Me; 4.76, s, **C**H_2; 6.92, s, H5.

N.O.e. experiments gave the following results: irradiation at δ 2.31 gave an enhancement at δ 6.92 (2.9%); irradiation at δ 2.39 gave an enhancement at δ 4.76 (1.7%); irradiation at δ 2.41 gave enhancements at δ 4.76 (1.7%) and at δ 6.92 (2.8%); irradiation at δ 4.76 gave enhancements at δ 2.39 (1.4%) and at δ 2.41 (1.0%); irradiation at δ 6.92 gave enhancements at δ 2.31 (0.6%) and at δ 2.41 (0.4%). ^{13}C n.m.r. ($CDCl_3$) δ 15.7, 2-Me and 3-Me; 19.4, 6-Me; 20.7, 4-Me; 59.6, **C**H_2; 129.6, C5; 133.2, C3; 133.9, C6; 134.2, C1; 136.0, 136.3, C2, C4. The above assignments were confirmed by reverse detected heteronuclear correlation spectra (HMQC, HMBC).

The labile benzyl nitrates (257) and (258) and benzyl nitrites (259) and (260) were identified from the ^1H n.m.r. ($CDCl_3$) signal assigned to the C**H**$_2$-O-X function in each case, where X = NO_2 or NO, respectively: (257) (δ 5.56[16], s), (258) (δ 5.42[16], s), (259) [δ 5.73, br s (c.f. ref. 12)], (260) [δ 5.65, br s (c.f. ref. 12)].

5.3.3.2 Photonitration of Pentamethylbenzene (135) in 1,1,1,3,3,3-Hexafluoropropan-2-ol (HFP)

Reaction of pentamethylbenzene (135) / tetranitromethane in HFP at +20°, as above, for 24 h gave a product which was shown by ^1H n.m.r. spectral analysis to be a mixture of predominantly 2,3,4,5,6-pentamethylnitrobenzene (250) (68%), 2,3,4,5-tetramethyl-1-(2',2',2'-trinitroethyl)-benzene (247) (8%), 2,3,4,5-tetramethylphenylnitromethane (252) (11%), minor amounts of compounds (246), (249), (251), (253), (255) and (256) (total 8%) and unidentified aromatics (total 5%). The reaction was slow, only a low conversion (*c.* 17%) occurring in 3 h.

5.3.3.3 Photonitration of Pentamethylbenzene (135) in Dichloromethane Containing Trifluoroacetic Acid

Reaction of pentamethylbenzene (135) / tetranitromethane in dichloromethane containing trifluoroacetic acid (0.71 mol L^{-1}) at +20°, as above, for 3 h resulted in a low conversion (*c.* 26%) into the 2',2',2'-trinitroethyl compounds (246) (20%) and (247) (5%), nonamethyldiphenylmethanes (248) (9%) and (249) (31%), 2,3,4,5-tetramethylphenylnitromethane (252) (18%), and minor amounts of compounds (251), (253), (255)-(258) (total 7%) and unidentified aromatic compounds (total 10%) (Table 3.12).

5.3.3.4 Nitration of Pentamethylbenzene (135) with Nitrogen Dioxide in Dichloromethane

A solution of pentamethylbenzene (135) (0.42 mol L^{-1}) in dichloromethane saturated with nitrogen dioxide was stored at +20° in the dark. Aliquots were removed at appropriate time intervals, the excess nitrogen dioxide and solvent were removed under reduced pressure at ≤0°, and the product composition determined by ^1H n.m.r. spectral analysis (Table 3.13). After 3 h the products formed were shown to be predominantly 2,3,4,5-tetramethylphenylnitromethane (252) (39%), the benzyl nitrates (257) (14%) and (258) (39%) and small amounts of aromatic compounds (248), (249), (251), (253), (255) and (256) (total 7%), and unidentified aromatic compounds (total 1%).

5.3.3.5 Photonitration of Pentamethylbenzene (135) with Nitrogen Dioxide in Dichloromethane

A solution of pentamethylbenzene (135) (0.42 mol L^{-1}) in dichloromethane saturated with nitrogen dioxide was irradiated with filtered light ($\lambda_{cut\text{-}off}$<435 nm) at +20°. Aliquots were removed at appropriate time intervals, the excess nitrogen dioxide and solvent were removed under reduced pressure at ≤0°, and the product composition determined by ^1H n.m.r. spectral analysis (Table 3.13). After 3 h the products formed were shown to be similar to those of the "dark" reaction, above, i.e. predominantly 2,3,4,5-tetramethylphenylnitromethane (252) (32%), the benzyl nitrates (257) (13%) and (258) (48%) and small amounts of aromatic compounds (248), (249), (251), (253), (255) and (256) (total 6%), and unidentified aromatic compounds (total 2%).

5.3.3.6 Rearrangement of 1,2,3,4,6-Pentamethyl-*r*-3-nitro-*t*-6-trinitromethyl-cyclohexa-1,4-diene (244) in (D_2)-dichloromethane

A solution of adduct (244) in (D_2)-dichloromethane was stored at +22° and its ^1H n.m.r. spectrum monitored at appropriate time intervals. After 2 min. significant rearrangement (26%) of the adduct mixture had occurred, and the rearrangement was complete after 1 h (Fig. 3.52). At that time the major rearrangement products were 2,3,4,6-tetramethyl-1-(2',2',2'-trinitroethyl)-benzene (246) (11%), 2,3,4,5-tetramethylphenylnitromethane (252) (48%), 2,3,4,5-tetramethylbenzyl nitrate (258) (9%), 2,3,4,5-tetramethylbenzyl nitrite (260) (26%).

5.3.4 GENERAL PROCEDURE FOR THE PHOTONITRATION OF HEXAMETHYLBENZENE (136) WITH TETRANITROMETHANE.

A solution of hexamethylbenzene (136) (500 mg, 0.39 mol L^{-1}) and tetranitromethane (0.78 mol L^{-1}) in dichloromethane (at +20 or -20°) or acetonitrile (at +20°) was irradiated with filtered light ($\lambda_{cut\text{-}off}$<435 nm). Aliquots were withdrawn from the reaction mixture at appropriate time intervals, the volatile material removed under reduced pressure at ≤0°, and the product composition determined by ^1H n.m.r. spectral analysis (Tables 3.14 and 3.15).

5.3.4.1 Photonitration of Hexamethylbenzene (136) in Dichloromethane

Photochemistry in dichloromethane at -20° and the identification of aromatic products (279)-(287).

Reaction of hexamethylbenzene (136) / tetranitromethane in dichloromethane at -20°, as above, for 8 h gave a product which was shown by ^1H n.m.r. spectral analysis (Table 3.14) to be a mixture of pentamethyl-(2',2',2'-trinitroethylbenzene (279) (10%), pentamethylbenzyl nitrite (280) (6%), pentamethylbenzyl nitrate (281) (42%), pentamethylphenylnitromethane (282) (40%), and small amounts of compounds (283)-(287). The components of this mixture were separated by h.p.l.c. to give in elution order:

Pentamethyl-(2',2',2'-trinitroethyl)-benzene (279),[12] (Found: $M^{+\bullet}$ 311.1116. $C_{13}H_{17}N_3O_6$ requires 311.1117). ν_{max} (KBr) 1603, 1578 cm^{-1}. ^1H n.m.r. ($CDCl_3$) δ 2.12, s, 2-Me, 6-Me; 2.20, s, 3-Me, 5-Me; 2.24, s, 4-Me; 4.82, br s, CH_2. N.O.e. experiments gave the following results: irradiation at δ 2.12 gave an enhancement at δ 4.82 (3.6%); irradiation at δ 4.82 gave an enhancement at δ 2.12 (2.1%). ^{13}C n.m.r. ($CDCl_3$) δ 17.0, 3-Me, 4-Me,

5-Me; 17.1, 2-Me, 6-Me; 35.1, **C**H_2; 123.1, C1; 133.8, 133.9, C2, C3; 136.6, C4; resonance for **C**$(NO_2)_3$ not observed. The above assignments were confirmed by reverse detected heteronuclear correlation spectra (HMQC, HMBC).

Pentamethylbenzyl nitrite (280),[12] ν_{max} (liquid film) 1639, 1593 cm^{-1}. ^1H n.m.r. ($CDCl_3$) δ 2.23, s, 3-Me, 5-Me; 2.26, s, 4-Me; 2.27, s, 2-Me, 6-Me; 5.78, br s, C**H$_2$**. N.O.e. experiments gave the following results: irradiation at δ 2.27 gave an enhancement at δ 5.78 (2.5%); irradiation at δ 5.78 gave an enhancement at δ 2.27 (1.2%).

Pentamethylbenzyl nitrate (281),[12] (Found: $M^{+\bullet}$ 223.1207. $C_{12}H_{17}NO_3$ requires 223.1208). ν_{max} (KBr) 1624, 1611 cm^{-1}. ^1H n.m.r. ($CDCl_3$) δ 2.23, s, 3-Me, 5-Me; 2.26, s, 4-Me; 2.31, s, 2-Me, 6-Me; 5.63, s, C**H$_2$**. N.O.e. experiments gave the following results: irradiation at δ 2.31 gave an enhancement at δ 5.63 (3.4%); irradiation at δ 5.63 gave an enhancement at δ 2.31 (1.8%). ^{13}C n.m.r. ($CDCl_3$) δ 16.5, 2-Me, 6-Me; 16.7, 3-Me, 5-Me; 17.2, 4-Me; 71.5, **C**H_2; 124.8, C1; 133.2, C3, C5; 134.5, C2, C6; 137.3, C4. The above assignments were confirmed by reverse detected heteronuclear correlation spectra (HMQC, HMBC).

Pentamethylphenylnitromethane (282),[17] (Found: $M^{+\bullet}$ 207.1257. $C_{12}H_{17}NO_2$ requires 207.1259). ν_{max} (KBr) 1549 cm^{-1}. ^1H n.m.r. ($CDCl_3$) δ 2.25, s, 3-Me, 5-Me; 2.27, s, 4-Me; 2.31, s, 2-Me, 6-Me; 5.67, s, C**H$_2$**. N.O.e. experiments gave the following results: irradiation at δ 2.31 gave an enhancement at δ 5.67 (2.8%); irradiation at δ 5.67 gave an enhancement at δ 2.31 (1.3%). ^{13}C n.m.r. ($CDCl_3$) δ 16.6, 2-Me, 6-Me; 16.8, 3-Me, 5-Me; 17.2, 4-Me; 74.8, **C**H_2; 124.6, C1; 133.2, C3, C5; 134.1, C2, C6; 137.3, C4. The above assignments were confirmed by reverse detected heteronuclear correlation spectra (HMQC, HMBC).

Di-(pentamethylbenzyl) ether (283),[18] m.p. 168° (dec.) (Insufficient for elemental analysis. Found: $M^{+\bullet}$ 338.2603. $C_{24}H_{34}O$ requires

338.2610). ν_{max} (KBr) 1088, 1042 cm^{-1}. ^1H n.m.r. ($CDCl_3$) δ 2.19, s, 3-Me, 5-Me; 2.21, s, 4-Me; 2.32, s, 2-Me, 6-Me; 4.64, s, CH_2. N.O.e. experiments gave the following results: irradiation at δ 2.19 gave an enhancement at δ 2.32 (2.1%); irradiation at δ 2.32 gave enhancements at δ 2.19 (2.0%) and at δ 4.64 (5.2%); irradiation at δ 4.64 gave an enhancement at δ 2.32 (3.7%). ^{13}C n.m.r. ($CDCl_3$) δ 16.2, 2-Me, 6-Me; 16.6, 3-Me, 5-Me; 16.9, 4-Me; 67.4, CH_2; 131.6, C1; 132.3, C3, C5; 133.4, C2, C6; 134.7, C4. The above assignments were confirmed by reverse detected heteronuclear correlation spectra (HMQC, HMBC).

3,4,5,6-Tetramethyl-2-nitromethylbenzyl nitrate (284), m.p. 79-82° (Insufficient for elemental analysis. Found: $M^{+\bullet}$ 268.10545. $C_{12}H_{16}N_2O_5$ requires 268.1059). ν_{max} (KBr) 1628, 1541, 1279, 858 cm^{-1}. ^1H n.m.r. ($CDCl_3$) δ 2.29, s, 4-Me, 5-Me; 2.34, s, 3-Me; 2.36, s, 6-Me; 5.70, s, CH_2ONO_2; 5.72, s, CH_2NO_2. N.O.e. experiments gave the following results: irradiation at δ 2.34 gave an enhancement at δ 5.72 (1.8%); irradiation at δ 2.36 gave an enhancement at δ 5.70 (2.0%); irradiation at δ 5.70 gave an enhancement at δ 2.36 (1.9%); irradiation at δ 5.72 gave an enhancement at δ 2.34 (2.3%). ^{13}C n.m.r. ($CDCl_3$) δ 16.6, 4-Me or 5-Me; 16.7, 6-Me; 17.2, 3-Me; 17.3, 5-Me or 4-Me; 70.1, CH_2ONO_2; 74.1, CH_2NO_2; 126.4, C2; 127.2, C1; 135.4, C3; 135.8, C6; 138.4, 138.6, C4, C5. The above assignments were confirmed by reverse detected heteronuclear correlation spectra (HMQC, HMBC).

1,2-Bis(nitromethyl)-3,4,5,6-tetramethylbenzene (285),[12] (Found: $M^{+\bullet}$ 252.1103. $C_{12}H_{16}N_2O_4$ requires 252.1110). ν_{max} (KBr) 1541 cm^{-1}. ^1H n.m.r. ($CDCl_3$) δ 2.29, s, 4-Me, 5-Me; 2.37, s, 3-Me, 6-Me; 5.82, s, CH_2. N.O.e. experiments gave the following results: irradiation at δ 2.37 gave an enhancement at δ 5.82 (1.9%); irradiation at δ 5.82 gave an enhancement at δ 2.37 (2.4%). ^{13}C n.m.r. ($CDCl_3$) δ 16.7, 3-Me, 6-Me; 17.3, 4-Me, 5-Me; 74.3, CH_2; 126.6, C1, C2; 135.7, C3, C6; 138.7, C4, C5. The above

assignments were confirmed by reverse detected heteronuclear correlation spectra (HMQC, HMBC).

3,4,5,6-Tetramethyl-2-nitromethylbenzyl alcohol (286), as an oil which could not be induced to crystallize (Insufficient for elemental analysis. Found: $M^{+\bullet}$ 223.1203. $C_{12}H_{17}NO_3$ requires 223.1208). ν_{max} (liquid film) 3383, 1551 cm^{-1}. ^1H n.m.r. ($CDCl_3$) δ 2.27 and 2.28, both s, 4-Me, 5-Me; 2.30, s, 3-Me; 2.39, s, 6-Me; 4.84, s, C**H**$_2$OH; 5.80, s, C**H**$_2$$NO_2$. N.O.e. experiments gave the following results: irradiation at δ 2.30 gave an enhancement at δ 5.80 (1.6%); irradiation at δ 2.39 gave an enhancement at δ 4.84 (1.5%); irradiation at δ 4.84 gave enhancements at δ 2.39 (1.5%) and at δ 5.80 (2.8%); irradiation at δ 5.80 gave enhancements at δ 2.30 (1.1%) and at δ 4.84 (2.5%). ^{13}C n.m.r. ($CDCl_3$) δ 16.3, 6-Me; 16.4, 17.0, 17.2, 3-Me, 4-Me, 5-Me; 59.8, **C**H_2OH; 74.5, **C**$H_2$$NO_2$; 125.4, C2; 134.0, C6; 134.9, C3; 135.8, C1; 136.3, C4; 138.3, C5. The above assignments were confirmed by reverse detected heteronuclear correlation spectra (HMQC, HMBC).

Pentamethylbenzyl alcohol (287),[12] (Found: $M^{+\bullet}$ 178.1359. $C_{12}H_{18}O$ requires 178.1358). ν_{max} (KBr) 3285 cm^{-1}. ^1H n.m.r. ($CDCl_3$) δ 2.22, s, 3-Me, 5-Me; 2.24, s, 4-Me; 2.35, s, 2-Me, 6-Me; 4.78, s, C**H**$_2$. N.O.e. experiments gave the following results: irradiation at δ 2.35 gave an enhancement at δ 4.78 (3.0%); irradiation at δ 4.78 gave an enhancement at δ 2.35 (1.5%). ^{13}C n.m.r. ($CDCl_3$) δ 16.1, 2-Me, 6-Me; 16.6, 3-Me, 5-Me; 16.9, 4-Me, 60.0, **C**H_2; 132.7, C3, C5; 132.9, 133.9, C1, C2, C6; 135.0, C4. The above assignments were confirmed by reverse detected heteronuclear correlation spectra (HMQC, HMBC). This compound was isolated in higher yield than that present in the mixture prior to h.p.l.c. separation, and may be formed by hydrolysis of either/both of the benzyl esters (280) and (281) during chromatography.

Photochemistry in dichloromethane at +20° and identification of penta-methylbenzaldehyde (288).

Reaction of hexamethylbenzene (136) / tetranitromethane in dichloromethane at +20°, as above, for 5 h gave a product which was shown by ^{1}H n.m.r. spectral analysis (Table 3.14) to be a mixture of compounds (279) (16%), (280) (8%), (281) (31%), (282) (32%), and small amounts of compounds (283)-(288). Chromatography of the reaction mixture on a silica gel Chromatotron plate gave pentamethylbenzaldehyde (288) in a fraction eluted immediately after the di-(pentamethylbenzyl) ether (283):

Pentamethylbenzaldehyde (288),[15] (Found: $M^{+\bullet}$ 176.1198. $C_{12}H_{16}O$ requires 176.1201). ν_{max} ($CHCl_3$) 2928, 2855, 1684 cm^{-1}. ^{1}H n.m.r. ($CDCl_3$) δ 2.24, s, 3-Me, 5-Me; 2.29, s, 4-Me; 2.42, s, 2-Me, 6-Me; 10.63, s, C**H**O. N.O.e. experiments gave the following results: irradiation at δ 2.42 gave an enhancement at δ 10.63 (3.1%). ^{13}C n.m.r. ($CDCl_3$) δ 16.1, 2-Me, 3-Me, 5-Me, 6-Me; 17.6, 4-Me, 131.3, C1; 131.7, C3, C5; 132.5, C2, C6; 138.3, C4; 196.5, **C**HO. The above assignments were confirmed by reverse detected heteronuclear correlation spectra (HMQC, HMBC).

5.3.4.2 Photonitration of Hexamethylbenzene (136) in Acetonitrile

Photochemistry in acetonitrile at +20° and the identification of aromatic products (228), (289) *and* (290).

Reaction of hexamethylbenzene (136) / tetranitromethane in acetonitrile at +20°, as above, for 8 h gave a product which was shown by ^{1}H n.m.r. spectral analysis (Table 3.15) to be a mixture of compounds (279) (9%), (281) (21%), (282) (40%), (285) (10%), and small amounts of compounds (228), (280), (283), (284), (286), (287), 289), (289) and (290). The components of this mixture were separated by h.p.l.c. to give the

additional compounds (228), (289) and (290) in elution order:

N-*Nitroso*-N-*(pentamethylbenzyl)-acetamide* (228), as an oil which could not be induced to crystallize (Insufficient for elemental analysis. Found: M^+ 248.1526. $C_{14}H_{20}N_2O_2$ requires 248.1525. $M^{+\bullet}$-NO 218.1534. $C_{14}H_{20}NO$ requires 218.1545). ν_{max} (liquid film) 1719, 1504, 1121 cm^{-1}. ^1H n.m.r. ($CDCl_3$) δ 2.17, s, 2'-Me, 6'-Me, 2.20, s, 3'-Me, 5'-Me; 2.21, s, 4'-Me; 2.73, s, 1-Me; 4.99, s, C**H$_2$**. N.O.e. experiments gave the following results: irradiation at δ 2.17 gave enhancements at δ 2.73 (0.7%) and at δ 4.99 (3.9%); irradiation at δ 2.73 gave an enhancement at δ 2.17 (0.3%); irradiation at δ 4.99 gave an enhancement at δ 2.17 (2.3%). ^{13}C n.m.r. ($CDCl_3$) δ 16.7, 2'-Me, 4'-Me, 6'-Me; 16.9, 3'-Me, 5'-Me; 20.3, 1-Me; 39.7, **C**H_2; 128.3, C2', C6'; 132.9, C1', C3', C5'; 134.8, C4'; 174.5, C2. The above assignments were confirmed by reverse detected heteronuclear correlation spectra (HMQC, HMBC).

Pentamethylbenzyl acetate (289), identical with an authentic sample,[19] (Found: $M^{+\bullet}$ 220.1469. $C_{14}H_{20}O_2$ requires 220.1463). ν_{max} (KBr) 1732, 1240 cm^{-1}. ^1H n.m.r. ($CDCl_3$) δ 2.06, s, 1-Me; 2.24, s, 3'-Me, 5'-Me; 2.25, s, 4'-Me; 2.29, s, 2'-Me, 6'-Me; 5.25, s, C**H$_2$**. N.O.e. experiments gave the following results: irradiation at δ 2.29 gave an enhancement at δ 5.25 (3.5%); irradiation at δ 5.25 gave an enhancement at δ 2.29 (1.6%). ^{13}C n.m.r. ($CDCl_3$) δ 16.3, 2'-Me, 6'-Me; 16.7, 3'-Me, 5'-Me; 17.1, 4'-Me, 21.0, 1-Me; 62.2, **C**H_2; 129.2, C1'; 132.9, C3', C5'; 133.8, C2', C6'; 136.0, C4', 171.4, C2. The above assignments were confirmed by reverse detected heteronuclear correlation spectra (HMQC, HMBC).

N-(Pentamethylbenzyl)-acetamide(290),[20] (Found: $M^{+\bullet}$ 219.1624. $C_{14}H_{21}NO$ requires 219.1623). ν_{max} (KBr) 3304, 1643, 1537, 1385 cm^{-1}. ^1H n.m.r. ($CDCl_3$) δ 2.00, s, 1-Me; 2.24, s, 3'-Me, 4'-Me, 5'-Me; 2.27, s, 2'-Me, 6'-Me; 4.46, d, $J_{methylene,NH}$ 4.4 Hz, C**H$_2$**; 6.03, br s, N-**H**. N.O.e.

experiments gave the following results: irradiation at δ 2.00 gave an enhancement at δ 6.03 (2.7%); irradiation at δ 2.37 gave enhancements at δ 4.46 (4.3%) and at δ 6.03 (1.0%); irradiation at δ 4.46 gave enhancements at δ 2.27 (2.4%) and at δ 6.03 (2.1%); irradiation at δ 6.03 gave enhancements at δ 2.00 (1.2%), at δ 2.27 (0.3%) and at δ 4.46 (1.1%). ^{13}C n.m.r. ($CDCl_3$) δ 16.3, 2'-Me, 6'-Me; 16.7, 3'-Me, 5'-Me; 16.9, 4'-Me; 22.4, 1-Me; 39.6, **C**H_2; 130.4, C1'; 132.9, 133.0, C2', C3', C5', C6'; 135.0, C4'; 170.8, C2. The above assignments were confirmed by reverse detected heteronuclear correlation spectra (HMQC, HMBC).

5.3.4.3 Photonitration of Hexamethylbenzene (136) in 1,1,1,3,3,3-Hexafluoropropan-2-ol (HFP)

A solution of hexamethylbenzene (136) (250 mg, 0.39 mol L^{-1}) and tetranitromethane (0.78 mol L^{-1}) in HFP at +20° was irradiated with filtered light ($\lambda_{cut\text{-}off}$<435 nm) for 24 h. After workup the product composition was determined by ^1H n.m.r. spectral analysis (Table 3.16) and shown to be substantially a mixture of 2,3,4,5,6-pentamethyl-1-(2',2',2'-trinitroethyl)-benzene (279) (67%) and 2,3,4,5,6-pentamethylphenylnitromethane (282) (11%), with small amounts of the dibenzyl ether (283) (3%), 2,3,4,5,6-pentamethylbenzyl alcohol (287) (5%) and unidentified aromatic compounds (total 14%).

5.3.4.4 Nitration of Hexamethylbenzene (136) with Nitrogen Dioxide in Dichloromethane

A solution of hexamethylbenzene (136) (0.39 mol L^{-1}) in dichloromethane saturated with nitrogen dioxide was stored at +20° in the dark. Aliquots were removed at appropriate time intervals, the excess nitrogen

dioxide and solvent were removed under reduced pressure at ≤0°, and the product composition determined by ^{1}H n.m.r. spectral analysis (Table 3.17). After 8 h the products formed were shown to be predominantly 2,3,4,5,6-pentamethylbenzyl nitrate (281) (50%) and 2,3,4,5,6-pentamethylphenyl-nitromethane (282) (40%) and a small amount of 2,3,4,5,6-pentamethyl-benzyl nitrite (280) (7%).

5.3.4.5 Photonitration of Hexamethylbenzene (136) with Nitrogen Dioxide in Dichloromethane

A solution of hexamethylbenzene (136) (0.39 mol L^{-1}) in dichloro-methane saturated with nitrogen dioxide was irradiated with filtered light ($\lambda_{cut\text{-}off}$<435 nm) for 8 h at +20°. Aliquots were removed at appropriate time intervals, the excess nitrogen dioxide and solvent were removed under reduced pressure at ≤0°, and the product composition determined by ^{1}H n.m.r. spectral analysis (Table 3.17). After 8 h the products formed were shown to be similar to those of the "dark" reaction, i.e. predominantly 2,3,4,5,6-pentamethylbenzyl nitrate (281) (56%) and 2,3,4,5,6-pentamethyl-phenylnitromethane (282) (35%) and a small amount of 2,3,4,5,6-penta-methylbenzyl nitrite (280) (4%).

5.3.4.6 Nitration of Hexamethylbenzene (136) with Nitrogen Dioxide in Acetonitrile

A solution of hexamethylbenzene (136) (0.39 mol L^{-1}) in acetonitrile saturated with nitrogen dioxide was stored at +20° in the dark. After 1 h complete reaction of hexamethylbenzene (136) had occurred, the excess nitrogen dioxide and solvent were removed under reduced pressure at ≤0°, and the product composition determined by ^{1}H n.m.r. spectral analysis.

The products formed were shown to be predominantly 2,3,4,5,6-pentamethylbenzyl nitrate (281) (19%), 2,3,4,5,6-pentamethylphenylnitromethane (282) (63%), 1,2-bis(nitromethyl)-3,4,5,6-tetramethylbenzene (285) (9%) and the *N*-nitroso acetamide (228) (4%).

5.3.4.7 Photonitration of Hexamethylbenzene (136) with Nitrogen Dioxide in Acetonitrile

A solution of hexamethylbenzene (136) (0.39 mol L^{-1}) in acetonitrile saturated with nitrogen dioxide was irradiated with filtered light ($\lambda_{cut\text{-}off}$<435 nm) at +20°. After 1 h complete reaction of hexamethylbenzene (136) had occurred, the excess nitrogen dioxide and solvent were removed under reduced pressure at ≤0°, and the product composition determined by ^1H n.m.r. spectral analysis. The products formed were shown to be predominantly 2,3,4,5,6-pentamethylbenzyl nitrate (281) (13%), 2,3,4,5,6-pentamethylphenylnitromethane (282) (63%), 1,2-bis(nitromethyl)-3,4,5,6-tetramethylbenzene (285) (11%) and the *N*-nitroso acetamide (228) (2%).

5.4 Experimental Relating to Chapter Four

GENERAL PROCEDURE FOR THE PHOTONITRATION OF 2,3-DIMETHYL-ANISOLE (307) WITH TETRANITROMETHANE.

A solution of 2,3-dimethylanisole (307) (500 mg, 0.46 mol L^{-1}) and tetranitromethane (0.92 mol L^{-1}) in dichloromethane or acetonitrile (at +20 or -20°) or 1,1,1,3,3,3-hexafluoropropan-2-ol (at +20°) was irradiated with filtered light ($\lambda_{cut\text{-}off}$<435 nm). Aliquots were withdrawn from the reaction

mixture at appropriate time intervals, the volatile material removed under reduced pressure at ≤0°, and the product composition determined by ^{1}H n.m.r. spectral analysis (Tables 4.1-4.3).

5.4.1 Photonitration of 2,3-Dimethylanisole (307) in Dichloromethane

Photochemistry of 2,3-dimethylanisole (307) *in dichloromethane at +20° and the identification of products* (314)-(324).

Reaction of 2,3-dimethylanisole (307) / tetranitromethane in dichloromethane at +20°, as above, for 8 h resulted in essentially complete conversion into a product which was shown by ^{1}H n.m.r. spectral analysis (Table 4.1) to be a mixture of nitro/trinitromethyl adducts (314) (15%) and (315) (9%), hydroxy/trinitromethyl adducts (316) (3%) and (317) (1%), and aromatic compounds (318) (10%), (319) (1%), (320) (7%), (321) (42%), (322) (5%), (323) (1%) and hydroxy dinitro compound (324) (1%). H.p.l.c. allowed the partial separation of these products in the elution order given below.

5,6-Dimethyl-3-trinitromethylanisole (318), m.p. 94° (dec.) (Insufficient for elemental analysis. Found: $M^{+\bullet}$ 285.0593. $C_{10}H_{11}N_3O_7$ requires 285.0597). ν_{max} (KBr) 1614, 1587 cm^{-1}. ^{1}H n.m.r. ($CDCl_3$) δ 2.22, s, 6-Me; 2.34, s, 5-Me; 3.84, s, OMe; 6.87, d, $J_{H2,H4}$ 2.5 Hz, H2; 6.96, d, $J_{H4,H2}$ 2.5 Hz, H4. N.O.e. experiments gave the following results: irradiation at δ 2.34 gave an enhancement at δ 6.96 (5.3%); irradiation at δ 3.84 gave an enhancement at δ 6.87 (9.7%); irradiation at δ 6.87 gave an enhancement at δ 3.84 (1.4%); irradiation at δ 6.96 gave an enhancement at δ 2.34 (0.7%). ^{13}C n.m.r. ($CDCl_3$) δ 12.2, 6-Me; 20.4, 5-Me; 55.9, OMe; 108.1, C2; 119.6, C3; 123.5, C4; 133.4, C5; 139.2, C6; 157.9, C1; a resonance for **C**$(NO_2)_3$ was not observed. The above assignments were confirmed by reverse detected heteronuclear correlation spectra (HMQC,

HMBC).

4-Methoxy-2,3-dimethylbenzonitrile N-*oxide* (319), m.p. 112° (sublim.) (Insufficient for elemental analysis. Found: $M^{+\bullet}$ 177.0790. $C_{10}H_{11}NO_2$ requires 177.0790). ν_{max} (KBr) 2280, 1263 cm^{-1}. ^1H n.m.r. ($CDCl_3$) δ 2.15, s, 3-Me; 2.24, s, 2-Me; 3.80, s, OMe; 6.65, d, $J_{H5,H6}$ 8.8 Hz, H5; 6.92, d, $J_{H6,H5}$ 8.8 Hz, H6. N.O.e. experiments gave the following results: irradiation at δ 3.80 gave an enhancement at δ 6.65 (5.4%); irradiation at δ 6.65 gave enhancements at δ 3.80 (0.9%) and at δ 6.92 (10.2%); irradiation at δ 6.92 gave an enhancement at δ 6.65 (5.5%). ^{13}C n.m.r. ($CDCl_3$) δ 12.3, 3-Me; 15.2, 2-Me; 55.7, OMe; 108.3, C5; 122.8, C6; 124.9, C1; 126.3, C3; 132.3, C2; 155.3, C4; a resonance for **C**$(NO_2)_3$ was not observed. The above assignments were confirmed by reverse detected heteronuclear correlation spectra (HMQC, HMBC).

2,3-Dimethyl-4-trinitromethylanisole (320), m.p. 58-59° (Insufficient for elemental analysis. Found: No parent ion visible, $M^{+\bullet}$-NO_2 239.0664. $C_{10}H_{11}N_2O_5$ requires 239.0668). ν_{max} (KBr) 1622, 1580 cm^{-1}. ^1H n.m.r. ($CDCl_3$) δ 2.02, s, 3-Me; 2.21, s, 2-Me; 3.91, s, OMe; 6.83, d, $J_{H6,H5}$ 8.8 Hz, H6; 7.11, d, $J_{H5,H6}$ 8.8 Hz, H5. N.O.e. experiments gave the following results: irradiation at δ 2.02 gave an enhancement at δ 2.21 (1.5%); irradiation at δ 2.21 gave an enhancement at δ 2.02 (1.1%); irradiation at δ 3.91 gave an enhancement at δ 6.83 (7.1%); irradiation at δ 6.83 gave enhancements at δ 3.91 (1.5%) and at δ 7.11 (11.3%); irradiation at δ 7.11 gave an enhancement at δ 6.83 (5.3%). ^{13}C n.m.r. ($CDCl_3$) δ 12.0, 2-Me; 18.2, 3-Me; 55.8, OMe; 107.7, C6; 113.7, C4; 128.7, C2; 129.0, C5; 139.5, C3; 161.5, C1; a resonance for **C**$(NO_2)_3$ was not observed. The above assignments were confirmed by reverse detected heteronuclear correlation spectra (HMQC, HMBC).

2,3-Dimethyl-4-nitroanisole (321), m.p. 71-72° (Lit.[21] m.p. 70-73°), (Found: $M^{+\bullet}$ 181.0741. $C_9H_{11}NO_3$ requires 181.0739). ν_{max} (KBr) 1583,

1516 cm^{-1}. ^1H n.m.r. ($CDCl_3$) δ 2.21, 2.45, both s, 2-Me, 3-Me; 3.90, s, OMe; 6.75, d, $J_{H6,H5}$ 9.0 Hz, H6; 7.80, d, $J_{H5,H6}$ 9.0 Hz, H5. N.O.e. experiments gave the following results: irradiation at δ 2.21 gave an enhancement at δ 2.45 (0.8%); irradiation at δ 2.45 gave an enhancement at δ 2.21 (1.0%); irradiation at δ 3.90 gave an enhancement at δ 6.75 (5.9%); irradiation at δ 6.75 gave enhancements at δ 3.90 (1.2%) and at δ 7.80 (5.0%); irradiation at δ 7.80 gave an enhancement at δ 6.75 (2.5%).

5,6-Dimethyl-2,4-dinitrophenol (322), m.p. 84-85.5° (Lit.[22] m.p. 86.5-87°), (Found: $M^{+\bullet}$ 212.0432. $C_8H_8N_2O_5$ requires 212.0433). ν_{max} (KBr) 3209, 1614, 1591, 1549, 1522, 1354 cm^{-1}. ^1H n.m.r. ($CDCl_3$) δ 2.37, 2.54, both s, 5-Me, 6-Me; 8.61, s, H3; 11.32, br s, OH. N.O.e. experiments gave no enhancements on irradiation of the proton signals.

3-Methoxy-4,5-dimethylbenzoic acid (323), m.p. 153-154° (Insufficient for elemental analysis. Found: $M^{+\bullet}$ 180.0782. $C_{10}H_{12}O_3$ requires 180.0786). ν_{max} (KBr) 3421, 1684 cm^{-1}. ^1H n.m.r. ($CDCl_3$) δ 2.21, s, 4-Me; 2.33, s, 5-Me; 3.88, s, OMe; 7.42, br s, H2; 7.56, br s, H6. N.O.e. experiments gave the following results: irradiation at δ 2.21 gave an enhancement at δ 2.33 (1.1%); irradiation at δ 2.33 gave enhancements at δ 2.21 (0.9%) and at δ 7.56 (7.5%); irradiation at δ 3.88 gave an enhancement at δ 7.42 (10.8%); irradiation at δ 7.42 gave an enhancement at δ 3.88 (1.4%); irradiation at δ 7.56 gave an enhancement at δ 2.33 (1.1%).

1-Methoxy-5,6-dimethyl-*t*-6-nitro-*r*-3-trinitromethylcyclohexa-1,4-diene (314), as an oil containing an impurity (*c.* 5%). ν_{max} (liquid film) 1599, 1558 cm^{-1}. ^1H n.m.r. ($CDCl_3$) δ 1.80, dd, $J_{5\text{-Me},H4}$ 1.5 Hz, $J_{5\text{-Me},H3}$ 1.4 Hz, 5-Me; 1.82, s, 6-Me; 3.64, s, OMe; 4.91, br s, H3; 5.03, dd, $J_{H2,H3}$ 3.9 Hz, $J_{H2,H4}$ 1.5 Hz, H2; 5.77, ddq, $J_{H4,H3}$ 3.4 Hz, $J_{H4,H2}$ 1.5 Hz, $J_{H4,5\text{-Me}}$ 1.5 Hz, H4; the spin-spin coupling patterns above were confirmed by double irradiation experiments. N.O.e. experiments gave the following results:

irradiation at δ 1.80 gave an enhancement at δ 5.77 (4.6%); irradiation at δ 3.64 gave an enhancement at δ 5.03 (9.3%); irradiation at δ 4.91 gave an enhancement at δ 5.77 (2.1%); irradiation at δ 5.03 gave an enhancement at δ 3.64 (1.3%); irradiation at δ 5.77 gave enhancements at δ 1.80 (1.1%) and at δ 4.91 (2.7%). ^{13}C n.m.r. ($CDCl_3$) δ 18.0, 5-Me; 21.9, 6-Me; 43.6, C3; 55.9, OMe; 88.5, C2; 89.1, C6; 117.3, C4; 140.5, C5; 158.3, C1; a resonance for **C**$(NO_2)_3$ was not observed. The above assignments were confirmed by reverse detected heteronuclear correlation spectra (HMQC, HMBC).

1-Methoxy-5,6-dimethyl-*c*-6-nitro-*r*-3-trinitromethylcyclohexa-1,4-diene (315), as an oil containing an impurity (*c.* 5%). ν_{max} (liquid film) 1601, 1556 cm^{-1}. ^1H n.m.r. ($CDCl_3$) δ 1.82, dd, $J_{5\text{-Me,H4}}$ 1.4 Hz, $J_{5\text{-Me,H3}}$ 1.4 Hz, 5-Me; 1.85, s, 6-Me; 3.63, s, OMe; 4.81, br s, H3; 4.97, dd, $J_{H2,H3}$ 3.4 Hz, $J_{H2,H4}$ 2.0 Hz, H2; 5.68, ddq, $J_{H4,H3}$ 2.9 Hz, $J_{H4,H2}$ 2.0 Hz, $J_{H4,5\text{-Me}}$ 1.4 Hz, H4; the spin-spin coupling patterns above were confirmed by double irradiation experiments. N.O.e. experiments gave the following results: irradiation at δ 1.82 gave an enhancement at δ 5.68 (4.2%); irradiation at δ 3.63 gave an enhancement at δ 4.97 (9.5%); irradiation at δ 4.81 gave enhancements at δ 4.97 (2.3%) and at δ 5.68 (1.7%); irradiation at δ 4.97 gave enhancements at δ 3.63 (1.4%) and at δ 4.81 (2.5%); irradiation at δ 5.68 gave enhancements at δ 4.81 (2.2%) and at δ 1.82 (0.9%). ^{13}C n.m.r. ($CDCl_3$) δ 18.0, 5-Me; 21.4, 6-Me; 42.6, C3; 55.9, OMe; 88.5, C2, C6; 117.2, C4; 139.3, C5; 157.7, C1; a resonance for **C**$(NO_2)_3$ was not observed. The above assignments were confirmed by reverse detected heteronuclear correlation spectra (HMQC, HMBC).

2-Methoxy-1,6-dimethyl-*t*-4-trinitromethylcyclohexa-2,5-dien-*r*-1-ol (316), isolated only in admixture with hydroxy/trinitromethyl adduct (317) (*c.* 15%) below. ν_{max} (liquid film) 3460, 1597, 1576 cm^{-1}. ^1H n.m.r. ($CDCl_3$) δ 1.45, s, 1-Me; 1.95, d, $J_{6\text{-Me,H5}}$ 1.5 Hz, 6-Me; 3.66, s, OMe; 4.71,

d, $J_{H4,H5}$ 2.9 Hz, H4; 4.71, s, H3; 5.45, dq, $J_{H5,H4}$ 2.9 Hz, $J_{H5,6\text{-Me}}$ 1.5 Hz, H5; the spin-spin coupling patterns above were confirmed by double irradiation experiments. N.O.e. experiments gave the following results: irradiation at δ 1.45 gave an enhancement at δ 1.95 (1.3%); irradiation at δ 1.95 gave enhancements at δ 1.45 (0.9%) and at δ 5.45 (4.5%); irradiation at δ 3.66 gave an enhancement at δ 4.71 (5.7%); irradiation at δ 4.71 gave enhancements at δ 3.66 (1.2%) and at δ 5.45 (2.4%); irradiation at δ 5.45 gave enhancements at δ 1.95 (0.7%) and at δ 4.71 (1.3%). ^{13}C n.m.r. ($CDCl_3$) δ 17.5, 6-Me; 26.9, 1-Me; 43.9, C4; 55.4, OMe; 68.6, C1; 84.6, C3; 112.2, C5; 147.2, C6; 163.6, C2; a resonance for **C**$(NO_2)_3$ was not observed. The above assignments were confirmed by reverse detected heteronuclear correlation spectra (HMQC, HMBC).

2-Methoxy-1,6-dimethyl-*c*-4-trinitromethylcyclohexa-2,5-dien-*r*-1-ol (317), isolated only as the minor component in admixture with hydroxy/trinitromethyl adduct (316) above. ^1H n.m.r. ($CDCl_3$) δ 1.45, 1-Me; 1.94, dd, $J_{6\text{-Me},H5}$ 1.5 Hz, $J_{6\text{-Me},H4}$ 1.5 Hz, 6-Me; 3.63, s, OMe; 4.61, ddq, $J_{H4,H5}$ 3.0 Hz, $J_{H4,H3}$ 2.5 Hz, $J_{H4,6\text{-Me}}$ 1.5 Hz, H4; 4.66, dd, $J_{H3,H4}$ 2.5 Hz, $J_{H3,H5}$ 2.0 Hz, H3; 5.40, ddq, $J_{H5,H4}$ 3.0 Hz, $J_{H5,H3}$ 2.5 Hz, $J_{H5,6\text{-Me}}$ 1.5 Hz, H5; the spin-spin coupling patterns above were confirmed by double irradiation experiments. N.O.e. experiments gave the following results: irradiation at δ 1.94 gave an enhancement at δ 5.40 (3.9%); irradiation at δ 3.63 gave an enhancement at δ 4.66 (2.5%); irradiation at δ 4.61 gave an enhancement at δ 3.63 (0.6%). ^{13}C n.m.r. ($CDCl_3$) δ 17.7, 6-Me; 24.4, 1-Me; 42.8, C4; 55.4, OMe; 85.2, C3; 112.7, C5; the above assignments were confirmed by short range reverse detected heteronuclear correlation spectra (HMQC); resonances for C1, C2, C6 and **C**$(NO_2)_3$ were not observed for a sample in which adduct (317) was the minor component.

2-(4'-Hydroxy-3'-methoxy-4',5'-dimethylcyclohexa-2',5'-dienylidene)-1,1-dinitroethene (324), as an oil (Insufficient for elemental analysis.

Found: $M^{+\bullet}$ 256.0693. $C_{10}H_{12}N_2O_6$ requires 256.0695). ν_{max} (liquid film) 3427, 1657, 1541 cm^{-1}. λ_{max} (ethanol) 386 nm (ε 32 400), 342 nm (sh, ε 23 600). ^1H n.m.r. ($CDCl_3$) δ 1.55, s, 4'-Me; 2.16, d, $J_{5'\text{-Me},H6'}$ 1.0 Hz, 5'-Me; 2.43, br s, 4'-OH; 3.94, s, OMe; 6.38, dq, $J_{H6',H2'}$ 1.5 Hz, $J_{H6',5'\text{-Me}}$ 1.0 Hz, H6'; 6.44, d, $J_{H2',H6'}$ 1.5 Hz, H2'; the spin-spin coupling patterns above were confirmed by double irradiation experiments. N.O.e. experiments gave the following results: irradiation at δ 1.55 gave an enhancement at δ 2.16 (1.5%); irradiation at δ 2.16 gave enhancements at δ 1.55 (0.8%) and at δ 6.38 (5.8%); irradiation at δ 3.94 gave an enhancement at δ 6.44 (10.4%); irradiation at δ 6.38 gave an enhancement at δ 2.16 (0.8%); irradiation at δ 6.44 gave an enhancement at δ 3.94 (1.0%). ^{13}C n.m.r. ($CDCl_3$) δ 18.6, 5'-Me; 27.2, 4'-Me; 56.9, OMe; 70.9, C4'; 89.9, C2'; 114.9, C6'; 146.6, C2; 158.5, C5'; 175.8, C3'; a resonance for **C**$(NO_2)_2$ was not observed. The above assignments were confirmed by reverse detected heteronuclear correlation spectra (HMQC, HMBC).

5.4.2 Photonitration of 2,3-Dimethylanisole (307) in 1,1,1,3,3,3-Hexafluoropropan-2-ol (HFP)

Reaction of 2,3-dimethylanisole (307) / tetranitromethane in HFP at +20°, as above, for 24 h gave a product which was shown by ^1H n.m.r. spectral analysis (Table 4.3) to be a mixture of nitro/trinitromethyl adducts (314) (1%) and (315) (2%), hydroxy/trinitromethyl adducts (316) (0.3%) and (317) (trace), and aromatic compounds (318) (19%), (320) (4%), (321) (61%), (322) (0.3%), and unidentified aromatic compounds (total 12%). After a reaction time of 8 h the conversion of 2,3-dimethylanisole (307) into products was *c.* 30%, in contrast to essentially complete conversion in dichloromethane at +20°.

5.4.3 Photonitration of 2,3-Dimethylanisole (307) in Dichloromethane Containing Trifluoroacetic Acid

Reaction of 2,3-dimethylanisole (307) / tetranitromethane in dichloromethane containing trifluoroacetic acid (0.71 mol L^{-1}) at +20°, as above, for 8 h resulted in *c.* 20% conversion into a mixture of nitro/trinitromethyl adducts (314) (3%) and (315) (0.5%), aromatic compounds (318) (42%), (319) (7%), (320) (8%), (321) (23%), (322) (2%), and unidentified aromatic compounds (total 15%) (Table 4.4).

5.5 Appendix : Crystallography

Crystal data, established from precession photographs and measured accurately, by means of a Siemens R3m/V four-circle diffractometer (molybdenum X-radiation, λ(Mo Kα) 0.71069 Å, or copper X-radiation, λ(Cu Kα) 1.54180 Å, from a crystal monochromator) are given below. The space group was, in each case, determined unambiguously as a result of the structure analyses reported below, but initially indicated by conditions limiting possible reflections. ω-Scans were used to collect reflection intensities out to a maximum Bragg angle θ, given below. The cell parameters were determined by least-squares refinements for which the setting angles of 20-25 accurately centred high-angle reflections were used.

(a) Crystal Data

1,4,6,7-Tetramethyl-r-*1-nitro*-t-*4-trinitromethyl-1,4-dihydro-naphthalene* (75).—$C_{15}H_{16}N_4O_8$, *M* 380.32, monoclinic, space group $P2_1/c$, *a* 16.054(3), *b* 9.085(1), *c* 11.909(2) Å, β 107.69(2)°, *V* 1654.8(5) Å^3, D_c 1.527 g cm^{-3}, *Z* 4, μ(Cu Kα) 10.84 cm^{-1}. The crystal was colourless and of approximate dimensions 0.56 by 0.30 by 0.21 mm. Data were collected at 130 K out to a maximum Bragg angle θ 26.75°. Number of independent reflections measured 1938, 1424 with $I > 2\sigma(I)$; g_1 0.1531, g_2 0.0000; absorption corrections were not applied; $R_{(obs)}$ factor 0.080, $wR_{(all\ data)}$ 0.215.

1,4,6,7-Tetramethyl-1,2-dihydronaphthalene-r-*1,c-2-diol* (86).—$C_{14}H_{18}O_2$, *M* 218.28, triclinic, space group $P\bar{1}$, *a* 5.264(1), *b* 8.505(2), *c* 13.864(3) Å, α 104.08(3), β 100.04(3), γ 94.96(3)°, *V* 587.4(2) Å^3, D_c 1.234 g cm^{-3}, *Z* 2, μ(Mo Kα) 0.81 cm^{-1}. The crystal was colourless and of approximate dimensions 0.70 by 0.27 by 0.25 mm. Data were collected at 130 K out to a maximum Bragg angle θ 27.5°. Number of independent reflections measured 2667,1798 with $I > 2\sigma(I)$; g_1 0.0757, g_2 0.0000; absorption corrections were not applied; $R_{(obs)}$ factor 0.043, $wR_{(all\ data)}$ 0.114.

trans-*2,6-Dimethyl-1-nitro-4-trinitromethyl-1,4-dihydronaphthalene* (95).—$C_{13}H_{12}N_4O_8$, *M* 352.27, triclinic, space group $P\bar{1}$, *a* 9.621(2), *b* 9.708(2), *c* 9.720(2) Å, α 101.03(3), β 117.60(3), γ 105.00(3)°, *V* 723.9(3) Å^3, D_c 1.616 g cm^{-3}, *Z* 2, μ(Mo Kα) 1.37 cm^{-1}. The crystal was colourless and of approximate dimensions 0.52 by 0.40 by 0.16 mm. Data were collected at 130 K out to a maximum Bragg angle θ 22.5°. Number of independent reflections measured 2346, 2016 with $I > 2\sigma(I)$; g_1 0.0480,

g_2 0.5841; absorption corrections were not applied; $R_{(obs)}$ factor 0.037, $wR_{(all\ data)}$ 0.099.

cis-*2,6-Dimethyl-1-nitro-4-trinitromethyl-1,4-dihydronaphthalene* (97).—$C_{13}H_{12}N_4O_8$, *M* 352.27, triclinic, space group $P\bar{1}$, *a* 6.580(1), *b* 7.700(2), *c* 15.225(3) Å, α 80.44(3), β 89.95(3), γ 75.96(3)°, *V* 737.3(3) Å^3, D_c 1.587 g cm^{-3}, *Z* 2, μ(Mo Kα) 1.34 cm^{-1}. The crystal was colourless and of approximate dimensions 0.55 by 0.50 by 0.42 mm. Data were collected at 130 K out to a maximum Bragg angle θ 22.88°. Number of independent reflections measured 1931, 1542 with $I > 2\sigma(I)$; g_1 0.0578, g_2 0.7244; absorption corrections were not applied; $R_{(obs)}$ factor 0.045, $wR_{(all\ data)}$ 0.118.

Nitro Cycloadduct (101).—$C_{13}H_{12}N_4O_8$, *M* 352.27, monoclinic, space group $P2_1/c$, *a* 15.234(3), *b* 11.663(2), *c* 8.531(2) Å, β 105.23(3)°; *V* 1462.5(5) Å^3, D_c1.600 g cm^{-3}, *Z* 4, μ(Mo Kα) 1.35 cm^{-1}. The crystal was colourless and of approximate dimensions 0.80 by 0.44 by 0.38 mm. Data were collected at 132 K out to a maximum Bragg angle θ 22.5°. Number of independent reflections measured 2532, 1895 with $I > 2\sigma(I)$; g_1 0.0571, g_2 0.2816; absorption corrections were not applied; $R_{(obs)}$ factor 0.0425, $wR_{(all\ data)}$ 0.108.

Hydroxy Cycloadduct (104).—$C_{13}H_{13}N_3O_7$, *M* 323.26, orthorhombic, space group *Pbca*, *a* 15.028(3), *b* 10.710(2), *c* 16.779(3) Å, *V* 2700.6(9) Å^3, D_c 1.590 g cm^{-3}, *Z* 8, μ(Mo Kα) 1.32 cm^{-1}. The crystal was colourless and of approximate dimensions 0.42 by 0.40 by 0.10 mm. Data were collected at 130 K out to a maximum Bragg angle θ 22.5°. Number of independent reflections measured 2372, 1060 with $I > 2\sigma(I)$; g_1 0.0498, g_2 0.0000;

absorption corrections were not applied; $R_{(obs)}$ factor 0.073, $wR_{(all\ data)}$ 0.166.

trans-*6,8-Dimethyl-1-nitro-4-trinitromethyl-1,4-dihydronaphthalene* (111).—$C_{13}H_{12}N_4O_8$, *M* 352.27, triclinic, space group $P\bar{1}$, *a* 9.423(2), *b* 9.830(2), *c* 10.039(2) Å, α 101.61(3), β 112.01(3), γ 112.23(3)°, *V* 731.5(3) Å^3, D_c 1.599 g cm^{-3}, *Z* 2, μ(Cu Kα) 11.76 cm^{-1}. The crystal was colourless and of approximate dimensions 0.67 by 0.58 by 0.39 mm. Data were collected at 120 K out to a maximum Bragg angle θ 26.75°. Number of independent reflections measured 1639, 1526 with $I > 2\sigma(I)$; g_1 0.0582, g_2 0.01788; absorption corrections were not applied; $R_{(obs)}$ factor 0.041, $wR_{(all\ data)}$ 0.108.

Nitro cycloadduct (112).—$C_{13}H_{12}N_4O_8$, *M* 352.27, monoclinic, space group $P2_1/c$, *a* 7.594(2), *b* 23.672(5), *c* 8.179(2) Å, β 104.63(3)°, *V* 1422.6(6) Å^3, D_c 1.645 g cm^{-3}, *Z* 4, μ(Cu Kα) 12.09 cm^{-1}. The crystal was colourless and of approximate dimensions 0.80 by 0.37 by 0.28 mm. Data were collected at 120 K out to a maximum Bragg angle θ 26.75°. Number of independent reflections measured 1677, 1410 with $I > 2\sigma(I)$; g_1 0.0706, g_2 2.4846; absorption corrections were not applied; $R_{(obs)}$ factor 0.060, $wR_{(all\ data)}$ 0.161.

cis-*6,8-Dimethyl-1-nitro-4-trinitromethyl-1,4-dihydronaphthalene* (113).—$C_{13}H_{12}N_4O_8$, *M* 352.27, monoclinic, space group $P2_1/c$, *a* 7.881(2), *b* 17.684(4), *c* 10.973(2) Å, β 102.29(3)°, *V* 1494.2(6) Å^3, D_c 1.566 g cm^{-3}, *Z* 4, μ(Cu Kα) 11.51 cm^{-1}. The crystal was colourless and of approximate dimensions 0.52 by 0.50 by 0.22 mm. Data were collected at 130 K out to a maxiumum Bragg angle θ 26.75°. Number of independent reflections measured 1762, 1537 with $I > 2\sigma(I)$; g_1 0.0989,

g_2 2.2498; absorption corrections were not applied; $R_{(obs)}$ factor 0.059, $wR_{(all\ data)}$ 0.171.

Nitro cycloadduct (122).—$C_{13}H_{12}N_4O_8$, *M* 352.27, orthorhombic, space group *Pbca*, *a* 7.361(2), *b* 16.023(4), *c* 24.491(6) Å, *V* 2889(1) Å^3, D_c 1.620 g cm^{-3}, *Z* 8, μ(Mo Kα) 1.4 cm^{-1}. The crystal was colourless and of approximate dimensions 0.49 by 0.24 by 0.13 mm. Data were collected at 120 K out to a maximum Bragg angle θ 24.99°. Number of independent reflections measured 2533, 1022 with $I > 2\sigma(I)$; g_1 0.0080, g_2 0.0000; absorption corrections were not applied; $R_{(obs)}$ factor 0.035, $wR_{(all\ data)}$ 0.045.

Nitro cycloadduct (153).—$C_{10}H_{12}N_4O_8$, *M* 316.24, monoclinic, space group *P* $2_1/c$, *a* 10.440(2), *b* 6.812(4), *c* 18.844(4) Å, *β* 101.17(1)°, *V* 1314.7(9) Å^3, D_c 1.598 g cm^{-3}, *Z* 4, *μ*(Mo Kα) 1.40 cm^{-1}. The crystal was colourless and of approximate dimensions 0.90 by 0.25 by 0.17 mm. Data were collected at 130 K out to a maximum Bragg angle *θ* 25°. Number of independent reflections measured 2316, 1598 with $I > 2\sigma(I)$; g_1 0.0700, g_2 0.0000; absorption corrections were not applied; $R_{(obs)}$ factor 0.045, $wR_{(all\ data)}$ 0.149.

1,2,3-Trimethyl-r-*3*,c-*4*,c-*6-trinitro*-t-*5-trinitromethylcyclohex-1-ene* (157).—$C_{10}H_{12}N_6O_{12}$, *M* 408.26, monoclinic, space group *P* $2_1/n$, *a* 10.187(2), *b* 13.904(4), *c* 12.348(3) Å, *β* 110.84(3)°, *V* 1634.5(7) Å^3, D_c 1.659 g cm^{-3}, *Z* 4, *μ*(Mo Kα) 1.54 cm^{-1}. The crystal was colourless and of approximate dimensions 1.02 by 0.21 by 0.16 mm. Data were collected at 173 K out to a maximum Bragg angle *θ* 24.66°. Number of independent reflections measured 2122, 1222 with $I > 2\sigma(I)$; g_1 0.0396, g_2 0.0000;

absorption corrections were not applied; $R_{(obs)}$ factor 0.036, $wR_{(all\ data)}$ 0.077.

Crystal data for a poor-quality crystal of trinitro nitronic ester (160), $C_{10}H_{12}N_4O_8$. X-solvate, *a* 8.119(3), *b* 9.623(2), *c* 10.903(2) Å, α 73.501(9), β 74.40(1), γ 68.46(2) °, *V* 746.6(3) Å^3.

Trinitro nitronic ester (161).—$C_{10}H_{12}N_4O_8$, *M* 316.24, orthorhombic, space group, *Pbca*, *a* 6.480(7), *b* 14.840(9), *c* 26.79(2) Å, *V* 2576(4) Å^3, D_c 1.631 g cm^{-3}, *Z* 8, μ(Mo Kα) 1.43 cm^{-1}. The crystal was colourless and of approximate dimensions 0.40 by 0.10 by 0.06 mm. Data were collected at 130 K out to a maximum Bragg angle θ 22.49°. Number of independent reflections measured 1671, 837 with $I > 2\sigma(I)$; g_1 0.0405, g_2 0.0000; absorption corrections were not applied; $R_{(obs)}$ factor 0.047, $wR_{(all\ data)}$ 0.097.

Hydroxy dinitro nitronic ester (162).—$C_{10}H_{13}N_3O_7$, *M* 287.23, monoclinic, space group *P* $2_1/c$, *a* 10.004(2), *b* 8.287(3), *c* 14.671(3) Å, β 96.93(1)°, *V* 1207.4(6) Å^3, D_c 1.580 g cm^{-3}, *Z* 4, μ(Mo Kα) 1.36 cm^{-1}. The crystal was colourless and of approximate dimensions 0.97 by 0.91 by 0.15 mm. Data were collected at 130 K out to a maximum Bragg angle θ 27.5°. Number of independent reflections measured 2769, 2064 with $I > 2\sigma(I)$; g_1 0.0735, g_2 0.0000; absorption corrections were not applied; $R_{(obs)}$ factor 0.037, $wR_{(all\ data)}$ 0.124.

t-*6-Hydroxy-4,5,6-trimethyl-2,*r-*4,*t-*5-trinitrocyclohex-2-enone* (172).—$C_9H_{11}N_3O_8$, *M* 289.21, monoclinic, space group *P* $2_1/n$, *a* 6.943(4), *b* 20.410(3), *c* 8.281(1) Å, β 101.23(3)°, *V* 1151.0(7) Å^3, D_c 1.669 g cm^{-3}, *Z* 4, μ(Mo Kα) 1.49 cm^{-1}. The crystal was colourless and of approximate

dimensions 0.62 by 0.30 by 0.19 mm. Data were collected at 173 K out to a maximum Bragg angle θ 25.0°. Number of independent reflections measured 2031, 1307 with $I > 2\sigma(I)$; g_1 0.0285, g_2 0.0000; absorption corrections were not applied; $R_{(obs)}$ factor 0.030, $wR_{(all\ data)}$ 0.059.

(b) Structure Determination

The structures were solved by direct methods and difference-Fourier synthesis. Full-matrix least-squares refinements (SHELXL-93)[23] were employed. This program is based on intensities and uses all data. The observed threshold $I > 2\sigma(I)$ was used only for calculating $R_{(obs)}$, shown here as a comparison for the refinements based on F. Reflection weights $1/[\sigma^2(F_o^2) + (g_1P)^2 + g_2P]$, where $P = [F_o^2 + 2F_c^2]/3$, were used.

All non-hydrogen atoms were assigned anisotropic thermal parameters. Methyl hydrogen atoms were included as rigid groups pivoting about their carbon atoms. Final Fourier syntheses show no significant residual electron density, and there were no abnormal discrepancies between observed and calculated structure factors.

Table 5.1 Fractional coordinates for atoms in 1,4,6,7-tetramethyl-*r*-1-nitro-*t*-4-trinitromethyl-1,4-dihydronaphthalene (75).

Atom	$10^4X/a$	$10^4Y/b$	$10^4Z/c$	10^3U [a]
O(11)	8284(2)	-2933(4)	7746(4)	39(1)
O(12)	8173(2)	-3931(4)	9339(4)	47(1)
O(21)	5031(2)	1311(4)	7376(4)	42(1)
O(22)	6213(2)	1368(4)	8861(4)	37(1)
O(31)	5481(2)	1473(4)	5087(3)	37(1)
O(32)	5266(2)	3598(4)	5790(3)	39(1)
O(41)	7058(2)	4215(4)	6828(4)	40(1)
O(42)	6485(3)	4178(4)	8259(4)	43(1)
N(1)	7981(3)	-2992(4)	8570(5)	32(1)
N(2)	5794(3)	1563(4)	7817(4)	32(1)
N(3)	5635(2)	2404(5)	5847(4)	30(1)
N(4)	6668(3)	3647(4)	7439(5)	33(1)
C(1)	7309(3)	-1766(5)	8635(5)	27(1)
C(2)	6692(3)	-1693(5)	7409(5)	29(1)
C(3)	6568(3)	-541(5)	6741(5)	29(1)
C(4)	7050(3)	915(5)	7040(5)	27(1)
C(4a)	7749(3)	843(5)	8265(4)	25(1)
C(5)	8330(3)	2012(5)	8644(5)	29(1)
C(6)	8982(3)	2005(5)	9714(5)	30(1)
C(7)	9054(3)	778(5)	10455(5)	30(1)
C(8)	8502(3)	-382(5)	10064(5)	29(1)
C(8a)	7859(3)	-377(5)	8975(5)	27(1)
C(9)	6856(3)	-2222(5)	9520(5)	35(1)
C(10)	7487(3)	1253(5)	6091(5)	33(1)
C(11)	9583(3)	3296(5)	10062(5)	36(1)

Table 5.1 cont.

Atom	$10^4X/a$	$10^4Y/b$	$10^4Z/c$	10^3U [a]
C(12)	9738(3)	723(6)	11648(5)	38(1)
C(13)	6334(3)	2084(5)	7045(5)	27(1)

[a] The equivalent isotropic temperature factor, U (in Å^2), in Tables 1-15 is defined as one-third of orthogonalized U_{ij} tensor.

Table 5.2 Fractional coordinates for atoms in 1,4,6,7-tetramethyl-1,2-dihydronaphthalene-*r*-1,*c*-2-diol (86).

Atom	$10^4X/a$	$10^4Y/b$	$10^4Z/c$	10^3U
O(1)	7039(2)	3863(1)	9217(1)	24(1)
O(2)	1790(2)	4518(1)	8787(1)	24(1)
C(1)	4928(3)	2554(2)	8740(1)	17(1)
C(2)	2717(3)	3209(2)	8141(1)	17(1)
C(3)	3575(3)	3764(2)	7288(1)	20(1)
C(4)	5143(3)	2968(2)	6745(1)	18(1)
C(4a)	6150(3)	1535(2)	7024(1)	17(1)
C(5)	7365(3)	445(2)	6386(1)	19(1)
C(6)	8487(3)	-839(2)	6665(1)	20(1)
C(7)	8347(3)	-1076(2)	7624(1)	21(1)
C(8)	7101(3)	-10(2)	8254(1)	20(1)
C(8a)	6014(3)	1292(2)	7986(1)	16(1)
C(9)	3669(3)	1894(2)	9559(1)	22(1)
C(10)	5998(3)	3510(2)	5881(1)	24(1)
C(11)	9956(3)	-1892(2)	5976(1)	27(1)
C(12)	9574(3)	-2426(2)	7979(1)	29(1)

Table 5.3 Fractional coordinates for atoms in *trans*-2,6-dimethyl-1-nitro-4-trinitromethyl-1,4-dihydronaphthalene (95).

Atom	$10^4X/a$	$10^4Y/b$	$10^4Z/c$	10^3U
O(11)	6045(2)	4669(2)	2415(2)	29(1)
O(12)	4521(2)	3290(2)	-202(2)	33(1)
O(21)	8793(2)	1109(2)	469(2)	25(1)
O(22)	8845(2)	-537(2)	1702(2)	29(1)
O(31)	11569(2)	1432(2)	5695(2)	29(1)
O(32)	12247(2)	298(2)	4097(2)	33(1)
O(41)	12140(2)	2307(2)	1635(2)	30(1)
O(42)	13761(2)	3369(2)	4326(2)	26(1)
N(1)	5776(2)	3732(2)	1194(2)	21(1)
N(2)	9404(2)	700(2)	1646(2)	20(1)
N(3)	11647(2)	1153(3)	4475(2)	22(1)
N(4)	12404(2)	2586(2)	3017(2)	19(1)
C(1)	7097(3)	3051(2)	1422(2)	19(1)
C(2)	7291(3)	2295(2)	2674(2)	19(1)
C(3)	8818(3)	2402(2)	3802(2)	19(1)
C(4)	10436(2)	3197(2)	3895(2)	16(1)
C(4a)	10307(2)	4321(2)	2999(2)	15(1)
C(5)	11785(2)	5447(2)	3360(2)	18(1)
C(6)	11727(3)	6512(2)	2587(2)	19(1)
C(7)	10130(3)	6463(2)	1477(2)	21(1)
C(8)	8657(3)	5375(2)	1130(2)	20(1)
C(8a)	8717(2)	4283(2)	1867(2)	17(1)
C(9)	5602(3)	1369(3)	2537(3)	27(1)
C(10)	13339(3)	7662(2)	2926(3)	24(1)
C(11)	10948(2)	1951(2)	3254(2)	17(1)

Table 5.4 Fractional coordinates for atoms in *cis*-2,6-dimethyl-1-nitro-4-trinitromethyl-1,4-dihydronaphthalene (97).

Atom	$10^4X/a$	$10^4Y/b$	$10^4Z/c$	10^3U
O(11)	4501(4)	2910(3)	1646(2)	31(1)
O(12)	6416(4)	1439(3)	2806(2)	31(1)
O(21)	828(3)	6534(3)	1279(2)	35(1)
O(22)	1940(4)	5417(3)	2645(2)	33(1)
O(31)	2100(4)	10422(3)	744(2)	35(1)
O(32)	-833(4)	10178(3)	1342(2)	36(1)
O(41)	1516(3)	10628(3)	2897(2)	30(1)
O(42)	427(4)	8241(3)	3432(2)	34(1)
N(1)	5884(4)	2746(3)	2208(2)	21(1)
N(2)	1557(4)	6616(3)	1998(2)	23(1)
N(3)	1066(4)	9779(3)	1306(2)	25(1)
N(4)	1280(4)	9110(3)	2889(2)	22(1)
C(1)	7095(5)	4228(4)	2162(2)	17(1)
C(2)	6570(4)	5525(4)	1303(2)	16(1)
C(3)	5479(4)	7222(4)	1282(2)	17(1)
C(4)	4626(4)	8009(4)	2087(2)	16(1)
C(4a)	5662(4)	6864(4)	2958(2)	16(1)
C(5)	5619(4)	7638(4)	3724(2)	17(1)
C(6)	6594(4)	6665(4)	4523(2)	18(1)
C(7)	7656(5)	4867(4)	4542(2)	21(1)
C(8)	7788(4)	4098(4)	3789(2)	20(1)
C(8a)	6793(4)	5072(4)	2988(2)	16(1)
C(9)	7457(5)	4820(5)	486(2)	26(1)
C(10)	6578(5)	7558(4)	5325(2)	28(1)
C(11)	2220(5)	8330(4)	2076(2)	18(1)

Table 5.5 Fractional coordinates for atoms in nitro cycloadduct (101).

Atom	$10^4X/a$	$10^4Y/b$	$10^4Z/c$	10^3U
O(11)	7633(1)	1813(1)	7944(2)	23(1)
O(12)	6166(1)	1463(1)	6932(2)	19(1)
O(21)	8477(1)	1082(2)	5588(2)	41(1)
O(22)	8175(1)	-713(2)	5051(2)	45(1)
O(31)	6482(2)	794(2)	3348(2)	50(1)
O(32)	5783(1)	-486(1)	4401(2)	32(1)
O(41)	6540(1)	-912(2)	10724(2)	36(1)
O(42)	6203(2)	-2226(2)	8900(3)	54(1)
N(1)	6998(1)	1505(2)	6492(2)	21(1)
N(2)	8015(1)	231(2)	5512(2)	29(1)
N(3)	6400(1)	174(2)	4441(2)	27(1)
N(4)	6349(1)	-1237(2)	9320(3)	29(1)
C(1)	7376(2)	1219(2)	9277(3)	20(1)
C(2)	6372(1)	870(2)	8501(3)	18(1)
C(3)	6301(2)	-384(2)	7977(3)	18(1)
C(4)	7108(1)	-646(2)	7257(3)	18(1)
C(4a)	7951(1)	-653(2)	8669(3)	18(1)
C(5)	8571(2)	-1540(2)	8994(3)	22(1)
C(6)	9285(2)	-1533(2)	10397(3)	26(1)
C(7)	9248(2)	-633(2)	11480(3)	28(1)
C(8)	8723(2)	254(2)	11177(3)	26(1)
C(8a)	8033(2)	250(2)	9772(3)	20(1)
C(9)	5677(2)	1294(2)	9331(3)	24(1)
C(10)	9970(2)	-2488(2)	10749(3)	35(1)
C(11)	7139(2)	302(2)	6044(3)	21(1)

Table 5.6 Fractional coordinates for atoms in hydroxy cycloadduct (104).

Atom	$10^4X/a$	$10^4Y/b$	$10^4Z/c$	10^3U
O(11)	878(2)	3994(3)	1734(2)	17(1)
O(12)	47(2)	3338(4)	2740(2)	18(1)
O(21)	-36(3)	3502(4)	352(2)	25(1)
O(22)	-348(3)	1524(4)	277(3)	29(1)
O(31)	-1633(3)	2846(4)	1612(3)	27(1)
O(32)	-1265(3)	995(4)	2008(3)	28(1)
O(4)	1359(3)	532(4)	2903(2)	22(1)
N(1)	13(3)	3568(5)	1904(3)	18(1)
N(2)	-172(3)	2487(6)	639(3)	20(1)
N(3)	-1101(3)	2014(5)	1739(3)	19(1)
C(1)	1503(3)	3266(6)	2232(3)	17(1)
C(2)	890(4)	2679(6)	2869(4)	17(1)
C(3)	661(4)	1333(6)	2680(3)	18(2)
C(4)	500(4)	1275(6)	1775(3)	14(1)
C(4a)	1411(4)	1406(5)	1388(3)	13(1)
C(5)	1729(4)	594(6)	823(3)	17(2)
C(6)	2601(4)	686(6)	554(3)	20(2)
C(7)	3139(4)	1601(6)	885(3)	19(2)
C(8)	2817(4)	2449(6)	1439(4)	17(1)
C(8a)	1945(4)	2351(5)	1687(3)	14(1)
C(9)	1166(4)	2908(6)	3721(3)	24(1)
C(10)	2951(4)	-221(6)	-59(4)	31(2)
C(11)	-123(4)	2325(5)	1542(3)	13(1)

Table 5.7 Fractional coordinates for atoms in *trans*-6,8-dimethyl-1-nitro-4-trinitromethyl-1,4-dihydronaphthalene (111).

Atom	$10^4X/a$	$10^4Y/b$	$10^4Z/c$	10^3U
O(11)	5679(3)	7006(3)	11590(2)	33(1)
O(12)	7770(3)	9265(2)	12039(2)	26(1)
O(21)	8187(3)	4510(2)	8640(2)	22(1)
O(22)	6270(3)	3462(2)	6157(2)	24(1)
O(31)	8052(3)	4760(2)	4694(2)	26(1)
O(32)	7138(3)	6461(2)	5025(2)	26(1)
O(41)	11068(3)	5570(2)	8285(2)	26(1)
O(42)	11330(3)	7383(2)	7319(2)	22(1)
N(1)	6934(4)	7805(3)	11469(3)	20(1)
N(2)	7627(3)	4515(3)	7341(3)	17(1)
N(3)	7875(3)	5737(3)	5484(3)	18(1)
N(4)	10536(3)	6337(3)	7659(2)	17(1)
C(1)	7429(4)	6889(3)	10453(3)	16(1)
C(2)	6256(4)	6648(3)	8829(3)	18(1)
C(3)	6809(4)	6960(3)	7845(3)	16(1)
C(4)	8678(4)	7480(3)	8218(3)	15(1)
C(4a)	9961(4)	8109(3)	9964(3)	12(1)
C(5)	11750(4)	9019(3)	10505(3)	14(1)
C(6)	13006(4)	9576(3)	12063(3)	16(1)
C(7)	12399(4)	9208(3)	13075(3)	19(1)
C(8)	10619(4)	8328(3)	12595(3)	16(1)
C(8a)	9373(4)	7791(3)	11013(3)	15(1)
C(9)	8687(4)	6056(3)	7231(3)	14(1)
C(10)	14937(4)	10481(4)	12598(3)	23(1)
C(11)	10102(4)	7976(4)	13790(3)	24(1)

Table 5.8 Fractional coordinates for atoms in nitro cycloadduct (112).

Atom	$10^4X/a$	$10^4Y/b$	$10^4Z/c$	10^3U
O(11)	3277(5)	3385(2)	590(4)	24(1)
O(12)	4378(5)	4225(2)	1267(4)	24(1)
O(21)	-1088(5)	3649(2)	147(4)	27(1)
O(22)	232(5)	4393(2)	-546(4)	29(1)
O(31)	3426(4)	4538(1)	4144(4)	18(1)
O(32)	417(4)	4587(1)	3554(4)	18(1)
O(41)	104(5)	2697(1)	5221(4)	22(1)
O(42)	731(4)	3360(1)	7108(4)	23(1)
N(1)	3284(5)	3848(2)	1231(5)	16(1)
N(2)	103(6)	4007(2)	392(5)	20(1)
N(3)	1891(5)	4527(2)	2761(5)	16(1)
N(4)	366(5)	3196(2)	5641(5)	18(1)
C(1)	1437(6)	3449(2)	3114(6)	15(1)
C(2)	158(6)	3634(2)	4246(6)	15(1)
C(3)	885(6)	4198(2)	4980(6)	16(1)
C(4)	2988(6)	4235(2)	5577(6)	16(1)
C(4a)	3938(6)	3672(2)	5650(6)	14(1)
C(5)	5497(6)	3526(2)	6853(6)	15(1)
C(6)	6368(6)	3019(2)	6738(6)	17(1)
C(7)	5676(6)	2655(2)	5424(6)	18(1)
C(8)	4093(6)	2790(2)	4219(6)	14(1)
C(8a)	3243(6)	3296(2)	4323(6)	15(1)
C(9)	1656(6)	3953(2)	2008(6)	13(1)
C(10)	-1908(6)	3642(2)	3442(6)	19(1)
C(11)	3633(7)	4610(2)	7104(6)	20(1)

Table 5.9 Fractional coordinates for atoms in *cis*-6,8-dimethyl-1-nitro-4-trinitromethyl-1,4-dihydronaphthalene (113).

Atom	$10^4X/a$	$10^4Y/b$	$10^4Z/c$	10^3U
O(11)	9690(4)	6970(2)	5414(3)	41(1)
O(12)	8461(4)	7587(2)	3786(3)	31(1)
O(21)	5674(4)	6660(2)	2554(3)	39(1)
O(22)	5838(4)	5550(2)	3410(3)	33(1)
O(31)	2508(4)	5052(2)	2745(3)	36(1)
O(32)	2234(4)	5369(2)	4608(3)	34(1)
O(41)	1434(5)	6666(2)	1299(3)	60(1)
O(42)	553(4)	6560(2)	2464(3)	30(1)
N(1)	8494(4)	7334(2)	4816(3)	18(1)
N(2)	5103(4)	6134(2)	3066(3)	23(1)
N(3)	2644(4)	5486(2)	3616(3)	23(1)
N(4)	2011(5)	6531(2)	2272(3)	24(1)
C(1)	7006(5)	7520(2)	5475(3)	15(1)
C(2)	6442(5)	6797(2)	5997(3)	17(1)
C(3)	4909(5)	6496(2)	5589(3)	16(1)
C(4)	3572(5)	6813(2)	4523(3)	15(1)
C(4a)	3954(5)	7628(2)	4200(3)	13(1)
C(5)	2602(5)	8063(2)	3538(3)	14(1)
C(6)	2825(5)	8826(2)	3300(3)	16(1)
C(7)	4451(5)	9142(2)	3766(4)	18(1)
C(8)	5819(5)	8734(2)	4448(3)	16(1)
C(8a)	5577(5)	7955(2)	4662(3)	13(1)
C(9)	3366(5)	6276(2)	3397(4)	16(1)
C(10)	1327(5)	9297(2)	2620(4)	24(1)
C(11)	7515(5)	9126(2)	4963(4)	24(1)

Table 5.10 Fractional coordinates for atoms in nitro cycloadduct (122).

Atom	$10^4X/a$	$10^4Y/b$	$10^4Z/c$	10^3U
O(11)	5953(1)	-3899(3)	5791(1)	25(1)
O(12)	5945(1)	-4349(3)	6671(1)	24(1)
O(21)	7025(1)	180(3)	5778(1)	25(1)
O(22)	7490(1)	-1697(3)	6400(1)	27(1)
O(31)	5268(1)	-1278(3)	7167(1)	17(1)
O(32)	6111(1)	1014(3)	6966(1)	17(1)
O(41)	4577(1)	2416(3)	5397(1)	27(1)
O(42)	4242(1)	3640(3)	6177(1)	27(1)
N(1)	5973(2)	-3375(4)	6268(1)	19(1)
N(2)	6937(1)	-902(4)	6151(1)	18(1)
N(3)	6065(1)	-921(4)	6939(1)	17(1)
N(4)	4672(1)	2646(4)	5891(1)	20(1)
C(1)	5392(2)	-361(4)	5979(1)	12(1)
C(2)	5383(2)	1638(4)	6158(1)	14(1)
C(3)	5302(2)	1635(4)	6782(1)	15(1)
C(4)	4691(2)	176(4)	6994(1)	16(1)
C(4a)	4132(2)	-651(4)	6566(1)	13(1)
C(5)	3296(2)	-1098(4)	7758(1)	14(1)
C(6)	2885(2)	-2023(4)	6244(1)	19(1)
C(7)	3253(2)	-2518(4)	5754(1)	16(1)
C(8)	4086(2)	-2018(4)	5670(1)	16(1)
C(8a)	4511(2)	-1103(4)	6069(1)	11(1)
C(9)	6032(2)	-1327(4)	6338(1)	11(1)
C(10)	2851(2)	-648(4)	7186(1)	24(1)
C(11)	2784(2)	-3514(4)	5310(1)	25(1)

Table 5.11 Fractional coordinates for atoms in nitro cycloadduct (153).

Atom	$10^4X/a$	$10^4Y/b$	$10^4Z/c$	10^3U
O(11)	7001(2)	5670(3)	2565(1)	29(1)
O(12)	5547(2)	3401(4)	2579(1)	34(1)
O(21)	8471(2)	2574(4)	3664(1)	30(1)
O(22)	7680(2)	-246(4)	4258(1)	28(1)
O(31)	8634(2)	4229(3)	1635(1)	14(1)
O(32)	9656(2)	1687(3)	2240(1)	16(1)
O(41)	6435(2)	-2612(3)	1063(1)	24(1)
O(42)	8117(2)	-1938(3)	582(1)	28(1)
N(1)	6627(2)	3995(4)	2522(1)	19(1)
N(2)	7949(2)	1465(4)	3187(1)	19(1)
N(3)	8817(2)	3301(4)	2315(1)	15(1)
N(4)	7472(2)	-1708(4)	1059(1)	19(1)
C(1)	8022(3)	-509(4)	1699(1)	14(1)
C(2)	6926(3)	839(4)	1866(1)	14(1)
C(3)	6285(3)	1781(4)	1143(2)	14(1)
C(4)	7082(3)	2520(4)	734(1)	13(1)
C(5)	8532(3)	2654(4)	1076(1)	15(1)
C(6)	9078(3)	845(4)	1540(1)	14(1)
C(7)	7577(3)	2357(4)	2415(1)	15(1)
C(8)	4820(3)	1624(5)	947(2)	20(1)
C(9)	6646(3)	3352(5)	-12(2)	18(1)
C(10)	9434(3)	3271(5)	576(2)	19(1)

Table 5.12 Fractional coordinates for atoms in 1,2,3-trimethyl-*r*-3,*c*-4,*c*-6-trinitro-*t*-5-trinitromethylcyclohex-1-ene (157).

Atom	$10^4X/a$	$10^4Y/b$	$10^4Z/c$	10^3U
O(11)	-126(3)	6513(2)	4394(2)	69(1)
O(12)	1820(2)	6430(2)	4112(2)	39(1)
O(21)	2819(3)	5671(2)	2383(2)	45(1)
O(22)	858(3)	4958(2)	1463(2)	51(1)
O(31)	3353(2)	8137(2)	4177(2)	37(1)
O(32)	1557(3)	8802(2)	4412(2)	55(1)
O(41)	3864(3)	6865(2)	487(2)	62(1)
O(42)	1720(2)	6336(2)	-106(2)	38(1)
O(51)	1135(3)	8199(2)	-995(2)	55(1)
O(52)	83(2)	8639(2)	162(2)	38(1)
O(61)	4391(2)	8216(2)	2178(2)	40(1)
O(62)	3185(2)	9242(2)	859(2)	44(1)
N(1)	553(3)	6516(2)	3775(2)	35(1)
N(2)	1542(3)	5670(2)	1894(2)	32(1)
N(3)	2141(3)	8415(2)	3827(2)	31(1)
N(4)	2653(3)	6903(2)	396(2)	35(1)
N(5)	1004(3)	8231(2)	-52(2)	30(1)
N(6)	3369(3)	8472(2)	1361(3)	32(1)
C(1)	-270(3)	8376(2)	2306(3)	26(1)
C(2)	-1018(3)	7582(2)	2268(3)	27(1)
C(3)	-284(3)	6604(2)	2455(3)	25(1)
C(4)	715(3)	6607(2)	1762(3)	22(1)
C(5)	1761(3)	7456(2)	1998(3)	20(1)
C(6)	1268(3)	8330(2)	2513(2)	22(1)
C(7)	-897(3)	9375(2)	2164(3)	43(1)

Table 5.12 cont.

Atom	$10^4X/a$	$10^4Y/b$	$10^4Z/c$	10^3U
C(8)	-2557(3)	7605(2)	2060(3)	41(1)
C(9)	-1273(2)	5753(2)	2180(3)	39(1)
C(10)	2146(3)	7749(2)	947(3)	23(1)

Table 5.13 Fractional coordinates for atoms in trinitro nitronic ester (161).

Atom	$10^4X/a$	$10^4Y/b$	$10^4Z/c$	10^3U
O(11)	907(5)	2191(2)	1869(1)	17(1)
O(12)	3552(5)	2811(2)	2237(1)	22(1)
O(21)	3347(5)	4544(2)	2415(1)	28(1)
O(22)	1881(5)	5262(2)	1798(1)	25(1)
O(31)	-809(6)	5284(2)	638(1)	34(1)
O(32)	-2463(5)	4089(2)	403(1)	28(1)
O(41)	-4483(5)	2572(2)	1023(1)	31(1)
O(42)	-4778(4)	3929(2)	1330(1)	24(1)
N(1)	1998(6)	2987(3)	1991(1)	18(1)
N(2)	2254(6)	4571(3)	2042(1)	21(1)
N(3)	-1103(6)	4471(3)	641(1)	22(1)
N(4)	-3874(6)	3194(3)	1286(1)	21(1)
C(1)	-1939(7)	3092(3)	1593(2)	15(1)
C(2)	-515(7)	6877(3)	1506(2)	14(1)
C(3)	341(7)	3894(3)	964(2)	16(1)
C(4)	715(7)	2991(3)	732(2)	16(1)
C(5)	281(7)	2233(3)	977(2)	14(1)
C(6)	-774(7)	2222(3)	1482(2)	15(1)
C(7)	1234(7)	3765(3)	1854(2)	13(1)
C(8)	1794(6)	3052(3)	237(2)	19(1)
C(9)	904(8)	1308(3)	779(2)	24(1)
C(10)	-1949(8)	1376(3)	1626(2)	24(1)

Table 5.14 Fractional coordinates for atoms in hydroxy dinitro nitronic ester (162).

Atom	$10^4X/a$	$10^4Y/b$	$10^4Z/c$	10^3U
O(1)	7433(1)	6909(1)	6835(1)	16(1)
O(11)	8456(1)	10482(1)	8190(1)	16(1)
O(12)	10236(1)	11051(1)	9151(1)	20(1)
O(21)	12072(1)	8818(2)	9498(1)	30(1)
O(22)	11163(1)	6437(2)	9514(1)	25(1)
O(31)	8611(1)	3959(1)	7786(1)	24(1)
O(32)	6625(1)	4137(2)	8212(1)	25(1)
N(1)	9612(2)	9924(2)	8740(1)	15(1)
N(2)	11138(2)	7883(2)	9301(1)	18(1)
N(3)	7760(2)	4640(2)	8181(1)	17(1)
C(1)	8312(2)	7997(2)	7353(1)	13(1)
C(2)	9146(2)	7140(2)	8156(1)	13(1)
C(3)	8183(2)	6204(2)	8704(1)	14(1)
C(4)	6999(2)	7164(2)	8927(1)	14(1)
C(5)	6707(2)	8606(2)	8532(1)	14(1)
C(6)	7472(2)	9253(2)	7777(1)	13(1)
C(7)	9908(2)	8387(2)	8744(1)	14(1)
C(8)	6248(2)	6491(2)	9678(1)	20(1)
C(9)	5626(2)	9690(2)	8816(1)	21(1)
C(10)	6619(2)	10227(2)	7050(1)	18(1)

Table 5.15 Fractional coordinates for atoms in *t*-6-hydroxy-4,5,6-trimethyl-2,*r*-4,*t*-5-trinitrocyclohex-2-enone (172).

Atom	$10^4X/a$	$10^4Y/b$	$10^4Z/c$	10^3U
O(1)	4824(2)	108(1)	1672(2)	24(1)
O(6)	6662(2)	-1052(1)	1573(2)	21(1)
O(11)	1033(2)	559(1)	1030(2)	33(1)
O(12)	-457(2)	314(1)	3017(2)	28(1)
O(21)	230(2)	-1946(1)	1995(2)	28(1)
O(22)	151(2)	-2528(1)	4105(2)	33(1)
O(31)	6157(2)	-637(1)	4880(2)	24(1)
O(32)	7650(2)	-1569(1)	5223(2)	32(1)
N(1)	798(2)	216(1)	2196(2)	20(1)
N(2)	1368(2)	-2026(1)	3302(2)	20(1)
N(3)	6303(2)	-1220(1)	4572(2)	20(1)
C(1)	3966(3)	-373(1)	1995(2)	16(1)
C(2)	2082(3)	-359(1)	2588(2)	14(1)
C(3)	1505(3)	-842(1)	3438(2)	16(1)
C(4)	2711(3)	-1441(1)	3974(2)	16(1)
C(5)	4640(3)	-1511(1)	3245(2)	16(1)
C(6)	4678(2)	-1065(1)	1725(2)	16(1)
C(7)	3066(3)	-1492(1)	5847(2)	21(1)
C(8)	5193(3)	-2214(1)	2945(2)	21(1)
C(9)	3371(3)	-1324(1)	146(2)	19(1)

5.6 References for Chapter Five

1 Kinns, M., and Sanders, J. K. M., *J. Magn. Reson.*, 1984, **56**, 518.

2 Tschinkel, J. G., *Ind. Eng. Chem.*, 1965, **48**, 732.

3 Davis, A., and Warren, K. D., *J. Chem. Soc. B*, 1969, 873.

4 Greenland, H., Pinhey, J. T., and Sternhell, S., *Aust. J. Chem.*, 1987, **40**, 325.

5 Barnes, C. E., Fieldman, K. S., Johnson, M. W., Lee, H. W. H., and Myhre, P. C., *J. Org. Chem.*, 1979, **44**, 3925.

6 Hartshorn, M. P., Judd, M. C., Vannoort, R. W., and Wright, G. J., *Aust. J. Chem.*, 1989, **42**, 689; Blackstock, D. J., Hartshorn, M. P., Lewis, A. J., Richards, K. E., Vaughan, J., and Wright, G. J., *J. Chem. Soc. B*, 1971, 1212.

7 Young, D. A. W., *B. Sc. (Hons. III) project*, University of Canterbury, 1994.

8 Myhre, P. C., *Personal communication.*

9 Banwell, T., Morse, C. S., Myhre, P. C., and Vollmar, A., *J. Am. Chem. Soc.*, 1977, **99**, 3042.

10 Baciocchi, E., Cort, A. D., Eberson, L., Mandolini, L., and Rol, C., *J. Org. Chem.*, 1986, **51**, 4544.

11 Fischer, A., and Leonard, D. R. A., *Can. J. Chem.*, 1976, **54**, 1795.

12 Masnovi, J. M., Sankararaman, S., and Kochi, J. K., *J. Am. Chem. Soc.*, 1989, **111**, 2263.

13 Nyberg, K., and Wistrand, L. G., *Chem. Scripta*, 1974, **5**, 234.

14 Nyberg, K., *Chem. Scripta*, 1974, **5**, 115.

15 Kim, F. K., and Kochi, J. K., *J. Org. Chem.*, 1989, **54**, 1692.

16 Suzuki, H., and Nakamura, K., *Bull. Chem. Soc. Jpn.*, 1970, **43**, 473.

17 Suzuki, H., *Bull. Chem. Soc. Jpn.*, 1970, **43**, 879.

18 Mori, K., Yukitake, K., and Matsui, S., *Japan. Kokai*, 75 35, 123; Chem. Abs., 1975, **83**, 96715z.

19 Baciocchi, E., Rol, C., and Mandolini, L., *J. Org. Chem.*, 1977, **42**, 3682.

20 Suzuki, H., and Hanafusa, T., *Bull. Chem. Soc. Jpn.*, 1973, **46**, 3607.

21 Pouchert, C. J., *The Aldrich Library of FT-IR Spectra, Edn. I, vol. 1*, 1985; Pouchert, C. J., *The Aldrich Library of NMR Spectra, Edn. II, vol. 1*, 1983.

22 Holler, A. C., Huggett, C., and Rathmann, F. H., *J. Am. Chem. Soc.*, 1950, **72**, 2034.

23 Sheldrick, G. M., *J. Appl. Crystallogr.*, In preparation.

Acknowledgements

I would like to express my gratitude to my supervisor, Professor Michael P. Hartshorn, for his encouragement and guidance throughout the duration of this work.

In addition, my thanks go to Professor Ward T. Robinson for his assistance with the X-ray structure analysis work; Bruce Clark for seemingly endless mass spectrometry; Rewi Thompson for help especially with the initial n.m.r., infrared and ultraviolet work; and the other academic and technical staff of the Chemistry Department, University of Canterbury for their assistance whenever required. I would also like to thank Craig P. Butts, Karen L. Fulton, Bryan R. Woods and Dawson A. W. Young - the 'TNM' team.

Finally, I would like to extend a special thanks to my wife, Gail, for her support, encouragement and understanding during this time and also to my ever interested family.